

Olga Gladkova

Doktorander i reglerteknik

Ref nr: PA2020/3049-173 Datum för ansökan: 2020-11-01 11:41



Födelsedatum	1991-12-31
Adress	Zavodskoi proezd 105037 Moscow Russian Federation
E-post	gladkova.olga.ig@gmail.com
Kön	Kvinna
Mobiltelefon	+79851912827
Telefon	+79851912827

Frågor

1. *Har du avlagt masterexamen?*
Ja Rätt svar
2. *Vid vilket universitet har du avlagt masterexamen?*
Bauman Moscow State Technical University
3. *Ange namn på din(a) referens(er).*
Vadim V. Veltishev
Sergey A. Egorov
Alexey A. Makashov
4. *Vilket är det främsta skälet till att du söker denna tjänst?*
The theory of automatic control was my favourite subject at the university. That is why I want to continue my research in this field as a PhD student.

Olga Gladkova

Doktorander i reglerteknik

Ref nr: PA2020/3049-17 Datum för ansökan: 2020-11-01 11:41

Eget uppladdat CV

Egna filer och portfolio

Diploma-Tr-Gladkova.pdf

Diploma-Tr-Gladkova.pdf

Diploma-Original-Gladkova.pdf

Diploma-Original-Gladkova.pdf

Transcript-Gladkova.pdf

Transcript-Gladkova.pdf

Transcript-Original-Gladkova.pdf

Transcript-Original-Gladkova.pdf

Reference-from-Veltishev-to-Gladkova.pdf

Reference-from-Veltishev-to-Gladkova.pdf

Reference-from-Egorov-to-Gladkova.pdf

Reference-from-Egorov-to-Gladkova.pdf

Reference-from-Makashov-to-Gladkova.pdf

Reference-from-Makashov-to-Gladkova.pdf

Utbildningar

Titel	Skola/Företag	Ort	Land	Från-Till
Master's degree in Engineering	Bauman Moscow State Technical University	Moscow	Russian Federation	2008-2014
	<i>Specialist / Master's degree in Engineering, speciality – Mechatronics and Robotics</i>			

Språk

ryska	Flytande	<i>Modersmål</i>
engelska	Mycket bra	

Körkort



Referenser

Namn Vadim V. Veltishev
Företag Bauman Moscow State Technical University
E-post vvv@bmstu.ru
Telefon +74992636115

Namn Sergey A. Egorov
Företag Bauman Moscow State Technical University
E-post egorovsa@bmstu.ru
Telefon +74992635784

Namn Alexey Makashov
Företag Bauman Moscow State Technical University
E-post amakashov@bmstu.ru
Telefon +79164335281

Dear Sir/Madam,

I got very encouraged and inspired when I found an open PhD student position in Automatic Control at Lund University. I find myself as an active, enthusiastic, and hardworking person who has a strong addiction to science.

I studied at the Bauman Moscow State Technical University (BMSTU), "Underwater robots and vehicles" department at the specialist degree program for six years (it is an analogue of a bachelor's and master's degree in Russia).

Besides being a student, I was working in the Research Institute of Special Machinery, Department of Underwater Robotics. My major both at university and at work was the control systems engineering. My main duties included mathematical modelling of the vehicle's movements development. I worked with the programming and simulations software MATLAB, sensor fusion, programming (C++) and testing of the proposed algorithms, bench and field-trials of complex systems. Development of complex systems gave me a valuable experience of work both independently and as a team member of professionals from different fields.

During my university years, I demonstrated not only excellent academic results but also a desire to broaden my horizons in science. I took part in conferences and published my research results in scientific journals. After graduation, I decided to continue my work with research about motion control of that special Remotely Operated Vehicle for periodic monitoring of the technical conditions of such underwater structures as ship hulls, harbours, pipelines, etc. It became the starting point of my career as a teacher as well. Nowadays, when the prototype of that remotely operated vehicle was successfully tested, I can return to my dream of getting a PhD degree in the field of automatic control.

I have to admit that underwater robotics is an interesting but highly specialized field and I wish to work on a larger scale, in the scientific field with a cut of the edge investigation and in the international collective. From all my life experience I know that my curiosity, assertiveness, goal-orientation and active life position always helps me to get to the bottoms of all the difficult questions. That is why I truly believe that becoming a PhD student at the Department of Automatic Control is the perfect opportunity where I can work with enormous motivation and fulfil my potential.

Sincerely,
Olga Gladkova.

Olga Gladkova

Address: 105037, Russia, Moscow, Zavodskoi proezd, 3, app.2

Telephone: +7 985 191 28 27

E-mail: gladkova.olga.ig@gmail.com

Date of birth: 31 December 1991

Research interests

Control theory, simulations and modeling, robotics.

Education

September 2008 – July 2014: Specialist / Master's degree in Engineering, speciality – Mechatronics and Robotics, Bauman Moscow State Technical University (Mechanical Engineering Faculty, Department of Underwater Robots and Vehicles).

Principal subjects: Control theory; electronics.

GPA: 5.0 out of 5.

October 2015 – October 2019: High-Research teacher, Bauman Moscow State Technical University (Mechanical Engineering Faculty, Department of Underwater Robots and Vehicles).

Awards: 2011 – Schlumberger Scholarship award in recognition of talent and perseverance in science and engineering; 2012 – personal scholarship of Imperial Technical College Club (Bauman Moscow State Technical University); 2012 – President of Russian Federation grant.

Publications list appended below.

Work experience

September 2010 – present: Bauman Moscow State Technical University (Research Institute of Special Machinery, Department of Underwater Robotics), Moscow, Russia
Research Fellow

Duties included:

- control systems engineering: development of motion control systems of remotely operated vehicles (with different types of propulsion systems), sensors selection and processing (sensor fusion, calibration), prototype design, programming and testing proposed algorithms, bench and field-trials of complex systems;
- analyzing data: updating knowledge database, working with datasets from simulations and trials, troubleshooting, making research, preparing reports.
- electronic engineering: development of special electronic devices for underwater robots (f. e. compact control unit for zoom and focus drives of a video camera, digital interface modules with RS-485 and RS-232, power boards) including components selection, PCB layout, controllers programming and debugging.

September 2015 – present: Bauman Moscow State Technical University
Research teacher at the Department of Underwater Robots and Vehicles

Duties included:

- managing seminars at “Introduction to profile training” and “Control of Robots and Robotic Systems” courses;
- supervision: bachelors pre-diploma projects and final qualifying works (4 B.Sc. qualification works, 3 of those with distinction);
- research: developing and testing new algorithms of unmanned underwater vehicles motion control; publishing obtained results.

Courses and trainings

2013 – “Student of Business Administration” course: personal effectiveness, business effectiveness, international business; “Recruiter” course of volunteer’s center “Kazan 2013” (the XXVII Summer Universiade). **Volunteer:** Greenpeace Russia.

Personal skills and competencies

Native language: Russian.

Other languages: English (Upper Intermediate); practice at International Workshop “Space Development: Theory and Practice” (2010), “Work and Travel USA” (2011).

Technical skills and competences: analytical skills (performing research, understanding of sophisticated technical solutions, analyzing data, exploring the ways of systems improvement).

Social skills and competences: a flexible team player with an excellent ability to adapt to various working conditions. These skills were gained through my experience in development and testing complex systems and because of communications with different types of people and professionals from various fields (electronics, software, design, management, etc.).

Organizational skills and competences: responsible and organized person with the ability to enhance these skills of the team members (and/or students).

Computer skills and competences:

- numerical-analysis and simulation software (MATLAB, Mathcad);
- CAD and 3D graphic products (AutoCAD, SolidWorks);
- programming skills (C++ with QtCreator IDE, Assembler);
- distributed version control systems (Git), issue tracking software (Jira);
- electronic design automation software packages (P-CAD, Altium Designer);
- excellent command of Microsoft Office tools (Word, Excel, PowerPoint, Visio);
- a user of OS Linux, QNX, Windows.

Other skills and competences

Driving license: B category.

Interests & extra information

Scuba diving (OWD certificate from SSI), mountaineering and rock climbing, hiking, ecotourism, swimming, surfing, kitesurfing, yacht sailing.

Publications (<https://bit.ly/33ADQwP>):

1. Prospects of underwater gliders usage

Author(s): Gladkova O.I.

Student scientific spring 2010: Collection of abstracts of the university scientific and technical conference, April 1-30, 2010 / Bauman Moscow State Technical University, Moscow, 2010. T.10, part 2. pp. 302-303. (in Russian)

2. Using underwater gliders to study the ocean of Jupiter's moon "Europa"

Author(s): Gladkova O.I., Igritsky V.A.

Actual problems of Russian cosmonautics: Proceedings of XXXV Academic Readings on Cosmonautics / Edited by A.K. Medvedeva. - Moscow: Commission of the Russian Academy of Sciences on the development of the scientific heritage of pioneers of space exploration, 2011. 624 p. (in Russian)

3. Monitoring and control system for lithium-ion batteries in remotely operated and autonomous unmanned underwater vehicles

Author(s): Gladkova O.I., Shipovskoi D.M.

Online journal "Youth science and technology newsletter, Bauman Moscow State Technical University, No ФС77-51038. ISSN 2307-0609" [electronic resource]. Moscow: BMSTU. 2013. No.12. URL: <http://ainsnt.ru/doc/641120.html> (date of access 09.09.2020). (in Russian)

4. Investigation of the mutual influence of the control loops of the autonomous unmanned underwater vehicle "Imperator" taking into account the peculiarities of the organization of its propulsion and steering complex

Author(s): Gladkova O.I.

Online journal "Youth science and technology newsletter, Bauman Moscow State Technical University, No ФС77-51038. ISSN 2307-0609" [electronic resource]. Moscow: BMSTU. 2014. No.8. URL: <http://ainsnt.ru/doc/724988.html> (date of access 09.09.2020). (in Russian)

5. Information and control system of a hybrid remotely operated vehicle

Author(s): Gamazov N.I., **Gladkova O.I.**, Egorov S.A., Lyamina E.A.

Modern methods and means of oceanological research: Proceedings of the XIV International Scientific and Technical Conference "MSOI-2015". Moscow: IO RAN, 2015. - T.2. pp. 209-213. (in Russian)

6. Features of development and testing of the information and control system of a hybrid remotely operated vehicle

Author(s): Gamazov N.I., **Gladkova O.I.**, Inozemtsev V.V., Egorov S.A., Lyamina E.A.

Sixth Russian Scientific and Technical Conference "Technical Problems of World Ocean Development" (TPOMO-6): September 28 - October 2, 2015: Conference proceedings. / Vladivostok: FEB RAS, 2015. pp. 401-405. (in Russian)

7. Underwater Survey of Vessels with Robotic Technology

Authors: Veltischev V.V., Egorov S.A., **Gladkova O.**, Grigoriev M., Baskakova E.V.

Underwater investigations and robotics: a scientific and technical journal about exploration ocean problems. / FEB RAS. 2016. Vladivostok: Dalnauka. 2016, No. 1 (21). pp. 15-24. (in Russian)

8. Mathematical model of curvilinear movement of remotely operated vehicle with a hybrid propulsion system

Author(s): Veltischev V.V., **Gladkova O.I.**, Mashkov K.Y.

Collection of scientific articles "TRUDY NAMI". 2017. No. 3 (270). pp. 82-90. (in Russian)

9. Application of hybrid propulsion UUV for ship hull survey without dry docking

Authors: Gladkova O.I.

Transactions of the Krylov State Research Centre. 2018; special issue 1. DOI: 10.24937/2542-2324-2018-1-5-1-213-223. pp. 213-223. (in Russian)

10. Development of an Information Control System for a Remotely Operated Vehicle with Hybrid Propulsion System

Author(s): Gladkova O.I., Veltischev V.V., Egorov S.A.

Robotics: Industry 4.0 Issues & New Intelligent Control Paradigms. Springer. Cham. 2020. DOI: 10.1007/978-3-030-37841-7_17. pp. 205-217.

References

Doctor of Technical Science

Vadim V. Veltischev

Head of "Underwater Robots and Vehicles" department,

Bauman Moscow State Technical University,

head of "Underwater Robotics" division,

Research Institute of Special Machinery of

Bauman Moscow State Technical University

e-mail: vvv@bmstu.ru

phone: +74992636115

mobile phone: +79162794220

Candidate of Technical Science

Sergey A. Egorov

Head of "Information and Control systems of Underwater Robotics" laboratory,

Research Institute of Special Machinery of

Bauman Moscow State Technical University

e-mail: egorovsa@bmstu.ru

phone: +74992635784

mobile phone: +79163859599

RUSSIAN FEDERATION

[Emblem of the Russian Federation]

**Diploma of Specialist
with honors**



СЕРТИФИКАТ
СРЕДНЕГО ПРОФЕССИОНАЛЬНОГО ОБРАЗОВАНИЯ
ДЕПАРТАМЕНТ ОБРАЗОВАНИЯ
СРЕДНЕГО ПРОФЕССИОНАЛЬНОГО ОБРАЗОВАНИЯ
МИНИСТЕРСТВО ОБРАЗОВАНИЯ И НАУКИ
РОССИЙСКОЙ ФЕДЕРАЦИИ

[Emblem of the Russian Federation]

RUSSIAN FEDERATION

Federal State Budgetary Educational Institution
of Higher Professional Education
"Moscow State Technical University
named after N.E. Bauman"

City of Moscow

**Diploma of Specialist
with honors**

107704 0003-007

Document of Education and of Qualification

Registration Number

102

Issue date

June 30, 2014

This Diploma is to certify that

**Gladkova
Olga Igorevna**

has mastered a Specialist Curriculum in Speciality
220402

"Robots and Robotic Systems"

and passed successfully the Final State Attestation

By the decision of the State Attestation Commission
the qualification of
ENGINEER
is conferred on him.

The Minutes № 4/SM11 of 19 June 2014

Chairman of the State Qualification Commission

(signature) G.K. Borovin

Head of the Educational Institution

(signature) B.V. Padalkin

Seal affixed



РОССИЙСКАЯ ФЕДЕРАЦИЯ



**ДИПЛОМ
СПЕЦИАЛИСТА
С ОТЛИЧИЕМ**





РОССИЙСКАЯ ФЕДЕРАЦИЯ

Федеральное государственное бюджетное образовательное учреждение
высшего профессионального образования
«Московский государственный технический университет
имени Н.Э. Баумана»
г. Москва

ДИПЛОМ СПЕЦИАЛИСТА С ОТЛИЧИЕМ

107704 0003407

ДОКУМЕНТ ОБ ОБРАЗОВАНИИ И О КВАЛИФИКАЦИИ

Регистрационный номер

102

Дата выдачи

30 июня 2014 года

Настоящий диплом свидетельствует о том, что

**Гладкова
Ольга Игоревна**

окончила(а) программу специалитета по специальности

220402

«Роботы и робототехнические системы»

и успешно прошла(а) государственную итоговую аттестацию

Решением Государственной экзаменационной комиссии
присвоена квалификация

инженер

Протокол №4/СМ11 от «19» июня 2014 г.

Председатель
Государственной
экзаменационной комиссии

Руководитель образовательной
организации



Г.И. Серов

Б.В. Садловник

Bauman Moscow State University, Faculty of Mechanical Engineering

Academic transcript

Name: Olga Gladkova

Birthday: 31 December 1991

Documents concerning previous education:

Secondary School Certificate of Education, issued in 2008 year

Entrance examinations: passed

Accepted to Bauman Moscow State University: 2008 (full-time student)

Date of graduation: June 2014

Program duration for full-time study: 5 years 10 months

Specialty: Mechatronics and Robotics

Major: Underwater robotics

List of term papers:

Term paper Total number of hours: 102	Machine parts and fundamentals of machine design excellent
Term paper Total number of hours: 51	Automatic control theory excellent
Term paper Total number of hours: 102	Electronics of robots excellent
Term paper Total number of hours: 102	Special purpose technology excellent
Term paper Total number of hours: 78	Design of underwater robots excellent
Term paper Total number of hours: 102	Management systems of robots and its



CERTIFY THAT
ПОДПИСАНО И СООТВЕТСТВУЕТ

	excellent
Term paper Total number of hours: 51	Electrical engineering
	excellent

List of practicums

Technological practicum Total number of hours: 144	excellent
Design and technological practicum Total number of hours: 144	excellent
Maintenance practicum Total number of hours: 144	excellent
Final practicum Total number of hours: 144	excellent

Final thesis Total number of hours: 1000	Special theme
	excellent

List of courses

Course title	Total number of hours	Final mark
History of Russia	102	Passed
Philosophy	136	Passed
Economics	204	Passed
Political science	102	Passed
Law	102	Passed
Economics of enterprise	102	Passed
Industrial engineering and planning	119	Excellent
Management basics	65	Passed
Ecology		Passed
Foreign language (English)		Excellent



CERTIFY THAT
INFORMATION IS ACCURATE

Physical education	408	Passed
Mathematical analysis	170	Excellent
Analytic geometry	102	Excellent
Ordinary differential equations	153	Excellent
Linear algebra and multivariable calculus	102	Passed
Multiple integrals	102	Excellent
Basics of probability theory and math statistics	68	Passed
Series, complex analysis and operational calculus	102	Excellent
Special themes in advanced mathematics	51	Passed
Computer science	221	Excellent
Theoretical mechanics	272	Excellent
Physics	374	Excellent
Chemistry	136	Excellent
Descriptive geometry	85	Excellent
Technical drawing	204	Excellent
Study and technological practicum	68	Passed
Strength of materials	136	Excellent
Metrology, standartization and certification	102	Excellent
Machine parts and fundamentals of machine design	272	Excellent
Materials science	102	Excellent
Design of special mechanisms	85	Passed
Special purpose technology	238	Excellent
Electrical engineering	204	Excellent
Automated mechanical and instrumentation manufacturing	68	Passed
Robotic manufacturing technology	68	Passed
Information processing systems of robots	85	Excellent
Probability theory	102	Passed
Intellectual property law	68	Passed
Special electronic devices	85	Excellent
Fundamentals of Automated Modeling	153	Excellent
Automatic control theory	595	Excellent
Electronics of robots	476	Excellent
Robot modeling	136	Excellent
Electronic drivers of robots	102	Excellent
Hydraulic systems of robots	136	Excellent



IDENTIFY THAT
SACCORAT R

Microprocessor systems of robots and its software	323	Excellent
Modelling and research of robots and robotic systems	214	Excellent
Artificial intelligence methodologies	65	Passed
Computer-aided design	102	Excellent
Design of underwater robots	231	Excellent
Control systems of underwater vehicles and robots	266	Excellent
Introduction to robotics	51	Passed
Cultural studies	102	Passed
Student's research activities	180	Passed
Civil defense	51	Passed
Health studies	34	Passed
Russian language and standards of speech	51	Passed
Life safety	85	Passed
Applied Hydro-acoustics	68	Passed
Modern design methodologies for underwater vehicles	208	Passed

Grade point average: 5.00 / 5.00

According to the Russian grading system:

Grade		Description
Excellent	5	The best possible grade
Good	4	Next highest grade, given for performance that meet the standard completely and is above average
Satisfactory	3	The lowest passing grade, indicates "average" performance
Unsatisfactory	2	Failure
Passed		Pass/Fail basis



**WE HEREBY CERTIFY THAT
THE INFORMATION IS ACCURATE**

[Handwritten signature]

РОССИЙСКАЯ
ФЕДЕРАЦИЯ



Федеральное государственное
бюджетное образовательное
учреждение высшего
профессионального
образования «Московский
государственный технический
университет
имени Н.Э. Баумана»
г. Москва

1. СВЕДЕНИЯ О ЛИЧНОСТИ ОБЛАДАТЕЛЯ ДИПЛОМА

Фамилия **Гладкова**
Имя **Ольга**
Отчество **Игоревна**
Дата рождения **31 декабря 1991 года**

Предшествующий документ об образовании или
об образовании и о квалификации

Аттестат о среднем (полном) общем образовании, 2008 год

2. СВЕДЕНИЯ О КВАЛИФИКАЦИИ

Решением Государственной экзаменационной
комиссии присвоена квалификация

инженер

по специальности

220402 «Роботы и робототехнические системы»

Срок освоения программы бакалавриата/специалитета
в очной форме обучения

5 лет 10 месяцев

ПРИЛОЖЕНИЕ
к ДИПЛОМУ
специальности с отличием
107718 0233984

Регистрационный
номер
102

Дата выдачи
30 июня 2014 года

3. СВЕДЕНИЯ О СОДЕРЖАНИИ И РЕЗУЛЬТАТАХ ОСВОЕНИЯ
ПРОГРАММЫ БАКАЛАВРИАТА/СПЕЦИАЛИТЕТА

Наименование дисциплины (модулей) программы, вид занятий	Количество зачетных единиц/ академических часов	Оценка
Отечественная история	102	ЗАЧТЕНО
Философия	136	ЗАЧТЕНО
Экономика	204	ЗАЧТЕНО
Политология	102	ЗАЧТЕНО
Правоведение	102	ЗАЧТЕНО
Экономика предприятия	102	ЗАЧТЕНО
Организация и планирование производства	119	ОТЛИЧНО
Основы менеджмента	65	ЗАЧТЕНО
Экология	68	ЗАЧТЕНО
Иностранный язык	561	ОТЛИЧНО
Физическая культура	408	ЗАЧТЕНО
Математический анализ	170	ОТЛИЧНО
Аналитическая геометрия	102	ОТЛИЧНО
Интегралы и дифференциальные уравнения	153	ОТЛИЧНО
Линейная алгебра и функции нескольких переменных	102	ЗАЧТЕНО
Кратные интегралы, теория поля, ряды	102	ОТЛИЧНО
Основы теории вероятностей и математической статистики	68	ЗАЧТЕНО
Теория функций комплексного переменного и операционное исчисление	102	ОТЛИЧНО
Высшая математика (спец. главы)	51	ЗАЧТЕНО
Информатика	221	ОТЛИЧНО
Теоретическая механика	272	ОТЛИЧНО
Физика	374	ОТЛИЧНО
Химия	136	ОТЛИЧНО
Начертательная геометрия	85	ОТЛИЧНО
Инженерная графика	204	ОТЛИЧНО
Учебно-технологический практикум	68	ЗАЧТЕНО
Сопротивление материалов	136	ОТЛИЧНО
Метрология, стандартизация и сертификация	102	ОТЛИЧНО
Детали машин и основы конструирования	272	ОТЛИЧНО
Материаловедение	102	ОТЛИЧНО
Конструкция спец. машин и устройств	85	ЗАЧТЕНО
Специальные технологии	238	ОТЛИЧНО
Электротехника	204	ОТЛИЧНО
Технология автоматизированного машиностроения и приборостроения	68	ЗАЧТЕНО
Технология роботизированного производства	68	ЗАЧТЕНО
Информационные устройства и системы роботов		
Теория вероятностей и теория случайных процессов	85	ОТЛИЧНО
Защита интеллектуальной собственности	102	ЗАЧТЕНО
Специальные электронные устройства	68	ЗАЧТЕНО
Основы автоматизированного проектирования	85	ОТЛИЧНО
Теория автоматического управления	153	ОТЛИЧНО
Электронные устройства роботов	595	ОТЛИЧНО
Основы робототехники	476	ОТЛИЧНО
	136	ОТЛИЧНО

Наименование дисциплины (модулей) программ, вид практики	Количество зачетных единиц/ недельные часы	Оценка
Электрические приводы роботов	102	отлично
Гидроэлектромеханические приводы роботов	136	отлично
Микропроцессорные устройства роботов и их программное обеспечение	323	отлично
Моделирование и исследование роботов и робототехнических систем	214	отлично
Методы искусственного интеллекта	65	зачтено
Проектирование робототехнических систем	102	отлично
Проектирование подводных робототехнических систем	231	отлично
Управление роботами и подводными робототехническими системами	266	отлично
Введение в специальность	51	зачтено
Культурология	102	зачтено
Научно-исследовательская работа студента	180	зачтено
Безопасность жизнедеятельности: защита в чрезвычайных ситуациях и гражданская оборона		
Валеология	51	зачтено
Русский язык и культура речи	34	зачтено
Безопасность жизнедеятельности	51	зачтено
Гидроакустические поисковые и измерительные системы	85	зачтено
Проектирование движительных комплексов подводных аппаратов	68	зачтено
	208	зачтено
Практика в том числе:	16 недель	
Технологическая		
Конструкторско-технологическая	4 недели	отлично
Эксплуатационная	4 недели	отлично
Преддипломная	4 недели	отлично
4 недели	4 недели	отлично
Государственная итоговая аттестация в том числе:	17 недель	
государственный экзамен		
выпускная квалификационная работа (дипломный проект) на тему «Разработка системы управления углом крена автономного необитаемого аппарата «Император»		не предусмотрен
		отлично
Общая трудоемкость образовательной программы в том числе объем работ обучающихся во взаимодействии с преподавателем:	215 недель 5123 час.	

4. КУРСОВЫЕ РАБОТЫ (ПРОЕКТЫ)	ОЦЕНКА
Курсовой проект по деталям машин и основам конструирования	отлично
Курсовая работа по теории автоматического управления	отлично
Курсовой проект по электронным устройствам роботов	отлично
Курсовой проект по специальной технологии	отлично
Курсовой проект по проектированию подводных робототехнических систем	отлично
Курсовой проект по микропроцессорным устройствам роботов и их программному обеспечению	отлично
Курсовая работа по электротехнике	отлично

5. ДОПОЛНИТЕЛЬНЫЕ СВЕДЕНИЯ

Форма обучения: очная

Специализация: Подводные роботы и робототехнические системы

Образовательная организация переименована в 2011 году.

Старое полное официальное наименование образовательной организации – Государственное образовательное учреждение высшего профессионального образования Московской государственной технический университет имени Н.Э. Баумана

Руководитель образовательной организации



Б.В. Падалкин

Подпись обучающегося (подпись)

4

Dear Sir/Madam,

I am writing this letter of recommendation in order to support the application of Olga Gladkova. She studied at the Bauman Moscow State Technical University (BMSTU), "Underwater robots and vehicles" department at the specialist degree program for six years (it is an analogue of a bachelor's and master's degree in Russia). I have worked with Olga as a supervisor and as a head of division where she is employed. I can characterize her as an extremely enthusiastic, ambitious and hard-working person.

As the head of the department, I interviewed all the school graduates who have honour degrees and intention to study at "Underwater robots and vehicles" department. Olga was one of them. During that interview, she showed herself as a perspective student and later it was proved by her excellent academic results and few scholarship awards. Olga has a great aspiration for learning. She started her research from the second year of education. She wrote her diploma work and conducted research under my supervision. Being proactive and well-organized Olga demonstrated her ability to handle sophisticated problems and provided remarkable analytical skills. Moreover, she revealed brilliant presentation skills as an articulate speaker at conferences. Her writing skills at academic papers in research fields both in Russian and English are impressive as well.

I had an excellent opportunity to watch how this student turned out into an experienced engineer. From the third course of her study, she entered the "Underwater Robotics" division of Scientific and Research Institute of Special Machinery and grown up from a technician to engineer and research teacher at the department. She successfully fulfilled few projects, recommended herself as a responsible person and made a valuable contribution to the studying process. She showed that she can work well both independently and as a team member, with professionals and students.

Worth mentioning, she managed to balance her time productively as she has also practiced in extracurricular activities. Olga was a group leader and representative, she was a member of the university's swimming team and participated in international programs.

As an enthusiastic person, Olga was always on the lookout for new information and ideas. And I knew that one day she would like to try herself in another interesting sphere where she can fulfil her potential. I reckon that you will find her an equally motivated, goal-seeking and persistent candidate. That is why I highly recommend her for admission to your university.

Sincerely,

Head of "Underwater robots and vehicles" department

Bauman Moscow State Technical University,

Head of "Underwater Robotics" division of

Scientific and Research Institute of Special Machinery

Bauman Moscow State Technical University,

Doctor of Technical Science,

Prof. Vadim Veltichev.



Dear Sir/Madam,

I have worked with Olga Gladkova from the time she studied at Bauman Moscow State Technical University (BMSTU) and during this time got to know her very well. She is a reliable, hardworking and active person. Combination of these skills is the reason why I have a professional and personal respect for her.

Being a lecturer and examiner for "Information processing systems of robots" and "Control systems of underwater vehicles and robots" courses at Bauman Moscow State Technical University, I have noticed that Olga has got a tireless curiosity for broadening her horizons and expanding her knowledge. After her graduation, she became an engineer at "Information and Control systems of Underwater Robotics" laboratory at Scientific and Research Institute of Special Machinery at BMSTU and started working under my supervision. Her determination, dedication to work and reliability were characteristics which helped Olga to succeed. She is not afraid challenging tasks and setting high. During our projects, she showed that she can push herself to the limits to complete critical tasks as soon as possible. Diligence, assiduity, accuracy – all these skills helped her to become a valuable researcher and development engineer.

Apart from that, Olga also has a great sense of humour, which helped her to overcome obstacles and challenges. Also, she has excellent communication and teamwork skills. She can be a leader and organizer, as she is capable of motivating groups of people and direct their efforts in the right way. She has a long list of activities being involved during her studies and work. That helps her to keep a firm mind and show her best at all the stages of development (from making a software to testing a system at the field trials) regardless of workplace conditions.

Personal skills, maturity level and dedication make Olga an exceptional student. I believe that Olga will make a valuable addition to any research group, as her abilities and determination will continue to grow.

Sincerely,

Head of "Information and Control systems of Underwater Robotics" laboratory

Scientific and Research Institute of Special Machinery

Bauman Moscow State Technical University,

Candidate of Technical Science

Sergey Igorov



Dear Sir/Madam,

It was a fortune for me to work with Olga Gladkova for almost 6 years at the Scientific and Research Institute of Special Machinery of Bauman Moscow State Technical University. Based on my experience of working with Olga during several projects in "Information and Control systems of Underwater Robotics" laboratory, I can say that she is intelligent, ambitious and energetic individual.

Olga possesses a multidisciplinary vision and impressive analytical skills, which are necessary for assessment and troubleshooting during the research and development process. She has repeatedly demonstrated her resourcefulness, precise attention to details and her persistence in finding the solutions. She does not avoid difficult tasks and always shows her best. Worth mentioning her work as a team member. Despite the heavy workload, she always can lend a helping hand and boost the motivation of her colleagues. Olga is opened for the opinions, perspectives and feelings of other members even if they differ from her own thoughts. She is a kind and caring person who's energy and optimism creates a positive and pleasant atmosphere.

I would be eager to characterize Olga not only as a competent specialist but also as an extremely self-organised person. Her wide circle of interests from mountaineering and climbing to piano shows her as a bright and inquisitive individual.

I know that Olga wishes to work on the cut of the edge, in a culture of freedom and responsibility, in collaboration with other researchers and without having language restrictions. I am certain that Olga is going to continue to show herself in the best light. That is why I advised her to take an advantage of any opportunity she gets and finally achieve her cherished dream - become a PhD candidate.

Kind regards,

Research fellow

"Information and Control systems of Underwater Robotics" laboratory

Scientific and Research Institute of Special Machinery

Bauman Moscow State Technical University.

Alexey Makashov.



Yifan Liu

Doktorander i reglerteknik

Ref nr: PA2020/3049-17 Datum för ansökan: 2020-11-01 11:21



Födelsedatum 1996-06-12
Adress 1037#Luoyu Road
430074 Wuhan
Hubei Sheng
Kina
E-post liu_yifan@hust.edu.cn
Kön Kvinna
Mobiltelefon +86 159 2642 4938
Telefon +86 159 2642 4938

Frågor

1. *Har du avlagt masterexamen?*
Nej Fel svar
2. *Vid vilket universitet har du avlagt masterexamen?*
Huazhong University of Science and Technology
3. *Ange namn på din(a) referens(er).*
Housheng Su, Zhigang Zeng
4. *Vilket är det främsta skälet till att du söker denna tjänst?*
The position at LTH is very attractive to me. I am willing to devote most of my time to the corresponding research project for pursuing a PhD degree.

Yifan Liu

Doktorander i reglerteknik

Ref nr: PA2020/3049-17 Datum för ansökan: 2020-11-01 11:21

Eget uppladdat CV

Egna filer och portfolio

Contact Information_Yifan Liu.pdf

Contact Information_Yifan Liu.pdf

transcript of courses_Yifan Liu .pdf

transcript of courses_Yifan Liu .pdf

Published Papers.pdf

Published Papers.pdf

Språk

kinesiska (mandarin) Flytande
engelska Mycket bra

Modersmål

Körkort

Saknas

Cover Letter

I am applying for a position as PhD student at the Department of Automatic Control because the requirements of this position are very attractive to me. I am willing to devote most of my time to the corresponding research project, and I am also willing to spend part of my time on courses learning, and the teaching part is what I am willing to do due to my experience as a teaching assistant in graduate school.

My interests are designing distributed and advanced control methods for multiple multi-agent systems based on the knowledge of control theory, stability theory, and game theory. Due to my strong interest in mathematics and robotic coordination, I got a B.E. in automation in the School of Artificial Intelligence and Automation, where I am pursuing my master's degree in control science and engineering. For three years, I have been designing suitable control algorithms for several types of multi-agent systems to achieve an agreement about certain interest such as consensus or containment. So, I am very familiar with the knowledge about algebraic graph theory, control theory and stability theory. After unremitting research on the above issues, I have achieved some output with 8 publications in the international journals, which are about multi-agent systems with sampled data control, intermittent control, switched dynamics and so on.

Robotic coordination and social networks do not take full advantages of those advanced control methods in combination with game theory and machine learning insights. However, there are many problems in these networked systems that need to be optimized, such as time delay, nonlinear disturbance, unreliable information channels, coupling constraints and input constraints, etc. Due to the complexity of multi-agent systems, to make systems stable or achieve certain interests is much more challenging, this is what attracts me most about this research. Using control theory and the related knowledge of optimization to solve coordination problems for multi-agent systems is also what I particularly want to study during my Ph.D. career. This is related to what I studied before and is a more challenging cross-cutting field that I have been fascinated with for many years, so I want a breakthrough in this area. I want to take my full advantages of the knowledge about algebraic graph theory, control theory and stability theory to conduct theoretical and algorithmic research on multi-agent systems, utilizing ideas from sampled data control, iterative learning, game theory and optimization.

As I became more interested in these research areas, I investigated the project groups at Lund University. The research carried out at LTH is of a high international standard, standing out as doing work I would like to be involved in.

In conclusion, I am an experienced student ready to enter the academic field with the support of the excellent researchers at LTH. The research carried out at LTH matches my research goals, and I feel that my research experience would be a benefit for your department. I hope I can have this opportunity to enter this department to fulfill my academic dream.

Yifan Liu

Address: Wuhan, China

Telephone: (86) 159-2642-4938

Email: liu_yifan@hust.edu.cn

EDUCATION BACKGROUND

Huazhong University of Science and Technology, Wuhan, China

M.S.E., Control Science and Engineering, in School of Artificial Intelligence and Automation

Advisor: Prof. Housheng Su

Expected June 2021

Huazhong University of Science and Technology, Wuhan, China

B.E., Automation, in School of Artificial Intelligence and Automation

June 2018

Thesis: Second-Order Consensus for Multi-agent Systems via Intermittent Sampled Position Data Control. (IN CHINESE)

SKILLS

- Proficient in MATLAB, familiar with Mathematica, proficient in C Programming
 - Familiar with design based on MCU, PID control design in process control system
 - Proficient in writing with Latex
 - Fluent in English and native Mandarin
-

AWARDS

National scholarship for Postgraduates **2019, 2020**

Only 5 of 400 students in Graduate School of Artificial Intelligence and Automation awarded

Merit Student for Postgraduates **2019**

Less than 15% of the total number of graduate students in my grade awarded

First Prize of "Siemens Cup" China Intelligent Manufacturing Challenge **2017**

Participated in the preliminary competition of continuous process design and development as the main participant

RESEARCH INTERESTS

- Stability analysis and control of switched systems
 - Reinforcement learning, especially Q-learning method
 - Modeling and control of a system/process model
 - Distributed cooperative control of multi-agent systems
 - Discontinuous control strategies such as sampled data control, intermittent control
-

PROJECT EXPERIENCES

Researcher, The Edge-Consensus Control in Networked Multi-agent System **2018-2020**

(Program of National Natural Science Foundation of China)

For networked multi-agent systems, based on the fact that information is difficult to obtain continuously in real life, some novel discontinuous control strategies are proposed, such as sampled position data

control, intermittent control, etc., which achieve breakthroughs in controller methods of agent. In this project, I have improved my ability of C programming. Besides, I can use MATLAB more proficiently and I have a deeper understanding of control methods.

Researcher, Continuous Process Design and Development in "Siemens Cup" China Intelligent Manufacturing Challenge **2017**

According to the industrial process given in the competition, by analyzing the characteristics of the process and the object, we designed the control method of the process and put it into operation, which satisfies all indicators (steady-state indicators, dynamic indicators, accumulation indicators, and safety indicators). In this project, I learned how to select appropriate data or sensors to monitor and model the process and how to satisfy all the control objectives by design the suitable control methods.

PUBLICATIONS

- 1) **Yifan Liu**, Housheng Su and Zhigang Zeng, "Second-Order Consensus for Multi-agent Systems with Switched Dynamics," in *IEEE Transactions on Cybernetics*, doi: 10.1109/TCYB.2020.3015977.
- 2) **Yifan Liu** and Housheng Su, "General Second-Order Consensus of Discrete-time Multi-agent Systems via Q-learning Method," in *IEEE Transactions on Systems, Man, and Cybernetics: Systems*, doi: 10.1109/TSMC.2020.3019519.
- 3) **Yifan Liu** and Housheng Su, "Second-Order Consensus for Multi-agent Systems with Switched Dynamics and Sampled Position Data," in *IEEE Transactions on Systems, Man, and Cybernetics: Systems* (submitted).
- 4) **Yifan Liu** and Housheng Su, "Necessary and Sufficient Conditions for Containment in Fractional-Order Multiagent Systems via Sampled Data," in *IEEE Transactions on Systems, Man, and Cybernetics: Systems*, doi: 10.1109/TSMC.2020.2997294.
- 5) Housheng Su, **Yifan Liu** and Zhigang Zeng, "Second-Order Consensus for Multiagent Systems via Intermittent Sampled Position Data Control," in *IEEE Transactions on Cybernetics*, vol. 50, no. 5, pp. 2063-2072, May 2020.
- 6) **Yifan Liu** and Housheng Su, "Containment Control of Second-Order Multi-agent Systems via Intermittent Sampled Position Data Communication," in *Applied Mathematics and Computation*, vol. 362, Dec. 2020.
- 7) **Yifan Liu** and Housheng Su, "Some Necessary and Sufficient Conditions for Containment of Second-Order Multi-agent Systems with Sampled Position Data," in *Neurocomputing*, vol. 378, pp. 228-237, Feb. 2020.
- 8) **Yifan Liu** and Housheng Su, "Some Necessary and Sufficient Conditions for Containment of Second-order Multi-agent Systems with Intermittent Sampled Data," in *ISA Transactions*, doi: 10.1016/j.isatra.2020.08.014

FULL CITATIONS: 39

Contact Information

REFERENCES

Prof. Housheng Su
Telephone: 027-87540210
Email: houshengsu@qq.com

Prof. Zhigang Zeng
Telephone: 027-87543630
Email: zgzen@hust.edu.cn

Transcripts and Degree Certificates

Of Yifan Liu

This file consists of:

- One Graduate School Academic Record
- One Undergraduate Academic Record
- One Certificate of the Degree of Bachelor
- One Certificate of Graduation



GRADUATE SCHOOL ACADEMIC RECORD

Name: Liu Yifan

Date of Enrollment: September, 2018

Student ID: M201872770

Date of Printing: August, 2020

College: School of Artificial Intelligence and Automation

Academic Program: Master's Program

Major: Control Science and Engineering

NO.	Courses Name	Hours	Credit	Score	Duration of Study
1	Foreign language (English)	32	2.0	exemption	Autumn of 2018
2	Nonlinear Control Theory high-level international courses	32	2.0	90	Autumn of 2018
3	Complex networks and control full English, high-level international courses	32	2.0	100	Autumn of 2018
4	Theory of matrices	48	3.0	80	Autumn of 2018
5	Analysis of Time Series	32	2.0	79	Autumn of 2018
6	Mathematical Statistics	48	3.0	90	Autumn of 2018
7	linear system theory	32	2.0	94	Autumn of 2018
8	Project Management	32	2.0	96	Autumn of 2018
9	Optimum control	32	2.0	87	Autumn of 2018
10	Information Retrieval	24	1.5	89	Spring of 2019
11	Theory and Practice of Socialism with Chinese Characteristics	36	2.0	89	Spring of 2019
12	Dialectics of Nature	18	1.0	78	Spring of 2019

Total credits: 24.50

Courses weighted average score: 88.51

Remarks: Two grading systems we employ are as follows:

1. The Percentage System: 60 is passing, 100 is full mark;

2. Two-Degree Grading: pass or fail.

3. Courses weighted average score $= \frac{\sum(\text{credits} * \text{grade})}{\sum \text{credits}}$, only count marks of the Percentage System.

Graduate School

Dean: 

Huazhong University of Science and Technology



华中科技大学

HUAZHONG UNIVERSITY OF SCIENCE AND TECHNOLOGY

UNDERGRADUATE ACADEMIC RECORD

Name: Liu Yifan Department: School of Artificial Intelligence and Automation

Date of Entrance: 09/2014

Student ID: U201414362 Major: Automation

Length of Schooling: 4 years

Course	Credits/Hours	Result	Course	Credits/Hours	Result
2014-2015 1st Semester			China's Foreign Policy--Case Analysis	1.5	85
Physical Education(I)	1	82	Signal Analysis	2	77
Engineering Graphics (I)	2.5	87	China's World Natural & Cultural Heritage	1.5	78
Metalworking Practice	1	91	2016-2017 1st Semester		
Military Theory	1	89	Sensor and Detecting Technology	3	84
Military Training	1	85	Principle of Process Control	5	86
Fundamentals of Ideological and Ethical Standards & Law	2.5	84	Control Theory Integrated Lab	1	85
Calculus (I) (A)	5.5	73	Japanese Society and Culture	2	90
Introduction to Information Technologies	1.5	Pass	Principles of Microcomputer	3.5	78
Chinese	2	76	Principles of Microcomputer Lab	1	77
Comprehensive English (I)	3.5	90	System Simulation and Matlab	2	92
2014-2015 2nd Semester			Operations Research (I)	2	99
Advanced Programming Language C	3.5	60	Control Theory (I)	4	90
Physics (I)	4	66	2016-2017 2nd Semester		
Global Human Geography	1.5	90	Electronic Technology Project	1	80
Social Practice in Ideological and Political Education	1.5	87	Engineering Management	2	80
National Conditions Outside China and Global Focus	1.5	90	Process Control Technology Integrated Lab	1.5	90
Calculus (I) (B)	5.5	80	Process Control System	3.5	90
Physics Lab(I)	2	73	Computer Control Technology	2.5	92
Linear Algebra	2.5	77	Computer Networks	3	98
Yoga (I)	1	90	Field Practice	1	94
Survey of Modern Chinese History	2	90	Digital Image Processing	2	92
Comprehensive English (III)	3.5	83	Situation and Policy	2	80
2015-2016 1st Semester			Intelligent Instruments and Microcontrollers	3	90
Course Project of Advanced Programming Language C	1.5	79	Principles of Automatic Control (II)	3	95
Physics (II)	4	73	2017-2018 1st Semester		
Circuit Theory (V)	4	72	Introduction to Guided Missile	1	84
Complex Function and Integral Transform	2.5	84	Process Control Technology Integrated Lab	1.5	80
Probability Theory and Mathematical Statistics (II)	2.5	85	Process Control System Project	1.5	95
Introduction to Basic Principles of Marxism	2.5	71	Robotic Principles	1.5	89
History and Development of Top American Universities	2	85	Distribution Control System and Configuration Software	2.5	87
Data Structure	3	79	2017-2018 2nd Semester		
Mathematic Model	2	88	Graduation Thesis	8	93
Experiment of Physics(III)	0.8	77	<hr/>		
Football (Elementary)	1	89	Total Credits	153.3	
2015-2016 2nd Semester			Total Weighted Average Scores		81.92
Game Theory	2	99	CET4		618
Electrical Skills Practice	1	89	CET6		467
Electronic Circuit Design: Testing and Experiment(II)	1	70	<hr/>		
Electronic Circuit Design Test and Experiment(II)	1	83	Remarks:		
Numerical Methods(III)	2	90	1. Hundred-mark system: (1)85--100=4.8; (2)60--84=1.5--3.9		
General Introduction to Mao Zedong Thought and Socialist Theory with Chinese Characteristics	3.5	79	(add 0.1 for every one more point)		
Analog Electronic Technology(II)	3.5	75	2. Five-grade marking system: Excellent (A)=4.0; good (B)=3.5;		
Digital Circuit and Logic Design (I)	3.5	70	satisfactory(C)=2.5; pass (D)=1.5		
Taikwondo (Elementary)	1		3. Two-grade marking system: Pass=3.0		

Director of Archives: Fan Yizhen

Huazhong University of Science and Technology

Date of Printing: August 5, 2020





Archives
Huazhong University of
Science and Technology

Wuhan, 430074, P.R.China
Tel: (827)87559510
Fax: (827)87559510

华中科技大学档案馆
中华人民共和国 湖北 武汉

CERTIFICATE OF THE DEGREE OF BACHELOR

Certificate No.1048742018006376

This is to certify that Ms. Liu Yifan, female, born on June 12, 1996, was enrolled in the School of Artificial Intelligence and Automation, Huazhong University of Science and Technology in September, 2014, majoring in Automation, having passed all the required examinations of Bachelor courses and thesis defense in Huazhong University of Science and Technology and satisfied all the requirements, graduated in June, 2018.

In accordance with the Degree Evaluation Committee of Huazhong University of Science and Technology, she is awarded the Degree of Bachelor of Engineering.

Dong Lieyun
President
Huazhong University of
Science and Technology
Archives
Verification

Date of Issue: June 30, 2018



Archives
Huazhong University of
Science and Technology

Wuhan, 430074, P.R.China
Tel: (827)87559510
Fax: (827)87559510

华中科技大学档案馆
中华人民共和国 湖北 武汉

CERTIFICATE OF GRADUATION

Certificate No.104871201805006376

This is to certify that Ms. Liu Yifan, female, born on June 12, 1996, was enrolled in the School of Artificial Intelligence and Automation, Huazhong University of Science and Technology in September, 2014, majoring in Automation, having passed all the examinations and thesis required by the four-year undergraduate program, graduated in June, 2018.



Qing Lieyun
President
Huazhong University of
Science and Technology

Date of Issue: June 30, 2018

Published Papers

Of Yifan Liu

This file consists of three representative papers, they are:

- 1) Second-Order Consensus for Multi-agent Systems with Switched Dynamics
- 2) General Second-Order Consensus of Discrete-time Multi-agent Systems via Q-learning Method
- 3) Second-Order Consensus for Multiagent Systems via Intermittent Sampled Position Data Control

Second-Order Consensus for Multiagent Systems With Switched Dynamics

Yifan Liu^{ID}, Housheng Su^{ID}, and Zhigang Zeng^{ID}, *Fellow, IEEE*

Abstract—This article investigates the consensus control problem for second-order multiagent systems with switched dynamics, consisting of a continuous-time subsystem and a discrete-time subsystem. Under a fixed directed topology, two linear control protocols are proposed for achieving consensus. One is that two subsystems use different control inputs, where the continuous-time system uses continuous-time control, and the discrete-time system uses discrete-time control. In order to reach consensus for this kind of control protocol, some necessary and sufficient conditions are derived. The other is to use the same control algorithm for the two subsystems, which is a sampled-data control input. Similar consensus conditions are also obtained. Finally, a few simulation examples are given to verify the theoretical results.

Index Terms—Consensus, sampled-data control, second-order multiagent system (MAS), switched dynamics.

I. INTRODUCTION

A GROUP of autonomous agents working in the same networked environment is defined as multiagent systems (MASs). Recently, distributed cooperative control of MAS has received great attention due to its wide applications in sensor networks [1], [2]; information control [3], [4]; and so on. Designing algorithms for MAS to accomplish specific global control goals is the main purpose of researchers. The global control goals include consensus problem [5], [6]; controllability analysis [7], [8]; optimization control [9], [10]; etc.

The popular research topic in these control goals is the consensus problem, which suggests that agents are able to achieve an agreement about certain interests under an appropriate algorithm. For decades, a lot of theoretical results on consensus for MASs have been developed [11], [12]. Olfati-Saber *et al.* [5] studied the consensus issues of first-order MAS (FOMAS) and

obtained an important distributed condition suggesting that the FOMAS can reach consensus if a spanning tree always exists in the networked topology. Recently, the research of the consensus issues for FOMAS has been widely investigated in [13]–[15]. Considering the reality, second-order consensus algorithms should be paid more attention to because some typical models, such as mobile robot dynamics models, can be linearized into double integrators. The consensus for second-order MAS (SOMAS) means that a set of agents controlled by double integrators is able to achieve agreement on certain states. For the consensus of FOMAS, the convergence result is usually affected by the network topology. As for the consensus of SOMAS, the convergence result will be affected not only by topology but also by the coupling strength of the system. In this case, a lot of literature was studied in [16]–[20] to reach second-order consensus for MAS, which is more challenging than the first-order consensus.

In reality, continuously measuring information is quite difficult because of unreliable information channels and limited network transmission bandwidth. Therefore, using sampled-data control is more practical with more advantages like robustness. Besides, the sampled-data control method was used in many practical systems, such as radar tracking systems and power systems. Recently, researchers have widely studied the sampled-data control problem for SOMAS to achieve consensus. Some novel conditions were achieved by the methods like zero-order holds and direct discretization in [21]–[23]. To deal with the problem that time-varying topology or communication delays occurred in MAS, the method of sampled-data control was discussed in [24]–[27]. Hong *et al.* [28] proposed a novel protocol to solve the problem to measure speed data with only current and some sampled previous position data used. More results about achieving consensus for FOMAS or SOMAS via sampled-data control were discussed in [29]–[32].

Consider that all of the above works are only relevant for continuous-time (CT) MAS or discrete-time (DT) MAS. However, switching is a common phenomenon in reality. Not only can switching behaviors occur in network topology but also in the dynamic behaviors of agents. Many real-world processes and systems can be modeled as switching systems, such as power systems, aircraft, and air-traffic control systems, automatic speed control systems, and many other fields. Considering a UAV formation, each agent is equipped with a hybrid quadrotor (HQ), which is an innovative airframe technology that combines the vertical takeoff and landing capabilities of a quadrotor and the efficiency, speed, and the range of a normal fixed-wing aircraft. Since the advantages

Manuscript received December 29, 2019; revised June 2, 2020; accepted August 7, 2020. This work was supported in part by the National Natural Science Foundation of China under Grant U1913602, Grant 61991412, and Grant 61873318; in part by the Frontier Research Funds of Applied Foundation of Wuhan under Grant 2019010701011421; in part by the 111 Project on Computational Intelligence and Intelligent Control under Grant B18024; and in part by the Program for HUST Academic Frontier Youth Team under Grant 2018QYTD07. This article was recommended by Associate Editor L. Liu. (Corresponding author: Housheng Su.)

The authors are with the School of Artificial Intelligence and Automation, Huazhong University of Science and Technology, Wuhan 430074, China, and also with the Key Laboratory of Image Processing and Intelligent Control, Education Ministry of China, Huazhong University of Science and Technology, Wuhan 430074, China (e-mail: liuyifanhust@126.com; houshengsu@gmail.com; zgzeng@hust.edu.cn).

Color versions of one or more of the figures in this article are available online at <http://ieeexplore.ieee.org>.

Digital Object Identifier 10.1109/TCYB.2020.3015977

of a quadrotor and a normal fixed-wing aircraft are obviously different and complementary, in order to realize the specific coordination tasks of takeoff, navigation, and landing, the UAV formation switches between the quadrotor control system, the fixed-wing platform control system, and the quadrotor control system. This is a typical example of a kind of switched MAS that switches its dynamics in order to achieve different coordination tasks. In this article, a novel type of switched MAS is proposed, in which the dynamics of agents switch between CT dynamics and DT dynamics. In real life, some systems are multimodel in nature, where CT-DT switched behaviors usually occur. Taking a CT plant as an example, it is controlled by physically implemented regulators or computer-implemented regulators, and there are switching rules between the regulators. Since the controller can only be implemented in a DT model in any computer-aided system. In this kind of system, when the sampling period is not necessarily small, only the changing values at the sampling points need to be dealt with and the discretization model of CT dynamics needs to be considered accordingly. On the contrary, when the entire system requires more precision and the sampling period is necessarily small, we need to deal with the values that change at all times and consider the CT dynamics model accordingly. Therefore, this entire system is able to be regarded as a switching system composed of a CT and a DT subsystem [33]. Liberzon [34] proposed a concept of a hybrid system, which refers to a system controlled by both continuous and discrete dynamics. As is known to all, when the CT subsystem and the DT subsystem are, respectively, stable, the CT-DT switched system may also be unstable. Therefore, compared with analyzing only the CT subsystem or the DT subsystem, the stability analysis of the CT-DT switched system is more difficult. The stability of CT-DT switched systems was studied via a Lie algebraic method in [35]. Zheng *et al.* [36] combined the classic CT and DT consensus protocols to obtain a novel control protocol to make the CT-DT switched FOMAS reach consensus. Moreover, the finite-time control and quantized control for CT-DT switched MAS to achieve consensus were investigated in [37]–[39], respectively. In addition, Zhu *et al.* [40] discussed the containment conditions for CT-DT switched SOMAS, while for general CT-DT switched SOMAS, the containment control issue was studied in [41].

Inspired by the aforementioned works, this article investigates the consensus control issue for SOMAS with the CT-DT switched dynamic model. Unlike most of the highly related papers, which focused more on FOMAS [36]–[39], this article studies a new type of SOMAS with CT-DT switched dynamics. Compared with the containment control issues for CT-DT switched SOMAS [40], [41], two novel protocols are proposed for SOMAS under a directed graph to reach consensus in our paper. One is that CT and DT subsystems use different control inputs, that is, the CT subsystem uses CT control, and the DT subsystem uses DT control. So the difficulties and challenges, such as the stability problems of the switched system, need to be solved since a switched system may be unstable even when all subsystems are stable. The application of the stability principle and iterative algorithm solve this existing problem, and some necessary and sufficient conditions are obtained for

SYMBOLS AND NOMENCLATURE

i	imaginary number
\otimes	Kronecker product
$\lambda_i(Q)$	the i^{th} eigenvalue of matrix Q
$ \cdot $	the determinant
$\ \cdot\ $	the Euclidean norm
\mathbb{R}	the set of all real numbers
\mathbb{R}^n	the set of n -dimensional real vectors
$\mathbb{R}^{m \times n}$	the set of $m \times n$ -dimensional real matrices
I_M	the $M \times M$ dimensional identity matrix
$\Re(\cdot)$	the real part of a complex number
$\Im(\cdot)$	the imaginary part of a complex number
$\text{triag}\{\dots\}$	the upper triangular matrices

the SOMAS to reach consensus. In addition, for the proof of consensus, we convert it into the proof of the stability of the final states, which is, in turn, beneficial to the proof of the stability of the switched system. The other protocol is to use the same control strategy for both CT and DT subsystems, that is, to use sampled-data control inputs for different subsystems, which is more challenging and practical because of the wide application of sampled-data control in reality. Also, similar conditions are derived to achieve consensus for CT-DT switched SOMAS via sampled-data control. The specific contributions are as follows.

- 1) This article is the first one to design linear distributed consensus control protocols for SOMAS, which combines classic CT and DT consensus control protocols to overcome the problems caused by multimodel and CT-DT switched behaviors.
- 2) Two novel control protocols for the SOMAS with CT-DT switched dynamics are proposed to reach consensus. In particular, one control protocol uses the same control strategy for both CT and DT subsystems, that is, sampled-data control, so that the controller does not need to switch back and forth between the two control protocols when the system switches. It is more practical for using this algorithm, and it is robust and low cost.
- 3) Two necessary and sufficient conditions for these two control protocols are obtained. The network topology and the coupling strength should be of both concern to achieve consensus. In particular, for the protocol that uses sampled-data control, the size of the sampling period also has an impact on reaching consensus.

The remainder of this article is arranged as follows. Section II shows a few crucial preliminaries. The main results are obtained in Sections III and IV. In Section V, we provide several simulation examples. Finally, a brief conclusion is reached in Section VI.

II. PRELIMINARIES

A. Algebraic Graph Theory

Assume that $\mathcal{G} = (\mathcal{V}, \mathcal{E}, \mathcal{A})$ is a digraph with a set of vertices $\mathcal{V} = \{v_1, \dots, v_N\}$, a set of directed edges $\mathcal{E} \subseteq \mathcal{V} \times \mathcal{V}$, and the adjacency matrix $\mathcal{A} = [a_{ij}] \in \mathbb{R}^{N \times N}$. A directed edge e_{ij} in \mathcal{G} is defined as the ordered pair (v_i, v_j) , which describes information that can be passed from the latter to the former. If $e_{ij} \in \mathcal{E}$, $a_{ij} > 0$, else $a_{ij} = 0$, and if $i = 1, \dots, N$, $a_{ii} = 0$. Furthermore, apparently $a_{ij} = a_{ji}$ for an undirected

topology. The Laplacian matrix of the graph \mathcal{G} is defined as $\mathcal{L} = [l_{ij}] \in \mathbb{R}^{N \times N}$, in which

$$l_{ij} = \begin{cases} \sum_{j \in N_i} a_{ij}, & i = j \\ -a_{ij}, & i \neq j. \end{cases}$$

An undirected graph with paths between any pair of different nodes is called connected. A connected subgraph without cycles is called a tree. In a directed graph, a directed tree containing all nodes in \mathcal{G} is called a directed spanning tree.

B. Formulation

The second-order dynamic is considered for MAS, where the CT-DT switched dynamics will be applied to all agents. The CT dynamic is described as

$$\begin{cases} \dot{x}_i(t) = v_i(t) \\ \dot{v}_i(t) = u_i(t), \quad i = 1, 2, \dots, n \end{cases} \quad (1)$$

and the DT dynamic is described as

$$\begin{cases} x_i(t_{k+1}) = x_i(t_k) + v_i(t_k) \\ v_i(t_{k+1}) = v_i(t_k) + u_i(t_k), \quad i = 1, 2, \dots, n \end{cases} \quad (2)$$

where $x_i(\cdot) \in \mathbb{R}^n$, $v_i(\cdot) \in \mathbb{R}^n$, and $u_i(\cdot) \in \mathbb{R}^n$ are the position state, the velocity state, and the control input of agent i , respectively. For convenience, $n = 1$ is studied in this article. The case of $n > 1$ can be studied by utilizing the Kronecker product.

The linear control input is designed as

$$\begin{aligned} u_i(\cdot) = & \alpha \sum_{j \in N_i} a_{ij} [x_j(\cdot) - x_i(\cdot)] \\ & + \beta \sum_{j \in N_i} a_{ij} [v_j(\cdot) - v_i(\cdot)] \end{aligned} \quad (3)$$

where α and β are the coupling gains, \cdot represents t for the CT system, and represents t_k for the DT system.

Definition 1: The switched SOMAS (1) and (2) is said to reach consensus if, for any initial state

$$\begin{aligned} \lim_{t \rightarrow \infty} \|x_i(t) - x_j(t)\| &= 0 \\ \lim_{t \rightarrow \infty} \|v_i(t) - v_j(t)\| &= 0 \end{aligned}$$

where $i = 1, \dots, N$.

A few useful lemmas and some important assumptions are described here.

Lemma 1 [42]: For the block matrix

$$\Omega = \begin{bmatrix} \Omega_{11} & \Omega_{12} \\ \Omega_{21} & \Omega_{22} \end{bmatrix}$$

where $\Omega_{11}, \Omega_{12}, \Omega_{21}, \Omega_{22} \in \mathbb{R}^{n \times n}$, the determinant of this block matrix satisfies $\det(\Omega) = \det(\Omega_{11}\Omega_{22} - \Omega_{12}\Omega_{21})$, if Ω_{11} and Ω_{22} commute.

Lemma 2 [43]: Give a second-order complex coefficient polynomial as

$$h(s) = s^2 + (\epsilon_1 + \mathbf{i}\kappa_1)s + \epsilon_0 + \mathbf{i}\kappa_0$$

where the constants $\epsilon_1, \kappa_1, \epsilon_0$, and κ_0 are real. Then, if and only if $\epsilon_1 > 0$ and $\epsilon_1\kappa_1\kappa_0 + \epsilon_1^2\epsilon_0 - \kappa_0^2 > 0$, $h(s)$ is stable.

Assumption 1: The directed graph \mathcal{G} has a directed spanning tree.

Lemma 3 [5]: Under Assumption 1, the Laplacian matrix \mathcal{L} of the directed graph has a simple eigenvalue 0 and all the real parts of the other eigenvalues are positive.

III. MAIN RESULTS

The CT-DT switched systems (1) and (2) are cast to

$$\begin{cases} \dot{x}_i(t) = v_i(t) \\ \dot{v}_i(t) = -\alpha \sum_{j \in N_i} l_{ij} x_j(t) - \beta \sum_{j \in N_i} l_{ij} v_j(t) \end{cases} \quad (4)$$

and

$$\begin{cases} x_i(t_{k+1}) = x_i(t_k) + v_i(t_k) \\ v_i(t_{k+1}) = v_i(t_k) - \alpha \sum_{j \in N_i} l_{ij} x_j(t_k) \\ \quad - \beta \sum_{j \in N_i} l_{ij} v_j(t_k) \end{cases} \quad (5)$$

where $i = 1, \dots, N$.

For the CT system, let $y_i(t) = (x_i(t), v_i(t))^T$, $A = \begin{pmatrix} 0 & 1 \\ \alpha & 0 \end{pmatrix}$, and $B = \begin{pmatrix} 0 & 0 \\ \alpha & \beta \end{pmatrix}$. Then, the CT system (1) is

$$\dot{y}_i(t) = Ay_i(t) - \sum_{j=1}^N l_{ij} B y_j(t). \quad (6)$$

Let $y(t) = (y_1^T(t), \dots, y_N^T(t))^T$, then

$$\dot{y}(t) = [(I_N \otimes A) - (\mathcal{L} \otimes B)]y(t). \quad (7)$$

The Jordan form associated with the Laplacian matrix \mathcal{L} is defined as \mathcal{J} , that is, $\mathcal{L} = P\mathcal{J}P^{-1}$, where P is a nonsingular matrix. Then, letting $\eta(t) = (P^{-1} \otimes I_2)y(t)$, the matrix form (7) is cast to

$$\begin{aligned} \dot{\eta}(t) &= (P^{-1} \otimes I_2)[(I_N \otimes A) - (\mathcal{L} \otimes B)]y(t) \\ &= [(P^{-1} \otimes A) - (\mathcal{J}P^{-1} \otimes B)]\eta(t) \\ &= [(I_N \otimes A) - (\mathcal{J} \otimes B)]\eta(t). \end{aligned} \quad (8)$$

As for a digraph \mathcal{G} , the Jordan form can be defined as $\mathcal{J} = \text{diag}(\mathcal{J}_1, \mathcal{J}_2, \dots, \mathcal{J}_r)$, where \mathcal{J}_d are Jordan blocks as follows:

$$\mathcal{J}_d = \begin{pmatrix} \mu_d & 1 & 0 & 0 \\ 0 & \ddots & \ddots & 0 \\ 0 & 0 & \ddots & 1 \\ 0 & 0 & 0 & \mu_d \end{pmatrix}_{N_d \times N_d}$$

in which μ_d are the eigenvalues of the \mathcal{L} , with multiplicity N_d , $d = 1, 2, \dots, r$, and $N_1 + N_2 + \dots + N_r = N$.

For the DT system, by similar transformation, we have

$$\eta(t_{k+1}) = [(I_N \otimes C) - (\mathcal{J} \otimes B)]\eta(t_k) \quad (9)$$

where $y_i(t_k) = (x_i(t_k), v_i(t_k))^T$, $y(t_k) = (y_1^T(t_k), \dots, y_N^T(t_k))^T$, $\eta(t_k) = (P^{-1} \otimes I_2)y(t_k)$, and $C = \begin{pmatrix} 1 & 0 \\ 0 & 1 \end{pmatrix}$.

Let $P = (p_1, \dots, p_N)$, $P^{-1} = (\tilde{p}_1, \dots, \tilde{p}_N)^T$, $\eta(\cdot) = (P^{-1} \otimes I_2)y(\cdot) = (\eta_1^T(\cdot), \dots, \eta_N^T(\cdot))^T$, and $\eta_i(\cdot) = (\eta_{i1}(\cdot), \eta_{i2}(\cdot))$. Under Assumption 1 and Lemma 3, zero is a simple eigenvalue of the Laplacian matrix, so (8) and (9) are cast to

$$\dot{\eta}_1(t) = A\eta_1(t) \quad (10)$$

and

$$\eta_1(t_{k+1}) = C\eta_1(t_k). \quad (11)$$

Lemma 4: Under Assumption 1, the CT-DT switched SOMAS formed by (1) and (2) can achieve consensus if and only if

$$\begin{aligned} \lim_{t \rightarrow \infty} \|\eta_i(t)\| &= 0 \\ \lim_{k \rightarrow \infty} \|\eta_i(t_k)\| &= 0 \end{aligned}$$

where $i = 2, \dots, N$.

Proof:

Sufficiency: Under Assumption 1 and Lemma 3, $p_1 = 1_N/\sqrt{N}$ can be defined as the unit right eigenvector of the simple zero eigenvalue $\mu_1 = 0$ of the Laplace matrix \mathcal{L} , where $\mathcal{L}P = P\mathcal{J}$ and $P = (p_1, \dots, p_N)$.

From $\lim_{t \rightarrow \infty} \|\eta_i(t)\| = 0$ for $i = 2, \dots, N$, for the CT subsystem, one has

$$\begin{aligned} \lim_{t \rightarrow \infty} \left\| y(t) - \frac{1}{\sqrt{N}} (\eta_1^T(t), \dots, \eta_1^T(t))^T \right\| \\ = \lim_{t \rightarrow \infty} \left\| (P \otimes I_2) \eta(t) - \frac{1}{\sqrt{N}} (\eta_1^T(t), \dots, \eta_1^T(t))^T \right\| = 0 \end{aligned} \quad (12)$$

where $\eta_1(t)$ satisfies (10).

From $\lim_{k \rightarrow \infty} \|\eta_i(t_k)\| = 0$ for $i = 2, \dots, N$, for the DT subsystem, one has

$$\begin{aligned} \lim_{k \rightarrow \infty} \left\| y(t_k) - \frac{1}{\sqrt{N}} (\eta_1^T(t_k), \dots, \eta_1^T(t_k))^T \right\| \\ = \lim_{k \rightarrow \infty} \left\| (P \otimes I_2) \eta(t_k) - \frac{1}{\sqrt{N}} (\eta_1^T(t_k), \dots, \eta_1^T(t_k))^T \right\| = 0 \end{aligned} \quad (13)$$

where $\eta_1(t_k)$ satisfies (11). Therefore, the SOMAS (4) and (5) with CT-DT dynamics can reach consensus.

Necessity: If the SOMAS (4) and (5) can reach consensus, then there exist two vectors $y^*(t) \in R^2$ and $y^*(t_k) \in R^2$ such that $\lim_{t \rightarrow \infty} \|y(t) - 1_N \otimes y^*(t)\| = 0$ and $\lim_{k \rightarrow \infty} \|y(t_k) - 1_N \otimes y^*(t_k)\| = 0$. Then, $0_N = P^{-1}\mathcal{L}1_N = \mathcal{J}P^{-1}1_N = \mathcal{J}(\tilde{p}_1^T 1_N, \dots, \tilde{p}_N^T 1_N)^T$, from the Jordan form and Lemma 3; thus, $\tilde{p}_i^T 1_N = 0$ for $i = 2, \dots, N$ can be obtained. Hence, $\|\eta_i(t)\| = \|(\tilde{p}_i^T \otimes I_2)y(t)\| \rightarrow \|(\tilde{p}_i^T 1_N) \otimes y^*(t)\| = 0$ and $\|\eta_i(t_k)\| = \|(\tilde{p}_i^T \otimes I_2)y(t_k)\| \rightarrow \|(\tilde{p}_i^T 1_N) \otimes y^*(t_k)\| = 0$, as $t \rightarrow \infty$ and $k \rightarrow \infty$, for all $i = 2, \dots, N$. ■

Remark 1: The switching method between CT dynamics and DT dynamics is arbitrary switching. That is to say, the system can be controlled by CT dynamics or DT dynamics at any time, but not both. Since the system can be controlled only by CT dynamics or DT dynamics, the following theorem is derived.

Theorem 1: Under Assumption 1, this CT-DT switched MAS, formed by (1) and (2) with protocol (3), can reach second-order consensus if and only if conditions 1) and 2) hold simultaneously.

1)

$$\begin{cases} \alpha > 0, & \beta > 0 \\ \frac{\beta^2}{\alpha} > \frac{3^2(\mu_i)}{3\Re(\mu_i)\|\mu_i\|^2} \end{cases} \quad (14)$$

2)

$$\begin{cases} \beta > \alpha > 0 \\ (2\alpha - 2\beta)^2 \left(\alpha - 2\beta + \frac{4\Re(\mu_i)}{\|\mu_i\|^2} \right) \\ - \alpha \cdot \frac{16\Im^2(\mu_i)}{\|\mu_i\|^4} > 0 \end{cases} \quad (15)$$

where μ_i are the eigenvalues of \mathcal{L} , $i = 2, \dots, N$.

Proof:

Sufficiency: Meanwhile, the CT-DT switched behaviors are meant to be simultaneous for all agents. Then, systems (4) and (5) are rewritten as

$$\begin{aligned} \dot{\eta}(t) &= H_1 \eta(t) \\ \eta(t_{k+1}) &= S_1 \eta(t_k) \end{aligned} \quad (16)$$

where

$$\begin{aligned} H_1 &= I_N \otimes A - \mathcal{J} \otimes B \\ S_1 &= I_N \otimes C - \mathcal{J} \otimes B. \end{aligned}$$

For $t > 0$, $t = t_c + dh$ can be defined, where t_c and dh represent the total working hours of working on a CT system of (16) and a DT system of (16), respectively. Note that $H_1 S_1 = S_1 H_1$ and (16), one has

$$\eta(t) = e^{H_1 t_c} S_1^d \eta(0). \quad (17)$$

Since $\mathcal{J} = P^{-1}\mathcal{L}P = \text{triag}\{\mu_1, \dots, \mu_N\}$, where P is a nonsingular matrix. Then, we have

$$\begin{aligned} S_1 &= I_N \otimes C - \mathcal{J} \otimes B \\ &= I_N \otimes C - \text{triag}\{\mu_1, \dots, \mu_N\} \otimes B \\ &= \text{triag} \left\{ \begin{pmatrix} 1 & h \\ -\alpha\mu_1 & 1 - \beta\mu_1 \end{pmatrix}, \dots, \begin{pmatrix} 1 & h \\ -\alpha\mu_N & 1 - \beta\mu_N \end{pmatrix} \right\}. \end{aligned} \quad (18)$$

Hence, the eigenvalues of S_1 are derived by the following equation:

$$\begin{aligned} \det(\lambda I_{2N} - S_1) \\ &= \prod_{i=1}^N \det \begin{pmatrix} \lambda - 1 & -1 \\ \alpha\mu_i & \lambda - 1 + \beta\mu_i \end{pmatrix} \\ &= \prod_{i=1}^N \det(\lambda^2 - (2 - \beta\mu_i)\lambda + 1 + \alpha\mu_i - \beta\mu_i) \\ &= \prod_{i=1}^N h_i(\lambda) \end{aligned} \quad (19)$$

where $h_i(\lambda) = \lambda^2 - (2 - \beta\mu_i)\lambda + 1 + \alpha\mu_i - \beta\mu_i$. Introducing the bilinear transformation $\lambda = \frac{s+1}{s-1}$ into $h_i(\lambda)$, one has

$$\begin{aligned} w_i(s) &= (s-1)^2 h_i \left(\frac{s+1}{s-1} \right) \\ &= \alpha\mu_i s^2 + (-2\alpha\mu_i + 2\beta\mu_i)s \\ &\quad + \alpha\mu_i - 2\beta\mu_i + 4. \end{aligned} \quad (20)$$

If $\alpha\mu_i \neq 0$, then

$$\begin{aligned} \tilde{w}_i(s) &= \frac{w_i(s)}{\alpha\mu_i} \\ &= s^2 + \left(-2 + \frac{2\beta}{\alpha} \right) s + 1 - \frac{2\beta}{\alpha} + \frac{4}{\alpha\mu_i}. \end{aligned} \quad (21)$$

Then, $\tilde{w}_i(s)$ being Hurwitz stable can lead to $h_i(\lambda)$ being Schur stable. Then, $\tilde{w}_i(s)$ is rewritten as

$$\tilde{w}_i(s) = s^2 + \left(-2 + \frac{2\beta}{\alpha}\right)s + 1 - \frac{2\beta}{\alpha} + \frac{4\Re(\mu_i)}{\alpha\|\mu_i\|^2} + \mathbf{i}\frac{4\Im(\mu_i)}{\alpha\|\mu_i\|^2}. \quad (22)$$

Then, based on Lemma 2, the following conditions should be satisfied to make $\tilde{w}_i(s)$ Hurwitz stable:

$$-2 + \frac{2\beta}{\alpha} > 0$$

and

$$\left(-2 + \frac{2\beta}{\alpha}\right)^2 \cdot \left(1 - \frac{2\beta}{\alpha} + \frac{4\Re(\mu_i)}{\alpha\|\mu_i\|^2}\right) - \frac{16\Im^2(\mu_i)}{\alpha^2\|\mu_i\|^4} > 0. \quad (23)$$

After simplification, the DT subsystem of (16) is Schur stable if 2) of Theorem 1 holds. Then, all eigenvalues of S_1 are in the unit circle.

Similarly, for the CT subsystem of (16), H_1 is rewritten as

$$\begin{aligned} H_1 &= I_N \otimes A - \mathcal{J} \otimes B \\ &= I_N \otimes A - \text{triang}\{\mu_1, \dots, \mu_N\} \otimes B \\ &= \text{triang}\left\{\begin{pmatrix} 0 & 1 \\ -\alpha\mu_1 & -\beta\mu_1 \end{pmatrix}, \dots, \begin{pmatrix} 0 & 1 \\ -\alpha\mu_N & -\beta\mu_N \end{pmatrix}\right\}. \end{aligned} \quad (24)$$

Then, the characteristic polynomial of H_1 is that

$$\begin{aligned} \det(\lambda I_{2N} - H_1) &= \prod_{i=1}^N \det\begin{pmatrix} \lambda & -1 \\ \alpha\mu_i & \lambda + \beta\mu_i \end{pmatrix} \\ &= \prod_{i=1}^N \det(\lambda^2 + \beta\mu_i\lambda + \alpha\mu_i) \\ &= \prod_{i=1}^N f_i(\lambda) \end{aligned} \quad (25)$$

where $f_i(\lambda) = \lambda^2 + \beta\mu_i\lambda + \alpha\mu_i$. Then, $f_i(\lambda)$ can be rewritten as $f_i(\lambda) = \lambda^2 + (\Re(\mu_i) + \mathbf{i}\Im(\mu_i))\beta\lambda + (\Re(\mu_i) + \mathbf{i}\Im(\mu_i))\alpha$. Based on Lemma 2, the following conditions should be met to make $f_i(\lambda)$ Hurwitz stable:

$$\begin{cases} \beta\Re(\mu_i) > 0 \\ \beta\Re(\mu_i) \cdot \beta\Im(\mu_i) \cdot \alpha\Im(\mu_i) + \beta^2\Re(\mu_i)^2 \cdot \alpha\Re(\mu_i) - \alpha^2\Im(\mu_i)^2 > 0. \end{cases}$$

After simplification, we can obtain

$$\begin{cases} \beta > 0 \\ \frac{\beta^2}{\alpha} > \frac{\Im^2(\mu_i)}{\Re(\mu_i)\|\mu_i\|^2} \end{cases} \quad (26)$$

which is condition 1) of Theorem 1. In this circumstance, the CT subsystem is Hurwitz stable, that is, all the eigenvalues of H_1 have negative real parts.

Therefore, if (14) and (15) in Theorem 1 are met, $\lim_{t \rightarrow \infty} \eta(t) = 0$ and $\lim_{k \rightarrow \infty} \eta(t_k) = 0$ from (17) can be obtained. Then, from Lemma 4, the CT-DT switched SOMAS can achieve consensus.

Necessity: If the switched SOMAS can reach consensus under arbitrary switching, the CT subsystem (1) and the DT subsystem (2) can achieve consensus control asymptotically, respectively. Then, $\lim_{t \rightarrow \infty} \|\eta_i(t)\| = 0$ and $\lim_{k \rightarrow \infty} \|\eta_i(t_k)\| = 0$ can be easily obtained based on Lemma 4. Meanwhile, from (16), one has

$$\eta(t) = e^{H_1 t} \eta(0) \quad (27)$$

and

$$\eta(t_k) = S_1^k \eta(0). \quad (28)$$

Hence, we can conclude that H_1 and S_1 are Hurwitz stable and Schur stable, respectively, which can indicate the necessity of conditions 1) and 2) in Theorem 1 from the above proof. ■

IV. CONTROL INPUT WITH SAMPLED DATA

The linear control input is designed as

$$\begin{aligned} u(\cdot) &= \alpha \sum_{j \in N_i} a_{ij} [x_j(t_k) - x_i(t_k)] \\ &\quad + \beta \sum_{j \in N_i} a_{ij} [v_j(t_k) - v_i(t_k)]. \end{aligned} \quad (29)$$

The CT-DT switched systems (1) and (2) are cast to

$$\begin{cases} \dot{x}_i(t) = v_i(t) \\ \dot{v}_i(t) = -\alpha \sum_{j \in N_i} l_{ij} x_j(t_k) - \beta \sum_{j \in N_i} l_{ij} v_j(t_k) \end{cases} \quad (30)$$

and

$$\begin{cases} x_i(t_{k+1}) = x_i(t_k) + v_i(t_k) \\ v_i(t_{k+1}) = v_i(t_k) - \alpha \sum_{j \in N_i} l_{ij} x_j(t_k) - \beta \sum_{j \in N_i} l_{ij} v_j(t_k) \end{cases} \quad (31)$$

where $i = 1, \dots, N$.

Remark 2: Note that this protocol uses the same control strategy for both CT and DT subsystems, that is, sampled-data control, so that the controller does not need to switch back and forth between the two control protocols when the system switches. It is more practical to use this algorithm, as it is robust and low cost. Compared to the existing work on switching dynamics [36], [40], [41], this is the first article to use the same control strategy for a CT or DT subsystem. Therefore, compared with previous works, it is more difficult to prove that the CT subsystem can reach consensus under sampled control.

For the CT system, let $z_i(t) = (x_i(t), v_i(t))^T$, $A = \begin{pmatrix} 0 & 1 \\ \alpha & 0 \end{pmatrix}$, and $B = \begin{pmatrix} 0 & 0 \\ \alpha & \beta \end{pmatrix}$. Then, the CT system (1) is cast to

$$\dot{z}_i(t) = Az_i(t) - \sum_{j=1}^N l_{ij} Bz_j(t_k). \quad (32)$$

Let $z(t) = (z_1^T(t), \dots, z_N^T(t))^T$, and the system (32) is rewritten as

$$\dot{z}(t) = (I_N \otimes A)z(t) - (\mathcal{L} \otimes B)z(t_k). \quad (33)$$

\mathcal{J} and P are defined as those in Section III, that is, $\mathcal{L} = P\mathcal{J}P^{-1}$. Then, letting $\zeta(t) = (P^{-1} \otimes I_2)z(t)$, the matrix form (7) is cast to

$$\dot{\zeta}(t) = \left(P^{-1} \otimes I_2\right) \left[(I_N \otimes A)\zeta(t) - (\mathcal{L} \otimes B)\zeta(t_k) \right]$$

$$= (I_N \otimes A)\zeta(t) - (\mathcal{J} \otimes B)\zeta(t_k). \quad (34)$$

For the DT system, by the similar transformation, we have

$$\zeta(k+1) = [(I_N \otimes C) - (\mathcal{J} \otimes B)]\zeta(t_k) \quad (35)$$

where $z_i(t_k) = (x_i(t_k), v_i(t_k))^T$, $z(t_k) = (z_1^T(t_k), \dots, z_N^T(t_k))^T$, $\zeta(t_k) = (P^{-1} \otimes I_2)z(t_k)$, and $C = \begin{pmatrix} 1 & \\ 0 & 1 \end{pmatrix}$.

Lemma 5: Under Assumption 1, the CT-DT switched SOMAS formed by (30) and (31) can achieve consensus if

$$\begin{aligned} \lim_{t \rightarrow \infty} \|\zeta_i(t)\| &= 0 \\ \lim_{k \rightarrow \infty} \|\zeta_i(t_k)\| &= 0 \end{aligned} \quad (36)$$

where $i = 2, \dots, N$.

Proof: The proof here is similar to the proof of Lemma 4; thus, it is omitted here.

Theorem 2: Under Assumption 1, the CT-DT switched SOMAS, formed by (1) and (2) with protocol (29), can achieve consensus if and only if conditions 1) and 2) hold simultaneously

$$1) \quad \begin{cases} T < \frac{2\beta}{\alpha} \\ (\alpha T - 2\beta)^2 \left(-2\beta T + \frac{4\Re(\mu_i)}{\|\mu_i\|^2} \right) - \alpha \cdot \frac{16\Im^2(\mu_i)}{\|\mu_i\|^4} > 0 \end{cases} \quad (37)$$

$$2) \quad \begin{cases} \beta > \alpha > 0 \\ (2\alpha - 2\beta)^2 \left(\alpha - 2\beta + \frac{4\Re(\mu_i)}{\|\mu_i\|^2} \right) \\ \quad - \alpha \cdot \frac{16\Im^2(\mu_i)}{\|\mu_i\|^4} > 0 \end{cases} \quad (38)$$

where μ_i are the eigenvalues of \mathcal{L} , $i = 2, \dots, N$.

Proof:

Sufficiency: From (34), for the CT subsystem, one has

$$\dot{\zeta}_i(t) = A\zeta_i(t) - \mu_i B\zeta_i(t_k), \quad i = 2, \dots, N. \quad (39)$$

Then, the above formula can be changed into

$$\left(e^{-At} \zeta_i(t) \right)' = -e^{-At} \mu_i B \zeta_i(t_k). \quad (40)$$

Integrating both sides of the above formula from t_k to t and referring to $e^{-At} = \begin{pmatrix} 1 & -t \\ 0 & 1 \end{pmatrix}$, one obtains

$$\begin{aligned} \zeta_i(t) &= e^{A(t-t_k)} \zeta_i(t_k) - e^{At} \int_{t_k}^t e^{-As} \mu_i B \zeta_i(t_k) ds \\ &= \begin{pmatrix} 1 & t-t_k \\ 0 & 1 \end{pmatrix} \zeta_i(t_k) - \begin{pmatrix} 1 & t \\ 0 & 1 \end{pmatrix} \\ &\quad \times \begin{pmatrix} t-t_k & -\frac{t^2}{2} + \frac{t_k^2}{2} \\ 0 & t-t_k \end{pmatrix} \times \mu_i B \zeta_i(t_k) \\ &= \left[\begin{pmatrix} 1 & t-t_k \\ 0 & 1 \end{pmatrix} - \begin{pmatrix} \frac{\alpha}{2} \mu_i (t-t_k)^2 & \frac{\beta}{2} \mu_i (t-t_k)^2 \\ \alpha \mu_i (t-t_k) & \beta \mu_i (t-t_k) \end{pmatrix} \right] \\ &\quad \times \zeta_i(t_k) \\ &= \begin{pmatrix} 1 - \frac{\alpha}{2} \mu_i (t-t_k)^2 & (t-t_k) - \frac{\beta}{2} \mu_i (t-t_k)^2 \\ -\alpha \mu_i (t-t_k) & 1 - \beta \mu_i (t-t_k) \end{pmatrix} \zeta_i(t_k). \end{aligned} \quad (41)$$

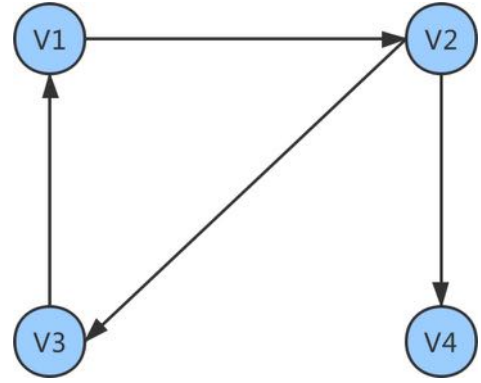


Fig. 1. Directed graph of CT-DT switched MASs.

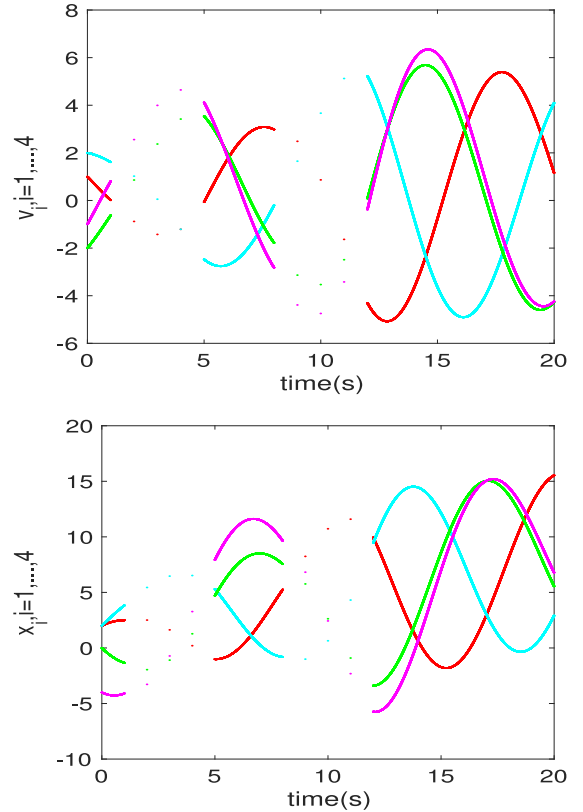


Fig. 2. States of agents when $\alpha = 0.2$ and $\beta = 0.2$.

It can be rewritten as

$$\zeta_i(t) = M_i(t-t_k) \zeta_i(t_k) \quad (42)$$

with $M_i(t) = \begin{pmatrix} 1 - \frac{\alpha}{2} \mu_i t^2 & t - \frac{\beta}{2} \mu_i t^2 \\ -\alpha \mu_i t & 1 - \beta \mu_i t \end{pmatrix}$. Since $M_i(t)$ is bounded on $[0, T]$, one has

$$\zeta_i(t) = M_i(t-t_k) M_i^k(T) \zeta_i(t_0) \quad (43)$$

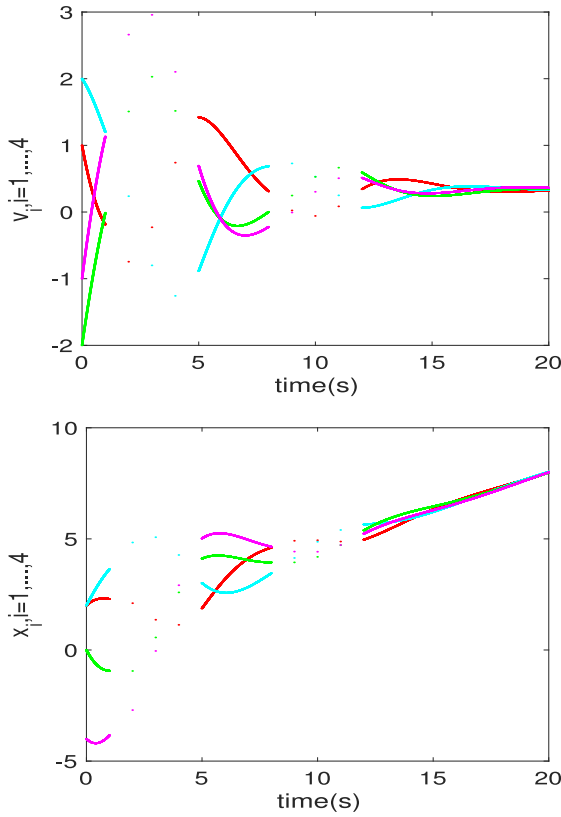
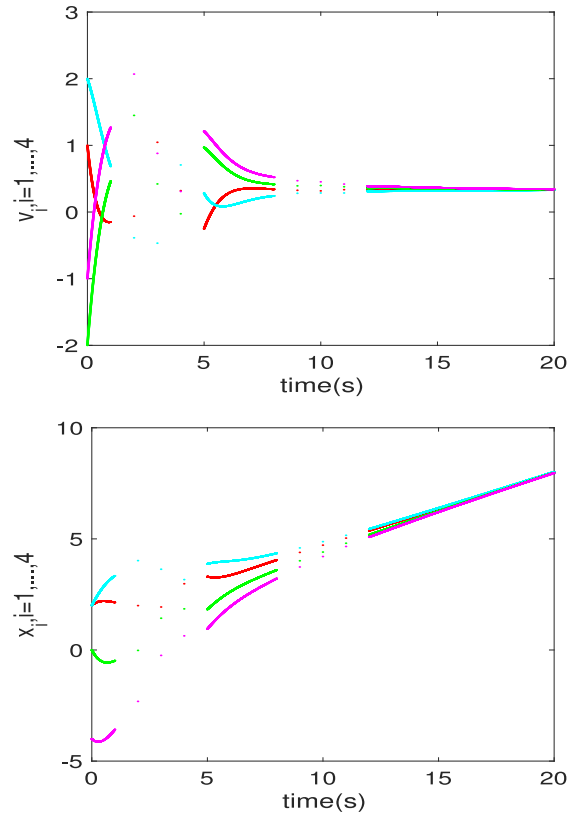
where $t_{k+1} - t_k = T$.

For the DT system (35), one has

$$\zeta(k+1) = N_i \zeta(t_k) = N_i^k \zeta(t_0) \quad (44)$$

where $N_i = [(I_N \otimes C) - (\mathcal{J} \otimes D)]$.

So, for $t > 0$, $t = t_c + kT$ can be defined, where $t_c (t_c \in [t_k, t_{k+1}))$ and kT represent the total working hours of


 Fig. 3. States of agents when $\alpha = 0.2$ and $\beta = 0.5$.

 Fig. 4. States of agents when $\alpha = 0.2$ and $\beta = 1$.

working on a CT system of (30) and a DT system of (31), respectively. From the above analysis, one has

$$\zeta_i(t) = M_i(t_c - t_k)M_i^k(T)N_i^k\zeta_i(t_0). \quad (45)$$

Since $M_i(t_c - t_k)$ are delimited when $t_c \in [t_k, t_{k+1})$, $\zeta_i(t) \rightarrow 0$ as long as the amplitudes of all eigenvalues of $M_i(T)$ and N_i are less than 1. Then, the characteristic polynomial of $M_i(T)$ is that

$$\begin{aligned} \det(\lambda I_2 - M_i(T)) &= \lambda^2 + \left(\frac{\alpha}{2}\mu_i T^2 + \beta\mu_i T - 2\right)\lambda + \frac{\alpha}{2}\mu_i T^2 - \beta\mu_i T + 1 \\ &= \hat{f}_i(\lambda) \end{aligned} \quad (46)$$

where $\hat{f}_i(\lambda) = \lambda^2 + (\frac{\alpha}{2}\mu_i T^2 + \beta\mu_i T - 2)\lambda + \frac{\alpha}{2}\mu_i T^2 - \beta\mu_i T + 1$, with μ_i representing the i th eigenvalue of \mathcal{L} . Letting $\lambda = \frac{s+1}{s-1}$, then one has

$$\begin{aligned} g_i(s) &= (s-1)^2 \hat{f}_i\left(\frac{s+1}{s-1}\right) \\ &= T^2\alpha\mu_i s^2 + (-T^2\alpha\mu_i + 2T\beta\mu_i)s - 2T\beta\mu_i + 4. \end{aligned}$$

If $T^2\alpha\mu_i \neq 0$, then

$$\begin{aligned} \tilde{g}_i(s) &= \frac{g_i(s)}{T^2\alpha\mu_i} \\ &= s^2 + \left(-1 + \frac{2\beta}{\alpha T}\right)s - \frac{2\beta}{\alpha T} + \frac{4}{T^2\alpha\mu_i}. \end{aligned} \quad (47)$$

Then, $\tilde{g}_i(s)$ being Hurwitz stable can lead to $\hat{f}_i(\lambda)$ being Schur stable. Then, $\tilde{g}_i(s)$ can be rewritten as

$$\begin{aligned} \tilde{g}_i(s) &= s^2 + \left(-1 + \frac{2\beta}{\alpha T}\right)s - \frac{2\beta}{\alpha T} \\ &\quad + \frac{4\Re(\mu_i)}{\alpha\|\mu_i\|^2 T^2} + \mathbf{i} \frac{4\Im(\mu_i)}{\alpha\|\mu_i\|^2 T^2}. \end{aligned} \quad (48)$$

Then, based on Lemma 2, $\tilde{g}_i(s)$ is Hurwitz stable if and only if

$$-1 + \frac{2\beta}{\alpha T} > 0$$

and

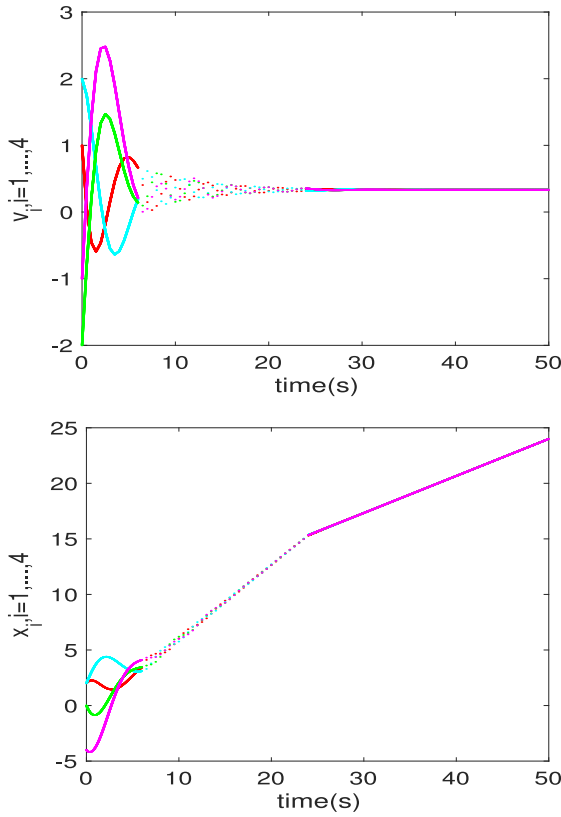
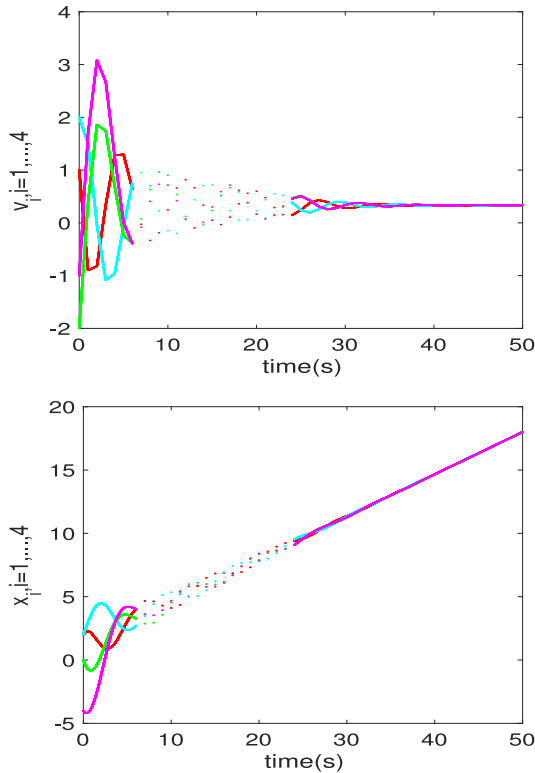
$$\left(-1 + \frac{2\beta}{\alpha T}\right)^2 \cdot \left(-\frac{2\beta}{\alpha T} + \frac{4\Re(\mu_i)}{\alpha\|\mu_i\|^2 T^2}\right) - \frac{16\Im^2(\mu_i)}{\alpha^2\|\mu_i\|^4 T^4} > 0.$$

After simplification, the CT subsystem of (30) is Schur stable if and only if 1) and the first condition of 2) in Theorem 3 holds. Then, all eigenvalues of $M_i(T)$ are in the unit circle.

Similar to the proof of the DT subsystem of (16) in Section III, the DT subsystem of (31) is Schur stable if 2) of Theorem 3 holds.

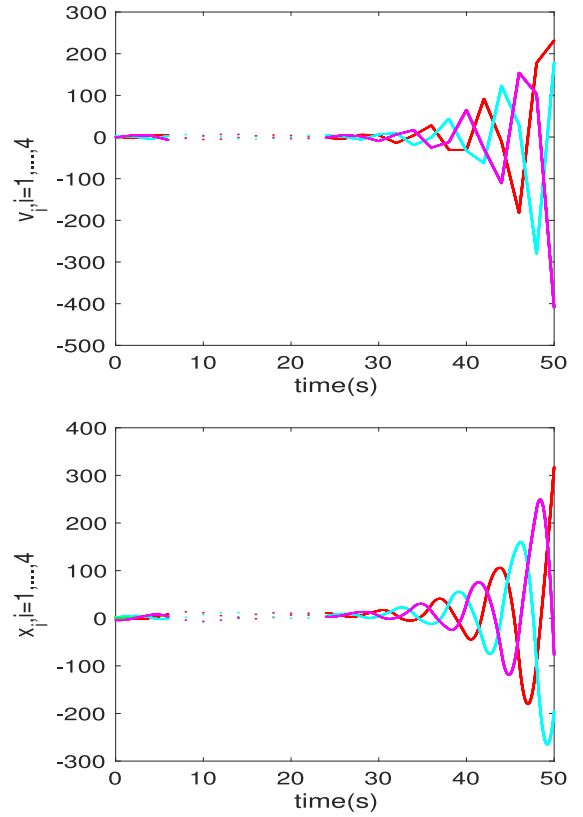
Therefore, under conditions (37) and (38) in Theorem 3, we can obtain that $\lim_{t \rightarrow \infty} \zeta(t) = 0$ and $\lim_{k \rightarrow \infty} \zeta(t_k) = 0$ from (45). Then, from Lemma 5, the CT-DT switched SOMAS can achieve consensus.

Necessity: If the switched SOMAS can reach consensus under arbitrary switching, the CT subsystem (1) and the DT subsystem (2) can achieve consensus control asymptotically, respectively. Then, $\lim_{t \rightarrow \infty} \|\zeta_i(t)\| = 0$ and

Fig. 5. States of agents when $\alpha = 0.2$, $\beta = 0.5$, and $T = 0.5$.Fig. 6. States of agents when $\alpha = 0.2$, $\beta = 0.5$, and $T = 1$.

$\lim_{k \rightarrow \infty} \|\zeta_i(t_k)\| = 0$ can be easily obtained based on Lemma 5. Meanwhile, from (43) and (44), one has

$$\zeta_i(t) = M_i(t - t_k) M_i^k(T) \zeta_i(t_0) \quad (49)$$

Fig. 7. States of agents when $\alpha = 0.2$, $\beta = 0.5$, and $T = 2$.

and

$$\zeta(t_{k+1}) = N_i \zeta(t_k) = N_i^k \zeta(t_0). \quad (50)$$

Hence, we can conclude that $M_i(h)$, N_i are both Schur stable, which can indicate the necessity of conditions 1) and 2) in Theorem 1 from the above proof. ■

V. SIMULATIONS

A. Consensus Under Protocol (3)

Consider four agents under a digraph as Fig. 1 satisfying Assumption 1, where the Laplace matrix is

$$\mathcal{L} = \begin{bmatrix} 1 & 0 & -1 & 0 \\ -1 & 1 & 0 & 0 \\ 0 & -1 & 1 & 0 \\ 0 & -1 & 0 & 1 \end{bmatrix}$$

with $\mu_1 = 0$, $\mu_2 = 1$, $\mu_3 = 1.5 + 0.866j$, and $\mu_4 = 1.5 - 0.866j$. For the CT-DT switched system (1) and (2) under protocol (3) and randomly switching, first, we can assume $\alpha = 0.2$. Then, from Theorem 1, the appropriate range of β is calculated as $0.4217 < \beta < 1.0543$. Then, we take $\beta = 0.2$, $\beta = 0.5$, and $\beta = 1$ to explore the consensus behavior of the CT-DT switched SOMAS under a directed graph. Figs. 2–4 describe the velocity and position states of all agents. It is obvious to see that when $\beta = 0.2$, the CT-DT switched SOMAS cannot reach consensus. When $\beta = 0.5$ and $\beta = 1$, the CT-DT switched SOMAS can reach consensus, which can prove the correctness of Theorem 1.

B. Consensus Under Protocol (29)

The same topology and the same dynamics of each agent are considered as Section V-A. Under protocol (29) and randomly switching, first we can assume $\alpha = 0.2$. From Theorem 2, the appropriate range of β is calculated as $0.4217 < \beta < 1.0543$. Then, we take $\beta = 0.5$ to obtain the appropriate range of T that $0 < T < 1.4662$. After that, we take $T = 0.5$, $T = 1$, and $T = 2$ to explore the consensus behavior of the CT-DT switched SOMAS under the directed graph. Figs. 5–7 describe the velocity and position states of all agents. It is obvious to see that when $T = 2$, the CT-DT switched SOMAS cannot reach consensus. When $T = 0.5$ and $T = 1$, the CT-DT switched SOMAS can reach consensus, which can prove the correctness of Theorem 2.

VI. CONCLUSION

The consensus issues for SOMAS with CT-DT switched dynamics have been studied in this article. Under a digraph, two control protocols are designed to reach consensus. One is that the CT subsystem uses CT control, and the DT subsystem uses DT control. For this kind of control protocol, some necessary and sufficient conditions about the network structure and the coupling gains to reach consensus are derived. The other is to use the same control strategy for both CT and DT subsystems, and similarly, some consensus conditions are also obtained for the protocol with the sampled-data control inputs applied in different subsystems. Finally, a few simulation examples are obtained to show the correctness of theorems. In the future, the consensus control problem for SOMAS with switched dynamics via the sampled position data control or time delays will be discussed.

REFERENCES

- [1] H. Su, Y. Ye, Y. Qiu, Y. Cao, and M. Z. Q. Chen, "Semi-global output consensus for discrete-time switching networked systems subject to input saturation and external disturbances," *IEEE Trans. Cybern.*, vol. 49, no. 11, pp. 3934–3945, Nov. 2019.
- [2] X. Wang, X. Wang, H. Su, and J. Lam, "Coordinated control for uncertain networked systems using interval observers," *IEEE Trans. Cybern.*, early access, Oct. 28, 2019, doi: [10.1109/TCYB.2019.2945580](https://doi.org/10.1109/TCYB.2019.2945580).
- [3] H. Li, C. Huang, G. Chen, X. Liao, and T. W. Huang, "Distributed consensus optimization in multiagent networks with time-varying directed topologies and quantized communication," *IEEE Trans. Cybern.*, vol. 47, no. 8, pp. 2044–2057, Aug. 2017.
- [4] M. Long, H. Su, and Z. Zeng, "Output-feedback global consensus of discrete-time multiagent systems subject to input saturation via q-learning method," *IEEE Trans. Cybern.*, early access, May 7, 2020, doi: [10.1109/TCYB.2020.2987385](https://doi.org/10.1109/TCYB.2020.2987385).
- [5] R. Olfati-Saber, J. A. Fax, and R. M. Murray, "Consensus and cooperation in networked multi-agent systems," *Proc. IEEE*, vol. 95, no. 1, pp. 215–233, Jan. 2007.
- [6] H. Su, J. Chen, X. Chen, and H. He, "Adaptive observer-based output regulation of multiagent systems with communication constraints," *IEEE Trans. Cybern.*, early access, Jun. 10, 2020, doi: [10.1109/TCYB.2020.2995147](https://doi.org/10.1109/TCYB.2020.2995147).
- [7] M. Long, H. Su, and B. Liu, "Second-order controllability of two-time-scale multi-agent systems," *Appl. Math. Comput.*, vol. 343, pp. 299–313, Feb. 2019.
- [8] H. Su, M. Long, and Z. Zeng, "Controllability of two-time-scale discrete-time multiagent systems," *IEEE Trans. Cybern.*, vol. 50, no. 4, pp. 1440–1449, Apr. 2020.
- [9] H. Li, Q. Lü, and T. Huang, "Distributed projection subgradient algorithm over time-varying general unbalanced directed graphs," *IEEE Trans. Autom. Control*, vol. 64, no. 3, pp. 1309–1316, Mar. 2019.
- [10] H. Li, Q. Lü, X. Liao, and T. Huang, "Accelerated convergence algorithm for distributed constrained optimization under time-varying general directed graphs," *IEEE Trans. Syst., Man, Cybern., Syst.*, vol. 50, no. 7, pp. 2612–2622, Jul. 2020.
- [11] H. Su, Y. Sun, and Z. Zeng, "Semiglobal observer-based non-negative edge consensus of networked systems with actuator saturation," *IEEE Trans. Cybern.*, vol. 50, no. 6, pp. 2827–2836, Jun. 2020.
- [12] Y. Sun, H. Su, and Z. Zeng, "H_∞ control for observer-based non-negative edge consensus of discrete-time networked systems," *IEEE Trans. Cybern.*, early access, Jul. 10, 2020, doi: [10.1109/TCYB.2020.3003279](https://doi.org/10.1109/TCYB.2020.3003279).
- [13] A. Jadbabaie, J. Lin, and A. S. Morse, "Coordination of groups of mobile autonomous agents using nearest neighbor rules," *IEEE Trans. Autom. Control*, vol. 48, no. 6, pp. 988–1001, Jun. 2003.
- [14] Y. Fan, G. Feng, Y. Wang, and C. Song, "Distributed event-triggered control of multi-agent systems with combinational measurements," *Automatica*, vol. 49, no. 2, pp. 671–675, 2013.
- [15] Y. Wan, G. H. Wen, J. D. Cao, and W. W. Yu, "Distributed node-to-node consensus of multi-agent systems with stochastic sampling," *Int. J. Robust Nonlin. Control*, vol. 26, no. 1, pp. 110–124, 2016.
- [16] W. Yu, G. Chen, and M. Cao, "Some necessary and sufficient conditions for second-order consensus in multi-agent dynamical systems," *Automatica*, vol. 46, no. 6, pp. 1089–1095, 2010.
- [17] H. Su, Y. Liu, and Z. Zeng, "Second-order consensus for multiagent systems via intermittent sampled position data control," *IEEE Trans. Cybern.*, vol. 50, no. 5, pp. 2063–2072, May 2020.
- [18] H. Su, X. Wang, X. Chen, and Z. Zeng, "Second-order consensus of hybrid multiagent systems," *IEEE Trans. Syst., Man, Cybern., Syst.*, early access, Jan. 14, 2020, doi: [10.1109/TSMC.2019.2963089](https://doi.org/10.1109/TSMC.2019.2963089).
- [19] H. Yu and X. Xia, "Adaptive consensus of multi-agents in networks with jointly connected topologies," *Automatica*, vol. 48, no. 8, pp. 1783–1790, 2012.
- [20] H. Su, X. Wang, and Z. Zeng, "Consensus of second-order hybrid multiagent systems by event-triggered strategy," *IEEE Trans. Cybern.*, early access, Nov. 8, 2019, doi: [10.1109/TCYB.2019.2948209](https://doi.org/10.1109/TCYB.2019.2948209).
- [21] Y. Gao, L. Wang, G. Xie, and B. Wu, "Consensus of multi-agent systems based on sampled-data control consensus of multi-agent systems based on sampled-data control," *Int. J. Control*, vol. 82, no. 12, pp. 2193–2205, 2009.
- [22] H. Su, Y. Ye, X. Chen, and H. He, "Necessary and sufficient conditions for consensus in fractional-order multiagent systems via sampled-data over directed graph," *IEEE Trans. Syst., Man, Cybern., Syst.*, early access, May 21, 2019, doi: [10.1109/TSMC.2019.2915653](https://doi.org/10.1109/TSMC.2019.2915653).
- [23] H. Zhao, S. Xu, and D. Yuan, "Consensus of data-sampled multi-agent systems with Markovian switching topologies," *Asian J. Control*, vol. 14, no. 5, pp. 1366–1373, 2012.
- [24] Y. Zhang and Y. P. Tian, "Consensus of data-sampled multi-agent systems with random communication delay and packet loss," *IEEE Trans. Autom. Control*, vol. 55, no. 4, pp. 939–943, Apr. 2010.
- [25] H. Su, J. Zhang, and Z. Zeng, "Formation-containment control of multi-robot systems under a stochastic sampling mechanism," *Sci. China Technol. Sci.*, vol. 63, no. 6, pp. 1025–1034, 2020.
- [26] Y. Gao and L. Wang, "Sampled-data based consensus of continuous-time multi-agent systems with time-varying topology," *IEEE Trans. Autom. Control*, vol. 56, no. 5, pp. 1226–1231, May 2011.
- [27] H. Su, J. Zhang, and Z. Zeng, "A stochastic sampling mechanism for time-varying formation of multiagent systems with multiple leaders and communication delays," *IEEE Trans. Neural Netw. Learn. Syst.*, vol. 30, no. 12, pp. 3699–3707, Dec. 2019.
- [28] Y. Hong, J. Hu, and L. Gao, "Tracking control for multi-agent consensus with an active leader and variable topology," *Automatica*, vol. 42, no. 7, pp. 1177–1182, 2007.
- [29] N. Huang, Z. Duan, and G. Chen, "Some necessary and sufficient conditions for consensus of second-order multi-agent systems with sampled position data," *Automatica*, vol. 63, pp. 148–155, Jan. 2016.
- [30] Y. Liu and H. Su, "Necessary and sufficient conditions for containment in fractional-order multiagent systems via sampled-data," *IEEE Trans. Syst., Man, Cybern., Syst.*, early access, Jun. 11, 2020, doi: [10.1109/TSMC.2020.2997294](https://doi.org/10.1109/TSMC.2020.2997294).
- [31] N. Huang, Z. Duan, and Y. Zhao, "Leader-following consensus of second-order non-linear multi-agent systems with directed intermittent communication," *IET Control Theory Appl.*, vol. 8, no. 10, pp. 782–795, 2014.
- [32] Z. Yu, H. Jiang, and C. Hu, "Second-order consensus for multiagent systems via intermittent sampled-data control," *IEEE Trans. Syst., Man, Cybern., Syst.*, vol. 48, no. 11, pp. 1986–2002, Nov. 2018.

- [33] G. Zhai, H. Lin, A. Michel, and K. Yasuda, "Stability analysis for switched with continuous-time and discrete-time subsystems," in *Proc. Amer. Control Conf.*, 2004, pp. 4555–4560.
- [34] D. Liberzon, *Switching in Systems and Control*. Boston, MA, USA: Birkhäuser, 2003.
- [35] G. Zhai, D. Liu, J. Imae, and T. Kobayashi, "Stability analysis for switched systems with continuous-time and discrete-time subsystems: A Lie algebraic approach," in *Proc. IEEE Int. Symp. Circuits Syst. (ISCAS)*, 2005, pp. 3183–3186.
- [36] Y. Zheng, J. Ma, and L. Wang, "Consensus of switched multi-agent systems," *IEEE Trans. Circuits Syst. II, Exp. Briefs*, vol. 63, no. 3, pp. 314–318, Mar. 2016.
- [37] X. Lin, Y. Zheng, and L. Wang, "Consensus of switched multi-agent systems with random networks," *Int. J. Control*, vol. 90, no. 5, pp. 1113–1122, 2017.
- [38] X. Lin and Y. Zheng, "Finite-time consensus of switched multiagent systems," *IEEE Trans. Syst., Man, Cybern., Syst.*, vol. 47, no. 7, pp. 1535–1545, Jul. 2017.
- [39] Y. Zhu, Y. Zheng, and Y. Guan, "Consensus of switched multi-agent systems under quantised measurements," *Int. J. Syst. Sci.*, vol. 48, no. 9, pp. 1796–1804, 2017.
- [40] Y. Zhu, Y. Zheng, and L. Wang, "Containment control of switched multi-agent systems," *Int. J. Control*, vol. 88, no. 12, pp. 2570–2577, 2015.
- [41] F. Wang, Y. Ni, Z. Liu, and Z. Chen, "Containment control for general second-order multiagent systems with switched dynamics," *IEEE Trans. Cybern.*, vol. 50, no. 2, pp. 550–560, Feb. 2020.
- [42] F. R. Gantmakher, *The Theory of Matrices*. New York, NY, USA: Chelsea, 1959.
- [43] P. C. Parks and V. Hahn, *Stability Theory*. Englewood Cliffs, NJ, USA: Prentice-Hall, 1993.



Yifan Liu received the B.S. degree in automatic control from the Huazhong University of Science and Technology, Wuhan, China, in 2018, where she is currently pursuing the M.S. degree with the School of Artificial Intelligence and Automation.

Her current research interests include multiagent systems and second-order systems.



Housheng Su received the B.S. degree in automatic control and the M.S. degree in control theory and control engineering from the Wuhan University of Technology, Wuhan, China, in 2002 and 2005, respectively, and the Ph.D. degree in control theory and control engineering from Shanghai Jiao Tong University, Shanghai, China, in 2008.

From December 2008 to January 2010, he was a Postdoctoral Researcher with the Department of Electronic Engineering, City University of Hong Kong, Hong Kong. Since November 2014, he has been a Full Professor with the School of Artificial Intelligence and Automation, Huazhong University of Science and Technology, Wuhan. His research interests lie in the areas of multiagent coordination control theory and its applications to autonomous robotics and mobile sensor networks.

Dr. Su is an Associate Editor of *IET Control Theory and Applications*.



Zhigang Zeng (Fellow, IEEE) received the Ph.D. degree in systems analysis and integration from the Huazhong University of Science and Technology, Wuhan, China, in 2003.

He is currently a Professor with the School of Artificial Intelligence and Automation and also the Key Laboratory of Image Processing and Intelligent Control, Education Ministry of China, Huazhong University of Science and Technology. He has published over 180 international journal papers. His current research interests include theory of func-

tional differential equations and differential equations with discontinuous righthand sides, and their applications to dynamics of neural networks, memristive systems, and control systems.

Prof. Zeng was an Associate Editor of the IEEE TRANSACTIONS ON NEURAL NETWORKS from 2010 to 2011, and has been an Associate Editor of the IEEE TRANSACTIONS ON CYBERNETICS since 2014 and the IEEE TRANSACTIONS ON FUZZY SYSTEMS since 2016, and a member of the editorial board of *Neural Networks* since 2012, *Cognitive Computation* since 2010, and *Applied Soft Computing* since 2013.

General Second-Order Consensus of Discrete-Time Multiagent Systems via Q-Learning Method

Yifan Liu¹ and Housheng Su¹

Abstract—A consensus control issue is studied for general second-order multiagent systems via Q-learning method in this article. A novel second-order type with discrete-time dynamics is investigated to solve the corresponding consensus issues. Under fixed directed topology, in order to achieve general second-order consensus for the systems, a model-free Q-learning method is proposed, which can derive the coupling gains matrix without any information from the system dynamics. Moreover, applying the obtained coupling gains matrix, this general second-order multiagent systems can achieve consensus. Then, for undirected graphs, a similar corollary is obtained for this system to achieve general second-order consensus by means of the Q-learning method. Finally, the correctness of the new method is confirmed by several simulation examples.

Index Terms—Discrete-time control, general second-order consensus, multiagent systems, Q-learning method.

I. INTRODUCTION

A GROUP of multiple individuals in the same networked environment is defined as a multiagent system (MAS), which can be divided into continuous-time MAS (CTMAS), discrete-time MAS (DTMAS), and hybrid MAS. Recently, many results about distributed cooperative control of MAS have been derived [1]–[7]. The main purpose of these research is to design algorithms for MAS to achieve global control goals, which include consensus problem [8]–[11], containment problem [12]–[14], controllability analysis [15], [16], formation control [17]–[19], convergence rate [20]–[22], and so on.

Consensus control is the most concerned issue. Designing an appropriate algorithm with the help of local information is the key to solve this issue so that all agents in the network can achieve an agreement about certain interest. Olfati-Saber and Murray [23] proposed a groundbreaking work, which applied the algebraic graph theory and frequency domain analysis into

consensus issue of first-order MAS (FOMAS). So far, a lot of theoretical results on consensus for FOMAS have been obtained and widely known [24]–[27]. Considering reality, second-order MAS (SOMAS), including position and velocity states is more common. However, the conditions under which FOMAS can reach consensus may not guarantee the consensus of SOMAS because the latter includes the position and velocity states, which has a more complex structure. Moreover, for the consensus of SOMAS, the convergence result will not only be affected by the network communication topology but also by the coupling strength of the system. For this case, lots of literatures were studied in [28]–[30] to reach consensus for SOMAS, which are more challenging than FOMAS. As we known, only a few literatures focus on the consensus control problem of general SOMAS because it is more universal than SOMAS. Hou *et al.* [31] proposed a novel consensus protocol for general SOMAS to achieve consensus. The bounds on delay consensus margin for general SOMAS were studied in [32] to reach robust consensus. Furthermore, Wang *et al.* [33] discussed the containment issue for general SOMAS, where the dynamics of agents can switch between different dynamics. Note that all the above articles have studied the continuous-time control of general SOMAS instead of the discrete-time control.

In some practical applications, the situation is common where the dynamic information of agents cannot be available to get. To deal with this problem, a reinforcement learning (RL) techniques for the discrete-time system is proposed in [34], which is inspired by the Q-learning (QL) algorithm. Some adaptive and optimal control problems were investigated in [35] and [36] by using the QL algorithm. The discrete-time system with saturation in [37] can reach global stabilization, which uses the low-gain feedback matrix computed by the QL method. Some model-free iterative algorithms like the QL method are applied to MAS to solve optimal consensus issue [38]–[41]. For DTMAS, Abouheaf *et al.* [38] proposed an RL Nash solution to solve the problem of dynamic graphics games, where the information of agent dynamics is not utilized. Furthermore, a model-free algorithm for heterogeneous DTMAS was derived in [39] to solve the optimal output synchronization problems. Zhang *et al.* [40] focused on distributed optimal consensus problems for nonlinear CTMAS requiring no information of agent dynamics. Moreover, a data-based optimal control for DTMAS was investigated in [41] by utilizing the input–output QL algorithm without system dynamics.

Manuscript received January 6, 2020; revised April 17, 2020; accepted August 15, 2020. This work was supported in part by the National Natural Science Foundation of China under Grant 61991412 and Grant 61873318; in part by the Frontier Research Funds of Applied Foundation of Wuhan under Grant 2019010701011421; and in part by the Program for HUST Academic Frontier Youth Team under Grant 2018QYTD07. This article was recommended by Associate Editor L. Cao. (Corresponding author: Housheng Su.)

The authors are with the School of Artificial Intelligence and Automation, Image Processing and Intelligent Control Key Laboratory of Education Ministry of China, Huazhong University of Science and Technology, Wuhan 430074, China (e-mail: liuyifanhust@126.com; houshengsu@gmail.com).

Color versions of one or more of the figures in this article are available online at <http://ieeexplore.ieee.org>.

Digital Object Identifier 10.1109/TSMC.2020.3019519

Inspired by the aforementioned works, we study the consensus control issue for general SOMAS via the QL method without the information of agent dynamics in this article. Under fixed directed topology, a model-free QL algorithm is proposed for the DTMAS to achieve general second-order consensus. Unlike most of the systems studied in the aforementioned works like CTMAS, we consider a new type of general SOMAS with discrete-time dynamics. Besides, for the difficulty where any information of agent dynamics of DTMAS cannot be available, the QL method is proposed to derive the coupling gains matrix via model-free iterative algorithms. Moreover, using the coupling gains matrix derived by QL method, the consensus problem is still a challenge of this algorithm. The contributions are as follows.

- 1) This article is the first one to study the general SOMAS with discrete-time dynamics and design a linear distributed consensus control protocol. The general SOMAS is more universal than the double-integrator MAS. Regarding the consensus of general SOMAS, limited results have been studied by continuous-time control. Compared with [40], this article uses the QL method for the first time to study the general second-order consensus of DTMAS, which describes more realistic dynamics of the general SOMAS.
- 2) For a fixed directed topology, a model-free QL algorithm is proposed for the DTMAS to achieve general second-order consensus, which can derive the coupling gains matrix requiring no information of dynamics. Moreover, for an undirected topology, the general second-order DTMAS can still reach consensus by means of the QL method.
- 3) Unlike the optimal output synchronization problems in [39] and data-based optimal control problem in [41], this article studies the consensus problem using QL method. Besides, by means of the method of the Lyapunov function, the QL method can be proved to make the DTMAS achieve general second-order consensus.

The main content of this article is summarized as follows. Section II introduces a few preliminaries and gives the general second-order models, besides, the definition of general second-order consensus is given for DTMAS. Section III shows the main results of this article, where Algorithm 1 is given to derive the coupling gains matrix and Theorem 1 is given to prove that the DTMAS can reach consensus with the obtained coupling gains matrix. Section IV provides some simulation examples to verify the correctness of the theorems. At last, a short conclusion is drawn in Section V.

II. PRELIMINARIES

A. Algebraic Graph Theory

A directed graph \mathbb{G} consisting of N dynamic agents is defined as $\mathbb{G} = (\mathbb{V}, \mathbb{E}, \mathbb{D})$, and we can define that $\mathbb{V} = \{v_1, \dots, v_N\}$, $\mathbb{E} = \{(v_i, v_j) : v_i, v_j \in \mathbb{V}\}$, and a row stochastic matrix $\mathbb{D} \in \mathfrak{R}^{N \times N}$, the definitions of which can be seen as the following table.

\mathbb{G} a directed graph with N nodes

\mathbb{V} a collection of all nodes in the graph \mathbb{G}

\mathbb{E} all edges of the graph \mathbb{G}

\mathbb{D} the interconnection among all agents

$\mathfrak{R}^{m \times n}$ the set of $m \times n$ -dimensional real matrices.

Then we define that $\mathbb{D} = [d_{ij}]$, where $d_{ii} > 0$, $\sum_{j=1}^N d_{ij} = 1$, and

$$\begin{cases} d_{ij} > 0, & (v_i, v_j) \in \mathbb{E} \\ d_{ij} = 0, & (v_i, v_j) \notin \mathbb{E}. \end{cases}$$

Note that an undirected graph is connected if there is a path existing between any two different nodes; A directed graph is strongly connected if there is a directed path existing between any two different nodes. Moreover, define the input and output degree of agent i in the graph \mathbb{G} as \mathbb{I}_i and \mathbb{O}_i , respectively. If $\mathbb{I}_i = \mathbb{O}_i$ for all $i = 1, 2, \dots, N$ satisfies, then \mathbb{G} is balanced. For DTMAS, $I - \mathbb{D}$ is considered as a special Laplacian matrix [42], besides, the eigenvalues of which satisfy

$$\operatorname{Re}(\lambda_1(I - \mathbb{D})) < \operatorname{Re}(\lambda_2(I - \mathbb{D})) \leq \dots \leq \operatorname{Re}(\lambda_N(I - \mathbb{D})).$$

SYMBOLS AND NOMENCLATURE

\otimes Kronecker product

$|\cdot|$ the determinant

$\|\cdot\|$ the Euclidean norm

\mathbf{i} imaginary number

$\lambda_i(Q)$ the i th eigenvalue of matrix Q

I_Z the $Z \times Z$ dimensional identity matrix

$\mathfrak{R}, \mathfrak{R}^n$ the set of all real numbers, n -dimensional real vectors.

B. Formulation

The general second-order dynamic has been considered for the DTMAS as follows:

$$\begin{cases} \dot{x}_i(k+1) = x_i(k) + hv_i(k) \\ \dot{v}_i(k+1) = v_i(k) + ahx_i(k) + bhv_i(k) + hu_i(k) \end{cases} \quad (1)$$

where $x_i(k) \in \mathfrak{R}^n$, $v_i(k) \in \mathfrak{R}^n$, and $u_i(k) \in \mathfrak{R}^p$ represent the position, the velocity state, and the control input of agent i , respectively; $i = 1, 2, \dots, N$; $a \in \mathfrak{R}$ and $b \in \mathfrak{R}$ are real numbers; $h > 0$ is the sampling period.

Let $z_i(k) = [x_i^T(k), v_i^T(k)]^T$, $A = \begin{pmatrix} 1 & h \\ ah & 1 + bh \end{pmatrix}$, and $B = \begin{pmatrix} 0 \\ h \end{pmatrix}$, then system (1) is cast to

$$z_i(k+1) = Az_i(k) + Bu_i(k). \quad (2)$$

Definition 1: The DTMAS (1) can achieve general second-order consensus if

$$\begin{aligned} \lim_{k \rightarrow \infty} \|x_i(k) - x_j(k)\| &= 0 \\ \lim_{k \rightarrow \infty} \|v_i(k) - v_j(k)\| &= 0 \end{aligned}$$

where $i = 1, \dots, N$.

Remark 1: There are few literatures on the consensus control problem of general SOMAS because the general SOMAS is more universal than the double-integrator MAS. Hou *et al.* [31] and Ma *et al.* [32] both studied the consensus protocols via continuous-time control for general

SOMAS to achieve consensus. As far as we known, limited results have been studied for general SOMAS by discrete-time control. Our work is the first one to study the general SOMAS with discrete-time dynamics and design a linear distributed consensus control protocol by means of the model-free QL method.

The most important thing is to get a state feedback controller to make the system achieve general second-order consensus, that is, to make Definition 1 hold. For these purposes, a few important assumptions and useful lemmas are described here.

Assumption 1: The pair (A, B) is stabilizable.

Assumption 2: The digraph \mathbb{G} is strongly connected and balanced. The undigraph \mathbb{G} is connected.

Lemma 1 [42]: Under Assumption 2, for a DTMAS with a directed graph \mathbb{G} , $(2/[N(N-1)]) \leq \text{Re}(\lambda_2(I_N - \mathbb{D}))$ can be obtained.

Lemma 2 [42]: Under Assumption 2, for a DTMAS with a directed graph \mathbb{G} , $(4/[N(N-1)]) \leq \lambda_2(I_N - \mathbb{D})$ can be obtained.

III. MAIN RESULTS

For DTMAS, a new iterative QL method will be proposed to find the coupling gains matrix without knowing the system dynamics (A, B) to make the system achieve general second-order consensus.

The linear control input is designed as

$$\begin{aligned} u(k) &= \alpha \sum_{j \in N_i} d_{ij} [x_j(k) - x_i(k)] + \beta \sum_{j \in N_i} d_{ij} [v_j(k) - v_i(k)] \\ &= K \sum_{j \in N_i} d_{ij} [z_j(k) - z_i(k)] \end{aligned} \quad (3)$$

where α, β are the coupling gains, and $K = (\alpha \beta)$ is the coupling gains matrix.

Then, we propose an iterative model-free QL method to get the coupling gains matrix K .

The DTMAS (1) can be recalled as

$$z_i(k+1) = Az_i(k) + B\omega_i(k) \quad (4)$$

where $\omega_i(k) = mKz_i(k)$ is the test control input to derive the coupling gains matrix K .

Then a quadratic utility function can be cast to

$$r_{ik}(z_{ik}, \omega_{ik}) = z_{ik}^T z_{ik} + \omega_{ik}^T \omega_{ik} \quad (5)$$

where $z_i(k)$ and $\omega_i(k)$ are denoted as z_{ik} and ω_{ik} . Equation (5) can be regarded as the utility function with the performance matrices $Q = I$ and $R = I$.

Then, a cost function of agent i with state z_{ik} is defined as follow:

$$V_i(z_{ik}, \omega_{ik}) = \sum_{j=k}^{\infty} r_{ij}(z_{ij}, \omega_{ij}). \quad (6)$$

Define a unique positive definite matrix as P , the total cost of agent i is quadratic in its state as follows:

$$V_{ik}(z_{ik}) = z_{ik}^T P z_{ik} \quad (7)$$

where $P = P^T > 0$.

According to the Bellman optimality principle, the cost function (6) is rewritten as

$$V_{ik}(z_{ik}) = r_{ik}(z_{ik}, \omega_{ik}) + V_{ik}(z_{i(k+1)}) \quad (8)$$

Furthermore, define a Q-function as

$$Q_{ik}(z_{ik}, \omega_{ik}) = r_{ik}(z_{ik}, \omega_{ik}) + V_{ik}(z_{i(k+1)}) \quad (9)$$

which can be rewritten as

$$\begin{aligned} Q_{ik}(z_{ik}, \omega_{ik}) &= z_{ik}^T z_{ik} + \omega_{ik}^T \omega_{ik} + z_{i(k+1)}^T P z_{i(k+1)} \\ &= z_{ik}^T z_{ik} + \omega_{ik}^T \omega_{ik} + (Az_i(k) + B\omega_i(k))^T \\ &\quad \times P(Az_i(k) + B\omega_i(k)) \\ &= \begin{pmatrix} z_{ik} \\ \omega_{ik} \end{pmatrix}^T \begin{pmatrix} I + A^T P A & A^T P B \\ B^T P A & B^T P B + I \end{pmatrix} \begin{pmatrix} z_{ik} \\ \omega_{ik} \end{pmatrix}. \end{aligned} \quad (10)$$

Let $\varsigma_{ik} = (z_{ik}^T, \omega_{ik}^T)^T$, and

$$S = \begin{pmatrix} S_{zz} & S_{z\omega} \\ S_{\omega z} & S_{\omega\omega} \end{pmatrix} = L \begin{pmatrix} I + A^T P A & A^T P B \\ B^T P A & B^T P B + I \end{pmatrix}$$

defined as the Q-function matrix. Then the Q-function (9) is cast to

$$Q_{ik}(\varsigma_{ik}) = \varsigma_{ik}^T S \varsigma_{ik}. \quad (11)$$

From (8) and (9), we have

$$Q_{ik}(z_{ik}, \omega_{ik}) = V_{ik}(z_{ik}). \quad (12)$$

Then, from (8) and (12), the Q-function is cast to

$$Q_{ik}(z_{ik}, \omega_{ik}) = z_{ik}^T z_{ik} + \omega_{ik}^T \omega_{ik} + Q_{ik}(z_{i(k+1)}, \omega_{i(k+1)}) \quad (13)$$

which is in a recursive form.

From (11) and (13), the matrix S can be estimated by the following equation:

$$\varsigma_{ik}^T S \varsigma_{ik} = z_{ik}^T z_{ik} + \omega_{ik}^T \omega_{ik} + \varsigma_{i(k+1)}^T S \varsigma_{i(k+1)} \quad (14)$$

where the Q-function matrix S can be rewritten as

$$S = \begin{pmatrix} s_{11} & s_{12} & \cdots & s_{1(n+p)} \\ s_{21} & s_{22} & \cdots & s_{2(n+p)} \\ \vdots & \ddots & \ddots & \vdots \\ s_{(n+p)1} & s_{(n+p)2} & \cdots & s_{(n+p)(n+p)} \end{pmatrix}$$

in which s_{ij} represents the i th row and the j th column component of matrix S and $s_{ij} = s_{ji}$.

Then define that

$$Q_{ik}(\varsigma_{ik}) = \varsigma_{ik}^T S \varsigma_{ik} = \bar{S}^T \bar{\varsigma}_{ik} \quad (15)$$

therefore, the (14) can be recalled as

$$\bar{S}^T \bar{\varsigma}_{ik} = z_{ik}^T z_{ik} + \omega_{ik}^T \omega_{ik} + \bar{S}^T \bar{\varsigma}_{i(k+1)} \quad (16)$$

with

$$\begin{aligned} \bar{S} \triangleq & [s_{11}, 2s_{12}, \dots, 2s_{1(n+p)}, s_{22}, 2s_{23}, \dots \\ & 2s_{2(n+p)}, \dots, s_{(n+p)(n+p)}]^T \end{aligned} \quad (17)$$

Algorithm 1 An Iterative Model-Free QL Algorithm

Step 1 (Initialization): the iteration $j = 0$; a Q-function matrix $S^0 > 0$; an arbitrary coupling gains matrix K^0 ; a test control input $\omega_{ik} = mK^0 z_{ik} + \delta_{ik}$ with an exploration signal δ_{ik} ; an agent i starting with ω_{ik} .

Step 2: For the j th iteration ($j > 0$), R datasets of $(z_{ik}, \omega_{ik}, z_{i(k+1)}, \omega_{i(k+1)})$ at time k need to be collected, where $\omega_{i(k+1)}$ is measured by utilizing the test control input policy $\omega_{i(k+1)} = mK^{j-1} z_{i(k+1)}$, and $R \geq (n+p)(n+p+1)/2$.

Step 3: Obtain the Q-function matrix S^j from the following QL Bellman equation:

$$\bar{S}^{jT} \bar{S}_{ik} = z_{ik}^T \omega_{ik} + \omega_{ik}^T \omega_{ik} + \bar{S}^{(j-1)T} \bar{S}_{i(k+1)}. \quad (19)$$

Step 4: Update $\omega_{i(k)} = mK^j z_{i(k)} + \delta_{ik}$ by selecting

$$K^j = -c(S_{\omega\omega}^j)^{-1} S_{\omega z}^j, \quad (20)$$

where $c = \frac{1}{4N(N-1)}$.

Step 5: If $\|K^j - K^{j-1}\|_2 < \varepsilon$, where the constant $\varepsilon > 0$ is very small, then turn to Step 6; else, return to the Step 2 by setting $j = j + 1$.

Step 6: Terminate.

and

$$\bar{S}_{ik} \triangleq \left[S_{ik(1)}^2, S_{ik(1)} S_{ik(2)}, \dots, S_{ik(1)} S_{ik(n+p)}, S_{ik(2)}^2, S_{ik(2)} S_{ik(3)}, \dots, S_{ik(2)} S_{ik(n+p)}, \dots, S_{ik(n+p)}^2 \right]^T \quad (18)$$

where $S_{ik(j)}$ is the j th component of vector S_{ik} .

Based on the (16) about Q-function, we design a novel method to derive the coupling gains matrix K , which is called as the model-free QL method.

Algorithm 1 is completely model-free, which can learn the coupling gains matrix K for the system (1) to reach consensus. To learn a suitable coupling gains matrix K , starting from arbitrarily selecting an agent, we initialize a Q-function matrix $S^0 > 0$ and an arbitrary coupling gains matrix K^0 . Then, based on a test input ω_{ik} , the datasets of $(z_{ik}, \omega_{ik}, z_{i(k+1)}, \omega_{i(k+1)})$ can be collected and updated to solve the QL Bellman (19) and obtain the Q-function matrix S , which is used to derive the coupling gains matrix K . From [34], after repeating the steps 2–4 finitely multiple times, the suitable coupling gains matrix K can be derived. In step 5, we will check whether the coupling gains matrix K has stabilized during the iteration. If K remains unchanged, the required K is found and the iteration is completed. The DTMAS (1) can reach general second-order consensus by utilizing the obtained coupling gains matrix K in the control protocol (3). Otherwise return to step 2 and perform the next iteration until it finds that K remains unchanged.

In step 3 of Algorithm 1, to solve the QL Bellman (19), we get

$$\bar{S}^j = (\Phi \Phi^T)^{-1} \Phi \Psi \quad (21)$$

where

$$\Phi = \begin{bmatrix} \bar{S}_{ik}^1, \bar{S}_{ik}^2, \dots, \bar{S}_{ik}^R \end{bmatrix}$$

$$\Psi = \begin{bmatrix} r_{ik}^1 + (\bar{S}^{j-1})^T \bar{S}_{i(k+1)}^1, \dots, r_{ik}^R + (\bar{S}^{j-1})^T \bar{S}_{i(k+1)}^R \end{bmatrix}^T$$

where $\Phi \in \mathbb{R}(((n+p)(n+p+1))/2) \times R$ and $\Psi \in \mathbb{R}^{R \times 1}$. To get the unique solution of (19), $\text{rank}(\Phi)$ needs to satisfy that

$$\text{rank}(\Phi) = \frac{(n+p)(n+p+1)}{2} \quad (22)$$

which suggests the full rank condition of Φ . To satisfy that, we add an exploration signal δ_{ik} into the test input ω_{ik} in Algorithm 1, defined as persistence of excitation (PE). This is discussed further in the literature on adaptive control [43].

Remark 2: From Algorithm 1, we can know that the QL method only needs to know the total number N of agents, and it is not necessary to know the system matrices A and B , so the QL method can be called as a model-free algorithm. Second, after initializing the states of agents and a Q-function matrix S^0 , the coupling gains matrix K can be calculated through several iterative calculation which can guarantee the second-order consensus of the systems. Therefore, the coupling gains matrix K does not need to be given, but is calculated by the QL method, which can be a zero matrix when iteratively initialized.

Next, we will utilize the method of Lyapunov function to prove that the QL method can make the DTMAS reach consensus.

Theorem 1: Under Assumptions 1 and 2, for the directed graph \mathbb{G} , the general SOMAS formed by (1) with protocol (3) can reach global consensus if and only if the coupling gains matrix K is obtained by Algorithm 1 with

$$4N(N-1) + 2\sqrt{4N^2(N-1)^2 - 3} \leq m < 8N(N-1). \quad (23)$$

Proof: From (7) and (12), the Q-function (13) can be rewritten as

$$Q_{ik}(z_{ik}, \omega_{ik}) = V_{ik}(z_{ik}) = z_{ik}^T P z_{ik}. \quad (24)$$

Then, substitute the test input $\omega_i(k) = mK z_i(k)$ into Q-function (24), one has

$$\begin{aligned} z_{ik}^T P z_{ik} &= z_{ik}^T z_{ik} + [mK z_i(k)]^T [mK z_i(k)] + Q_{ik}(z_{i(k+1)}) \\ &= z_{ik}^T z_{ik} + [mK z_i(k)]^T [mK z_i(k)] \\ &\quad + (A z_{ik} + mB K z_{ik})^T P (A z_{ik} + mB K z_{ik}) \\ &= z_{ik}^T z_{ik} + m^2 z_{ik}^T K^T K z_{ik} + z_{ik}^T A^T P A z_{ik} \\ &\quad + m z_{ik}^T A^T P B K z_{ik} + m z_{ik}^T K^T B^T P A z_{ik} \\ &\quad + m^2 z_{ik}^T K^T B^T P B K z_{ik}. \end{aligned} \quad (25)$$

Since $K = -c(S_{\omega\omega})^{-1} S_{\omega z} = -c(B^T P B + I)^{-1} B^T P A$, then (25) is

$$\begin{aligned} z_{ik}^T P z_{ik} &= z_{ik}^T z_{ik} + c^2 m^2 z_{ik}^T \left[A^T P B (B^T P B + I)^{-1} B^T P A \right] \\ &\quad \times z_{ik} - 2cm z_{ik}^T \left[A^T P B (B^T P B + I)^{-1} B^T P A \right] z_{ik} \\ &\quad + z_{ik}^T A^T P A z_{ik} \end{aligned}$$

$$= z_{ik}^T z_{ik} + z_{ik}^T A^T P A z_{ik} + (c^2 m^2 - 2cm) z_{ik}^T \times \left[A^T P B (B^T P B + I)^{-1} B^T P A \right] z_{ik}. \quad (26)$$

The general SOMAS (1) can be proved to reach consensus with control input $u(k) = K \sum_{j \in N_i} d_{ij} [z_j(k) - z_i(k)]$, $i = 1, 2, \dots, N$, where K is obtained by Algorithm 1. The error function is defined as $\xi(k) = [\Phi(I_N - \mathbb{D}) \otimes I_N] Z(k)$, where $Z(k) = [z_1^T(k), \dots, z_N^T(k)]^T$, and $I_N - \mathbb{D} = \Phi^{-1} \mathbb{J} \Phi$, with $\mathbb{J} \in \mathbb{R}^{N \times N}$ being an upper-triangular matrix with $\lambda_i (I_N - \mathbb{D}) (i = 1, \dots, N)$ as its diagonal entries. Obviously, the consensus can be achieved if $\xi(k) = 0$, i.e., $z_1 = \dots = z_N(k)$. According to $K = -c(S_{\omega\omega})^{-1} S_{\omega z} = -c(B^T P B + I)^{-1} B^T P A$ obtained by Algorithm 1, then $Z(k+1) = (I_N \otimes A) z(k) - [c(I_N - \mathbb{D}) \otimes B] (B^T P B + I)^{-1} B^T P A z(k)$ can be gotten. $\xi(k)$ is cast to

$$\begin{aligned} \xi(k+1) &= [\Phi(I_N - \mathbb{D}) \otimes I_N] Z(k) \\ &= [\Phi(I_N - \mathbb{D}) \otimes I_N] \left[(I_N \otimes A) - c((I_N - \mathbb{D}) \otimes B) \right. \\ &\quad \left. \times (B^T P B + I)^{-1} B^T P A \right] z(k) \\ &= \left[I_N \otimes A - c(\mathbb{J} \otimes B) (B^T P B + I)^{-1} B^T P A \right] \xi(k). \end{aligned} \quad (27)$$

Since the matrix $[I_N \otimes A - c(\mathbb{J} \otimes B) (B^T P B + I)^{-1} B^T P A]$ is block upper-triangular, (27) is asymptotically stable if

$$\bar{\xi}(k+1) = \left[I_N \otimes A - c(\bar{\mathbb{J}} \otimes B) (B^T P B + I)^{-1} B^T P A \right] \bar{\xi}(k) \quad (28)$$

is asymptotically stable, where $\bar{\mathbb{J}} = \text{diag}(\lambda_1 (I_N - \mathbb{D}), \dots, \lambda_N (I_N - \mathbb{D}))$, and $\bar{\xi}(k) = \xi(k)$.

Then, we design a Lyapunov function

$$V(k) = \bar{\xi}^H(k) (I_N \otimes P) \bar{\xi}(k). \quad (29)$$

For any bounded set $\chi \subset \mathbb{R}^n$, there must be a positive constant κ satisfying

$$\kappa \geq \sup_{z_i \in \chi, i=1, \dots, N} \left(\bar{\xi}^H(k) (I_N \otimes P) \bar{\xi}(k) \right). \quad (30)$$

Define a level set

$$L_V(\kappa) := \{ \bar{\xi} \in \mathbb{R}^{nN} : V(\bar{\xi}) \leq \kappa \}. \quad (31)$$

Within $L_V(\kappa)$, the variation of Lyapunov function $V(k)$ is cast to

$$\begin{aligned} \Delta V &= V(k+1) - V(k) \\ &= \bar{\xi}^H(k+1) (I_N \otimes P) \bar{\xi}(k+1) - \bar{\xi}^H(k) (I_N \otimes P) \bar{\xi}(k) \\ &= \bar{\xi}^H(k) \left[I_N \otimes A - c(\bar{\mathbb{J}} \otimes B) (B^T P B + I)^{-1} B^T P A \right]^H \\ &\quad \times (I_N \otimes P) \left[I_N \otimes A - c(\bar{\mathbb{J}} \otimes B) (B^T P B + I)^{-1} \right. \\ &\quad \left. \times B^T P A \right] \bar{\xi}(k) - \bar{\xi}^H(k) (I_N \otimes P) \bar{\xi}(k) \\ &= \bar{\xi}^H(k) \left[I_N \otimes A^T P A - c(\bar{\mathbb{J}}^H + \bar{\mathbb{J}}) \otimes A^T P B \right. \\ &\quad \times (B^T P B + I)^{-1} B^T P A + c^2 \bar{\mathbb{J}}^H \bar{\mathbb{J}} \otimes A^T P B \\ &\quad \times (B^T P B + I)^{-1} B^T P B (B^T P B + I)^{-1} B^T P A \\ &\quad \left. - I_N \otimes P \right] \bar{\xi}(k) \end{aligned}$$

$$\begin{aligned} &= \sum_{i=1}^N \bar{\xi}_i^H(k) \left[A^T P A - 2c \Re(\lambda_i) A^T P B (B^T P B + I)^{-1} \right. \\ &\quad \times B^T P A + c^2 |\lambda_i|^2 A^T P B (B^T P B + I)^{-1} B^T P B \\ &\quad \left. \times (B^T P B + I)^{-1} B^T P A - P \right] \bar{\xi}_i^H(k) \end{aligned} \quad (32)$$

where λ_i represents the eigenvalue of the matrix $I_N - \mathbb{D}$, $i = 1, \dots, N$.

Since $\bar{\xi}(k) = [\bar{\xi}_1^T(k), \bar{\xi}_2^T(k), \dots, \bar{\xi}_N^T(k)]^T$ and $(B^T P B + I)^{-1} B^T P B (B^T P B + I)^{-1} = (B^T P B + I)^{-1} - (B^T P B + I)^{-2}$, then the variation of Lyapunov function $V(k)$ is cast to

$$\begin{aligned} \Delta V &= \sum_{i=1}^N \bar{\xi}_i^H(k) \left[A^T P A - 2c \Re(\lambda_i) A^T P B (B^T P B + I)^{-1} \right. \\ &\quad \times B^T P A + c^2 |\lambda_i|^2 A^T P B (B^T P B + I)^{-1} B^T P A \\ &\quad \left. - c^2 |\lambda_i|^2 A^T P B (B^T P B + I)^{-2} B^T P A - P \right] \bar{\xi}_i(k) \\ &\leq \sum_{i=1}^N \bar{\xi}_i^H(k) \left[A^T P A - 2c \Re(\lambda_i) A^T P B (B^T P B + I)^{-1} \right. \\ &\quad \times B^T P A + c^2 |\lambda_i|^2 A^T P B (B^T P B + I)^{-1} \\ &\quad \left. \times B^T P A - P \right] \bar{\xi}_i(k). \end{aligned} \quad (33)$$

From Lemma 1, we can obtain that $\Re(\lambda_i (I_N - \mathbb{D})) \geq (2/[N(N-1)])$ and $|\lambda_i (I_N - \mathbb{D})| < 2$, then (33) is

$$\begin{aligned} \Delta V &\leq N \bar{\xi}_i^H(k) \left[A^T P A - P - c \cdot \frac{4}{N(N-1)} A^T P B \right. \\ &\quad \times (B^T P B + I)^{-1} B^T P A + 4c^2 A^T P B \\ &\quad \left. \times (B^T P B + I)^{-1} B^T P A \right] \bar{\xi}_i(k). \end{aligned} \quad (34)$$

Furthermore, since $4N(N-1) + 2\sqrt{4N^2(N-1)^2 - 3} \leq m < 8N(N-1)$ and $c = (1/[4N(N-1)])$, then $c^2 m^2 - 2cm \geq -(3/[4N^2(N-1)^2])$ and $2cm - c^2 m^2 \in (0, 1]$. Thus the variation of Lyapunov function $V(k)$ is

$$\begin{aligned} \Delta V &\leq N \bar{\xi}_i^H(k) \left[A^T P A - P + (c^2 m^2 - 2cm) A^T P B \right. \\ &\quad \left. \times (B^T P B + I)^{-1} B^T P A \right] \bar{\xi}_i(k). \end{aligned} \quad (35)$$

Then from (26), we have

$$\begin{aligned} z_{ik}^T P z_{ik} &= z_{ik}^T z_{ik} + z_{ik}^T A^T P A z_{ik} + (c^2 m^2 - 2cm) z_{ik}^T \\ &\quad \times \left[A^T P B (B^T P B + I)^{-1} B^T P A \right] z_{ik}. \end{aligned}$$

Obviously

$$\begin{aligned} z_{ik}^T A^T P A z_{ik} - z_{ik}^T P z_{ik} &+ (c^2 m^2 - 2cm) \\ &\times z_{ik}^T \left[A^T P B (B^T P B + I)^{-1} B^T P A \right] z_{ik} = -z_{ik}^T z_{ik} \leq 0 \end{aligned}$$

can be derived. Hence, the following inequality can be easily give:

$$\begin{aligned} A^T P A - P + (c^2 m^2 - 2cm) A^T P B (B^T P B + I)^{-1} \\ \times B^T P A < 0 \end{aligned} \quad (36)$$

which can lead to $\Delta V < 0$. Hence, according to the Lyapunov stability theory, the discrete-time trajectory ξ starting from

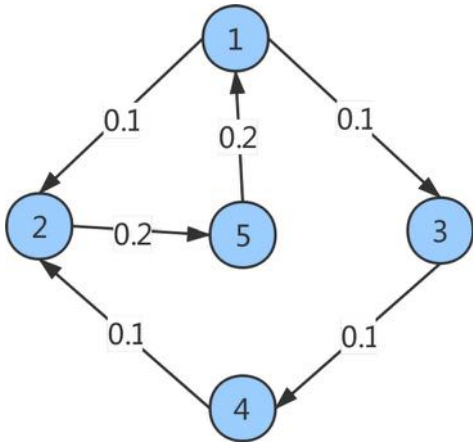


Fig. 1. Connected and balanced digraph.

the level set $L_V(\kappa)$ will converge exponentially to the origin $\xi = 0$ as $t \rightarrow \infty$, which implies that $z_1 = z_2 = \dots = z_N$, $i = 1, \dots, N$ as $t \rightarrow \infty$. ■

Remark 3: For an undirected graph, the dynamics and control inputs of the system are as shown previously. The algorithm to obtain the coupling gains matrix K is the same as Algorithm 1, except that all the eigenvalues of $I_N - \mathbb{D}$ for the undirected graph are real numbers, so the value of m is different from Theorem 1. The specific results and proofs are as follows.

Corollary 1: Under Assumptions 1 and 2, for an undirected graph \mathbb{G} , the general SOMAS formed by (1) with protocol (3) can reach consensus if and only if the coupling gains matrix K is obtained by Algorithm 1 with

$$4N(N-1) + 2\sqrt{4N^2(N-1)^2 - 7} \leq m < 8N(N-1). \quad (37)$$

Proof: The construction of the Lyapunov function is the same as Theorem 1, then the variation of Lyapunov function $V(k)$ is cast to

$$\begin{aligned} \Delta V &= V(k+1) - V(k) \\ &= \bar{\xi}^H(k+1)(I_N \otimes P)\bar{\xi}(k+1) - \bar{\xi}^H(k)(I_N \otimes P)\bar{\xi}(k) \\ &= \bar{\xi}^H(k) \left[I_N \otimes A - c(\bar{\mathbb{J}} \otimes B)(B^T PB + I)^{-1} B^T PA \right]^H \\ &\quad \times (I_N \otimes P) \left[I_N \otimes A - c(\bar{\mathbb{J}} \otimes B)(B^T PB + I)^{-1} \right. \\ &\quad \left. \times B^T PA \right] \bar{\xi}(k) - \bar{\xi}^H(k)(I_N \otimes P)\bar{\xi}(k) \\ &= \bar{\xi}^H(k) \left[I_N \otimes A^T PA - c(\bar{\mathbb{J}}^H + \bar{\mathbb{J}}) \otimes A^T PB \right. \\ &\quad \times (B^T PB + I)^{-1} B^T PA + c^2 \bar{\mathbb{J}}^H \bar{\mathbb{J}} \otimes A^T PB \\ &\quad \times (B^T PB + I)^{-1} B^T PB (B^T PB + I)^{-1} B^T PA \\ &\quad \left. - I_N \otimes P \right] \bar{\xi}(k) \\ &= \sum_{i=1}^N \bar{\xi}_i^H(k) \left[A^T PA - c \cdot 2\lambda_i A^T PB (B^T PB + I)^{-1} \right. \\ &\quad \times B^T PA + c^2 |\lambda_i|^2 A^T PB (B^T PB + I)^{-1} \\ &\quad \left. \times B^T PB \times (B^T PB + I)^{-1} B^T PA - P \right] \bar{\xi}_i^H(k) \end{aligned} \quad (38)$$

where λ_i represents the eigenvalue of the matrix $I_N - \mathbb{D}$, $i = 1, \dots, N$.

Since $\bar{\xi}(k) = [\bar{\xi}_1^T(k), \bar{\xi}_2^T(k), \dots, \bar{\xi}_N^T(k)]^T$ and $(B^T PB + I)^{-1} B^T PB (B^T PB + I)^{-1} = (B^T PB + I)^{-1} - (B^T PB + I)^{-2}$, then the variation of Lyapunov function $V(k)$ is cast to

$$\begin{aligned} \Delta V &\leq \sum_{i=1}^N \bar{\xi}_i^H(k) \left[A^T PA - 2c\lambda_i A^T PB (B^T PB + I)^{-1} \right. \\ &\quad \times B^T PA + c^2 |\lambda_i|^2 A^T PB (B^T PB + I)^{-1} \\ &\quad \left. \times B^T PA - P \right] \bar{\xi}_i(k). \end{aligned} \quad (39)$$

From Lemma 2, we can obtain that $\lambda_i(I_N - \mathbb{D}) \geq (4/[N(N-1)])$ and $|\lambda_i(I_N - \mathbb{D})| < 2$, then (39) is

$$\begin{aligned} \Delta V &\leq N \bar{\xi}_i^H(k) \left[A^T PA - P - c \cdot \frac{8}{N(N-1)} A^T PB \right. \\ &\quad \times (B^T PB + I)^{-1} B^T PA + 4c^2 A^T PB \\ &\quad \left. \times (B^T PB + I)^{-1} B^T PA \right] \bar{\xi}_i(k). \end{aligned} \quad (40)$$

Since $4N(N-1) + 2\sqrt{4N^2(N-1)^2 - 7} \leq m < 8N(N-1)$ and $c = (1/[4N(N-1)])$, then $c^2 m^2 - 2cm \geq -(7/[4N^2(N-1)^2])$ and $2cm - c^2 m^2 \in (0, 1]$. Thus the variation of Lyapunov function $V(k)$ is

$$\begin{aligned} \Delta V &\leq N \bar{\xi}_i^H(k) \left[A^T PA - P + (c^2 m^2 - 2cm) A^T PB \right. \\ &\quad \left. \times (B^T PB + I)^{-1} B^T PA \right] \bar{\xi}_i(k). \end{aligned} \quad (41)$$

Then from (26), we have

$$\begin{aligned} z_{ik}^T P z_{ik} &= z_{ik}^T z_{ik} + z_{ik}^T A^T PA z_{ik} + (c^2 m^2 - 2cm) z_{ik}^T \\ &\quad \times \left[A^T PB \times (B^T PB + I)^{-1} B^T PA \right] z_{ik}. \end{aligned}$$

Obviously

$$\begin{aligned} z_{ik}^T A^T PA z_{ik} - z_{ik}^T P z_{ik} &+ (c^2 m^2 - 2cm) z_{ik}^T \\ &\quad \times \left[A^T PB \times (B^T PB + I)^{-1} B^T PA \right] z_{ik} = -z_{ik}^T z_{ik} \leq 0 \end{aligned}$$

can be derived. Therefore, the following inequality can be easily given:

$$\begin{aligned} A^T PA - P + (c^2 m^2 - 2cm) A^T PB \\ \times (B^T PB + I)^{-1} B^T PA < 0 \end{aligned} \quad (42)$$

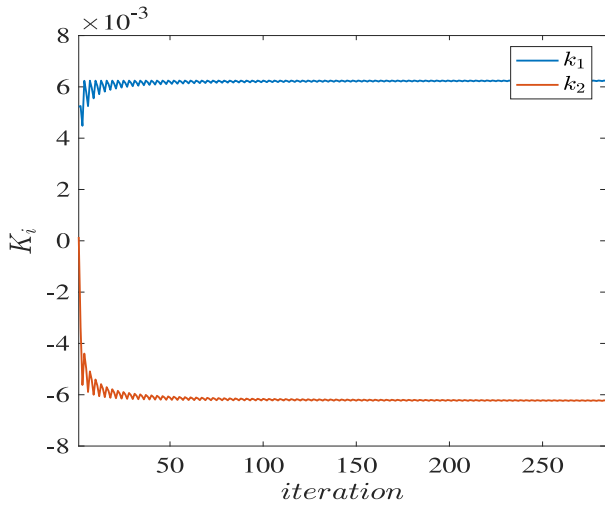
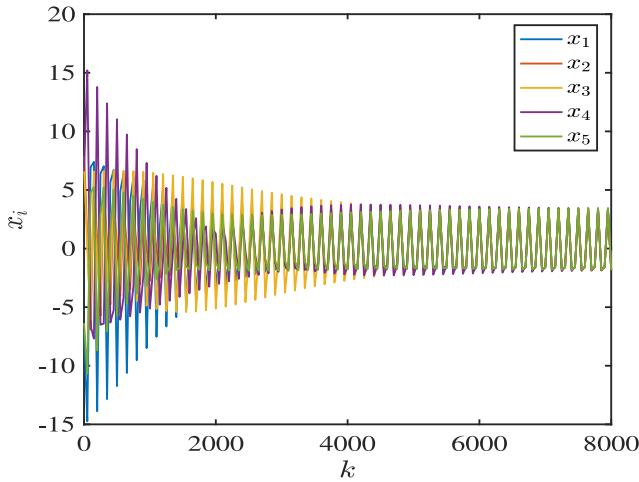
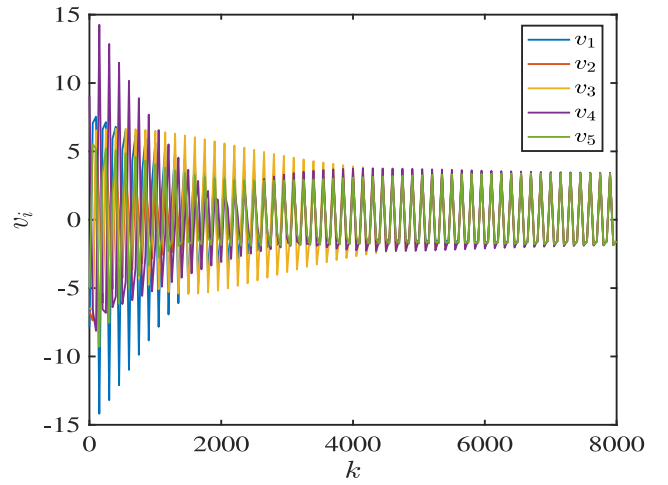
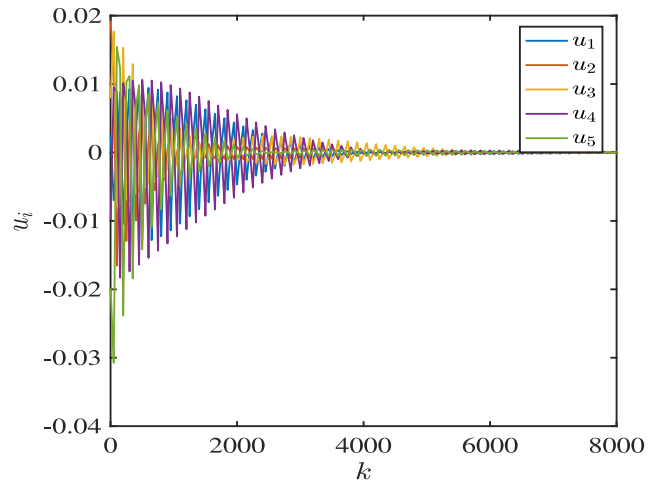
which can lead to $\Delta V < 0$. Then $z_1 = z_2 = \dots = z_N$, $i = 1, \dots, N$ as $t \rightarrow \infty$ can be obtained according to the Lyapunov stability theory. Therefore the general second-order consensus can be reached under undirected graphs. ■

IV. SIMULATIONS

Consider a general SOMAS with five agents and choose $h = 1$, $a = b = -1$, then system matrices are

$$A = \begin{bmatrix} 1 & 1 \\ -1 & 0 \end{bmatrix}, \quad B = \begin{bmatrix} 0 \\ 1 \end{bmatrix}$$

which satisfies Assumption 1.

Fig. 2. Convergence of coupling gains matrix K under the digraph.Fig. 3. Position state x_i of each agent under the digraph.Fig. 4. Velocity state v_i of each agent under the digraph.Fig. 5. Control input u_i of each agent under the digraph.

Example 1: The graph \mathbb{G} is strongly connected and balanced as Fig. 1, where

$$I_N - \mathbb{D} = \begin{bmatrix} 0.2 & 0 & 0 & 0 & -0.2 \\ -0.1 & 0.2 & 0 & -0.1 & 0 \\ -0.1 & 0 & 0.1 & 0 & 0 \\ 0 & 0 & -0.1 & 0.1 & 0 \\ 0 & -0.2 & 0 & 0 & 0.2 \end{bmatrix}.$$

Then, the initial position states of five agents are defined as $x_1(0) = -7.13$, $x_2(0) = 7.86$, $x_3(0) = 6.96$, $x_4(0) = 6.60$, $x_5(0) = -6.36$, and the initial velocity states of five agents are defined as $v_1(0) = -7.85$, $v_2(0) = -6.72$, $v_3(0) = -6.48$, $v_4(0) = 9.06$, $v_5(0) = -5.04$. With $N = 5$, the initial parameters are defined as $c = 1/80$, $m = 159.95$, $\mathbb{K}^0 = [0 \ 0]$, $S^0 = I$, $\varepsilon = 1 \times 10^{-5}$ and $R = 1000$. Then apply Algorithm 1 to the system, and the coupling gains matrix K is eventually computed as $K = [0.0062 \ -0.0062]$, and Fig. 2 shows the convergence process of K . With K computed by Algorithm 1, the convergences of the position states, velocity states, and the control input of each agent are shown in Figs. 3–5, respectively. It is easy to conclude that under Algorithm 1 and Theorem 1, the general second-order consensus for MAS (1)

can be achieved. The correctness of Theorem 1 can be proved.

Example 2: The graph \mathbb{G} is undirected and connected as Fig. 6, where

$$I_N - \mathbb{D} = \begin{bmatrix} 0.8 & -0.5 & -0.2 & -0.1 \\ -0.5 & 0.5 & 0 & 0 \\ -0.2 & 0 & 0.7 & -0.5 \\ -0.1 & 0 & -0.5 & 0.6 \end{bmatrix}.$$

Then the initial position states of five agents are defined as $x_1(0) = 5.66$, $x_2(0) = 7.86$, $x_3(0) = 4.30$, $x_4(0) = -6.33$, and the initial velocity states of five agents are defined as $v_1(0) = -4.32$, $v_2(0) = -7.28$, $v_3(0) = 5.46$, $v_4(0) = -5.45$. With $N = 4$, the initial parameters are defined as $c = 1/48$, $m = 95.8$, $\mathbb{K}^0 = [0 \ 0]$, $S^0 = I$, $\varepsilon = 1 \times 10^{-5}$ and $R = 1000$. Then apply Algorithm 1 to the system, and the coupling gains matrix K is eventually computed as $K = [0.0104 \ -0.0104]$, and Fig. 7 shows the convergence process of K . With K computed by Algorithm 1, the convergences of the position states, velocity states, and the control input of each agent are shown in Figs. 8–10, respectively. It is easy to conclude that

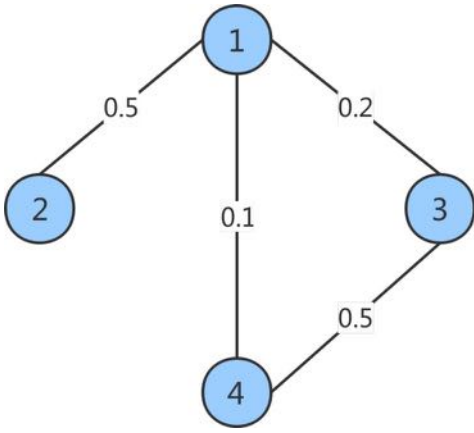
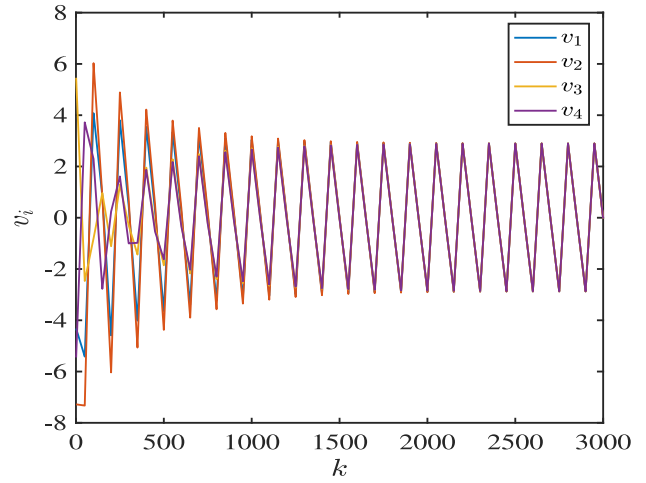
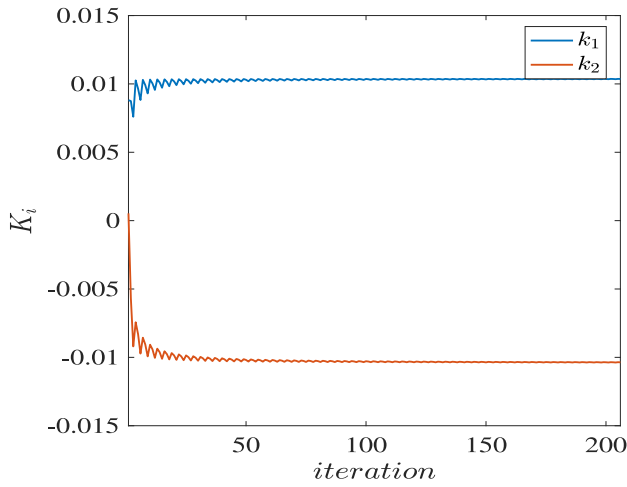
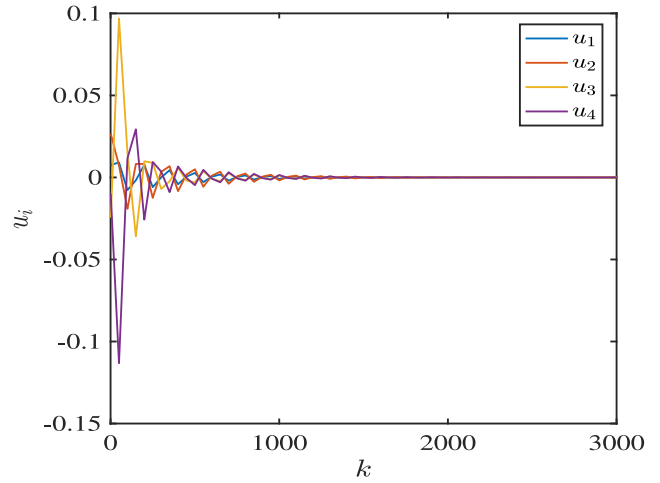
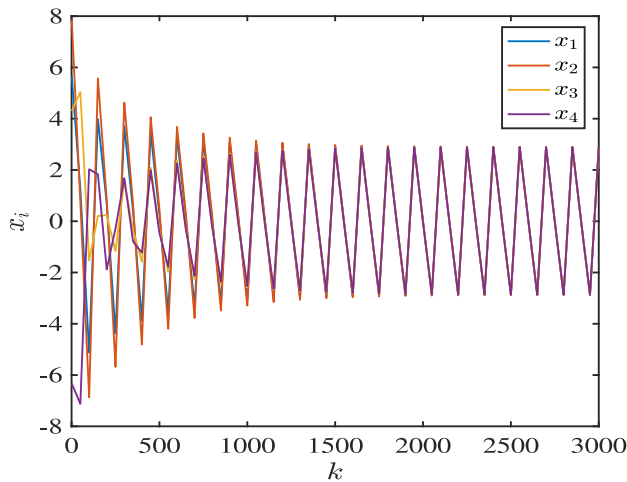


Fig. 6. Connected and undirected graph.

Fig. 9. Velocity state v_i of each agent under the undirected graph.Fig. 7. Convergence of coupling gains matrix K under the undirected graph.Fig. 10. Control input u_i of each agent under the undirected graph.Fig. 8. Position state x_i of each agent under the undirected graph.

under Algorithm 1 and Corollary 1, the general second-order consensus for MAS (1) can be achieved. The correctness of Corollary 1 can be proved.

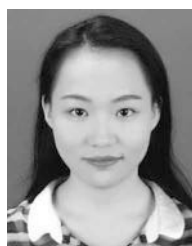
V. CONCLUSION

A novel consensus control problem is studied in this article for general SOMAS via the QL method with no knowledge of agent dynamics. Besides, this article is the first to study the type of general SOMAS with discrete-time dynamics. Under fixed directed topology, a QL algorithm with no knowledge of agent dynamics is obtained for MAS via discrete-time control to achieve general second-order consensus. Moreover, the obtained model-free QL algorithm is able to derive the coupling gains matrix without any information of dynamics. With this obtained coupling gains matrix, general second-order consensus can be achieved. In the future, the general second-order consensus control issue for MAS with switched dynamics via QL method will be investigated.

REFERENCES

- [1] Z. Yu, H. Jiang, and C. Hu, "Second-order consensus for multiagent systems via intermittent sampled data control," *IEEE Trans. Syst., Man, Cybern., Syst.*, vol. 48, no. 11, pp. 1986–2002, Nov. 2018.
- [2] H. Su, H. Wu, X. Chen, and M. Z. Q. Chen, "Positive edge consensus of complex networks," *IEEE Trans. Syst., Man, Cybern., Syst.*, vol. 48, no. 12, pp. 2242–2250, Dec. 2018.

- [3] D. Chen, Y. Wang, G. Wu, M. Kang, Y. Sun, and W. Yu, "Inferring causal relationship in coordinated flight of pigeon flocks," *Chaos*, vol. 29, no. 11, 2019, Art. no. 113118.
- [4] D. Chen, W. Li, X. Liu, W. Yu, and Y. Sun, "Effects of measurement noise on flocking dynamics of cuckoo-smale systems," *IEEE Trans. Circuits Syst. II, Exp. Briefs*, early access, Oct. 16, 2019, doi: [10.1109/TCSII.2019.2947788](https://doi.org/10.1109/TCSII.2019.2947788).
- [5] H. Su, Y. Sun, and Z. Zeng, "Semiglobal observer-based non-negative edge consensus of networked systems with actuator saturation," *IEEE Trans. Cybern.*, vol. 50, no. 6, pp. 2827–2836, Jun. 2020, doi: [10.1109/TCYB.2019.2917006](https://doi.org/10.1109/TCYB.2019.2917006).
- [6] D. Chen, H. Su, and G. J. Pan, "Framework based on communicability to measure the similarity of nodes in complex networks," *Inf. Sci.*, vol. 524, pp. 241–253, Jul. 2020.
- [7] X. Wang, X. Wang, H. Su, and J. Lam, "Coordination control for uncertain networked systems using interval observers," *IEEE Trans. Cybern.*, vol. 50, no. 9, pp. 4008–4019, Sep. 2020, doi: [10.1109/TCYB.2019.2945580](https://doi.org/10.1109/TCYB.2019.2945580).
- [8] R. Agha, M. Rehan, C. K. Ahn, G. Mustafa, and S. Ahmad, "Adaptive distributed consensus control of one-sided Lipschitz nonlinear multiagents," *IEEE Trans. Syst., Man, Cybern., Syst.*, vol. 49, no. 3, pp. 568–578, Mar. 2019.
- [9] H. Su, Y. Liu, and Z. Zeng, "Second-order consensus for multiagent systems via intermittent sampled position data control," *IEEE Trans. Cybern.*, vol. 50, no. 5, pp. 2063–2072, May 2020.
- [10] X. Wang, G. P. Jiang, H. Su, and X. Wang, "Robust global coordination of networked systems with input saturation and external disturbances," *IEEE Trans. Syst., Man, Cybern., Syst.*, early access, Mar. 30, 2020, doi: [10.1109/TSMC.2020.2980295](https://doi.org/10.1109/TSMC.2020.2980295).
- [11] H. Meng, H. T. Zhang, Z. Wang, and G. Chen, "Event-triggered control for semiglobal robust consensus of a class of nonlinear uncertain multiagent systems," *IEEE Trans. Autom. Control*, vol. 65, no. 4, pp. 1683–1690, Apr. 2020, doi: [10.1109/TAC.2019.2932752](https://doi.org/10.1109/TAC.2019.2932752).
- [12] Y. Liu and H. Su, "Containment control of second-order multi-agent systems via intermittent sampled position data communication," *Appl. Math. Comput.*, vol. 362, Dec. 2019, Art. no. 124522.
- [13] J. Zhang and H. Su, "Formation-containment control for multi-agent systems with sampled data and time delays," *Neurocomputing*, to be published, doi: [10.1016/j.neucom.2019.11.030](https://doi.org/10.1016/j.neucom.2019.11.030).
- [14] Y. Liu and H. Su, "Some necessary and sufficient conditions for containment of second-order multi-agent systems with sampled position data," *Neurocomputing*, vol. 378, pp. 228–237, Feb. 2020.
- [15] H. Su, M. Long, and Z. Zeng, "Controllability of two-time-scale discrete-time multiagent systems," *IEEE Trans. Cybern.*, vol. 50, no. 4, pp. 1440–1449, Apr. 2020.
- [16] M. Long, H. Su, and B. Liu, "Second-order controllability of two-time-scale multi-agent systems," *Appl. Math. Comput.*, vol. 343, pp. 299–313, Feb. 2019.
- [17] H. Su, J. Zhang, and X. Chen, "A stochastic sampling mechanism for time-varying formation of multiagent systems with multiple leaders and communication delays," *IEEE Trans. Neural Netw. Learn. Syst.*, vol. 30, no. 12, pp. 3699–3707, Dec. 2019.
- [18] H. Su, J. Zhang, and Z. Zeng, "Formation-containment control of multi-robot systems under a stochastic sampling mechanism," *Sci. China Technol. Sci.*, vol. 63, pp. 1025–1034, Apr. 2020, doi: [10.1007/s11431-019-1451-6](https://doi.org/10.1007/s11431-019-1451-6).
- [19] B. Liu *et al.*, "Collective dynamics and control for multiple unmanned surface vessels," *IEEE Trans. Control Syst. Technol.*, early access, Aug. 14, 2019, doi: [10.1109/TCST.2019.2931524](https://doi.org/10.1109/TCST.2019.2931524).
- [20] X. Mo, Z. Chen, and H. T. Zhang, "Effects of adding a reverse edge across a stem in a directed acyclic graph," *Automatica*, vol. 103, pp. 254–260, May 2019.
- [21] X. Wang, H. Su, and X. Wang, "The infimum on Laplacian Eigenvalues of a connected extended graph: An edge-grafting perspective," *IEEE Trans. Circuits Syst. II, Exp. Briefs*, early access, Dec. 5, 2019, doi: [10.1109/TCSII.2019.2957944](https://doi.org/10.1109/TCSII.2019.2957944).
- [22] Q. Tang, D. Chen, and X. He, "Integration of enhanced flux linkage observer and i-f starting method for wide-speed-range sensorless SPMSM drives," *IEEE Trans. Power Electron.*, vol. 35, no. 8, pp. 8374–8393, Aug. 2020, doi: [10.1109/TPEL.2019.2963208](https://doi.org/10.1109/TPEL.2019.2963208).
- [23] R. Olfati-Saber and R. M. Murray, "Consensus problems in networks of agents with switching topology and time-delays," *IEEE Trans. Autom. Control*, vol. 49, no. 9, pp. 1520–1533, Sep. 2004.
- [24] X. Wang and H. Su, "Consensus of hybrid multi-agent systems by event-triggered/self-triggered strategy," *Appl. Math. Comput.*, vol. 359, pp. 490–501, Oct. 2019.
- [25] H. Su, Y. Ye, X. Chen, and H. He, "Necessary and sufficient conditions for consensus in fractional-order multiagent systems via sampled data over directed graph," *IEEE Trans. Syst., Man, Cybern., Syst.*, early access, May 21, 2019, doi: [10.1109/TSMC.2019.2915653](https://doi.org/10.1109/TSMC.2019.2915653).
- [26] X. Wang and H. Su, "Self-triggered leader-following consensus of multi-agent systems with input time delay," *Neurocomputing*, vol. 330, pp. 70–77, Feb. 2019.
- [27] Y. Wan, G. H. Wen, J. D. Cao, and W. W. Yu, "Distributed node-to-node consensus of multi-agent systems with stochastic sampling," *Int. J. Robust Nonlinear Control*, vol. 26, no. 1, pp. 110–124, 2016.
- [28] W. Yu, G. Chen, and M. Cao, "Some necessary and sufficient conditions for second-order consensus in multi-agent dynamical systems," *Automatica*, vol. 46, no. 6, pp. 1089–1095, 2010.
- [29] H. Su, X. Wang, X. Chen, and Z. Zeng, "Second-order consensus of hybrid multiagent systems," *IEEE Trans. Syst., Man, Cybern., Syst.*, early access, Jan. 14, 2020, doi: [10.1109/TSMC.2019.2963089](https://doi.org/10.1109/TSMC.2019.2963089).
- [30] H. Su, X. Wang, and Z. Zeng, "Consensus of second-order hybrid multiagent systems by event-triggered strategy," *IEEE Trans. Cybern.*, early access, Nov. 8, 2019, doi: [10.1109/TCYB.2019.2948209](https://doi.org/10.1109/TCYB.2019.2948209).
- [31] W. Hou, M. Fu, H. Zhang, and Z. Wu, "Consensus conditions for general second-order multi-agent systems with communication delay," *Automatica*, vol. 75, pp. 293–298, Jan. 2017.
- [32] D. Ma, R. Tian, A. Zulfiqar, J. Chen, and T. Chai, "Bounds on delay consensus margin of second-order multiagent systems with robust position and velocity feedback protocol," *IEEE Trans. Autom. Control*, vol. 64, no. 9, pp. 3780–3787, Sep. 2019.
- [33] F. Wang, Y. Ni, Z. Liu, and Z. Chen, "Containment control for general second-order multiagent systems with switched dynamics," *IEEE Trans. Cybern.*, vol. 50, no. 2, pp. 550–560, Feb. 2020, doi: [10.1109/TCYB.2018.2869706](https://doi.org/10.1109/TCYB.2018.2869706).
- [34] R. S. Sutton and A. G. Barto, "Reinforcement learning: An introduction," *IEEE Trans. Neural Netw.*, vol. 9, no. 5, pp. 1054–1078, Sep. 1998.
- [35] K. G. Vamvoudakis, "Q-learning for continuous-time graphical games on large networks with completely unknown linear system dynamics," *Int. J. Robust Nonlinear Control*, vol. 27, pp. 2900–2920, Nov. 2017.
- [36] K. G. Vamvoudakis, "Q-learning for continuous-time linear systems: A model-free infinite horizon optimal control approach," *Syst. Control Lett.*, vol. 100, pp. 14–20, Feb. 2017.
- [37] S. A. A. Rizvi and Z. Lin, "An iterative Q-learning scheme for the global stabilization of discrete-time linear systems subject to actuator saturation," *Int. J. Robust Nonlinear Control*, vol. 29, no. 9, pp. 2660–2672, 2019.
- [38] M. I. Abouheaf, F. L. Lewis, M. S. Mahmoud, and D. G. Mikulski, "Discrete-time dynamic graphical games: Model-free reinforcement learning solution," *Control Theory Technol.*, vol. 13, no. 1, pp. 55–69, 2015.
- [39] B. Kiumarsi and F. L. Lewis, "Output synchronization of heterogeneous discrete-time systems: A model-free optimal approach," *Automatica*, vol. 84, pp. 86–94, Oct. 2017.
- [40] J. Zhang, H. Zhang, and T. Feng, "Distributed optimal consensus control for nonlinear multiagent system with unknown dynamic," *IEEE Trans. Neural Netw. Learn. Syst.*, vol. 29, no. 8, pp. 3339–3348, Aug. 2018.
- [41] J. Zhang, Z. Wang, and H. Zhang, "Data-based optimal control of multiagent systems: A reinforcement learning design approach," *IEEE Trans. Cybern.*, vol. 49, no. 12, pp. 4441–4449, Dec. 2019.
- [42] H. Su, H. Wu, and X. Chen, "Observer-based discrete-time nonnegative edge synchronization of networked systems," *IEEE Trans. Neural Netw. Learn. Syst.*, vol. 28, no. 10, pp. 2446–2455, Oct. 2017.
- [43] G. Tao, *Adaptive Control Design and Analysis*. Hoboken, NJ, USA: Wiley, 2003.



Yifan Liu received the B.S. degree in automatic control from the Huazhong University of Science and Technology, Wuhan, China, in 2018, where she is currently pursuing the M.S. degree in control theory and control engineering with the School of Artificial Intelligence and Automation.

Her current research interests include multiagent systems and second-order systems.



Housheng Su received the B.S. degree in automatic control and the M.S. degree in control theory and control engineering from the Wuhan University of Technology, Wuhan, China, in 2002 and 2005, respectively, and the Ph.D. degree in control theory and control engineering from Shanghai Jiao Tong University, Shanghai, China, in 2008.

From December 2008 to January 2010, he was a Postdoctoral Researcher with the Department of Electronic Engineering, City University of Hong Kong, Hong Kong. Since November 2014, he has been a Full Professor with the School of Artificial Intelligence and Automation, Huazhong University of Science and Technology, Wuhan. His research interests lie in the areas of multiagent coordination control theory and its applications to autonomous robotics and mobile sensor networks.

Dr. Su is an Associate Editor of *IET Control Theory and Applications*.

Second-Order Consensus for Multiagent Systems via Intermittent Sampled Position Data Control

Housheng Su^{id}, Yifan Liu, and Zhigang Zeng^{id}, *Senior Member, IEEE*

Abstract—In this paper, a second-order consensus for multiagent systems with a directed communication topology is studied. A novel consensus strategy is first proposed, where a periodic intermittent control strategy only with casual sampled position data is used, which not only decreases the operating time and the update rates of conditioners for every individual but also responds effectively to the case of missing velocity information. A necessary and sufficient consensus condition based on the coupling gains, the sampling period, the communication width, and the spectrum of the Laplacian matrix is established to reach the consensus, and the right intervals of the sampling period are given. Furthermore, a delay-induced consensus protocol is designed, and a necessary and sufficient condition is also given, by which the sampling period and the communication width can easily be chosen to achieve the consensus. At last, some simulation examples are given to verify the correctness of the theoretical results.

Index Terms—Communication width, intermittent sampled position data, multiagent system, sampling period, second-order consensus.

I. INTRODUCTION

A MULTIAGENT system means a group of autonomous agents working in a networked environment. Designing protocols for a multiagent system to achieve certain global control aims attracts the attention of many control engineers. One of the certain global control aims is the consensus, which means that individuals can achieve an agreement about certain interest under a suitable algorithm. It is found that in a networked environment, a group of individuals can accomplish some complicated tasks together while not being able to fulfill them individually. So far, the study of consensus in

multiagent systems has got great attention [1], [2] because of its widespread applications in robotic teams, biological systems [3], information control [4], sensor networks [5], [6], and so on.

Many of the significant results presented earlier were to reach the consensus. A general framework of first-order consensus problems for networked multiagent systems with fixed and switching topologies was discussed in [1]. Then a crucial distributed consensus condition was proposed in [1], which concluded that the condition to reach the first-order consensus is a spanning tree always existing. So far, the research boom in the first-order consensus has passed, and many significant results have been obtained in [7]–[10]. Considering the reality, much attention is paid to second-order consensus algorithms. For this case, some conditions were obtained in [11] to reach the consensus. Moreover, a lot of significant results were studied in [12]–[16] focused on the second-order consensus via nonlinear dynamics, adaptive control, or coupling delay. With the deepening of research, more complicated multiagent systems such as nonlinear, high-order, and stochastic dynamics were studied in [17]–[20].

To overcome the shortage that the controllers have difficulty in obtaining continuous information in reality, the second-order consensus with sampled data has been proposed, which has more advantages like robustness and low cost. Some conditions were achieved in [21]–[23] with the help of zero-order holds and direct discretization in order to reach the consensus with sampled control. More conditions with sampled control were discussed in [24]–[26] with communication delays or time-varying topology. The studies in [27] put forward some protocols using the current and some sampled previous position data without velocity data to overcome the difficulty in measuring the velocity information. Recently, in order to overcome the problem that the current position data cannot be obtained successfully, Huang *et al.* [28] considered the consensus using only sampled position information. However, most of the works mentioned previously studied continuous time control, requiring continuous communication between the controllers of agents to update information all the time. To reduce the operating time of the controllers, an intermittent control strategy was proposed. In [29], the first-order consensus with nonlinear topologies via intermittent communication was discussed. To reach the second-order consensus by using intermittent communication, the protocols with and without time delay were designed in [30]. Yu *et al.* [31] proposed a novel protocol via intermittent control to reach the second-order consensus, which can reduce the operating time

Manuscript received September 12, 2018; revised October 28, 2018; accepted October 29, 2018. This work was supported in part by the National Natural Science Foundation of China under Grant 61873318 and Grant 61473129, in part by the Foundation for Innovative Research Groups of Hubei Province of China under Grant 2017CFA005, in part by the Natural Science Foundation of Hubei Province of China under Grant 2018CFA058, in part by the Wuhan Morning Light Plan of Youth Science and Technology under Grant 2017050304010288, in part by the Fundamental Research Funds for the Central Universities under Grant HUST: 2017KFYXJJ178, and in part by the Program for HUST Academic Frontier Youth Team. This paper was recommended by Associate Editor T. H. Lee. (*Corresponding author: Housheng Su.*)

The authors are with the School of Automation, Huazhong University of Science and Technology, Wuhan 430074, China, and also with the Key Laboratory of Image Processing and Intelligent Control of Education Ministry of China, Huazhong University of Science and Technology, Wuhan 430074, China (e-mail: houshengsu@gmail.com; liuyifanhust@126.com; zgzeng@hust.edu.cn).

Color versions of one or more of the figures in this paper are available online at <http://ieeexplore.ieee.org>.

Digital Object Identifier 10.1109/TCYB.2018.2879327

of conditioners compared to other protocols that have been derived. This reminds us whether utilizing past sampled position data via intermittent communication for a second-order multiagent systems can still achieve the consensus so that not only the operating time and the update rates of conditioner for every individual can be shortened but also the problem that some information unavailable states can be overcome. Note that the above conclusions are based on multiagent systems.

Inspired by the above discussions, two novel control protocols in this paper are proposed via intermittent sampled position data control. The contributions of this paper are as follows.

- 1) There is a novel control strategy proposed for multiagent systems with second-order dynamics by utilizing the intermittent communication and the sampled position data. So it is able to decrease the operating time and the update rates of conditioners for every individual and effective to respond to the situation when the velocity and current position information cannot be obtained.
- 2) To reach the second-order consensus under a digraph, a necessary and sufficient condition is obtained, which concludes that the consensus via intermittent sampled position data control can be reached if two inequalities about the network structure and the parameters, including the sampling period, the communication width, the coupling gains, and the spectrum of the Laplacian matrix are satisfied. More advanced than the previous works of Huang *et al.* [28], this paper considers the consensus by using not only the sampled position information but also intermittent communication. On the one hand, in applications, by controlling the operating time and the update rates of conditioners, it can be effective to cut back communication cost and energy consumption. On the other hand, in calculation, by adding intermittent communication, this paper obtains fewer and simpler inequalities to achieve the consensus, and the order of inequality about the sampling period is lower, so it is easier to calculate.
- 3) By means of the utilizing time delay and the discussions about the relationship between various parameters regarding time, a necessary and sufficient condition is derived similarly. Under the circumstance where other parameters regarding time are given, it is simple to find that as long as the sampling period is within the range calculated by the inequality, the consensus can be achieved. It is found that this inequality is easier to calculate when compared to the protocol without time delay since the inequality to determine the interval of sampling period is first-order not third-order.

The rest of this paper is summarized as follows. Some important preliminaries are given in Section II. The main results are derived and presented in Section III. In Section IV, several simulation examples are given to verify the theoretical results. At last, a short conclusion is drawn in Section V.

Notations: Throughout this paper, \mathbb{R} and \mathbb{N} are real and natural numbers, respectively. Suppose that \mathbb{R}^n and $\mathbb{R}^{n \times n}$ are

the n -dimensional real vector space and $n \times n$ real matrix, respectively. \mathbb{N}_+ represents the positive integer. A^T represents the transpose of matrix A . $\lambda_i(A)$ represents the i th eigenvalue of matrix A . \otimes is the Kronecker product. For a vector s , $\|s\|$ denotes its Euclidean norm. For a complex number z , $\|z\|$ represents its modulus, and $\Re(z)$ and $\Im(z)$ denote its real part and imaginary part, respectively.

II. PRELIMINARIES

Next, some significant preliminaries about algebraic graph theory, useful lemmas, and model formulation are introduced.

A. Graph Theory and Useful Lemmas

Assume that $\mathcal{G} = (\mathcal{V}, \mathcal{E}, \mathcal{A})$ is a digraph of N agents with a set of nodes $\mathcal{V} = \{v_1, \dots, v_N\}$, a set of directed edges $\mathcal{E} \subseteq \mathcal{V} \times \mathcal{V}$, and the adjacency matrix $\mathcal{A} = [a_{ij}] \in \mathbb{R}^{N \times N}$ drawing the communication topology of agents. In network \mathcal{G} , an edge e_{ij} is described as $e_{ij} = (v_i, v_j)$, meaning the i th agent can get information from the j th agent. If $e_{ij} \in \mathcal{E}$, $a_{ij} > 0$, else $a_{ij} = 0$. Furthermore, for all $i = 1, \dots, N$, suppose that $a_{ii} = 0$. While for an undirected topology, apparently $a_{ij} = a_{ji}$. The Laplacian matrix of the graph \mathcal{G} is defined as $\mathcal{L} = [l_{ij}] \in \mathbb{R}^{N \times N}$ with $l_{ij} = -a_{ij}$, $i \neq j$, and $l_{ii} = \sum_{j \in N_i} a_{ij}$, $i = j$, which satisfies that $\sum_{j \in N_i} l_{ij} = 0$. If there is a path among any pair of dissimilar nodes, a connected undirected graph is obtained, which means they can communicate with each other. A connected subgraph without loops is called a tree. A directed spanning tree is defined if a directed tree contains all the nodes in \mathcal{G} .

Lemma 1 [1]: A Laplacian matrix \mathcal{L} has a simple eigenvalue 0, and all the other eigenvalues are positive if and only if the undirected network is connected. A Laplacian matrix \mathcal{L} has a simple eigenvalue 0, and all the real parts of the other eigenvalues are positive if and only if the directed network has a directed spanning tree.

Lemma 2 [32]: Given a complex coefficient polynomial of order two as follows:

$$g(s) = s^2 + (\xi_1 + \mathbf{i}\gamma_1)s + \xi_0 + \mathbf{i}\gamma_0$$

where ξ_1 , γ_1 , ξ_0 , and γ_0 are real constants. And then $g(s)$ is stable if and only if $\xi_1 > 0$ and $\xi_1\gamma_1\gamma_0 + \xi_1^2\xi_0 - \gamma_0^2 > 0$.

Lemma 3 [1]: For an undirected graph, \mathcal{L} is a symmetric matrix with real eigenvalues; i.e., the eigenvalues of \mathcal{L} satisfy $\Im(\mu) = 0$, $\Re(\mu) = \mu$.

B. Formulation

Assume a multiagent system consisting of N agents. The second-order dynamic of each agent i is defined as

$$\begin{aligned} \dot{x}_i(t) &= v_i(t) \\ \dot{v}_i(t) &= u_i(t), i \in \mathcal{V} \end{aligned} \quad (1)$$

where $x_i(t) \in \mathbb{R}^n$, $v_i(t) \in \mathbb{R}^n$, and $u_i(t) \in \mathbb{R}^n$ represent the position, velocity states of agent i , and control input, respectively. For simplicity, the case $n = 1$ is studied. But when $n > 1$, more conclusions can be introduced by utilizing the Kronecker product.

Definition 1: If for any $i, j \in \mathcal{V}$ and for any initial states

$$\begin{aligned} \lim_{t \rightarrow \infty} \|x_i(t) - x_j(t)\| &= 0 \\ \lim_{t \rightarrow \infty} \|v_i(t) - v_j(t)\| &= 0 \end{aligned}$$

it is said to be the second-order consensus.

Two novel consensus protocols are introduced as follows, which not only can reduce the operating time and the update rates of conditioners for individuals but also can respond effectively to the case of missing velocity information:

$$u_i(t) = \begin{cases} \alpha \sum_{j=1}^N a_{ij}(x_j(t_k) - x_i(t_k)) \\ - \beta \sum_{j=1}^N a_{ij}(x_j(t_k - hT) - x_i(t_k - hT)) \\ t \in [t_k, t_k + \theta) \\ 0, t \in [t_k + \theta, t_{k+1}), h \in \mathbb{N}_+, k \in \mathbb{N}, i \in \mathcal{V} \end{cases} \quad (2)$$

and

$$u_i(t) = \begin{cases} \alpha \sum_{j=1}^N a_{ij}(x_j(t_k) - x_i(t_k)) \\ - \beta \sum_{j=1}^N a_{ij}(x_j(t_k - \tau) - x_i(t_k - \tau)) \\ t \in [t_k, t_k + \theta) \\ 0, t \in [t_k + \theta, t_{k+1}), k \in \mathbb{N}, i \in \mathcal{V} \end{cases} \quad (3)$$

where $t_k, k \in \mathbb{N}$, are the sampling instants, T is the sampling period, α and β are the coupling gains, h is the out-dated degree of the past data, τ is the time delay, and θ is the communication width. For simplicity, let $t_{k+1} - t_k = T, 0 < \tau < T, 0 < \theta < T$.

Remark 1: What deserves our attention is that protocol (2) is designed via intermittent communication control with the communication width θ , and based on the causal sampled position data $x_i(t_k)$ and $x_i(t_k - hT), i \in \mathcal{V}$. However, protocol (3) is devised via intermittent communication control by using only $x_i(t_k)$ and by the help of time delay. These two strategies improve the main results in [28] and [31] by utilizing only sampled position data control with intermittent communication so that the good points of sampled position data control can be maintained, but also the operating time of conditioners for every individual can be decreased.

III. MAIN RESULTS

A. Consensus With Cooperative Protocol (2)

In this section, some conditions about how to reach the second-order consensus in protocol (2) are provided when $h = 1$. So system (1) is obtained

$$\begin{aligned} \dot{x}_i(t) &= v_i(t) \\ \dot{v}_i(t) &= \begin{cases} -\alpha \sum_{j=1}^N l_{ij}x_j(t_k) \\ + \beta \sum_{j=1}^N l_{ij}x_j(t_{k-1}), & t \in [t_k, t_k + \theta) \\ 0, t \in [t_k + \theta, t_{k+1}), & k \in \mathbb{N}, i \in \mathcal{V}. \end{cases} \end{aligned} \quad (4)$$

Let $\delta_i = (x_i, v_i)^T$, $C = \begin{pmatrix} 0 & 1 \\ 0 & 0 \end{pmatrix}$, and $D = \begin{pmatrix} 0 & 0 \\ 1 & 0 \end{pmatrix}$. Thus, system (4) is cast to

$$\dot{\delta}_i(t) = \begin{cases} C\delta_i(t) - \alpha \sum_{j=1}^N l_{ij}D\delta_i(t_k) \\ + \beta \sum_{j=1}^N l_{ij}D\delta_i(t_{k-1}), & t \in [t_k, t_k + \theta) \\ C\delta_i(t), t \in [t_k + \theta, t_{k+1}), & k \in \mathbb{N}, i \in \mathcal{V}. \end{cases} \quad (5)$$

Let $\delta = (\delta_1^T, \delta_2^T, \dots, \delta_N^T)^T$ and system (5) is transformed to a matrix form

$$\dot{\delta}(t) = \begin{cases} (I_N \otimes C)\delta(t) - \alpha(\mathcal{L} \otimes D)\delta(t_k) \\ + \beta(\mathcal{L} \otimes D)\delta(t_{k-1}), & t \in [t_k, t_k + \theta) \\ (I_N \otimes C)\delta(t), & t \in [t_k + \theta, t_{k+1}), k \in \mathbb{N}. \end{cases} \quad (6)$$

The Jordan form related to \mathcal{L} is defined as \mathcal{J} , i.e., $\mathcal{L} = P\mathcal{J}P^{-1}$, where P is a nonsingular matrix. Let $\zeta(t) = (P^{-1} \otimes I_2)\delta(t)$, and then (6) can be transformed to

$$\dot{\zeta}(t) = \begin{cases} (I_N \otimes C)\zeta(t) - \alpha(\mathcal{J} \otimes D)\zeta(t_k) \\ + \beta(\mathcal{J} \otimes D)\zeta(t_{k-1}), & t \in [t_k, t_k + \theta) \\ (I_N \otimes C)\zeta(t), t \in [t_k + \theta, t_{k+1}), & k \in \mathbb{N}. \end{cases} \quad (7)$$

When the graph \mathcal{G} is undirected, \mathcal{J} is a diagonal matrix having real diagonal elements, which are the eigenvalues of \mathcal{L} . However, for directed graphs \mathcal{G} , some of the eigenvalues of \mathcal{L} may be complex and $\mathcal{J} = \text{diag}(\mathcal{J}_1, \mathcal{J}_2, \dots, \mathcal{J}_r)$, where \mathcal{J}_d are Jordan blocks as follows:

$$\mathcal{J}_d = \begin{pmatrix} \mu_d & 0 & 0 & 0 \\ 1 & \ddots & 0 & 0 \\ 0 & \ddots & \ddots & 0 \\ 0 & 0 & 1 & \mu_d \end{pmatrix}_{N_d \times N_d}$$

in which μ_d are the eigenvalues of the \mathcal{L} , with multiplicity $N_d, d = 1, 2, \dots, r$ and $N_1 + N_2 + \dots + N_r = N$.

Before continuing, the following assumptions and lemma are presented.

Assumption 1: The graph \mathcal{G} contains a directed spanning tree.

Assumption 2: The graph \mathcal{G} is undirected and connected.

Lemma 4: Suppose that Assumption 1 is established. In the aforementioned system, the consensus can be reached if $\lim_{t \rightarrow \infty} \|\zeta_i(t)\| = 0, i = 1, 2, \dots, N$, in (7).

Proof: This can be demonstrated in a similar way in [11]. ■

Corollary 1: Suppose that Assumption 1 is established. The aforementioned system can reach the consensus if the following $N - 1$ systems are asymptotically stable:

$$\begin{aligned} \dot{w}_i(t) &= Cw_i(t) - \alpha\mu_i y(t)Dw_i(t_k) + \beta\mu_i y(t)Dw_i(t_{k-1}) \\ t &\in [t_k, t_{k+1}) \end{aligned} \quad (8)$$

where $i \in \mathcal{V}$, μ_i is a nonzero eigenvalue of \mathcal{L} , and

$$y(t) = \begin{cases} 1, & t \in [t_k, t_k + \theta) \\ 0, & t \in [t_k + \theta, t_{k+1}), k \in \mathbb{N}. \end{cases} \quad (9)$$

Proof (Necessity): From Lemma 4, we can obtain $\lim_{t \rightarrow \infty} \|\zeta_i(t)\| = 0, i = 1, 2, \dots, N$, in (7). For $t \in [t_k, t_k + \theta)$ and $t \in [t_k + \theta, t_{k+1})$, since the variables in the $N - 1$ systems (8) are the first term of each Jordan block in system (7), it is obvious to obtain that $\lim_{t \rightarrow \infty} \|w_i(t)\| = 0$, which indicates that the system (8) is asymptotically stable.

(Sufficiency): It is easy to see that if the $N - 1$ systems (12) are asymptotically stable, then $\lim_{t \rightarrow \infty} \|w_i(t)\| = 0, i = 1, 2, \dots, N$, in (8). From the properties of the Jordan form, the asymptotical behavior in system (7) is dominated

by the diagonal terms, therefore we can easily conclude that $\lim_{t \rightarrow \infty} \|\zeta_i(t)\| = 0$, $i = 1, 2, \dots, N$, in (7) and the conclusion follows. ■

The following theorem is obtained for reaching consensus, revealing how internal parameters of the system impact on consensus behavior.

Theorem 1: Under Assumption 1, system (1) with protocol (2) can reach the consensus if and only if

$$T > \max \left\{ \theta, \frac{\alpha - \beta}{2\beta} \cdot \theta \right\}, \quad \beta(\alpha - \beta) > 0 \quad (10)$$

and

$$c_{i1}T^3 + c_{i2}T^2 + c_{i3}T + c_{i4} > 0, \quad i = 1, 2, \dots, N \quad (11)$$

with

$$\begin{aligned} c_{i1} &= \frac{-4\beta^2(\alpha + \beta)}{(\alpha - \beta)^3}, \quad c_{i2} = \frac{4\beta(\alpha + 2\beta)}{(\alpha - \beta)^2} \cdot \theta \\ &+ \frac{16\beta^2\Re(\mu_i)}{(\alpha - \beta)^3 \|\mu_i\|^2 \theta} \\ c_{i3} &= \frac{-(\alpha + 5\beta)\theta^2}{\alpha - \beta} - \frac{16\beta\Re(\mu_i)}{(\alpha - \beta)^2 \|\mu_i\|^2} \\ &- \frac{16\Im^2(\mu_i)}{(\alpha - \beta)^2 \|\mu_i\|^4 \theta^2} \end{aligned}$$

and

$$c_{i4} = \theta^3 + \frac{4\Re(\mu_i)}{(\alpha - \beta) \|\mu_i\|^2} \cdot \theta.$$

Proof: From (8), one obtains

$$\begin{aligned} (e^{-Ct}w_i(t))' &= e^{-Ct}(-\alpha\mu_i y(t)Dw_i(t_k) \\ &+ \beta\mu_i y(t)Dw_i(t_{k-1})), \quad t \in [t_k, t_{k+1}). \end{aligned} \quad (12)$$

Integrating both sides of (12) from t_k to t ($t \leq t_k + \theta$) and referring to $e^{-Ct} = \begin{pmatrix} 1 & -t \\ 0 & 1 \end{pmatrix}$, one obtains

$$\begin{aligned} w_i(t) &= e^{C(t-t_k)}w_i(t_k) + e^{Ct} \int_{t_k}^t e^{-Ct}(-\alpha\mu_i Dw_i(t_k) \\ &+ \beta\mu_i Dw_i(t_{k-1}))dt \\ &= \begin{pmatrix} 1 & t-t_k \\ 0 & 1 \end{pmatrix} w_i(t_k) + \begin{pmatrix} 1 & t \\ 0 & 1 \end{pmatrix} \begin{pmatrix} -\frac{1}{2}t^2 + \frac{1}{2}t_k^2 & 0 \\ t-t_k & 0 \end{pmatrix} \\ &\quad \times (-\alpha\mu_i w_i(t_k) + \beta\mu_i w_i(t_{k-1})) \\ &= \begin{pmatrix} 1 & t-t_k \\ 0 & 1 \end{pmatrix} w_i(t_k) + \begin{pmatrix} -\frac{\alpha}{2}\mu_i(t-t_k)^2 & 0 \\ -\alpha\mu_i(t-t_k) & 0 \end{pmatrix} w_i(t_k) \\ &\quad + \begin{pmatrix} -\frac{\beta}{2}\mu_i(t-t_k)^2 & 0 \\ -\beta\mu_i(t-t_k) & 0 \end{pmatrix} w_i(t_{k-1}) \\ &= \begin{pmatrix} 1 - \frac{\alpha}{2}\mu_i(t-t_k)^2 & t-t_k \\ -\alpha\mu_i(t-t_k) & 1 \end{pmatrix} w_i(t_k) \\ &\quad + \begin{pmatrix} \frac{\beta}{2}\mu_i(t-t_k)^2 & 0 \\ \beta\mu_i(t-t_k) & 0 \end{pmatrix} w_i(t_{k-1}). \end{aligned} \quad (13)$$

It can be rewritten as

$$\begin{aligned} w_i(t) &= M_i(t-t_k)w_i(t_k) + N_i(t-t_k)w_i(t_{k-1}) \\ &\quad t \in [t_k, t_k + \theta) \end{aligned} \quad (14)$$

$$\text{with } M_i(t) = \begin{pmatrix} 1 - \frac{\alpha}{2}\mu_i t^2 & t \\ -\alpha\mu_i t & 1 \end{pmatrix} \text{ and } N_i(t) = \begin{pmatrix} \frac{\beta}{2}\mu_i t^2 & 0 \\ \beta\mu_i t & 0 \end{pmatrix}.$$

Therefore, one has

$$\begin{aligned} w_i(t_k + \theta) &= \begin{pmatrix} 1 - \frac{\alpha}{2}\mu_i\theta^2 & \theta \\ -\alpha\mu_i\theta & 1 \end{pmatrix} w_i(t_k) \\ &\quad + \begin{pmatrix} \frac{\beta}{2}\mu_i\theta^2 & 0 \\ \beta\mu_i\theta & 0 \end{pmatrix} w_i(t_{k-1}). \end{aligned} \quad (15)$$

Then, for $t \in [t_k + \theta, t_{k+1})$, one obtains

$$\begin{aligned} w_i(t) &= e^{C(t-(t_k+\theta))}w_i(t_k + \theta) \\ &= \begin{pmatrix} 1 + \alpha\mu_i\theta(\frac{\theta}{2} - (t-t_k)) & t-t_k \\ -\alpha\mu_i\theta & 1 \end{pmatrix} w_i(t_k) \\ &\quad + \begin{pmatrix} -\beta\mu_i\theta(\frac{\theta}{2} - (t-t_k)) & 0 \\ \beta\mu_i\theta & 0 \end{pmatrix} w_i(t_{k-1}) \\ &= M'_i(t-t_k)w_i(t_k) + N'_i(t-t_k)w_i(t_{k-1}) \end{aligned} \quad (16)$$

with

$$\begin{aligned} M'_i(t) &= \begin{pmatrix} 1 + \alpha\mu_i\theta(\frac{\theta}{2} - t) & t \\ -\alpha\mu_i\theta & 1 \end{pmatrix} \\ N'_i(t) &= \begin{pmatrix} -\beta\mu_i\theta(\frac{\theta}{2} - t) & 0 \\ \beta\mu_i\theta & 0 \end{pmatrix}. \end{aligned}$$

Then, we show that the state in (14) and (16) only utilizing past sampled position data is asymptotically stable.

For $t_k \in [t_k + \theta, t_{k+1})$, $k \in \mathbb{N}$, let $t_0 = 0$, by using (16), and it follows that

$$\begin{aligned} w_i(t_k) &= M'_i(T)w_i(t_{k-1}) + N'_i(T)w_i(t_{k-2}) \\ w_i(t_{k-1}) &= M'_i(0)w_i(t_{k-1}) + N'_i(0)w_i(t_{k-2}). \end{aligned}$$

Let $W_i(t) = \begin{pmatrix} M'_i(t) & N'_i(t) \\ M'_i(t-T) & N'_i(t-T) \end{pmatrix}$ and $\varepsilon_i(t) = (w_i^T(t), w_i^T(t-T))^T$. One obtains

$$\varepsilon_i(t) = H_i \varepsilon_i(t_k - T) = H_i \varepsilon_i(t_{k-1}) = H_i W_i^{k-1}(T) \varepsilon_i(t_0)$$

with $H_i = \begin{pmatrix} H_{i1} & H_{i2} \\ H_{i3} & H_{i4} \end{pmatrix}$, in which $H_{i1} = M'_i(t-t_k)M'_i(T) + N'_i(t-t_k)$, $H_{i1} = M'_i(t-t_k)N'_i(T)$, $H_{i3} = M'_i(t-t_k)$, $H_{i4} = N'_i(t-t_k)$. Similarly, when $t_k \in [t_k, t_k + \theta)$, using the same method, one has

$$\varepsilon_i(t) = Q_i \varepsilon_i(t_k - T) = Q_i \varepsilon_i(t_{k-1}) = Q_i W_i^{k-1}(T) \varepsilon_i(t_0)$$

with $Q_i = \begin{pmatrix} Q_{i1} & Q_{i2} \\ Q_{i3} & Q_{i4} \end{pmatrix}$, in which $Q_{i1} = M_i(t-t_k)M_i(t) + N_i(t-t_k)$, $Q_{i2} = M_i(t-t_k)N_i(T)$, $Q_{i3} = M_i(t-t_k)$, $Q_{i4} = N_i(t-t_k)$. Combining the above two results, one has

$$\varepsilon_i(t) = \begin{cases} Q_i W_i^{k-1}(T) \varepsilon_i(t_0), & t \in [t_k, t_k + \theta) \\ H_i W_i^{k-1}(T) \varepsilon_i(t_0), & t \in [t_k + \theta, t_{k+1}), k \in \mathbb{N}. \end{cases} \quad (17)$$

It is easy to see that $w_i(t) \rightarrow 0$ if $\varepsilon_i(t) \rightarrow 0$. Since Q_i and H_i are delimited when $t \in [t_k, t_k + \theta)$ and $t \in [t_k + \theta, t_{k+1})$, $\varepsilon_i(t) \rightarrow 0$ as long as the amplitudes of all eigenvalues of $W_i(T)$ are less than 1. Let $|\lambda J_4 - W_i(T)| = 0$. It yields

$$\lambda^4 + a_1 \lambda^3 + a_0 \lambda^2 = 0 \quad (18)$$

where $a_1 = -2 - \alpha\mu_i\theta^2/2 + \beta\mu_i\theta^2/2 + \alpha\mu_i\theta T$ and $a_0 = 1 + \alpha\mu_i\theta^2/2 - \beta\mu_i\theta^2/2 - \beta\mu_i\theta T$. Note that $W_i(T)$ has two

eigenvalues $\lambda_1 = \lambda_2 = 0$. Let $\lambda = (s + 1/s - 1)$ in (18), and one obtains

$$(1 + a_1 + a_0)s^2 + (2 - 2a_0)s + 1 - a_1 + a_0 = 0 \quad (19)$$

with $1 + a_1 + a_0 = (\alpha\mu_i\theta - \beta\mu_i\theta)T$, $2 - 2a_0 = -\alpha\mu_i\theta^2 + \beta\mu_i\theta^2 + 2\beta\mu_i\theta T$, $1 - a_1 + a_0 = 4 + \alpha\mu_i\theta^2 - \beta\mu_i\theta^2 - (\alpha\mu_i\theta + \beta\mu_i\theta)T$. Then, one has

$$s^2 + \left(-\frac{\theta}{T} + \frac{2\beta}{\alpha - \beta}\right)s + \frac{4}{(\alpha - \beta)\mu_i\theta T} + \frac{\theta}{T} - \frac{\alpha + \beta}{\alpha - \beta} = 0. \quad (20)$$

To make $\|\lambda\| < 1$ in (18), as long as $\Re(s) < 0$ in (20) is established. Therefore, when all real parts of roots in (20) are negative, $w_i(t) \rightarrow 0$ can be obtained. According to Lemma 2, (20) is stable if and only if

$$-\frac{\theta}{T} + \frac{2\beta}{\alpha - \beta} > 0 \quad (21)$$

and

$$\left(-\frac{\theta}{T} + \frac{2\beta}{\alpha - \beta}\right)^2 \left(\frac{\theta}{T} - \frac{\alpha + \beta}{\alpha - \beta} + \frac{4\Re(\mu_i)}{(\alpha - \beta)\|\mu_i\|^2\theta T}\right) - \frac{16\Im^2(\mu_i)}{(\alpha - \beta)^2\|\mu_i\|^4\theta^2 T^2} > 0. \quad (22)$$

So one can easily get (10) and (11) from the above two inequalities. According to the aforementioned analysis, that the conditions (10) and (11) are satisfied means $w_i(t) \rightarrow 0$, i.e., system (1) under protocol (2) can reach consensus. This proof is completed. ■

Remark 2: From Theorem 1, (10) and (11) both contain the sampling period T , the coupling gains α , β , and the communication width θ . So it is hard to choose α only by using β or β only by using α . Therefore, one can identify a general range of α and β at first by satisfying $\beta(\alpha - \beta) > 0$, then give a suitable θ and calculate the appropriate range of T according to Theorem 1, or give a suitable T and then calculate the appropriate range of θ based on Theorem 1. The benefit of doing this is that when the other three parameters are determined first, by the two inequality conditions of Theorem 1, we can determine the range of values for the remaining parameter and then select the most friendly value in the range to apply to the system in order to reach the consensus. The choice of the corresponding value is in the range and can be modified to get the most suitable value.

Remark 3: According to Remark 2, one can choose α , β , and θ first, and then obtain the right interval of T by using the results (10) and (11). To do so, let $f_i(T) = c_{i1}T^3 + c_{i2}T^2 + c_{i3}T + c_{i4}$, $\mathbb{U}_i = \{T | f_i(T) > 0\}$, and $\mathbb{U} = \bigcap_{i=2}^N \mathbb{U}_i$. So the mission is to solve \mathbb{U} . For the reason that $f_i(T) = 0$ has three real roots generally, it is simple to solve \mathbb{U}_i . Hence, based on (10) and (11), the sampling period T satisfying $T \in \mathbb{U} \cap (\max\{\theta, (\alpha - \beta/2\beta) \cdot \theta\}, \infty)$ can guarantee to achieve the consensus. For an undirected graph, an oversimplified corollary is obtained as follows.

Corollary 2: Under Assumption 2, this system can reach the consensus if

$$T > \frac{(\alpha - \beta) \cdot \theta}{2\beta}, \alpha\beta - \beta^2 > 0 \quad (23)$$

and

$$\theta < T < \frac{\alpha - \beta}{\alpha + \beta} \cdot \theta + \frac{4}{(\alpha + \beta)\mu_N\theta} \quad (24)$$

with μ_N being the maximum eigenvalue of \mathcal{L} .

Proof: Under Lemma 3, all eigenvalues of \mathcal{L} of the undirected graph are real, i.e., $\Im(\mu_i) = 0$ and $\Re(\mu_i) = \mu_i$ for $i = 2, \dots, N$. Then (22) is equal to

$$\left(-\frac{\theta}{T} + \frac{2\beta}{\alpha - \beta}\right)^2 \left(\frac{\theta}{T} - \frac{\alpha + \beta}{\alpha - \beta} + \frac{4}{(\alpha - \beta)\mu_i\theta T}\right) > 0 \quad i = 2, \dots, N. \quad (25)$$

Thus, for an undirected graph, the consensus can be reached if conditions (23) and (24) hold. ■

Remark 4: Though one can choose the sampling period appropriately from Theorem 1 and Remark 3, and how to choose the communication width θ under the given α , β , and T remains unknown. From (22), one has $\theta^5 + d_{i1}\theta^4 + d_{i2}\theta^3 + d_{i3}\theta^2 + d_{i4}\theta + d_{i5} > 0$, $i = 1, 2, \dots, N$, with

$$\begin{aligned} d_{i1} &= \frac{-(\alpha + 5\beta)T}{\alpha - \beta}, d_{i2} = \frac{4\beta(\alpha + 2\beta)T^2}{(\alpha - \beta)^2} + \frac{4\Re(\mu_i)}{(\alpha - \beta)\|\mu_i\|^2} \\ d_{i3} &= \frac{-4\beta^2T^3(\alpha + \beta)}{(\alpha - \beta)^3} - \frac{16\beta\Re(\mu_i)T}{(\alpha - \beta)^2\|\mu_i\|^2} \\ d_{i4} &= \frac{16\beta^2\Re(\mu_i)T^2}{(\alpha - \beta)^3\|\mu_i\|^2}, d_{i5} = -\frac{16\Im^2(\mu_i)T}{(\alpha - \beta)^2\|\mu_i\|^4}. \end{aligned}$$

Let $g_i(\theta) = \theta^5 + d_{i1}\theta^4 + d_{i2}\theta^3 + d_{i3}\theta^2 + d_{i4}\theta + d_{i5}$, $\mathbb{S}_i = \{\theta | g_i(\theta) > 0\}$, and $\mathbb{S} = \bigcap_{i=2}^N \mathbb{S}_i$. Hence, the mission is to solve \mathbb{S} . Then based on (10), the communication width θ satisfying $\theta \in \mathbb{S} \cap (0, \min\{T, (2\beta/\alpha - \beta) \cdot T\})$ can guarantee to achieve the consensus. For an undirected graph, an oversimplified corollary can be obtained as follows.

Corollary 3: Under Assumption 2, this system can reach the consensus if

$$0 < \theta < \min\left\{T, \frac{2\beta}{\alpha - \beta} \cdot T\right\}, \beta(\alpha - \beta) > 0 \quad (26)$$

and

$$\theta^2 - \frac{(\alpha + \beta)T}{\alpha - \beta} \cdot \theta + \frac{4}{(\alpha - \beta)\mu_i} > 0. \quad (27)$$

Proof: This can be demonstrated in a similar way in Corollary 2. ■

Remark 5: From (22), one has $h(\alpha, \beta, T, \theta, \mu_i) = (-\theta/T + (2\beta/\alpha - \beta))^2((\theta/T) - (\alpha + \beta/\alpha - \beta) + [4\Re(\mu_i)/((\alpha - \beta)\|\mu_i\|^2\theta T)]) - [(16\Im^2(\mu_i))/((\alpha - \beta)^2\|\mu_i\|^4\theta^2 T^2)] > 0$. Find a stable consensus region [33] as $\mathbb{V}_i = \{\mu_i | h(\alpha, \beta, T, \theta, \mu_i) > 0\}$, and $\mathbb{V} = \bigcap_{i=2}^N \mathbb{V}_i$. So the mission is changed to find whether all the nonzero eigenvalues $\mu_i (i = 2, \dots, N)$ are in the stable consensus region \mathbb{V} . Under Assumption 1, the consensus can be reached if (10) holds and $\mu_i \in \mathbb{V}$ for all $i = 2, \dots, N$.

Remark 6: For $h > 1$, a similar result can be developed. Taking $h = 2$ as an example, we have $\varepsilon_i(t) = (z_i^T(t), z_i^T(t - T), z_i^T(t - 2T))^T$ and for $t_k \in [t_k + \theta, t_{k+1})$, and one obtains $\varepsilon_i(t) = H_i^* \varepsilon_i(t_k - 2T) = H_i^* \varepsilon_i(t_{k-2}) = H_i^* \hat{W}_i^{k-2}(T) \varepsilon_i(t_0)$, where $\hat{W}_i^k(T) = [\hat{W}_{ij}^k]$ with $\hat{W}_{11}^k = [M_i^k(T)]^2$, $\hat{W}_{12}^k = \hat{W}_{23}^k =$

$N'_i(T)$, $\hat{W}_{13}^i = M'_i(T)N'_i(T)$, $\hat{W}_{21}^i = M'_i(T)$, $\hat{W}_{31}^i = M'_i(0)$, and the rest are zeros. Similarly, when $t_k \in [t_k, t_k + \theta)$, using the same method, one has $\varepsilon_i(t) = \mathcal{S}_i^* \varepsilon_i(t_k - 2T) = \mathcal{S}_i^* \varepsilon_i(t_{k-2}) = \mathcal{S}_i^* \hat{W}_i^{k-2}(T) \varepsilon_i(t_0)$. Combining the above two results, one has

$$\varepsilon_i(t) = \begin{cases} \mathcal{S}_i^* \hat{W}_i^{k-2}(T) \varepsilon_i(t_0), & t \in [t_k, t_k + \theta) \\ H_i^* \hat{W}_i^{k-2}(T) \varepsilon_i(t_0), & t \in [t_k + \theta, t_{k+1}), k \in \mathbb{N}. \end{cases}$$

It is obvious to see that S_i^* and H_i^* are all determined by $M'_i(T)$, $N'_i(T)$, $M'_i(t - t_k)$, and $N'_i(t - t_k)$; therefore, they are bounded when $t \in [t_k, t_k + \theta)$ and $t \in [t_k + \theta, t_{k+1})$. Then, one can also analyze the eigenvalues of $\hat{W}_i(T)$ to obtain the corresponding conditions for reaching the consensus.

B. Consensus With Cooperative Protocol (3)

Obviously, the time delay always existing in practical applications cannot be ignored. Under the distributed protocol (3) considering the time delay, one obtains

$$\dot{\delta}(t) = \begin{cases} (I_N \otimes C)\delta(t) - \alpha(\mathcal{L} \otimes D)\delta(t_k) \\ + \beta(\mathcal{L} \otimes D)\delta(t_k - \tau), & t \in [t_k, t_k + \theta) \\ (I_N \otimes C)\delta(t), & t \in [t_k + \theta, t_{k+1}), k \in \mathbb{N}. \end{cases} \quad (28)$$

The Jordan form related to the Laplacian matrix \mathcal{L} is defined as \mathcal{J} , i.e., $\mathcal{L} = P\mathcal{J}P^{-1}$, where P is as defined previously. Let $\zeta(t) = (P^{-1} \otimes I_2)\delta(t)$, and then (28) can be transformed to

$$\dot{\zeta}(t) = \begin{cases} (I_N \otimes C)\zeta(t) - \alpha(\mathcal{J} \otimes D)\zeta(t_k) \\ + \beta(\mathcal{J} \otimes D)\zeta(t_k - \tau), & t \in [t_k, t_k + \theta) \\ (I_N \otimes C)\zeta(t), & t \in [t_k + \theta, t_{k+1}), k \in \mathbb{N}. \end{cases} \quad (29)$$

Through similar calculations, in this case, the corresponding Lemma 4 and Corollary 1 can be obtained. It follows that:

$$\dot{w}_i(t) = Cw_i(t) - \alpha\mu_i y(t)Dw_i(t_k) + \beta\mu_i y(t)Dw_i(t_k - \tau) \quad t \in [t_k, t_{k+1}) \quad (30)$$

where $i \in \mathcal{V}$, μ_i is a nonzero eigenvalue of \mathcal{L} , and

$$y(t) = \begin{cases} 1, & t \in [t_k, t_k + \theta) \\ 0, & t \in [t_k + \theta, t_{k+1}), k \in \mathbb{N}. \end{cases} \quad (31)$$

Furthermore, the conditions are established as follows.

Theorem 2: Under Assumption 1, system (1) with protocol (3) can reach the consensus if and only if

$$0 < \theta < \frac{2\beta}{\alpha - \beta} \cdot \tau \quad (32)$$

and

$$\left[\left(\frac{2\beta\tau}{\alpha - \beta} - \theta \right)^2 + \frac{16\Im^2(\mu_i)}{(\alpha - \beta)^2 \|\mu_i\|^4 \theta^2} \right] \cdot T < \frac{4\Re(\mu_i) \left(\frac{2\beta\tau}{\alpha - \beta} - \theta \right)^2}{(\alpha - \beta) \|\mu_i\|^2 \theta} - \left(\frac{2\beta\tau}{\alpha - \beta} - \theta \right)^3. \quad (33)$$

Proof: From (30), one has

$$\left(e^{-Ct} w_i(t) \right)' = e^{-Ct} (-\alpha\mu_i y(t)Dw_i(t_k) + \beta\mu_i y(t)Dw_i(t_k - \tau)) \quad t \in [t_k, t_{k+1}), i = 2, \dots, N. \quad (34)$$

Then according to the aforementioned analysis, one obtains

$$w_i(t) = \begin{cases} M_i(t - t_k)w_i(t_k) + N_i(t - t_k)w_i(t_k - \tau) \\ t \in [t_k, t_k + \theta) \\ M'_i(t - t_k)w_i(t_k) + N'_i(t - t_k)w_i(t_k - \tau) \\ t \in [t_k + \theta, t_{k+1}). \end{cases} \quad (35)$$

Considering the relationship between various parameters regarding time. The following cases are discussed.

Case 1: $0 < \tau < \min\{\theta, T - \theta\}$.

For $t \in [t_k, t_k + \tau)$

$$\begin{aligned} w_i(t) &= M_i(t - t_k)w_i(t_k) + N_i(t - t_k)w_i(t_k - \tau), \\ w_i(t - \tau) &= M'_i(t - t_{k-1} - \tau)w_i(t_{k-1}) \\ &\quad + N'_i(t - t_{k-1} - \tau)w_i(t_{k-1} - \tau). \end{aligned}$$

For $t \in [t_k + \tau, t_k + \theta)$

$$\begin{aligned} w_i(t) &= M_i(t - t_k)w_i(t_k) + N_i(t - t_k)w_i(t_k - \tau) \\ w_i(t - \tau) &= M_i(t - t_k - \tau)w_i(t_k) \\ &\quad + N_i(t - t_k - \tau)w_i(t_k - \tau). \end{aligned}$$

For $t \in [t_k + \theta, t_k + \theta + \tau)$

$$\begin{aligned} w_i(t) &= M'_i(t - t_k)w_i(t_k) + N'_i(t - t_k)w_i(t_k - \tau) \\ w_i(t - \tau) &= M_i(t - t_k - \tau)w_i(t_k) \\ &\quad + N_i(t - t_k - \tau)w_i(t_k - \tau). \end{aligned}$$

For $t \in [t_k + \theta + \tau, t_{k+1})$

$$\begin{aligned} w_i(t) &= M'_i(t - t_k)w_i(t_k) + N'_i(t - t_k)w_i(t_k - \tau) \\ w_i(t - \tau) &= M'_i(t - t_k - \tau)w_i(t_k) \\ &\quad + N'_i(t - t_k - \tau)w_i(t_k - \tau). \end{aligned}$$

Then

$$\begin{aligned} w_i(t_{k+1}) &= M'_i(T)w_i(t_k) + N'_i(T)w_i(t_k - \tau) \\ w_i(t_{k+1} - \tau) &= M'_i(T - \tau)w_i(t_k) \\ &\quad + N'_i(T - \tau)w_i(t_k - \tau). \end{aligned}$$

Let $\varepsilon_i(t) = (w_i^T(t), w_i^T(t - \tau))^T$, $\vartheta = t - t_k$, and one has the following.

For $t \in [t_k, t_k + \tau)$

$$\varepsilon_i(t) = M_{i0}(\vartheta)\varepsilon_i(t_{k-1}) = M_{i0}(\vartheta)M_{i3}^{k-1}(T)\varepsilon_i(t_0).$$

For $t \in [t_k + \tau, t_k + \theta)$

$$\varepsilon_i(t) = M_{i1}(\vartheta)\varepsilon_i(t_k) = M_{i1}(\vartheta)M_{i3}^k(T)\varepsilon_i(t_0).$$

For $t \in [t_k + \theta, t_k + \theta + \tau)$

$$\varepsilon_i(t) = M_{i2}(\vartheta)\varepsilon_i(t_k) = M_{i2}(\vartheta)M_{i3}^k(T)\varepsilon_i(t_0).$$

For $t \in [t_k + \theta + \tau, t_{k+1})$

$$\varepsilon_i(t) = M_{i3}(\vartheta)\varepsilon_i(t_k) = M_{i3}(\vartheta)M_{i3}^k(T)\varepsilon_i(t_0)$$

where $M_{i0}(t) = \begin{pmatrix} S_{i1} & T_{i1} \\ M'_i(t+T-\tau) & N'_i(t+T-\tau) \end{pmatrix}$ with $S_{i1} = M_i(t)M_i(t) + N_i(t)M'_i(T - \tau)$, $T_{i1} = M_i(t)N_i(T) + N_i(t)N'_i(T - \tau)$, $M_{i1}(t) = \begin{pmatrix} M_i(t) & N_i(t) \\ M_i(t-\tau) & N_i(t-\tau) \end{pmatrix}$, $M_{i2}(t) = \begin{pmatrix} M'_i(t) & N'_i(t) \\ M'_i(t-\tau) & N'_i(t-\tau) \end{pmatrix}$, $M_{i3}(t) = \begin{pmatrix} M'_i(t) & N'_i(t) \\ M'_i(t-\tau) & N'_i(t-\tau) \end{pmatrix}$.
Case 2: $T - \theta \leq \tau < \theta$ ($\theta > (T/2)$).

Similarly, one has the following.

For $t \in [t_k, t_{k-1} + \theta + \tau)$

$$\varepsilon_i(t) = M_{i4}(\vartheta)\varepsilon_i(t_{k-1}) = M_{i4}(\vartheta)M_{i3}^{k-1}(T)\varepsilon_i(t_0).$$

For $t \in [t_{k-1} + \theta + \tau, t_k + \tau)$

$$\varepsilon_i(t) = M_{i0}(\vartheta)\varepsilon_i(t_{k-1}) = M_{i0}(\vartheta)M_{i3}^{k-1}(T)\varepsilon_i(t_0).$$

For $t \in [t_k + \tau, t_k + \theta)$

$$\varepsilon_i(t) = M_{i1}(\vartheta)\varepsilon_i(t_k) = M_{i1}(\vartheta)M_{i3}^k(T)\varepsilon_i(t_0).$$

For $t \in [t_k + \theta, t_{k+1})$

$$\varepsilon_i(t) = M_{i3}(\vartheta)\varepsilon_i(t_k) = M_{i3}(\vartheta)M_{i3}^k(T)\varepsilon_i(t_0)$$

where $M_{i4}(t) = \begin{pmatrix} S_{i2} & T_{i2} \\ M'_i(t+T-\tau) & N'_i(t+T-\tau) \end{pmatrix}$ with $S_{i2} = M'_i(t)M_i(t) + N'_i(t)M_i(T-\tau)$, $T_{i2} = M'_i(t)N_i(T) + N'_i(t)N_i(T-\tau)$.
Case 3: $\theta < \tau < T - \theta$ ($\theta < T/2$).

Similarly, one has the following.

For $t \in [t_k, t_k + \theta)$

$$\varepsilon_i(t) = M_{i0}(\vartheta)\varepsilon_i(t_{k-1}) = M_{i0}(\vartheta)M_{i3}^{k-1}(T)\varepsilon_i(t_0).$$

For $t \in [t_k + \theta, t_k + \tau)$

$$\varepsilon_i(t) = M_{i5}(\vartheta)\varepsilon_i(t_{k-1}) = M_{i5}(\vartheta)M_{i3}^{k-1}(T)\varepsilon_i(t_0).$$

For $t \in [t_k + \tau, t_k + \theta + \tau)$

$$\varepsilon_i(t) = M_{i2}(\vartheta)\varepsilon_i(t_k) = M_{i2}(\vartheta)M_{i3}^k(T)\varepsilon_i(t_0).$$

For $t \in [t_k + \theta + \tau, t_{k+1})$

$$\varepsilon_i(t) = M_{i3}(\vartheta)\varepsilon_i(t_k) = M_{i3}(\vartheta)M_{i3}^k(T)\varepsilon_i(t_0)$$

where $M_{i5}(t) = \begin{pmatrix} S_{i3} & T_{i3} \\ M'_i(t+T-\tau) & N'_i(t+T-\tau) \end{pmatrix}$ with $S_{i3} = M'_i(t)M'_i(T) + N'_i(t)M'_i(T-\tau)$, $T_{i3} = M'_i(t)N'_i(T) + N'_i(t)N'_i(T-\tau)$.

Case 4: $\tau > \max\{\theta, T - \theta\}$.

Similarly, one has the following.

For $t \in [t_k, t_{k-1} + \theta + \tau)$

$$\varepsilon_i(t) = M_{i4}(\vartheta)\varepsilon_i(t_{k-1}) = M_{i4}(\vartheta)M_{i3}^{k-1}(T)\varepsilon_i(t_0).$$

For $t \in [t_{k-1} + \theta + \tau, t_k + \theta)$

$$\varepsilon_i(t) = M_{i0}(\vartheta)\varepsilon_i(t_{k-1}) = M_{i0}(\vartheta)M_{i3}^{k-1}(T)\varepsilon_i(t_0).$$

For $t \in [t_k + \tau, t_k + \theta + \tau)$

$$\varepsilon_i(t) = M_{i2}(\vartheta)\varepsilon_i(t_k) = M_{i2}(\vartheta)M_{i3}^k(T)\varepsilon_i(t_0).$$

For $t \in [t_k + \theta + \tau, t_{k+1})$

$$\varepsilon_i(t) = M_{i3}(\vartheta)\varepsilon_i(t_k) = M_{i3}(\vartheta)M_{i3}^k(T)\varepsilon_i(t_0).$$

According to cases 1–4 and the previous analysis, since $M_{ij}(\vartheta)$ are bounded when $t \in [t_k, t_k + \theta)$ and $t \in [t_k + \theta, t_{k+1})$ for all $i = 2, \dots, N$ and $j = 0, 1, 2, 3, 4, 5$, we can draw that $w_i(t) \rightarrow 0$ if $\varepsilon_i(t) \rightarrow 0$. So one can obtain the conclusion that $w_i(t) \rightarrow 0$ if and only if all eigenvalues of $M_{i3}(T)$ satisfy $\|\lambda\| < 1$. Let $|\lambda I_4 - M_{i3}(T)| = 0$. It yields

$$\lambda^4 + a_1\lambda^3 + a_0\lambda^2 = 0 \quad (36)$$

where $a_1 = -2 - \alpha\mu_i\theta^2/2 + \beta\mu_i\theta^2/2 + \alpha\mu_i\theta T - \beta\mu_i\theta T + \beta\mu_i\theta\tau$ and $a_0 = 1 + \alpha\mu_i\theta^2/2 - \beta\mu_i\theta^2/2 -$

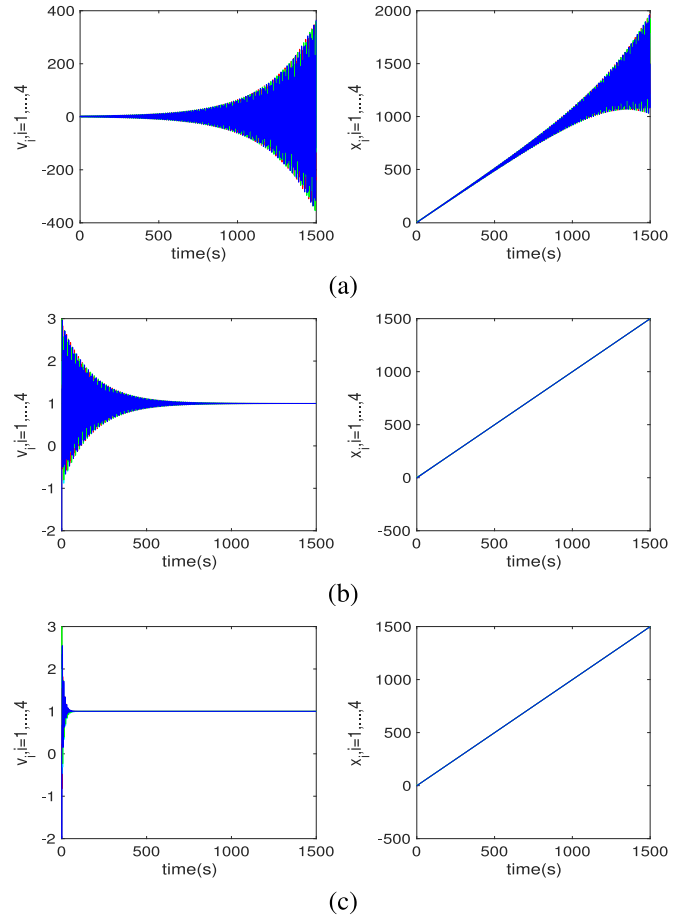


Fig. 1. Velocity and position states of agents when $\theta = 0.5$, where (a) $T = 2.15$, (b) $T = 2.1$, and (c) $T = 0.8$.

$\beta\mu_i\theta\tau$. Note that $W_i(T)$ has two eigenvalues $\lambda_1 = \lambda_2 = 0$. Then the following proof can be completed with Lemma 2, which is similar to Theorem 1. The proof is completed. ■

Remark 7: According to Theorem 2, (32) is independent of the sampling period T , so the right boundary of the communication width θ can be calculated first for the given coupling gains α, β and the time delay τ , i.e., $\theta \in (0, \min\{T, (2\beta/\alpha - \beta) \cdot \tau\})$. Since (33) can be considered as a first-order inequality of T , it is quite easy to calculate T . Hence, based on (32) and (33), the sampling period T satisfying $T \in (0, [(4\Re(\mu_i)((2\beta\tau/\alpha - \beta) - \theta)^2)/((\alpha - \beta)\|\mu_i\|^2\theta)] - ((2\beta\tau/\alpha - \beta) - \theta)^3/[(2\beta\tau/\alpha - \beta) - \theta)^2 + [(16\Im^2(\mu_i))/((\alpha - \beta)^2\|\mu_i\|^4\theta^2)]]$) can guarantee to reach the consensus. For an undirected graph, an oversimplified corollary is derived as follows.

Corollary 4: Under Assumption 2, this system can reach the consensus if

$$0 < \theta < \frac{2\beta}{\alpha - \beta} \cdot \tau \quad (37)$$

and

$$0 < T < \theta - \frac{2\beta\tau}{\alpha - \beta} + \frac{4}{(\alpha - \beta)\mu_i\theta}. \quad (38)$$

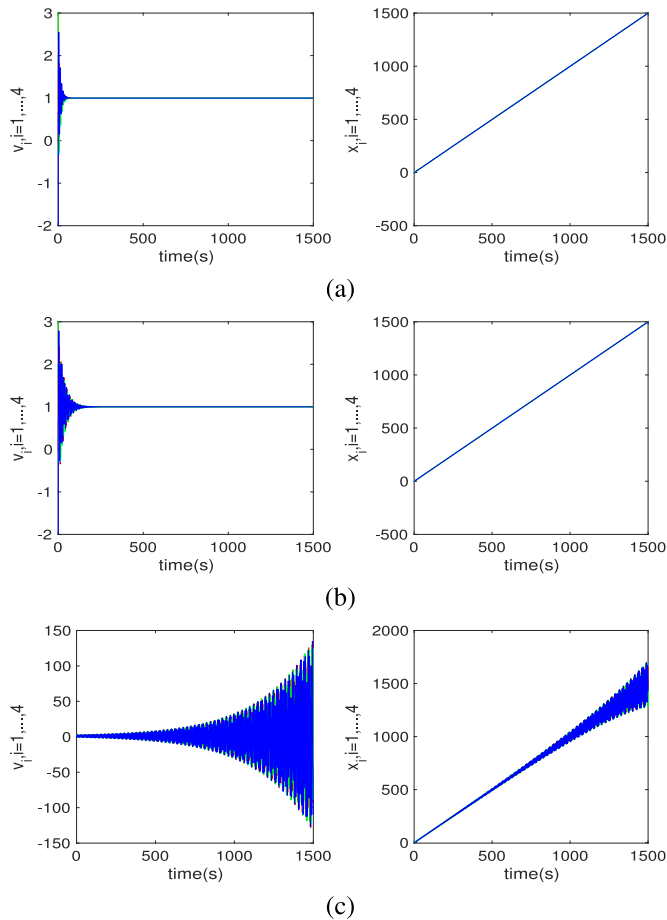


Fig. 2. Velocity and position states of agents when $\theta = 0.4$, where (a) $T = 2.15$, (b) $T = 2.5$, and (c) $T = 2.7$.

Proof: This can be demonstrated in a similar way in Corollary 2. ■

It is amazing to find that whether in a directed or undirected topology, the conclusions obtained from the previous theorem indicate that due to time delay, the inequality of the sampling period T is first-order rather than third-order, which is more convenient for calculation and implementation. Hence, we can find that sometimes the existence of time delay does not necessarily have no advantage, and time delay may lead to better algorithms.

IV. SIMULATIONS

A. Consensus With Protocol (2)

Consider a system (1) consisting of four agents with cooperative protocol (2) under a digraph with a spanning tree, where $\mathcal{L} = \begin{pmatrix} 1 & 0 & 0 & -1 \\ -1 & 1 & 0 & 0 \\ -1 & 0 & 1 & 0 \\ 0 & 0 & -1 & 1 \end{pmatrix}$ with $\mu_1 = 0$, $\mu_2 = 1$, $\mu_3 = 1.5 + 0.866j$, and $\mu_4 = 1.5 - 0.866j$. Choosing $\alpha = 1$, $\beta = 0.9$, and $\theta = 0.5$, from Theorem 1, one has that $0.09 < T < 2.1$. Hence, this system is able to achieve the consensus when the condition $0.5 < T < 2.1$ satisfies. The velocity and position states of all agents are presented in Fig. 1, which shows us the difference of convergence when (a) $T = 2.15$, (b) $T = 2.1$, and (c) $T = 0.8$. It is obvious to

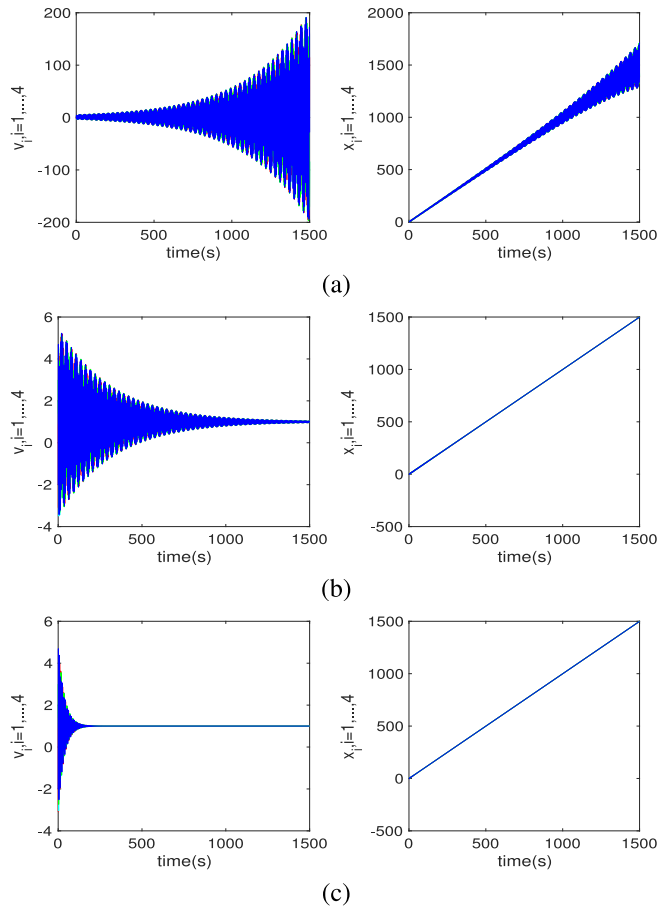


Fig. 3. Velocity and position states of agents when $\theta = 1$, where (a) $T = 2.1$, (b) $T = 2$, and (c) $T = 1.6$.

see that when (a) $T = 2.15$, the system cannot reach the consensus as $t \rightarrow \infty$. While when (b) $T = 2.1$ and (c) $T = 0.8$, the system can reach the consensus as $t \rightarrow \infty$, and the latter is faster than the former in achieving the consensus, which indicates that in the interval of the obtained T , the smaller the T is, the faster the agreement can be achieved.

From the above example, we can see that the sampling period is significant for achieving the consensus. Define the obtained upper bound \bar{T} as the threshold. When $\theta = 0.4$, the velocity and position states are presented in Fig. 2 with (a) $T = 2.15$, (b) $T = 2.5$, and (c) $T = 2.7$. Comparing Fig. 2 with Fig. 1, one can obtain that when $\theta = 0.4$, the threshold of the sampling period is greater than the one when $\theta = 0.5$. Hence, it is amazing to find that the threshold of the sampling period is getting greater, while the communication width is getting smaller.

B. Consensus With Protocol (3)

Consider a system (1) consisting of four agents with cooperative protocol (3) under a digraph as above. Choosing $\alpha = 1$, $\beta = 0.9$, $\tau = 1$, and when $\theta = 1$, according to Theorem 2, one has that $T < 2.05$. Thus, this system is able to achieve the consensus when the condition $1 < T < 2.05$ satisfies. The velocity and position states of all agents are presented in Fig. 3, which shows us the difference of convergence when

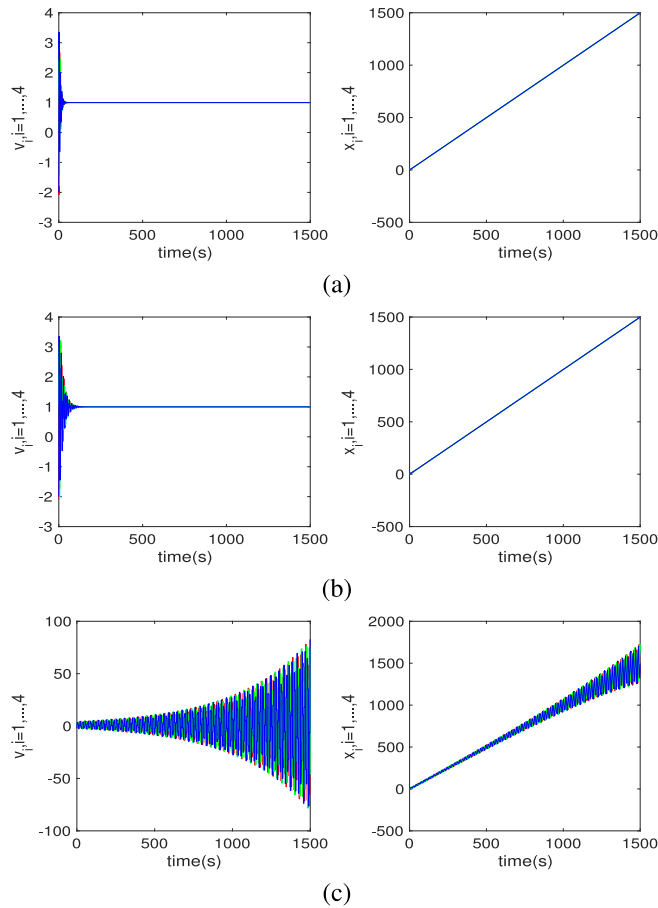


Fig. 4. Velocity and position states of agents when $\theta = 0.8$, where (a) $T = 2.1$, (b) $T = 3.2$, and (c) $T = 4.68$.

(a) $T = 2.1$, (b) $T = 2$, and (c) $T = 1.6$. It is obvious to see that when (a) $T = 2.1$, the system cannot reach the consensus as $t \rightarrow \infty$. While when (b) $T = 2$ and (c) $T = 1.6$, the system can reach the consensus as $t \rightarrow \infty$, and the latter is faster than the former in achieving the consensus, which also can indicate that in the interval of the obtained T , the smaller the T is, the faster the agreement can be achieved.

Similarly when $\theta = 0.8$, the velocity and position states are presented in Fig. 4, with (a) $T = 2.1$, (b) $T = 3.2$, and (c) $T = 4.68$. Comparing Fig. 4 with Fig. 3, it can still find that when the time delay exists, the threshold of the sampling period is getting greater, while the communication width is getting smaller.

V. CONCLUSION

In this paper, the second-order consensus in multiagent systems has been studied by intermittent sampled position data control. By using sampled position information and intermittent control, two novel consensus protocols with or without time delay have been designed. A necessary and sufficient condition has been obtained for the given protocol without time delay, which concludes that if and only if two inequalities about the internal parameters of system are satisfied, this system can achieve the consensus. Then we have discussed that the right intervals of the sampling period under other

parameters are given. Furthermore, a delay-induced consensus protocol is designed. Similarly, by discussing four cases about the relationship between various parameters regarding time, a necessary and sufficient condition is obtained for the delay-induced consensus protocol. In the future, the consensus for multiagent systems via event-triggered and intermittent sampled position data control will be studied.

REFERENCES

- [1] R. Olfati-Saber, J. A. Fax, and R. M. Murray, "Consensus and cooperation in networked multi-agent systems," *Proc. IEEE*, vol. 95, no. 1, pp. 215–233, Jan. 2007.
- [2] H. Su *et al.*, "Decentralized adaptive pinning control for cluster synchronization of complex dynamical networks," *IEEE Trans. Cybern.*, vol. 43, no. 1, pp. 394–399, Feb. 2013.
- [3] H. Su, H. Wu, and J. Lam, "Positive edge-consensus for nodal networks via output feedback," *IEEE Trans. Autom. Control*, to be published, doi: [10.1109/TAC.2018.2845694](https://doi.org/10.1109/TAC.2018.2845694).
- [4] H. Li, C. Huang, G. Chen, X. Liao, and T. W. Huang, "Distributed consensus optimization in multiagent networks with time-varying directed topologies and quantized communication," *IEEE Trans. Cybern.*, vol. 47, no. 8, pp. 2044–2057, Aug. 2017.
- [5] H. Su, Y. Ye, Y. Qiu, Y. Cao, and M. Z. Q. Chen, "Semi-global output consensus for discrete-time switching networked systems subject to input saturation and external disturbances," *IEEE Trans. Cybern.*, to be published, doi: [10.1109/TCYB.2018.2859436](https://doi.org/10.1109/TCYB.2018.2859436).
- [6] J. Sandhu, M. Mesbahi, and T. Tsukamaki, "On the control and estimation over relative sensing networks," *IEEE Trans. Autom. Control*, vol. 54, no. 12, pp. 2859–2863, Dec. 2009.
- [7] H. Su, H. Wu, X. Chen, and M. Z. Q. Chen, "Positive edge consensus of complex networks," *IEEE Trans. Syst., Man, Cybern., Syst.*, vol. 48, no. 12, pp. 2242–2250, Dec. 2018.
- [8] M. Long, H. Su, and B. Liu, "Group controllability of two-time-scale multi-agent networks," *J. Frankl. Inst.*, vol. 355, no. 13, pp. 6045–6061, 2018.
- [9] A. Jadbabaie, J. Lin, and A. S. Morse, "Coordination of groups of mobile autonomous agents using nearest neighbor rules," *IEEE Trans. Autom. Control*, vol. 48, no. 6, pp. 988–1001, Jun. 2003.
- [10] Y. Fan, G. Feng, Y. Wang, and C. Song, "Distributed event-triggered control of multi-agent systems with combinatorial measurements," *Automatica*, vol. 49, no. 2, pp. 671–675, 2013.
- [11] W. Yu, G. Chen, and M. Cao, "Some necessary and sufficient conditions for second-order consensus in multi-agent dynamical systems," *Automatica*, vol. 46, no. 6, pp. 1089–1095, 2010.
- [12] K. Liu, G. Xie, W. Ren, and L. Wang, "Consensus for multi-agent systems with inherent nonlinear dynamics under directed topologies," *Syst. Control Lett.*, vol. 62, no. 2, pp. 152–162, 2013.
- [13] H. Su, G. Chen, X. Wang, and Z. Lin, "Adaptive second-order consensus of networked mobile agents with nonlinear dynamics," *Automatica*, vol. 47, no. 2, pp. 368–375, 2011.
- [14] M. Long, H. Su, and B. Liu, "Second-order controllability of two-time-scale multi-agent systems," *Appl. Math. Comput.*, vol. 343, pp. 299–313, Feb. 2019.
- [15] H. Yu and X. Xia, "Adaptive consensus of multi-agents in networks with jointly connected topologies," *Automatica*, vol. 48, no. 8, pp. 1783–1790, 2012.
- [16] H. Yu, Y. Shen, and X. Xia, "Adaptive finite-time consensus in multi-agent networks," *Syst. Control Lett.*, vol. 62, no. 10, pp. 880–889, 2013.
- [17] H. Wu and H. Su, "Discrete-time positive edge-consensus for undirected and directed nodal networks," *IEEE Trans. Circuits Syst. II, Exp. Briefs*, vol. 65, no. 2, pp. 221–225, Feb. 2018.
- [18] H. Su, H. Wu, and X. Chen, "Observer-based discrete-time nonnegative edge synchronization of networked systems," *IEEE Trans. Neural Netw. Learn. Syst.*, vol. 28, no. 10, pp. 2446–2455, Oct. 2017.
- [19] H. Wu and H. Su, "Observer-based consensus for positive multiagent systems with directed topology and nonlinear control input," *IEEE Trans. Syst., Man, Cybern., Syst.*, to be published, doi: [10.1109/TSMC.2018.2852704](https://doi.org/10.1109/TSMC.2018.2852704).
- [20] H. Su, Y. Qiu, and L. Wang, "Semi-global output consensus of discrete-time multi-agent systems with input saturation and external disturbances," *ISA Trans.*, vol. 67, pp. 131–139, Mar. 2017.

- [21] Y. Gao, L. Wang, G. Xie, and B. Wu, "Consensus of multi-agent systems based on sampled-data control," *Int. J. Control*, vol. 82, no. 12, pp. 2193–2205, 2009.
- [22] H. Liu, G. Xie, and L. Wang, "Necessary and sufficient conditions for solving consensus problems of double-integrator dynamics via sampled control," *Int. J. Robust Nonlin. Control*, vol. 20, no. 15, pp. 1706–1722, 2010.
- [23] H. Zhao, S. Xu, and D. Yuan, "Consensus of data-sampled multi-agent systems with Markovian switching topologies," *Asian J. Control*, vol. 14, no. 5, p. 1366–1373, 2012.
- [24] Y. Zhang and Y.-P. Tian, "Consensus of data-sampled multi-agent systems with random communication delay and packet loss," *IEEE Trans. Autom. Control*, vol. 55, no. 4, pp. 939–943, Apr. 2010.
- [25] Y. Gao and L. Wang, "Consensus of multiple dynamic agents with sampled information," *IET Control Theory Appl.*, vol. 4, no. 6, pp. 945–956, Jun. 2010.
- [26] Y. Gao and L. Wang, "Sampled-data based consensus of continuous-time multi-agent systems with time-varying topology," *IEEE Trans. Autom. Control*, vol. 56, no. 5, pp. 1226–1231, May 2011.
- [27] Y. Hong, J. Hu, and L. Gao, "Tracking control for multi-agent consensus with an active leader and variable topology," *Automatica*, vol. 42, no. 7, pp. 1177–1182, 2007.
- [28] N. Huang, Z. Duan, and G. Chen, "Some necessary and sufficient conditions for consensus of second-order multi-agent systems with sampled position data," *Automatica*, vol. 63, pp. 148–155, Jan. 2016.
- [29] G. Wen, Z. Duan, Z. Li, and G. Chen, "Consensus and its \mathcal{L}_2 -gain performance of multi-agent systems with intermittent information transmissions," *Int. J. Control*, vol. 85, no. 4, pp. 384–396, 2012.
- [30] N. Huang, Z. Duan, and Y. Zhao, "Leader-following consensus of second-order non-linear multi-agent systems with directed intermittent communication," *IET Control Theory Appl.*, vol. 8, no. 10, pp. 782–795, Jul. 2014.
- [31] Z. Yu, H. Jiang, and C. Hu, "Second-order consensus for multiagent systems via intermittent sampled data control," *IEEE Trans. Syst., Man, Cybern., Syst.*, vol. 48, no. 11, pp. 1986–2002, Nov. 2018, doi: [10.1109/TSMC.2017.2687944](https://doi.org/10.1109/TSMC.2017.2687944).
- [32] P. C. Parks and V. Hahn, *Stability Theory*. Englewood Cliffs, NJ, USA: Prentice-Hall, 1993.
- [33] Z. Duan, G. Chen, and L. Huang, "Disconnected synchronized regions of complex dynamical networks," *IEEE Trans. Autom. Control*, vol. 54, no. 4, pp. 845–849, Apr. 2009.



Housheng Su received the B.S. degree in automatic control and the M.S. degree in control theory and control engineering from the Wuhan University of Technology, Wuhan, China, in 2002 and 2005, respectively, and the Ph.D. degree in control theory and control engineering from Shanghai Jiao Tong University, Shanghai, China, in 2008.

From 2008 to 2010, he was a Post-Doctoral Researcher with the Department of Electronic Engineering, City University of Hong Kong, Hong Kong. Since 2014, he has been a Full Professor with the School of Automation, Huazhong University of Science and Technology, Wuhan. His current research interests include multiagent coordination control theory and its applications to autonomous robotics and mobile sensor networks.

Dr. Su is an Associate Editor of *IET Control Theory and Applications*.



Yifan Liu received the B.S. degree from the Department of Control Science and Engineering, Huazhong University of Science and Technology, Wuhan, China, in 2018, where she is currently pursuing the M.S. degree with the School of Automation.

Her current research interests include multiagent systems and second-order systems.



Zhigang Zeng (SM'07) received the Ph.D. degree in systems analysis and integration from the Huazhong University of Science and Technology, Wuhan, China, in 2003.

He is currently a Professor with the School of Automation and also with the Key Laboratory of Image Processing and Intelligent Control of Education Ministry of China, Huazhong University of Science and Technology. He has published over 180 international journal papers. His current research interests include theory of functional differential equations and differential equations with discontinuous righthand sides, and their applications to dynamics of neural networks, memristive systems, and control systems.

Dr. Zeng was an Associate Editor of the IEEE TRANSACTIONS ON NEURAL NETWORKS from 2010 to 2011. He has been an Associate Editor of the IEEE TRANSACTIONS ON CYBERNETICS (since 2014) and the IEEE TRANSACTIONS ON FUZZY SYSTEMS (since 2016), and an Editorial Board Member of *Neural Networks* (since 2012), *Cognitive Computation* (since 2010), and *Applied Soft Computing* (since 2013).

Callum Kingstree

Doktorander i reglerteknik

Ref nr: PA2020/3049-165 Datum för ansökan: 2020-10-31 21:02

Födelsedatum	1998-12-15
Adress	7 Castleview Gardens DG11 1ND Lochmaben Dumfries and Galloway Storbritannien
E-post	callum.kingstree124@gmail.com
Kön	Man
Mobiltelefon	+447810170001
Telefon	+441387810966

Frågor

1. *Har du avlagt masterexamen?*
Ja Rätt svar
2. *Vid vilket universitet har du avlagt masterexamen?*
The University of Edinburgh, Scotland (graduating with Master's degree in May 2021)
3. *Ange namn på din(a) referens(er).*
Prof. Sigurd Skogestad (sigurd.skogestad@ntnu.no)
Dr. Gregory Francois (gregory.francois@hevs.ch)
4. *Vilket är det främsta skälet till att du söker denna tjänst?*
After doing my Master's thesis on the topic of control I wish to further my knowledge in the field and the best way to do this is through a PhD.

Callum Kingstree

Doktorander i reglerteknik

Ref nr: PA2020/3049-165 Datum för ansökan: 2020-10-31 21:02

Eget uppladdat CV

Egna filer och portfolio

Sigurd_Skogestad_Letter_of_Recommendation.pdf

Sigurd_Skogestad_Letter_of_Recommendation.pdf

Gregory_Francois_Letter_of_Recommendation.pdf

Gregory_Francois_Letter_of_Recommendation.pdf

Callum_Kingstree_Edinburgh_transcript.pdf

Callum_Kingstree_Edinburgh_transcript.pdf

Callum_Kingstree_NUS_transcript.pdf

Callum_Kingstree_NUS_transcript.pdf

Utbildningar

Titel	Skola/Företag	Ort	Land	Från-Till
Exchange Year	National University of Singapore	Singapore	Singapore	2018-2019
	<i>Spent third year of degree on exchange at National University of Singapore.</i>			
University	University of Edinburgh	Edinburgh	Storbritannien	2016-Nuvarande
	<i>Five-year Chemical Engineering with Management (MEng Hons) degree, with third year spent on exchange. Will graduate in May 2021 with the projected result of a first-class.</i>			

Språk

engelska Flytande Modersmål

Körkort



Referenser

Namn Sigurd Skogestad
Företag Norwegian University of Science and Technology (NTNU)
E-post sigurd.skogestad@ntnu.no
Telefon +47 73 59 40154

Namn Gregory Francois
Företag University of Applied Sciences Western Switzerland (previously University of Edinburgh)
E-post gregory.francois@hevs.ch
Telefon +41 58 606 82 19

7 Castleview Gardens
Lochmaben
Dumfries and Galloway
DG11 1ND
Scotland
30/10/20

Department of Automatic Control
Faculty of Engineering
Lund University
Lund
Sweden

Dear Sir/Madam,

Re: PhD Position in Department of Automatic Control at Lund University

I am writing to apply for the above role, after reading about it on the Lund University website. Please find my CV attached appropriately. This role appeals to me as I wish to expand my knowledge and contribute within the field of automatic control. Being able to complete my PhD at Lund University, with the prestige and the high level of internationalisation that this brings, would be an honour.

The Automatic Control Group at Lund has previously been recommended to me, and also in my own research I am impressed with both the quality and range of research within the group, especially the Innovative Control Applications research area. Being able to make an impact to the world around us is a passion of mine, particularly through sustainability. Seeing the group addressing several of the UN's Sustainable Development Goals is outstanding.

Currently, I am doing my Master's thesis (remotely due to Covid-19) with Prof. Skogestad at Norwegian University of Science and Technology (NTNU) in his Process Systems group. My work is focussed on an extension of feedback linearization which has been developed in the research group. I am applying the theory to different case studies and running simulations in order to validate it. Working remotely has vastly improved my interpersonal skills, requiring to communicate with ease and clarity, and while maintaining a good relationship with the rest of the research group in Norway.

The change to remote working has been difficult and created division within the University community as everyone is working on different timetables and in different time zones. As a pro-active self-starter, I decided to start a new project to improve communication within the Chemical Engineering community at the University of Edinburgh. Using my initiative, I decided that this will take the form of weekly videos with staff and students, discussing what they are currently working on, what change it is making to the world and what the outcome will be. I hope my skills match what you are looking for in new PhD students in the group.

I look forward to hearing from you soon and would like to thank you for reading my letter.

Yours faithfully



Callum Kingstree

callum.kingstree124@gmail.com

CALLUM ROSS KINGSTREE

+44 7810170001 / callum.kingstree124@gmail.com / www.linkedin.com/in/callumrk/

PERSONAL STATEMENT

I am a fifth year Chemical Engineering with Management (MEng) student at the University of Edinburgh and I will graduate in May 2021. As a global-minded individual and having previously been chosen to study in China, Singapore and Norway, I am now seeking a PhD position at a University with a high international reputation in my chosen area of Automatic Control. I am keen to build on knowledge learned through previous control modules taken at university, and past projects such as my Master's thesis, spent with Prof. Skogestad at NTNU. I am always willing to learn and consistently seek to go beyond expectations.

EDUCATION

2020 – Present: Norwegian University of Science and Technology (NTNU)

Masters Research Project

Six-month work experience placement with Prof. Sigurd Skogestad in the Process Control Research group. This work is focussed on simplifying the control structure of non-linear processes. For example; concentration control of a CSTR reactor and temperature control of a semi-batch polymerization reactor. Some of this work is planned to be published in 2021.

2016 – Present: University of Edinburgh

MEng (Hons) Chemical Engineering with Management (Average grade: 83%)

Key Modules: Fluid Mechanics, Separation Processes, Plant Engineering, Supply Chain Management, Operations Management, Thermodynamics and Engineering Mathematics.

Software: Mathcad, MATLAB, R Studio, gPROMS and UniSim (ThermoWorkbench, STE and Design)

2018 – 2019: National University of Singapore (NUS)

Chemical Engineering Exchange Year (Average grade: A)

Recipient of Erasmus+ International Credit Mobility Scholarship.

Key Modules: Process Dynamics and Control, Advanced Process Control, Process Synthesis and Simulation, Process Modelling and Numerical Simulation and Fluid-Solid Systems.

Software: Aspen HYSYS, Simulink and LaTeX.

2010-2016: Lockerbie Academy

Held position of Head Boy and was awarded Dux.

Advanced Highers: Physics (A), Chemistry (A) and Mathematics (A)

Highers: Physics (A), Chemistry (A), Biology (A), Mathematics (A) and Geography (A).

ENGINEERING EXPERIENCE

- **University of Edinburgh Summer Vacation Scholarship (2019)** - Last summer I was a recipient of the Summer Vacation Scholarship from University of Edinburgh. I was researching within the Chemical Engineering department to simplify the liquid pendular bridge model. I was working with ASTEC, Inc. who use the current model to simulate the coating of aggregate with bitumen to use on the roads in America. They wish to use a simpler model in order to speed up these simulations but still capture a similar degree of accuracy. I was using the discrete element method (DEM) software, EDEM, along with basic Python coding. With regard to this, I also attended the UK-China International Particle Technology Forum. Through this I have learned key **research skills**; both undertaking my own studies and being able to present my findings to an industry representative.

- **Nanjing University of Aeronautics and Astronautics (2018)** - Spending a month at Nanjing University of Aeronautics and Astronautics in 2018 demonstrated my **adaptability** to fit in to completely new surroundings. I developed skills required to work in a different country and strived on this by embracing the language and culture. Working in a diverse environment helped me foster new world-views, fuel new ideas and broaden my horizons. The summer course was focused on computer numerically controlled (CNC) machines; in a group of mixed students we had the task to code a machine to produce a prototype metal desk vice. There was often a language barrier but through **team-work** and **perseverance** we made this work.

SKILLS DEVELOPED

- After studying at The National University of Singapore I have developed my **independent skills**, such as problem solving, and how to cope with stressful and challenging situations after having to sort out all accommodation and visas on my own. The difference in academic standards and the general university style challenged me and put me outside of my comfort-zone but I worked hard to become **versatile** and maintain my high grades. This is where I was first introduced to process control and after my excellent performance and class participation in the basic process control course I was allowed to be admitted to the advanced process control course – not usually offered to exchange students. This covered topics such as robust control, digital control and MIMO systems.
- While in Singapore I felt as though the welcoming experience for international students was fairly minimal. Working on **my own initiative**, to improve the exchange experience for students coming to Edinburgh, I joined the Tandem committee. This year, I am the events coordinator for the committee and with this role I help to organise ‘*Language Cafes*’ - these encourage international students to interact and become a part of the University community.
- I am an **efficient communicator** - in both listening and talking - demonstrated while presenting at Royal Society’s Summer Science Exhibition in London, building on existing skills gained while Head Boy at Lockerbie Academy. Furthermore, I **organised** the inaugural Remembrance Week in Lockerbie for the victims of the Lockerbie Air Disaster – this was run in collaboration with the Remembrance week at Syracuse University, New York State – a very important week in the University’s calendar where they remember the students who sadly never returned from their year abroad. This was a very moving experience but it was an honour to organise.
- I am **very hard working**, this is evident in achieving the top mark in Scotland for my Higher Geography exam, the Dux award (academic prize for highest grades) for my school and also the Horsburgh Award for my Mathematics results at University. Furthermore, being awarded a First-class grade for my design project is a highlight of mine. This project was focused on designing a plant to produce hydrogen, while capturing the carbon dioxide released.

INTERESTS

- Through playing hockey and rowing for my university I have become a **team player** and an **effective contributor**. I am always reliable, organised and maintain positivity within the team. I thoroughly enjoy wearing my colours and representing with pride. In my spare time I enjoy running and I am currently training to run a marathon- requiring strict commitment and the ability to never give up.
- In 2017 I became a STEM ambassador for East Scotland, this involves being **pro-active** and going into local schools to help with STEM related activities. I always enjoy helping others and giving back to people who have previously helped me. Furthermore, last year at university I was involved in the peer mentoring scheme, for this we had to undergo training sessions to be able to help a first-year student who was struggling to adapt to university life. This was very interesting and taught me lots of transferable skills, for example **time management** techniques. I have also played a role in peer-support for students going abroad next year, to try to share my experience and tell them what to expect.

To: Whom It May Concern

Letter of recommendation for Mr. Callum Kingstree

This letter is in support of Mr. Callum Kingstree who I understand is applying for a PhD position.

Callum is presently a Master student at the University of Edinburgh, and he contacted me about one year ago about the possibility to do a Master Thesis with me in Trondheim on process control. We agreed on a very good topic and he started working with me on the Master thesis in early June 2020. Unfortunately, because of the COVID situation he has yet not been able to come physically to Trondheim, but we have interacted closely on video phone (zoom) and by email.

The topic of his master thesis is "input transformations for disturbance rejection, decoupling and linearization". It may be viewed as an extension of feedback linearization, with focus on process control applications. The emphasis is on the transformation of variables and on making this simple and robust. Callum has contributed with several very interesting simulation examples, some of which we are planning to publish.

We have many good Master students in Trondheim, but I have been very impressed about Callum, both with respect to his knowledge, independence, motivation and work ethics. He works very efficiently, and he is simply an excellent student. I would be happy to have him as a PhD student for myself if I had the funding.

I am sure Callum Kingstree will be an excellent candidate for any PhD program in process control and systems engineering. Please do not hesitate to contact me for further information.



Sigurd Skogestad
Professor of Chemical Engineering

Address	Org.no. 974 767 880	Location	Phone
NO-7491 Trondheim	E-mail:	Kjemiblokk 5, 1. etg	+ 47 73 59 40154
	postmottak@chemeng.ntnu.no	Sem Sælandsvei 4	Fax
	http://www.chemeng.ntnu.no	NO-7034 Trondheim	+ 47 73 59 40 80

All correspondence that is part of the case being processed is to be addressed to the relevant unit at NTNU, not to individuals. Please use our reference with all inquires.

Prof Dr. Grégory Francois, HDR
HES-SO Valais-Wallis
Route du Rawyl 47, CP 2134
CH - 1950 Sion 2 Switzerland
gregory.francois@hevs.ch

Sion, Switzerland, October 30, 2020

To whomsoever it may concern

This is with great pleasure that I am writing this letter of recommendation to support the application of M. Callum Kingstree. I have known Callum for a couple of years, having been the course organiser and the academic supervisor of his chemical engineering design project in 2019-2020, before I moved back to Switzerland to take a position of Professor of Automatic Control in a Systems Engineering department, while being still affiliated at the University of Edinburgh as Invited Senior Lecturer.

The design project course is a whole-year 40-credits 4th year course (~20 ECTS credits). Callum has therefore been working for 14 weeks on the joined industrial remit of Energaia (<https://energaia.com>) and SSE (<https://sse.co.uk/home>) with his group. As their academic advisor, I had weekly meetings with him and his group from November 2019 to April 2020, the last ones having been online team meetings, and I have thus witnessed his performances over a relatively long time-period, in the context of a challenging project with a heavy workload, made more complicated by the CoVid-19 outbreak, by the end of their project.

I must say that his performances during the project have been outstanding. He has shown patience, diligence, commitment, curiosity, creativity and a strong engineering insight and common sense combined to an excellent level of scientific (research) skills, from the very beginning until the end of the project. At this stage, I have also to underline his interpersonal and communication skills, which have been a strong asset for him and his group during the project. His responsiveness to supervision and constructive criticism has been excellent, and his dedication to the project, his capacity to argue and collaborate with his teammates, preserving always a very pleasant working atmosphere, have been impressive.

He indeed very quickly took a major role in his group, thanks to his natural leadership skills, becoming one of the main contributors. He always did it to the benefits of the whole group, leaving enough space to everybody to propose and discuss individual and collective ideas. Callum is certainly committed to excellence and achieved significantly more than what can be expected from an undergrad student, in particular for his individual design report. He showed evidences of a very good combination of engineering and research skills and his capacity to excel in teamwork, as well as for independent work. In addition, while the global situation in March was getting worse and most his groupmates having to go back to their home countries or home towns, he managed to kept the group focused for the last weeks of the project and we did not miss any meeting.

Coming back to Callum's academic performances, you will have seen his level of marks, which put him in the top 5% of his cohort (if not top 2%), and could lead him to a 1st class degree, which is the highest degree classification in the UK, and which is very difficult to obtain at the University of Edinburgh. Of note

is that a 2:1 degree classification (i.e. the second best degree classification, after the 1st class degree) is a typical requirement for acceptance by doctoral programs in the UK.

His performances have been very consistent and he obtained excellent marks in almost all courses, irrespective of them dealing with theoretical, scientific, applied or engineering topics. He has excellent analytical reasoning skills, he grasps concepts and creates connections quickly, and he always keeps in mind the necessity to contextualise, quantify, criticise and communicate his results, four major skills for a PhD student.

Callum and I have discussed several times about PhD studies over the past year, and his motivation seems to me very deep, sincere and solid. We also discussed his motivation as he has always shown interest for automatic control, especially since his year abroad at the National University in Singapore. We discussed about automatic control at many different occasions, also when he decided to do his masters project with Prof. Sigurd Skogestad at NTNU in Norway. This is because he knew I was teaching process dynamics and control in Edinburgh since 2015, after having spent among other academic positions more than 10 years at the Automatic Control Laboratory of EPFL in Lausanne. He wanted to discuss research and career opportunities in the field of automatic control right after he came back from Singapore where he developed this very deep interest for the field. I have been impressed by the strength of his motivation, and even though our discussion also covered career opportunities in control in the industry, several of his questions and the nature of most of our early conversations made me think that I would not be surprised if Callum would decide to go for a PhD thesis.

I am convinced that his motivation, his curiosity, his creativity and his commitment to excellence are very strong assets, on top of his excellent to outstanding level of academic performances, to excel in a PhD programme, and would he have applied for a PhD in my group, would I have had open positions, I would have certainly considered very seriously his application.

For all the reasons above and others that I will not include in this letter to keep it short, I strongly recommend Callum, without any reservation.

With best regards,

Prof. Dr. Grégory Francois
University of Applied Sciences
and Arts Western Switzerland
(HES-SO), Valais Wallis

Invited Senior Lecturer, The
University of Edinburgh





Information identifying the holder of the qualification

Full Name: Callum Ross Kingstree
 Date of Birth: 15 December 1998
 Matric / HUSID Number: S1621206 / 1611670122827

(HUSID (HESA Unique Student Identifier) is the unique identifying number for students registered at a UK university. It is defined by the UK's Higher Education Statistics Agency)

Information identifying the qualification

The qualification has not yet been awarded, the student is studying Chemical Engineering with Management (MEng Hons)

(The power to award degrees is regulated by law in the UK.)

Main field(s) of study for the qualification: Chemical Engineering with Management

Name and status of awarding institution: The University of Edinburgh

(The University of Edinburgh is a recognised body granted powers by the Privy Council to award degrees.)

Language(s) of instruction/examination: English

Information on the level of the qualification

Official length of programme: 5 Years

Access requirement(s): Detailed information regarding admission to the programme is available in the University's [Prospectus](#)

Information on the contents and results gained

Mode of study: Full-time

Programme requirements: <http://www.drps.ed.ac.uk/20-21/dps/utchemm.htm>

Further Information Sources

Further information sources: <http://www.see.ed.ac.uk/drupal> Any enquiries regarding the above should be addressed to: Engineering and Electronics Teaching Organisation, Faraday Building, King's Buildings, Mayfield Road, EH9 3JL; Tele: +44 (0) 131 650 5687; Web: <http://www.see.ed.ac.uk/>; email: eeoall@eng.ed.ac.uk

Further information regarding the University of Edinburgh HEAR: <http://www.ed.ac.uk/schools-departments/student-administration/other-info/overview>

This Higher Education Achievement Report incorporates the model developed by the European Commission, Council of Europe and UNESCO/CEPS for the European Diploma Supplement. The purpose of the report is to provide sufficient recognition of qualifications (diplomas, degrees, certificates etc). It is designed to provide a description of the nature, level, context and status of the studies that were purposed and successfully completed by the individual named on the original qualification to which this report should be appended. It should be free from any value judgements, equivalence statements or suggestions about recognition. Information in all eight sections should be provided. Where information is not provided, an explanation should be given.

Programme details, and the individual grades/marks/credits obtained

Programme Start Date: 19 September 2016

This is an interim transcript, the student is currently studying Chemical Engineering with Management (MEng Hons)

Academic Year	Code	Name	Mark	Grade	Result	SCQF Level	No. of attempts	Credits Achieved*
2016/17	CHEE08001	Chemical Engineering 1	83	A2	P	08	1	20
2016/17	CHEM08028	Chemistry for Chemical Engineers 1A	89	A2	P	08	1	20
2016/17	CHEM08029	Chemistry for Chemical Engineers 1B	89	A2	P	08	1	20
2016/17	MATH08074	Engineering Mathematics 1a	90	A1	P	08	1	20
2016/17	MATH08075	Engineering Mathematics 1b	96	A1	P	08	1	20
2016/17	SCEE08001	Engineering 1	74	A3	P	08	1	20
								Sub Total: 120
2017/18	CHEE08006	Plant Engineering 2	89	A2	P	08	1	10
2017/18	CHEE08007	Chemistry and Processes 2	81	A2	P	08	1	20
2017/18	CHEE08011	Computational Methods for Chemical Engineers 2	81	A2	P	08	1	10
2017/18	CHEE08013	Separation Processes 2	77	A3	P	08	1	10
2017/18	CHEE08014	Process Calculations 2	85	A2	P	08	1	10
2017/18	CHEE08015	Chemical Engineering Thermodynamics 2	88	A2	P	08	1	10
2017/18	MAEE08002	Techniques of Management	86	A2	P	08	1	20
2017/18	SCEE08003	Fluid Mechanics 2	82	A2	P	08	1	10
2017/18	SCEE08009	Engineering Mathematics 2A	89	A2	P	08	1	10
2017/18	SCEE08010	Engineering Mathematics 2B	80	A2	P	08	1	10
								Sub Total: 120
2018/19	XXXX09001	Non-compulsory year abroad (full year) – level 9		P	P	09	1	120
								Sub Total: 120
2019/20	CHEE10002	Chemical Engineering Design: Projects 4	73	A3	P	10	1	40
2019/20	CHEE10004	Fluid Mechanics (Chemical) 4	98	A1	P	10	1	10
2019/20	CHEE10005	Chemical Engineering Design: Synthesis and Economics 4	91	A1	P	10	1	10
2019/20	CHEE10008	Chemical Reaction Engineering 4	83	A2	P	10	1	10
2019/20	CHEE10009	Chemical Engineering Study Project 4	67	B	P	10	1	10
2019/20	CHEE10010	Chemical Engineering Design 4	74	A3	P	10	1	10
2019/20	MAEE10002	Supply Chain Management 4	75	A3	P	10	1	10
2019/20	MAEE10003	Operations Management 4	70	A3	P	10	1	10
2019/20	MAEE10005	Engineering Project Management 4	76	A3	P	10	1	10
								Sub Total: 120
								Total: 480

* 1 European Credit Transfer Scheme (ECTS) credit = 2 University of Edinburgh credits

Additional Information

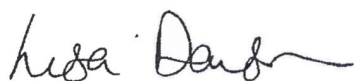
Prizes and Medals:

2016/17: Horsburgh Prize for the best Engineering students in the Pre-Honours Year 1 Mathematics courses.

Additional Recognised Activities: None recorded

Additional Notes: 2018/19 Optional Erasmus+ ICM Full Year Abroad at National University of Singapore, Singapore
2020/21 Part Year Work Placement at Norwegian University of Science and Technology, Norway, Remote work from Scotland

Certification:



Lisa Dawson, Director of Student Systems and Administration

Grading Scheme

Grade Expectations: <https://www.ed.ac.uk/student-systems/support-guidance/admin-support-staff/student-admin-colleges-schools/assessment-hub/recording-of-course-assessment-results-within-eucl>

Grades followed by 'A' = Fail (Credits Awarded on Aggregation)

Grades 'ES' and 'PS' = fail result of 38 or 39 but pass and credits awarded due to special circumstances

Grade CD = Course delivery disrupted, awarded on aggregate

Common Marking Scheme from 2005/2006

With effect from Academic Session 2005/2006, the marking scheme for undergraduate degree examinations in all Schools is as follows, except for the Royal (Dick) School of Veterinary Studies and the M.B.,Ch.B. curriculum in the College of Medicine and Veterinary Medicine.

HONOURS		NON HONOURS		
Honours Class	Mark (%)	Grade	Description	
I	90-100	A1	Excellent	
I	80-89	A2	Excellent	
I	70-79	A3	Excellent	
II.1	60-69	B	Very Good	
II.2	50-59	C	Performance at a level showing the potential to achieve at least a lower second class honours degree	
III	40-49	D	Pass, may not be sufficient for progression to an honours programme	
Fail	30-39	E	Marginal Fail	
Fail	20-29	F	Clear Fail	
Fail	10-19	G	Bad Fail	
Fail	0-9	H	Bad Fail	

Bachelor of Veterinary Medicine and Surgery (BVMS), Royal (Dick) School of Veterinary Studies

70-100 = A (Excellent); 60-69 = B (Very Good); 55-59 = C (Good); 50-54 = D (Satisfactory); 46-49 = E (Marginal Fail); 35-45 = F (Clear Fail); 0-34 = G (Bad Fail)

BVMS is a Masters level degree and is not classified into any other GPA or similar system. Due to differences in examining systems, it is rare for students to receive a mark greater than 80% with 70% or greater equating to a distinction.

Postgraduate Extended Common Marking Scheme (with effect from Academic Session 2005/2006)

Mark (%)	Grade	Description
90-100	A1	An excellent performance, satisfactory for a distinction
80-89	A2	An excellent performance, satisfactory for a distinction
70-79	A3	An excellent performance, satisfactory for a distinction
60-69	B	A very good performance
50-59	C	A good performance, satisfactory for a master's degree
40-49*	D	A satisfactory performance for the diploma, but inadequate for a master's degree
30-39**	E	Marginal Fail***
20-29	F	Clear Fail***
10-19	G	Bad Fail ***
0-9	H	Bad Fail***

* Assessment of the dissertation: A mark of 47-49 may be used to denote the possibility that by minor revision the work may be upgraded to a Masters standard.

** Assessment of the dissertation: A mark of 37-39 may be used to denote the possibility that by minor revision the work may be upgraded to a diploma standard.

*** Assessment of the dissertation: In those programmes where a diploma may be awarded for the taught component only, a failed dissertation may be put aside for the diploma.

Information on the National Higher Education System

Description of Higher Education in Scotland

Scotland's distinctive higher education system has 20 higher education institutions (HEIs). The 14 Universities, the Open University in Scotland, 2 colleges of higher education, 2 art schools and a conservatoire are part-funded for research, teaching and learning through the Scottish Funding Council.

The HEIs are independent, self-governing bodies, active in teaching, research and scholarship. They decide the degrees they offer; the conditions on which they are awarded and the admissions arrangements. Degrees and other higher education qualifications are legally owned by the awarding institution, not by the state. The HEIs offer qualifications at undergraduate (Bologna first cycle) and postgraduate (Bologna second and third cycle) levels. In Scotland, the law distinguishes the power to award degrees on the basis of completion of taught programmes from the power to award research degrees. Universities have powers to award taught and research degrees. Some other HEIs have powers to award degrees while others offer programmes leading to degrees awarded by HEIs with degree powers.

Lists of institutions with powers toward degrees and institutions recognised by authorities in Scotland as being able to offer courses leading to a degree of another HEI may be found at (<http://www.universities-scotland.ac.uk>). A small number of degrees are available in colleges of further education by the authority of a duly empowered HEI.

Qualifications

The types of qualification awarded at the undergraduate (first cycle) and postgraduate level (second and third cycles) in Scotland are described in the Framework for Higher Education qualifications in Scotland which includes qualifications descriptors, developed with the higher education sector (<http://www.qaa.ac.uk>). The Framework is an integral part of a wider national framework: the Scottish Credit and Qualifications Framework that covers all forms of programmes and qualifications from School to Doctorates (see table 1 and <http://www.scf.org.uk>). Institutions use SCQF credit points for students entering or transferring between programmes or institutions, and use ECTS for transfers within the European area.

Admission

Requirements for particular programmes are set by the HEIs which offer a range of routes for entry and/or credit transfer into their programmes, and admit students whom they believe have the potential to complete their programmes successfully. The Open University is an open entry institution. The most common qualification for entry to higher education is the Higher or Advanced Higher or, for entrants from the rest of the U.K., the General Certificate of Education at 'Advanced' level (including the "advanced supplementary") or comparable qualifications. Four or five Highers are normally taken in the 5th and 6th year of secondary school or at college or further education and studied in considerable depth, involving coursework and final examinations. Advanced Highers are taken in the 6th year. A major route into Degrees, often with transfer of credit, is the higher National Qualifications offered in colleges or further education.

Quality Assurance

Standards of qualification and the quality of the student learning experience are maintained by the HEIs using a range of processes including extensive use of external examiners. In some subject areas, Professional and Statutory Bodies have a role to ensure that programmes meet the needs and standards of the particular profession. HEIs in Scotland demonstrate their public accountability for quality and standards through a national quality and standards through a national quality assurance framework that has a strong focus on enhancement as follows: HEIs take account of a QAA published U.K.-wide code of practice for quality assurance, and U.K. subject level 'benchmark' statements on standards (see <http://www.qaa.ac.uk>). Subject level issues are addressed by HEIs internal reviews conducted in accordance with guidance issued by the Scottish Funding Council (SHEFC) (see <http://www.scf.ac.uk>). External reviews are conducted by the Quality Assurance Agency for Higher Education in Scotland (QAA). The Agency is an independent body established to provide public confidence in the quality and standards of higher education. It involves students in its quality enhancement activities. The Agency publishes reports on the outcomes of reviews and the confidence that can be placed in the HEIs' arrangements for assuring and enhancing standards and quality, and for ensuring that they provide public information that is complete, accurate and fair (see <http://www.qaa.ac.uk>). A national development service supports students in their role as active participants in assuring and enhancing quality and standards (see <http://www.sparqs.org.uk>).

Table 1: The Scottish Credit and Qualifications Framework (SCQF)

The SCQF covers all the major qualifications in Scotland from school to Doctorate and including work based Scottish Vocational Qualifications (SVQs)

SCQF Level	Qualifications of Higher Education Institutions	SQA Higher National and National Units, Courses and Group Awards	SVQs
12	Doctoral Degrees (Minimum 540 SCQF credits)	-	-
11	Masters Degrees (Minimum 180 SCQF credits) Postgraduate Diploma (Minimum 120 SCQF credits) Integrated Masters Degrees (Minimum 600 SCQF credits)	-	SVQ 5
10	Bachelors Degree with Honours (Minimum 480 SCQF credits) Graduate Diplomas and Certificates	-	-
9	Bachelors Degree (Minimum 360 SCQF credit) Graduate Diplomas and Certificates	-	-
8	Diploma of Higher Education (Minimum 240 SCQF credits)	Higher National Diploma	SVQ 4
7	Certificate of Higher Education (Minimum 120 SCQF credits)	Advanced Higher Higher National Certificate	-
6	-	Higher	SVQ 3
5	-	Intermediate 2 Credit Standard Grade	SVQ 2
4	-	Intermediate 1 General Standard Grade	SVQ 1
3	-	Access 3 Foundation Standard Grade	-
2	-	Access 2	-
1	-	Access 1	-

Notes

- SCQF levels represent increasing complexity and demand in learning outcome.
- One credit represents the outcomes achievable by the average through 10 notional hours of learner effort. In general terms, one full-time undergraduate year is considered to be 120 credits worth of learning. A postgraduate year is 180 credits. 1 ECTS credit is deemed equivalent to 2 SCQF credits. Research degrees – Master of Philosophy (MPhil) and Doctor of Philosophy (PhD) are not credit rated.
- Graduate Certificates (minimum of 60 SCQF credits) and Graduate Diplomas (minimum of 120 credits) are offered at levels 9 and 10 within the SCQF framework. They are offered for programmes that are for graduates but do not have outcomes that are at postgraduate level.
- The Bachelors Degree (level 9) leads to employment and in some instances can give access to postgraduate study particularly when accompanied by relevant work or professional experience.
- At Postgraduate levels, the framework and the higher education qualifications are the same as those for the rest of the UK. The Honours Degree levels of the frameworks are considered to be in broad alignment (the Honours Degree in Scotland normally takes 4 years and that in the rest of the UK takes 3 years). Below Honours level the frameworks reflect the different educational structures of Scotland and the rest of the UK.
- Scotland has a distinctive higher education system and also operates under a devolved government, including for higher education. There is a separate Description of Higher Education in England, Wales and Northern Ireland where the system is different to that of Scotland.
- This national description is endorsed by the Quality Working Group which is a national committee with members from The Quality Assurance Agency for Higher Education, Scotland; The Scottish Funding Council; Universities Scotland and the National Union of Students in Scotland.

Description of the University of Edinburgh

The University of Edinburgh was founded in 1583, and has 22 Schools in 3 Colleges: Humanities and Social Science, Medicine and Veterinary Medicine and Science and Engineering. It offers more than 300 degree programmes to its approximately 29,000 students. It is one of around a hundred universities in the United Kingdom and of 14 in Scotland. Higher Education, including universities, within Scotland is the responsibility of the Scottish Parliament, which has powers devolved from the U.K. Parliament.

The University is an independent, self-governing body that is active in both teaching and research. Its mission is the advancement and dissemination of knowledge and understanding. (See http://www.planning.ed.ac.uk/Strategic_Planning/MissionStatement.htm for fuller details of the University's mission and plan). Like all universities in the UK, its degrees are its own responsibility, not that of the State. The University is funded from a variety of sources, including a block grant from the Scottish government, academic fees, research grants, and other sources.

About 4,500 students graduate every year with a Bachelors degree with honours and after four-years of study. For long-standing historical reasons, many degrees at this level in humanities subjects are designated Master of Arts. There are also some "undergraduate masters degrees" in science subjects that require five years of study and take students to a postgraduate level of achievement without their having achieved an intermediate bachelors degree. The outcome of these honours degrees is quoted in terms of the "classification" of the degree: first (the highest), upper second, lower second, or third. Some students graduate with a non-honours "ordinary" degree, which is not classified, although a transcript showing their marks is available. This system is common to all the universities in the UK.

About 2,000 students each year graduate with postgraduate degrees, generally designated as Master or Doctor. These degrees are not classified.



NATIONAL UNIVERSITY
of SINGAPORE

OFFICIAL TRANSCRIPT

NAME: KINGSTREE CALLUM ROSS

STUDENT NO.: A0192888E

DATE OF BIRTH: 15/12/1998

DATE ISSUED: 02/07/2019

PROGRAMME: NON GRADUATING PROGRAMME

MODULE

GRADE CREDITS

ACADEMIC YEAR 2018/2019 SEMESTER 1

CN2116	CHEMICAL KINETICS & REACTOR DESIGN	A+	4.00
CN1125	HEAT & MASS TRANSFER	A	4.00
CN321	PROCESS DYNAMICS & CONTROL	A-	4.00
CN3135	PROCESS SAFETY, HEALTH AND ENVIRONMENT	B+	3.00

ACADEMIC YEAR 2018/2019 SEMESTER 2

CN3124	FLUID-SOLID SYSTEMS	A+	3.00
CN3421	PROCESS MODELING AND NUMERICAL SIMULATION	A	4.00
CN4122*	PROCESS SYNTHESIS AND SIMULATION	AUD	3.00
CN4227R	ADVANCED PROCESS CONTROL	A	4.00

CN4122 - Module was not included in the computation of the Cumulative Average Point.

*****END OF TRANSCRIPT*****



NATIONAL UNIVERSITY OF SINGAPORE (NUS)
 Registrar's Office, University Hall (Lee Kong Chian Wing),
 #UHL-04-01, 21 Lower Kent Ridge Road,
 Singapore 119077

Telephone : (65) 6516 2301 / (65) 6516 2304
 Facsimile : (65) 6778 6371
 Website : <http://www.nus.edu.sg/registrar>

TRANSCRIPT INFORMATION
Applicable to Undergraduate and Graduate programmes (unless specified otherwise)

MEDIUM OF INSTRUCTION
 The medium of instruction used in the University is English, unless specified otherwise.

GRADE LEGEND

Grade	Grade Point	Additional Grading Options
A+, A	5.00	S Satisfactory
A-	4.50	U Unsatisfactory
B+	4.00	CS Completed (Satisfactory)
B	3.50	CU Completed (Unsatisfactory)
B-	3.00	IC Incomplete
C+	2.50	IP In Progress
C	2.00	AUD Audit
D+	1.50	EXE Exempted
D	1.00	W Withdrawn
F	0.00	WU Withdrawal from University

CUMULATIVE AVERAGE POINT (CAP)

The Cumulative Average Point (CAP) was introduced for students admitted from the Academic Year (AY) 1998/1999 onwards to track the progress of students under the Modular System. It is the weighted average grade point of all modules taken by the student. Modules with no assigned modular credit or grade point are excluded from the calculation of CAP.

MODULAR CREDIT (MC)

A modular credit (MC) is a unit of the effort, stated in terms of time, expected of a typical student in managing his/her workload. One MC is equivalent to 2.5 hours of study and preparation per week. Thus, a 4-MC module would require 10 hours of work a week, including lectures, tutorials, laboratory sessions, assignments, and independent or group study, over 13 Instructional Weeks in a semester.

GRADE-FREE SCHEME (GFS)

The Grade-free Scheme (GFS), in the form of 32 MCs of Satisfactory/Unsatisfactory (S/U) option, was introduced for **undergraduate** students admitted from AY2014/2015 onwards to provide a supportive and enabling environment for them to make a successful transition into

The following information is specific to the respective Faculties/Schools:

**FACULTY OF DENTISTRY (BDS)/
 YONG LOO LIN SCHOOL OF MEDICINE (MBBS)**

Grade	Descriptor	Additional Grading Options
A+	Distinction	DT Distinction
A	Merit	M Merit
A-	Pass	P Pass
B+	Incomplete	IC Incomplete
B	In Progress	IP In Progress
B-	Withdrawn	W Withdrawn
C+	Withdrawal from University	WU Withdrawal from University
C		
F		

SUPPLEMENTARY EXAMINATION AND RE-EXAMINATION

Students who sit for Supplementary Examination or Re-examination are awarded the grade appropriate to the marks they obtain.

FACULTY OF LAW (LLB)

DEGREE CLASSIFICATION

The criteria for degree classification applicable to students conferred their LLB degrees from 30 June 2016 are as follows:

Degree Classification

First Class Honours
 Obtained a Cumulative Weighted Numerical Average for all modules taken at NUS that is equivalent to a grade of A- or better, or finished in the top 10% of the graduating class.

Second Class (Upper Division) Honours
 Obtained a Cumulative Weighted Numerical Average for all modules taken at NUS that is equivalent to a grade of B or better, and do not qualify for First Class Honours.

Second Class (Lower Division) Honours
 Obtained a Cumulative Weighted Numerical Average for all modules taken at NUS that is equivalent to a grade of C or better, and do not qualify either for First Class or Second Class (Upper Division) Honours.

Third Class Honours
 Completed the number of credits required for a LLB (Honours) degree but do not qualify for First Class, Second Class (Upper Division) or Second Class (Lower Division) Honours.

- (i) No student will be eligible for First Class or Second Class (Upper Division) Honours if the student has failed more than 12 credits of modules at NUS (or while on an approved exchange programme); or
- b) the student has taken more than 9 semesters to complete the 4-year LLB programme or 7 semesters to complete the 3 year Graduate LLB programme (excluding periods where the student has been granted a leave of absence).

SUPPLEMENTARY EXAMINATION

Unless otherwise indicated, a student who passes a subject by supplementary examination is awarded only a 'D' grade irrespective of his/her performance.

the academic and social culture of university life. It serves to facilitate a transition in students' mindsets towards grades and learning in the university setting, as well as enable them to leverage opportunities for a holistic education. It was enhanced from a grade-free first semester to a grade free first year for undergraduate students admitted from AY2016/2017 onwards.

At the end of a semester, students may choose to retain the letter grade or to exercise the S/U option on a module, in which case the letter grade will not be shown on the transcript nor computed towards the CAP. An 'S' grade is assigned if students receive a C grade or above while a 'U' grade is assigned if the grade obtained is D+, D or F. Students will receive credits towards the degree only if they attain an 'S' grade.

DEGREE CLASSIFICATION

The criteria for degree classification applicable to students admitted from AY2012/2013 onwards are as follows:

Honours Degree Classification (i)
 Honours (Highest Distinction) CAP 4.50 and above (ii)
 Honours (Distinction) CAP 4.00 - 4.49
 Honours (Merit) CAP 3.50 - 3.99
 Pass CAP 3.00 - 3.49
 Pass CAP 2.00 - 2.99

Bachelor's Degree Classification (iii)

Pass with Merit CAP 3.00 and above
 Pass CAP 2.00 - 2.99

(i) This refers to 160-MC degree programmes.

(ii) Particular Faculties/Schools may stipulate other requirements.

(iii) This refers to 120-MC degree programmes.

LEAVE OF ABSENCE

Only leave of absence of one semester or longer is recorded in the transcript.

NUS BULLETIN

More information on the University's programmes is available in the NUS Bulletin at: <http://www.nus.edu.sg/nusbulletin>.

This transcript shows the latest information. For information on earlier grade legends, please visit: <http://www.nus.edu.sg/registrar/adminpolicy/transcripts.html>.

For degree verification, please visit: <http://www.nus.edu.sg/registrar/administrative-policies/degree-verification.html>.

CHECK FOR AUTHENTICITY:

NUS official transcript is printed in landscape format on paper with security fibres and displays the NUS coat of arms as a watermark with a smaller NUS coat of arms in full colour as part of the letterhead. Each page of the official transcript is individually validated with the NUS seal and the Registrar's endorsement (on a tri-colour background) or by an authorised staff of the University.

Peter Hallstadius

Doktorander i reglerteknik

Ref nr: PA2020/3049-15 Datum för ansökan: 2020-10-31 16:21

Personnummer	960726-3770
Adress	Magistratsvägen 55 NB 1220 226 44 Lund Sverige
E-post	peter@hallstadius.se
Kön	Man
Mobiltelefon	0703823125
Telefon	0703823125

Frågor

1. *Har du avlagt masterexamen?*
Nej Fel svar
2. *Vid vilket universitet har du avlagt masterexamen?*
Lund University. I will finish my master thesis and receive my master's degree in January 2021.
3. *Ange namn på din(a) referens(er).*
Eskil Andreasson
4. *Vilket är det främsta skälet till att du söker denna tjänst?*
I have a burning passion for science and research and my curiosity and desire to learn has not been satisfied after five years of Engineering Physics.

Peter Hallstadius

Doktorander i reglerteknik

Ref nr: PA2020/3049-15 Datum för ansökan: 2020-10-31 16:21

Eget uppladdat CV

Egna filer och portfolio

Official National Transcript of Records Peter Hallstadius.pdf

Official National Transcript of Records Peter Hallstadius.pdf

20201029_External_letter_of_reccomendation_Peter_Hallstadius.pdf

20201029_External_letter_of_reccomendation_Peter_Hallstadius.pdf

2015 Cambridge English Peter Hallstadius.pdf

2015 Cambridge English Peter Hallstadius.pdf

Anställningar

Titel	Företag	Ort	Land	Från-Till
Student Talent	Tetra Pak / Adecco	Lund	Sverige	2016-2020

General description:

"Student Talent Programme is a programme for ambitious students with an interest in getting to know a potential future employer already during your education. It is an opportunity for you to gain valuable experience and inspiration for your future career goals. By offering you summer internship, extra work, master thesis project and a dedicated mentor, the intention of the program is a collaboration that extends throughout your education and hopefully longer. As a Student Talent you will be hired by Adecco as a consultant working for Tetra Pak."

My work tasks have ranged from evaluation of test procedures for package integrity, development of new such methods (chemical, optical and electrical), to scientific programming, simulation, and development of new models for the interaction between water and paper material.

Språk

svenska

engelska

tyska

Flytande

Flytande

Nybörjare

Modersmål

Körkort



Dear Mr. Cervin and Mr. Rantzer,

I am writing to apply for the position as PhD student at the Department of Automatic Control. My MSc in Engineering Physics is nearing its completion. However, after five years, I am still every bit as curious as when I started the program. I am still eager to learn more, so the opportunity to continue as a PhD student seems very appealing to me. Apart from postgrad courses, large-scale systems and control applications (in particular the robotics lab) are areas I find really interesting.

My interest in robotics and control engineering has been lifelong – already at the age of eleven I designed my own four-legged walkers in Lego, and continued with maze-solving and balancing robots built with Lego Mindstorms. During my education, Automatic Control has easily been one of the most enjoyable subjects and one which I wish to pursue.

During my master-level studies, I have taken courses in a wide variety of different subjects. Most were related to numerical modelling of solids and fluids, programming, material science, but also machining – all relevant to automatic control and its applications. I have taken the Multivariable Control course (FRTN10) and was an opponent for Jonas Hansson's and Magnus Svensson's thesis on autotuners.

I am fluent in both spoken and written English. Before my university studies, I achieved grade A corresponding to CEFR level C2 in the Cambridge Advanced English test. I have since then also lived in Canada during my exchange semester at University of British Columbia.

I believe my single most relevant experience has been my position as a Student Talent at Tetra Pak. There I was a part of the Virtual Engineering group for the past two years. The focus was on research and development, and I had the opportunity to contribute with what I regard as my greatest strength – bridging the gap between theory and practical experiments. This summer, I worked on quantifying the chromatographic effect of glue pressed into paper. I designed and machined the experiment setup, developed a model and ran simulations based on the results. This experience has given me a taste for innovative environments where creativity, communication, and problem-solving are important skills.

Thank you for your time and consideration. I look forward to hearing from you.

Peter Hallstadius

tfy15pha@student.lu.se

0703-823125

PETER HALLSTADIUS

CURRICULUM VITAE



PERSONAL DATA

Born Lund, Sweden, 1996-07-26
Citizenship Swedish
Home address Magistratsvägen 55NB 1220, 226 44 Lund, Sweden
Mobile phone +46 (0)703 823125
Email peter@hallstadius.se

EDUCATION

2015 – Engineering Physics, Faculty of Engineering, Lund University

WORK EXPERIENCE

2016 – 2020 Student Talent (formerly Technical Talent) at Tetra Pak Packaging Solutions AB, Lund, Sweden.
2020 Summer job, 2020-05-14 – 2020-08-14, Tetra Pak Packaging Solutions AB, Lund, Sweden.
2019 Summer job, 2019-08-05 – 2019-08-23, Tetra Pak Packaging Solutions AB, Lund, Sweden.
2018 Summer job, 2018-06-04 – 2018-06-21, 2018-08-01 – 2018-08-24 Tetra Pak Packaging Solutions AB, Lund, Sweden.
2017 Summer job, 2017-06-05 – 2017-06-22, 2017-07-31 – 2017-08-18 Tetra Pak Packaging Solutions AB, Lund, Sweden.
2016 Summer job, 2016-08-01 – 2016-08-19, Tetra Pak Packaging Solutions AB, Lund, Sweden.
2015 Summer job, 2015-08-03 – 2015-08-21, Tetra Pak Packaging Solutions AB, Lund, Sweden.
2014 Summer job, 2014-07-28 – 2014-08-15, Tetra Pak Packaging Solutions AB, Lund, Sweden.

2013 Summer job, 2013-07-29 – 2013-08-16, Tetra Pak Packaging Solutions AB, Lund, Sweden.

2012 Summer job, 2012-07-30 – 2012-08-10, Tetra Pak Packaging Solutions AB, Lund, Sweden.

OTHER EXPERIENCES

2019 – 2020 President of LundaPyrot (Pyrotechnic Association at TLTH)

2017 – 2018 Vice President of LundaPyrot (Pyrotechnic Association at TLTH)

2015 Contestant in the International Physics Olympiad.

2015 Kemiolympiaden, contestant in the Swedish national final.

2011 PRAO at Tetra Pak, 2011-10-10 – 2011-10-14.

PROFESSIONAL TRAINING

2015 English, Cambridge Advanced English; Folkuniversitetet, Lund, Sweden

Official National Transcript of Records Peter Hallstadius.pdf

**The file could not be included.
This can be because the file is protected.
Please check the original file!**



Letter of Recommendation

Peter Hallstadius has worked at Tetra Pak® during the summers and partly during the semesters since 2012. The last 3 years, Peter have been involved and a part of a student program between our company and eminent students at Lund University, called “student talent”-program. The tasks have differed a lot during the years, ranging from experimental tests, building rigs/equipment’s, packaging material evaluation, method development, theoretical studies, scientific programming and numerical simulations. Different software’s and tools have also been tested and evaluated during the time.

The work that Peter has done lately has increased the awareness at Tetra Pak® of the moisture/water transport in the packaging material occurring during the glue application when producing paper straws. A combination of theoretical, practical and simulation work in a scientific manner has been the focus the last summer to increase the understanding of the physics behind and the mechanisms involved during the gluing process of paper sheets.

Peter has worked both independently and has collaborated with engineers during the summers and he has finalized a good workflow. All the work has been well documented and great skills in communication were also shown. Several written reports and presentations were made and presented during the work to the project team. The last years have been focused on that Peter has driven projects by his own with support and guidance from colleagues, domain experts and project members.

Peter has with deep dedication and precision done his work with outstanding quality. He has been an appreciated team member by his friendly, curios and interested attitude. I consider him hard working, reliable and committed. Therefore, I strongly recommend him for further employment and wish him good luck in his future work.

29th of October 2020

Tetra Pak in Lund

Eskil Andreasson

Technology Specialist

Virtual Modelling, Materials and Package

Packaging Solutions AB

+46 733 36 32 69

eskil.andreasson@tetrapak.com



Cambridge English Level 3 Certificate in ESOL International (Advanced)*

This is to certify that

PETER HALLSTADIUS

has been awarded

Grade A

in the

Certificate in Advanced English

Performance at Grade A demonstrates an ability at Level 3*
and Council of Europe Level C2

Overall Score 204

Reading	210
Use of English	204
Writing	193
Listening	201
Speaking	210

Date of Examination **MARCH (CAE2) 2015**
Place of Entry **LUND**
Reference Number **153SE0085435**
Accreditation Number **500/7558/5**

Saul Nassé
Chief Executive

*This level refers to the UK National Qualifications Framework



Date of Issue 26/04/15
Certificate Number 004890002

CERTIFICATE IN ADVANCED ENGLISH (CAE)

CAE is a general proficiency examination at Level C1 in the Council of Europe's Common European Framework of Reference. It is at Level 2 in the UK National Qualifications Framework.

Further details of CAE are given in the CAE Handbook, and at www.cambridgeenglish.org

CAE results are reported using scores on the Cambridge English Scale. CAE certificates are awarded to candidates who achieve the following grades:

Grade A – CEFR Level C2 (score 200-210)

Grade B – CEFR Level C1 (score 190-199)

Grade C – CEFR Level C1 (score 180-190)

Candidates who have achieved a score between 200 and 210 (Grade A) have demonstrated ability at CEFR Level C2. Candidates who have not achieved a CAE passing grade, but score between 180 and 199, receive a Cambridge English certificate stating they demonstrated ability at CEFR Level B2.

A T symbol next to the grade indicates that the candidate was exempt from satisfying the full range of assessment objectives in the examination.

The Council of Europe's Common European Framework of Reference covers six levels of language proficiency. Research carried out by the Association of Language Testers in Europe (ALTE) shows what learners can typically do at each level. The table below gives examples of typical ability in each of the skill areas for Council of Europe Levels C2, C1 and B2.

Level C2	Listening and Speaking	Reading and Writing
Overall general ability	CAN advise on or talk about complex or sensitive issues, understand colloquial references and deal confidently with difficult questions.	CAN understand various documents, including the finer points of complex texts, and CAN write letters and meeting notes with good expression and accuracy.
Level C1	Listening and Speaking	Reading and Writing
Overall general ability	CAN contribute effectively to meetings and seminars within own area of work or keep up a casual conversation with a good degree of fluency, coping with abstract expressions.	CAN read quickly enough to cope with an academic course, and CAN take reasonably accurate notes in meetings or write a piece of work which shows an ability to communicate.
Social & Tourist	CAN pick up nuances of meaning/opinion. CAN keep up conversations of a casual nature for an extended period of time and discuss abstract/cultural topics with a good degree of fluency and range of expression.	CAN understand complex opinions/arguments as expressed in serious newspapers. CAN write most letters (s/he is likely to be asked to do, such errors as occur will not prevent understanding of the message).
Work	CAN follow discussion and argument with only occasional need for clarification, employing good compensation strategies to overcome inadequacies. CAN deal with unpredictable questions.	CAN understand the general meaning of more complex articles without serious misunderstanding. CAN, given enough time, write a report that communicates the desired message.
Study	CAN follow up questions by probing for more detail. CAN make critical remarks/express disagreement without causing offence.	CAN scan texts for relevant information, and grasp main topic of text. CAN write a piece of work whose message can be followed throughout.
Level B2	Listening and Speaking	Reading and Writing
Overall general ability	CAN follow a talk on a familiar topic. CAN keep up a conversation on a fairly wide range of topics.	CAN scan texts for relevant information. CAN make notes while someone is talking or write a letter including non-standard requests.

Further information and examples of the ability statements can be found at www.alfz.org

Any alteration to this certificate renders it invalid and use of an altered certificate could constitute a criminal offence.

Cambridge English Language Assessment provides a results verification service to help organisations and agencies quickly and securely validate candidates' Cambridge English examination results at <https://cambridgeenglish.org/verify>

Mingjing Sun

Doktorander i reglerteknik

Ref nr: PA2020/3049-148 Datum för ansökan: 2020-10-31 12:39

Födelsedatum	1996-09-08
Adress	Shanghai Jiao Tong University, 800 Dongchuan Road, Minhang District, Shanghai 200240 ??? Shanghai Shi Kina
E-post	mj.sun@sjtu.edu.cn
Kön	Man
Mobiltelefon	?86?18601719920
Telefon	?86?18601719920

Frågor

1. *Har du avlagt masterexamen?*
Ja Rätt svar
2. *Vid vilket universitet har du avlagt masterexamen?*
Shanghai Jiao Tong University
3. *Ange namn på din(a) referens(er).*
1. Daniel E. Quevedo E-mail: dquevedo@ieee.org
Professor, School of Electrical Engineering and Robotics, Queensland University of Technology
2. Jianping He E-mail: jphe@sjtu.edu.cn
Associate Professor, Department of Automation, Shanghai Jiao Tong University
4. *Vilket är det främsta skälet till att du söker denna tjänst?*
My research background suits well with this position.

Mingjing Sun

Doktorander i reglerteknik

Ref nr: PA2020/3049-148 Datum för ansökan: 2020-10-31 12:39

Eget uppladdat CV

Egna filer och portfolio

Awards&Honors_mjsun.pdf

Awards&Honors_mjsun.pdf

Publikationer

Titel	Förlag	Ort	År
Privacy-Preserving Correlated Data Publication with Noise Adding Mechanism	IEEE International Conference on Control & Automation	Sapporo, Hokkaido, Japan	2020
	<i>First author; accepted</i>		
Privacy-Preserving Correlated Data Publication: Privacy Analysis and Optimal Noise Design	IEEE Transactions on Network Science and Engineering	-	2020
	<i>First author; minor revision</i>		

Språk

engelska Flytande

Körkort

c1

Mingjing Sun

Shanghai Jiao Tong University

800 Dongchuan Rd
Shanghai 200240, China
☎ (+86) 18601719920
✉ mj.sun@sjtu.edu.cn



Education

- Sep 2018–
Mar 2021 (expected) **Shanghai Jiao Tong University**,
Department of Automation, Shanghai, China.
- M.S. Degree (Control Science and Engineering)
 - Supervisor: Professor Jianping He
 - Thesis Topic: *Privacy-Preserving High-dimensional Data Publication and Optimal Noise Design*
- Sep 2014–
Jun 2018 **Northwestern Polytechnical University**,
Department of Automation, Xi'an, China.
- B.S. Degree (GPA 90.68/100, Rank: 3/149)
 - Thesis Topic: *Machine-vision-based Screw Defect Detection Algorithm*

Research of Interests

Security and privacy in network systems, information-theoretically optimal mechanism design, consensus, distributed optimization

Publications

- J1 **Mingjing Sun**, Chengcheng Zhao, Jianping He, Peng Cheng, and Daniel E. Quvedo. “Privacy-Preserving Correlated Data Publication: Privacy Analysis and Optimal Noise Design”. *IEEE Transactions on Network Science and Engineering* (T-NSE), minor revision, 2020.
- C1 **Mingjing Sun**, Chengcheng Zhao, and Jianping He. “Privacy-preserving Correlated Data Publication with Noise Adding Mechanism”, in *IEEE International Conference on Control & Automation*, accepted, 2020.

Scientific Achievements

- **Design: A Non-invasive Diabetes Detector**
 - 1) Traditional blood-sampling-based diabetes detectors are traumatic to human body, and with slow response speed. To overcome this drawback, we developed a non-invasive, automatic and real-time diabetes detector, based on acetone concentration detection. We won **National Award** in energy saving and emission reduction contest and excellent conclusion from numerous experts.

2) The patent "Breath-type diabetes detection system based on automatic acetone recognition" has been issued (CN201720868245.5).

○ Screw Defect Detection Algorithm

In order to handle traditional screw defect detection algorithms insufficient robustness, unsatisfactory running speed and hard-applying to industrial vision systems, we propose a precise, robust, fast and industry-oriented detection algorithm.

Academic Activity

Academic Talk ○ 2020.9.25 | Attending the **IEEE International Conference on Control & Automation 2020**, and making oral presentation.

Academic Services **Served to review** the manuscripts including

- IEEE Transactions on Visualization and Computer Graphics
- IEEE Conference on Decision and Control
- IEEE Vehicular Technology Conference

Projects and Competitions

Projects ○ National innovation and entrepreneurship training program (**Leader**)
○ Industrial defect inspection/shape recognition project

Competitions ○ National energy saving and emission reduction contest (**Leader**)

- Mathematical modeling competition (**Leader**)
- Advanced mathematics competition
- Electronic design competition
- Computer programming contest

Selected Awards

2014–2019 First Class Scholarship

2018 Second Prize in National Energy Saving and Emission Reduction Contest

2017 **First Prize** in Mathematical Modeling Competition

2015 **First Prize** in Mathematical Modeling Competition

Skills

Programming C/C++, Python, MATLAB

Software/ Labview, Robot Operating System, Engineering Drawing;

Hardware skill Circuit Board Design

English TOEFL 92

References

Jianping He *E-mail: jphe@sjtu.edu.cn*

Associate Professor, Department of Automation, Shanghai Jiao Tong University

Daniel E. Quevedo *E-mail: dquevedo@ieee.org*

Professor, School of Electrical Engineering and Robotics, Queensland University of Technology

List

Publications..... Page 2

Selected awards..... Page 3-9

Transcript..... Page 10-11

Publications

IEEE Transactions on Network Science and Engineering provisional acceptance:

(First Author)

RE: TNSESI-2020-04-0203.R1, "Privacy-Preserving Correlated Data Publication: Privacy Analysis and Optimal Noise Design"
Manuscript Type:

08-Sep-2020

Dear Miss Zhao,

We have completed the review process of the above referenced paper for the IEEE Transactions on Network Science and Engineering and recommend that your paper undergo a Minor Revision.

IEEE ICCA acceptance:

(First Author)

Message from PaperCept Conference Management System

Message originated by IEEE ICCA 2020

To: Ms. Chengcheng Zhao

From: IEEE ICCA 2020

Re: (231) Privacy-preserving Correlated Data Publication with Noise Adding Mechanism

Dear Ms. Zhao,

It is our great pleasure to inform you that the paper referenced above, for which you are listed as an author, has been accepted for oral presentation and publication in the proceedings of The 16th IEEE International Conference on Control and Automation (ICCA 2020). Attached please find reviewers' comments and associate editor's summary. You may also log into author's workspace at <https://controls.papercept.net> to see them. It is important that you adequately address any critical comments therein when you prepare your final paper.

Leader of National Innovation Project (Funded by 20000 RMB)

国家级大学生创新创业训练项目重点在研证明

项目编号：201610699041

项目名称：基于电子鼻技术的呼气式糖尿病检测仪

立项日期：2016年6月

项目成员：

	姓名	学号	班级	所在学院	项目中的分工
项目组主要成员	孙明靖	2014303003	自动化/ 09011404	自动化学院	整体结构设计，传感器的筛选
	熊瑞婧	2014301672	飞行器动力工程/ 07011403	动力与能源学院	单片机的编程设计，模拟实验，找出最优方法
	蒋昱晨	2014301485	飞行器动力工程/ 07011401	动力与能源学院	硬件电路设计，仪器的性能测试
	曹志远	2015301553	飞行器动力工程/ 07011504	动力与能源学院	丙酮的制备与检测，参与实验
	周书萱	2015301339	工程力学/ 06011502	力学与土木建筑学院	设计实验，记录分析数据

特此证明。



2016年9月23日

Patent



中华人民共和国国家知识产权局

710072

陕西省西安市友谊西路 127 号
西北工业大学专利中心 陈星(029-88494370)

发文日:

2017年07月18日



申请号或专利号: 201720868245.5

发文序号: 2017071800808680

专利申请受理通知书

根据专利法第 28 条及其实施细则第 38 条、第 39 条的规定, 申请人提出的专利申请已由国家知识产权局受理。现将确定的申请号、申请日、申请人和发明创造名称通知如下:

申请号: 201720868245.5

申请日: 2017 年 07 月 18 日

申请人: 西北工业大学

发明创造名称: 基于紫外光丙酮识别的呼气式糖尿病检测系统

经核实, 国家知识产权局确认收到文件如下:

说明书附图 每份页数:2 页 文件份数:1 份

专利代理委托书 每份页数:2 页 文件份数:1 份

说明书 每份页数:5 页 文件份数:1 份

摘要附图 每份页数:1 页 文件份数:1 份

权利要求书 每份页数:1 页 文件份数:1 份 权利要求项数: 4 项

说明书摘要 每份页数:1 页 文件份数:1 份

实用新型专利请求书 每份页数:4 页 文件份数:1 份

提示:

1. 申请人收到专利申请受理通知书之后, 认为其记载的内容与申请人所提交的相应内容不一致时, 可以向国家知识产权局请求更正。
2. 申请人收到专利申请受理通知书之后, 再向国家知识产权局办理各种手续时, 均应当准确、清晰地写明申请号。
3. 国家知识产权局收到向外国申请专利保密审查请求书后, 依据专利法实施细则第 9 条予以审查。

审查员: 自动受理

审查部门:



200101
2010.4

纸件申请, 回函请寄: 100088 北京市海淀区蓟门桥西土城路 6 号 国家知识产权局受理处收
电子申请, 应当通过电子专利申请系统以电子文件形式提交相关文件。除另有规定外, 以纸件等其他形式提交的文件视为未提交。

National Award in Energy Saving Competition

“神雾杯”第十届全国大学生节能减排社会实践与科技竞赛

二等奖名单

经 2017 年 8 月 10 日节能减排竞赛委员会会议表决通过，共有 116 件作品被评为“神雾杯”第十届全国大学生节能减排社会实践与科技竞赛二等奖，现公布如下（排名不分先后）：

证书编号	作品名称	作品类别	队长姓名	团队其他成员	所在学校
2017-C-001	新型高效汽车发动机在线增氧装置	科技作品	徐航	彭传喆、戚玉玲、卫林、 管玲娟、王政、朱浩	安徽工程大学
2017-C-002	基于道路侧向风及振动发电绿色储能装置	科技作品	宋超宇	袁翔、陈嘉豪、刘坤	安徽工程大学
2017-C-003	废旧塑料低温融化处理技术与装置	科技作品	傅左强	杨二瑞、李志行、李秀儒、 程雨露、占学宽	安徽理工大学
2017-C-004	一种节能高效的小型污水处理装置	科技作品	李玉呈	左俊怡、徐智炜、孙凤仪、 江光敏、陈琪	安庆师范大学
2017-C-005	基于能源互联网的云端电力预测调控系统	科技作品	陈婉怡	苗盼、谢旭、刁成永、胡道欢	北方工业大学
2017-C-006	沥青路面智能贴缝机	科技作品	蔡文渊	周思齐、王章陶、郭启进	北京航空航天大学
2017-C-007	应用旋转阀式定容燃烧技术的航空动力系统	科技作品	何欢	王章、程如玥、彭黎明、 佟若均	北京航空航天大学
2017-C-008	智慧能源车控系统	科技作品	魏琦	白寅良、余柯、刘亚楠、 连武雄、杨正文	北京交通大学
2017-C-009	基于双级跟踪的智能太阳能车	科技作品	高平蒙	吴庆兵、李万全、李瑶、 唐得成	北京交通大学
2017-C-010	太阳能辅助间接蒸发式制冷空调	科技作品	林晓	陈俊斌、陈湘敏、刘家平、 滕依达、曹彪、宋高明	北京科技大学
2017-C-011	新型海洋转轮器	科技作品	梁育	丛浩、王健琛、梁之海、 黄朝伟、蓝映	大连理工大学



2017-C-069	一种环保铅笔的研发	科技作品	魏亚鲁	刘绪超、王绪坤、韩忠祥、 包会丹、安森、刘新宇	潍坊职业学院
2017-C-070	基于肠道仿生的无动力农村生活污水处理设施	科技作品	沈王政	李亚敏、徐素、苏思倩	武汉大学
2017-C-071	基于灰色系统理论的农村生活垃圾处理方案优化及对策研究——以西安市非主城区为例	社会实践调查	丁浩	张雍宇、陈信、赵柘栋、 李星星、陈常伦、侯雪妍	西安建筑科技大学
2017-C-072	用于含磷废水处理的石墨烯基磁性粒子	科技作品	计怡	韩优花、陈闯、莫鑫、赵佳 伟、朱文玉、宋庆飞	西北工业大学
2017-C-073	纸币整理机	科技作品	刘志丹	李景超、刘煦洋、郭俊睿、 崔杰、孙瑞亮、江天牧	西北工业大学
2017-C-074	基于介孔材料的多功能检测吸附仪	科技作品	赵佳伟	王继启、孙明靖、邓白雪、 计怡、贾乐敏、王子继	西北工业大学
2017-C-075	新型多功能智能吸附剂——三重响应性磁性多孔微球	科技作品	邓白雪	丁栋梁、邹敏浩、赵佳伟、 李蓓、陈闯、狄萌	西北工业大学
2017-C-076	一种漂浮式磁力光伏污水制氢装置	科技作品	敬婧	罗安妮、程杰、付仁鲜、 袁冬梅	西华大学
2017-C-077	一种新型秸秆（或物料）功能性碳化处理装置与工艺方法	科技作品	江志伟	李焯晴、杨苻贻、毛路遥、 王燕	西南交通大学
2017-C-078	“Guidance”——重载货运列车平稳节能优化操纵指导装置	科技作品	尤冰涛	陈鸿辉、王晓文、陈南匡、 徐云松	西南交通大学（峨眉校区）
2017-C-079	一种新型节能景观路灯	科技作品	冉方圆	范登鑫、杨运涛、沈玉妹、 吴清清	西南科技大学
2017-C-080	农村秸秆处理和资源化利用技术、产业发展及示范——以中国凉都（六盘水）为例	社会实践调查	薛祝缘	陈婉心、夏羽、龚蕾、 赵琛琦、涂孙伟	西南科技大学
2017-C-081	湘西龙山县百合产业精准扶贫绿色行动——基于机器视觉的太阳能绿色农业喷药智能机器人	科技作品	刘泽辉	江奥、刘沁蕊、刘浩林、 谢尚位、赵浩武	湘潭大学





孙明靖 同学在 2014—2015 学
年成绩优秀，表现突出，被评
为校 优秀学生
并获 一等奖学金。

荣誉证书
CERTIFICATE

西北工业大学

2015年11月

荣誉证书

公 诚 勇 毅

基础扎实
工作踏实
作风朴实
开拓创新

孙明靖 同学在2015-2016学年
学习成绩优秀，综合表现突出，
被评为校 优秀学生 ，
并获 一等奖学金。


西北工业大学

2016 年 12 月

First Prize in Mathematical Modeling Competition

获奖证书

孙明靖, 王继启, 赵佳伟同学在二〇一五年“工大出版社杯”第十六届西北工业大学大学生数学建模竞赛中获得**一等奖**。

特发此证, 以资鼓励。

西北工业大学教务处

二〇一五年六月

Transcript

条形码



西北工业大学本科生成绩单

编号: 2014303003170606094537

院系	专业	学号	2014303003	性别	男	证件号	321088199409080012	照片	
院系	专业	学号	09011404	入学日期	2014-09-01	毕业日期	2018-07-01		
院系	专业	学号	自动化学院	专业	智能	专业	自动化		
课程名称	学分	成绩	课程属性	学期	课程名称	学分	成绩	课程属性	学期
大学英语	3.5	89	必修	2014-2015(春)	英语听力4	2	80	集中课程教学	2015-2016(春)
大学英语	2	85	必修	2014-2015(春)	英语1(听力)	1	86	必修	2015-2016(春)
大学英语(下)	6	80	必修	2014-2015(春)	英语综合与阅读(下)	1	80	集中课程教学	2014-2015(春)
大学英语	2	88	必修	2014-2015(春)	英语听力	1	88	集中课程教学	2014-2015(春)
大学英语(上)	1.5	82	必修	2014-2015(春)	英语听力(听力)	4	84	集中课程教学	2014-2017(春)
大学英语(下)	2	83	必修	2014-2015(春)	大学英语(上)	2	84	集中课程教学	2014-2017(春)
大学英语(上)	3.5	81	必修	2014-2015(春)	大学英语(下)	6.5	87	必修	2014-2017(春)
大学英语(下)	1.5	80	必修	2014-2015(春)	大学英语(上)	1.5	86	必修	2014-2017(春)
大学英语(上)	1.5	85	必修	2014-2015(春)	大学英语(下)	2	100	集中课程教学	2014-2017(春)
大学英语(下)	2	84	必修	2014-2015(春)	大学英语(上)	2	87	集中课程教学	2014-2017(春)
大学英语(上)	2	78	必修	2014-2015(春)					
大学英语(下)	6	76	必修	2014-2015(春)					
英语(听力)	1	88	必修	2014-2015(春)					
英语(阅读)	0.5	84	必修	2014-2015(春)					
大学英语(听力)	2	81	必修	2014-2015(春)					
大学英语(听力)	1.5	84	必修	2014-2015(春)					
英语(听力)	2	82	必修	2014-2015(春)					
英语(听力)	3.5	84	必修	2014-2015(春)					
大学英语(听力)	1	80	必修	2014-2015(春)					
英语(听力)	3	85	必修	2014-2015(春)					
大学英语(听力)	1.5	80	必修	2014-2015(春)					
英语(听力)	2	85	必修	2014-2015(春)					
英语(听力)	2	85	必修	2014-2015(春)					
英语(听力)	1	80	必修	2014-2015(春)					
英语(听力)	2	87	必修	2014-2015(春)					
英语(听力)	1	88	必修	2014-2015(春)					
英语(听力)	4	82	必修	2014-2015(春)					
英语(听力)	1	85	必修	2014-2015(春)					
英语(听力)	4	85	必修	2014-2015(春)					
英语(听力)	2	84	必修	2014-2015(春)					
英语(听力)	2	89	必修	2014-2015(春)					
英语(听力)	2	81	必修	2014-2015(春)					
英语(听力)	1	80	必修	2014-2015(春)					
英语(听力)	4	87	必修	2014-2015(春)					
英语(听力)	2	77	必修	2014-2015(春)					
英语(听力)	2	80	必修	2014-2015(春)					
英语(听力)	2	80	必修	2014-2015(春)					
英语(听力)	2	88	必修	2014-2015(春)					
英语(听力)	1	80	必修	2014-2015(春)					
英语(听力)	4	83	必修	2014-2015(春)					
英语(听力)	1.5	80	必修	2014-2015(春)					
英语(听力)	3	88	必修	2014-2015(春)					
英语(听力)	2	84	必修	2014-2015(春)					
英语(听力)	3	81	必修	2014-2015(春)					
英语(听力)	1.5	84	必修	2014-2015(春)					
英语(听力)	2	84	必修	2014-2015(春)					
国家英语六级						817			
国家英语四级						578			
毕业设计	题目		成绩		指导教师				
课程总学分	142	课程总学分	134	平均成绩	/				

制表人: [Signature]

审核人: 吴心华

打印日期: 2017-06-06 09:45:37



GPA Rank: 3/149

孙明靖，学号 2014303003，自动化学院自动化专业 1404 班
学生，其专业排名为第 3 名，专业年级人数为 149 人。

2017 年 6 月 7 日



2017. 6. 8

西北工业大学 自动化学院

王新昆

2017. 6. 9

AMNA Khan

Doktorander i reglerteknik

Ref nr: PA2020/3049-140 Datum för ansökan: 2020-10-30 16:22

Födelsedatum	1992-06-07
Adress	street 34, house 81, G-9/1, Islamabad, Pakistan 440000 Islamabad Pakistan
E-post	amna.khan.434@hotmail.com
Kön	Kvinna
Mobiltelefon	+393883863976
Telefon	+393883863976

Frågor

1. *Har du avlagt masterexamen?*
Ja Rätt svar
2. *Vid vilket universitet har du avlagt masterexamen?*
Air University, Islamabad
3. *Ange namn på din(a) referens(er).*
Dr Zafar Ulla Koreshi, Dr Yasir Ayaz
4. *Vilket är det främsta skälet till att du söker denna tjänst?*
My research interest in robotics, IoT, autonomous systems, statistical analysis of data sets (acquired using biosensors), pattern recognition

AMNA Khan

Doktorander i reglerteknik

Ref nr: PA2020/3049-14 Datum för ansökan: 2020-10-30 16:22

Eget uppladdat CV

Egna filer och portfolio

Letter of Motivation.pdf

Letter of Motivation.pdf

BEDegree.pdf

BEDegree.pdf

BETranscript.pdf

BETranscript.pdf

ielts 2019-02-19 08.48.29.pdf

ielts 2019-02-19 08.48.29.pdf

MS Degree.pdf

MS Degree.pdf

MS Transcript.pdf

MS Transcript.pdf

Recommendation_Letter_by_Dr_Yasar.pdf

Recommendation_Letter_by_Dr_Yasar.pdf

Recommendation_Letter_by_Prof_Dr_Zafar(1).pdf

Recommendation_Letter_by_Prof_Dr_Zafar(1).pdf

Språk

engelska

Flytande



1.AMNA KHAN
MECHATRONICS ENGINEER
(PEC number: MECHATRO1524)

amna.khan.434@Hotmail.com(+393883863976)

Date: October 20, 2020

Research Interests:

robotics, human-machine interface, IoT, autonomous systems, signal processing, statistical analysis of data sets (acquired using biosensors), machine learning algorithms, programming languages

2.Educational Degrees

Date of certificate	Degree title	Major subject/Degree program	Educational Institute	Awarded	Locality and Country
2017	Masters in Mechatronics Engineering	Mechatronics	Air University	3.80 GPA	E-9, Islamabad, Pakistan
2014	Bachelors in Mechatronics Engineering	Mechatronics	Air University	3.63 GPA	E-9, Islamabad, Pakistan
2010	Fsc	Pre-Engineering	Islamabad Model College	75 %	F-7/4, Islamabad, Pakistan
2008	Matriculation	Science	Islamabad Model College	79%	F-7/4, Islamabad, Pakistan

3.Internships

Organization	Position Held	Duration
Pakistan Aeronautical Complex (PAC), Kamra (Avonics Production Factory (APF))	Internee	June – July 2012
Comcept Pvt. Ltd	Internee	July – August 2011
Air University (Admission Office)	Internee	June – July 2011

4. Languages	
1	Urdu (National)
2	English (Ielts Result attached)
3	Italian (Basic level)

Seminars		
Organization	Title	Held on
Air University in collaboration with Pakistan Engineering Council	One Day International Workshop on Outcome Based Education and Implementation	May 2017
YUNUS Textiles for Life	Give & Get Initiative on Employability Skills	Feb 2014
Air University Bits & Bytes Society	Three Days Hands on Workshop on Solid works 2012	April 2012
Ace Pressure weld Singapore	Procurement Engineering Workshop	Dec 2014
EDCONS Institute of Business & Technology	Introduction to Drilling & Well Operations	Sep 2015

5-6. Job Experience

Organization	Job title	Duration
Air University (Department of Mechatronics Engineering)	Lecturer	September 9/2017 – January 2/2020
Air University (Department of Mechatronics Engineering)	Lab Engineer	January 10/2016 – August 20/2017
Tek-Oro Pvt Ltd (Oil and Gas)	Senior Procurement Engineer	May 1/2015 – January 8/2016
Seronic Pvt Ltd	Procurement Engineer	Sept 3/2014 – April 30 2/2015

8. Research Grants

Awarded Travel Grant from Higher Education Commission (HEC) Pakistan and presented my paper at International Conference on Mechatronics and Control Engineering (ICMCE 2018) held from Nov 27-29 at Amsterdam, Netherlands 2018 (one hundred ninety thousand rupees)

9. Publications

- Afaq Ahmed Abbasi, Hayat Muhammad Khan, Ehtisham ul Hasan, **Amna Khan**, Muqteet Ahmad, *A Novel Analytical Approach for Validating Serial Manipulators Kinematics; Simulation and Practical Implementation*, **Journal of Mechanical Science and Technology** [Submitted]
- **Amna Khan**, Ehtisham Ul Hasan, Zareena Kausar, *Effective Electrode Extraction Procedure for Myoelectric data of upper limb*, **Journal of Neural Engineering** [Submitted]
- Ehtisham Ul Hasan, **Amna Khan**, *Robot Assisted Physiotherapy Device for Knee Joint Rehabilitation*, **International Conference on Mechatronics and Control Engineering ICMCE 2018, Amsterdam, Netherlands** [Published]
- **Khan, Z.** Kausar E.U Hasan, S Malik, *Elbow Joint Position Estimation and Myoelectric Control for Upper Limb Rehabilitation: A Simple Approach*, **International Journal of Human Computer Studies** [Submitted]
- Ehtisham Ul Hasan, **Amna Khan**, Afaq Ahmed Abbasi, *fNIRS based position control of Upper Limb at extreme positions*, **ICBBE 2018 : 20th International Conference on Biosignals and Biorobotics Engineering** [Submitted]
- Ehtisham ul Hasan, **Amna Khan** and Afaq Ahmed Abbasi, *Lateral Acceleration Control of aircraft using PID, Linear Quadratic Regulator (LQR) and Linear Quadratic Integral (LQI); a comparative case study*, **2018 5th IEEE International Conference on Electrical and Electronics Engineering (ICEEE 2018)** to be held in **Istanbul, Turkey during May 03-05, 2018** [Published]
- Afaq Ahmed Abbasi, Ehtisham ul Hasan, **Amna Khan**, *Static Force, Torque and Structural Analysis of 5R Robotics Arm-Simulation and Practical Implementation*, **2018 The 4th International Conference on Control, Automation and Robotics (ICCAR 2018)** to be held in **Auckland, New Zealand during April 20-23, 2018** [Published]
- **Khan A**, Kausar Z, Malik S. *Comparison of Linear Discriminant Analysis and Support Vector Machine Classifications for Electromyography Signals Acquired at Five Positions of Elbow Joint*. **World Academy of Science, Engineering and Technology, International Journal of Mechanical and Materials Engineering**. 2017 Jul 27;4(7). [Published]
- **Khan A**, Kausar Z. *Intention realization of intermittent angular positions of elbow using myo armband sensor*. In **Proceedings of the 5th International Conference on Mechatronics and Control Engineering** 2016 Dec 14 (pp. 108-112). ACM. [Published]
- **Khan A**, Sair AR, Ekram A, Malik S, Afzal MR, Junaid AB, Eizad A. *An automated object retrieval system for warehouses*. In **2015 15th International Conference on Control, Automation and Systems (ICCAS)** 2015 Oct 13 (pp. 95-100). IEEE. [Published]

11. Project completed with Department of Mechatronics Engineering

- Officer In charge of MS program
- Part of rubrics deciding committee of subjects related to electronics
- Developed Self Assessment Report (SAR) for PEC accreditation of Mechatronics Engineering at Air University
- Supervised and co supervised projects
- Conducted Workshops on LEGO Mindstorms EV3 Kits at Schools for awareness on career selection in collaboration with Higher Education Commission through its Social Integration Outreach Program

10-11. Additional Duties in Job

Lecturer Sep 2017 to January 2019	Faculty of Engineering, Department of Mechatronics Engineering, Air University, E-9, Islamabad
Lab Engineer Jan 2016 to Aug 2017	Faculty of Engineering, Department of Mechatronics Engineering, Air University, E-9, Islamabad
Member Technical Committee (Reviewer)	2018 5th IEEE International Conference on Electrical and Electronics Engineering
Supervised	1) EMG based Power Grip Strength Tester 2) Smart Stick for visually impaired 3) Defect detection in textile industry using image processing 4) Augmented Reality Warehouse Management System
Projects Co-Supervisor	1) Iron Rod Cutting and Ring Making Machine 2) Automation of Distribution Box Assembly Line 3) Automated Physiotherapy Device (Completed) 4) fNIRS based Position control of Elbow Joint at extreme positions (Completed)
Administrative Positions	Officer-In-charge MS Mechatronics Research Program Department of Mechatronics Engineering Air University, E-9, Islamabad Website Coordinating Officer Department of Mechatronics Engineering Air University, E-9, Islamabad
Research Area	Bio-Mechatronics (<i>Rehabilitation Studies Using EMG, EEG and fNIRS</i>), Robotics and Control Systems for people suffering from Parkinson's stroke or muscle injury

Courses Taught

Electronic Devices & Circuits, Electric Circuit Analysis, Electronics II, Fluid Mechanics, Electromechanical Systems

12. Achievements and Awards

- Awarded **Excellent Oral Presentation Certificate** at 5TH International Conference on Mechatronics and Control Engineering (ICMCE 2016) held on December 14-17, 2016, in Venice, Italy
- Participant DICE CONNECT held on **19-20 December, 2012** at University of Engineering & Technology (JET), Taxila
- Participant Fly Move & Speed Wiring Competition of PARADIGM 2012 held on **3rd April, 2012** at Air University, PAF Complex, E-9, Islamabad
- Participant Techkriti'13 Global Robotics Competition (GRC) Pakistan Round held on **6th February, 2012** at international level, India

15. Skills and Abilities

Programming and Simulation Software: MATLAB, C++ and Assembly language programming, Rockwell, PLC Programming, CNC Programming (G Codes and M Codes), FPGA coding on Xilinx® ISE, Microcontroller Programming on KIEL® and Arduino®

Computer Aided Drawing Software: Auto-CAD®, Pro-Engineering®, SolidWorks® **Simulation and Analysis Software:** Proteus®, Lab View®, Electronics Workbench®, ANSYS®, ModelSim® **Projects**

15. Bachelors Projects

- Implemented a code for Digital Clock using Xilinx and FPGA based platform
- G Codes for part Jobs on CNC Milling
- Following and maintaining distance of Robots using IR sensors and Microcontroller
- Numerical Solution of ODE's and PDE's on Matlab
- Online banking system using C++
- Measuring and displaying speed of robot using self-made optical encoder
- Engine piston working model based on engine working

Bachelors Final Year Project: Autonomous Warehouse Robot

The system developed in the project autonomously retrieves boxes placed in the shelves according to the part number fed in the system by the user. The system uses A* algorithm to determine the shortest path for retrieving the objects. Line tracking sensors were used for robot navigation. Telescoping arms mounted on the robot were used to retrieve objects from the shelves.

MS Thesis: EMG based Intermittent Position Control of Upper Limb Exoskeleton

The field of bio-Mechatronics has extended applications in rehabilitation of upper limb power assist mechanisms. Most of the work is done on EMG based control of upper limb robotic arm movements at extreme positions only. This research, in addition to attaining extreme positions has used EMG signals to attain intermittent positions of elbow between a modified range of elbow flexion and extension. Initially, two extreme and three intermittent positions are specified. EMG signals are then recorded using Myo Armband Sensor at five specified positions. Features are extracted from the logged data. Based on a combination of distinguishing features, Linear discriminant analysis (LDA) is applied for classification of three intermittent positions from one of the two extreme positions. The applicability of the research has been strengthened by generating the control commands from classified results. The control commands are given to actuate a 6 Degree of Freedom ExoArm model (*developed in PeterCorke Robotics Toolbox in MATLAB®*) through a Proportional Derivative (PD) controller. A comparison between the reference trajectory

Letter of Motivation

I am Amna Khan, currently located in Italy and looking for a doctoral position. I came across the PhD position in **Automatic Control** at **University of Lund (Department of Automatic Control)**. I would like to present my credentials. Previously I worked as Lecturer in Department of Mechatronics Engineering, Air University, Islamabad, Pakistan. I have obtained a Master of Science and Bachelor degree in Mechatronics Engineering.

It seems very interesting and aligned to my educational as well as professional background. Looking at the similarities of working with robotics, motivates me to carry out research in this domain for futuristic benefits of the society. I am confident that my research interests and qualifications are very much in line with the requirements of your well reputed and interdisciplinary group.

My research interest in **robotics, IoT, autonomous systems, statistical analysis of data sets** (acquired using biosensors), **pattern recognition** (behavior analysis), **identification of disorders** and implementation of **machine learning algorithms** or **neural networks** significantly reflects me as a potential candidate for the advertised doctoral position.

My Masters dissertation is in the field of **bio-Mechatronics**. It was based on rehabilitation of upper limb power assist mechanisms. The inspiration of this work was patients suffering from **Parkinson's**. The main idea was intention realization using **Electro myography (EMG)**. EMG signals were recorded using Myo Armband Sensor, Features were extracted from the logged data. Machine learning algorithms were utilized to identify positions. The applicability of the research was strengthened by generating the control commands from classified results, which were then used to actuate exoskeleton arm. Majority of my publications are related to diagnostic support and rehabilitation. Moreover, I have worked with **fNIRs sensor** to distinguish human brain activation in the prefrontal region of the brain from rest state.

My bachelors final year project was **autonomous warehouse robot**. The system developed in the project **autonomously** retrieved boxes placed in the shelves according to the part number fed in the system by the user. **Machine learning algorithms** were used to determine the shortest path for retrieving the objects. Robotic arms mounted on the robot were used to retrieve objects from the shelves. I have also supervised and co-supervised various projects in the field of industrial automation and bio-medical engineering.

I am very much interested to contribute through research for the health and wellbeing of special people that can enable them to improve their quality of life. I feel motivated to work with such team who is contributing towards wellbeing of society through evolving research trends.

In parallel to my research interests, I also held various administrative posts like Officer In charge Mechatronics Engineering MS Research Program, responsible for advising students with the streams of emerging technological advancements and streamline their ideas as per their area of interest before they take up their MS Thesis Research Topic. Besides, I have reviewed numerous conference and journal papers. Furthermore, I have organized number of events including International Conferences, Seminars and Hand-on Training Workshops. In addition to my professional activities, I like to stay up-to-date about new studies underway in my research area, writing research papers and moving around the world to interact with people working in different fields. I presented a paper titled **Robot Assisted Physiotherapy** Device for Knee Joint Rehabilitation at an International Conference held in Amsterdam, Netherlands from Nov 26-30, 2018. I was awarded Travel grant by Higher Education Commission (HEC) of Pakistan for traveling and presenting the above mentioned paper.

Resume is attached for reference.

Yours's Sincerely

Amna Khan

Email: amna.khan.434@hotmail.com

Ph no : +393883863976

S.No. 011013

AIR UNIVERSITY

Be it known that by virtue of the authority vested in it by law,
and upon the recommendation of the faculty, the Board of Governors has conferred upon

AMNA KHAN

the degree of

Bachelor of Mechatronics Engineering

With all rights, privileges and honours.

Awarded at Islamabad, this 31st day of March, 2016.


Registrar




Vice Chancellor

Registration No : 100434

Session: 2010-2014

Degree Completion Date: 25-Jul-2014

Prepared by :

(Tariq Ali Abbasi)
Registration Assistant

Checked by :

(Kunjad Mehmood)
Assistant Registrar



AIR UNIVERSITY

TRANSCRIPT

Bachelor of Mechatronics Engineering

Roll No: 100434
 Name: Anna Khan
 Date of Birth: June 7, 1992

FALL-2010					SEMESTER-4					SPRING-2011					SEMESTER-6						
14-SEP-10 - 04-JAN-11					26-JAN-11 - 27-MAY-11					26-JAN-11 - 27-MAY-11					SEMESTER-6						
Code	Course	Cr. Hrs	Grade	GP	Code	Course	Cr. Hrs	Grade	GP	Code	Course	Cr. Hrs	Grade	GP	Code	Course	Cr. Hrs	Grade	GP		
MA101	Calculus I	3	B+	9.00	MT242	Digital Logic Design	4	A-	14.00	MT141	Electric Circuit Analysis	4	B+	13.33							
HU101	Communication Skills	3	B+	9.00	MT111	Engineering Statics	3	C	8.00	MA107	Matrix Algebra and Differential Equations	4	A-	14.00							
MT271	Computer Aided Drawing	3	A	12.00	MA105	Multivariable Calculus	3	A-	11.00	HU116	Pakistan Studies	2	A-	7.34							
CS161	Computer Programming	4	A-	14.00	HU121	Workshop Technology	1	A-	3.67												
PH103	Physics	4	A-	14.00																	
SGPA: 3.61 CGPA: 3.61 Honors					Cr.Hrs.: 17.0					SGPA: 3.37 CGPA: 3.47 Good					Cr.Hrs.: 38.0						

FALL-2011					SEMESTER-III					SPRING-2012					SEMESTER-IV							
13-SEP-11 - 14-JAN-12					23-JAN-12 - 23-MAY-12					23-JAN-12 - 23-MAY-12					SEMESTER-IV							
Code	Course	Cr. Hrs	Grade	GP	Code	Course	Cr. Hrs	Grade	GP	Code	Course	Cr. Hrs	Grade	GP	Code	Course	Cr. Hrs	Grade	GP			
MT243	Analog Electronics	4	B+	13.33	MT245	Electromechanical Systems	4	A	16.00	MT201	Energy and Society	2	A-	7.34								
MA201	Complex Analysis	3	A-	11.00	MT162	Instrumentation and Measurement Systems	4	A	16.00	MT203	Probability Methods in Engineering	3	A	12.00								
MT2	Engineering Dynamics	3	C+	8.99	HU104	Technical Writing	3	B+	9.99	MT221	Thermodynamics	3	A	12.00								
MT220	Engineering Materials	3	A	12.00																		
HU118	Islamic Studies	2	A	8.00																		
MT214	Mechanics of Materials	4	A-	14.00																		
SGPA: 3.47 CGPA: 3.47 Good					Cr.Hrs.: 67.0					SGPA: 3.86 CGPA: 3.87 Honors					Cr.Hrs.: 76.0							

FALL-2012					SEMESTER-V					SPRING-2013					SEMESTER-VI						
01-SEP-12 - 02-JAN-13					21-JAN-13 - 06-JUN-13					21-JAN-13 - 06-JUN-13					SEMESTER-VI						
Code	Course	Cr. Hrs	Grade	GP	Code	Course	Cr. Hrs	Grade	GP	Code	Course	Cr. Hrs	Grade	GP	Code	Course	Cr. Hrs	Grade	GP		
HU114	Contemporary International Relations	2	A-	7.34	MT353	Control Engineering	4	A	16.00	MT396	Final Year Project I	1	A	4.00							
MT304	Engineering Management and Entrepreneurship	2	A	8.00	MT320	Heat and Mass Transfer	4	A-	14.00	MT305	Manufacturing Processes	3	A	12.00							
MT330	Fluid Mechanics	4	A	16.00	MT364	Mechatronics Design Lab	2	A-	7.34	MA302	Numerical Analysis and Computation	3	B+	9.99							
MT315	Machine Design	3	A-	11.00																	
MT261	Microprocessors and Microcontrollers in Mechatronics	4	B+	13.32																	
MT372	Modeling and Simulation of Dynamic Systems	3	A	12.00																	
SGPA: 3.76 CGPA: 3.61 Honors					Cr.Hrs.: 94.0					SGPA: 3.77 CGPA: 3.63 Honors					Cr.Hrs.: 111.0						

FALL-2013					SEMESTER-VII					SPRING-2014					SEMESTER-VIII						
01-SEP-13 - 14-JAN-14					20-JAN-14 - 20-MAY-14					20-JAN-14 - 20-MAY-14					SEMESTER-VIII						
Code	Course	Cr. Hrs	Grade	GP	Code	Course	Cr. Hrs	Grade	GP	Code	Course	Cr. Hrs	Grade	GP	Code	Course	Cr. Hrs	Grade	GP		
MT434	Advanced Control and Simulation Techniques	3	B+	9.99	MT424	Computer Aided Engineering	3	B	9.00	MT400	Final Year Project II	3	A	12.00							
MT464	Advanced Mechatronics	4	A-	14.00	MT408	Industrial Mechatronics	4	A	16.00	MT418	Mechanical Vibrations	3	A	12.00							
MT466	Final Year Project I	2	A	8.00	MT467	Power Electronics	4	A-	14.00												
MT460	Path Planning for Mobile Robots	4	B+	13.32																	
MT	Total Quality Management	2	A	8.00																	
SGPA: 3.60 CGPA: 3.63 Honors					Cr.Hrs.: 126.0					SGPA: 3.67 CGPA: 3.63 Honors					Cr.Hrs.: 147.0						

Credit Hrs. - Successfully Completed 147.00
 Total Credit Hours 147.00

Degree Status: **COMPLETED**

CGPA: 3.63
 Academic Standing: Honors

Obseey

Controller of Examinations
 October 01, 2014

Program Completion Date: July 25, 2014
 Session: 2010 - 2014

Muhammad

(GHULAM MUADDID)
 Air Core (Retd)
 Registrar

TRANSCRIPT INTERPRETATION

The normal duration of the undergraduate program is four years. However, students have the option to complete the program in more time depending on the workload they take. After enrollment, the program must be completed within six years. The academic year is comprised of two semesters, i.e., Spring and Fall Semester. Students are not allowed to take advanced courses in Summer.

ACADEMIC STANDING

1st Semester

CGPA	Academic Standing
3.75 ≤ CGPA < 4.00	High Honors
3.50 ≤ CGPA < 3.75	Honors
3.00 ≤ CGPA < 3.50	Good
2.50 ≤ CGPA < 3.00	Fair
2.00 ≤ CGPA < 2.50	Satisfactory
1.80 ≤ CGPA < 2.00	Warning
1.75 ≤ CGPA < 1.80	Serious Warning
1 ≤ CGPA < 1.75	Dismissal (Eligible to rejoin first Semester when offered without admission test)
CGPA < 1	Dismissal


2nd Semester Onwards

CGPA	Academic Standing
3.75 ≤ CGPA < 4.00	High Honors
3.50 ≤ CGPA < 3.75	Honors
3.00 ≤ CGPA < 3.50	Good
2.50 ≤ CGPA < 3.00	Fair
2.00 ≤ CGPA < 2.50	Satisfactory
1.80 ≤ CGPA < 2.00	Warning
1.50 ≤ CGPA < 1.80	Serious Warning
CGPA < 1.50	Dismissal


GRADING POLICY

Letter Grades	Grade Points
A	4.00
A-	3.67
B+	3.33
B	3.00
B-	2.67
C+	2.33
C	2.00
C-	1.67
D	1.00
W	Withdrawal

Prepared by:


(Hina Azeem)
Examination Assistant

Checked by:


(Anjar Mahmood)
Assistant Registrar

When signed, dated and sealed, the transcript provides a certified copy of the student's academic performance. An official, confidential transcript can only be obtained directly from the Registrar's Office, Air University, PAF Complex, Sector E-9, Islamabad, Pakistan. Tel: (0092-51) 9262557-9261781. Fax: (0092-51) 9260158. Air web: www.au.edu.pk

BAND 9**EXPERT USER**

Has fully operational command of the language: appropriate, accurate and fluent with complete understanding.

BAND 8**VERY GOOD USER**

Has fully operational command of the language with only occasional unsystematic inaccuracies and inappropriacies. Misunderstandings may occur in unfamiliar situations. Handles complex detailed organisation well.

BAND 7**GOOD USER**

Has operational command of the language, though with occasional inaccuracies, inappropriacies and misunderstandings in some situations. Generally handles complex language well and understands detailed reasoning.

BAND 6**COMPETENT USER**

Has generally effective command of the language despite some inaccuracies, inappropriacies and misunderstandings. Can use and understand fairly complex language, particularly in familiar situations.

BAND 5**MODEST USER**

Has partial command of the language, coping with overall meaning in most situations, though is likely to make many mistakes. Should be able to handle basic communication in own field.

BAND 4**LIMITED USER**

Basic competence is limited to familiar situations. Has frequent problems in understanding and expression. Is not able to use complex language.

BAND 3**EXTREMELY LIMITED USER**

Comprehends and understands only general meaning in very familiar situations. Frequent breakdowns in communication occur.

BAND 2**INTERMITTENT USER**

No real communication is possible except for the most basic information using isolated words or short formulae in familiar situations and to meet immediate needs. Has great difficulty understanding spoken and written English.

BAND 1**NON USER**

Essentially has no ability to use the language beyond possibly a few isolated words.

BAND 0**DID NOT ATTEMPT THE TEST**

No assessable information provided.

SN# 013467

AIR UNIVERSITY

Be it known that by virtue of the authority vested in it by law,
and upon the recommendation of the faculty, the Board of Governors has conferred upon

AMNA KHAN

the degree of

Master of Science in Mechatronics Engineering

With all rights, privileges and honours.

Awarded at Islamabad, this 27th day of September, 2017.


Registrar




Vice Chancellor

Registration No : 140950

Session: 2014 - 2016

Degree Completion Date: January 17, 2017

Prepared by :



(Tariq Ali Abbas)
Registration Assistant

Checked by :



(Anjaral Mehmood)
Assistant Registrar



AIR UNIVERSITY

Grade Report Master of Science in Mechatronics Engineering

Roll No: 140950
 Name: Amna Khan
 Date of Birth: June 7, 1992

FALL-2014 02-SEP-14 - 30-DEC-14 SEMESTER-I

Code	Course	Cr. Hrs	Grade	GP
MA644	Advanced Engineering Mathematics	3	B+	8.00
MT571	Advanced Robotics Mechanisms	3	B+	8.00
MT634	Control Engineering I	3	A	12.00
SGPA: 3.55 CGPA: 3.55 Good		Cr.hrs.: 9.0		

SPRING-2015 02-FEB-15 - 02-JUN-15 SEMESTER-II

Code	Course	Cr. Hrs	Grade	GP
MT622	Embedded Systems for Mechatronics	3	A	12.00
MT624	Optimization in Engineering Systems	3	A	12.00
SGPA: 4.00 CGPA: 3.73 Good		Cr.hrs.: 15.0		

FALL-2015 01-SEP-15 - 01-JAN-16 SEMESTER-III

Code	Course	Cr. Hrs	Grade	GP
MT763	Bio Robotics	3	A-	11.00
MT3020	Numerical Computing in Engineering	3	A-	11.00
SGPA: 3.67 CGPA: 3.71 Good		Cr.hrs.: 21.0		

SPRING-2016 21-JAN-16 - 18-MAY-16 SEMESTER-IV

Code	Course	Cr. Hrs	Grade	GP
MT600	Advanced Modeling and Simulation in Mechatronics	3	A	12.00
MT799	Thesis	6	B	
SGPA: 4.00 CGPA: 3.75 Honors		Cr.hrs.: 24.0		

FALL-2016 01-SEP-16 - 30-DEC-16 SEMESTER-V

Code	Course	Cr. Hrs	Grade	GP
MT799	Thesis	6	A	24.00
SGPA: 4.00 CGPA: 3.80 Honors		Cr.hrs.: 30.0		

Credit Hrs. - Successfully Completed 30.00

Total Credit Hours 30.00

Degree Status: ENROLLED

Date of Final Defense Evaluation: January 17, 2017

Title of Thesis: EMG-based Intermittent Position Control of Upper Limb Exoskeleton

Supervisor: Dr. Zareena Kausar

CGPA: 3.80

Academic Standing: Honors

* This is a computer generated report which is not valid for academic evaluation until authenticated by the Registrar.

Amjad Ali Khan
 Assistant Registrar
 AIR UNIVERSITY PAF Complex
 PAF, Islamabad



Defining futures

SCHOOL OF MECHANICAL AND MANUFACTURING ENGINEERING
NATIONAL UNIVERSITY OF SCIENCE & TECHNOLOGY

TO WHOM IT MAY CONCERN

It gives me immense pleasure to write this letter of recommendation for Amna Khan. I believe that a letter of recommendation is a serious responsibility and I write one, only when I am convinced that the candidate is right for the program that he/she is applying for. Amna has worked from January 2016 to September 2017 in Mechatronics Engineering Department at Air University, Islamabad, Pakistan. For the time frame mentioned above, Amna served as a Lab Engineer and was a MS scholar. She was promoted to Lecturer, in September 2017 and is currently employed with Department of Mechatronics Engineering, Air University in the same capacity. I have been her MS Thesis advisor and have also known her at institution level because of her affiliation with MS Mechatronics Engineering Research Program.

As an MS student, Amna was an easy to manage researcher, and she always gave that extra effort to meet deadlines. She demonstrated superior analytical capabilities in the field of Bio-robotics. She scored an 'A' grade in her MS dissertation titled EMG based Intermittent Position Control of Upper Limb Exoskeleton. Her commitment made her publish a paper during her MS research work in 5th International Conference on Mechatronics and Control Engineering (ICMCE) held from December 14-17, 2016 in Venice Italy. She was awarded best presenter award in the conference.

As a faculty member at the Department of Mechatronics Engineering, Amna carries out various administrative tasks and organizes numerous technical conferences, seminars, on and off campus robotics workshops. Also, she currently holds the post of Officer In-charge MS Mechatronics Research Program. I not only know Amna as a sound researcher but had also witnessed her management skills very closely. She was the organizer of Open House/Project Exhibition 2017 and I was invited as Judge to evaluate the Projects being displayed. She managed every matter with patience and confidence. In vein of achieving higher technological insight, Amna has always been a competent researcher and an effective individual for the department/lab she works in. She was a reviewer (*member technical committee*) in 2018 5th IEEE International Conference on Electrical and Electronics Engineering and is still part of the technical committee for the upcoming edition of the conference in April 2019.

While I will certainly cherish the working relationship I have with Amna through the years, I'm confident she will be able to make an immediate as well as positive impact on your institution/lab. If you have any questions or concerns about Amna's capabilities, experience or credentials don't hesitate to call or email me on the details given below.

I wish her the best of luck in her future projects and endeavors.

Please feel free to contact me with queries, if you have any, regarding my recommendation.




Dr. Yasar Ayaz
Head of Department
Dept of Robotics & AI
School of Mech & Mfg Engg
(SMME), NUST, Islamabad
HOD R&AI
(Dr. Yasar Ayaz)



AIR UNIVERSITY

Sector E-9, Islamabad

Ph: (+92-51) 9262557-9, 9261781 Fax: (+92-51) 9260158

Web: www.au.edu.pk

Prof. Dr. Zafar Ullah Koresbi

Senior Dean

Faculty of Engineering

Air University, Islamabad

☎ Off: +92519262557-9 Ext 213

zafar@mail.au.edu.pk

Recommendation Letter

Every year, I am approached by several dozens of students who request a recommendation letter. However, I end up recommending only a few of them. This is to recommend Amna Khan for admission to a postgraduate program in Engineering at your esteemed institution.

I have known her for more than 8 years in my capacity as Chair, Department of Mechatronics Engineering and Senior Dean, Faculty of Engineering. Amna Khan has been a full time student in the Department of Mechatronics Engineering at Air University till December 2016. She was hired as Lab Engineer/Research Assistant during the research phase of her MS dissertation in January 2016. She served as a Lab Engineer for a period of one year and six months. Amna was promoted to Lecturer, in September 2017 on open merit and is still serving at the same post.

Her MS Thesis was on: EMG based Intermittent Position Control of Upper Limb Exoskeleton. I have come across many students with a sharp understanding and knowledge of biomedical signal processing, machine learning and pattern recognition. It is the rare student who is able to develop a multi-dimensional perspective of the course of and implement in one's research work. Amna is one such rare student. She had developed a conceptual understanding of fact-based subjects like Artificial Intelligence and Machine Learning of which her MS research work is a true reflection.

She has shown the motivation, intelligence, preserving nature and analytical aptitude for graduate study. Her attendance and presence of mind has been a key part of her study program that has helped her to contribute positively while working as an individual and as part of the team in numerous research projects.

In my view, Ms Amna Khan compares favorably with the best among my students. I am sure, she will make an outstanding performance at her postgraduate studies. I recommend her in the strongest term for provision of opportunity to present position at your institution.

Zafar Ullah Koresbi

Martin Gemborn Nilsson

Doktorander i reglerteknik

Ref nr: PA2020/3049-136 Datum för ansökan: 2020-10-13 11:39



Personnummer 940603-3432
Adress Baldersgatan 5B
58244 Linköping
Östergötlands län
Sverige
E-post martin.gemborn.nilsson@gmail.com
Kön Man
Mobiltelefon 0703383943
Telefon 0703383943

Frågor

1. *Har du avlagt masterexamen?*
Nej Fel svar
2. *Vid vilket universitet har du avlagt masterexamen?*
Lund University (I do not have the degree yet, but I have successfully finished all required courses and presented the master's thesis)
3. *Ange namn på din(a) referens(er).*
Héctor Caltenco (Ericsson - Device Software Research)

Anders Robersson (LTH - Dept. of Automatic Control) - I have done some projects including the master's thesis with Anders as supervisor, so a second opinion from him might be useful to you.
4. *Vilket är det främsta skälet till att du söker denna tjänst?*
A strong interest in automatic control and many other closely related fields as well as the positive and encouraging atmosphere at the department.

Martin Gemborn Nilsson

Doktorander i reglerteknik

Ref nr: PA2020/3049-136 Datum för ansökan: 2020-10-13 11:39

Eget uppladdat CV

Egna filer och portfolio

Official-Transcript-2020-10-11-english.pdf

Official-Transcript-2020-10-11-english.pdf

Transcript-University-of-California-Santa-Barbara.pdf

Transcript-University-of-California-Santa-Barbara.pdf

DeansHonors67.pdf

DeansHonors67.pdf

Språk

svenska

Flytande

Modersmål

engelska

Flytande

Körkort



Referenser

Namn

Héctor Caltenco

Företag

Ericsson - Device Software Research

E-post

hector.caltenco@ericsson.com

Telefon

+46725078918

Namn

Anders Robertsson

Företag

LTH - Dept. of Automatic Control

E-post


anders.robertsson@control.lth.se

Telefon

0768649416

Martin Gemborn Nilsson

Electrical Engineering Student • Automatic Control

☎ (+46) 0703-383943 | ✉ martin.gemborn.nilsson@gmail.com |  LinkedIn



Application for doctoral studies in automatic control

Hi!

My name is Martin and I am currently about to finish the final year of my M.Sc. in electrical engineering here at Lund University. I have been specializing in automatic control but I am also interested in many closely related fields such as mathematics, computer science and electronics. A combination of an extensive interest in technology and the fact that I really enjoy to learn new things, make me find almost everything within the fields of science and engineering to be both exciting and fascinating.

I think doctoral studies could suit me well as it would provide further opportunities for me to continue learning new things, and thus grow on both an intellectual and a personal level. It would also feel meaningful to contribute to research, and hopefully in the long run, to society as well. In the future I see myself spending my time with new emerging technologies having potential to help society and nature. I feel that doctoral studies could be a big leap in the right direction to achieve this goal.

I am interested in this particular position mainly for two reasons. Firstly, I am familiar with the department as I have taken several courses here, including the master's thesis. I have always felt very welcome and included while also getting inspired by the positive and encouraging atmosphere. Secondly, as I previously mentioned, I have a wide interest in technology and science. I can think of no better field than automatic control where many of those areas are intersecting and overlapping, thus making it an attractive area for me.

A couple of things that permeate all my work and commitments are positivity, accuracy and cooperation. To do things thoroughly and with high precision is very important to me since I think this is a key component in being able to feel confident in and take responsibility for the work I am doing. I believe this mindset could be useful both in research and for teaching. I do like to work independently trying to solve problems, but I also put great value in good teamwork and communication. This as I know that mutual efforts and discussions can result in creative environments, possibly leading to synergies both in individual work and by cooperation in joint projects.

I hope to hear from you and I look forward to discuss and learn more about possible areas of research as well as giving you a more complete picture of me.

Best regards,

Martin Gemborn Nilsson

Martin Gemborn Nilsson

Baldersgatan 5B, 58244 Linköping, Sweden

✉ martin.gemborn.nilsson@gmail.com **in** LinkedIn ☎ (+46) 0703383943

EDUCATION

Lund University, Faculty of Engineering

M.Sc. in Electrical Engineering

- Specialising in automatic control, additional coursework in data science.

Master's Thesis - collaboration with the Swedish Sea Rescue Society

- Title: Robust Relative Positioning and Autonomous Landing for a Flying-Wing MAV
- Personal focus on control systems and landing strategy using model predictive control.

University of California Santa Barbara, College of Engineering

University of California Education Abroad Program, Deans Honors

Liljeholmens Folkhögskola

Music Studies, Jazz Ensemble

Katedralskolan, Natural Science Program

Upper Secondary School

Lund, Sweden

Aug 2014 - present

Jan 2020 - Aug 2020

Goleta, California

Sep 2017 - Jun 2018

Rimforsa, Sweden

Aug 2013 - Jun 2014

Linköping, Sweden

Aug 2010 - Jun 2013

WORK EXPERIENCE

Ericsson AB

Engineering Intern at Device Software Research

- Automation of data collection and data labeling.
- Visual-inertial SLAM in ROS environment.

SAAB AB

Summer Engineering Intern

- Geometric computations with mesh grids in Matlab.

Lunds Tekniska Högskola

Supplemental Instruction (SI) Leader

- Supplemental Instruction (SI) Leader in *Calculus in One Variable* at Lund University, Faculty of Engineering. Planning and execution of discussion exercises in mathematics for engineering students.

Adecco

Forklift Operator, holiday substitute during summers

Attendo

Elderly Care, holiday substitute during summers

Lund, Sweden

Apr 2019 - Jan 2020

Linköping, Sweden

Summer 2017

Lund, Sweden

Aug 2015 - Jan 2016

Linköping, Sweden

Jun 2014 - Sep 2015

Linköping, Sweden

Jun 2011 - Aug 2013

OTHER EXPERIENCE

Lund Formula Student

Driverless

- Camera pipeline and state estimation for the LFS20 driverless team.

Electronics and Software

- Development, construction and programming of electronic control units for the LFS19 car.

E-sektionen inom TLTH

Head of the Social Committee

- Member of the board of the E-guild at Lund University, Faculty of Engineering.
- Responsible for planning and executing of social events, mainly for members of the E-guild.

Lund, Sweden

Sep 2019 - May 2020

Aug 2018 - Aug 2019

Lund, Sweden

Jan 2016 - Dec 2016

SKILLS

Programming Languages

Matlab, Python, C++, Java

Software & Tools

ROS, git, LaTeX, Simulink, Eagle - PCB design

LANGUAGES

Swedish

Native Language

English

Fluent

French

Basic Skills

OTHER

Driver's License, B

Forklift Operating Licence, A and B

Official-Transcript-2020-10-11-english.pdf

**The file could not be included.
This can be because the file is protected.
Please check the original file!**

University of California, Santa Barbara

Office of the Registrar, Santa Barbara, CA 93106-2011

PRINTED: 07/09/18

OFFICIAL TRANSCRIPT

PAGE: 1

STUDENT NAME: WALTER ERIC JO SEMBORN NILSSON

PERM NUMBER: 647118

SSN

Birth Date: 06/02/84

LAST ACTIVE ACADEMIC PROGRAM:

COLLEGE: College of Engineering
OBJECTIVE: No Objective
MAJOR: Undeclared (Engineering)

COURSE	TITLE	GRADE	COMPLETE		GRADE POINTS	GPA
			UNITS	UNITS		
2017 Fall Quarter EAP Reciprocity student						
ENR19	10 ANTARCTICA	A+	4.0	4.0	16.00	
EE	176 INTRO DIG IMAGE	A	4.0	4.0	16.00	
ES	1- 24A ELEMENTARY GOLF	F	0.5	0.0	0.00	
ES	1- 408 INTERMED VOLLEYBALL	F	0.5	0.0	0.00	
ME	179D ROBOTICS: CONTROL	A	4.0	4.0	16.00	
Quarterly Total:			12.0	12.0	48.00	4.00 Dean's Honors
THRU F17 Total:			12.0	12.0	48.00	4.00
2018 Winter Quarter EAP Reciprocity student						
ASTRO	1 BASIC ASTRONOMY	A+	4.0	4.0	16.00	
CMPE	100A DATA STRUCT ALGOR	B+	4.0	4.0	13.20	
EE	181 INTRO COMP VISION	A+	4.0	4.0	16.00	
ES	1- 49 LIFE/EN ACT INVERTE	F	0.5	0.0	0.00	
ME	22A NONLINEAR CONT. SYS	B-	4.0	4.0	14.80	
Quarterly Total:			16.5	16.0	60.00	3.75 Dean's Honors
THRU W18 Total:			28.5	28.0	108.00	3.85
2018 Spring Quarter EAP Reciprocity student						
CMPE	161B MACHINE LEARNING	A+	4.0	4.0	16.00	
ES	1- 24A ELEMENTARY SWIMMING	F	0.5	0.0	0.00	
ME	125 INTRO MACHINE SHOP	A+	3.0	3.0	12.00	
ME	104A ADV WECH ENGR LAB	A	2.0	2.0	12.00	
ME	179P ROBOTICS: PLANNING	A+	4.0	4.0	16.00	
Quarterly Total:			12.5	12.0	48.00	4.00 Dean's Honors
THRU S18 Total:			42.0	40.0	156.00	3.90
UC Credit Limited Total:			42.0	40.0	156.00	3.90

** END OF RECORD **

THE REGISTRAR'S WHITE SIGNATURE IS IMPOSED UPON A LIGHT BLUE INSTITUTIONAL SEAL. THE DOCUMENT SHOULD BE REJECTED IF EITHER IS DISTORTED.

ISSUED TO

EAP RECIPROCALITY

Leesa Beck
University Registrar

This officially sealed and signed transcript is printed on blue security paper with the signature printed in white. A raised seal is not required. When photocopied, a security statement containing the name of the institution will appear. A BLACK ON WHITE OR A COLOR COPY SHOULD NOT BE ACCEPTED!

UNIVERSITY OF CALIFORNIA • SANTA BARBARA

TRANSCRIPT GUIDE

UNITS OF CREDIT

Until September 1966, credits were recorded as semester units. Since that time, the University of California, Santa Barbara has operated on a quarter calendar, with three quarters per academic year and an optional summer session. Each quarter has ten weeks of instruction at the rate of one unit for every three hours of student work required each week.

CURRENT GRADING SYSTEM

The grades A, B, C, and D may be modified by plus (+) or minus (-) suffixes. Grade points for each unit are assigned as follows:

A+ = 4.0	A = 4.0	A- = 3.7
B+ = 3.3	B = 3.0	B- = 2.7
C+ = 2.3	C = 2.0	C- = 1.7
D+ = 1.3	D = 1.0	D- = 0.7

Grades of F, I, IP, P, NP, S, U and W = 0.0 grade points

Unit credit, but not grade-point credit, is assigned for P and S grades.

P = Passed (C- or better)	Undergraduate Course Only
NP = Not Passed (C- or below)	Undergraduate Course Only
S = Satisfactory (B or better)	Graduate Course Only
U = Unsatisfactory (B- or below)	Graduate Course Only
I = Incomplete	
W = Withdrawal after established deadline	
IP = Grade to be assigned at the end of the final course in the sequence	

GOOD ACADEMIC STANDING

A student is in good standing academically unless otherwise indicated.

TRANSFER CREDIT

Only credit that is accepted by the University is shown on the transcripts of UCSB students. Credit from other UC campuses may be shown either by individual course records or as a unit summary by campus. Individual courses from schools outside of the UC system are not shown.

ADVANCED PLACEMENT CREDIT

Examinations and the credits accepted for them are shown on the transcript in the same format and location as transfer credit.

COURSE NUMBERING SYSTEM

1 - 99	Lower Division Courses
100 - 199	Upper Division Courses
200 - 299	Graduate Courses
300 - 399	Professional courses for teachers
400 & above	Other professional and graduate courses

REPEATED COURSES

An undergraduate student may repeat only those courses for which an NP or letter grade of C- or lower is recorded. If the grade from a previous attempt had been included in the GPA calculations, its effect is then removed by a "repeat adjustment" up to a maximum of 16 units over the student's career.

ACCREDITATION

Western Association of Schools and Colleges (WASC)

TO TEST FOR AUTHENTICITY: Translucent globe icons AU, SJ be visible from both sides when held toward a light source. The face of this transcript is printed on blue SCRIP-SAFE® paper with the name of the institution appearing in white type over the face of the entire document.

UNIVERSITY OF CALIFORNIA-SANTA BARBARA • UNIVERSITY OF CALIFORNIA-SANTA BARBARA • UNIVERSITY OF CALIFORNIA-SANTA BARBARA
UNIVERSITY OF CALIFORNIA-SANTA BARBARA • UNIVERSITY OF CALIFORNIA-SANTA BARBARA • UNIVERSITY OF CALIFORNIA-SANTA BARBARA
UNIVERSITY OF CALIFORNIA-SANTA BARBARA • UNIVERSITY OF CALIFORNIA-SANTA BARBARA • UNIVERSITY OF CALIFORNIA-SANTA BARBARA

ADDITIONAL TESTS: When photocopied, the institutional NAME and the words COPY COPY will appear prominently on alternating lines on the face of the entire document, and in the signature box. ALTERATION OR FORGERY OF THIS DOCUMENT MAY BE A CRIMINAL OFFENSE! A black on white or a color copy is not an original and should not be accepted as an official institutional document. This transcript cannot be released to a third party without the written consent of the student. This is in accordance with the Family Educational Rights and Privacy Act of 1974, as amended. If you have any questions about this document, please contact the UCSB Office of the Registrar at (805) 893-2681.

09/01/99

SCRIP-SAFE® Security Products, Inc., Cincinnati, OH 45226-3171-099

UNIVERSITY OF CALIFORNIA, SANTA BARBARA

BERKELEY • DAVIS • IRVINE • LOS ANGELES • MERCED • RIVERSIDE • SAN DIEGO • SAN FRANCISCO
SANTA CRUZ



SANTA BARBARA •

Glenn E. Beltz
Associate Dean for Undergraduate Studies
College of Engineering
Santa Barbara, California 93106-5130

beltz@engineering.ucsb.edu

(805) 893-3354 Phone
(805) 893-8124 Fax

June 27, 2018

Dear Martin,

Congratulations on earning grades during the fall 2017, winter 2018, and spring 2018 quarters which placed you on the College of Engineering Dean's Honors List.

The criterion for such recognition is a quarter grade point average of at least 3.5 while completing a minimum of 12 letter-graded units.

My colleagues and I know how challenging and rigorous the academic curriculum is, and how much is expected of the average student in terms of workload. It is especially encouraging and gratifying to see students not only meet these high expectations, but also to receive academic honors because of their efforts.

Once again, congratulations – keep up the good work.

Best wishes,

A handwritten signature in blue ink that reads "Glenn E. Beltz".

Glenn E. Beltz
Associate Dean for Undergraduate Studies
Professor, Mechanical Engineering

Hossein Abdi

PhD students in Automatic Control

Ref nr: PA2020/3049-99 Application date: 2020-10-24 16:52



Date of birth 1994-01-31
Address C/O: Hossein Abdi
NO. 31, Eastern 4th Street, Shohadaye 7 Tir town, 5th Square
3176775141 Fardis, Alborz
Iran
Email address mr.hossein.abdi@gmail.com
Gender Male
Mobile phone +989369016997
Phone +982636530109

Questions

1. *Do you have a master's degree?*
Yes

Correct answer

2. *From which university is your master's degree?*
Sharif University of Technology

3. *Give the name(s) of your reference(s).*

- Dr. Hossein Nejat Pishkenari
Associate Professor
Department of Mechanical Engineering, Sharif University of Technology
Email: nejat@sharif.ir
- Prof. Hassan Salarieh
Professor
Department of Mechanical Engineering, Sharif University of Technology
Email: salarieh@sharif.ir
- Dr. Azadeh Kebriaee
Assistant Professor
Department of Aerospace Engineering, Sharif University of Technology
Email: kebriaee@sharif.edu

4. *What is your main reason for applying for this position?*
Continuing my study in a Ph.D. program and pursuing postdoctoral research at a high rank university with a high quality education and research system

Hossein Abdi

PhD students in Automatic Control

Ref nr: PA2020/3049-99 Application date: 2020-10-24 16:52

The person has uploaded a CV

Files and portfolio

Hossein Abdi-SOP.pdf

Hossein Abdi-SOP.pdf

Transcript (MSc and BSc).pdf

Transcript (MSc and BSc).pdf

International Program.pdf

International Program.pdf

Certification (Oral Presentation).pdf

Certification (Oral Presentation).pdf

Education

Title	University / College/Company	City	Country	From-To
International Summer Program	National Research University	Saint Petersburg	Russian Federation	2019-2019
	<i>International Summer Program (Summer 2019)</i>			
	<ul style="list-style-type: none">• <i>Field: Modern Machine Learning</i>• <i>National Research University, Saint Petersburg, Russia</i>• <i>Grade: 10/10 (A+)</i>			
M.Sc. in Mechanical Engineering	Sharif University of Technology	Thran	Iran	2017-2019
	<i>M.Sc. in Mechanical Engineering (2017-2019)</i>			
	<ul style="list-style-type: none">• <i>Field: Applied Mechanics (Control & Dynamics)</i>• <i>Sharif University of Technology, Tehran, Iran</i>• <i>Thesis Title: Control of Swarm Micro-Swimmers in the Low-Reynolds Number Fluid to Reduce Energy Consumption</i>• <i>Supervisor: Dr. Hossein Nejat Pishkenari</i>• <i>GPA: 4/4</i>			
Double Major B.Sc. in Mechanical Engineering & Aerospace Engineering	Sharif University of Technology	Thran	Iran	2012-2017
	<i>Double Major B.Sc. in Mechanical Engineering & Aerospace Engineering (2012-2017)</i>			
	<ul style="list-style-type: none">• <i>Sharif University of Technology, Tehran, Iran</i>• <i>Thesis Title: Dynamic Modeling and Designing a Dynamic Based Control Algorithm for Legged Quadruped Robot Locomotion</i>• <i>Supervisor: Dr. Hassan Salarieh</i>• <i>GPA: 3.88/4</i>			
High School	Allameh Helli	Thran	Iran	2008-2012
	<i>High School (2008-2012)</i>			
	<ul style="list-style-type: none">• <i>Major: Mathematics and Physics</i>• <i>National Organization for Development of Exceptional Talents (NODET)</i>• <i>GPA: 4/4</i>			

Work experience

Hossein Abdi

PhD students in Automatic Control

Ref nr: PA2020/3049-99 Application date: 2020-10-24 16:52

Title	Company	City	Country	From-To
NDT Ultrasonic Design	Iran's National Elites Foundation (INEF) <i>NDT Ultrasonic Design (January 2019 – September 2019)</i> <i>Mechanical Engineer at NDT Ultrasonic Design Project under supervision of Dr. Nejat & Prof. Salarieh at Sharif University of Technology, Tehran, Iran. Supported by INEF.</i>	Thran	Iran	2019-2019
Research Assistant	Sharif University of Technology <i>Research Assistant, under supervision of Dr. Nejat, at Nano Robotics Laboratory, Department of Mechanical Engineering, Sharif University of Technology, Tehran, Iran</i>	Thran	Iran	2017-Current
CubeSat Design and Fabrication	Iranian Space Agency (ISA) <i>CubeSat Design Competition (April 2016 – November 2017)</i> <i>Head of Thermal Control subsystem at SUTAC group (Sharif University of Technology) under supervision of Dr. Asadian, The Competition held by Iranian Space Agency (ISA)</i>	Thran	Iran	2016-2017
Teaching Assistant	Sharif University of Technology <i>Dynamics: Dr. Nejat, Fall 2018</i> <i>Dynamics of Machinery: Prof. Zohoor, Spring 2018</i> <i>Engineering Graphics: Dr. Haghshenas, Fall 2017</i> <i>Thermodynamics II: Dr. Kebriaee, Fall 2016</i> <i>Thermodynamics I: Dr. Kebriaee, Spring 2016</i>	Thran	Iran	2016-2018
Trainee Student	MAPNA Turbine Engineering and Manufacturing Company <i>MAPNA Turbine Engineering and Manufacturing Company (TUGA)</i> <i>Trainee Student in R&D (Combustion Chamber Design Section) under supervision of Dr. Kebriaee, July 2015 – September 2015</i>	Thran	Iran	2015-2015

Course

Title	University / College	City	Year
AI For Everyone	<i>AI For Everyone</i> <i>Prof. Andrew Ng, (In Progress)</i>		2020
Fundamentals of Reinforcement Learning	<i>Fundamentals of Reinforcement Learning</i> <i>Dr. Martha White & Dr. Adam White, University of Alberta, (In Progress)</i>		2020
Neural Networks and Deep Learning	<i>Neural Networks and Deep Learning</i> <i>Prof. Andrew Ng, (In Progress)</i>		2020
Advanced Python Programming	<i>Advanced Python Programming</i> <i>July 2019 – August 2019</i>		2019
Introduction to IOT	<i>Introduction to IOT</i> <i>July 2019</i>		2019
Machine Learning	Stanford University <i>Machine Learning</i> <i>Prof. Andrew Ng, Stanford University, April – June 2019</i>		2019
Intelligent Systems	Sharif University of Technology <i>Dr. Boroushaki, Sharif University of Technology, Spring 2018</i>		2018
Mechatronics	Sharif University of Technology		2018

Hossein Abdi

PhD students in Automatic Control

Ref nr: PA2020/3049-99 Application date: 2020-10-24 16:52

Nonlinear Control	<i>Prof. Vossoughi, Sharif University of Technology, Fall 2018</i> Sharif University of Technology	2018
Robust Control	<i>Prof. Vossoughi, Sharif University of Technology, Spring 2018</i> Sharif University of Technology	2018
Advanced Control	<i>Dr. Moradi, Sharif University of Technology, Spring 2018</i> Sharif University of Technology	2017
Advanced Dynamics	<i>Dr. Salarieh, Sharif University of Technology, Fall 2017</i> Sharif University of Technology	2017
Robotics	<i>Dr. Nejat Pishkenari, Sharif University of Technology, Fall 2017</i> Sharif University of Technology <i>Dr. Behzadipour, Sharif University of Technology, Fall 2016</i>	2016

Certifications

Title	University / College	Year
A jump start workshop on Deep learning for driverless cars	Sharif University of Technology	2019
Modern Machine Learning	National Research University, Saint Petersburg, Russia <i>International Summer Program (Summer 2019)</i> <ul style="list-style-type: none">• <i>Field: Modern Machine Learning</i>• <i>National Research University, Saint Petersburg, Russia</i>• <i>Grade: 10/10 (A+)</i>	2019
PLC (S7-300/400)	Sharif University of Technology	2019
Wearable biomedical device development	Sharif University of Technology	2019

Publications

Title	Publisher	City	Year
Controlled Swarm Motion of Self-Propelled Microswimmers for Energy Saving	Journal of Micro-Bio Robotics		2020
Reinforcement Learning Control of a High Maneuverable Microswimmer	<i>Abdi, H., H. Nejat Pishkenari. "Controlled Swarm Motion of Self-Propelled Microswimmers for Energy Saving." Journal of Micro-Bio Robotics. (under review)</i>		2020
Dynamic modeling and Designing a dynamic based control algorithm for legged quadruped robot locomotion	<i>Abdi, H., H. Nejat Pishkenari. "Reinforcement Learning Control of a High Maneuverable Microswimmer." (ongoing project)</i> Modares Mechanical Engineering		2019
Optimal Control of a	<i>Abdi, H., M. J. Shaker Arani, H. Salarieh, and M. M. Kakaei. "Dynamic modeling and Designing a dynamic based control algorithm for legged quadruped robot locomotion." Modares Mechanical Engineering 19, no. 11 (2019): 2635-2644.</i>		

Hossein Abdi

PhD students in Automatic Control

Ref nr: PA2020/3049-99 Application date: 2020-10-24 16:52

High Maneuverable
Micro-Swimmer in
Low Reynolds Number
Flow to Reduce Energy
Consumption

7th RSI International Conference on
Robotics and Mechatronics
ICRoM'19

2019

Abdi, H., H. Nejat Pishkenari. "Optimal Control of a High Maneuverable Micro-Swimmer in Low Reynolds Number Flow to Reduce Energy Consumption." 7th RSI International Conference on Robotics and Mechatronics ICRoM'19.

Language

Persian	Fluent	<i>Native language</i>
English	Fluent	

Websites

http://www.en.sharif.edu/	Sharif University of Technology
https://spb.hse.ru/en/	National Research University, Saint Petersburg, Russia
https://www.linkedin.com/in/hossein-abdi-b7389a116/	Linkedin
https://www.researchgate.net/profile/Hossein_Abdi5	Researchgate

References

Name	Dr. Hossein Nejat Pishkenari
Company	Department of Mechanical Engineering, Sharif University of Technology
Email address	nejat@sharif.ir
Phone	-
Name	Prof. Hassan Salarieh
Company	Department of Mechanical Engineering, Sharif University of Technology
Email address	salarieh@sharif.ir
Phone	-
Name	Dr. Azadeh Kebriaee
Company	Department of Aerospace Engineering, Sharif University of Technology
Email address	kebriaee@sharif.edu
Phone	-



To whom it may concern,

I am writing to express my interest in doing research at the **Faculty of Engineering, LTH** in the **Lund University**. I have reviewed your vacancies website, and found the Ph.D. position in **Automatic Control**. I found that interesting and aligned with my current research.

I'm majoring in Mechanical Engineering at Sharif University of Technology. My M.Sc. thesis focused on **optimal control of multi-agent micro-robots**, and the B.Sc. thesis centralized on **control of legged robots**. In parallel with my thesis work, I have published journal and conference papers as the first author, and become top participant in the international summer program on **Modern Machine Learning** in Russia. Nowadays, I am working on reinforcement learning control of a micro-robot, as a researcher at the Nano Robotics Laboratory, in collaboration with my supervisor Dr. Nejat.

During my Master and Bachelor program, I have taken courses related to control, dynamics, and robotics such as **Nonlinear Control, Robust Control, Advanced Automatic Control, Mechatronics, Intelligent Systems, and Robotics**. Additionally, I have been trying to increase my knowledge, and keep myself updated on Artificial Intelligence and Learning methods by self-studying or taking online courses on **Machine Learning, Reinforcement Learning, and Advanced Python Programming**.

Based on my research and academic background, I think the Ph.D. position is aligned with my experience and academic goals. So, I would like to join your team and continue my studies in Ph.D. program at the **Faculty of Engineering, LTH** in the **Lund University**. I would appreciate it if you would consider my application.

Yours Sincerely,

Hossein Abdi

Nano Robotics Laboratory,
Department of Mechanical Engineering
Sharif University of Technology, Tehran, Iran

Email: Mr.Hosein.Abdi@gmail.com

Hossein Abdi



General Information

Email: Mr.Hossein.Abdi@gmail.com

Phone: +989369016997

Address: Nano Robotics Laboratory,
Department of Mechanical Engineering,
Sharif University of Technology, Tehran, Iran.



Education

- **International Summer Program (Summer 2019)**
 - Field: **Modern Machine Learning**
 - National Research University, Saint Petersburg, Russia
 - Grade: **10/10 (A+)**

- **M.Sc. in Mechanical Engineering (2017-2019)**
 - Field: Applied Mechanics (Control & Dynamics)
 - Sharif University of Technology, Tehran, Iran
 - Thesis Title: **Control of Swarm Micro-Swimmers in the Low-Reynolds Number Fluid to Reduce Energy Consumption**
 - Supervisor: Dr. Hossein Nejat Pishkenari
 - GPA: **4/4**

- **Double Major B.Sc. in Mechanical Engineering & Aerospace Engineering (2012-2017)**
 - Sharif University of Technology, Tehran, Iran
 - Thesis Title: **Dynamic Modeling and Designing a Dynamic Based Control Algorithm for Legged Quadruped Robot Locomotion**
 - Supervisor: Dr. Hassan Salarieh
 - GPA: **3.88/4**

- **High School (2008-2012)**
 - Major: Mathematics and Physics
 - **National Organization for Development of Exceptional Talents (NODET)**
 - GPA: **4/4**

Honor & Award

- **Gold Medal (First Rank) in the Olympiad** of Mechanical Engineering, among top undergraduate students in Iran.
- **Merit-Based Admission Offer to Ph.D. Program** in Mechanical Engineering at Sharif University of Technology
- **Merit-Based Admission Offer to M.Sc. Program** in both Mechanical Engineering and Aerospace Engineering at Sharif University of Technology
- **Top 5% GPA** among all **graduate** students in the **Mechanical** Engineering Department
- **Top 5% GPA** among all **undergraduate** students in both **Mechanical** and **Aerospace** Engineering Department
- **Rank 10th** in the Nationwide **Mechanical Engineering** Entrance Examination of **M.Sc.** Program among more than 20'000 participants in Iran
- **Rank 4th** in the Nationwide **Aerospace Engineering** Entrance Examination of **M.Sc.** among more than 2'000 participants in Iran
- **Rank 149th** in the Nationwide Entrance Examination of **B.Sc.** among more than 260'000 participants in Iran
- Selected as a member of **Iran's National Elites Foundation (INEF)** based on outstanding academic and research background and Receiving INEF's **Scholarship** as an **honor student**, 2014-Present
- **Double Major B.Sc. Program** at Sharif University of Technology
- **Admitted** to study at Allameh Helli **High School** under supervision of **NODET** (National Organization of Developing Exceptional Talents) in Iran

Publication

➤ **Journal Papers:**

- **Abdi, H.**, H. Nejat Pishkenari. "Controlled Swarm Motion of Self-Propelled Microswimmers for Energy Saving." *Journal of Micro-Bio Robotics*. (under review)
- **Abdi, H.**, H. Nejat Pishkenari. "Reinforcement Learning Control of a High Maneuverable Microswimmer." (ongoing project)
- **Abdi, H.**, M. J. Shaker Arani, H. Salarieh, and M. M. Kakaei. "Dynamic modeling and Designing a dynamic based control algorithm for legged quadruped robot locomotion." *Modares Mechanical Engineering* 19, no. 11 (2019): 2635-2644.

➤ **Conference Papers:**

- **Abdi, H.**, H. Nejat Pishkenari. "Optimal Control of a High Maneuverable Micro-Swimmer in Low Reynolds Number Flow to Reduce Energy Consumption." *7th RSI International Conference on Robotics and Mechatronics ICRoM'19*.

Research Interests

- Machine Learning
- Micro/Nano-Robotic
- Intelligent Control
- Swarm Formation of Multi-agent Systems
- Mechatronics & Robotics

Academic Experience

- **Research Assistant (2017-Present)**
 - Nano Robotics Laboratory, Department of Mechanical Engineering, Sharif University of Technology, Tehran, Iran
- **Teaching Assistant**
 - **Dynamics:** Dr. Nejat, Sharif University of Technology, Fall 2018
 - **Dynamics of Machinery:** Prof. Zohoor, Sharif University of Technology, Spring 2018
 - **Engineering Graphics:** Dr. Haghshenas, Sharif University of Technology, Fall 2017
 - **Thermodynamics II:** Dr. Kebriaee, Sharif University of Technology, Fall 2016
 - **Thermodynamics I:** Dr. Kebriaee, Sharif University of Technology, Spring 2016
- **International Conference Committee Member (November 2019)**
 - Volunteer in the student committee of the 7th RSI International Conference on Robotics and Mechatronics ICROM'19 (IEEE), Sharif University of Technology, Tehran, Iran

Professional Experience

- **NDT Ultrasonic Design (January 2019 – September 2019)**
Mechanical Engineer at **NDT Ultrasonic Design** Project under supervision of Dr. Nejat & Prof. Salarieh at Sharif University of Technology, Tehran, Iran. Supported by **INEF**.
- **CubeSat Design Competition (April 2016 – November 2017)**
Head of Thermal Control subsystem at SUTAC group (Sharif University of Technology) under supervision of Dr. Asadian, The Competition held by **Iranian Space Agency (ISA)**
- **MAPNA Turbine Engineering and Manufacturing Company (TUGA)**
Trainee Student in R&D (Combustion Chamber Design Section) under supervision of Dr. Kebriaee, July 2015 – September 2015

Educational Workshop

- **A jump start workshop on Deep learning for driverless cars**
Sharif University of Technology, November 2019
- **Wearable biomedical device development**
Sharif University of Technology, November 2019

- **An Introduction to AI and Python programming**
Sharif University of Technology, April 2019
- **Ultrasound Imaging with Born Approximations and Compressive Sensing**
Sharif University of Technology, December 2018
- **PLC (S7-300/400)**
Sharif University of Technology, July 2019
- **Satellite Thermal Analysis by Thermal Desktop & Sinda**
Iranian Space Agency (ISA), May 2017

Online Courses

- **Machine Learning**
Prof. Andrew Ng, Stanford University, April – June 2019
- **Neural Networks and Deep Learning**
Prof. Andrew Ng, (In Progress)
- **Fundamentals of Reinforcement Learning**
Dr. Martha White & Dr. Adam White, University of Alberta, (In Progress)
- **AI For Everyone**
Prof. Andrew Ng, (In Progress)
- **Advanced Python Programming**
July 2019 – August 2019
- **Introduction to IOT**
July 2019

Selected Courses

- **Intelligent Systems:** Dr. Boroushaki, Sharif University of Technology, Spring 2018
- **Mechatronics:** Prof. Vossoughi, Sharif University of Technology, Fall 2018
- **Nonlinear Control:** Prof. Vossoughi, Sharif University of Technology, Spring 2018
- **Advanced Control:** Dr. Salarieh, Sharif University of Technology, Fall 2017
- **Advanced Dynamics:** Dr. Nejat Pishkenari, Sharif University of Technology, Fall 2017
- **Robotics:** Dr. Behzadipour, Sharif University of Technology, Fall 2016

Selected Course Projects

- **Inverted Pendulum Control** (Mechatronics Lab)
- **Optimization by GA Controller to Reduce Energy of the Micro-Robot** (Intelligent Systems)
- **Nonlinear Control of a Biped Robot** (Nonlinear Control)
- **Puma Robot Simulation** (Robotics)
- **Sudoku Programming by C Language** (Fundamental of Programming)

Skills & Ability

- **Programming:** MATLAB/Simulink, Python, C/C++
- **Engineering Software:** SolidWorks, Fluent & Gambit, Maple, AutoCAD, COMSOL, CATIA, Thermal Desktop & Sinda, Proteus, EES
- **Ability:** Decision Making, Teamwork, Time Management, Adaptability, Flexibility

Language

- **Persian:** Native
- **English:** Fluent (Preparing for TOEFL exam)
- **Arabic:** Elementary

Favorite Activity and Hobby

- Twitter
- Traveling
- Free Discussion
- Book Reading
- Swimming
- Biking
- Soccer

Reference

- **Dr. Hossein Nejat Pishkenari**
Associate Professor
Department of Mechanical Engineering, Sharif University of Technology
Email: nejat@sharif.ir
- **Prof. Hassan Salarieh**
Professor
Department of Mechanical Engineering, Sharif University of Technology
Email: salarieh@sharif.ir
- **Dr. Azadeh Kebriaee**
Assistant Professor
Department of Aerospace Engineering, Sharif University of Technology
Email: kebriaee@sharif.edu
- **Prof. Hassan Zohoor**
Professor
Department of Mechanical Engineering, Sharif University of Technology
Email: zohoor@sharif.edu

Statement of Purpose

Hossein Abdi

To whom it may concern,

I was born in an educated Persian family with strong social values of hard work and resilience in the face of adversity. I have a twin and an old brother. During our childhood, our parents took their most effort to educate us. They always counseled us to study hard and keep our mind disengaged from the existing difficulties. Consequently, currently, my old brother is a professor at one of the best universities in Iran and both my twin brother and I have graduated from the high rank universities in the country.

Back to my childhood, I was always among top students in both elementary and secondary school. When I was fifteen, I was admitted by **NODET (National Organization for Developing Exceptional Talents)** to enter the Allame Helli high school which is a school with a different curriculum for talented students. After four years being the first rank student at high school, since every prospective undergraduate student has to take nationwide university entrance exam (Konkoor) in Iran, I participated in the Konkoor in 2012, and ranked 149th out of more than 260,000 participants in the country. So, I achieved the chance to study my undergraduate program at **Sharif University of Technology (SUT)**, ranked first in Iran.

Due to my deep interest in Mechanical and Aerial systems, I decided to continue my study in double major B.Sc. program, in both Mechanical Engineering and Aerospace Engineering. During my undergraduate program, I was trying my best. Therefore, I was always among high GPA, and top undergraduate students. Hence, based on my outstanding academic and research achievements, I was selected as a member of **Iran's National Elites Foundation (INEF)** in 2014, and have been receiving INEF's **Scholarship** as an honor student since 2014. In the final year of my B.Sc. program, I gained **Gold Medal** (first rank) in the Iranian National Mechanical Engineering **Olympiad** which is a very tricky and competitive exam held among nationwide top undergraduate students. In principle, it became a motivation for me to continue my studies on Mechanical Engineering in future!

To continue my studies in M.Sc. program, I had a **Merit-Based Admission** offer from the department of Mechanical Engineering at SUT. Nonetheless, to evaluate my knowledge and academic background, I participated in the nationwide entrance exam for M.Sc. program, and honorably, gained rank 10th and 4th in Mechanical Engineering and Aerospace Engineering respectively, among more than 20000 participants in the country. Based on my interest in Control of Dynamical systems, and gaining a professional experience on **Robotics** in my **B.Sc. project**, finally, I decided to continue my M.Sc. program in the field of **Applied Mechanics (Control & Dynamics)** at SUT.

During my M.Sc. studies, I was trying to take fundamental courses which were also relevant to hot ongoing research topics of my field such as Intelligent Systems, Nonlinear Control, Advanced Control, Advanced Dynamics, and Mechatronics in which various mathematical and practical aspects of control of dynamic systems methods were discussed and developed. Because of my enthusiasm in research at the cutting edge of knowledge, I defined my M.Sc. thesis on the Micro-Robotics with the title of “**Control of Swarm Micro-Swimmers in the Low-Reynolds Number Fluid to Reduce Energy Consumption.**” In my thesis, which was under supervision of Dr. Hossein Nejat, I have used optimal multi-agent control method to control motion of a swarm Micro-Swimmers in order to reduce their energy consumption.

Along with the classes I have attended, I have been trying to expand my knowledge, and keep myself updated on **Intelligent Control Methods** by self-studying, participating in workshops, and taking online courses on **Artificial Intelligence, Machine Learning, Reinforcement Learning, and Advanced Python Programming**. To enrich my knowledge and gain a professional background on this area, in summer 2019, I participated to an **International Summer Program on Modern Machine Learning at National Research University in Saint Petersburg, Russia**, and honorably gained full mark and became top participant.

In parallel with my B.Sc. and M.Sc. program, I have published journal and conference papers as the first author. Nowadays, I am working on reinforcement learning control of a micro-robot, as a researcher at the **Nano Robotics Laboratory**, in collaboration with my supervisor Dr. Nejat.

Personally, I believe that continuing the study in a Ph.D. program and pursuing a postdoctoral research at a high rank university with a high quality education and research system is the first step toward chasing my childhood dream which is becoming a great researcher and professor. Therefore, although, I have currently an admission offer for Ph.D. program at SUT, I am looking for a Ph.D. position in a much better university with more research potentials for graduate students. Regarding my research interests which focus on **Control of Dynamic Systems**, this is a big chance for me to research on my favorite subjects at the **Lund University** because the research being carried out at your **Faculty of Engineering** in the fields of **Automatic Control** is both diverse and exhaustive. I am aware that joining your university involves working diligently, and I can assure you that I am absolutely motivated and totally prepared.

Yours Sincerely,

Hossein Abdi

SHARIF UNIVERSITY OF TECHNOLOGY
UNOFFICIAL TRANSCRIPT

Page 1 of 1
ISSUED ON: 11.26.2019

LAST NAME: KHU
FIRST NAME: MOHAMMAD
M. S. 1994
M. S. NO. 901 0040942
CUA ID: 901

STUDENT NUMBER: 9000021
DEPT: MECHANICAL ENG
PROGRAM NAME: MECHANICAL ENGINEERING
MAJOR: APPLIED DESIGN

COURSE NO.	COURSE TITLE	UNITS	GRADE	COURSE NO.	COURSE TITLE	UNITS	GRADE
26.201	MECH (LABORATORY)	3	199	26.461	MSC THESIS	6	P_YO
26.361	ADV. FLUID CONTROL	3	18.2	SEMESTER UNITS AVERAGE			
26.366	ADV. DYNAMICS	3	18.2				
SEMESTER UNITS AVERAGE				TOTAL UNITS GAINED (CUM. AVG)			
TOTAL UNITS GAINED (CUM. AVG)				TOTAL UNITS GAINED & DPN EXCLUDING COURSES FAILED AND PASSED AFTERWARDS			

SPRING SEM 2018-2019							
26.261	MECHANISMS	3	19.8	NO ENTRY BELOW THIS LINE			
26.264	ROBUST CONTROL	3	18.0				
26.265	NON-LINEAR CONTROL	3	18.8	SEMESTER UNITS AVERAGE			
44.332	INTELLIGENT SYS	3	17.6				
SEMESTER UNITS AVERAGE				TOTAL UNITS GAINED (CUM. AVG)			

FALL SEM 2018-2019							
26.110	MECHANISMS LAB	3	18.0	SEMESTER UNITS AVERAGE			
26.111	MECHATRONICS	3	18.2				
26.401	ROBOTS	3	18.2	TOTAL UNITS GAINED (CUM. AVG)			
26.366	MSC THESIS	6	P_YO				
SEMESTER UNITS AVERAGE				TOTAL UNITS GAINED (CUM. AVG)			

SPRING SEM 2014-2015							
26.266	MSC THESIS	6	P_YO	SEMESTER UNITS AVERAGE			
SEMESTER UNITS AVERAGE				TOTAL UNITS GAINED (CUM. AVG)			

W	Withdraw	J	In Progress	P,SB	Transfer	NR	Credits Earned
F	Fail	S	Satisfactory	P,VO	Very Good	NC	No Credits/Project Complete
F	Fail	N	Not Available	P,GR	Good	EP	Examinations Postponed
D	Distinction	V	Value-Cy Course	P,JA	Fair	-	3.3x, 3M Sc. Course
X	Audited	A	At-Risk	NP	Not Passed	6	Optional M.Sc. (Ph.D.) Course
F	26.11	S	Satisfactory	①	Course of First Major	②	Course of Second Major
D	Distinction	NP	Not Passed (Exam) (Year)	NP	Withdraw (Failed Exam)	R	Research in Progress
NR	Required Course	P,MR	Missing Requirement				

9000021 1. Numerical Grade Range from 0 to 20, Passing Grade is 10
2. Cum- & Dept Avg Based on Last Recorded Term, see Regimen/entry 15, 20, 25, 30. Dept GPA for this class of students is 15.50

This unofficial transcript has been issued solely for the student information and possible use for personal reference to the graduate school. The official transcript will be provided upon the applicant direct request to ACADEMIC VICE CHANCELLOR, SHARIF UNIVERSITY OF TECH.

NOT VALID WITHOUT SIGNATURE AND EMBROIDERED SEAL OF THE REGISTRAR

SHARIF UNIVERSITY OF TECHNOLOGY
UNOFFICIAL TRANSCRIPT

Page 1 of 2
ISSUED ON: 07-02-2019

LAST NAME: SAFA
FIRST NAME: MOHAMMAD
S. Y. 1994
S. T. NO: 0014001000

STUDENT NUMBER: 0010010
DEPT: AEROSPACE ENG./MECHANICAL ENG.
PROGRAM 1: B.Sc. / AEROSPACE ENGINEERING
MAJOR 1: B.Sc. /
PROGRAM 2: B.Sc. / MECHANICAL ENGINEERING
MAJOR 2: B.Sc. /
COURSE TITLE: **فقط برای اطلاع دانشجویان**

COURSE NO	COURSE TITLE	CREDITS	GRADE	COURSE NO	COURSE TITLE	CREDITS	GRADE
FALL SEMESTER 2013-2014							
22-004	GEN MATH 1	4	11.7	22-011	GEN MATH 1	4	18.0
24-001	PHYSICS LAB 1	1	17.8	24-261	EXP. OF MECHANICS 1	1	17.0
24-011	PHYSICS 1	1	18.1	31-011	MATH TECH. WORKSHOP	1	18.0
36-001	PHYSICAL EDUCATION 1	1	18.0	35-111	ENG GRAPHICS 2 1H	2	18.0
31-010	INTRO PROGRAM LITERATURE	1	18.1	25-426	ISLAMIC REVOLUTION OF IRAN	2	18.0
31-111	FOREIGN LANG.	1	18.0	45-111	AERODYNAMICS 1	3	20.0
35-011	GENERAL WORKSHOP	1	18.0	45-119	NUMERICAL METHOD	3	19.1
	SEMESTER UNITS AVERAGE	18	17.96	45-124	FLUID MECHANICS 1	3	20.0
	TOTAL UNITS CUMULATIVE AVERAGE	18	17.96	45-407	ORBITAL MECHANICS	3	18.0
SPRING SEMESTER 2013-2014							
22-004	GEN MATH 2	4	18.0		SEMESTER UNITS AVERAGE	21	18.30
22-024	DIFF. EQN.	1	17.2		TOTAL UNITS CUMULATIVE AVERAGE	39	18.01
24-002	PHYSICS LAB 2	1	18.1	SUMMER 2013-2014			
24-011	PHYSICS 2	1	18.2		THE KNOWLEDGE OF FAMILY & POPULATION	2	F
35-111	ENG GRAPHICS 1	1	18.1		SEMESTER UNITS AVERAGE	-	-
45-111	STATS	1	18.5		TOTAL UNITS CUMULATIVE AVERAGE	41	18.01
45-112	INTRO TO AEROSPACE	1	22.0	FALL SEMESTER 2014-2015			
	SEMESTER UNITS AVERAGE	18	18.77		ENGINEERING & ENROLLMENT IN THE 2ND PROGRAM MECHANICAL ENGINEERING		
	TOTAL UNITS CUMULATIVE AVERAGE	57	18.07				
FALL SEMESTER 2014-2015							
24-001	FUNDAMENTALS I	3	20.0	24-111	QUAL. DESIGN	1	17.0
25-441	ISLAMIC TECHNOLOGY	2	19.1	24-122	FLUID MECHANICS 2	3	18.0
45-131	INTRO PROGRAM GRAPHIC	3	17.0	26-042	FLUID MECH 1	1	17.7
45-400	ADV. WORKSHOP WORKSHOP 1	1	18.0	26-044	VIBRATIONS	1	14.0
45-414	DYNAMICS	3	17.7	26-043	MATERIALS SCIENCE	1	10.0
45-124	FLUID MECHANICS 1	4	18.2	35-423	ISLAMIC CULTURE & CIVILIZATION	2	19.0
45-131	STRENGTH OF MATERIALS	4	18.0	40-278	INDUSTRIAL WORKSHOP 1	1	19.1
	SEMESTER UNITS AVERAGE	19	18.06	45-111	AERODYNAMICS 2	3	19.3
	TOTAL UNITS CUMULATIVE AVERAGE	76	18.26		SEMESTER UNITS AVERAGE	21	18.30
					TOTAL UNITS CUMULATIVE AVERAGE	97	18.27
SPRING SEMESTER 2014-2015							
				22-011	FUNDAMENTALS II	3	18.0

Abv.	W: Withdraw	F: In Progress	F: S.S. Failed	CR: Credit Received
	F: Pass	F: Re-enrolled	F: No. Re-enrolled	NC: No Credit Project Complete
	F: Fail	CR: Not Available	F: 20% Credit	EP: Examination Proposed
	D: Dismissed	C: Make Up Course	F: 75% Fail	-: B.Sc. M.Sc. Course
	S: Audited	V: MCN	EP: Not Failed	&: Optional M.Sc./Ph.D. Course
	+ : Ph.D.	S: Suspend	①: Courses of First Major	②: Courses of Second Major
	U: Unofficial	WF: Withdraw (Failed State)	WF: Withdraw (Failed Term)	R: Research in Progress
	RR: Repeated Course	F: Job: Manual Requirement		
NOTES:	1. Successful Grades Range from 0 to 20, Passing Grade is 10			
	2. Pass & Dept. Avg. Based on Last Successful Term (see Requirements 11.43.14.4. Dept. GPa for this class of students is 16.1)			
	This unofficial transcript has been issued solely for the student information and possible use for professional admission to the graduate school. The official transcript will be provided upon the applicant direct request. ACADEMIC DEAN/CHAIRMAN, SHARIF UNIVERSITY OF TECH.			
	NOT VALID WITHOUT SIGNATURE AND EMPLOYED SEAL OF THE DEPARTMENT			

SHARQ UNIVERSITY OF TECHNOLOGY
UNOFFICIAL TRANSCRIPT

Page: 1 of 2
ISSUED ON: 05-03-2019

CADITHAB, 9882
FIRSTNAME: SUKSEEN
S. V. 2004
S.C. NO: 000000194

STUDENT NUMBER: 9104702
DEPT: AEROSPACE (ENG) / MECHANICAL (ENG)
PROGRAM 1: B.Sc. / AEROSPACE ENGINEERING
MAJOR: B.Sc. / -
PROGRAM 2: B.Sc. / MECHANICAL ENGINEERING
MAJOR 2: B.Sc. / -
COLLEGE NO: 01
CITY: DUBAI

COURSE NO	COURSE TITLE	CREDIT	GRADE	COURSE NO	COURSE TITLE	CREDIT	GRADE
SEMESTER 2014-2015 (PREREQ)							
28-402	AC/DC CONTROL	1	18.7	SEMESTER 2015-2016			
28-407	DYN OF MACHINERY	1	18.1	41-041	STRUCTURE LAB	1	20.0
28-411	MACHINE ELEMENT DESIGN I	1	15.5	41-040	AERODYNAMICS LAB I	1	16.8
28-702	THERMODYN LAB	1	17.1	SEMESTER UNITS, AVERAGE			
27-444	FLUID MECH THERMODYN	2	17.0	TOTAL UNITS GAINED/CUM AV			
45-124	HEAT TRANSFER I	3	20.0	FALL SEM 2016-2017			
45-126	AC STRUCTURAL ANALYSIS	1	17.9	28-708	DYN & VIB LAB	1	17.3
SEMESTER UNITS, AVERAGE				28-444	ROBOTIC & LAB	1	15.4
TOTAL UNITS GAINED/CUM AV				28-664	SPORTS	1	15.3
SEMESTER 2014-2015				29-480	APPLIED PROJECT MANAGEMENT	1	18.3
41-040	STRUCTURAL DESIGN WORKSHOP	1	18.0	45-127	AC STRUCTURAL DESIGN	1	19.0
41-044	INDUSTRIAL TRAINING	0	F	45-171	AIRCRAFT DESIGN I	1	16.3
SEMESTER UNITS, AVERAGE				45-270	HYDRO MECHANICAL DESIGN	1	16.9
TOTAL UNITS GAINED/CUM AV				SEMESTER UNITS, AVERAGE			
FALL SEM 2016-2017				TOTAL UNITS GAINED/CUM AV			
29-440	ENG FROM A TO Z	1	18.0	SPRING SEM 2016-2017			
28-280	PROBABILISTICA	1	17.0	29-667	FINITE STRUC TNO LAB	1	19.2
28-404	MACHINE DESIGN I (DESIGN I)	1	17.0	28-211	PROB APPROACH	1	19.0
28-701	FLUID MECH LAB	1	17.4	28-640	HEAT EXCHG TYP	2	17.1
33-011	WELDING WORKSHOP	1	17.7	28-641	APPL ELECTRONICS	1	18.1
27-444	NAVIGAL BALANCE & ORBITAL DYN DEVELOPMENT	2	19.0	28-900	PROJECT	1	F
45-127	PROPULSION PRINC	4	14.1	33-011	WELD WORKSHOP	1	18.0
45-124	FLIGHT DYNAMICS I	1	17.7	41-040	STRUCTURAL DESIGN	1	16.8
44-404	INTRO TO CFD	1	16.5	SEMESTER UNITS, AVERAGE			
SEMESTER UNITS, AVERAGE				TOTAL UNITS GAINED/CUM AV			
FALL SEM 2017-2018				SEMESTER UNITS, AVERAGE			
28-121	HEAT TRANSFER 2	1	15.5	TOTAL UNITS GAINED/CUM AV			
28-241	HYDRAULIC & PNEU	1	17.9	SEMESTER 2016-2017			
28-244	HYDRAULIC & PNEU LAB	1	15.8	28-900	PROJECT	0	NC
27-427	LIFE STYLE	2	17.7	28-121	HEAT TRANSFER 2	0	F 15.5
41-011	ENGINE WORKSHOP 1	1	20.0	SEMESTER UNITS, AVERAGE			
41-040	CONTR. SYSTEMS LABORATORY	1	18.3	TOTAL UNITS GAINED/CUM AV			
41-101	FLIGHT DYNAMICS 2	1	14.0	COMPLETION RATIO FOR B.Sc. DEGREE (Aerospace Engineering -)			
41-411	MATERIALS & CONSTRUCTION	1	14.0	COMPLETION RATIO FOR B.Sc. DEGREE (Mechanical Engineering -)			
41-401	AIRBORN FLIGHT ENG DESIGN	1	17.9	NO ENTRY BELOW THIS LINE			
41-407	GAS TURBO-COMPRESSOR DESIGN	1	17.3	1777			
SEMESTER UNITS, AVERAGE				1777			
TOTAL UNITS GAINED/CUM AV				142 17.81			

NOT VALID WITHOUT SIGNATURE AND EMPRESSED SEAL OF THE REGISTRAR
FOR ABBREVIATIONS REFER TO THE FIRST PAGE



HIGHER SCHOOL OF ECONOMICS
NATIONAL RESEARCH UNIVERSITY
SAINT PETERSBURG

CERTIFICATE

awarded to

Hossein Abdi

who participated in HSE Saint Petersburg Summer School 2019 and completed the following course held at National Research University Higher School of Economics, St. Petersburg, Russia from August 12 to August 16, 2019

Modern Machine Learning

Director of HSE University, St. Petersburg



Sergey M. Kadochnikov

SAINT PETERSBURG
2019

Федеральное государственное автономное образовательное
учреждение высшего образования

НАЦИОНАЛЬНЫЙ ИССЛЕДОВАТЕЛЬСКИЙ УНИВЕРСИТЕТ
ВЫСШАЯ ШКОЛА ЭКОНОМИКИ
САНКТ-ПЕТЕРБУРГСКИЙ ФИЛИАЛ

В

TRANSCRIPT OF RECORDS

I. STUDENT PROFILE

NAME OF STUDENT: HOSSEIN ABDI

Date of Birth: 31.01.1994

NAME OF HOST UNIVERSITY: National Research University Higher School of Economics in St. Petersburg

II. ACADEMIC REPORT

1. Modern Machine Learning

Grade: 10 out of 10

Credits: 3 ECTS

Total ECTS credits: 3

Date of Issue: 16 August, 2019

Director of Centre for International Education

National Research University Higher School of Economics (St. Petersburg)
Russian Federation



Martina V. Samikova

CERTIFICATE



The Robotics Society of Iran Presents

The 7th RSI International Conference on
Robotics & Mechatronics

20-21 Nov 2019 - Shahrood University of Technology - Tehran, Iran



This is to certify that an oral presentation of

**Optimal Control of a High Maneuverable Micro-Swimmer in
Low Reynolds Number Flow to Reduce Energy Consumption**

Hossein Abdi and Hossein Nejat Pishkenari

has been presented in the 7th RSI International Conference on Robotics and Mechatronics
ICRoM'19, held on November 20-21, 2019, Shahrood University of Technology, Tehran, Iran.

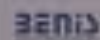
Prof. S Ali A Moosavian

S. A. Moosavian
Conference Chair



Prof. Hassan Zohoor

RSI Chair



Saeed Ansari Rad

Doktorander i reglerteknik

Ref nr: PA2020/3049-38 Datum för ansökan: 2020-10-06 20:16



Födelsedatum 1992-10-02
Adress Salman Farsi Alley, Navab
1345848743 Tehran
Tehr?n
Iran
E-post saeedansari71@ut.ac.ir
Kön Man
Mobiltelefon +989141599475
Telefon +984533350847

Frågor

1. *Har du avlagt masterexamen?*

Ja

Rätt svar

2. *Vid vilket universitet har du avlagt masterexamen?*

University of Tehran, Iran

3. *Ange namn på din(a) referens(er).*

Here are information of professional references:

1- Mehdi Tale Masouleh, Assistant Professor, University of Tehran, School of Electrical and Computer Engineering, Director of Human and Robot Interaction Laboratory

Faculty webpage: <http://ece.ut.ac.ir/~m.t.masouleh>

Email : m.t.masouleh@ut.ac.ir, mehdi.tale.masouleh@taarlab.com

Tel. : +98-21-61118413

2- Ahmad Kalhor, Assistant Professor, Control and Intelligent Processing Center of Excellence, School of Electrical and Computer Engineering, University of Tehran, Tehran, Iran, Office 322, PO Box: 14395-515, Tel: +(98 21)6111 9780

Fax: +(98 21)8801 3199

Email: akalhor@ut.ac.ir

3- Prof. B. Nadjar Aarabi, Control and Intelligent Processing Center of Excellence, School of Electrical and Computer Engineering, University of Tehran, Tehran, Iran

Email: araabi@ut.ac.ir

4- Moosa Ayati, PhD. Assistant professor, School of Mechanical Engineering, College of Engineering, University of Tehran.

Email: smoosa_ayati@yahoo.com, m.ayati@ut.ac.ir

Homepage: <https://rtis.ut.ac.ir/cv/m.ayati> or www.moosaayati.com

4. *Vilket är det främsta skälet till att du söker denna tjänst?*

Pursuing my researches in Automatic Control, improving knowledge in this field, Access to cutting-edge information in LTH

Saeed Ansari Rad

Doktorander i reglerteknik

Ref nr: PA2020/3049-38 Datum för ansökan: 2020-10-06 20:16

Eget uppladdat CV

Egna filer och portfolio

Recomm_Letter1.pdf

Recomm_Letter1.pdf

Recomm_Letter2.pdf

Recomm_Letter2.pdf

names and contact information, references.pdf

names and contact information, references.pdf

Language Test Results.pdf

Language Test Results.pdf

MSc Certificate.pdf

MSc Certificate.pdf

BSc Certificate.pdf

BSc Certificate.pdf

BSc Transcript.pdf

BSc Transcript.pdf

MSc Trascript.pdf

MSc Trascript.pdf

Accepted_Journal_Measurement.pdf

Accepted_Journal_Measurement.pdf

Accepted_Journal_Evolving Systems.pdf

Accepted_Journal_Evolving Systems.pdf

Accepted_Journal_Mechanical Engineering Science.pdf

Accepted_Journal_Mechanical Engineering Science.pdf

Accepted_Conference_ACC2018.pdf

Accepted_Conference_ACC2018.pdf

Accepted_Journal_MMT.pdf

Accepted_Journal_MMT.pdf

Accepted_Journal_Dynamic&Control.pdf

Accepted_Journal_Dynamic&Control.pdf

Utbildningar

Titel	Skola/Företag	Ort	Land	Från-Till
Master of Science Student	College of Engineering, University of Tehran, School of ECE. 2016-2018 <i>University of Tehran M.Sc. Student at College of Engineering, University of Tehran, School of ECE. Electrical and Control Engineering GPA: 3.88/4</i>	Tehran	Iran	2016-2018
Bachelor of Science	College of Engineering, University of Tehran, School of ECE 2012-2016 <i>University of Tehran B.Sc. Student at College of Engineering, University of Tehran, School of ECE. Electrical and Control Engineering GPA: 4/4</i>	Tehran	Iran	2012-2016

Saeed Ansari Rad

Doktorander i reglerteknik

Ref nr: PA2020/3049-38 Datum för ansökan: 2020-10-06 20:16

Anställningar

Titel	Företag	Ort	Land	Från-Till
Research Assistant	Human & Robotic Interaction Laboratory <i>Research Assistant at Human & Robotic Interaction Laboratory Under supervision of Dr. Tale Masouleh</i>	Tehran	Iran	2018-Nuvarande
Research Assistant	<i>2018-Now</i> Instrumentations Laboratory <i>Research Assistant at Instrumentations Laboratory Under supervision of Dr. Moosa Ayati</i>	Tehran	Iran	2016-2017
	<i>2016-2017</i>			

Kurser

Titel	Skola	Ort	År
Data Analysis and Deep Learning	University of Tehran	Tehran	2019
Machine Learning	University of Tehran	Tehran	2019
Adaptive Control	University of Tehran	Tehran	2018
Game Theory	University of Tehran	Tehran	2018
Neural Networks and Deep Learning	University of Tehran	Tehran	2018
Optimal Control	University of Tehran	Tehran	2018
Robust Control	University of Tehran	Tehran	2018
Stochastic System Control	University of Tehran	Tehran	2018
Pattern Recognition	University of Tehran	Tehran	2017

Certifieringar

Titel	Skola	År
M.Sc. Certification, Electrical and Control Engineering	College of Engineering, University of Tehran, School of ECE. <i>GPA: 3.88/4</i>	2018
B.S. Certification, Electrical and Control Engineering	College of Engineering, University of Tehran, School of ECE <i>GPA: 4/4</i>	2016

Publikationer

Titel	Förlag	Ort	År
-------	--------	-----	----

Classification-Based
Fuel Injection Fault
Detection of a Trainset
Diesel Engine Using
Vibration Signature
Analysis

Journal of Dynamic Systems,
Measurement, and Control

2020

Diesel engines are crucial components of trainsets. Automated fault detection of diesel engines can play an important role for increasing reliability of passenger trains. In this research, vibration-based fuel injection fault detection of a high-power 12-cylinder trainset diesel engine is studied. Vibration signals are analyzed in frequency and time-frequency domains to obtain possible patterns of faults. Fast Fourier transform (FFT) and wavelet packet transform (WPT) of vibration signals are used to extract several uncorrelated features. These features are chosen to increase the ability of classifiers to separate healthy and faulty engine sides, automatically. Different classification methods including multilayer perception (MLP), support vector machines (SVM), K-nearest neighbor (KNN), and local linear model tree (LOLIMOT) are used to process captured features; these methods are utilized in both "Single-sensor condition monitoring" and "Classification and fault detection" sections. It is shown that KNN networks are practical tools in the proposed fault detection procedure. The main novelty of this work comes from introducing a rich feature-extraction method based on a combination of FFT and db4 features. In addition, the complexity of computations and average running-time decrease while classification accuracy in the fuel injection fault detection procedure increases.

Experimental study on
robust adaptive control
with insufficient
excitation of a 3-DOF
spherical parallel robot
for stabilization
purposes

Mechanism and Machine Theory

2020

In this paper, a robust adaptive control approach has been proposed for under insufficient excitation Multi-Input Multi-Output (MIMO) systems. The stability and performance of adaptive controllers are highly dependent on initial conditions and speed of convergence of identified parameters. Moreover, the corresponding adaptation rules suffer from system uncertainties, disturbances, and insufficient excitation. In order to overcome such crucial challenges, in this paper a robust adaptive control is proposed. By inspiring from the classic Damped Least Squares (DLS) and Singular Value Decomposition (SVD) methods, a novel algorithm namely, SVD-DLS, is introduced which obtains an optimal solution to the estimation wind-up. Above all, the proposed approach is implemented on a 3 degree-of-freedom spherical parallel robot for stabilization purposes. By avoiding from challenges of model-based approaches, the unknown parameters are obtained without having any prior knowledge which makes the proposed approach more interesting for robotic having complex models. Based on the practical implementation, the oscillations of identified parameters are dampened much smoother than other identification methods in which the ratio of end-effector to base orientation, as a stabilization index, is acquired as 0.134.

Control of Quad-rotor
in Cooperation with an
Attached 3-DOF
Manipulator

2019 5th Conference on Knowledge
Based Engineering and Innovation
(KBEI)

2019

Autonomous quad-rotor flight systems have grabbed considerable attention for varied missions in rescue, inspection devices, and so forth. Accordingly, various control methods have been employed for hovering these devices. Recently, in order to extend the applications of quad-rotors, including, among the others, the pick-and-place, a robotic arm has been attached, which requires the analysis of both dynamic equations and control procedures. However, considering the coupled system as a case of robot-robot interaction, these state-of-the-art flight systems have rarely received attention due to much higher complexity of dynamic equations. Moreover, flight

time expense is revealed as another critical issue in the flight systems with the attached arm, which requires effective solution due to excessive arm loads and power source limitations. To this end, in this paper, the dynamic equations of quad-rotor with a 3-link arm are obtained in order to be employed in designing suitable control methods. In this regard, by stabilizing the quad-rotor in desired coordinations and tracking desired paths for robotic arm, the dynamic interaction as the main challenge of the robot-robot interaction is successfully handled. Thereafter, a Linear Quadratic Regulator (LQR) is proposed to tackle the flight time issue in which by assigning optimal values to the state input weighting matrix, the motion of arm links reduced and as the result, the flight time effectively increases. In order to demonstrate the superiority of the proposed method, two well-known control approaches, namely, Sliding Mode Control (SMC) and Pole Placement are implemented in the same conditions. In simulation with Matlab software, the performance of the forgoing methods is compared by employing different indices, where it is inferred that despite presence of an external force resembling windy condition, the proposed LQR decreases the motion index by 24.14% in compare with SMC and Pole Placement methods, with approximately similar tracking index to them.

Fault detection and diagnosis of a 12-cylinder trainset diesel engine based on vibration signature analysis and neural network

Proceedings of the Institution of Mechanical Engineers, Part C: Journal of Mechanical Engineering Science

2019

This paper presents a condition monitoring and combustion fault detection technique for a 12-cylinder 588?kW trainset diesel engine based on vibration signature analysis using fast Fourier transform, discrete wavelet transform, and artificial neural network. Most of the conventional fault diagnosis techniques in diesel engines are mainly based on analyzing the difference of vibration signals amplitude in the time domain or frequency spectrum. Unfortunately, for complex engines, the time- or frequency-domain approaches do not provide appropriate features solely. In the present study, vibration signals are captured from both intake manifold and cylinder heads of the engine and were analyzed in time-, frequency-, and time-frequency domains. In addition, experimental data of a 12-cylinder 588?kW diesel engine (of a trainset) are captured and the proposed method is verified via these data. Results show that power spectra of vibration signals in the low-frequency range reliably distinguish between normal and faulty conditions. However, they cannot identify the fault location. Hence, a feature extraction method based on discrete wavelet transform and energy spectrum is proposed. The extracted features from discrete wavelet transform are used as inputs in a neural network for classification purposes according to the location of sensors and faults. The experimental results verified that vibration signals acquired from intake manifold have more potential in fault detection. In addition, the capacity of discrete wavelet transform and artificial neural network in detection and diagnosis of faulty cylinders subjected to the abnormal fuel injection was revealed in a complex diesel engine. Beside condition monitoring of the engine, a two-step fault detection method is proposed, which is more reliable than other one-step methods for complex engines. The average condition monitoring performance is from 93.89% up to 99.17%, based on fault location and sensor placement, and the minimum classification performance is 98.34%.

Partial identification and control of MIMO systems via switching linear reduced-order models under weak stimulations

Evolving Systems

2019

In closed loop identification of an unknown control system, the stability is a big concern particularly when the system does not proceed with sufficient excitation. In this paper, under insufficient excitation of the system, identification and control are investigated by employing Evolving Linear Models (ELMs). It is explained that under weak stimulation, linear correlations between input and output signals and their derivations are occurred. Removing some correlated variables through the time, an equivalent reduced order model of the original system is

Pseudo DVL reconstruction by an evolutionary TS-fuzzy algorithm for ocean vehicles	<i>appeared, which can be identified as an ELM. Defining control law based on the sliding mode control (SMC) and using appropriate adaptation rules for parameters of the model, the tracking errors converge to zero and the stability of the system is guaranteed. Then, convergence of the parameters to their true values is studied and discussed. Different simulations are given to demonstrate the efficacy of the proposed closed loop identification approach.</i>	Measurement	2019
Identification and Control of MIMO Linear Systems under Sufficient and Insufficient Excitation	<i>By development of ocean exploration, autonomous vehicles are employed to perform on-water and underwater tasks. Using an extended Kalman filter, Inertial Navigation System/Doppler Velocity Log (INS/DVL) integrated systems are trying to navigate in oceans and underwater environments when Global Positioning System (GPS) signals are not accessible. The dependency of DVL signals on acoustic environments may cause any DVL malfunction due to sea creatures or strong wave-absorbing material. In this paper, an improved version of evolutionary TS-fuzzy (eTS) is proposed in order to predict DVL sensor outputs at DVL malfunction moment, by utilizing an artificial intelligent (AI) aided integrated system. According to lack of input selection and shrinking, while the classic eTS suffers from soaring prediction errors and may result in instability, by adding these properties to eTS, the performance increases in long-term DVL outage. The proposed eTS-aided system makes ocean navigation purposes possible during long-term and simultaneous outage of GPS and DVL. These evolutionary fuzzy systems change their structure depending on the path which makes the trained fuzzy system more flexible with non-stationary and varying environments. The real sensor data is collected online with a test setup on a lake and then the algorithms are applied. The powerful capacity of the proposed data fusion method is demonstrated in analysis results.</i>	2018 Annual American Control Conference (ACC)	Milwaukee, WI, USA 2018
Stabilization of a Two-DOF Spherical Parallel Robot via a Novel Adaptive Approach	<i>In closed-loop identification of unknown control systems, stability is a major concern. Particularly, when the system does not proceed with sufficient excitation. In this paper, a closed-loop identification strategy for Multi-Input Multi-Output (MIMO) linear systems is intended via a robust adaptive control law based on Sliding Mode Control (SMC). Under both sufficient and insufficient excitation of the system, Evolving Linear Models (ELMs) are deployed to identify and control the system. It is explained that under insufficient excitation, linear correlations between input and output signals and their derivatives can be removed. An equivalent reduced-order model of the original system results which can be identified as an ELM. Defining the control law based on the SMC and using appropriate adaptation rules for parameters of the model, the tracking errors converge to zero and the stability of the system is guaranteed. Meanwhile, the parameters of the model converge to their true values. Simulation results demonstrate the efficacy of the proposed approach.</i>	2018 6th RSI International Conference on Robotics and Mechatronics (IcRoM)	2018

Saeed Ansari Rad

Doktorander i reglerteknik

Ref nr: PA2020/3049-38 Datum för ansökan: 2020-10-06 20:16

structure, the performance of the adaptive controller is validated. The proposed method leads to better performance in compare with the decay algorithm, from view point of quantitative indices of tracking, stabilization and smoothness.

Språk

persiska
turkiska
engelska

Flytande
Flytande
Flytande

Modersmål
Modersmål

Körkort

Saknas

Webbsidor

<http://taarlab.com/en/members/9-taarlab/members/244-saeed-ansari-rad> My web page in the TAARLab's website, including introduction, bio

Referenser

Namn Mehdi Tale Masouleh
Företag Human and Robot Interaction Laboratory
E-post m.t.masouleh@ut.ac.ir
Telefon +98-21-61118413

Namn Ahmad Kalhor
Företag University of Tehran
E-post akalhor@ut.ac.ir
Telefon +(98 21)6111 9780

My name is Saeed Ansari Rad, and I got my Master degree in control engineering, University of Tehran, the oldest and most prestigious university in Iran, with a total GPA of 3.88 on the scale of 4.

I received the B.Sc. degree in Electrical Engineering from University of Tehran, Iran, in 2015. The corresponding B.Sc. thesis concentrated on analysis and extension of the epoch robots. After acquiring outstanding rank among the Electrical Engineering students, I attended School of Electrical and Computer Engineering, University of Tehran in M.Sc and joined Iran's National Elites Foundation. Meanwhile, I pursued some of my researches, under supervision of Dr. Ayati, at Instrumentations Laboratory. My M.Sc thesis has carried out under supervision of Dr. Kalhor and Dr. Nadjar Arabi, which is entitled "Design a Robust Adaptive Operational Control Based on Identification and Following Parameters for Evolving Linear Systems with Limited-variation Parameters" with numerous novelties in control, identification, learning as well as applications in robot control. I have research backgrounds in control and machine learning, which now help me to work as a research assistant in the human and robot interaction laboratory (TAARLab). From 2018, I participate actively in some of TAARLab's projects under supervision of Dr. Tale Masouleh and Dr. Kalhor; the control and identification of these projects are carried out based on my innovative achievements in these fields. I've some accepted journal and conference publications in my research interests (<http://taarlab.com/en/members/9-taarlab/members/244-saeed-ansari-rad>).

Nowadays, I am working on a project, involving combining the novel ideas of a robust adaptive approach with the reinforcement learning in order to improve the performance of a robotic system with unknown parameters; the idea of mixing a general model-based approach with the notion of learning has received considerable attention from control researchers, lately. I attend to improve the aforementioned idea as far as possible. The Automatic Control field is close to most of my researches and back ground knowledge and that is why I am interested in pursuing my researches as in the automatic control field. Most of my educational projects focus on Control, Robotics and Identification. Also, I have suitable backgrounds in AI (passing several courses such as Pattern Recognition, Data Analytic) and Game theory. I have several accepted papers in the aforementioned area, and also have passed the required language test, TOEFL iBT, with the total score of 101 and each task with R24L29S23W25. There are several having teacher assistant experiences in control courses in M.Sc and B.Sc, including in the Industrial Control, Neural Network, Identification, and so forth. I'm so eager to pursue my studies in the LTH Faculty of Engineering. This institute is a prestigious university on the scale of international institutes and in the Sweden. There are no limitation from educational point to take up positions. All in all, it will be my pleasure to work under your headship, and I am ready for answering any question you might have.

Saeed Ansari Rad

#12, Salman Farsi Alley, Navab, Tehran, Iran

Postal Code: 1345848743

Tel. +989141599475

Email: Saeedansari71@ut.ac.ir

Webpage: taarlab.com/blog

Birthday: October, 1992

EDUCATION

2016-2018 University of Tehran
M.Sc. Student at College of Engineering, University of Tehran, School of ECE.
Electrical and Control Engineering
GPA: 3.88/4

2012-2015 University of Tehran
B.S. Student at College of Engineering, University of Tehran, School of ECE.
Electrical and Control Engineering
GPA: 4/4

RESEARCH INTERESTS

- System Identification
- Adaptive Control
- Machine Learning
- Automatic Control
- Parallel Robots
- Neural Networks
- Evolving Systems
- Fault Detection
- Stochastic Control

RESEARCH PAPERS

J1 “Partial identification and control of MIMO systems via switching linear reduced-order models under weak stimulations”, *Evolving Systems*, 2017 – Springer, [Accepted](#)

- J2 “Fault Detection and Diagnosis of a 12-Cylinder Trainset Diesel Engine Based on Vibration Signature Analysis and Neural Network”, *Part C: Journal of Mechanical Engineering Science*, 2019, [Accepted](#)
- J3 “Pseudo DVL reconstruction by an evolutionary TS-fuzzy algorithm for ocean vehicles”, *Measurement*, 2019, [Accepted](#)
- J4 “Classification-based Fuel Injection Fault Detection of a Trainset Diesel Engine Using Vibration Signature Analysis”, *Dynamic Systems, Measurement and Control*, 2020, [Accepted](#)
- J5 “Experimental Study on Robust Adaptive Control with Insufficient Excitation of a 3-DOF Spherical Parallel Robot for Stabilization Purposes”, *Mechanisms and Machine Theory*, 2020, [Accepted](#)
- C1 “Identification and Control of MIMO Linear Systems under Sufficient and Insufficient Excitation”, *American Control Conference*, 2018, [Accepted](#)
- C2 “Stabilization of a Two-DOF Spherical Parallel Robot via a Novel Adaptive Approach”, *6th International Conference on Robotics and Mechatronics*, 2018, [Accepted](#)
- C3 “Control of Quad-rotor in Cooperation with an Attached 3-DOF Manipulator”, *5th International Conference on Knowledge-Based Engineering and Innovation*, 2019, [Accepted](#)
- C4 “Fuel Injection Fault Detection in a Diesel Engine Based on Vibration Signature Analysis”, *Proceedings of the 5th Iranian International NDT Conference*, [Accepted](#)
- C5 “A Critical Review of Machine Vision Applications in Construction”, *The International Association for Automation and Robotics in Construction*, 2020, [Accepted](#)
- J6 “Control of a Two-DOF Parallel Robot with Unknown Parameters Using a Novel Robust Adaptive Approach”, *ISA Transactions*, 2020, [Under review, third round](#)
- J7 “Dynamics Analysis, Offline-Online Tuning and Identification of Base Inertial Parameters for the 3-DOF Delta Parallel Robot Under Insufficient Excitations”, *Multibody System Dynamics*, 2020, [Under review](#)

HONORS AND REWARDS

- 2015-Now** Contribution in “**Iran's National Elites Foundation**”
- 2012-2015** Ranked in **top 10%** of entrance of Electrical Engineering of University of Tehran
- 2011** Ranked **179th** among approximately 650,000 participants in nationwide university entrance exam B.S. degree
- 2010 - 2011** Admitted in the first stage of nationwide competition to select national "Mathematics", "Physics", and "Chemistry" Olympiad team
- 2008 – 2010** **Ranked 1th** among high school students of Shahid Beheshti for 3 years
- 2009- 2010** **First rank** of Laboratory completion in Physics field

ACADEMIC EXPERIENCE

- 2018-Now** Research Assistant at Human & Robotic Interaction Laboratory Under supervision of Dr. Tale Masouleh
- 2016-2017** Research Assistant at Instrumentations Laboratory Under supervision of Dr. Moosa Ayati
- 2018-2019** Sub-reviewer of ICRoM 2018-2019, UT.
- 2013-2017** Teacher Assistant, UT: System Identification, Digital Control, Micro Processors, Industrial Control, Linear Control Laboratory, Linear Control, Electrical Machine

SELECTED COURSEWORK

- Neural Networks and Deep Learning
- Machine Learning
- Pattern Recognition
- Stochastic System Control
- Game Theory
- Data Analysis and Deep Learning
- Robust Control
- Adaptive Control
- Optimal Control
- Robotics
- Robot Ignite Academy (ROS, TF, Control)

SKILLS

Computer science:	C/C++, Python, Lpic1, Verilog/VHDL
Robotics Field:	Robot Operation System (ROS), Gazebo, SimMechanics
Engineering software:	Matlab, Altium Designer, Corel Draw, Visual studio, Modelsim, CodeVision, Keil uVision, R studio
Miscellaneous softwares:	LATEX, Microsoft Office, Photoshop
Operating Systems:	Linux, Windows
Languages:	Eng. TOEFL: 101, R24L29S23W25 Persian: Native Turkish: Native

REFERENCES

- Ass. Prof. Tale Masouleh [University of Tehran
m.t.masouleh@ut.ac.ir](mailto:m.t.masouleh@ut.ac.ir)
- Ass. Prof. A. Kalhor [University of Tehran
akalhor@ut.ac.ir](mailto:akalhor@ut.ac.ir)
- Ass. Prof. M. Ayati [University of Tehran
m.ayati@ut.ac.ir](mailto:m.ayati@ut.ac.ir)
- Prof. B. Nadjjar Aarabi [University of Tehran
araabi@ut.ac.ir](mailto:araabi@ut.ac.ir)



University of Tehran

Dear whom it may concern

I have known Mr. “Saeed Ansari Rad” for more than three years as his teacher and his advisor. As I remember, Saeed was one of the best undergraduate students and the “School of Electrical and Computer engineering” approved him in the graduate program as a strait student. He passed successfully “identification” and “neural networks” courses with me with the best grades. Due to his very good background in control and identification, I invited him to be my assistant for two semesters. Then, for his master thesis, I asked him to develop the evolving linear models in the identification and control of unknown affine dynamic systems. Due to his excellent background in linear algebra, robust control, and adaptive control, we could develop some control strategies and adaptation rules, which were potentially appropriate in the identification and control of unknown systems with a slow variation. We stated some mathematic theorems to support our proposed methods. Then, we successfully applied our methods to some known parallel and serial robots, experimentally. We have published several high impact journals and conferences from our methods and their application in robotic systems. Based on my experiences in working with him, Saeed is an ethical and organized student with a very good capacity in working cooperatively with others.

In my opinion, Saeed has a high motivation towards a successful and productive career and I strongly recommend him as an excellent choice for your Ph.D. Program.

Ahmad Kalhor, 2019 Oct. 22

Assistant Professor, Control and Intelligent Processing Center of Excellence
School of Electrical and Computer Engineering, University of Tehran, Tehran 1439957131, Iran
Office 322
PO Box: 14395-515
Tel: +(98 21)6111 9780, Fax: +(98 21)8801 3199
Email: akalhor@ut.ac.ir



School of Electrical and Computer Engineering
University of Tehran
Human and Robot Interaction Laboratory

October 17, 2019

Dear Sir or Madam,

Mr. Saeed Ansari Rad is a talented Electrical engineering researcher with a proven history of achievement throughout his career. Mr. Ansari Rad success in research is rooted in his strong background in education and research. He earned his BSc from University of Tehran, one of the most prestigious University in Iran, in Electrical Engineering. After that, Mr. Ansari Rad was accepted to the graduate program at the University of Tehran, where he earned his MSc in Electrical engineering, Control. After completing his MSc in 2016, he started to work at the Human and Robot Interaction Laboratory as research assistant under my supervision. He has been conducting research there since 2017. Mr. Ansari Rad research centers around learning-based control approach of robotic mechanical systems, with a emphasize on parallel robots. He is highly skilled in developing new control strategy based on reinforcement learning approach. These skills make Saeed a versatile researcher who is well-positioned for continued success in his field.

One of Mr. Ansari Rad 's most impressive research contributions conducted in the Human and Robot Interaction Laboratory, is his innovative in proposing model-free approach with unknown parameters for controlling robotic mechanical systems, automatic control. These projects have generated a total of two accepted IEEE-index conference papers, one under review journal paper and two submitted Journal papers.

Mr. Ansari Rad 's contributions are valuable beyond their implications for other systems engineers. His innovations in proposing new control approach are also pertinent. The performance and talent of Mr. Ansari Rad was so remarkable that I trusted him to be the head of control group of the Laboratory. On this regard he supervised several BSc and MSc students under my supervision. He also acted as a sub-reviewer of the International Conference of Robotic and Mechatronics and the quality of his review report indicates that he has a comprehensive insight into the literature of control of robots and mechanisms.

Mr. Ansari Rad is also very skillful in computer programming languages, such as Python and ROS, and always eager to learn more such languages in order to compare the proposed algorithms.

It is clear that Mr. Ansari Rad is an excellent researcher and that he will have a very successful career in research. His presentations and communication in English are excellent, which is a

... 2

clear indication of his teaching abilities. In addition, he is very industrious in writing scientific papers resulted from his academic research and writes his papers without difficulty.

Overall, I strongly recommend him for Ph.D study due to his research abilities and outstanding performance at the Human and Robot Interaction Laboratory and I believe that he would be a perfect student during this program.

Should I present any more details, please do not hesitate to contact me.

Cordially Yours,

Mehdi Tale Masouleh
Ph.D, Associate Professor
Director of Human and Robot Interaction Laboratory
School of Electrical and Computer Engineering
University of Tehran

Here are information of professional references:

1-Mehdi Tale Masouleh, Assistant Professor, University of Tehran, School of Electrical and Computer Engineering, Director of Human and Robot Interaction Laboratory

Faculty webpage: <http://ece.ut.ac.ir/~m.t.masouleh>

Email : m.t.masouleh@ut.ac.ir, mehdi.tale.masouleh@taarlab.com

Tel. :+98-21-61118413

2- Ahmad Kalhor, Assistant Professor, Control and Intelligent Processing Center of Excellence, School of Electrical and Computer Engineering, University of Tehran, Tehran, Iran, Office 322, PO Box: 14395-515, Tel: +(98 21)6111 9780

Fax: +(98 21)8801 3199

Email: akalhor@ut.ac.ir

3- Prof. B. Nadjar Aarabi, Control and Intelligent Processing Center of Excellence, School of Electrical and Computer Engineering, University of Tehran, Tehran, Iran

Email: araabi@ut.ac.ir

4- Moosa Ayati, PhD. Assistant professor, School of Mechanical Engineering, College of Engineering, University of Tehran.

Email: smoosa_ayati@yahoo.com, m.ayati@ut.ac.ir

Homepage: <https://rtis.ut.ac.ir/cv/m.ayati> or www.moosaayati.com

Name: Ansari-Rad, Saeed

Last (Family/Surname) Name, First (Given) Name Middle Name

Email: saeedansari71@ut.ac.ir

Gender: M

Date of Birth: October 02, 1992

Appointment Number: 0000 0000 3555 7375

Test Date: August 03, 2019



Ansari-Rad, Saeed
Navab
Dampezeski
Salman-farsi
Tehran, Tehran
Iran, Islamic Republic of

Inst. Code	Dept. Code
1579	99

Country of Birth: Iran, Islamic Republic of

Native Language: Farsi

Test Center: STN12390A - Amirbahador Educational Complex

Test Center Country: Iran, Islamic Republic of

Security Identification

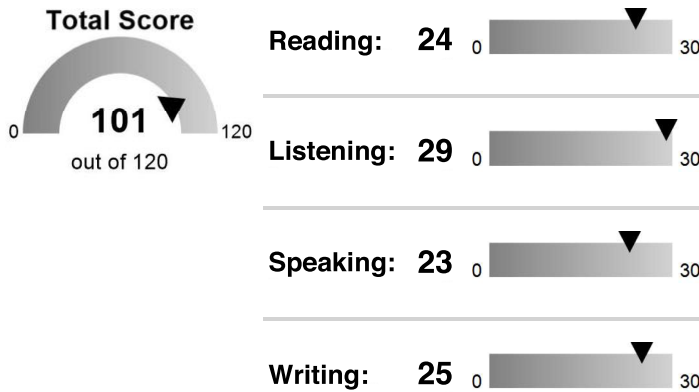
ID Type: National ID

ID No.: xxxxxxxxxxxxxxxxxxxx1685

Issuing Country: Iran, Islami

THIS IS A PDF SCORE REPORT, DOWNLOADED AND PRINTED BY THE TEST TAKER.

August 03, 2019 Test Date Scores

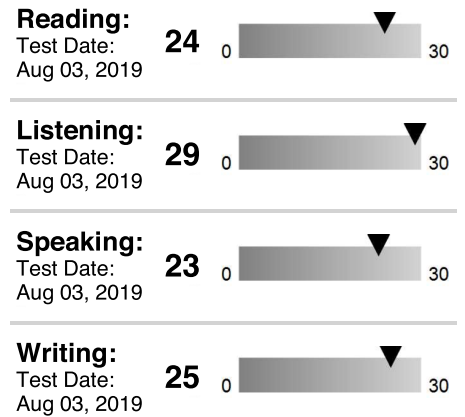


MyBest™ Scores

Your highest section scores from all valid test dates, as of August 09, 2019.

Sum of Highest Section Scores

101
out of 120



A total score is not reported when one or more sections have not been administered. Expired scores are not included in MyBest™ calculations.

THIS IS A PDF SCORE REPORT, DOWNLOADED AND PRINTED BY THE TEST TAKER.

Ansari-Rad, Saeed

Date of Birth: October 02, 1992

Appointment Number: 0000 0000 3555 7375

Test Date: August 03, 2019

SCORE RANGES

Total Score	0–120
Reading	0–30
Advanced	24–30
High - Intermediate	18–23
Low - Intermediate	4–17
Below Low - Intermediate	0–3
Listening	0–30
Advanced	22–30
High - Intermediate	17–21
Low - Intermediate	9–16
Below Low - Intermediate	0–8
Speaking	0–30
Advanced	25–30
High - Intermediate	20–24
Low - Intermediate	16–19
Basic	10–15
Below Basic	0–9
Writing	0–30
Advanced	24–30
High - Intermediate	17–23
Low - Intermediate	13–16
Basic	7–12
Below Basic	0–6

INSTITUTION CODES

The Institutions and Department code numbers shown on the front page are the ones you selected before you took the test.

Dept.	Where the Report Was Sent
00	Admissions office for undergraduate study
01, 04-41, 43-98	Admissions office for graduate study in a field other than management (business) or law according to the codes selected when you registered
02	Admissions office of a graduate school of management (business)
03	Admissions office of a graduate school of law
42	Admissions office of a school of medicine or nursing or licensing agency
99	Institution or agency that is not a college or university

For additional information about TOEFL iBT scores, score ranges, and how to improve your skills, visit www.ets.org/toefl/ibt/scores.

IMPORTANT NOTE TO SCORE USERS: This is a PDF score report, downloaded and printed by the test taker. Therefore, ETS cannot guarantee that it has not been altered. To verify the scores on this report, please contact the TOEFL Score Verification Service at **+1-800-257-9547** or **+1-609-771-7100**. Scores more than two years old cannot be reported or validated.

MATIN AMIRSHAHI

MPL, GradCert Australian Migration Law & Practice, NWS
Registered Migration Agent (MAARN 1683110)
NAATI Accredited Translator (NAATI No. 77495)
Official Translator to the Judiciary of LR (Licence No. RTI)

Unit 10, 2 Kashanchi Alley, Valian Street, Tajrish, Tehran
(+9821) 22704817 - 22705217
www.iranaustralia.org
info@iranaustralia.org

Translation from Persian
In the name of the Almighty
Islamic Republic of Iran
University of Tehran

Ref: 124/18196
Date: 18.05.2020

(Holder's photo affixed and sealed)

Provisional Certificate of Completion of Studies

This is to certify that:

Mr. Saeed ANSARI RAD, (holder of the above photo), son of Reza, holder of birth certificate No. 1450601685 and National ID No. 1450601685, born on 02.10.1992, has graduated with a **Discontinuous Master's Degree** in the field of **Electrical Engineering-Control** with an overall GPA of 18.28 (eighteen point two eight).

It is to be noted that the above-named commenced his studies at the University of Tehran-Campus of the Faculties of Engineering- Faculty of Electrical and Computer Engineering in the first semester of 2015-2016 and completed the curriculum on 08.07.2018 and is obligated to perform 2 years of service in Iran. It is noteworthy to mention that the above-named has a further service obligation with duration of 8 years for the Continuous Bachelor's Degree curriculum.

The present certificate has been issued solely for the enjoyment of any benefits thereof in Iran and shall not serve any other purpose. The testatur shall be issued after fulfillment of his service obligation.

All Taheri Mirghaedi
Director General of Academic Services of the University of Tehran
(Signed)

- To collect the testatur, the present certificate must be returned.
- A fiscal stamp at the amount of IRR 10,000 was stuck on this certificate and obliterated.

(Fiscal Stamp Stuck & Obliterated)

Affidavit: This is to certify that the present translation is accurate and complete and that the translator is competent to translate.

F.M.2020-05-308

May 21, 2020- Tehran, Iran



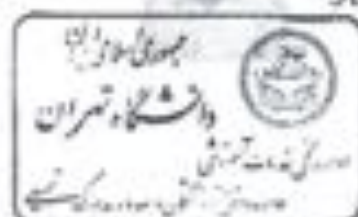
جمهوری اسلامی ایران

۱۳۹۷/۰۲/۱۷

دانشگاه تهران



بِسْمِ اللَّهِ الرَّحْمَنِ الرَّحِيمِ



گواهینامه موفقیت پایان تحصیلات

گواهی می شود:

آقای سعید انصاری راه (صاحب عکس فوق) فرزند رضا دارای شناسنامه شماره ۱۴۵۰۶۰۱۶۸۵ کنعلی ۱۴۵۰۶۰۱۶۸۵ متولد ۱۳۷۱/۰۷/۱۰ در مقطع کارشناسی ارشد ناپیوسته رشته مهندسی برق گرایش کنترل با معدل کل ۱۸/۲۸ (هیجده و بیست و هشت صدم) و با درجه تحصیلی کارشناسی ارشد ناپیوسته دانش آموخته گردیده است.

یادآور می شود نامبرده تحصیلات خود را در دانشگاه تهران - پردیس دانشکده های فنی - دانشکده مهندسی برق و کامپیوتر از نیمسال اول سال تحصیلی ۹۵-۹۴ شروع و در تاریخ ۱۳۹۷/۰۲/۱۷ به تمام رسانیده است. نامبرده مدت ۲ سال تعهد خدمت در ایران دارد. قبل ذکر است نامبرده در مقطع کارشناسی پیوسته نیز دارای ۸ سال تعهد خدمت آموزش رایگان می باشد.

این گواهی صرفاً برای بهره مندی از مزایای آن در ایران صادر شده و ارزش ترجمه ندارد. اصل مدرک تحصیلی پس از انجام تعهد خدمت تحویل خواهد شد. ۱۷-۱۳۹۷

علی طاهری مرفقاند
مدیرکل خدمات آموزشی
دانشگاه تهران



- برای دریافت دانشجویانه باید این گواهی همسر رد کرد.
- به این گواهی مبلغ ۱۰۰۰۰ ریال غیر الحاق و باطل گردیده است.



MATIN AMIRSHAHI

MPA, GradCert Australian Migration Law & Practice, NMI4

Registered Migration Agent (SEARN 1685110)

NAATI Accredited Translator (NAATI No. 77495)

Official Translator to the Judiciary of T.H.E.License No.813)

Unit 10, 2 Kashiuchi Alley, William Street, Tazrish, Tehran

(+9821) 22704817 - 22705217

www.iranaustralia.org

info@iranaustralia.org

*Translation from Persian
In the name of the Almighty
Islamic Republic of Iran
University of Tehran*

Ref.: 124/13043

Date: 27.04.2020

(Holder's photo affixed and sealed)

Provisional Certificate of Completion of Studies

This is to certify that:

Mr. Saeed ANSARI RAD, (holder of the above photo), son of Reza, holder of birth certificate No. 1450601685 and National ID No. 1450601685, born on 02.10.1992, has graduated with a **Continuous Bachelor's Degree** in the field of **Electrical Engineering-Control** with an overall GPA of 18.06 (eighteen point zero six).

It is to be noted that the above-named commenced his studies at the University of Tehran-Campus of the Faculties of Engineering- Faculty of Electrical and Computer Engineering in the first semester of 2011-2012 and completed the curriculum on 22.09.2015 and is obligated to perform 8 years of service in Iran.

The present certificate has been issued solely for the enjoyment of any benefits thereof in Iran and shall not serve any other purpose. The testamur shall be issued after fulfilment of his service obligation.

*Ah Taheri Mirghaied
Director General of Academic Services of the University of Tehran
(Signed)*

- To collect the testamur, the present certificate must be returned.
- A fiscal stamp of the amount of IRR 10,000 was stuck on this certificate and obliterated.

(Fiscal Stamp Stuck & Obliterated)

.....
Affidavit: This is to certify that the present translation is accurate and complete and that the translator is competent to translate.

F.M.2020-05-007

May 21, 2020- Tehran, Iran



جمهوری اسلامی ایران

دانشگاه تهران

۱۳۳/۱۲-۲۲
۱۳۹۹/۰۲/۰۸



بِسْمِ اللَّهِ الرَّحْمَنِ الرَّحِيمِ آمَنُوا بِمَنُكُمُ وَالَّذِينَ آمَنُوا بِاللَّيْمِ خَيْرًا

گواهینامه موفقیت پایان تحصیلات



گواهی می شود:

آقای سعید نصاری داد (ساحب عکس فوق) فرزند رضا دارای شناسنامه شماره ۱۴۵۰۶۰۱۶۸۵ کنشی ۱۴۵۰۶۰۱۶۸۵ متولد ۱۳۷۱/۰۷/۱۰ در مقطع کارشناسی پیوسته رشته مهندسی برق گرایش کنترل با معدل کلی ۱۸/۰۶ (هجده و شش صدم) و با درجه تحصیلی کارشناسی پیوسته دانش آموخته گردیده است.

بدآور می شود نامبرده تحصیلات خود را در دانشگاه تهران - پردیس دانشکده های فنی - دانشکده مهندسی برق و کامپیوتر از بهمن سال اول سال تحصیلی ۹۱-۱۳۹۰ شروع و در تاریخ ۱۳۹۲/۰۶/۳۱ به تمام رسانیده است. نامبرده مدت ۸ سال تعهد خدمت در ایران دارد. این گواهی صرفاً برای بهره مندی از مزایای آن در ایران صادر شده و ارزش ترجمه ندارد. اصل مدرک تحصیلی پس از انجام تعهد خدمت تحویل خواهد شد. ۱۳۹۲-۰۹-۰۲





علی طاهری میروانی
مدیرکل خدمات آموزشی
دانشگاه تهران

برای دریافت دانشگاه باید این گواهی صحیح گردید.
به این گواهی مبلغ ۱۰۰۰۰۰ ریال نمره الصاق و باطل گردیده است.

In The Name Of God
University of Tehran
Transcript of University Grades

Unofficial

	Student No. 911190273 First Name: Saeed Last Name: Asadollahi ID No. 1479603360 Date of Birth: 1992/09/02	Faculty: College of Engineering Major: Control Systems Total Passed Units: 142 GPA: 18.09 Level: Bachelor Graduate Date: 2015/09/22																																																																													
Academic Year 2011-2012 1st Semester EXCELLENT IN TERM Semester Status: Normal		Academic Year 2011-2012 2nd Semester EXCELLENT IN TERM Semester Status: Normal																																																																													
<table border="1" style="width: 100%; border-collapse: collapse;"> <thead> <tr> <th>Course Title</th> <th>Credits</th> <th>Grade</th> <th>Effect</th> </tr> </thead> <tbody> <tr><td>Introduction to Computers and Programming</td><td>3</td><td>17.5</td><td></td></tr> <tr><td>Physical Education 1</td><td>1</td><td>16</td><td></td></tr> <tr><td>English Language</td><td>3</td><td>16</td><td></td></tr> <tr><td>General Knowledge 1</td><td>3</td><td>16</td><td></td></tr> <tr><td>Industrial Training</td><td>1</td><td>20</td><td></td></tr> <tr><td>Physics 1</td><td>3</td><td>20</td><td></td></tr> <tr><td>Calculus 1</td><td>3</td><td>19.5</td><td></td></tr> <tr><td>Maths Workshop</td><td>1</td><td>17</td><td>0</td></tr> </tbody> </table>		Course Title	Credits	Grade	Effect	Introduction to Computers and Programming	3	17.5		Physical Education 1	1	16		English Language	3	16		General Knowledge 1	3	16		Industrial Training	1	20		Physics 1	3	20		Calculus 1	3	19.5		Maths Workshop	1	17	0	<table border="1" style="width: 100%; border-collapse: collapse;"> <thead> <tr> <th>Course Title</th> <th>Credits</th> <th>Grade</th> <th>Effect</th> </tr> </thead> <tbody> <tr><td>Engineering Probability and Statistics 1</td><td>3</td><td>17</td><td></td></tr> <tr><td>Foreign Language</td><td>1</td><td>20</td><td></td></tr> <tr><td>Islamic Studies</td><td>2</td><td>17</td><td></td></tr> <tr><td>Thermodynamics</td><td>3</td><td>18.5</td><td></td></tr> <tr><td>Differential Equations</td><td>3</td><td>18.5</td><td></td></tr> <tr><td>Physics 2</td><td>3</td><td>17</td><td></td></tr> <tr><td>Calculus 2</td><td>3</td><td>18</td><td></td></tr> </tbody> </table>		Course Title	Credits	Grade	Effect	Engineering Probability and Statistics 1	3	17		Foreign Language	1	20		Islamic Studies	2	17		Thermodynamics	3	18.5		Differential Equations	3	18.5		Physics 2	3	17		Calculus 2	3	18									
Course Title	Credits	Grade	Effect																																																																												
Introduction to Computers and Programming	3	17.5																																																																													
Physical Education 1	1	16																																																																													
English Language	3	16																																																																													
General Knowledge 1	3	16																																																																													
Industrial Training	1	20																																																																													
Physics 1	3	20																																																																													
Calculus 1	3	19.5																																																																													
Maths Workshop	1	17	0																																																																												
Course Title	Credits	Grade	Effect																																																																												
Engineering Probability and Statistics 1	3	17																																																																													
Foreign Language	1	20																																																																													
Islamic Studies	2	17																																																																													
Thermodynamics	3	18.5																																																																													
Differential Equations	3	18.5																																																																													
Physics 2	3	17																																																																													
Calculus 2	3	18																																																																													
<table border="1" style="width: 100%; border-collapse: collapse;"> <thead> <tr> <th>Semester</th> <th>Registered</th> <th>Semester Passed</th> <th>Total Passed Units</th> <th>Completion</th> </tr> <tr> <th>GPA</th> <th>Units</th> <th>Units</th> <th>GPA</th> <th>GPA</th> </tr> </thead> <tbody> <tr> <td>1st</td> <td>17</td> <td>17</td> <td>17</td> <td>17.81</td> </tr> </tbody> </table>		Semester	Registered	Semester Passed	Total Passed Units	Completion	GPA	Units	Units	GPA	GPA	1st	17	17	17	17.81	<table border="1" style="width: 100%; border-collapse: collapse;"> <thead> <tr> <th>Semester</th> <th>Registered</th> <th>Semester Passed</th> <th>Total Passed Units</th> <th>Completion</th> </tr> <tr> <th>GPA</th> <th>Units</th> <th>Units</th> <th>GPA</th> <th>GPA</th> </tr> </thead> <tbody> <tr> <td>2nd</td> <td>19</td> <td>19</td> <td>36</td> <td>18.24</td> </tr> </tbody> </table>		Semester	Registered	Semester Passed	Total Passed Units	Completion	GPA	Units	Units	GPA	GPA	2nd	19	19	36	18.24																																														
Semester	Registered	Semester Passed	Total Passed Units	Completion																																																																											
GPA	Units	Units	GPA	GPA																																																																											
1st	17	17	17	17.81																																																																											
Semester	Registered	Semester Passed	Total Passed Units	Completion																																																																											
GPA	Units	Units	GPA	GPA																																																																											
2nd	19	19	36	18.24																																																																											
Academic Year 2012-2013 1st Semester EXCELLENT IN TERM Semester Status: Normal		Academic Year 2012-2013 2nd Semester EXCELLENT IN TERM Semester Status: Normal																																																																													
<table border="1" style="width: 100%; border-collapse: collapse;"> <thead> <tr> <th>Course Title</th> <th>Credits</th> <th>Grade</th> <th>Effect</th> </tr> </thead> <tbody> <tr><td>Electromagnetics</td><td>3</td><td>17.5</td><td></td></tr> <tr><td>Engineering Mathematics</td><td>3</td><td>17.5</td><td></td></tr> <tr><td>Control Systems 1</td><td>3</td><td>17</td><td></td></tr> <tr><td>Logic Circuits</td><td>3</td><td>18.5</td><td></td></tr> <tr><td>Physics Laboratory 2</td><td>1</td><td>17</td><td></td></tr> <tr><td>Islamic Revolution and Challenges</td><td>1</td><td>18.5</td><td></td></tr> <tr><td>History of Iran</td><td>1</td><td>16</td><td></td></tr> <tr><td>Operations and Bulk Systems</td><td>1</td><td>20</td><td></td></tr> </tbody> </table>		Course Title	Credits	Grade	Effect	Electromagnetics	3	17.5		Engineering Mathematics	3	17.5		Control Systems 1	3	17		Logic Circuits	3	18.5		Physics Laboratory 2	1	17		Islamic Revolution and Challenges	1	18.5		History of Iran	1	16		Operations and Bulk Systems	1	20		<table border="1" style="width: 100%; border-collapse: collapse;"> <thead> <tr> <th>Course Title</th> <th>Credits</th> <th>Grade</th> <th>Effect</th> </tr> </thead> <tbody> <tr><td>An Introduction to the Study of Islamic Values</td><td>1</td><td>16</td><td></td></tr> <tr><td>Control Measurement Laboratory 1</td><td>1</td><td>18.5</td><td></td></tr> <tr><td>Control 2</td><td>3</td><td>18.5</td><td></td></tr> <tr><td>Systems Analysis</td><td>3</td><td>18.5</td><td></td></tr> <tr><td>Management 1</td><td>1</td><td>16</td><td></td></tr> <tr><td>Control Workshop</td><td>1</td><td>18.5</td><td></td></tr> <tr><td>Islamic Studies 2</td><td>1</td><td>19.5</td><td></td></tr> <tr><td>Islamic Mathematics 1</td><td>3</td><td>18.5</td><td></td></tr> </tbody> </table>		Course Title	Credits	Grade	Effect	An Introduction to the Study of Islamic Values	1	16		Control Measurement Laboratory 1	1	18.5		Control 2	3	18.5		Systems Analysis	3	18.5		Management 1	1	16		Control Workshop	1	18.5		Islamic Studies 2	1	19.5		Islamic Mathematics 1	3	18.5					
Course Title	Credits	Grade	Effect																																																																												
Electromagnetics	3	17.5																																																																													
Engineering Mathematics	3	17.5																																																																													
Control Systems 1	3	17																																																																													
Logic Circuits	3	18.5																																																																													
Physics Laboratory 2	1	17																																																																													
Islamic Revolution and Challenges	1	18.5																																																																													
History of Iran	1	16																																																																													
Operations and Bulk Systems	1	20																																																																													
Course Title	Credits	Grade	Effect																																																																												
An Introduction to the Study of Islamic Values	1	16																																																																													
Control Measurement Laboratory 1	1	18.5																																																																													
Control 2	3	18.5																																																																													
Systems Analysis	3	18.5																																																																													
Management 1	1	16																																																																													
Control Workshop	1	18.5																																																																													
Islamic Studies 2	1	19.5																																																																													
Islamic Mathematics 1	3	18.5																																																																													
<table border="1" style="width: 100%; border-collapse: collapse;"> <thead> <tr> <th>Semester</th> <th>Registered</th> <th>Semester Passed</th> <th>Total Passed Units</th> <th>Completion</th> </tr> <tr> <th>GPA</th> <th>Units</th> <th>Units</th> <th>GPA</th> <th>GPA</th> </tr> </thead> <tbody> <tr> <td>1st</td> <td>18</td> <td>18</td> <td>34</td> <td>18.25</td> </tr> </tbody> </table>		Semester	Registered	Semester Passed	Total Passed Units	Completion	GPA	Units	Units	GPA	GPA	1st	18	18	34	18.25	<table border="1" style="width: 100%; border-collapse: collapse;"> <thead> <tr> <th>Semester</th> <th>Registered</th> <th>Semester Passed</th> <th>Total Passed Units</th> <th>Completion</th> </tr> <tr> <th>GPA</th> <th>Units</th> <th>Units</th> <th>GPA</th> <th>GPA</th> </tr> </thead> <tbody> <tr> <td>2nd</td> <td>19</td> <td>19</td> <td>53</td> <td>17.96</td> </tr> </tbody> </table>		Semester	Registered	Semester Passed	Total Passed Units	Completion	GPA	Units	Units	GPA	GPA	2nd	19	19	53	17.96																																														
Semester	Registered	Semester Passed	Total Passed Units	Completion																																																																											
GPA	Units	Units	GPA	GPA																																																																											
1st	18	18	34	18.25																																																																											
Semester	Registered	Semester Passed	Total Passed Units	Completion																																																																											
GPA	Units	Units	GPA	GPA																																																																											
2nd	19	19	53	17.96																																																																											
Academic Year 2013-2014 1st Semester EXCELLENT IN TERM Semester Status: Normal		Academic Year 2013-2014 2nd Semester EXCELLENT IN TERM Semester Status: Normal																																																																													
<table border="1" style="width: 100%; border-collapse: collapse;"> <thead> <tr> <th>Course Title</th> <th>Credits</th> <th>Grade</th> <th>Effect</th> </tr> </thead> <tbody> <tr><td>Control Measurement Laboratory 2</td><td>1</td><td>17.5</td><td></td></tr> <tr><td>Control Laboratory 1</td><td>1</td><td>16</td><td></td></tr> <tr><td>Research and High Voltage Laboratory</td><td>1</td><td>20</td><td></td></tr> <tr><td>Control 2</td><td>3</td><td>18.5</td><td></td></tr> <tr><td>Plant System Analysis 1</td><td>3</td><td>18.5</td><td></td></tr> <tr><td>Local Control Systems</td><td>3</td><td>16</td><td></td></tr> <tr><td>High Voltage and Insulation</td><td>1</td><td>18.5</td><td></td></tr> <tr><td>Islamic Mathematics 2</td><td>1</td><td>16</td><td></td></tr> <tr><td>Islamic Studies (Philosophy and Literature)</td><td>1</td><td>18.5</td><td></td></tr> </tbody> </table>		Course Title	Credits	Grade	Effect	Control Measurement Laboratory 2	1	17.5		Control Laboratory 1	1	16		Research and High Voltage Laboratory	1	20		Control 2	3	18.5		Plant System Analysis 1	3	18.5		Local Control Systems	3	16		High Voltage and Insulation	1	18.5		Islamic Mathematics 2	1	16		Islamic Studies (Philosophy and Literature)	1	18.5		<table border="1" style="width: 100%; border-collapse: collapse;"> <thead> <tr> <th>Course Title</th> <th>Credits</th> <th>Grade</th> <th>Effect</th> </tr> </thead> <tbody> <tr><td>Local Control Systems Laboratory</td><td>1</td><td>20</td><td></td></tr> <tr><td>Control Laboratory 2</td><td>1</td><td>17.5</td><td></td></tr> <tr><td>Logic Circuits Laboratory</td><td>1</td><td>18.75</td><td></td></tr> <tr><td>Linear Algebra</td><td>3</td><td>18.75</td><td></td></tr> <tr><td>Digital and Practical Control Systems</td><td>3</td><td>18</td><td></td></tr> <tr><td>Electromagnetics 2</td><td>3</td><td>18.5</td><td></td></tr> <tr><td>Computer Architecture</td><td>1</td><td>19.5</td><td></td></tr> <tr><td>Physics Laboratory 1</td><td>1</td><td>17</td><td></td></tr> </tbody> </table>		Course Title	Credits	Grade	Effect	Local Control Systems Laboratory	1	20		Control Laboratory 2	1	17.5		Logic Circuits Laboratory	1	18.75		Linear Algebra	3	18.75		Digital and Practical Control Systems	3	18		Electromagnetics 2	3	18.5		Computer Architecture	1	19.5		Physics Laboratory 1	1	17	
Course Title	Credits	Grade	Effect																																																																												
Control Measurement Laboratory 2	1	17.5																																																																													
Control Laboratory 1	1	16																																																																													
Research and High Voltage Laboratory	1	20																																																																													
Control 2	3	18.5																																																																													
Plant System Analysis 1	3	18.5																																																																													
Local Control Systems	3	16																																																																													
High Voltage and Insulation	1	18.5																																																																													
Islamic Mathematics 2	1	16																																																																													
Islamic Studies (Philosophy and Literature)	1	18.5																																																																													
Course Title	Credits	Grade	Effect																																																																												
Local Control Systems Laboratory	1	20																																																																													
Control Laboratory 2	1	17.5																																																																													
Logic Circuits Laboratory	1	18.75																																																																													
Linear Algebra	3	18.75																																																																													
Digital and Practical Control Systems	3	18																																																																													
Electromagnetics 2	3	18.5																																																																													
Computer Architecture	1	19.5																																																																													
Physics Laboratory 1	1	17																																																																													
<table border="1" style="width: 100%; border-collapse: collapse;"> <thead> <tr> <th>Semester</th> <th>Registered</th> <th>Semester Passed</th> <th>Total Passed Units</th> <th>Completion</th> </tr> <tr> <th>GPA</th> <th>Units</th> <th>Units</th> <th>GPA</th> <th>GPA</th> </tr> </thead> <tbody> <tr> <td>3rd</td> <td>20</td> <td>20</td> <td>61</td> <td>17.96</td> </tr> </tbody> </table>		Semester	Registered	Semester Passed	Total Passed Units	Completion	GPA	Units	Units	GPA	GPA	3rd	20	20	61	17.96	<table border="1" style="width: 100%; border-collapse: collapse;"> <thead> <tr> <th>Semester</th> <th>Registered</th> <th>Semester Passed</th> <th>Total Passed Units</th> <th>Completion</th> </tr> <tr> <th>GPA</th> <th>Units</th> <th>Units</th> <th>GPA</th> <th>GPA</th> </tr> </thead> <tbody> <tr> <td>2nd</td> <td>19</td> <td>19</td> <td>70</td> <td>17.87</td> </tr> </tbody> </table>		Semester	Registered	Semester Passed	Total Passed Units	Completion	GPA	Units	Units	GPA	GPA	2nd	19	19	70	17.87																																														
Semester	Registered	Semester Passed	Total Passed Units	Completion																																																																											
GPA	Units	Units	GPA	GPA																																																																											
3rd	20	20	61	17.96																																																																											
Semester	Registered	Semester Passed	Total Passed Units	Completion																																																																											
GPA	Units	Units	GPA	GPA																																																																											
2nd	19	19	70	17.87																																																																											
Academic Year 2014-2015 1st Semester EXCELLENT IN TERM Semester Status: Normal		Academic Year 2014-2015 2nd Semester EXCELLENT IN TERM Semester Status: Normal																																																																													
<table border="1" style="width: 100%; border-collapse: collapse;"> <thead> <tr> <th>Course Title</th> <th>Credits</th> <th>Grade</th> <th>Effect</th> </tr> </thead> <tbody> <tr><td>Industrial Training</td><td>1</td><td>20</td><td>0</td></tr> </tbody> </table>		Course Title	Credits	Grade	Effect	Industrial Training	1	20	0	<table border="1" style="width: 100%; border-collapse: collapse;"> <thead> <tr> <th>Course Title</th> <th>Credits</th> <th>Grade</th> <th>Effect</th> </tr> </thead> <tbody> <tr><td>Industrial Electronics</td><td>1</td><td>16</td><td></td></tr> <tr><td>Management Research</td><td>1</td><td>18.5</td><td></td></tr> <tr><td>Control Workshop</td><td>1</td><td>20</td><td></td></tr> <tr><td>Industrial Control</td><td>3</td><td>19.5</td><td></td></tr> <tr><td>Computer Architecture Laboratory</td><td>1</td><td>18.75</td><td></td></tr> <tr><td>Fundamentals of Thermal Systems</td><td>1</td><td>18.5</td><td></td></tr> </tbody> </table>		Course Title	Credits	Grade	Effect	Industrial Electronics	1	16		Management Research	1	18.5		Control Workshop	1	20		Industrial Control	3	19.5		Computer Architecture Laboratory	1	18.75		Fundamentals of Thermal Systems	1	18.5																																									
Course Title	Credits	Grade	Effect																																																																												
Industrial Training	1	20	0																																																																												
Course Title	Credits	Grade	Effect																																																																												
Industrial Electronics	1	16																																																																													
Management Research	1	18.5																																																																													
Control Workshop	1	20																																																																													
Industrial Control	3	19.5																																																																													
Computer Architecture Laboratory	1	18.75																																																																													
Fundamentals of Thermal Systems	1	18.5																																																																													
<table border="1" style="width: 100%; border-collapse: collapse;"> <thead> <tr> <th>Semester</th> <th>Registered</th> <th>Semester Passed</th> <th>Total Passed Units</th> <th>Completion</th> </tr> <tr> <th>GPA</th> <th>Units</th> <th>Units</th> <th>GPA</th> <th>GPA</th> </tr> </thead> <tbody> <tr> <td>5th</td> <td>2</td> <td>2</td> <td>104</td> <td>17.87</td> </tr> </tbody> </table>		Semester	Registered	Semester Passed	Total Passed Units	Completion	GPA	Units	Units	GPA	GPA	5th	2	2	104	17.87	<table border="1" style="width: 100%; border-collapse: collapse;"> <thead> <tr> <th>Semester</th> <th>Registered</th> <th>Semester Passed</th> <th>Total Passed Units</th> <th>Completion</th> </tr> <tr> <th>GPA</th> <th>Units</th> <th>Units</th> <th>GPA</th> <th>GPA</th> </tr> </thead> <tbody> <tr> <td>4th</td> <td>18</td> <td>18</td> <td>122</td> <td>18.18</td> </tr> </tbody> </table>		Semester	Registered	Semester Passed	Total Passed Units	Completion	GPA	Units	Units	GPA	GPA	4th	18	18	122	18.18																																														
Semester	Registered	Semester Passed	Total Passed Units	Completion																																																																											
GPA	Units	Units	GPA	GPA																																																																											
5th	2	2	104	17.87																																																																											
Semester	Registered	Semester Passed	Total Passed Units	Completion																																																																											
GPA	Units	Units	GPA	GPA																																																																											
4th	18	18	122	18.18																																																																											



In The Name Of God
University of Tehran
Transcript of University Grades
Unofficial

	Student No. 400194601 First Name: Saeed Last Name: Arvan Eslami SSNO: 1450601665 Date of Birth: 1992/03/21	Faculty: College of Engineering Major: Control Systems Total Passed Units: 12 GPA: 18.28 Level: Master Graduate Date: 2018/07/08	
---	--	---	---

Academic Year 2015-2016 1st Semester					Academic Year 2015-2016 2nd Semester				
Semester Status: Normal					Semester Status: Normal				
Course Title	Credit	Grade	Effort		Course Title	Credit	Grade	Effort	
Mathematical Control Systems	3	CT			Estimation and System Identification	3	20		
Neural Networks	3	19			Robust Control	3	15.5		
Process Identification	3	19.1			Game Theory	3	16.5		
Semester GPA	Registered Units	Semester Passed Units	Total Passed Credits	Cumulative GPA	Semester GPA	Registered Units	Semester Passed Units	Total Passed Credits	Cumulative GPA
18.27	9	9	9	18.27	17.40	9	9	18	17.89

Academic Year 2016-2017 1st Semester					Academic Year 2016-2017 2nd Semester				
Semester Status: Normal					Semester Status: Normal				
Course Title	Credit	Grade	Effort		Course Title	Credit	Grade	Effort	
Signals	3	20			Special Topics in Control Engineering I	3	20		
Mathematical Systems Control	3	17.1			Thesis	6	20	1	
Thesis	6	20	1						
Semester GPA	Registered Units	Semester Passed Units	Total Passed Credits	Cumulative GPA	Semester GPA	Registered Units	Semester Passed Units	Total Passed Credits	Cumulative GPA
18.48	11	9	21	18.08	20.00	9	9	24	18.28

Academic Year 2017-2018 1st Semester					Academic Year 2017-2018 2nd Semester				
Semester Status: Normal					Semester Status: Normal				
Course Title	Credit	Grade	Effort		Course Title	Credit	Grade	Effort	
Thesis	6	20	1		Thesis	6	20/20	1	
Semester GPA	Registered Units	Semester Passed Units	Total Passed Credits	Cumulative GPA	Semester GPA	Registered Units	Semester Passed Units	Total Passed Credits	Cumulative GPA
8	6	6	24	18.28	8	6	6	24	18.28

Academic Status Full mark is 20 Last Name - Graduate Date : 2018/07/08	NOTE: In "Effort" column: "1" indicates that the total passed credits is not affected by this course. "2" indicates that the cumulative gpa is not affected by this course. "3" indicates that the total passed credits and cumulative gpa are not affected by this course. In "Grade" column the following abbreviations are used: B: Referred NC: Incomplete
--	---

GENERAL DIRECTOR OF ACADEMIC AFFAIRS
ALI TAHERI MORGHAIED Ph.D

Signed and sealed

NOTE: Since S/he has commitments with the government of the Islamic Republic of Iran, should S/he want to continue her/his studies, S/he is required to obtain an official permission from the Iranian government.



Date: 2020/04/26 END OF TRANSCRIPT



Pseudo DVL reconstruction by an evolutionary TS-fuzzy algorithm for ocean vehicles



Saeed Ansari-Rad ^a, Mojtaba Hashemi ^{b,*}, Hassan Salarieh ^c

^a School of Electrical and Computer Engineering, University of Tehran, Iran

^b School of Mechanical Engineering, University of Imam Hossein, Tehran, Iran

^c School of Mechanical Engineering, Sharif University of Technology, Tehran, Iran

ARTICLE INFO

Article history:

Received 6 January 2019

Received in revised form 9 July 2019

Accepted 12 July 2019

Available online 16 July 2019

Keywords:

AI-aided integration systems

Doppler Velocity Log (DVL) outage

Evolutionary TS-fuzzy

Extended Kalman Filter (EKF)

Inertial Navigation System (INS)

ABSTRACT

By development of ocean exploration, autonomous vehicles are employed to perform on-water and underwater tasks. Using an extended Kalman filter, Inertial Navigation System/Doppler Velocity Log (INS/DVL) integrated systems are trying to navigate in oceans and underwater environments when Global Positioning System (GPS) signals are not accessible. The dependency of DVL signals on acoustic environments may cause any DVL malfunction due to sea creatures or strong wave-absorbing material. In this paper, an improved version of evolutionary TS-fuzzy (eTS) is proposed in order to predict DVL sensor outputs at DVL malfunction moment, by utilizing an artificial intelligent (AI) aided integrated system. According to lack of input selection and shrinking, while the classic eTS suffers from soaring prediction errors and may result in instability, by adding these properties to eTS, the performance increases in long-term DVL outage. The proposed eTS-aided system makes ocean navigation purposes possible during long-term and simultaneous outage of GPS and DVL. These evolutionary fuzzy systems change their structure depending on the path which makes the trained fuzzy system more flexible with non-stationary and varying environments. The real sensor data is collected online with a test setup on a lake and then the algorithms are applied. The powerful capacity of the proposed data fusion method is demonstrated in analysis results.

© 2019 Elsevier Ltd. All rights reserved.

1. Introduction

By development of ocean exploration, remotely operated vehicles (ROVs) and autonomous underwater vehicles (AUVs) are employed to perform on-water and underwater tasks [1,2]. Navigation is the determination of position and orientation of an object at any moment. The inertial navigation system is a self-contained system with high reliability and complete independence, which has been widely used in military and civil applications. Inertial Navigation System (INS) usually uses the specific forces and angular rates of a vehicle in three dimensions measured by Inertial Measurement Unit (IMU) to provide velocity, position and attitude of the vehicle; however, inertial navigation is limited by time growing errors due to the inherent bias errors of gyroscopes and accelerometers [3–5].

Therefore, in order to improve the navigation performance, INS requires some measurements provided by auxiliary sensors. Inte-

grated navigation system consists of multiple navigation sensors and is widely adopted in ocean and underwater vehicles [6–8]. Global Positioning System (GPS) is often integrated with INS by a Kalman Filter (KF) to decrease the accumulated position error. Most of data fusion methods are based on the KF which optimally estimates the states of a linear system from observations. But in order to deal with nonlinear systems, an extended KF (EKF) is used whose performance depends on the accuracy of the system model and measurement dynamics [9]. For this purpose, authors in [10] and [11] have suggested the EKF in INS/GPS integration system. In ground navigation, the GPS and INS data fusion is using KF [12–14]. However, in ocean and underwater navigation, it is often necessary to exploit other auxiliary sensors due to quick attenuation of satellite signal and unavailability of GPS in water area.

Doppler Velocity Log (DVL) is a high-precision velocity measuring instrument, which increasingly becomes popular among acoustic sensors in standard underwater navigation systems [15]. DVL provides velocity relative to the seafloor or the current, based on the Doppler effect and by integration with KF can restrain the error accumulation of INS [16–18]. However, the dependence of DVL signal on the acoustic environment may cause DVL malfunction [4].

* Corresponding author.

E-mail addresses: saeedansari71@ut.ac.ir (S. Ansari-Rad), mo_hashemi@aut.ac.ir (M. Hashemi), salarieh@sharif.edu (H. Salarieh).

As a case, when the acoustic wave is emitted due to sea creatures or strong wave-absorbing materials and when an underwater vehicle sails over a trench or performs angular maneuvers with large roll and pitch. These situations could lead to the loss or sudden changes in the DVL signal, accumulation of INS errors and inaccurate navigation data obtained from the integrated system.

Over the past decades, two categories of solutions have been suggested to deal with auxiliary sensor malfunctions. One of them is to mask a faulty sensor by using the hardware redundancy [19,20] and the adjustment of sensors utilization [21–23]. This kind of approaches can deal with the malfunction for a long time, but requires high hardware cost. To provide a relatively high-precision solution, another category is working to find alternatives and pseudo auxiliary sensors for the KF [24–26]. Possible candidates for providing pseudo auxiliary sensors can be classified into data-driven, analytical model-based, and knowledge-based methods. The model-based approaches such as [27–30] fit mathematical models which are often constructed from time-consuming identification methods and accordingly, are only applicable to the systems with rich information. Thus, the autonomous underwater vehicles containing complex dynamics require relatively satisfactory models and numerous sensors, which practically rule out employing the model-based approaches for pseudo auxiliary sensors. On the other hand, the data-driven methods [31] only acquire information from direct measurement and as the result require large amount of data, reliable feature sets, and decision criteria in order to demonstrate meaningful results. Consequently, in the case of reconstructing auxiliary sensors, the performance of such methods decreases due to limited data sets and unexpected data range variations.

In contrast to model-based and data-driven, the knowledge-based approaches represent much more suitable candidate for applying to the systems with limited information, few sensors, or complex dynamics. These methods employ qualitative models with adaptable rules in order to effectively learn and then predict prevailing system behaviors. Therefore, some researches such as [14,25,32–38] recently have considered artificial intelligent knowledge-based modules for predicting the auxiliary sensor information. In [35], a hybrid predictor is proposed to deal with short-term DVL malfunctions for underwater integrated navigation systems; the approach can estimate the measurements of the DVL within its malfunction. However, in long-term malfunctions, the performance of the predictor decreases. To oppose with long-term malfunctions, evolutionary systems should be utilized in the prediction of missing DVL data. On the other hand, most of neural networks or neuro-fuzzy systems do not continue to learn, to improve, or to adapt after their designing. This problem imperils the prediction performance when these networks encounter non-stationary and changing environments. Therefore, it should begin considering evolving autonomous systems especially knowledge-based intelligent systems. In [32] a fault-tolerant integrated navigation system with an adaptive Kalman filter (AKF) based on evolutionary artificial neural networks (EANN) is proposed; but the evolutionary approach is only applied to the ground navigation system, where magnetic compass (MCP) data are available during DVL malfunctions.

This paper aims to use an evolutionary TS-fuzzy (eTS) algorithm for reconstruction of DVL signals for ocean navigation systems. The eTS is the subtopic of computational intelligence, whose property is the ability to self-adaptation, to online process of the system structure and parameters, to expand its structure, to adapt its parameters, and especially to evolve. Therefore, the problems of long-term DVL malfunctions, adaptive ocean and underwater navigation, and constructing an evolutionary pseudo DVL are solved in this paper. The remainder is organized as follows: In Section 2, the structure of the basic system, calculations of INS error dynamics

and integrated system with EKF are comprehensively studied. Thereafter in Section 3, the algorithm of eTS is explained and is improved in order to increase the predictability of the system. The description of the eTS aided fusion method is presented in Section 4. Finally, Section 5 is devoted to the simulation and field test studies.

2. Inertial navigation mechanization

Since GPS is not always available in ocean and underwater navigation, integrated navigation systems also adopt DVL as auxiliary sensor to reduce drift error and to increase high accuracy [39]. The DVL, without the need to use external sources, is a popular sensor to assist INS in the environments with attenuated GPS signals. While various versions of Kalman Filter [40], including Unscented KF and EKF, are used to augment INS measurements with auxiliary sensors, the proposed method in this research is not devoted to a specific type of Kalman Filter. In this section, EKF is studied as the corresponding filter to the integrated navigation system, but without losing any generality, other types of KF including UKF could be candidate for the proposed integrated system.

Fig. 1 shows the system structure of the INS/DVL integrated navigation system in the absence of GPS signals. Because of its less computational effort and high fault-tolerance, the federated filter is adopted to fuse the multi-sensor data. The measurement deviation between the INS and the assistant navigation observer is given to the corresponding local filter as input. Since the DVL provides the velocity measurements in the body frame, the outputs of the DVL need to be transformed to the navigation frame by the attitude matrix obtained from the INS.

2.1. Integration system using error-based EKF

A EKF [41,42] is applied for the navigation system, with the 15-state space vector as follows:

$$x = \left[\delta L \quad \delta l \quad \delta h \quad \delta V_{NE}^{1 \times 3} \quad \tilde{\epsilon}^{1 \times 3} \quad b_a^{1 \times 3} \quad b_g^{1 \times 3} \right]^T \quad (1)$$

where δL , δl , δh are the error of latitude, longitude and height, respectively. The vehicle velocity can be written as $V_{NE}^{1 \times 3} = [V_N V_E V_D]^T$ in north, east and down frame (NED). $\tilde{\epsilon}^{1 \times 3}$ is the perturbed quaternion elements vector. $b_a^{1 \times 3}$ and $b_g^{1 \times 3}$ represent the accelerometer biases and gyro biases in three directions of the body frame.

The nonlinear state space and the measurement vector (z) can be obtained as follows:

$$\dot{x} = f(x, u) + \Omega \xi(t), \quad \xi = N(0, Q)$$

$$z = h(x) + \kappa(t), \quad \kappa = N(0, R) \quad (2)$$

where $f(x, u)$ and $h(x)$ are the system vector and the observation vector. u denotes the input vector. Also, ξ and κ are process and measurement white noise vector, characterized by their corresponding covariance matrices Q and R , respectively. Ω is the system noise matrix. The first order Markov process is used for mathematical model of bias instability in inertial sensors.

The system in Eq. (2) is transformed to the discrete time form by using the forward Euler method with time step k . The state transition matrix is approximated as follows:

$$\Phi_k = \frac{\delta f_k}{\delta x_k^T}(x_k, u_k) \quad (3)$$

where x_k , u_k are the system state vector and the system input vector at stage k , respectively. The measurement matrix is calculated as follows:

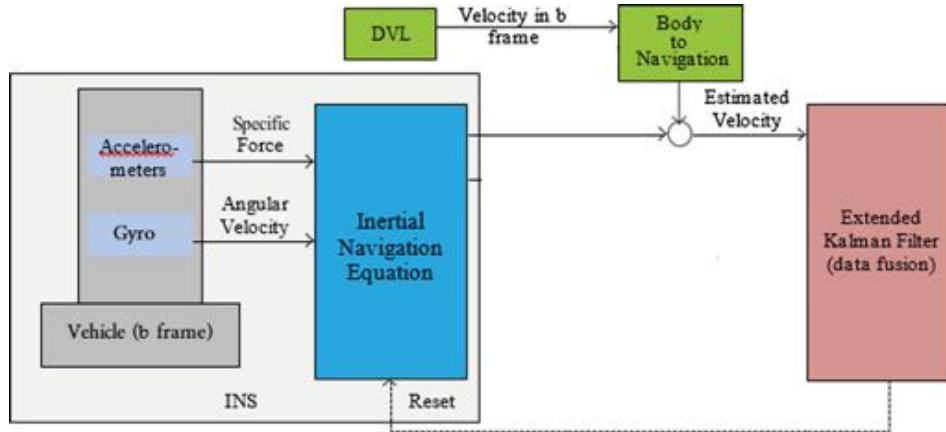


Fig. 1. Block diagram of the integration navigation system.

$$\theta_k^T = \frac{\delta z_k}{\delta x_k^T}(x_k) \quad (4)$$

where z_k denotes the measurement vector at step k . The implementation of EKF can be divided into two stages, the update and prediction. First, the Kalman gain (K_k) is computed and then, the estimated state vector (\hat{x}_k) and the error covariance matrix (\hat{X}_k) are updated using the prior estimate, \bar{x}_k , and its error covariance, \bar{X}_k at step k . Also, Q_k and R_k are covariance matrices of process and measurement white noise, and Ω_k is the system noise matrix, at step k [43–45]

$$K_k = X_k \theta_k^T (\theta_k X_k \theta_k^T + R_k)^{-1}$$

$$\hat{x}_k = \bar{x}_k + K_k (z_k - h_k(\bar{x}_k))$$

$$\hat{X}_k = (I - K_k \theta_k) \bar{X}_k (I - K_k \theta_k)^T + K_k R_k K_k^T \quad (5)$$

The prediction stage is formulated as the follows:

$$\bar{x}_{k+1} = f_k(\bar{x}_k, u_k)$$

$$\bar{X}_{k+1} = \Phi_k \hat{X}_k \Phi_k^T + \Omega_k Q_k \Omega_k^T. \quad (6)$$

3. Proposed predictor

In this part, the relationship between the INS outputs and the DVL measurements is going to be established. It is worth mentioning that INS results are corrected by EKF. Measurements of DVL can be predicted when it malfunctions. During navigation and in case of existing strong relevance between the variables, to improve the prediction accuracy and reliability, AI module should evolve, and also effective inputs should be selected. The main idea of an AI-aided integrated system is to explore the mathematical relationship between data of IMU, INS, and the navigation information of integrated system, trying to maintain high accuracy during DVL malfunction. In the case of availability of DVL signals, AI module is force to be trained. During DVL malfunction, the well-trained module is employed to reconstruct DVL signals. This part introduces eTS fuzzy system [46]. Thereafter, an improved version of eTS for AI-aided integrated systems is described.

3.1. ETS for the prediction of DVL measurements

Nowadays, facing with large data sets, demands for quick process with huge data streams, self-developing, and self-maintaining in advanced process industries which cannot be

covered with offline methods and adjusting parameters. These requirements call for new type of systems with flexibility, adaptability, and handling non-stationary environments. The Takagi-Sugeno fuzzy structures enable the flexibility, parallelism, and the development of effective learning techniques, which usually have consequent parts of linear form. The evolving TS-fuzzy system is defined as follows:

$$\text{Rule}^i : \text{IF } (x_1 \text{ is close to } x_1^{i*}) \text{ AND } \dots \text{ AND } (x_n \text{ is close to } x_n^{i*})$$

$$\text{Then } (y^i = x_e^T \pi^i) \quad (7)$$

where the number of fuzzy rules is shown with R ; the output of the i th sub-system is shown with y^i ; the extended input vector is formed as $x_e^T = [1, x_1, \dots, x_n]^T$, parameters of sub-models are shown with $\pi^i, i = 1, \dots, R$; and; x_j^{i*} is the j th index of the focal point of the i th rule.

Since the parameters of linear models are boundless, there is no general requirement for normalization of the inputs. However, to give more flexibility, a vector representation for data radius, $r = [r_1, r_2, \dots, r_n]^T$, is considered in the form of following:

$$r = \bar{r} (\bar{x} - \underline{x}) \quad (8)$$

where, $\bar{x} = [\bar{x}_1, \bar{x}_2, \dots, \bar{x}_n]^T$ and $\underline{x} = [x_1, x_2, \dots, x_n]^T$ represent respectively the vector of expected maximum and minimum of the inputs. Using different radius for each input variables, the membership function of fuzzy sets is formulated as Eq. (9).

$$\mu^i(x) = e^{-4 \sum_{j=1}^n \frac{(x_j - x_j^{i*})^2}{r_j^2}} \quad (9)$$

The overall model output is calculated with weighted average of individual rules' contribution,

$$y = \sum_{i=1}^R \lambda^i(x) y^i = \sum_{i=1}^R \lambda^i(x) x_e^T \pi^i \quad (10)$$

where $\lambda^i(x) = \mu^i(x) / \sum_{j=1}^R \mu^j(x)$ is the normalized firing level of the i th rule.

Both locally and globally optimal solutions can be adopted in using the RLS algorithm. In the following, basic stages for online learning is briefly reviewed. In Fig. 2, the scheme of the stages is visualized. For more details, the reader is referred to [47].

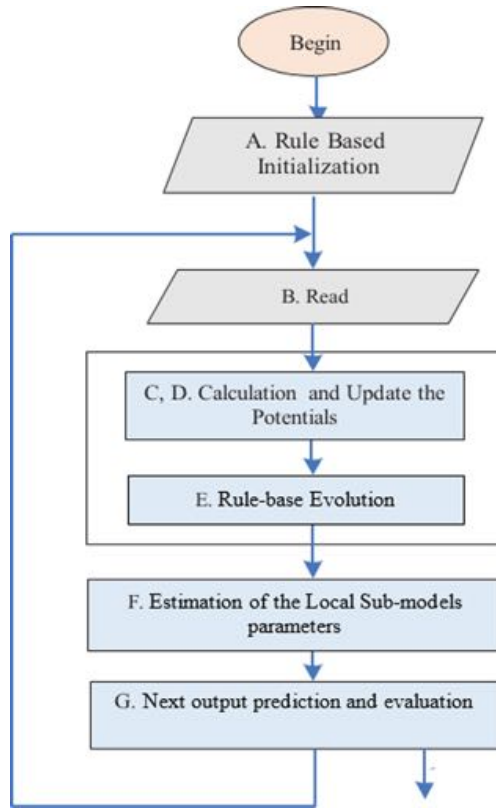


Fig. 2. The basic stages of the procedure in online learning [48].

3.1.1. Rule-base initialization

The on-line learning procedure starts with initialization of the first rule. The first data point is established as the focal point of the first cluster ($i = 1$). Parameters of the local linear model associated to the rule are also initialized with 0.

$$R = 1; x^{1*} = x_1; P_1(z^{1*}) = 1; \hat{\pi}_1^i = 0; c_1^i = \Omega I, \quad (11)$$

where z^{1*} is the first cluster center and I is the identity matrix. After this level, the time step is updated ($k := k + 1$), where k denotes the next time step.

3.1.2. Calculation of the potential of the new data point and updating the potentials of the centers

The potential of a data point is measured with a Cauchy type function and is recursively calculated as follows:

$$P_k(z_k) = k - \frac{1}{(k-1)(\vartheta_k + 1) + \sigma_k - 2v_k}; k = 2, 3, \dots \quad (12)$$

where $P_k(z_k)$ denotes the potential of the data point (z_k) calculated at step k . The remain parameters are calculated based on Eq. (13).

$$\vartheta_k = \sum_{j=1}^{n+1} (z_k^j)^2; v_k = \sum_{j=1}^{n+1} z_k^j \beta_k^j; \sigma_k = \sigma_{k-1} + \sum_{j=1}^{n+1} (z_{k-1}^j)^2$$

$$\beta_k^j = \beta_{k-1}^j + z_{k-1}^j; d_{ik}^j = z_i^j - z_k^j \quad (13)$$

Each new data point influences the potentials of the centers of the clusters. The potentials of the focal points of the existing clusters ($P_k(z^{l*})$) are recursively updated base on Eq. (14), where z^{l*} is the prototype of the l th rule at step k .

$$P_k(z^{l*}) = \frac{(k-1)P_{k-1}(z^{l*})}{k-2 + P_{k-1}(z^{l*}) + P_{k-1}(z^{l*}) \sum_{j=1}^{n+1} (d_{k(k-1)}^j)^2} \quad (14)$$

3.1.3. Rule base evolution

Condition 1: MODIFY

The new data point is replaced with the center of j th cluster with the following modifications:

$$x^{j*} = x_j; P_k(z^{j*}) = P_k(z_k). \quad (15)$$

When MODIFY principle is activated, the covariance matrices are taken from the previous step without change. Furthermore, parameters of all rules are not modified ($\hat{\pi}_k^i = \hat{\pi}_{k-1}^i; i = 1, 2, \dots, R$).

Condition 2: UPGRADE

The new data point is added as a new center and the number of rules increases, consequently.

$$R = R + 1; x^{R*} = x_R; P_k(z^{R*}) = P_k(z_k) \quad (16)$$

Parameters of the newly added rule are calculated as $\hat{\pi}_k^{R+1} = \sum_{i=1}^R \lambda^i \hat{\pi}_{k-1}^i$, and parameters of the rest of rules are not modified. The covariance matrix of the newly added rule is initialized with ΩI , and the rests are inherited ($c_k^i = c_{k-1}^i$).

Generally, the MODIFY condition includes the UPGRADE condition plus checking the closeness of the new rule center to the existing rule centers. The closeness is measured with Euclidean distance from the new data point to the closest existing rule centers. The condition of closeness is checked by monitoring $\delta_{min} < \|r\|/2$, where $\delta_{min} = \min_i (\delta^i = \|z_k - z^{i*}\|)$. Also, the condition of UPGRADE is activated when:

$$P_k(z_k) > \bar{P}_k \text{ or } P_k(z_k) < \underline{P}_k \quad (17)$$

where

$$\bar{P}_k = \max P_k(z^{i*}); \underline{P}_k = \min P_k(z^{i*}). \quad (18)$$

3.1.4. Estimation of the local sub-models parameters

The locally optimal estimation of parameters is calculated based on the weighted least square as follows:

$$\hat{\pi}_k^i = \hat{\pi}_{k-1}^i + c_k^i x_{ek-1} \lambda^i (x_{k-1}) (y_k - x_{ek-1}^T \hat{\pi}_{k-1}^i)$$

$$c_k^i = c_{k-1}^i - \frac{\lambda^i (x_{k-1}) c_{k-1}^i x_{ek-1} x_{ek-1}^T c_{k-1}^i}{1 + \lambda^i (x_{k-1}) x_{ek-1}^T c_{k-1}^i x_{ek-1}} \quad (19)$$

3.1.5. Next output prediction and evaluation

The next value of the output is predicted by employing the estimated parameters of the local sub-models:

$$\hat{y}_{k+1} = \Psi_k^T \hat{\theta}_k \quad (20)$$

where

$$\hat{\theta}_k = \left[(\hat{\pi}_k^1)^T, (\hat{\pi}_k^2)^T, \dots, (\hat{\pi}_k^R)^T \right]^T$$

$$\Psi_k = [\lambda^1 (x_k) x_{ek}^T, \lambda^2 (x_k) x_{ek}^T, \dots, \lambda^R (x_k) x_{ek}^T]^T. \quad (21)$$

Non-Dimensional Error Index (NDEI) is a tool to evaluate the performance of models which is the ratio of the root mean square error (RMSE) over the standard deviation of the target data.

$$\text{NDEI} = \frac{\text{RMSE}}{\text{Range}(y(t))} \quad (22)$$

3.2. Improved eTS

Condition 3: SHRINK

The structure of the ETS can grow by generating new fuzzy rules, but it can also shrink by removing a rule with low utility or detecting variation of data pattern with respect to the focal point of that rule. In the underwater navigation, due to the non-stationary and varying environment, clusters should grow or shrink through the learning phase. The focal point, which represents a cluster, should have generalization power regarding to the online nature of processes.

The population of the i th cluster at step k is the number of data samples which are assigned to the cluster ($N^i(k)$). By utilizing focal points of the rules, each data sample is assigned to the nearest existing focal points (one cluster only) based on Eq. (23) unless UPGARDE condition is activated. In UPGARDE, the population of the newly formed cluster is set to 1 and the rests are not modified.

$$N^i(k) = N^i(k) + 1; i = \arg \min_i \|x(k) - x^{i*}\|^2$$

$$\sum_{i=1}^R N^i(k) = k \quad (23)$$

From the moment of appearance of the i th cluster, it is judged by the existing data samples. Therefore, the population of each cluster should be monitored, and in the case of detecting clusters with less than 1% contribution with respect the total data samples, the cluster is ignored by setting its firing level to 0 ($\lambda^i = 0$). Unlike [49], in this paper, SHRINK condition is checked with a threshold described as the following condition:

$$\text{IF} \left(\frac{N^{i*}(k)}{\sum_{i=1}^R N^i(k)} < \eta \right), \text{THEN} (\lambda^{i*} = 0). \quad (24)$$

Suggested values for η are chosen between 0.001 and 0.1, depending on the application and data sample numbers.

Condition 4: Online VARIABLE SELECTION

So far it is assumed that the number of input variables is predefined and fixed; however, a large number of correlated inputs could be detected in many problems. Therefore, input variable selection becomes a crucial problem, especially for intelligent sensors. In off-line problems, input selection is usually approached by adopting principal component analysis (PCA), GA, partial least squares (PLS), and sensitivity analysis. It is often difficult to extract the best online subset of input variables for dynamic and non-stationary systems. Consequently, it is important to develop a method enabling automatic input variable selection.

The idea of automatic input variable selection is put forth based on the online monitoring and analysis of parameter values. If the parameters of rules are negligibly small for a certain input, a particular input would not significantly contribute with respect to the overall output. Hence, the input variable would be a candidate for removal. This can be mathematically represented with the accumulated sum of the consequent parameters ($|\pi_{jt}^i|$) for the specific j th input with respect to all inputs [50]:

$$\omega_{jk}^i = \frac{\varphi_{jk}^i}{\Phi_k^i} = \frac{\sum_{t=1}^k |\pi_{jt}^i|}{\sum_{r=1}^n \varphi_{rk}^i} \quad (25)$$

The value of ω_{jk}^i indicates the contribution of a particular input, which can be monitored. The online selection of input variables plays an important role in the intelligent sensor fusions. Unlike [50], in this paper, VARIABLE SELECTION condition is chosen as follows:

$$\text{IF} (\exists j^* | \omega_{j^*k}^i < \varepsilon), \text{THEN} (\text{remove } j^*) \quad (26)$$

where ε denotes a coefficient suggested between 0.001 and 0.1 and j^* denotes the candidate for removal. The mentioned researches [49,50] have tried to present automatic indices that measure the contribution of clusters and input features, and have considered the general applications of eTS scheme, which pose considerable complexities in system parameters. Nevertheless, applying eTS in the navigation procedure, the automatic indices lost their performance, and utilizing Eqs. (24) and (26) as indices leads to much more stable results rather than the automatic indices.

4. I-eTS aided ocean integrated navigation

By exploiting the improved eTS (I-eTS) algorithm, the AI-aided integrated system is constructed. Based on Fig. 3, in the learning stage by using IMU, INS, and ΔV_{DVL} online information, the I-eTS network is trained. Meanwhile, the INS/DVL integrated system is correcting the corresponding outputs. In Fig. 3, P_{INS} , V_{INS} and q_{INS} are the position, velocity, quaternions of INS sensors, respectively. Moreover, δP , δV , and δq denote estimation difference of the mentioned parameters calculated in EKF and f_b is the specific force measured from IMU. By detecting any malfunction in DVL signals, the training procedure is stopped and the well-trained network predicts DVL signals, $V_{\text{pseudo-DVL}}$. Thereafter, EKF uses these predicted signals instead of DVL signals to correct INS outputs.

The main concentration of the research is devoted to design a fault-tolerant integrated system employing an improved-eTS. Such fault-tolerant systems demand a robust methodology for detecting fault, which is currently out-of-box notion for this paper. On the other hand, varied strategies have been recently introduced, including [51], which are able to identify different auxiliary sensor faults, precisely. Hence, without losing any major points in the paper, it is assumed that in the DVL signal malfunction moment, the whole information is accessible, and the fault moments are completely known.

5. Test results

In order to evaluate the performance of the proposed method, a lake test was accomplished. An instrumented vessel was utilized for the experiment which is shown in Fig. 4. The instruments used in the test include a MEMS IMU assembled by Analog Devices Inc. with model ADIS16448, a DVL made by Link Quest Inc. model Nav-Quest 600 micro installed on the vessel, depicted in Fig. 4, and a GPS receiver FGPMMPA6B.

The GPS receiver and its measurements were used for initialization and reference purposes. The specifications of the instruments are listed in Table 1.

5.1. DVL signal estimation

This section is dedicated to the study the I-eTS and comparison with the performance of ordinary eTS. To meet with the target, by considering a portion of an ocean navigation path, the roll of design parameters from Section 3.2 is studied. The information of the path is acquired from an INS/GPS/DVL integrated navigation system, where the estimated values of auxiliary sensors are not involved in navigation correction. Therefore, in the learning stage, IMU, INS, and ΔV_{DVL} information are accessible for evolutionary structures, which are passed through eTS in the same order they have been obtained from the navigation path. Furthermore, the information is processed the same way as online eTS, which avoids accumulating data into a memory. Considering Fig. 5, 80% of path data is devoted to the training phase, which includes varied

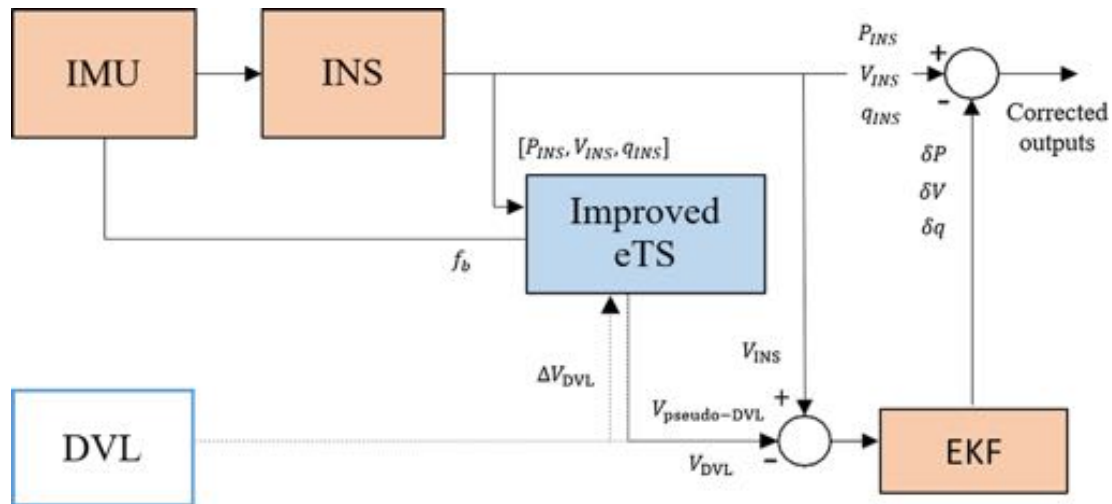


Fig. 3. Improved eTS aided INS/DVL integration navigation system.

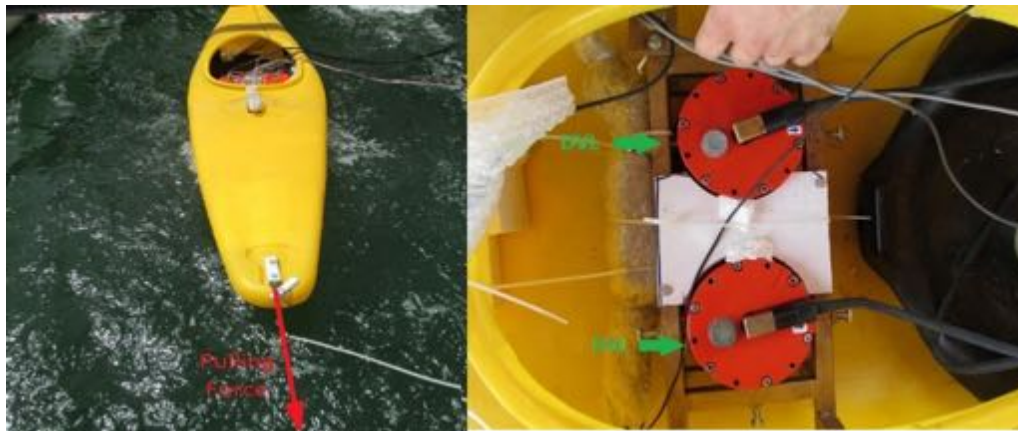


Fig. 4. Left) instrumented vessel for experiments and Right) instruments mounted on the vessel [29].

Table 1
Instrument specifications.

Gyroscope		Accelerometer		DVL		GPS	
Dynamic Range	$\pm 1200^\circ/\text{s}$	Dynamic Range	$\pm 18 \text{ g}$	Frequency	600 KHz	Frequency	1575.42 MHz
In-run Bias Stability	$14.5^\circ/\text{h} @ 1\sigma$	In-run Bias Stability	$0.25 \text{ mg} @ 1\sigma$	Accuracy	$0.2\% \pm 1 \text{ mm/s}$	Accuracy	2.5 m
Angular Random Walk	$0.066^\circ/\sqrt{\text{h}} @ 1\sigma$	Output Noise	5.1 mg rms	Maximum Altitude	110 m	Maximum Altitude	18,000 m
Output Noise	$0.27^\circ/\text{s rms}$	-3 dB Bandwidth	330 Hz	Minimum Altitude	0.3 m	Sensitivity	-148 dBm
-3 dB Bandwidth	330 Hz	Data Rate	100 Hz	Maximum Velocity	$\pm 20 \text{ knots}$	Maximum Velocity	515 m/s
Data Rate	100 Hz			Maximum Ping Rate	5/s	Maximum Acceleration	4 g

maneuvers making the online training procedure more challenging. On the other hand, the remaining data information for test path are based on the complete INS/GPS/DVL integrated system and accordingly, does not get feedback from eTS prediction results.

Afterward, the performance of eTS is compared with I-eTS in the Fig. 6. For each DVL output signal, the desired values (the red lines) obtained from the integrated navigation system and output prediction of eTS and I-eTS are demonstrated, as well. It is shown that for V_{DVLx} and V_{DVLy} , the performance of eTS (the green-lines) is impaired in some specific moments of test path mostly due to the redundant clusters, hardly contributing in learning process of DVL output signals. Nonetheless, I-eTS (the blue-lines) has improved the prediction ability and provided precise estimation of DVL output signals. In the third output, which is denoted by

V_{DVLz} , eTS and I-eTS demonstrate similar performance. The maneuver has been carried out on ocean surface; as a consequence, the third output signal remains fairly stable in the training and test phases, leading to precise prediction by both eTS and I-eTS structures.

Furthermore, effect of design parameters on the performance of I-eTS has been studied in Table 2 which is devoted to quantitative result of predicting the DVL outputs of the test path demonstrated in Fig. 5. Three major indices are selected for quantitative comparison between results of eTS and I-eTS: training and testing cost, and NDEI index obtained from Eq. (22). The first row of the table is related to the prediction results of eTS previously illustrated in Fig. 6 with the green lines. The remaining rows contain prediction results of I-eTS by considering different design parameters.

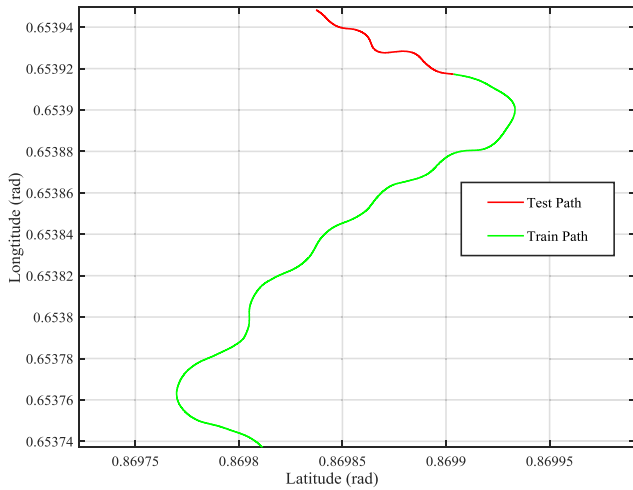


Fig. 5. Navigation trajectories for train and test phase of eTS and I-eTS (by choosing $\eta = 0.005$ and $\varepsilon = 0.01$).

The parameter η determines the limit for removing the excessive clusters in the training phase. In Table 2, it is demonstrated that by selecting a slightly small value for η such as 0.001, I-eTS performance bears resemblance to the ordinary eTS, and the vast majority of clusters are detected as influential one. On the other hand, choosing relatively substantial values such as 0.1 for η eliminates the clusters having significant contribution in predicting DVL output signals, and eventually decreases the performance of I-eTS. Selecting $\eta = 0.01$ as an optimal value, unimportant clusters are neglected, and the remaining clusters play conspicuous role in

improving the prediction ability of I-eTS in comparison with the ordinary eTS. The parameter ε is employed to determine the contribution of input regressors in I-eTS prediction ability. Similarly, assigning considerable values for ε such as 0.1 provides the possibility of ignoring the crucial input data, which dramatically increases the prediction error. Therefore, from what has been deduced from Table 2, the optimal values of $\eta = 0.01$ and $\varepsilon = 0.01$ are selected for the I-eTS prediction properties defined in Section 5.1.2. The main purpose of the table is to show behavior and effect of the assigned values on the DVL reconstruction accuracy. Moreover, the table represents ranges of chosen number which are available for the I-eTS index parameters. Consequently, all the numbers around $\eta = 0.01$ and $\varepsilon = 0.01$ mainly lead to the similar performance from NDEI point of view. As seen in Section 5.1.2, for other maneuvers, the assigned values bring about acceptable navigation accuracy during DVL malfunction.

5.2. ETS-aided integration navigation test

In this section, two ocean integrated navigation tests are conducted to show performance of the proposed algorithm in Section 4. For these tests, the signals measured by the instruments are logged by a computer carried by the vessel and then post processing of the collected data is carried out off-line in the laboratory.

Moreover, it has been tried to close the estimator initial conditions to real conditions as much as possible. To meet with the target, at the starting moment of navigation, the integration of INS/GPS/DVL via EKF is performed, and after a short time navigation is pursued without GPS. Accordingly, initial conditions utilized for INS/DVL navigation have the maximum accuracy. GPS outage

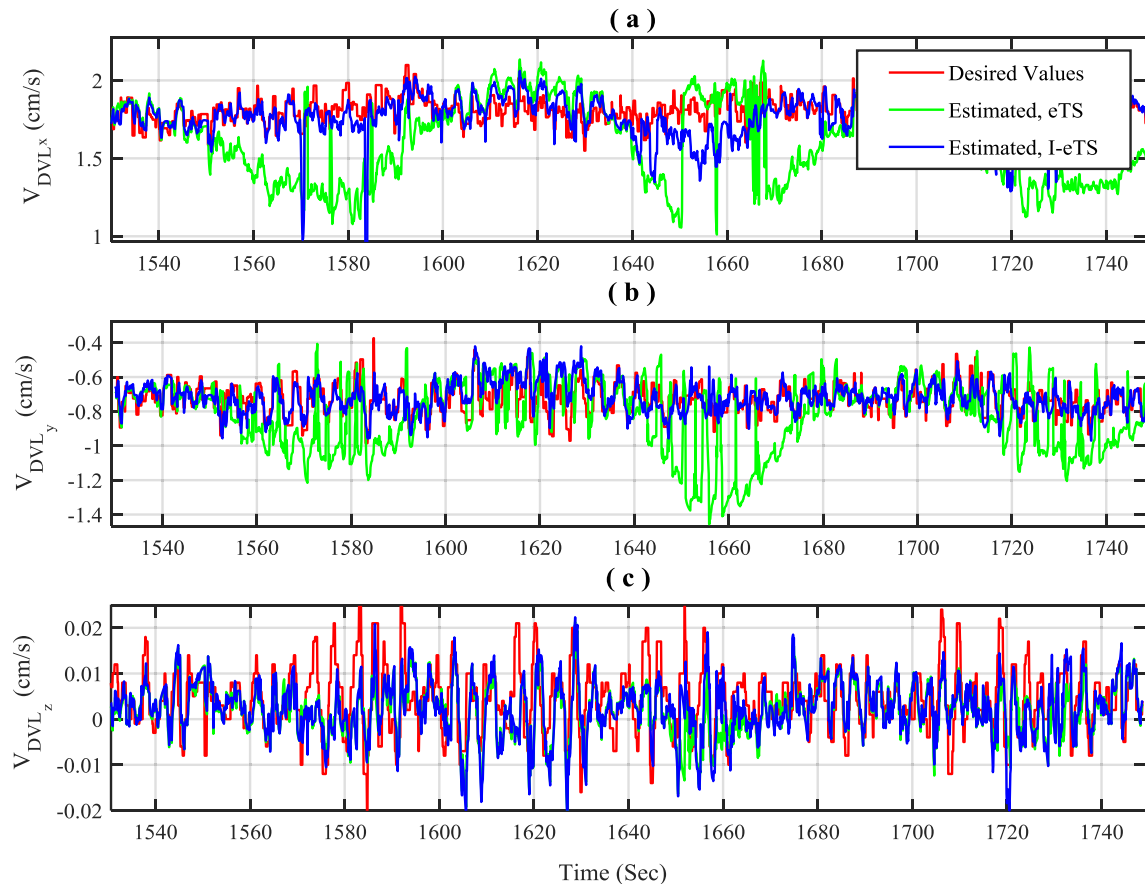


Fig. 6. Comparing prediction of DVL output ((a) V_{DVL_x} (b) V_{DVL_y} (c) V_{DVL_z}) between eTS and I-eTS during the prediction phase.

Table 2
Comparing effect of design parameters on the quantitative results of DVL output estimation.

Predictor	Parameter η	Parameter ε	Training cost (s)	Test cost (s)	NDEI Prediction
eTS	-	-	193.39	11.36	0.0316
I-eTS	0.001	0.001	191.18	11.32	0.0316
	0.01	0.001	187.17	9.13	0.0309
	0.1	0.001	94.34	6.39	0.0572
	0.001	0.01	181.65	11.18	0.0311
	0.01	0.01	107.17	8.36	0.0298
	0.1	0.01	51.75	4.62	0.0521
	0.001	0.1	160.24	6.63	0.0525
	0.01	0.1	79.01	4.08	0.0488
	0.1	0.1	45.55	3.43	0.125

always occurs after travelling 20% of the total path of the test. On the other hand, for each navigation test, results of conducting INS/GPS/DVL integration are demonstrated as a reference path, which show the accuracy of navigation without missing any auxiliary sensor information. Thereafter, the algorithm is applied to two different maneuvers. Second maneuver is flatter than the first one; as a result, different conditions of a path in navigation problem are considered. Travelled distance and the time of each test is presented in Table 3.

In Figs. 7 and 8 the navigation accuracy when 30% and 50% of the paths Test1 and Test2 are surveyed without the DVL information is plotted. Partial Least square Regression-Support Vector Regression (PLSR-SVR) is a hybrid predictor, which is employed

Table 3
Travelled distance and testing time.

	Time (s)	Travelled Distance (m)
Test 1	4371.6	9923.2
Test 2	1931.8	4209.0

in [35] to predict the residual components of the PLSR to estimate DVL measurements, precisely. To show the superiority of the proposed method in this paper, PLSR-SVR is utilized as a reference predictor. As pointed out, PLSR-SVR is designed for short-term prediction while losing long-term information impairs the performance of such hybrid methods. In this research, the same as [35], the optimal number of steps for PLSR is obtained as 4 steps. Moreover, when DVL works well, the memorizer sufficiently collects 20% of previous acquired data, and in the moment of malfunction, PLSR-SVR analyzes the information to train a reliable structure for predicting DVL output signals for the rest of path. Similar to the other regression-based methods, PLSR-SVR requires collected data sets to fit suitable models; however, obliges the integrated system to accumulate considerable volume of data, which in case of long distances or intricate maneuvers, encounters serious limitations on the memory or the processor. Therefore, these methods, regardless of their significant performance demonstrated in the papers, lack the ability to conform to the varying environments and are basically classified as off-line strategies whose performance is degraded in long-term navigation.

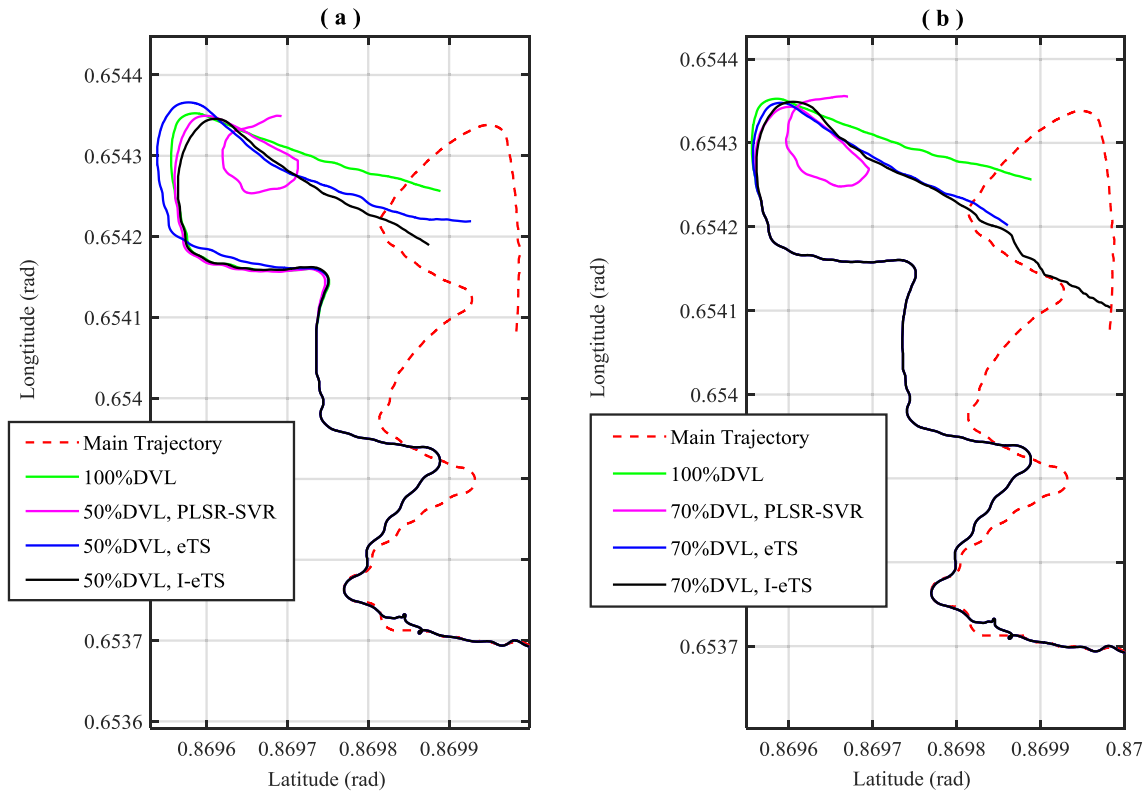


Fig. 7. Test1: Comparing navigation results when DVL signals are available at (a) 50% (b) 70% of the trajectory.

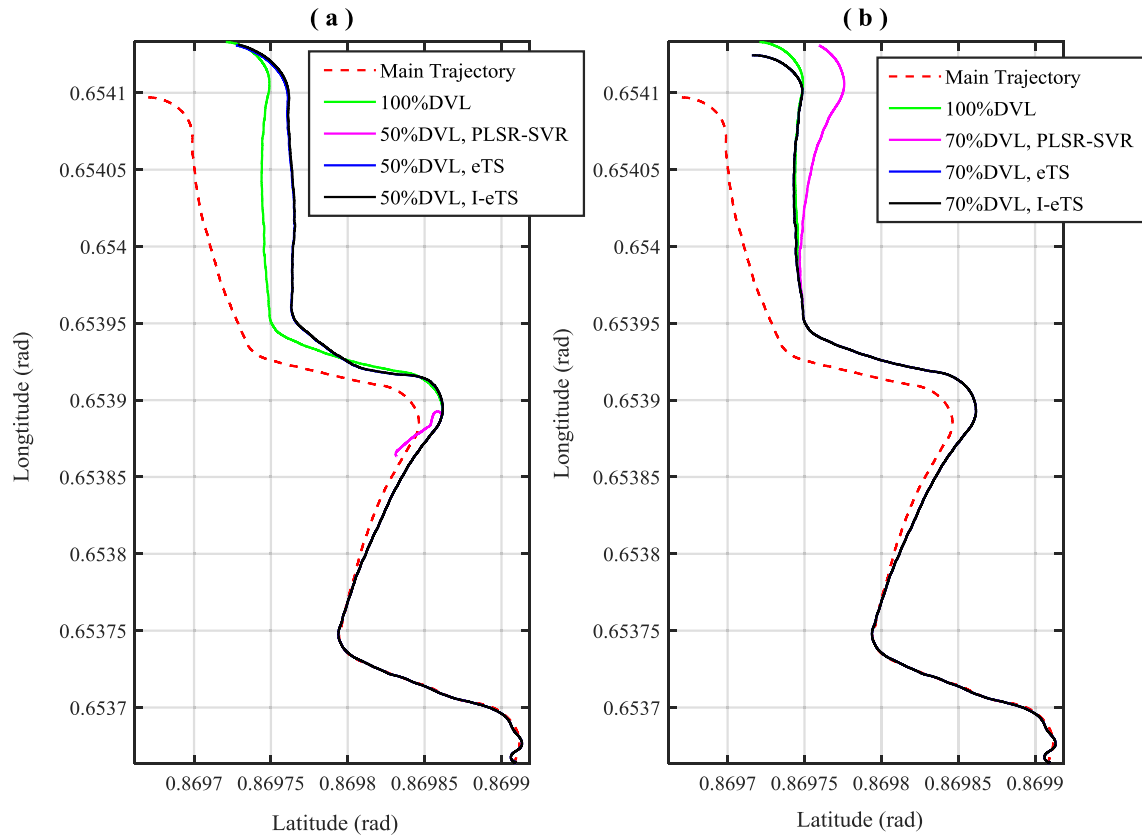


Fig. 8. Test2: Comparing navigation results when DVL signals are available at (a) 50% (b) 70% of the trajectory.

Another special demonstration in Figs. 7 and 8 lies in which by choosing the effective inputs and shrinking the outer clusters during training procedures, I-eTS (the black lines) results in more reliable navigation rather than the conventional eTS methods (the blue lines). In compared with the results of the complete INS/DVL integration systems (the green lines) and considering the long time malfunction period, the position errors are acceptable and limited by applying the strategy. Surprisingly, in some cases, such as scenario **b** of Test1 and Test2, the integrated navigation with I-eTS reveals slightly more reliable performance rather than complete INS/DVL integration system. Although the integrated system with PLSR-SVR behaves properly at the beginning of paths, but as the length of DVL malfunctioning increases, it is demonstrated that the performance of PLSR-SVR based navigation is dramatically declined.

In Tables 4 and 5, quantified results of different DVL malfunction for Test 1 and Test2 are shown. In order to compare quantitatively the improvement of strategy performance, the mean square error index which is calculated by the following equation is given for the entire tests:

$$\epsilon_{RMS} = \sqrt{\left(\frac{M_0^2 \sum (\phi_{est} - \phi_{real})^2}{N}\right) + \left(\frac{(N_0 \cos(\phi_0))^2 \sum (\lambda_{est} - \lambda_{real})^2}{N}\right)} \quad (27)$$

The *est* subscript stands for the estimated state variable by navigation algorithm and *real* subscript shows the real value of the state variable (measured by GPS). For converting the error of calculating geographical latitude and longitude to meter, latitude and longitude are multiplied by $N_0 \cos(\phi_0)$ and M_0 , respectively in which M_0 , N_0 and ϕ_0 are curvature radius in the meridian, geographical altitude at the start of movement. Also, N shows the total number of time steps in the navigation process. Positioning error at the final time is calculated as follows:

$$\epsilon_{final} = \sqrt{M_0^2 (\phi_{est}^f - \phi_{real}^f)^2 + (N_0 \cos(\phi_0))^2 (\lambda_{est}^f - \lambda_{real}^f)^2} \quad (28)$$

which superscript *f* denotes the final time of maneuver. The computational cost shows the whole running time of different navigation

Table 4
Test 1: Comparing quantitative results of different situation of the DVL sensor.

Test 1	Percentage of final error distance (50%)	Percentage of RMS error distance (50%)	Computational costs (s) (50%)	NDEI Prediction (50%)	Percentage of final distance error (70%)	Percentage of RMS distance error (70%)	Computational costs (s) (70%)	NDEI Prediction (70%)
Pure INS	1.8685e + 4	6.8610e + 4	172.22	-	5.262e + 3	2.6965e + 4	184.89	-
PLSR	15.02	25.96	237.18	0.058	15.37	27.67	269.56	0.065
PLSR-SVR	14.91	25.86	395.13	0.055	15.27	27.31	402.53	0.064
eTS	12.89	10.03	1378.97	0.019	12.38	9.24	1778.25	0.014
I-eTS	12.36	9.08	927.10	0.017	10.88	8.60	1042.03	0.011
Without DVL malfunctions	11.47	8.24	187.83	-	11.47	8.24	187.83	-

Table 5

Test2: Comparing quantitative results of different situation of the DVL sensor.

Test 2	Percentage of final distance error (50%)	Percentage of RMS distance error (50%)	Computational costs (s) (50%)	NDEI prediction (50%)	Percentage of final distance error (70%)	Percentage of RMS distance error (70%)	Computational costs (s) (70%)	NDEI prediction (70%)
Pure INS	1.6294e + 4	5.9294e + 4	59.33	–	1.156e + 3	5.7995e + 3	68.94	–
PLSR	18.37	42.59	77.76	0.524	6.59	20.04	91.82	0.069
PLSR-SVR	18.29	42.43	130.92	0.517	5.75	16.59	138.36	0.041
eTS	5.86	11.65	390.98	0.062	4.32	9.26	533.57	0.031
I-eTS	5.81	11.43	335.82	0.061	4.28	9.12	426.93	0.026
Without DVL malfunctions	4.49	10.53	77.72	–	4.49	10.53	77.72	–

systems in Tables 4 and 5. Moreover, the results are divided considering 50% or 70% DVL signals availability.

In Tables 4 and 5, navigation results are shown by using indices of Eqs. (22), (27) and (28), quantitatively. In general, with occurrence of DVL malfunction through the whole path, the integrated system operates as a pure INS system, which results in significant error values (The first row of Tables 4 and 5). The regression-based methods such as PLSR and PLS-SVR comparatively succeed to tackle the problem and limit the navigation error (second and third rows), but these limited errors are chiefly unaccepted, due to the mentioned drawbacks. Conversely, eTS and I-eTS reveal glowing performance in the integrated system in Tables 4 and 5 (4th and 5th rows). It is demonstrated that I-eTS improves the performance of eTS and limits the substantive errors at the long time malfunctions. Consequently, it can be concluded that I-eTS increases the stability and reliability of eTS-aided integrated systems, considering other mentioned strategies in the tables.

By increasing length of DVL malfunction, the performance of eTS-aided integrated system is reduced. Although, using the eTS-aided integrated system increases the computational cost, espe-

cially during the training phase, but I-eTS refines the cost. According the Fig. 9, in both scenarios, numbers of fuzzy rules reach the upper limitation after the moment of 500 s. Afterward, in the case of eTS, the predictor exploits the highest possible number of clusters, regardless of remaining parts of path, for the prediction phase. Hence, the prediction ability of eTS is generally attenuated in long-term training and the probability of instability increases, the evolving procedure does not involve the online input selection and shrinking. Conversely, in the case of I-eTS, by increasing the length of training phase or having straight navigation path, ineffective clusters and inputs are removed, which expectedly improves the prediction ability due to elimination of the dependency between input variables.

On the other hand, as it is demonstrated in Fig. 10, the prediction ability of eTS and I-eTS has been compared having 50% of DVL information. The illustration reveals that after the moment of 3400 Sec, the general eTS has lost reliability and the prediction error considerably increases. Nonetheless, according to online input selection and shrinking, I-eTS prediction error remains limited. Similarly, utilizing I-eTS has significantly improved the rela-

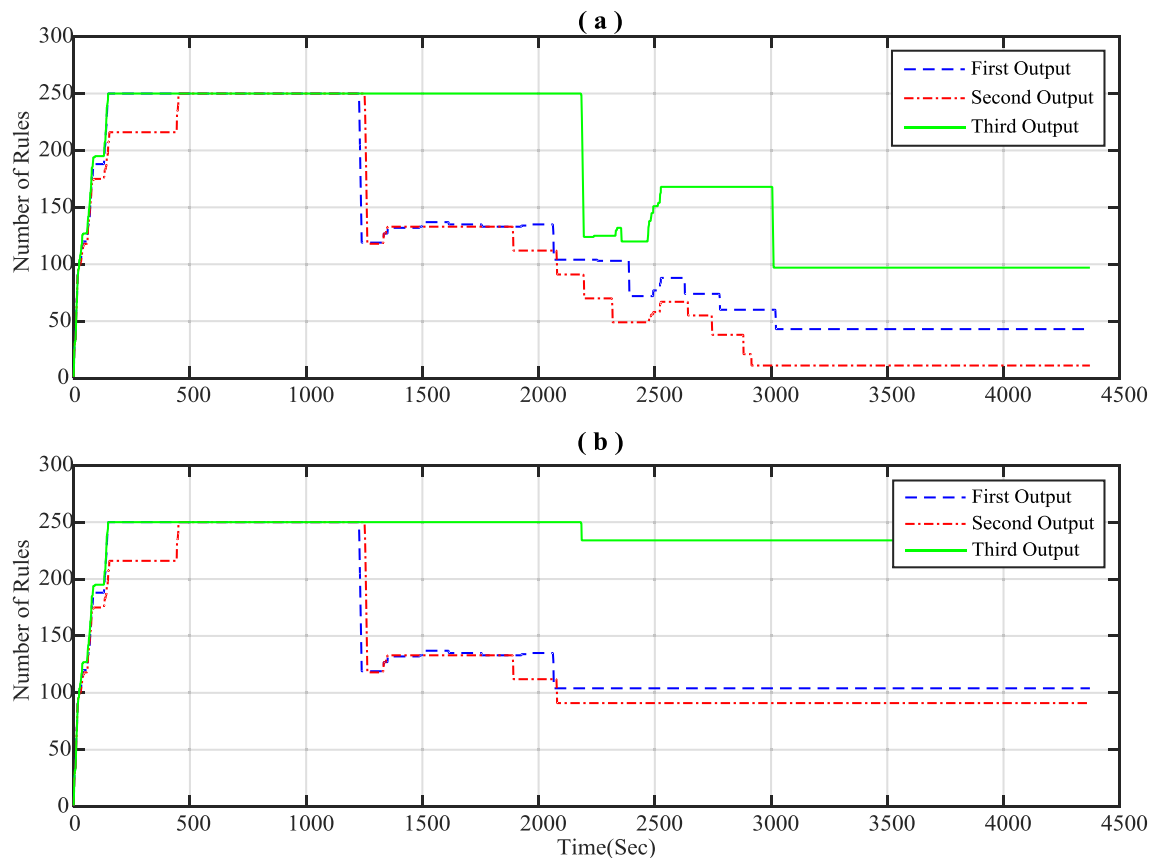


Fig. 9. Test1: Comparing number of rules in I-eTS at (a) 70% and (b) 50% of the DVL existence during the training phase.

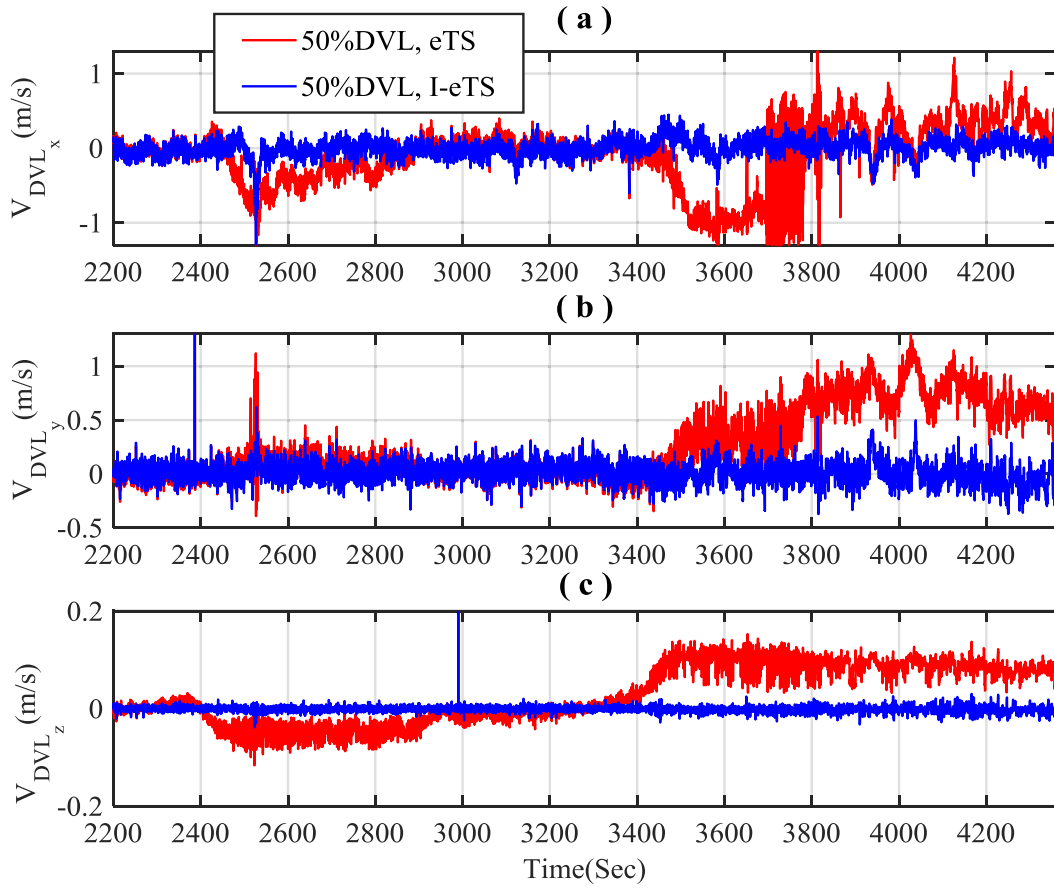


Fig. 10. Test1: Comparing prediction of DVL output ((a) V_{DVLx} (b) V_{DVLy} (c) V_{DVLz}) between eTS and I-eTS at 50% of the DVL existence during the prediction phase.

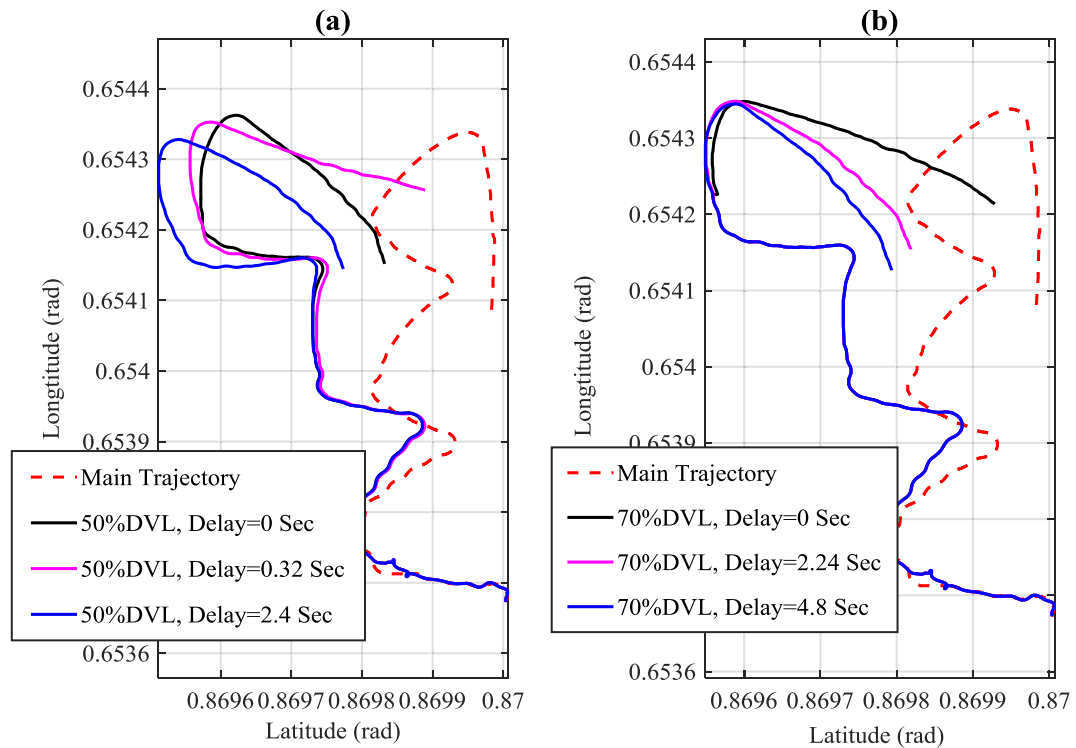


Fig. 11. Test1: Comparing effect of fault detection time delay on navigation when malfunction happens at (a) 50% (b) 70% of the trajectory.

bility of DVL output signal prediction, and quantitative results shown in 5th and 9th columns of Tables 4 and 5 (the NDEI index) obviously approve these demonstrations. Although the mentioned results demonstrate slight differences between eTS and I-eTS prediction NDEI in Table 5 which are chiefly related to invariant path of Test2 facilitating the prediction ability of eTS, but from time expense criterion point of view, reveal that I-eTS still improves the performance of eTS.

It worth noting that the introduced I-eTS based integrated navigation system is not confined to any specific type of fault. As demonstrated in the paper, the DVL malfunction is considered as the abrupt fault, regarding to the fact that such faulty signals influence the integrated system instantly, which makes them hard to deal with. Moreover, considering the harsh effect of abrupt fault on an integrated system, if a fault-tolerant method has the ability to handle the effect of abrupt faults, the other types of signal fault, including gradual or outliers, are more likely to be handled by the fault-tolerant system. Nevertheless, each fault detection mechanism leads to some fault detection time delay, which can influence on switching procedure between real DVL and pseudo-DVL. Therefore, in the following, for evaluating the effect of time delay on switching and navigation performance, two scenarios have been considered. In the first one, two time delay between fault occurrence and the fault detection moment have been chosen as 0.32 and 2.4 s in the case of having 50% of DVL information. In the second one, 2.24 and 4.8 s are selected as the fault detection time delay for occurrence of malfunction at the 70% of the trajectory. In both scenarios, the ideal fault detection results are plotted as a reference to provide the reader with a perspective of the effect of time delay amount on the performance of I-eTS based INS/DVL integrated navigation system. In Fig. 11, the results of the both scenarios are demonstrated in which as the amount of time delay increases, the navigation performance decreases as well. As a case, when the fault occurrence has been detected 4.8 s later, the RMS distance error increases by 8.59% for the scenario (b) in comparison with the ideal fault detection performance. Hence, as it is obvious, the navigation with the proposed I-eTS based signal reconstruction mechanism reveals nearly stable performance in confronting with fault detection time delay, which can be considered as a fault-tolerant navigation system.

6. Conclusion

In this paper, a novel AI-aided integrated system was introduced for the ocean navigation purposes. Due to the outage of GPS signals in these environments, the INS/DVL integration system was utilized for data fusion via an extended Kalman filter. Any long-term DVL malfunction converted the integrated system to the pure INS and resulted in instabilities. To tackle the problem, which was barely addressed in previous researches, an improved-version of evolutionary TS fuzzy system was adopted to predict DVL signals in long-term malfunctions. The evolving systems are powerful from computational point of view and was never utilized in integrated systems. Their structures are simple and this makes them agile. Adding online input selection and shrinking properties led to an optimal running time, and also prediction abilities were improved. By exploiting field test data of different maneuvers, the proposed AI-aided integrated system was applied to navigate under DVL malfunction conditions. Its performance was close to the perfect INS/DVL integrated system based on different simulation scenarios. The integrated system increased the time of stability during DVL malfunctions rather than other researches. The fuzzy system was trained in the presence of DVL signals and predicted the missing DVL signals while the rest of path information is never utilized in the training phase. These proper-

ties make the proposed integrated system more applicable and practical in oceanic environments for navigation purposes while with few changes, the underwater devices also can utilize the introduced scheme.

Declaration of Competing Interest

None.

References

- [1] S. Negahdaripour, P. Firoozfam, An ROV stereovision system for ship-hull inspection, *IEEE J. Oceanic Eng.* 31 (2006) 551–564.
- [2] L. Paull, S. Saeedi, M. Seto, H. Li, AUV navigation and localization: A review, *IEEE J. Oceanic Eng.* 39 (2014) 131–149.
- [3] X. Ning, M. Gui, Y. Xu, X. Bai, J. Fang, INS/VNS/CNS integrated navigation method for planetary rovers, *Aerosp. Sci. Technol.* 48 (2016) 102–114.
- [4] M. Shabani, A. Gholami, Improved underwater integrated navigation system using unscented filtering approach, *J. Navigation* 69 (2016) 561–581.
- [5] D. Wu, Z. Wang, Strapdown INS/GPS integrated navigation using geometric algebra, *Adv. Appl. Clifford Algebras* 23 (2013) 767–785.
- [6] M. Shabani, A. Gholami, N. Davari, Asynchronous direct Kalman filtering approach for underwater integrated navigation system, *Nonlinear Dyn.* 80 (2015) 71–85.
- [7] D. Li, D. Ji, J. Liu, Y. Lin, A multi-model EKF integrated navigation algorithm for deep water AUV, *Int. J. Adv. Rob. Syst.* 13 (2016) 3.
- [8] Ø. Hegrenæs, O. Hallingstad, K. Gade, Towards model-aided navigation of underwater vehicles, *Model. Ident. Control* 28 (2007) 113–123.
- [9] P. Aggarwal, D. Bhatt, V. Devabhaktuni, P. Bhattacharya, Dempster Shafer neural network algorithm for land vehicle navigation application, *Inf. Sci.* 253 (2013) 26–33.
- [10] C. Goodall, Z. Syed, N. El-Sheimy, Improving INS/GPS navigation accuracy through compensation of Kalman filter errors, *Vehicular Technology Conference, 2006. VTC-2006 Fall, 2006 IEEE 64th*, pp. 1–5.
- [11] J.J. Wang, J. Wang, D. Sinclair, L. Watts, A neural network and Kalman filter hybrid approach for GPS/INS integration, *12th IAIN Congress & 2006 Int. Symp. on GPS/GNSS*, Jeju, Korea, 2006, pp. 18–20.
- [12] E.-H. Shin, Accuracy Improvement of Low Cost INS/GPS for Land Applications, University of Calgary, 2001.
- [13] E. Ghotb Razmjou, S.K. Hosseini Sani, J. Sadati, Robust adaptive sliding mode control combination with iterative learning technique to output tracking of fractional-order systems, *Trans. Inst. Meas. Control* (2017), 0142331217691337.
- [14] Y. Yao, X. Xu, C. Zhu, C.-Y. Chan, A hybrid fusion algorithm for GPS/INS integration during GPS outages, *Measurement* 103 (2017) 42–51.
- [15] L. Whitcomb, D. Yoerger, H. Singh, Advances in Doppler-based navigation of underwater robotic vehicles, *Robotics and Automation, 1999 Proceedings IEEE International Conference on, IEEE, 1999*, pp. 399–406.
- [16] Z. Cao, D. Zhang, D. Sun, J. Yong, A method for testing phased array acoustic Doppler velocity log on land, *Appl. Acoust.* 103 (2016) 102–109.
- [17] B. Allotta, R. Costanzi, E. Meli, A. Ridolfi, L. Chisci, C. Fantacci, A. Caiti, F. Di Corato, D. Fenucci, An innovative navigation strategy for autonomous underwater vehicles: an unscented Kalman filter based approach, *ASME 2015 International Design Engineering Technical Conferences and Computers and Information in Engineering Conference, American Society of Mechanical Engineers, 2015*, pp. V05AT08A052–V005AT008A052.
- [18] W. Gao, Y. Zhang, J. Wang, A strapdown inertial navigation system/Beidou/Doppler velocity log integrated navigation algorithm based on a cubature Kalman filter, *Sensors* 14 (2014) 1511–1527.
- [19] A. Mirabadi, N. Mort, F. Schmid, Fault detection and isolation in multisensor train navigation systems, 1998.
- [20] B. Brumback, M. Srinath, A fault-tolerant multisensor navigation system design, *IEEE Trans. Aerosp. Electron. Syst.* (1987) 738–756.
- [21] M. Ushaq, F.J. Cheng, A Fault Tolerant Integrated Navigation Scheme Realized Through Online Tuning of Weighting Factors for Federated Kalman Filter, *Applied Mechanics and Materials*, Trans Tech Publ., 2014, pp. 1078–1085.
- [22] X. Li, W. Zhang, An adaptive fault-tolerant multisensor navigation strategy for automated vehicles, *IEEE Trans. Veh. Technol.* 59 (2010) 2815–2829.
- [23] Y. Liang, Y. Jia, A nonlinear quaternion-based fault-tolerant SINS/GNSS integrated navigation method for autonomous UAVs, *Aerosp. Sci. Technol.* 40 (2015) 191–199.
- [24] L.-Y. Zhao, X.-J. Liu, L. Wang, Y.-H. Zhu, X.-X. Liu, A pretreatment method for the velocity of DVL based on the motion constraint for the integrated SINS/DVL, *Appl. Sci.* 6 (2016) 79.
- [25] L. Semeniuk, A. Noureldin, Bridging GPS outages using neural network estimates of INS position and velocity errors, *Meas. Sci. Technol.* 17 (2006) 2783.
- [26] A. Hasan, K. Samsudin, A. Ramli, R. Azmir, Automatic estimation of inertial navigation system errors for global positioning system outage recovery, *Proc. Inst. Mech. Eng. G* 225 (2011) 86–96.
- [27] S. Ansari-Rad, A. Kalhor, B.N. Araabi, Partial identification and control of MIMO systems via switching linear reduced-order models under weak stimulations, *Evol. Syst.* (2017) 1–18.

- [28] S. Ansari-Rad, S. Jahandari, A. Kalhor, B.N. Araabi, Identification and control of MIMO linear systems under sufficient and insufficient excitation, in: 2018 Annual American Control Conference (ACC), IEEE, 2018, pp. 1108–1113.
- [29] A. Karmozdi, M. Hashemi, H. Salarieh, Design and practical implementation of kinematic constraints in Inertial Navigation System-Doppler Velocity Log (INS-DVL)-based navigation, *Navigation* 65 (2018) 629–642.
- [30] S. Ansari-Rad, M. Zarei, M.G. Tamizi, S.M. Nejati, M.T. Masouleh, A. Kalhor, Stabilization of a two-DOF spherical parallel robot via a novel adaptive approach, in: 2018 6th RSI International Conference on Robotics and Mechatronics (IcRoM), IEEE, 2018, pp. 369–374.
- [31] A. Zabihi-Hesari, S. Ansari-Rad, F.A. Shirazi, M. Ayati, Fault detection and diagnosis of a 12-cylinder trainset diesel engine based on vibration signature analysis and neural network, *Proc. Inst. Mech. Eng. C* (2018), 0954406218778313.
- [32] X. Xu, P. Li, J.-J. Liu, A fault-tolerant filtering algorithm for SINS/DVL/MCP integrated navigation system, *Math. Prob. Eng.* 2015 (2015).
- [33] J. Li, N. Song, G. Yang, M. Li, Q. Cai, Improving positioning accuracy of vehicular navigation system during GPS outages utilizing ensemble learning algorithm, *Inf. Fus.* 35 (2017) 1–10.
- [34] X. Tan, J. Wang, S. Jin, X. Meng, GA-SVR and pseudo-position-aided GPS/INS integration during GPS outage, *J. Navigation* 68 (2015) 678–696.
- [35] Y. Zhu, X. Cheng, J. Hu, L. Zhou, J. Fu, A novel hybrid approach to deal with DVL malfunctions for underwater integrated navigation systems, *Appl. Sci.* 7 (2017) 759.
- [36] W. Abdel-Hamid, A. Noureldin, N. El-Sheimy, Adaptive fuzzy prediction of low-cost inertial-based positioning errors, *IEEE Trans. Fuzzy Syst.* 15 (2007) 519–529.
- [37] N. El-Sheimy, K. Chiang, A. Noureldin, Developing a low cost MEMS IMU/GPS integration scheme using constructive neural networks, *IEEE Trans. Aerosp. Electron. Syst.* 44 (2008) 582–594.
- [38] Y.-W. Huang, K.-W. Chiang, An intelligent and autonomous MEMS IMU/GPS integration scheme for low cost land navigation applications, *GPS Sol.* 12 (2008) 135–146.
- [39] R.D. Christ, R.L. Wernli Sr, *The ROV Manual-A User Guide for Remotely Operated Vehicles*, Elsevier, Kidlington, 2014.
- [40] H.T. Foss, E.T. Meland, *Sensor Integration for Nonlinear Navigation System in Underwater Vehicles*, Institutt for teknisk kybernetikk, 2007.
- [41] G. Falco, G.A. Einicke, J.T. Malos, F. DAVIS, Performance analysis of constrained loosely coupled GPS/INS integration solutions, *Sensors* 12 (2012) 15983–16007.
- [42] F.A. Faruqi, K.J. Turner, Extended Kalman filter synthesis for integrated global positioning/inertial navigation systems, *Appl. Math. Comput.* 115 (2000) 213–227.
- [43] K.-W. Chiang, T.T. Duong, J.-K. Liao, Y.-C. Lai, C.-C. Chang, J.-M. Cai, S.-C. Huang, On-line smoothing for an integrated navigation system with low-cost MEMS inertial sensors, *Sensors* 12 (2012) 17372–17389.
- [44] N. Parnian, F. Golnaraghi, Integration of a multi-camera vision system and strapdown inertial navigation system (SDINS) with a modified Kalman filter, *Sensors* 10 (2010) 5378–5394.
- [45] Y. Bar-Shalom, X.R. Li, T. Kirubarajan, *Estimation with Applications to Tracking and Navigation: Theory Algorithms and Software*, John Wiley & Sons, 2004.
- [46] P. Angelov, D. Filev, On-line design of Takagi-Sugeno models, *Fuzzy Sets and Systems—IFSA 2003*, (2003) 92–165.
- [47] P.P. Angelov, D.P. Filev, An approach to online identification of Takagi-Sugeno fuzzy models, *IEEE Trans. Syst. Man Cybern. B (Cybernetics)* 34 (2004) 484–498.
- [48] P. Angelov, J. Victor, A. Dourado, D. Filev, On-line evolution of Takagi-Sugeno fuzzy models, *IFAC Proc.s Vol.* 37 (2004) 67–72.
- [49] P. Angelov, D. Filev, Simpl_eTS: a simplified method for learning evolving Takagi-Sugeno fuzzy models, *Fuzzy Systems, 2005. FUZZ'05. The 14th IEEE International Conference on*, IEEE, 2005, pp. 1068–1073.
- [50] P. Angelov, *Machine Learning (Collaborative Systems) Patent*, (2006).
- [51] Y. Zhu, X. Cheng, L. Wang, A novel fault detection method for an integrated navigation system using Gaussian process regression, *J. Navigation* 69 (2016) 905–919.



Partial identification and control of MIMO systems via switching linear reduced-order models under weak stimulations

Saeed Ansari-Rad¹ · Ahmad Kalhor¹ · Babak N. Araabi¹

Received: 27 August 2017 / Accepted: 30 November 2017
© Springer-Verlag GmbH Germany, part of Springer Nature 2017

Abstract

In closed loop identification of an unknown control system, the stability is a big concern particularly when the system does not proceed with sufficient excitation. In this paper, under insufficient excitation of the system, identification and control are investigated by employing Evolving Linear Models (ELMs). It is explained that under weak stimulation, linear correlations between input and output signals and their derivations are occurred. Removing some correlated variables through the time, an equivalent reduced order model of the original system is appeared, which can be identified as an ELM. Defining control law based on the sliding mode control (SMC) and using appropriate adaptation rules for parameters of the model, the tracking errors converge to zero and the stability of the system is guaranteed. Then, convergence of the parameters to their true values is studied and discussed. Different simulations are given to demonstrate the efficacy of the proposed closed loop identification approach.

Keywords Evolving linear models · Reduced-order models · Weak stimulation · Closed loop identification · Sliding mode control

1 Introduction

The complexity and dynamics of real-world problems require special methods for building online, adaptive systems. These intelligent systems, by analyzing conditions of environment, are trying to adapt themselves with non-stationary phenomena through time. Such systems should be able to grow as they operate, to update their knowledge and make the model better via interaction with the environment. Considering all complexities in control problems, makes us look for intelligent systems with higher adaptability to non-stationary environment.

A lot of natural processes are considered as MIMO systems. The closed-loop identifier introduced for MIMO linear

dynamic systems (Ng et al. 1977) is practically noticeable due to presence of noises in the feedback path assuming their distributions as random processes. (Zhu 1989) mentioned Order determination, while covariance of a MIMO transfer function is extracted and order of model is changing from low to infinite until tending to the optimal order. Thereafter, more identification procedures have been proposed for MIMO systems, like a closed-loop identifier for variable structured systems (Xu and Hashimoto 1996), a robust identifier for linear systems that assumes the cost function as quadratic time series (Pan and Basar 1996), two-stage closed-loop identification method (Leskens et al. 2002) and a method based on least squares SVM for linear dynamic systems (Goethals et al. 2005). Beside them, Identification procedures have been studied for linear transfer function of MIMO systems with different methods like shifting Legendre polynomials (Hwang and Guo 1984), Poisson moment functional (SAHA and RAO 1982) and Walsh functions (Rao and Sivakumar 1981). None of mentioned methods have given guarantee for stability during the identification procedure, although, most of systems have structured-complexities may cause instability during stimulation and identification procedures, so the methods guaranteeing

✉ Ahmad Kalhor
akalhor@ut.ac.ir
Saeed Ansari-Rad
saeedansari71@ut.ac.ir
Babak N. Araabi
araabi@ut.ac.ir

¹ Control and Intelligent Processing Center of Excellence, School of Electrical and Computer Engineering, University of Tehran, PO Box: 14395/515, Tehran 1439957131, Iran

stability of closed-loop system during identification have been more regarded.

On the other hand, controlling unknown systems has drawn a lot of attention recently. Many intelligent techniques based on conventional PID, Fuzzy, switching adaptive (Fu and Barmish 1986; Mårtensson 1985; Miller and Davison 1989, 1991), Model Predictive Controllers (Mayne et al. 2000; Qin and Badgwell 2003), sliding mode, evolving systems, and robust adaptive methods are elaborated to try to control unknown systems.

Another promising structure is imposing concept of control during identification of system behaviors. Self-tuning regulators (STR) has been developed by (Äström and Wittenmark 1989) for the control of systems with unknown parameters. In indirect STR schemes, the adaptive law generates on-line estimates of the parameters of the system. Due to its flexibility in choosing the controller design methodology (state feedback, compensator design, linear quadratic, etc.) and adaptive law (least squares, gradient, or SPR-Lyapunov type), indirect STRs are the most general class of adaptive control schemes (Ioannou and Sun 1996). The basic structure of presented article (in Algorithm 1) is emerged from indirect STRs: using sliding mode as the control methodology and continuous-time recursive least square (RLS) as the adaptive law. But the main contribution is the guaranteeing convergence of parameters to real values during control and within the Lyapunov function. In previous works, after the identification of parameters, following the desired behavior and the stability of the closed-loop system were possible. Therefore, initial conditions of the identification procedure and the speed of convergence of identified parameters were so important. Avoiding these problems was a motivation to design the current structure. Also, tracking the desired output is another advantage in compare with most STRs which are designed based on pole placement methods. This feature is useful in controlling robotic devices and most of drivers which are final purposes of authors in practical aspects. But the current scheme can handle practical plants like (Hou et al. 2012; Hovland et al. 2007; Sharifzadeh et al. 2017; Zeng et al. 2007), where the Lagrangian behavior of parallel systems is close to the basic model of the current scheme.

Evolvability of systems is one of the properties that makes models being more in rapport with reality. The concept itself exhibits many facets and is quite often linked with an idea of adaptive systems- the architectures, which have been around for a long time. The systems (models) have to evolve because the real world is often nonstationary. The perception of the world changes depending upon a certain observer (user) and his preferences and in this way the model evolves to adhere to the needs of the users (Jahandari et al. 2016).

In general terms, the evolvable systems are characterized by abilities to adjust their structure as well as parameters to the varying characteristics of the environment (with the

term of environment embracing processes/phenomena with which the system has to interact or deal with the users using the system) (Pedrycz 2010) which can change their structure in order to adapt to variations of systems. In (Kalhor et al. 2010, 2012), adaptive habitually linear and transiently evolving TS fuzzy model is suggested in which the parameters are updated quickly and the model can follow variations of the system with agility. However, such model is not agile enough in order to prevent when persistent excited (PE) order of the control signal is very low. A similar problem is demonstrated in the current proposed structure (in Algorithm 1) where insufficient PE signals challenge identification of system parameters. Some papers like (Cho et al. 2017; Ivanov and Orlovsky 2014; Vuthandam and Nikolaou 1997; Xu and Baird 1990) have presented different solution to cope with this problem. Here, a sort of ELM is introduced (in Algorithm 2) which is linear regression models whose number of regressors can increase or decrease over time span. A simple variant of such model has been introduced in (Angelov et al. 2011; Kalhor et al. 2012; Lughofer 2013; Lughofer et al. 2015; Precup et al. 2014). The concept of ELM is promising and between different schemes, only by choosing this concept, the stability of closed-loop system in the space of parameters with PE condition can still be guaranteed in a subspace while suffering from weak stimulation conditions.

The mentioned ELM consists of the basic model and reduced-order models (R-OM). (Zhang et al. 2008) construct a reduced-order switched model for a robustly stable switched system. (Leung Lai and Zong Wei 1986) study the problem concerning how much excitation should be introduced into the inputs in a multivariable ARMAX system. Industrial processes usually involve a large number of variables, many of which vary in a correlated manner. In (Qin 1993), a recursive partial least squares regression is used for online system identification and circumventing the ill-conditioned problem. In (Zhang and Shi 2008) a parameterized reduced-model is constructed for a discrete-time switched linear parameter varying systems. None of mentioned papers uses R-OMs in both control and identification procedures. In current scheme (in algorithm 2), R-OMs are used to adaptive the scheme with variation of stimulation degree. Therefore, besides tracking desired signals, we still are able to fit suitable model to system behaviors.

Our key contributions are: 1- How to use SMC and adaptation rules together in order to control of system outputs behavior and identification of system parameters at the same time. 2- Introducing a sort of ELM. When the excitation order of user-defined signals is low, identification of the basic model (model with the same dynamic order of system channels that fits behaviors of the basic system) turns into partially identification of system behaviors. By using R-OMs, important behaviors of system are still followed. 3- How to identify models whose parameters are guaranteed to converge asymptotically to their true values while

closed-loop procedure is proven to remain asymptotic stable. Also, by using these strategies, convergence of the R-OM parameters to their real values and stability of the closed-loop system with this R-OM can be guaranteed, as well.

The remainder of this paper is organized as follows: In Sect. 2.1, the basic model and equations of time-invarying R-OM are comprehensively studied. Section 2.2 presents the online identification procedure of R-OM and the SMC strategy. In Sect. 2.3, the stability of the closed-loop system and the convergence of parameters to their true values are studied. Then, in Sect. 2.4, the stability of the closed-loop system during switching and with ELM is covered. Also, Sect. 3 is devoted to simulation studies.

2 Control and Identification of MIMO systems via a robust adaptive algorithm

In the first part of this research, a closed-loop identification method for MIMO linear systems is proposed such that both the convergence of parameters to their true values

and stability of the closed-loop system are guaranteed. In Algorithm 1, the procedure of this method is presented. By imposing condition of sufficient PE to each channel, the identification of parameters is restricted to complex stimulations like independent sinusoidal signals applied to the system. Therefore, by facing any weak stimulations, the identifier is forced to stop the procedure. Under these circumstances, Algorithm 1 lost its control concept and it is not even applicable.

Nonetheless, by introducing a sort of ELM in the Sect. 2.1, the identification of model parameters is still carried on, no matter what excitation order applying signals have. The mentioned ELM consists of a basic model and linear switching models called reduced-order models. Also, the desired signals can be determined by user and none of mentioned constraints can stop the identifier. The applied strategy is shown in Algorithm 2. By using Algorithm 2, convergence of the R-OM parameters to their values and stability of the closed-loop system with this R-OM is guaranteed, as well. Details of both algorithms are explained in the Sect. 2.2.

Algorithm 1: Online identification of MIMO systems

- 1: **Procedure:** Online Identification method
 - 2: **Initialization** $\hat{a}_q(0) = 0_{n_q \times 1}$, $\hat{B}(0) = I_N$, $P_q^{-1}(0) = 0.01 \times I_{N+n_q}$, $\forall q = 1, \dots, N$
 - 3: Calculate desired signals and their derivatives
 - 4: Calculate output signals of the basic plant and form $\Phi_q = \begin{bmatrix} y_q \\ \underline{u} \end{bmatrix}$, $1 \leq \forall q \leq N$.
 - 5: Calculate the sliding surfaces Based on Eq. (10).
 - 6: Form control input signals as $\underline{u} = \hat{\underline{u}} - \eta \text{sgn}(\mathbf{S})$.
 - 7: Update the matrix $P_q^{-1}(t)$ based on $\dot{P}_q^{-1}(t) = -\alpha_q P_q^{-1}(t) + \Phi_q(t)\Phi_q^T(t)$, $\forall q = 1, \dots, N$.
 - 8: Calculate the estimation error:

$$e_q(t) = \tilde{\theta}_q^T(t)\Phi_q(t), \forall q = 1, \dots, N.$$
 - 9: Update parameters' adaptation rules:

$$\begin{bmatrix} \hat{a}_q \\ \hat{b}_q \end{bmatrix} = S_q(t)P_q(t) \begin{bmatrix} y_q \\ -\hat{\underline{u}} \end{bmatrix} + \gamma_q P_q(t)\Phi_q(t)e_q(t), \forall q = 1, \dots, N.$$
 - 10: Put $t = t + T$
 - 11: **If** $t < t_f$, **then**
 - 12: Return to line 3
 - 13: **else**
 - 14: Terminate the algorithm.
 - 15: **end if**
 - 16: **end procedure**
-

2.1 Time-invarying R-OMs

In this part, to fit the behaviors of the systems in the identification procedure, the basic model and R-OMs are nominated. The basic model is a MIMO square transfer function with no element zeros. The characteristic equation of each output channel is dissimilar to others and the system under these procedures should be minimum phase. Only data of inputs and outputs of the basic system are utilized and only information about this system, which is pre-required, is the dynamic rank of each output channel.

R-OMs, by removing some dependent regressors, fit the behavior of system channels under weak stimulations. In the following, important steps to gain R-OM equations from a basic model are expressed (model reduction). The other model switching procedures including transformation of R-OMs to each other or obtaining basic model from R-OM, in case of increasing richness of stimulations, can be extended with a few changes. These all switching models represent structure of an ELM. In different conditions from rich PE to weak stimulations, identification of system behaviors is still possible although we may have to be content with partial identification.

The transfer function of MIMO systems is considered as:

$$G(\mathbf{S}) = \left[\frac{b_{qj}}{\mathbf{S}^{n_q} - a_{qn_q} \mathbf{S}^{n_q-1} \dots - a_{q1}} \right]_{N \times N} \tag{1}$$

$$\forall q = 1, \dots, N, \forall j = 1, \dots, N$$

where Laplace variable is defined with symbol \mathbf{S} . The index q is a general channel indicator (When we refer to q th channel, in fact we refer to all channels.) and j refers to the index of input. Each output channel differential equation can be written as:

$$y_q^{[n_q]} = a_q^T y_{-q} + b_q^T u = \theta_q^T \Phi_q \tag{2}$$

where n_q denotes the dynamic rank of y_q . This is called basic model for each channel. The vector of input-output regres-

sors of the basic model is represented as $\Phi_q = \begin{bmatrix} y_{-q} \\ u \end{bmatrix} \in \mathbb{R}^{N+n_q}$.

Also for each channel, vectors of denominator coefficients, output signal regressors, nominator coefficients, and transfer function parameters are denoted as $a_q^T \in \mathbb{R}^{n_q}$, $y_{-q}^T \in \mathbb{R}^{n_q}$, $b_q^T \in \mathbb{R}^N$, $\theta_q^T \in \mathbb{R}^{N+n_q}$ respectively. The vector of input signals is shown as $u \in \mathbb{R}^N$.

$$\begin{aligned} a_q^T &= [a_{qn_q}, a_{q(n_q-1)}, \dots, a_{q1}] , b_q^T = [b_{qj}]_{1 \times N} \\ \theta_q^T &= [a_q^T, b_q^T] , y_{-q}^T = [y_q^{[n_q-1]}, y_q^{[n_q-2]}, \dots, y_q^{[1]}, y_q] , u = [u_j]_{N \times 1} \end{aligned} \tag{3}$$

While there are no dependencies between regressors of the basic model, Eq. (2) is still differential equation of the basic model. It is worth to mention that input and output signals are measured from the system, not the model. This becomes important when we substitute identified parameters in models, where their output signal regressors are different from y_{-q} in each channel.

On the contrary, if regressors of the basic model are correlated, channels of the system will not be sufficiently excited. Therefore the identifier is forced to stop Algorithm 1.

Assumption A1 To analyze these situations, it is assumed, by applying weak stimulation to one of system channels, we find non-zero nullity vectors in $\Phi_i^T(t)\Psi_i = 0, 0 \leq \tau_1 \leq t \leq \tau_2$ in one of channels as i th while the other channels are sufficiently excited. Index i refers to the channel with weak stimulation. The number of independent nullity vectors defines the number of regressors must be removed from models. But in the following, it is assumed $\Psi_i \in \mathbb{R}^{(n_i+N) \times 1}$ is the only non-zero nullity vector. In out of the interval $[\tau_1, \tau_2]$ the dependency relation is not established. The parameter τ_2 either can be finite or infinite based on excitation signals.

Remark 1 As it will be seen in the sect 3, it is too rare that system channels need model reduction at the same time. Changes of degree excitation of most known desired signals are such slow that the identifier can handle insufficient excitation with one model reduction at a proper interval. In Simulation 4, it is shown that by two consecutive model reductions, the identifier handles the rank deficiency of 2 in the second channel. Therefore, these assumptions do not bring any major limitations in the application of explained concepts in the research.

The nullity vector of i th output channel can be shown as:

$$\Psi_i^T = [\psi_{i(n_i+N)}, \psi_{i(n_i+N-1)}, \dots, \psi_{i1}] . \tag{4}$$

The dependency relation between regressors of i th channel is written as follows:

$$\begin{aligned} \psi_{i(n_i+N)} y_i^{[n_i-1]} + \psi_{i(n_i+N-1)} y_i^{[n_i-2]} + \dots + \psi_{i(n_i+1)} y_i \\ + \psi_{iN} u_N + \dots + \psi_{i1} u_1 = 0. \end{aligned} \tag{5}$$

To remove k th output regressor, Eq. (5) can be rearranged as Eq. (6). It is worth to mention that none of input regressors can remove from the basic models. Therefore, k th output regressor is the most effective output regressor in the nullity vector.

$$y_i^{[k]} = - \underbrace{\frac{\Psi_{i(n_i+N)}}{c_{i(n_i+N)}}}_{c_{i(n_i+N)}} y_i^{[n_i-1]} \dots - \underbrace{\frac{\Psi_{i(k+N+2)}}{c_{i(k+N+2)}}}_{c_{i(k+N+2)}} y_i^{[k+1]} - \underbrace{\frac{\Psi_{i(k+N)}}{c_{i(k+N)}}}_{c_{i(k+N)}} y_i^{[k-1]} \dots - \underbrace{\frac{\Psi_{iN}}{c_{iN}}}_{c_{iN}} u_N \dots - \underbrace{\frac{\Psi_{i1}}{c_{i1}}}_{c_{i1}} u_1 \quad (6)$$

By applying the dependency relation, the differential equation of *i*th channel can be written as Eq. (7).

$$y_i^{[n_i]} = \underbrace{(a'_{in_i} + a_{i(k+1)}c_{i(n_i+N)})}_{a'_{im_i}} y_i^{[n_i-1]} + \dots + \underbrace{(a_{i(m+1)} + a_{i(k+1)}c_{i(m+N+1)})}_{a'_{i(m+1)}} y_i^{[m]} + \dots + \underbrace{(b_{ij} + a_{i(k+1)}c_{ij})}_{b'_{ij}} u_j = \theta_i^T \Phi'_i(t) \quad (7)$$

where

$$\Phi_i^T(t) = [y_i^{[n_i-1]}, y_i^{[n_i-2]}, \dots, y_i^{[m]}, \dots, y_i^{[k+1]}, y_i^{[k-1]}, \dots, u^T] \theta_i^T = [a'_{in_i}, a'_{i(n_i-1)}, \dots, a'_{i(m+1)}, \dots, a'_{i(k+2)}, a'_{ik}, \dots, b_i^T], \quad \forall m = 0, \dots, k-1, k+1, \dots, n_i-1. \quad (8)$$

Hence, Eq. (7) is used to describe reduce-order differential equation of *i*th channel. It is called reduced-order model for *i*th channel. The accent ` is used to denote each parameter on R-OM to show its difference from the basic model. The transfer function of *j*th input and *i*th output can be written as Eq. (9), where the coefficient of S^k is set to zero.

$$g_{ij}(S) = \frac{b'_{ij}}{S^{n_i} - a'_{in_i} S^{n_i-1} \dots - a'_{i(m+1)} S^m \dots - a'_{i1}} \quad (9)$$

Applied sufficient PE signals to the system provide necessary information in order to identify all parameters of the

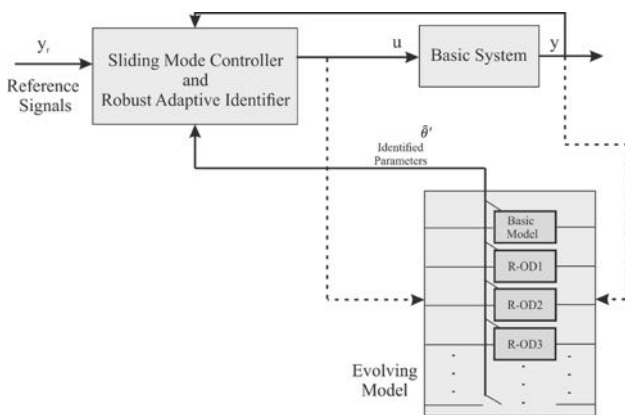


Fig. 1 The block diagram of closed-loop system and important signals

transfer function. Otherwise, the lack of information obstructs identification of $a_{i(m+1)}$ and $a_{i(k+1)}$ simultaneously. So, the identifier is just be able to identify and track $a'_{i(m+1)} = a_{i(m+1)} + a_{i(k+1)}c_{i(m+N+1)}$.

To gain a good view of what is happening in an ELM, consider the following scenario: Imagine you have a large suitcase containing all facilities you need. So, whenever you are going to a specific place or event or decide to do any activity, you select and take some of the means from your suitcase commensurate with what you anticipate you are going to need. Obviously you do not choose the same things when you are going to either camping in the forest or the beach or a formal ceremony although sometimes there might be some overlapping (Jahandari et al. 2016).

Inspired by the above story, the LTI models including the basic model and R-OMs establish an ELM to adapt behaviors of the identified model with behaviors of non-stationary environment. These behaviors, here, refer to changeable desired signals applied to the system. The desired signals are depending on users (degree of stimulation) and the environment (noises and other non-stationary effects). More concepts about ELMs can be found in reference (Jahandari et al. 2016).

2.2 Sliding mode control and robust adaptive identification

As you can see in Fig. 1, the ELM is sending identified parameters of switching models, whether from basic model or R-OM, to the control module. In the following, equations inside of this module and then, by using R-OM, concepts of algorithm are explained in detail.

Sliding rules force the system to gain our target features by sliding along a cross-section of the system's normal behavior. In order to track output signals and reduce the output error, the following sliding rules at each channel are defined:

$$s_q = \left(\frac{d}{dt} + \lambda_q \right)^{n_q-1} \tilde{y}_q = \Lambda \mu_q^T \tilde{y}_q \quad (10)$$

$$\tilde{y}_q = \underline{y}_q - \underline{y}_{r_q}, \quad \Lambda \mu_q^T = [1, \dots, (n_q - 1)\lambda_q^{n_q-2}, \lambda_q^{n_q-1}].$$

The vector of output desired regressors and output error regressors in each channel are shown with $\underline{y}_q^T = [y_{r_q}^{[n_q-1]}, \dots, y_{r_q}^{[1]}, y_{r_q}]$ and $\tilde{y}_q^T = [y_{r_q}^{[n_q-1]}, \dots, y_{r_q}^{[1]}, y_{r_q}] = [\tilde{y}_q^{[n_q-1]}, \dots, \tilde{y}_q^{[1]}, \tilde{y}_q]$, respectively. Desired signals are continuous and considerably smooth. The scaler s_q denotes sliding variable in each channel. Sliding rules are concerned with system properties, not models'. Therefore, any changes

in a model do not affect sliding surfaces and the system will track desired outputs anyway.

To analyze sliding surfaces, derivative of sliding rule of each channel is going to be studied. Based on these derivatives, control inputs are defined, which force the system to reach sliding surfaces. In the following, equations of R-OM are used to describe role of models in the module.

Considering Eq. (7), derivative of i th sliding variable is computed as Eq. (11). As mentioned, $a'_{i(m+1)}$ is obtained based on $a'_{i(m+1)} = a_{i(m+1)} + a_{i(k+1)}c_{i(m+1)}$. The summation $\sum_{l=0, l \neq k}^{n_i-1} a'_{i(l+1)}y^{[l]}$ is displayed as an inner product of reduced vectors of denominator coefficients $a'_i{}^k$ and output signal regressors y_{-ik} . The reduced vector of denominator coefficients contains all parameters except $a'_{i(k+1)}$.

$$\begin{aligned} \dot{s}_i &= \Lambda\mu_{s_i}{}^T \tilde{y}_{-i} + \tilde{y}_i^{[n_i]} = \Lambda\mu_{s_i}{}^T \tilde{y}_{-i} + \theta_i^{*T} \Phi'_i(t) - y_{ri}^{[n_i]} \\ &= \Lambda\mu_{s_i}{}^T \tilde{y}_{-i} + \sum_{l=0, l \neq k}^{n_i-1} a_{i(l+1)}y^{[l]} + b_i^{*T} u - y_{ri}^{[n_i]} \\ &= \Lambda\mu_{s_i}{}^T \tilde{y}_{-i} + a_i^{*kT} y_{-ik} + b_i^{*T} u - y_{ri}^{[n_i]} \end{aligned} \tag{11}$$

Derivative of the sliding vector, which is defined as $S = \begin{bmatrix} s_1 \\ \vdots \\ s_N \end{bmatrix} \in \mathbb{R}^N$, can be written as following:

$$\begin{aligned} \dot{S} &= \tilde{\Gamma} + \Gamma_a - \Gamma_r + B' u \\ \tilde{\Gamma} &= \begin{bmatrix} \Lambda\mu_{s_1}{}^T \tilde{y}_{-1} \\ \vdots \\ \Lambda\mu_{s_N}{}^T \tilde{y}_{-N} \end{bmatrix} \in \mathbb{R}^N, \Gamma_a = \begin{bmatrix} a_1^T y_{-1} \\ \vdots \\ a_i^{*kT} y_{-ik} \\ \vdots \\ a_N^T y_{-N} \end{bmatrix} \in \mathbb{R}^N, \\ \Gamma_r &= \begin{bmatrix} y_{r1}^{[n_1]} \\ \vdots \\ y_{rN}^{[n_N]} \end{bmatrix} \in \mathbb{R}^N, B' = \begin{bmatrix} b_1^T \\ \vdots \\ b_i^T \\ \vdots \\ b_N^T \end{bmatrix} \in \mathbb{R}^{N \times N}. \end{aligned} \tag{12}$$

Assumption A2 Matrices $B = [b_{aj}]_{N \times N}$ and B' are diagonally dominant.

Remark 2 As mentioned before, one of the main motivation of selected structure is the control of robotic systems while tracking of their dynamic behavior. By analyzing

the Lagrangian behavior of parallel robots in researches as (Briot and Bonev 2009; Li et al. 2006; Yahyapour et al. 2013), it is seen that these behaviors are close to decoupled equations. Therefore diagonally dominance of nominator matrices are demonstrated in these robotic systems.

System inputs are assigned based on the control input vector ($\hat{u} \in \mathbb{R}^N$) and the sliding vector.

$$\begin{aligned} u &= \hat{u} - \eta \operatorname{sgn}(S) \\ \hat{u} &= -\hat{B}'^{-1}(\tilde{\Gamma} + \Gamma_a - \Gamma_r), \eta = \begin{bmatrix} \eta_1 & 0 & 0 \\ 0 & \ddots & 0 \\ 0 & 0 & \eta_N \end{bmatrix} \in \mathbb{R}^{N \times N}, \\ \hat{B}' &= \begin{bmatrix} \hat{b}_1^T \\ \vdots \\ \hat{b}_i^T \\ \vdots \\ \hat{b}_N^T \end{bmatrix} \in \mathbb{R}^{N \times N}, \Gamma_a = \begin{bmatrix} \hat{a}_1^T y_{-1} \\ \vdots \\ \hat{a}_i^{*kT} y_{-ik} \\ \vdots \\ \hat{a}_N^T y_{-N} \end{bmatrix} \in \mathbb{R}^N \end{aligned} \tag{13}$$

The matrix η is a design parameter and is determined such that $\eta_q b_{qq} > 0$ and $\eta_i b'_{ii} > 0$. As we are going to investigate in next sections, the model reduction affects \hat{u} in Eq. (13). Therefore, the force needed to keep the system on reaching surfaces, is depending on identified model parameters ($\hat{\theta}$). The accent ^ on each parameter shows estimated value of that parameter by identifier. Substituting Eq. (13) in the derivative of the sliding vector results in Eq. (14), where $\tilde{a}_i^k = a_i^k - \hat{a}_i^k$. Likewise, the accent ~ on each parameter shows error value of identified parameter from its basic value.

$$\dot{S} = - \begin{bmatrix} \tilde{b}_1^T \\ \vdots \\ \tilde{b}_i^T \\ \vdots \\ \tilde{b}_N^T \end{bmatrix} \hat{u} + \begin{bmatrix} \tilde{a}_1^T y_{-1} \\ \vdots \\ \tilde{a}_i^{*kT} y_{-ik} \\ \vdots \\ \tilde{a}_N^T y_{-N} \end{bmatrix} - B' \eta \operatorname{sgn}(S) \tag{14}$$

To separate functionally between control and identification procedures, we need an energy function. This function shows how much energy the identifier needs to control system outputs and how much energy it needs to update model parameters. The Lyapunov function is considered as Eq. (15), where we define $\tilde{\theta}_i^T = [\tilde{a}_i^{*kT}, \tilde{b}_i^T]$ for i th channel and $\tilde{\theta}_q^T = [\tilde{a}_q^T, \tilde{b}_q^T]$ for the other channels. To keep the closed-loop system stable, the identifier should decrease this Lyapunov

function. Adaptation rules for updating identified model parameters are appropriate tools to reach this target. By designing suitable control input and adaptation rules, the stability of closed-loop system can be guaranteed. The matrix $P_q^{-1}(t) \in \mathbb{R}^{(N+n_q) \times (N+n_q)}$ denotes as the covariance matrix for channel q and the matrix $P_i'^{-1}(t)$ denotes as the reduced covariance matrix for i th channel.

$$V(t) = \frac{1}{2} \left[S^T S + \tilde{\theta}_i'^T(t) P_i'^{-1}(t) \tilde{\theta}_i'(t) + \sum_{q \neq i} \tilde{\theta}_q'^T(t) P_q^{-1}(t) \tilde{\theta}_q(t) \right], \quad \forall t : \tau_1 \leq t \leq \tau_2 \tag{15}$$

The structure of Lyapunov function changes with model reduction. In fact, reducing order of models helps the identifier to control output signals; this point is especially important when stimulation degree of desired signals is low. The RLS method is appropriate tool to update model parameters in order to decrease identification error. Updating rule in Eq. (16) is resulted from continuous RLS method, where scalar e_i is defined as $e_i = \tilde{y}_i^{[n_i]} = y_i^{[n_i]} - y_{r_i}^{[n_i]} = \tilde{\theta}_i'^T(t) \Phi_i'(t)$. For i th channel, updating rules should be stated with R-OM. It is obvious scalar $e_i(t)$ does not change with model reduction.

$$\hat{\theta}_i'(t) = P_i'(t) \Phi_i'(t) e_i(t) \tag{16}$$

Based on RLS method, the online updating of (invert of) reduced covariance matrix is expressed as following:

$$\dot{P}_i' = \alpha_i P_i'(t) - P_i'(t) \Phi_i'(t) \Phi_i'^T(t) P_i'(t) \tag{17}$$

where α_i denotes forgetting factor of i th channel. In RLS methods, basic model parameters of q th channel are traceable if vector of regressors in channel q is at least PE with degree $n_q + N$, which is the number of parameters needed to be estimated in the channel (Åström and Wittenmark 1989). Equation (13) shows that desired signals affect vectors of input signals and then output signals. It can be shown that a persistent excitation with degree n_q has sufficient stimulation for channel q . Also, any signals with degree less than n_q are weak stimulations for the channel.

If all desired signals are sufficient PE, basic model parameters are traceable and all covariance matrices remain positive definite. Therefore, two time-invarying scalars $\underline{\sigma}_q$ and $\bar{\sigma}_q$ can be found which $\forall t \geq 0 : 0 < \underline{\sigma}_q I \leq P_q^{-1}(t) \leq \bar{\sigma}_q I$ is established for. On the contrary, if at least for one channel (i th channel) desired signal is not sufficient PE, the covariance matrix becomes positive semi-defined after a while. Hence,

some dependency relations happen in vector of input–output regressors of i th channel.

Depending on degree of excitation in the channel, which determines number of dependency relations, the identifier switches the basic model to a suitable R-OM to fit the behavior of i th channel, while other channels remain intact. In this case, some correlated regressors are removed from the vector of input–output regressors and related model parameters are reduced in order to adapt model with low degree of excitation signal in i th channel. With these changes, the identifier carries on a partially identification method which is adapted to stimulation degree of desired signals. In this case the floating rank is less than the dynamic rank of i th channel. (The floating rank of i th channel determines the number of denominator parameters which can be identified in the online moment.)

Suggested adaptation rules for R-OM parameters are shown in Eq. (18). First part is concerned with adaptive updates based on sliding values. After reaching sliding surfaces, this part eliminates and only second part affects adaptation rules. The second part is mainly the same as Eq. (16); but parameter γ_i adjusts how much updating rule of RLS affects the adaptation rules. Number of adaptation rules are modified with model reduction.

$$\begin{bmatrix} \hat{a}_i^{k'} \\ \hat{b}_i' \end{bmatrix} = S_i(t) P_i'(t) \begin{bmatrix} y_{-ik} \\ -\hat{u} \end{bmatrix} + \gamma_i P_i'(t) \Phi_i'(t) e_i(t) \quad \tau_1 \leq t \leq \tau_2 \tag{18}$$

2.3 Stability and convergence

As it was discussed in the Sect. 1, giving guarantee of stability of system under any kind of identification procedure is important.

In Theorem 1, stability of the closed-loop system in presence of the basic model is studied. All conditions and assumptions are established before any switching. In another word, switching moment (if there is) is far enough to let model parameters converge and system reaches steady state.

Theorem 1 Regarding to the MIMO system described in Eq. (1) and based on A2, identification of the basic model is guaranteed. Also, the closed-loop system remains stable during identification procedures. In Appendix a, the proof of this theorem is presented.

In the following, by using R-OMs, stability of closed-loop system is going to be studied. Meanwhile, convergence of R-OM parameters to their true values is proven. Then, in

next section, stability of closed-loop system during switching and with ELM will be covered.

Theorem 1' After switching, by using the model formulated as Eq. (9), the closed-loop system under identification remains stable. Assumptions A1, A2, A3 are established in this theorem. In Appendix b, the proof of this theorem is presented.

Assumption A3 In Theorem 1, it is ideally assumed that after the stimulation degree decreases, the model is immediately reduced.

In Theorem 1, it has been proven a system under Algorithm1 before switching time is asymptotically stable. Now in Theorem 1 it is proven that after switching, by using R-OM, the system remains stable.

It is worth to mention that by switching between R-OMs, besides identification, the algorithm introduces much more sensible concept of control theory: Desired signals can be determined by user, not identifier. Based on the desired signal type and its stimulation degree, suitable models fit on system behaviors. For instant, if a user applies step signals to references, models with floating rank of 1 fit on basic system behaviors.

Hence, besides trying to fit suitable models on system behavior, this algorithm is trying to converge output signals of closed-loop system to user-defined desired signals. According to the variation of stimulation degree during identification, different models fit on a system in order to the identifier keeps tracking behavior of that system. This ELM can evolve from low floating rank R-OMs to the perfect order model (basic model).

2.4 Some discussions and details

Discussion D1 If until time $t = \tau_1^-$ sufficient excitation is applied to the system, as mentioned before, $\exists \underline{\sigma}_q, \bar{\sigma}_q, \forall t \leq \tau_1^- : 0 < \underline{\sigma}_q I \leq P_q^{-1}(t) \leq \bar{\sigma}_q I$ is established.

$$P_q^{-1}(t) = \int_0^t \exp(-\alpha_q(t - \tau)) \Phi_q(\tau) \Phi_q^T(\tau) d\tau \quad t \leq \tau_1, 1 \leq q \leq N \tag{19}$$

In the switching moment, due to reduction of stimulation degree and because $\underline{\sigma}_i$ almost vanish, Theorem 1 is not established any more. So a correlation happens in vector of regressors in $t = \tau_1$. Hence, the identifier must decrease the number of model parameters. By removing dependent

variable from vector $\Phi_i(t)$ and turning it into $\Phi'_i(t)$ for $\tau_1 \leq t$, equation $\Phi_i^T(t) \Psi_i = 0, \tau_1 \leq t \leq \tau_2$ has no non-zero answer.

$$P_i'^{-1}(t) = \int_0^t \exp(-\alpha_i(t - \tau)) \Phi'_i(\tau) \Phi_i^T(\tau) d\tau \quad \tau_1 \leq t \leq \tau_2 \tag{20}$$

It is concluded from Eq. (20) that $\exists \underline{\sigma}'_i, \bar{\sigma}'_i, \tau_1 \leq \forall t \leq \tau_2 : 0 < \underline{\sigma}'_i I \leq P_i'^{-1}(t) \leq \bar{\sigma}'_i I$. Based on A1, the other channels remain sufficient PE.

Discussion D2 In the above theorem, A3 was assumed. The switch time is defined based on when $\underline{\sigma}_i$ tends to zero, which in fact depends on the processor machine and its condition number. So despite A3, there might be a delay between changing the stimulation degree and switching time in setting up the algorithm. In this interval, the closed-loop system may run toward instability or identified parameters may get farther from their real values. Hence, it is important to observe the condition of the closed-loop system and parameter $\underline{\sigma}_i$ in order to reduce this delay.

Discussion D3 The stability of closed-loop system has been proven before and after switching time $t = \tau_1$, but more important problem happens during the switching time. The changes have been made to vectors $\theta_i^T, \underline{y}_{-ik}$ and matrix P_i' from $t = \tau_1^-$ to $t = \tau_1^+$ should be studied in detail. In this section, it is not necessary for parameters of the model to have converged to their real values before model reduction, but we should estimate Ψ_i^T close to its original value. Any sudden changes in system inputs can cause disturbances in the system condition. In the switching time, variation of control input signals may result in system instability. In order to switch the model, the dependent variable is removed; nevertheless, the sliding variable described as $s_i = \Lambda \mu_i^T \tilde{y}_i$ does not change because $\Lambda \mu_i$ and \tilde{y}_i are relevant to the system, not

the identified model. So during switching, vectors $\Gamma_{\hat{a}}$ and \hat{B}^{-1} are only parts which can affect on control input signals. The i th element of $\Gamma_{\hat{a}}$ changes from $\hat{a}_i^T \underline{y}_{-i}$ to $\hat{a}'_i{}^{kT} \underline{y}_{-ik}$.

$$\begin{aligned} \hat{a}_i^T(t) \underline{y}_{-i} &= \sum_{l=0}^{n_i-1} \hat{a}_{i(l+1)}(t) y_i^{[l]} = \hat{a}_{in_i} y_i^{[n_i-1]} + \dots \\ &+ \hat{a}_{i(m+1)} y_i^{[m]} + \dots + \hat{a}_{i(k+1)} y_i^{[k]} + \dots + \hat{a}_{i1} y_i, \quad t < \tau_1 \\ \hat{a}'_i{}^{kT}(t) \underline{y}_{-ik} &= \sum_{l=0, l \neq k}^{n_i-1} a'_{i(l+1)}(t) y_i^{[l]} = \hat{a}'_{in_i} y_i^{[n_i-1]} + \dots \\ &+ \underbrace{(\hat{a}'_{i(m+1)} + \hat{a}'_{i(k+1)} c_{i(m+1)})}_{\hat{a}'_{i(m+1)}} y_i^{[m]} + \dots + \hat{a}'_{i1} y_i, \quad \tau_1 \leq t \leq \tau_2 \end{aligned} \tag{21}$$

Considering Eq. (21), it is obvious that by choosing $\hat{a}'_{i(m+1)}(\tau_1) \leftarrow \hat{a}_{i(m+1)}(\tau_1) + \hat{a}_{i(k+1)}(\tau_1)c_{i(m+1)}$ two inner products become equivalent. On the contrary, the identifier doesn't change elements of \hat{B}'^{-1} in the switching moment and lets them converge to their real values, asymptotically. Also in the switching moment, the column and row $P_{i(k+1)}$ should be removed, where $P_{i(l+1)}$ denotes the row (or the column) of the matrix $P_i(t)$ related to $\hat{a}_{i(l+1)}$. By imposing mentioned variations, no impulses are exerted to closed-loop system during model reduction.

Discussion D4 Based on the previous discussion, it is necessary to observe the behavior of $\Psi_i^T(t)$, especially in the switching time. In fact, while this vector remains constant in a specified interval, the linear correlation in the vector of regressors results in a rank deficiency. Theoretically when $\underline{\sigma}_i$ tends to zero, Theorem 1 is not established and the identifier cannot track whole behaviors of the system. An interesting point is the rule of the forgetting factor. As α_i increases, the identifier finds the linear correlation faster and responses to the variation of stimulation degree; this happens because $\underline{\sigma}_i$ tends faster to zero. So it is clear that in switching time, the matrix $P_i^{-1}(t = \tau_1)$ has at least one non-zero null-vector. (As mention, we have assumed rank deficiency of one. So $P_i^{-1}(t = \tau_1)$ has exactly one non-zero null-vector.)

$$\begin{aligned}
 &P_i^{-1}(\tau_1)N_i \\
 &= \int_0^{\tau_1} \exp(-\alpha_i(\tau_1 - \tau))\Phi_i(\tau)\Phi_i^T(\tau)d\tau N_i = 0
 \end{aligned}
 \tag{22}$$

Theoretically, to establishing Eq. (22), the matrix $\Phi_i(t)\Phi_i^T(t)$ should have a joint null-vector for $\forall t : 0 \leq t \leq \tau_1$. It is worth to mention that $\Phi_i(t)\Phi_i^T(t)$ has different null-vectors in the interval, but due to the integration of matrices over time, just a joint null-vector leads to rank deficiency of $P_i^{-1}(t = \tau_1)$. This null-vector is the same as null-vector of $P_i^{-1}(t = \tau_1)$.

$$\Phi_i(t)\Phi_i^T(t)N_i = 0, \quad t \in [t_1, \tau_1]
 \tag{23}$$

So if Eq. (23) is established for a non-zero vector, $\Phi_i^T(t = \tau_1)\Psi_i = 0$ is established in switching time too. Hence, null-vector N_i , obtained from Eq. (22), is a good estimation for correlation vector Ψ_i . The parameter $c_{i(m+1)}$ is calculated based on this vector and the mentioned targets of evolving in the D3 are fulfilled.

Based on D2, there is a time difference between the variation of stimulation degree and nullity of P_i^{-1} ; the identifier needs to switch the model before mentioned instabilities happen. Above method is not applicable for detecting variations of stimulation degree (Eq. (22) doesn't have any valid solutions before the nullity of P_i^{-1} happens.) To fix this problem, a method is proposed which defines a limitation on the condition number of P_i^{-1} and detect the switching moment. In another word, by detecting ill-condition of the covariance matrix, variation of stimulation degree can easily be detected, no needed for the nullity of covariance matrix. By singular value decomposition (SDV) of $P_i^{-1} = U\Sigma V^*$ in the switching moment, the deficiency relation is obtained. The column of V , related to $\underline{\sigma}_i$, is a good estimation of Ψ_i . In the case of noisy regressors in matrix Φ_i or variant parameters of Ψ_i , the proposed method is more robust and leads to an efficient switching time.

Algorithm 2: Online identification of MIMO systems by an ELM

```

1: Procedure: Online Identification method
2:   Initialization  $\hat{a}_q(0) = 0_{n_q}$ ,  $\hat{B}(0) = I_N$ ,  $P_q^{-1}(0) = 0.01 \times I_{N+n_q}$ ,  $\forall q = 1, \dots, N$ 
3:   Calculate desired signals and their derivatives
4:   Calculate output signals of the basic plant and form  $\Phi_q = \begin{bmatrix} y_q \\ \underline{u} \end{bmatrix}$ ,  $1 \leq \forall q \leq N$ .
5:   Calculate sliding surfaces based on Eq. (10).
6:   Form control input signals as  $\underline{u} = \hat{\underline{u}} - \eta \operatorname{sgn}(\mathbf{S})$ .
7:   Update the matrix  $P_q^{-1}(t)$  based on  $\dot{P}_q^{-1} = -\alpha_q P_q^{-1}(t) + \Phi_q(t)\Phi_q^T(t)$ ,  $\forall q = 1, \dots, N$ .
8:   Calculate the condition number of  $P_q^{-1}(t)$ ,  $\forall q = 1, \dots, N$ .
9:   If the condition number of  $i$ th channel crosses the limitation, then
10:     Procedure: Model Reduction
11:       Calculate SVD of  $P_i^{-1}(t)$  as  $P_i^{-1} = U\Sigma V^*$ .
12:       Choose the last column of  $V$  as the vector  $\Psi_i$ .
13:       Choose  $k$  by searching the index of max element of  $\Psi_i$  and
         calculate  $c_{i(m+1)}$ ,  $0 \leq m \neq k \leq n_i - 1$ .
14:       Removed the column and row of  $P_{i(k+1)}$  and form  $P'_i$ .
15:       for  $m \neq k \rightarrow 0, n_i - 1$  do
16:          $\hat{a}'_{i(m+1)}(t) = \hat{a}_{i(m+1)}(t) + \hat{a}_{i(k+1)}(t)c_{i(m+1)}$ 
17:       end for
18:       Remove  $\hat{a}_{i(k+1)}$  from  $\hat{a}_i$  and form  $a_i'^k$ .
19:       Remove  $y_i^{[k]}$  from  $\underline{y}_i$  and form  $\Phi'_i = \begin{bmatrix} y_{ik} \\ \underline{u} \end{bmatrix}$ .
20:       Decrease one from the floating rank of  $i$ th channel.
21:       In the following, use reduced parameters  $(\Phi'_i, \hat{a}_i'^k, \hat{\theta}'_i, P'_i, \underline{y}_{ik})$  instead of their basic
         values.
22:     end procedure
23:   end if
24:   Calculate the estimation error  $e_q(t)$ :
         
$$e_q(t) = \tilde{\theta}_q^T(t)\Phi_q(t), \forall q = 1, \dots, N.$$

         Update parameters' adaptation rules:
25:     
$$\begin{bmatrix} \hat{\underline{a}}_q \\ \hat{\underline{b}}_q \end{bmatrix} = S_q(t)P_q(t) \begin{bmatrix} y_q \\ -\hat{\underline{u}} \end{bmatrix} + \gamma_q P_q(t)\Phi_q(t)e_q(t), \forall q = 1, \dots, N. \quad (24)$$

26:   Put  $t = t + T$ 
27:   If  $t < t_f$ , then
28:     Return to line 3
29:   else
30:     Terminate the algorithm.
31:   end if
32: end procedure

```

3 Simulation

In this part, we consider ELM and its effects on the identification procedure. A controllable linear MIMO system is studied under weak stimulations.

$$H(S) = \begin{bmatrix} \frac{1.7856}{S^2-1.0486S+0.4256} & \frac{-0.2567}{S^2-1.0486S+0.4256} \\ \frac{0.0533}{S^3-1.0635S^2-2.5088S-0.6607} & \frac{1.3986}{S^3-1.0635S^2-2.5088S-0.6607} \end{bmatrix}_{2 \times 2} \quad (25)$$

In Fig. 2, it is shown that Algorithm 1 under sufficient excitations is able to identify the system in Eq. (25), successfully. The dynamic rank of the second channel is 3 and the model needs stimulation degree of 3 to be identified perfectly. Therefore in second channel, 2-sinusoidal signal with stimulation degree of 4 is sufficient and stabilishes conditions of Theorem 1. Details of this simulation are listed in Table 1.

In the following, a sinusoidal signal is selected as the desired signal for each channel. Hence, the first channel is sufficiently excited due to its dynamic rank of 2. This time

by applying $y_{r2}(t) = 0.9 \sin 1.1t$ to the second channel and without model reduction, identified parameters are getting away from their real values and become swingy, as it is demonstrated in Fig. 3. The other details of this simulation are shown in Table 1. Hanging on this situation, condition number of P_2^{-1} is increasing intensely and stability of closed-system will be jeopardized.

To solve above problem, Algorithm 2 is applied with model reduction and results are demonstrated in Fig. 4.

According to D2, the time of switching of the model is obtained based on specified max limit of condition number of P_2^{-1} . Choosing this limitation, switching time would be before vanishing σ_2 . (To prevent any instabilities and control

problems, as it is clearly seen in Fig. 5, this max limit sets to 6000 in the simulation. So the system gets enough time to react against weak stimulations.) The identifier chooses 3rd regressor ($y_2^{[2]}$) of second channel and removes (Based on

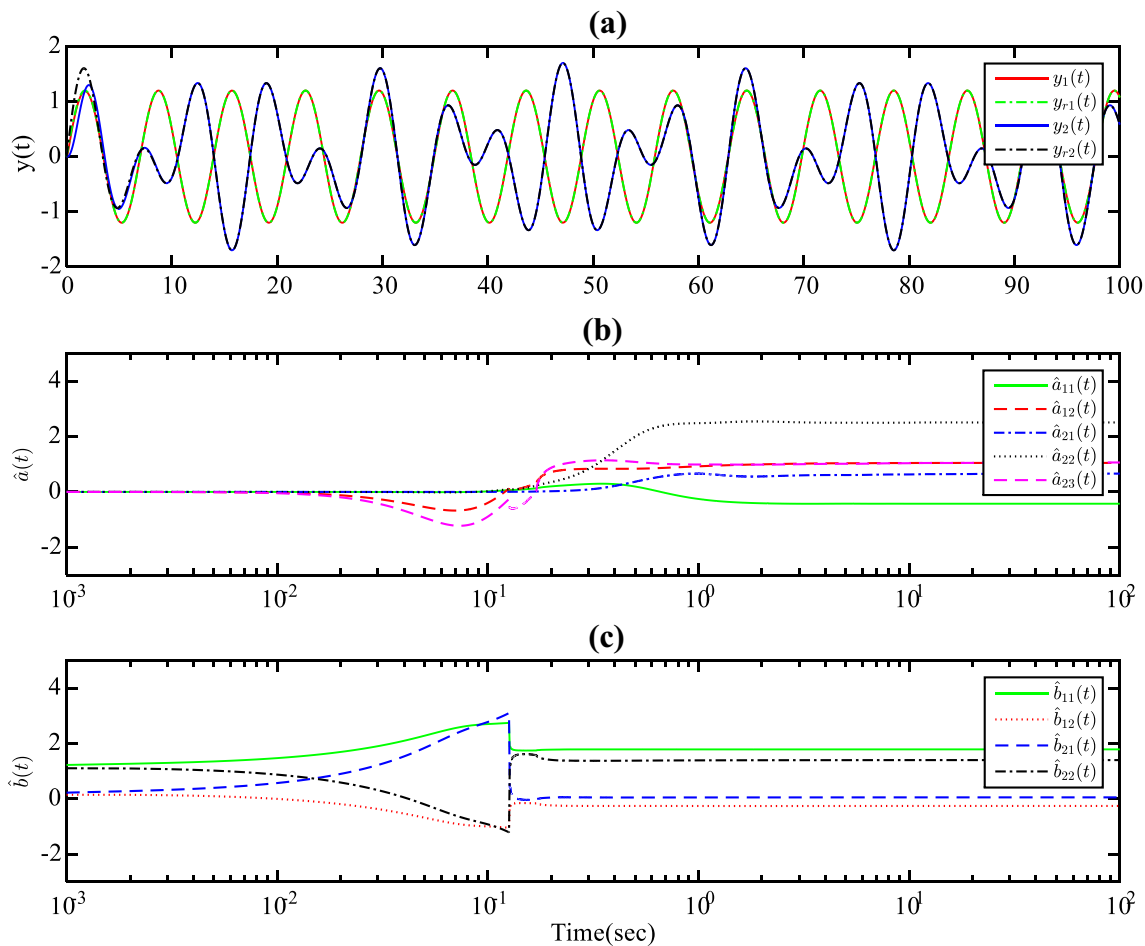


Fig. 2 Simulation 1: identification and control of the system under sufficient excitation. **a** Output and desired output signals. **b** The identified denominator parameters. **c** The identified nominator parameters

Table 1 Details of Simulation 1 including initial value, control parameters, desired signals and sampling period

Real parameters	Initial guess of parameters
$a_1^T = [1.0486, -0.4256]$	$\hat{a}_1^T = [0 \ 0], \hat{a}_2^T = [0 \ 0 \ 0]$
$a_2^T = [1.0635, 2.5088, 0.6607]$	$\hat{b}_1^T = [0 \ 1], \hat{b}_2^T = [1 \ 0]$
$b_1^T = [-0.2567, 1.7856], b_2^T = [1.3986, 0.0533]$	$P_1(0) = 100 I_4, P_2(0) = 100 I_5$
Control parameters	Sampling period
$\lambda_1 = 1, \lambda_2 = 1$	$\bar{dt} = 0.001$
$\gamma_1 = 1, \gamma_2 = 1$	Desired tracking signals
$\alpha_1 = 0.01, \alpha_2 = 0.01$	$y_{r1}(t) = 1.2 \sin 0.9t$
$\eta = \begin{bmatrix} 5 & 0 \\ 0 & 5 \end{bmatrix}$	$y_{r2}(t) = 0.9 \sin 1.1t + 0.8 \sin 0.7t$

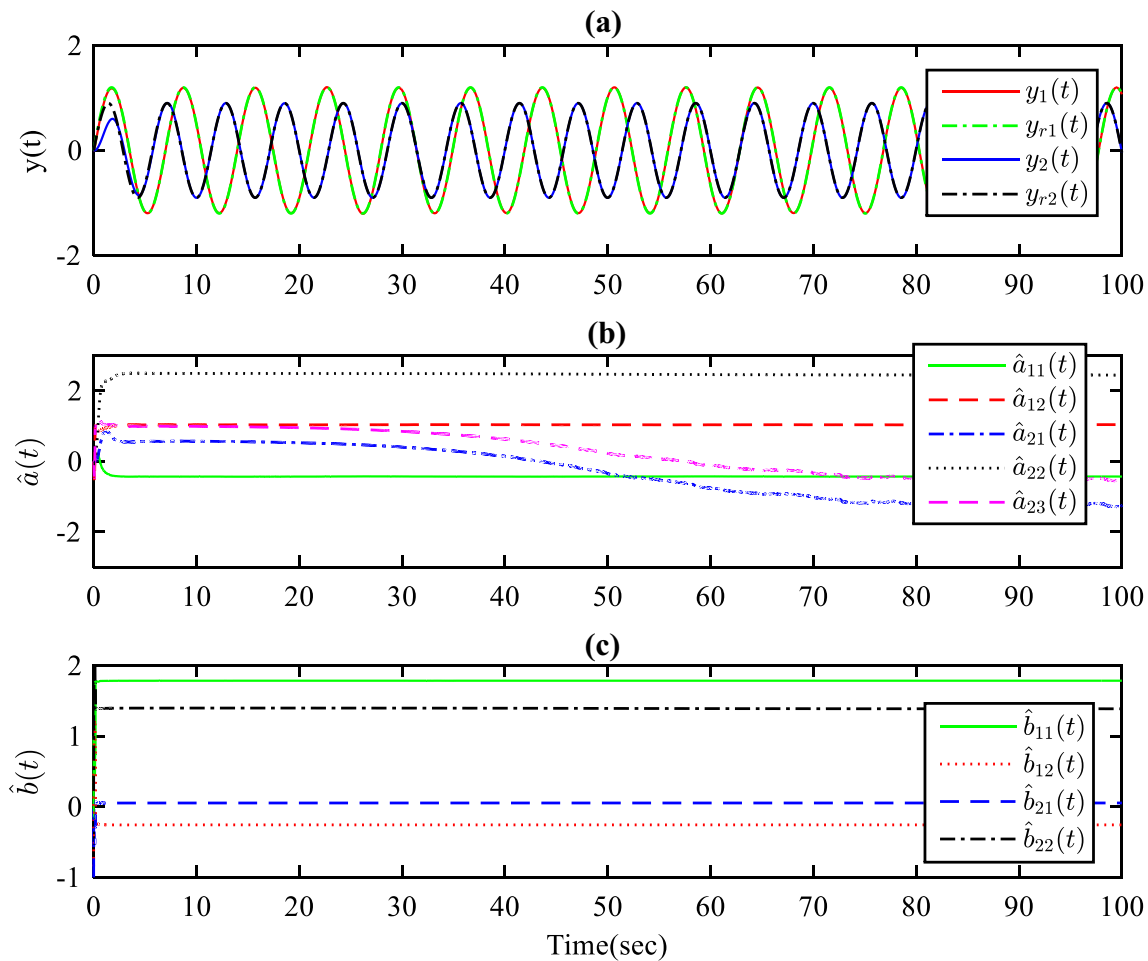


Fig. 3 Simulation 2: identification and control of the system under weak stimulation without model reduction. **a** Output and desired output signals. **b** The identified denominator parameters. **c** The identified nominator parameters

nullity vector) it. Then, another model with floating rank of two fits second channel.

After switching moment, identified R-OM on channel 2, input 2, is obtained as $\hat{H}'_{22}(S) = \frac{1.3985}{S^3 - 2.5072 S + 0.6169}$, while

before switching, the model on channel 2 was identified as $\hat{H}_{22}(S) = \frac{1.3985}{S^3 - 1.0079 S^2 - 2.5072 S - 0.5926}$.

The way of obtaining nullity vector is based on D4. After removing 3rd regressor, identified parameters of new model are initiated based on D3. The parameter C_{21} (from

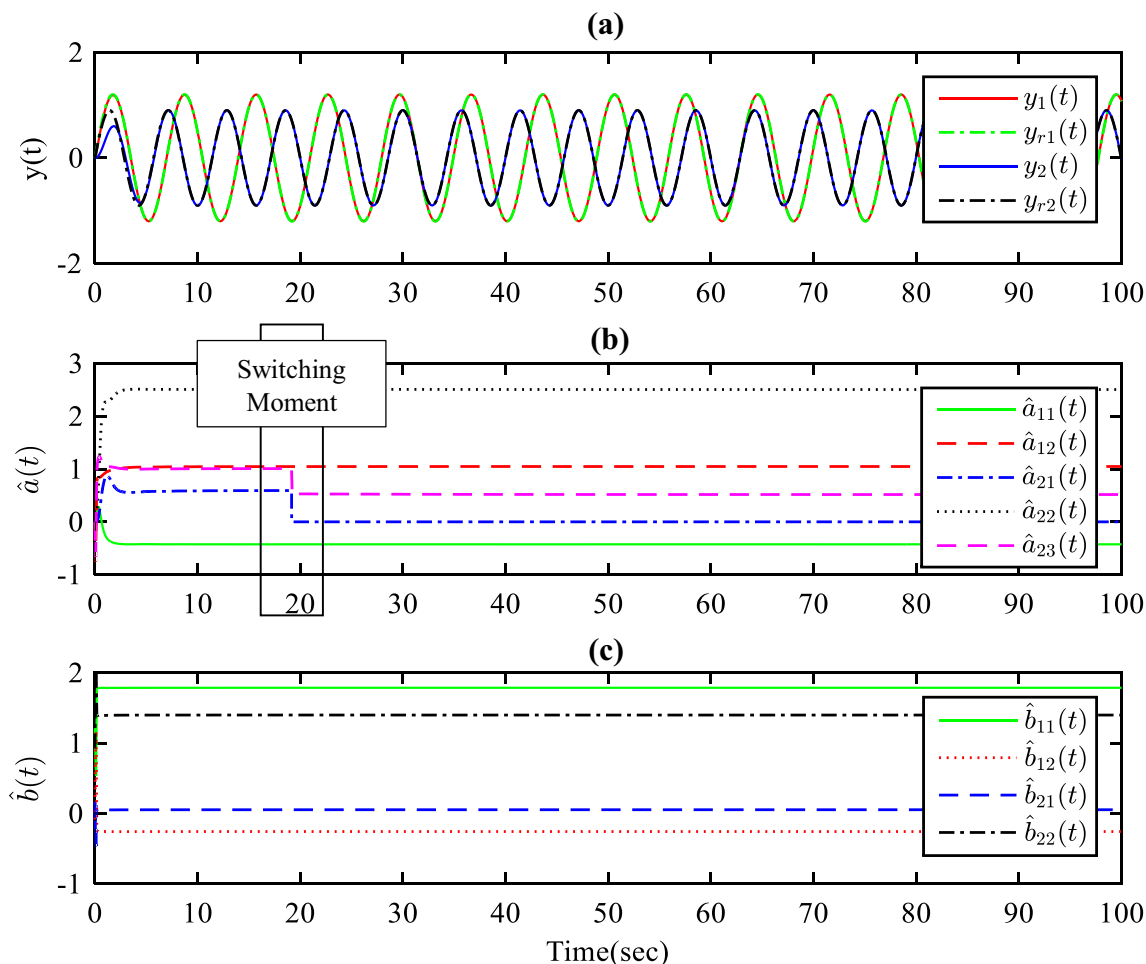


Fig. 4 Simulation 3: identification and control of the system under weak stimulation with model reduction. **a** Output and desired output signals. **b** The identified denominator parameters. **c** The identified nominator parameters

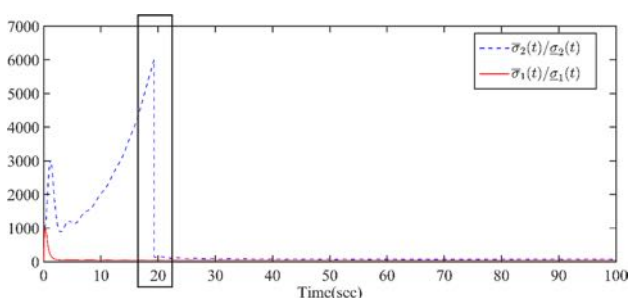


Fig. 5 Simulation 3: the status of condition numbers of P_1^{-1} and P_2^{-1} during identification

second channel and added to first regressor) is calculated about -1.22 ; other parameters are negligible. After initiating identified vector \hat{a}'_2 and matrix P'_2 in switching moment $\tau_1 = 19.272$, identification procedure is carried on.

It is demonstrated in Fig. 4 that based on Theorem 1', identified R-OM parameters converge to their values (The

characteristic equation of R-OM for second channel is calculated as $S^3 - 2.5088 S + 0.6261$, so identified parameters of second channel converge asymptotically to these values.) and none of input signals, output signals, or basic system parameters like S_i happens to discontinue. Since stimulation of second channel is rich now (1-sinusoidal signal can adequately excite R-OM with floating rank of two.), the identifier does not switch the model anymore and it is chosen as the best model fits to second channel, in presence of these excitation signals. Also, during these switching procedures, first channel with its basic model keeps tracking its parameters.

In Simulation 4, we study more complicated conditions: behavior of Algorithm 2 under very weak stimulations. The same basic system is studied, but two constant signals ($y_{r1}(t) = 0.9$ and $y_{r2}(t) = 1.1$) are chosen as desired signals. Both channels are excited by weak stimulations and need model-evolving. Table 1 contains the other details of this simulation.

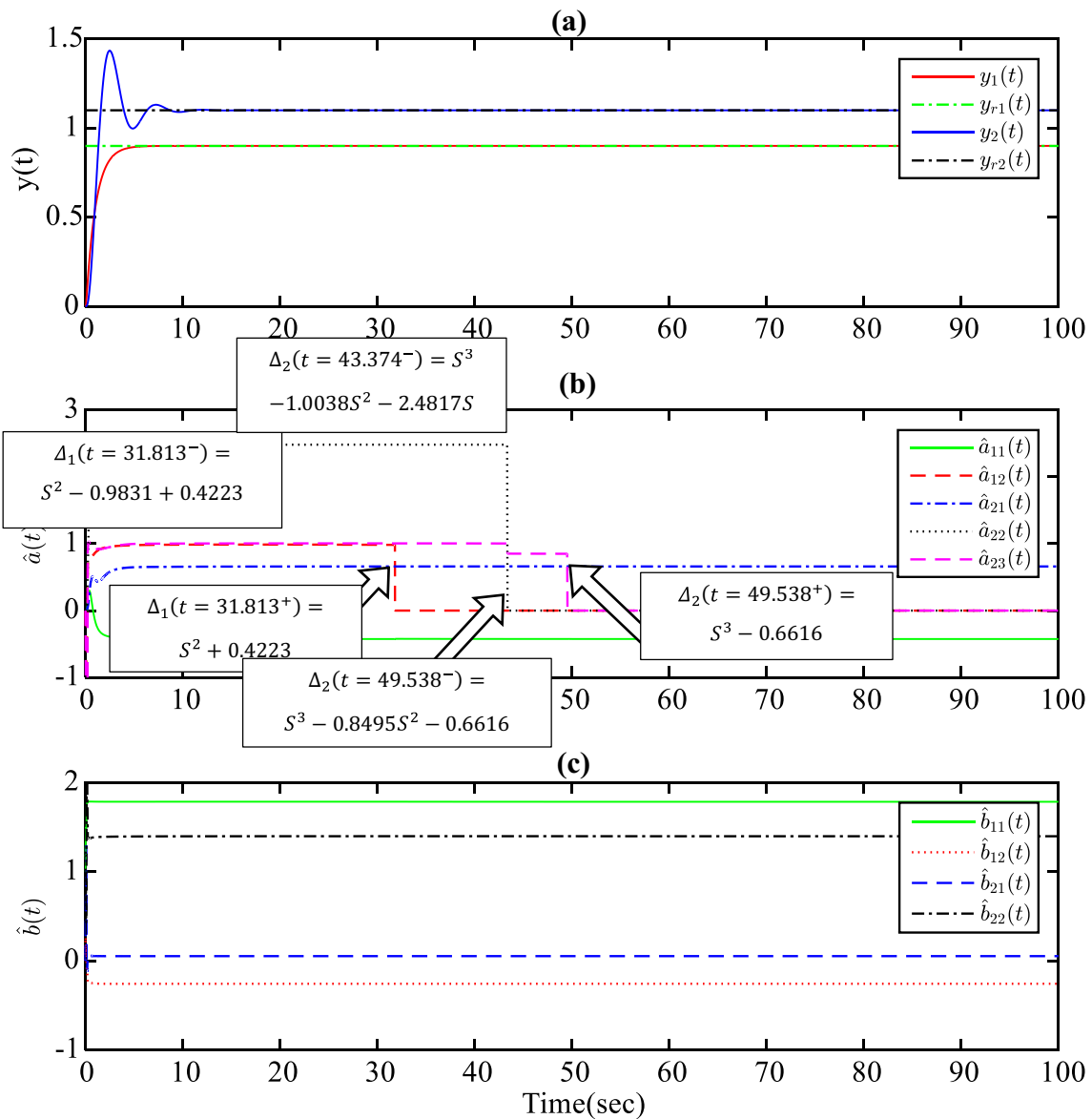


Fig. 6 Simulation 2: the identified denominator parameters and characteristic equations of channels under weak stimulation

It is demonstrated in Fig. 6 that channel one has been switched once. Then, second channel is imposed model reduction, twice. In Fig. 6 at each step, the characteristic equation of each channel and the models fitting on channels' behavior are shown. Also in Fig. 7, the nullity vector of the covariance matrix for each output channel in switching moment are demonstrated. In this simulation, limitation of condition number for covariance matrices is chosen to be 15,000.

By model switching, the identifier can track model parameters and fits suitable models on system behaviors in spite of constant desired signals. It is obvious that by multi-times switching and considering correlations between

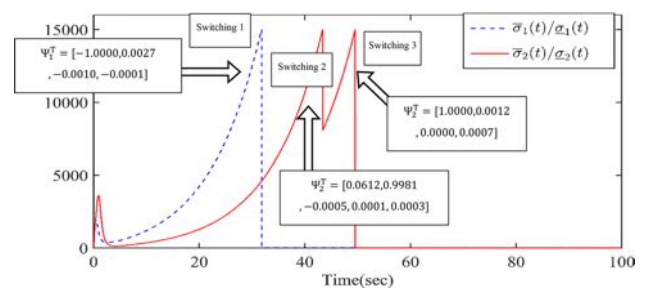


Fig. 7 Simulation 4: the status of condition numbers of P_1^{-1} and P_2^{-1} during identification

regressors, both controlling output signals and identifying model parameters are carried on.

In Simulation 4, the multi-times switching procedures can be briefed as one-time switching for each channel. Therefore, we should extract all correlation and deficiency relations at once for each channel. In this case, vector Ψ_2 has two non-zero answers each defines a correlation between input–output regressors. It is concluded that by choosing appropriate strategy while switching, no impulses are applied to the system during identification.

4 Conclusion and future works

The closed loop identification and control of a MIMO linear system under weak stimulation were investigated. Under weak stimulation of the system, by dropping out some input or output correlated variables, an equivalent reduced order model of the original system was appeared, where the system was identifying as an evolving linear model. Using SMC strategy and defining adaptation rules for parameters of the model, it was shown that the tracking errors converged to zero and the stability of the system was guaranteed. Also, the convergence of the parameters to their true values was studied and discussed.

When excitation order of user-defined signals was low, identification of the basic model turned into partially identification of system behaviors. By using linear models called R-OMs, important behaviors of the system were still followed. Also, convergence of the R-OM parameters to their real values and stability of the closed-loop system with this R-OM was guaranteed. Given different simulations showed clearly the proposed closed loop identification approach works under weak stimulation of a MIMO linear system.

The proposed schemes were restricted to linear systems. To extend for more robotic plants, nonlinearities of a system should be handled. In authors’ view, fuzzy evolving models can be a suitable solution. Convergence of parameters and tracking of outputs for a single model have been guaranteed in this paper. Giving guarantee for the stability of the closed-loop system with fuzzy models is the future challenge for

parameters on the sufficiently excitation of channels. By increasing the variation of parameters over time, the degree of persistent excitation needed for perfect tracking is increasing, which makes the possibility of sufficiently excitation much difficult. Extending the current structure to handle this problem is another future challenge for authors.

Appendix a

Theorem 1 Regarding to the MIMO system described in Eq. (1) and based on A2, identification of the basic model is guaranteed. Also, the closed-loop system remains stable during identification procedures.

Proof Consider following positive definite Lyapunov function including the sliding vector and parameters estimation errors (PEEs):

$$V(t) = \frac{1}{2} \left[S^T S + \sum_{q=1}^N \tilde{\theta}_q^T(t) P_q^{-1}(t) \tilde{\theta}_q(t) \right] \tag{26}$$

where

$$\tilde{\theta}_q^T(t) = [\tilde{a}_q^T, \tilde{b}_q^T] \tag{27}$$

Regarding to the differential equations in Eq. (2), the derivative of the Lyapunov function, formulated in Eq. (26), is computed as follows:

$$\dot{V}(t) = \frac{1}{2} \left[2S^T \dot{S} + 2 \sum_{q=1}^N \tilde{\theta}_q^T(t) P_q^{-1}(t) \dot{\tilde{\theta}}_q(t) + \sum_{q=1}^N \dot{\tilde{\theta}}_q^T(t) P_q^{-1}(t) \tilde{\theta}_q(t) \right] \tag{28}$$

Or

$$\dot{V}(t) = \frac{1}{2} \left[2S^T \dot{S} - 2 \sum_{q=1}^N \hat{\theta}_q^T(t) P_q^{-1}(t) \tilde{\theta}_q(t) + \sum_{q=1}^N \tilde{\theta}_q^T(t) \dot{P}_q^{-1}(t) \tilde{\theta}_q(t) \right] \tag{29}$$

By substituting the derivative of sliding vector from Eq. (14), the following formula is obtained:

$$\dot{V}(t) = \frac{1}{2} \left[-2S^T \begin{bmatrix} \tilde{b}_1^T \\ \vdots \\ \tilde{b}_N^T \end{bmatrix} \tilde{u} + 2S^T \begin{bmatrix} \tilde{a}_1^T y \\ \vdots \\ \tilde{a}_N^T y \end{bmatrix} - 2 \sum_{q=1}^N \hat{\theta}_q^T(t) P_q^{-1}(t) \tilde{\theta}_q(t) + \sum_{q=1}^N \tilde{\theta}_q^T(t) \dot{P}_q^{-1}(t) \tilde{\theta}_q(t) \right] - S^T B \eta \text{sign}(S). \tag{30}$$

authors. Another interesting point that authors demonstrated during simulations is the effect of variation of the system

Equation (30) can be written in summation format as follows:

$$\begin{aligned} \dot{V}(t) = & \sum_{q=1}^N \left(s_q \begin{bmatrix} y_q^T \\ -\hat{u}^T \end{bmatrix} - \begin{bmatrix} \hat{a}_q^T(t) \\ \hat{b}_q^T(t) \end{bmatrix} P_q^{-1}(t) \right) \tilde{\theta}_q(t) \\ & + \frac{1}{2} \sum_{q=1}^N \tilde{\theta}_q^T(t) \dot{P}_q^{-1}(t) \tilde{\theta}_q(t) - \sum_{q=1}^N \left(\eta_q \sum_{j=1}^N b_{qj} s_q \operatorname{sign}(s_j) \right). \end{aligned} \tag{31}$$

According to the design parameter, following inequality can be obtained:

$$\begin{aligned} \dot{V}(t) \leq & \sum_{i=1}^N \left(s_q \begin{bmatrix} y_q^T \\ -\hat{u}^T \end{bmatrix} - \begin{bmatrix} \hat{a}_q^T(t) \\ \hat{b}_q^T(t) \end{bmatrix} P_q^{-1}(t) \right) \tilde{\theta}_q(t) \\ & + \frac{1}{2} \sum_{q=1}^N \tilde{\theta}_q^T(t) \dot{P}_q^{-1}(t) \tilde{\theta}_q(t) \\ & - \sum_{q=1}^N \left| \eta_q \right| \left| s_q \right| \left(\left| b_{qq} \right| - \sum_{j=1, j \neq q}^N \left| b_{qj} \right| \right). \end{aligned} \tag{32}$$

Now, by using the given adaptation rules in Eq. (24), it is concluded that:

$$\begin{aligned} \dot{V}(t) \leq & -\frac{1}{2} \sum_{q=1}^N \alpha_q \tilde{\theta}_q^T(t) P_q^{-1}(t) \tilde{\theta}_q(t) \\ & - \sum_{q=1}^N \left(\gamma_q - \frac{1}{2} \right) \tilde{\theta}_q^T(t) \Phi_q(t) \Phi_q^T(t) \tilde{\theta}_q(t) \\ & - \sum_{q=1}^N \left| \eta_q \right| \left| s_q \right| \left(\left| b_{qq} \right| - \sum_{j=1, j \neq q}^N \left| b_{qj} \right| \right). \end{aligned} \tag{33}$$

By choosing $\gamma_q > \frac{1}{2}$, $\alpha_q > 0$ and according to A2:

$$\begin{aligned} \dot{V}(t) \leq & -\frac{1}{2} \sum_{q=1}^N \alpha_q \tilde{\theta}_q^T(t) P_q^{-1}(t) \tilde{\theta}_q(t) \\ & - \sum_{q=1}^N \left(\gamma_q - \frac{1}{2} \right) \tilde{\theta}_q^T(t) \Phi_q(t) \Phi_q^T(t) \tilde{\theta}_q(t) \\ & - \sum_{q=1}^N \left| \eta_q \right| \left| b_{qq} \right| \left| s_q \right|. \end{aligned} \tag{34}$$

Finally, it is concluded that:

$$\begin{aligned} \dot{V}(t) \leq & -W_3(\|S\|, \|\tilde{\theta}\|) = -\left(\frac{1}{2} a \sigma \|\tilde{\theta}\|^2 + \delta \|S\| \right) < 0 \\ 0 < a = & \min_{\forall q=1, \dots, N} \alpha_q, 0 < \delta = \min_{\forall q=1, \dots, N} \left(\left| \eta_q \right| \left| b_{qq} \right| \right). \end{aligned} \tag{35}$$

The derivative of Lyapunov function remains negative definite for PEE and the sliding vector. Hence, based on the Lyapunov theory, $W_3(\|S\|, \|\tilde{\theta}\|) \rightarrow 0$, asymptotically. As the result, estimated parameters of the basic model converge to their true values and output signals converge asymptotically to their corresponding desired signals.

Appendix b

Theorem 1' After switching, by using the model formulated as Eq. (9), the closed-loop system under identification remains stable. Assumptions A1, A2, A3 are established in this theorem.

The Lyapunov function stated in Eq. (15) is suitable for proving this theorem. Besides the system energy in sliding surfaces, it shows the energy of the identification error of R-OM in the input–output space. So the derivative of this function should be negative definite in order to vanish identification errors.

$$\begin{aligned} \dot{V}(t) = & \frac{1}{2} \left[2S^T \dot{S} - 2\hat{\theta}_i^T(t) P_i'^{-1}(t) \tilde{\theta}_i'(t) + \tilde{\theta}_i^T(t) \dot{P}_i'^{-1}(t) \tilde{\theta}_i'(t) \right. \\ & \left. - 2 \sum_{q \neq i}^N \hat{\theta}_q^T(t) P_q^{-1}(t) \tilde{\theta}_q(t) + \sum_{q \neq i}^N \tilde{\theta}_q^T(t) \dot{P}_q^{-1}(t) \tilde{\theta}_q(t) \right] \end{aligned} \tag{36}$$

By substitution of the derivative of the sliding vector in Eq. (14), it is calculated:

$$\begin{aligned} \dot{V}(t) = & \frac{1}{2} \left[-2S^T \begin{bmatrix} \tilde{b}_1^T \\ \vdots \\ \tilde{b}_i^T \\ \vdots \\ \tilde{b}_N^T \end{bmatrix} \hat{u} + 2S^T \begin{bmatrix} a_1^T y_{-1} \\ \vdots \\ a_i^{kT} y_{ik} \\ \vdots \\ a_N^T y_{-1} \end{bmatrix} - 2\hat{\theta}_i^T(t) P_i'^{-1}(t) \tilde{\theta}_i'(t) + \tilde{\theta}_i^T(t) \dot{P}_i'^{-1}(t) \tilde{\theta}_i'(t) - 2 \sum_{q \neq i}^N \hat{\theta}_q^T(t) P_q^{-1}(t) \tilde{\theta}_q(t) + \sum_{q \neq i}^N \tilde{\theta}_q^T(t) \dot{P}_q^{-1}(t) \tilde{\theta}_q(t) \right] - S^T B^T \eta \operatorname{sign}(S). \end{aligned} \tag{37}$$

By imposing adaptation rules and doing some calculations, it can be calculated:

$$\begin{aligned} \dot{V}(t) \leq & -\frac{1}{2} \alpha_i \tilde{\theta}_i^T(t) P_i^{-1}(t) \tilde{\theta}_i'(t) \\ & - \left(\gamma_i - \frac{1}{2} \right) \tilde{\theta}_i^T(t) \Phi_i'(t) \Phi_i^T(t) \tilde{\theta}_i'(t) \\ & - \frac{1}{2} \sum_{q \neq i}^N \alpha_q \tilde{\theta}_q^T(t) P_q^{-1}(t) \tilde{\theta}_q'(t) \\ & - \sum_{q \neq i}^N \left(\gamma_q - \frac{1}{2} \right) \tilde{\theta}_q^T(t) \Phi_q(t) \Phi_q^T(t) \tilde{\theta}_q'(t) \\ & - \sum_{q \neq i}^N \left| n_q \right| \left| b_{qq} \right| \left| S_q \right| - \left| n_i \right| \left| b'_{ii} \right| \left| S_i \right|. \end{aligned} \quad (38)$$

The whole calculations and steps of proof are the same as “Appendix a”. Even if τ_2 is finite and identifier cannot converges to real parameters, but still the energy of the sliding surfaces decreases and the closed-loop system remains stable. It is also concluded if τ_2 is far enough from the switching moment, parameters of identified R-OM can converge to their basic values in R-OM.

$$\dot{V}(t) \leq -W_3 \left(\|S\|, \|\tilde{\theta}'\| \right) = - \left(\frac{1}{2} a \sigma' \|\tilde{\theta}'\|^2 + \delta \|S\| \right) < 0 \quad (39)$$

References

- Angelov P, Sadeghi Tehran P, Ramezani R (2011) An approach to automatic real time novelty detection, object identification, and tracking in video streams based on recursive density estimation and evolving Takagi–Sugeno fuzzy systems International. *J Intell Syst* 26:189–205
- Äström K, Wittenmark B (1989) Adaptive control. Addison-Wesley, New York
- Briot S, Bonev I (2009) Pantopteron: a new fully decoupled 3DOF translational parallel robot for pick-and-place applications. *J Mech Robot* 1:021001
- Cho N, Shin H-S, Kim Y, Tsourdos A (2017) Composite model reference adaptive control with parameter convergence under finite excitation. *IEEE Trans Autom Control*. <https://doi.org/10.1109/TAC.2017.2737324>
- Fu M, Barmish B (1986) Adaptive stabilization of linear systems via switching control. *IEEE Trans Autom Control* 31:1097–1103
- Goethals I, Pelckmans K, Suykens JA, De Moor B (2005) Identification of MIMO Hammerstein models using least squares support. *Vector Mach Autom* 41:1263–1272
- Hou YL, Zeng DX, Zhang ZY, Wang CM, Hu XZ (2012) A novel two degrees of freedom rotational decoupled parallel mechanism. *Appl Mech Mater* 215–216:293–296
- Hovland G, Choux M, Murray M, Brogardh T (2007) Benchmark of the 3-dof gantry-tau parallel kinematic machine. In: Robotics and automation, 2007 IEEE international conference, pp 535–542
- Hwang C, Guo T-Y (1984) Transfer-function matrix identification in MIMO systems via shifted legendre polynomials. *Int J Control* 39:807–814
- Ioannou PA, Sun J (1996) Robust adaptive control, vol 1. PTR Prentice-Hall, Upper Saddle River
- Ivanov AV, Orlovsky IV (2014) Asymptotic properties of linear regression parameter estimator in the case of long-range dependent regressors and noise. *Theory Stoch Process* 19:1–10
- Jahandari S, Kalhor A, Araabi BN (2016) A self tuning regulator design for nonlinear time varying systems based on evolving linear models. *Evol Syst* 7:159–172
- Kalhor A, Araabi BN, Lucas C (2010) An online predictor model as adaptive habitually linear and transiently nonlinear model. *Evol Syst* 1:29–41
- Kalhor A, Araabi BN, Lucas C (2012) A new systematic design for habitually linear evolving TS fuzzy model. *Expert Syst Appl* 39:1725–1736
- Leskens M, Van Kessel L, Van den Hof P (2002) MIMO closed-loop identification of an. *MSW Inciner Control Eng Pract* 10:315–326
- Leung Lai T, Zong Wei C (1986) On the concept of excitation in least squares identification and adaptive control stochastics. *Int J Probab Stoch Process* 16:227–254
- Li W, Zhang J, Gao F, P-CUBE (2006) A decoupled parallel robot only with prismatic pairs. In: Mechatronic and embedded systems and applications, Proceedings of the 2nd IEEE/ASME International conference on 2006, pp 1–4
- Lughofer E (2013) On-line assurance of interpretability criteria in evolving fuzzy systems—achievements, new concepts and open issues. *Inf Sci* 251:22–46
- Lughofer E, Cernuda C, Kindermann S, Pratama M (2015) Generalized smart evolving fuzzy systems. *Evol Syst* 6:269–292
- Mårtensson B (1985) The order of any stabilizing regulator is sufficient a priori information for adaptive stabilization. *Syst Control Lett* 6:87–91
- Mayne DQ, Rawlings JB, Rao CV, Scokaert PO (2000) Constrained model predictive control. *Stab Optim Autom* 36:789–814
- Miller DE, Davison EJ (1989) An adaptive controller which provides Lyapunov stability. *IEEE Trans Autom Control* 34:599–609
- Miller DE, Davison EJ (1991) An adaptive controller which provides an arbitrarily good transient and steady-state response. *IEEE Trans Autom Control* 36:68–81
- Ng T, Goodwin G, Anderson B (1977) Identifiability of MIMO linear dynamic systems operating in closed loop. *Automatica* 13:477–485
- Pan Z, Basar T (1996) Parameter identification for uncertain linear systems with partial state measurements under an H_∞ criterion. *IEEE Trans Autom Control* 41:1295–1311
- Pedrycz W (2010) Evolvable fuzzy systems: some insights and challenges. *Evol Syst* 1:73–82
- Precup R-E, Filip H-I, Rădac M-B, Petriu EM, Preitl S, Dragoş C-A (2014) Online identification of evolving Takagi–Sugeno–Kang fuzzy models for crane systems. *Appl Soft Comput* 24:1155–1163
- Qin SJ (1993) Partial least squares regression for recursive system identification. In: Decision and control, proceedings of the 32nd IEEE conference on 1993, pp 2617–2622
- Qin SJ, Badgwell TA (2003) A survey of industrial model predictive control technology. *Control Eng Pract* 11:733–764
- Rao GP, Sivakumar L (1981) Transfer function matrix identification in MIMO systems via Walsh functions. *Proc IEEE* 69:465–466
- SAHA DC, RAO GP (1982) Transfer function matrix identification in MIMO systems via Poisson moment functionals. *Int J Control* 35:727–738
- Sharifzadeh M, Arian A, Salimi A, Masouleh MT, Kalhor A (2017) An experimental study on the direct and indirect dynamic identification of an over-constrained 3-DOF decoupled parallel mechanism. *Mech Mach Theory* 116:178–202
- Vuthandam P, Nikolaou M (1997) Constrained MPC: a weak persistent excitation approach. *AIChE J* 43:2279–2288
- Xu HY, Baird CR (1990) An identification technique for adaptive systems in the case of poor excitation. In: Bensoussan A, Lions JL

- (eds) Analysis and optimization of systems. Springer, Berlin, Heidelberg, pp 467–476
- Xu J-X, Hashimoto H (1996) VSS theory-based parameter identification scheme for MIMO systems. *Automatica* 32:279–284
- Yahyapour I, Hasanvand M, Masouleh MT, Yazdani M, Tavakoli S (2013) On the inverse dynamic problem of a 3-PRRR parallel manipulator, the tripteron. In: *Robotics and mechatronics (ICRoM)*, 2013 first RSI/ISM international conference on 2013. IEEE, pp 390–395
- Zeng D, Huang Z, Lu W (2007) A family of novel 2 DOF rotational decoupled parallel mechanisms. In: *Mechatronics and automation*, 2007. ICMA 2007. International conference on 2007. IEEE, pp 2478–2483
- Zhang L, Shi P (2008) l_2/l_∞ model reduction for switched LPV systems with average dwell time. *IEEE Trans Autom Control* 53:2443–2448
- Zhang L, Shi P, Basin M (2008) Model reduction for switched linear discrete-time systems with polytopic uncertainties and arbitrary switching. *IFAC Proc Vol* 41:7666–7671
- Zhu YC (1989) Black-box identification of mimo transfer functions: asymptotic properties of prediction error models. *Int J Adapt Control Signal Process* 3:357–373

Fault detection and diagnosis of a 12-cylinder trainset diesel engine based on vibration signature analysis and neural network

Proc IMechE Part C:
J Mechanical Engineering Science
0(0) 1–14
© IMechE 2018
Reprints and permissions:
sagepub.co.uk/journalsPermissions.nav
DOI: 10.1177/0954406218778313
journals.sagepub.com/home/pic



Alireza Zabihi-Hesari¹, Saeed Ansari-Rad², Farzad A Shirazi¹
and Moosa Ayati¹

Abstract

This paper presents a condition monitoring and combustion fault detection technique for a 12-cylinder 588 kW trainset diesel engine based on vibration signature analysis using fast Fourier transform, discrete wavelet transform, and artificial neural network. Most of the conventional fault diagnosis techniques in diesel engines are mainly based on analyzing the difference of vibration signals amplitude in the time domain or frequency spectrum. Unfortunately, for complex engines, the time- or frequency-domain approaches do not provide appropriate features solely. In the present study, vibration signals are captured from both intake manifold and cylinder heads of the engine and were analyzed in time-, frequency-, and time–frequency domains. In addition, experimental data of a 12-cylinder 588 kW diesel engine (of a trainset) are captured and the proposed method is verified via these data. Results show that power spectra of vibration signals in the low-frequency range reliably distinguish between normal and faulty conditions. However, they cannot identify the fault location. Hence, a feature extraction method based on discrete wavelet transform and energy spectrum is proposed. The extracted features from discrete wavelet transform are used as inputs in a neural network for classification purposes according to the location of sensors and faults. The experimental results verified that vibration signals acquired from intake manifold have more potential in fault detection. In addition, the capacity of discrete wavelet transform and artificial neural network in detection and diagnosis of faulty cylinders subjected to the abnormal fuel injection was revealed in a complex diesel engine. Beside condition monitoring of the engine, a two-step fault detection method is proposed, which is more reliable than other one-step methods for complex engines. The average condition monitoring performance is from 93.89% up to 99.17%, based on fault location and sensor placement, and the minimum classification performance is 98.34%.

Keywords

Fault detection, condition monitoring, vibration signal, neural network, discrete wavelet transform, trainset diesel engine

Date received: 14 April 2017; accepted: 26 April 2018

Introduction

Diesel engines are the heart of countless equipment including vehicles, trains, ships, and agricultural machinery. In order to maintain the overall efficiency, it is imperative to keep the engine in the best working conditions by using the condition-based maintenance strategies for detection and diagnosis of incipient faults.¹ Consequently, before any serious problem in main parts of the machinery, damaged components are replaced due to the predictability provided by the condition monitoring system.

Several types of signals can be measured for monitoring purposes including pressure,² rotational angle speed,³ temperature,⁴ fuel and oil quality,^{5–7} and

vibration.^{8–10} Vibration monitoring is a reliable method for detecting machine abnormality, considering the fact that different faults especially those related to combustion are the source of vibration.¹¹

The conventional vibration-based fault diagnosis techniques were focused on the amplitude difference

¹School of Mechanical Engineering, College of Engineering, University of Tehran, Tehran, Iran

²School of Electrical and Computer Engineering, College of Engineering, University of Tehran, Tehran, Iran

Corresponding author:

Moosa Ayati, School of Mechanical Engineering, College of Engineering, University of Tehran, North Kargar Street, Tehran 14399-5596, Iran.
Email: m.ayati@ut.ac.ir

in the time domain or frequency domain to detect different types of fault conditions. For example, fast Fourier transform (FFT) transfers test results from the time domain to the frequency domain. Meanwhile, the time–frequency techniques such as short-time Fourier transform,¹² time-average analysis,¹³ Winger–Ville distribution,^{5,14} continuous wavelet transform (CWT),¹⁵ and discrete wavelet transform (DWT)¹⁶ have been widely developed to analyze the vibration signals in both the time and frequency domains.

Vibration signal analyses using aforementioned approaches have been widely used for fault detection of diesel engines. For instance, Geng and Chen¹⁷ introduced a fast wavelet-packet decomposition and reconstruction algorithm in order to measure and extract the piston slap-induced vibration in a diesel engine. Teraguchi et al.¹⁸ investigated the influence of oil film between piston rings and cylinder walls on the induced vibration. A number of studies have been done to investigate the impact of different combustion factors on the engine block vibrations.^{11,19–21} Carlucci et al.²⁰ investigated the correlation between injection parameter variation and block vibration of a diesel engine using two accelerometers on two different zones on the engine block. Both classical Fourier analysis and time–frequency analysis were exploited to identify the degree of correlation between in-cylinder pressure and vibration signals. Shirazi et al.²² investigated the application of DWT in combustion failure detection of a four-cylinder internal combustion (IC) engine. Authors demonstrated the proof of concept of using DWT in detection and diagnosis of combustion failures in IC engines.

In diesel engines, an important source of noise and vibration is the injection system especially the seating of the injector needle and check valve. Valve train system also plays an important role in the combustion process. However, it is most likely to suffer from faults, inter alia, abnormal valve clearance and gas leakage from valves.²³ Measuring vibration and acoustic signals as nonintrusive methods is used to detect and overcome such problems at an early stage in order to avoid extremely severe faults.

Liu et al.²⁴ proposed a simple diagnostic technique combining partial sampling with future averaging (PSFA) for detection of abnormal valve clearance and combustion gas leakage. They measured the vibration signals of a four-cylinder diesel engine by installing four accelerometers on the cylinder head of the engine. The intake valve clearance of cylinder 1 was set to 0.15, 0.6, 0.9, 1.2, and 1.5 mm with a normal clearance of 0.3 mm. They presented tables of feature measurements for various fault levels. Jiang et al.²⁵ utilized a two-load acoustic approach for a four-cylinder diesel engine using two pressure sensors mounted on its exhaust system. Reduced injection pressure and increased valve clearance on one of the engine cylinders were detected by analyzing the pressure waveforms. Wang et al.²⁶

induced valve clearance faults on one cylinder of a four-cylinder diesel engine. A probabilistic neural network was used to classify the Winger–Ville distributions (WVD) of vibration acceleration signals. For eight combinations of normal and faulty cases of intake and exhaust valves a classification accuracy of 96% was obtained. Flett et al.²⁷ proposed a vibration-based method for detection and diagnosis of diesel ICE valve train faults requiring only one accelerometer. Deformed valve spring and abnormal valve clearance faults accurately were detected and classified using the naïve–Bayes classification method. For the spring faults occurring on individual valves the lowest detection accuracy and classification accuracy were both found to be 99.5%. The detection accuracy and classification accuracy for multiple faults occurring simultaneously were obtained to be 99.5% and 92.45%, respectively.

Even though the literature on fault detection and diagnosis methods is copious, relatively few papers have addressed the problem of abnormal fuel injection in diesel engines. In addition, the literature suffers from a lack of papers in which sophisticated engines with more than six cylinders are investigated. As the number of cylinders increases in diesel engines, the fault detection and diagnosis process based on the vibration signals becomes more complicated.

The basic aim of this paper is to present a novel fault detection method for a diesel engine based on analyzing the experimental data. The contribution is about how to use DWTs and ANNs as a tool to analyze a diesel engine with 12 cylinders. None of the previous studies mentioned about this kind of engines, but here time-, frequency-, and time–frequency-domain analyses are carried out to analyze the vibration signals. First, power spectral density (PSD) of vibration signals in low-frequency range is calculated and used to distinguish between faulty and normal engine. Nevertheless, the fault location (faulty cylinder) cannot be determined by this approach. In the next step, the engine vibration signals captured from the intake manifold and cylinder heads are pre-processed to obtain the different sub-band features by DWT. The fault features are clearly observed by energy spectrum. Finally, ANN is utilized to complete the fault detection process and classify it based on the location of the fault and sensor placement. The remainder of the paper is organized as follows. The test bed and signal acquisition process are described in the upcoming section. Next, signal processing methods are presented and ANN analysis is described. Subsequent section describes the classification and fault detection procedure. Finally, conclusions are provided.

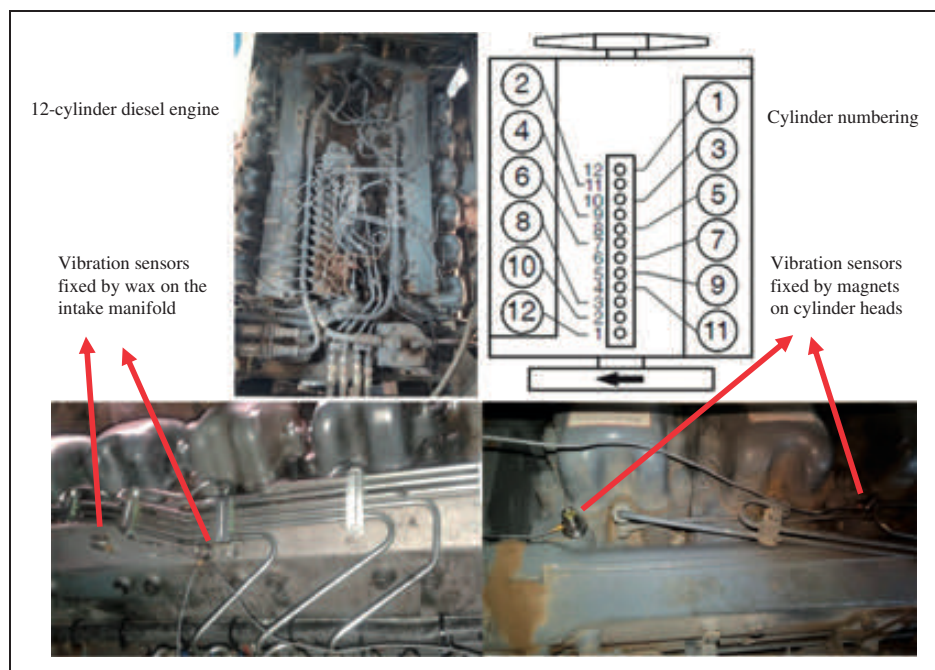
Experimental setup

Diesel engine and data acquisition system

The experimental tests were carried out on a 12-cylinder, D 2842 LE 602 diesel engine, which is

Table 1. Engine specifications.

Diesel	V 90°
Cycle	4-stroke diesel with turbocharger and intercooler
Number of cylinders	12
Compression ratio	16.5:1
Bore	128 mm
Stroke	142 mm
Engine capacity	21,930 cm ³
Direction of rotation viewed on flywheel	Anti-clockwise
Firing order	1-12-5-8-3-10-6-7-2-11-4-9
Firing interval	120°
Power based on DIN ISO 3046	588 kW at 2100 r/min

**Figure 1.** The instrumented engine and cylinder numbering.

commonly used in trainsets. The engine is a V-shaped, 4-stroke diesel engine with turbocharger and intercooler. The engine specifications are given in Table 1. All experiments were done at zero-load and a constant speed of 600 r/min. Vibration pickup was carried out by two DJB2784 accelerometers mounted on both intake manifold and cylinder heads. The accelerometers on the cylinder heads and intake manifold were firmly fixed by magnets and wax, respectively. In order to indicate the engine speed, a tachometer pointing to a reflective tape on the crankshaft pulley was utilized. Since the engine is a 4-stroke type, two complete crankshaft revolutions (720°) represents a full thermodynamic cycle. The vibration signals, measured by accelerometers, and tachometer signals were transferred through cables into a data logger/analyzer and then to the computer for further analysis. The

Bruel & Kajer-PULSE LabShop software version 12.5.1 was used in the course of data acquisition. The instrumented engine and the numbering of cylinders are illustrated in Figure 1.

Combustion failure may be the result of the malfunction in one or more cylinders. In order to test our proposed approach in fault detection, faulty conditions must be experimentally simulated on the engine. In this work, the fuel valve of cylinders was opened to let the fuel partially enter the combustion chamber. Therefore, the combustion failure was modeled by disabling fuel valve of known cylinders.

Signal acquisition

Vibration signals were obtained using two accelerometers mounted on either intake manifold or cylinder

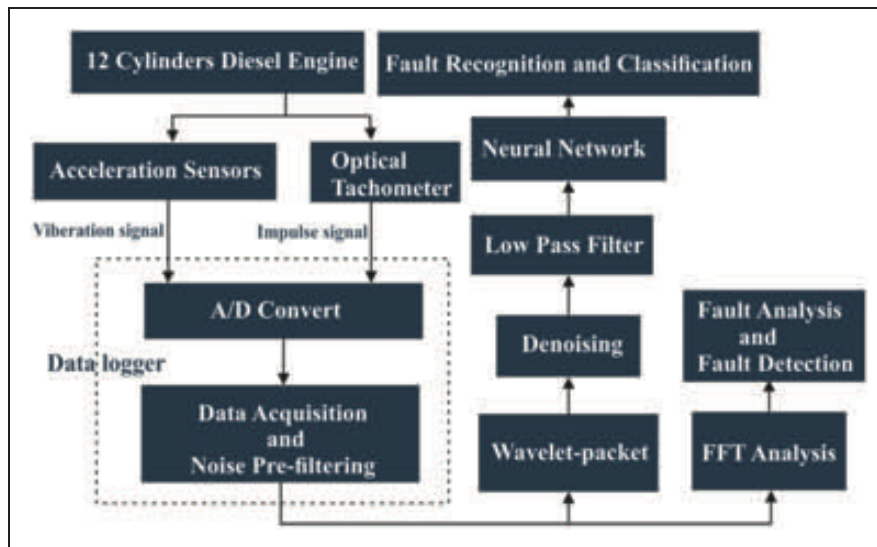


Figure 2. Schematic of data acquisition and signal processing system.

heads in two separate phases. Vibration data were collected using a four-channel data logger with a sampling frequency of 3.2 kHz and the span of 8.192 kHz. Each data set comprised 2 s of vibration signals with 16,384 data points. Using tachometer pulses, the engine vibration signals were split into segments with an equal length of 0.2 s corresponding to two of crankshaft revolutions (a complete thermodynamic cycle). Throughout the data acquisition process, the engine speed was set at 600 r/min (10 Hz) with zero load.

A few tests with higher sampling frequencies were also performed and results proved that the sampling frequency of 3.2 kHz is appropriate. By choosing aforementioned sampling frequency and consequently the span of 8.192 kHz, suitable information of vibration signals for condition monitoring and fault detection procedure were obtained. In fact, different faults became discriminable with these chosen frequencies.

In addition, to study the effect of load on the fault detection method, some tests were conducted. The data were obtained from the engine with a generator load and the speed of engine was set at 950 r/min. The process of signal acquisition and signal processing in this work is briefly shown in Figure 2.

Signal analysis

Time-domain analysis

A complete thermodynamic cycle for all cylinders takes 720° of revolution of the crankshaft (0.2 s at 600 r/min engine speed). According to the firing order of the engine, the combustion of each pair of cylinders ($C_{12}-C_7$, C_1-C_6 , C_9-C_{10} , C_2-C_5 , C_8-C_{11} , and C_3-C_4) occurs with 120° interval. According to the fundamentals of IC engine,²³ there are five main

impact forces that cause vibrations on the cylinder head, which are propagated to the intake manifold as well: intake valve closing (IVC), intake valve opening (IVO), exhaust valve closing (EVC), exhaust valve opening (EVO), and in-cylinder combustion pressure. Based on the datasheet of the engine, the theoretical valve timing for cylinder 1 is shown in Figure 3(a). If all cylinders are considered, as shown in Figure 3(b), the timing of main events including fuel injection (FI) and valve timings are closely located and very complicated.

The impact of fuel obstruction is more conspicuous in the fuel injection signal. After opening a fuel valve and implementing the faulty condition, the fuel injection signal of the faulty cylinder will be weakened and vibration signal of the engine changes. The vibration signal of the mounted sensor on the intake manifold in the vicinity of the cylinder 11 (M_{11}) in the healthy condition and also when cylinder 5 is faulty, are illustrated in Figure 4. The part of the vibration signal, which represents fuel injection phenomenon in a faulty situation is weakened although it is not completely eliminated due to the fuel injection of cylinder 8, which simultaneously occurs with cylinder 5. Even though the fault changes the vibration signal, it is not easily clarified in the time domain and more inter alia, frequency-, and time-frequency-domain analyses are required to interpret the changes caused by the faults.

As it is shown in Figure 3(b) for a crank angle interval of 720° , in addition to six large peaks, other small peaks are expected in the vibration signal. This pattern (composed of a large peak and three small peaks) is repeated six times in this interval, so theoretically the frequency of this pattern becomes 30 Hz as it is clear in Figure 5. In Figure 4(a), it is obvious that the pattern repeated six times during the mentioned interval.

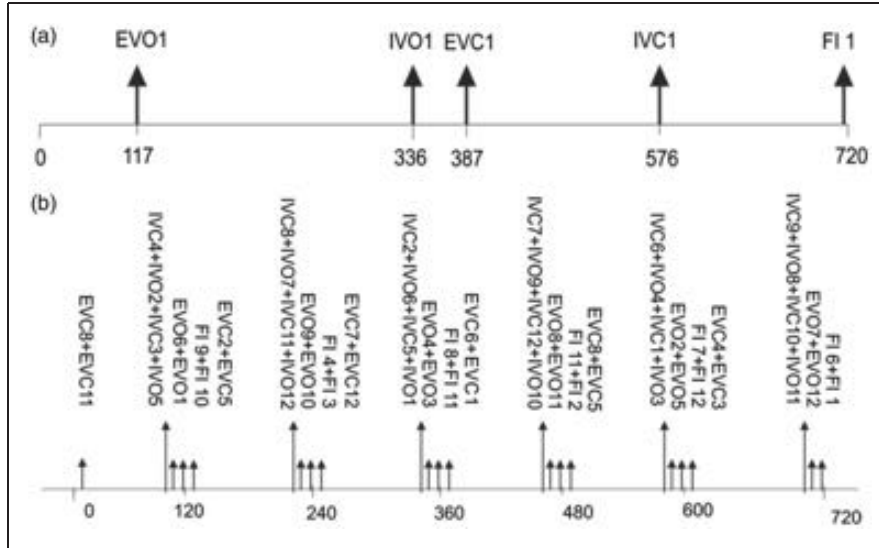


Figure 3. Theoretical occurrence of intake and exhaust valve opening and closing, and fuel injection of a D 2842 LE 602 diesel engine: (a) for C_{12} and (b) for all cylinders.

Frequency-domain analysis

The auto-spectrum of a vibration signal is defined as²⁸

$$P_{xx}(f) = X(f)X^*(f) = |X(f)|^2 \quad (1)$$

where, $X(f)$ refers to the FFT of the vibration signal, f is the frequency variable, and $*$ is the conjugate operator. Dividing $P_{xx}(f)$ by the sampling frequency (f_s) results in the power spectral density (PSD) of the signal assuming a uniform windowing

$$PSD = \frac{P_{xx}(f)}{f_s} \quad (2)$$

The PSD of vibration signals from different locations on the intake manifold are depicted in Figure 5. For a healthy engine (a, b, and c), the power spectrum of vibration signals has the same pattern for different locations on the intake manifold. In this case, there are two peaks in the PSD of vibration signals in frequencies of 10 Hz and 30 Hz, which refer to the engine speed (600 r/min) and the simultaneous combustion of a pair of cylinders in two complete revolutions of the crankshaft, respectively. The frequency-domain analysis has been done in a low-frequency interval of 0–180 Hz since it is more likely to distinguish between faulty and healthy conditions compared to a high-frequency range. Comparing healthy and faulty engine PSDs, it is concluded that in faulty conditions (d, e, and f) new peaks appeared between 10 Hz and 30 Hz in the frequencies of 15 Hz and 20 Hz. Similar results are demonstrated for the engine with generator load; but because of the different engine speed, the peaks resulted from faults happened in other frequencies (see Figure 6).

Based on FFT analysis and PSD of the vibration signals, we are able to distinguish between faulty and

healthy conditions; however, further time–frequency-domain analyses is presented in the following subsection to complete the fault detection and diagnosis process.

Time–frequency-domain analysis

Wavelet-based feature extraction provides multi-resolution analysis in the time–frequency domain for easier detection of abnormal vibration signals.²⁹ Hence, in this section wavelet-based feature extraction is used to analyze the vibration signals. The mathematics of wavelet transform is found in Burrus et al.³⁰ and Wu et al.³¹ A continuous wavelet transform (CWT) is defined by the following equation, which comprises time and frequency information simultaneously

$$CWT(a, b) = \frac{1}{|a|} \int_{-\infty}^{\infty} X(t) \psi^* \left(\frac{t-b}{a} \right) dt \quad (3)$$

where a is the scale parameter, b represents the translation parameter, ψ represents the basic or “mother” wavelet, and ψ^* is the complex conjugate of ψ . In CWT, different scales are used to analyze the signal and represent various frequency bands. Consequently, the signal generates a large number of wavelet coefficients with every possible scale. Therefore, a and b adopt the dyadic scale and translation to reduce computation wavelet coefficients and computation time. This method is called DWT and it is defined as

$$DWT(j, k) = \frac{1}{\sqrt{2^j}} \int_{-\infty}^{\infty} X(t) \psi^* \left(\frac{t-2^j k}{2^j} \right) dt \quad (4)$$

where a and b are replaced by 2^j and $2^j k$, respectively.²² Passing through two complementary filters, the original signal emerges as low-frequency

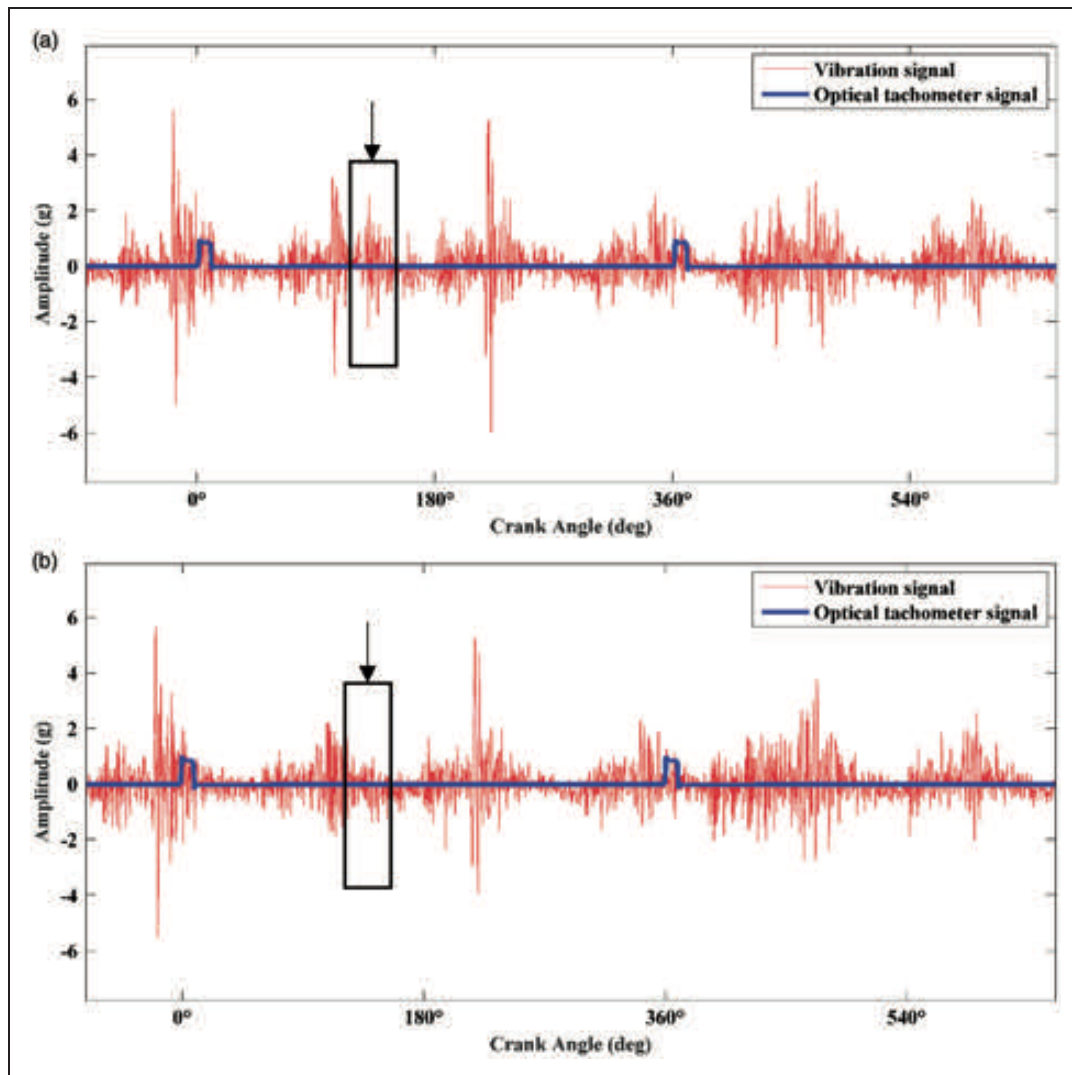


Figure 4. Vibration signal obtained from intake manifold in the vicinity of cylinder II (M_{II}) for a single engine cycle: (a) healthy condition and (b) when cylinder 5 is faulty.

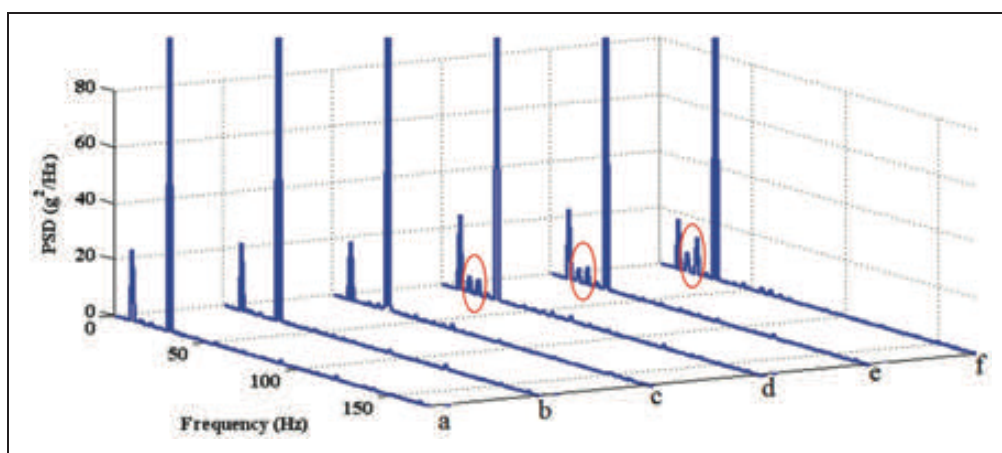


Figure 5. PSD of engine vibrations of the intake manifold: (a) in the vicinity of cylinder I for healthy condition, (b) in the vicinity of cylinder 3 for healthy condition, (c) in the vicinity of cylinder 8 for healthy condition, (d) in the vicinity of cylinder I when cylinder 5 is faulty, (e) in the vicinity of cylinder 3 when cylinder 5 is faulty, (f) in the vicinity of cylinder I when cylinder 4 is faulty.

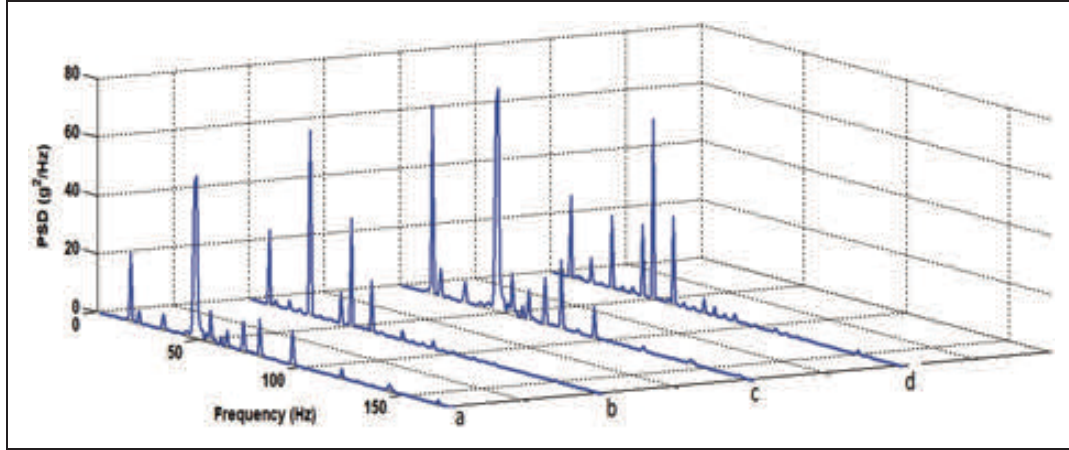


Figure 6. PSD of engine vibrations of the intake manifold (with load): (a) in the vicinity of cylinder 5 for healthy condition, (b) in the vicinity of cylinder 5 when cylinder 5 is faulty, (c) in the vicinity of cylinder 4 for healthy condition, (d) in the vicinity of cylinder 6 when cylinder 5 is faulty.

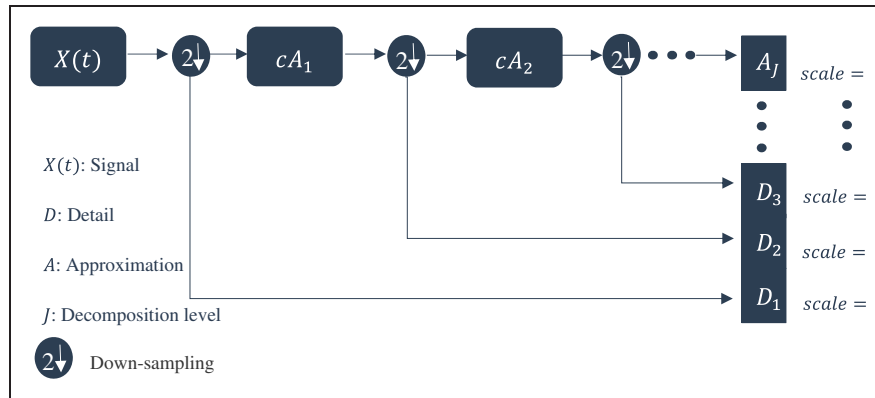


Figure 7. Decomposition process of multi-scale analysis.³¹

(approximations (A 's)) and high-frequency (details (D 's)) signals. Hence, the signal $X(t)$ is written as

$$X(t) = A_j + \sum_{j \leq J} D_j \tag{5}$$

where A_j and D_j are the approximation and the detail coefficients of j th level. The process of decomposition of the signal into J th level is shown in Figure 7. The decomposed signal is assembled back into the original signal throughout the reconstruction process, which consists of up-sampling and reconstruction filters as shown in Figure 8. Up-sampling is the process of extending signal components by inserting zeros between decomposition coefficients. The length of signal in each decomposition level is equal to the original signal after the reconstruction process. Although the DWT can improve the shortcomings of the CWT, it is still hard to find the fault conditions accuracy visually or by classifier since through the reconstruction process a large number of the signal features will be produced. The solution of this problem is energy

spectrum, which is based on Parseval's energy theorem³² and is expressed as

$$\sum_{t=0}^{N-1} |X(t)|^2 = \frac{1}{N} \sum_{f=0}^{N-1} |X(f)|^2 \tag{6}$$

where $X(t)$ is a time domain signal, $X(f)$ is the discrete form of the signal after applying Fourier transform, and N is the sampling period. By substituting equation (6) into equation (5) signal features based on DWT and energy spectrum are achieved as

$$\sum_{t=0}^{N-1} |X(t)|^2 = \frac{1}{N} \sum_{f=0}^{N-1} |A_j(f)|^2 + \sum_{j \leq J} \left[\frac{1}{N} \sum_{f=0}^{N-1} |D_j(f)|^2 \right] \tag{7}$$

Daubechies wavelet. Daubechies wavelets are a family of orthogonal wavelets that define a DWT. There is a

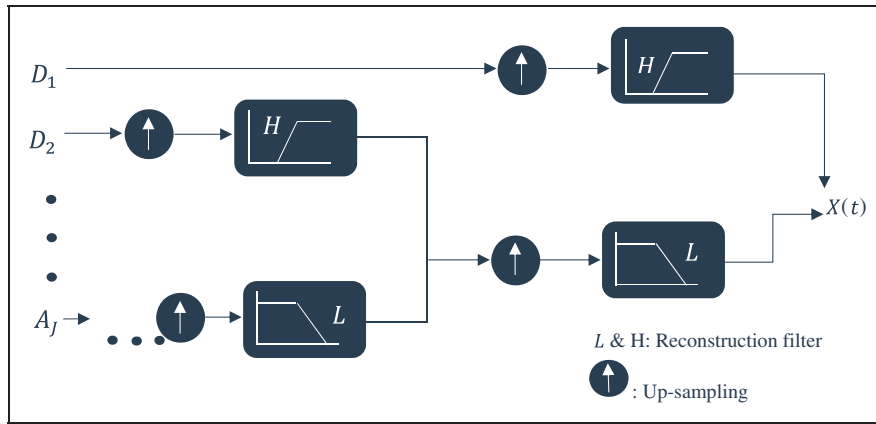


Figure 8. Flowchart of reconstruction process.³¹

scaling function with each wavelet type of this class that generates an orthogonal multiresolution analysis.³³ Here, Db4 (Daubechies 4) wavelet transform with eight layers and a filtering frequency of 4 kHz are chosen for the next analyses. The average energy of signals in each frequency range is calculated as a proper feature to distinguish between different sources of fault. The frequency features of the vibration signals are presented in Table 2.

Neural network analysis

Neural network methods have been used widely for condition monitoring purposes. The preference of ANN over other techniques, such as numerical methods, are complex and parallel processing using basis functions, adaptability, ability to learn, and to be trained.³⁴ In this research, a multilayer perceptron (MLP) network is used to process data features extracted from the time–frequency-domain analysis. As mentioned before, these features indicate the average energy of signals in each frequency range. The feature values are mapped to the interval $[-0.5, 0.5]$ to avoid saturation and to increase the network predictability.

The MLP network consists of an input layer with nine neurons (the number of features for each data sets), two hidden layers, and output layer; the number of neurons in the hidden layers is found by searching best validities. The number of output layer neurons is equal to the number of classes, and the tangent sigmoid is chosen as the activation functions. Training of the MLP network is based on back propagation (BP) algorithm.³⁵ For test data, 20% of datasets for each case of Tables 3, 6, 7, and 8 were selected randomly, which improves generalization of results for any similar test.

Back propagation algorithm

The BP of errors is a supervisory training algorithm for training a neural network. In this subsection, the

Table 2. Frequency features of the extracted signals from wavelet bank.

Extracted signal from wavelet bank	Beginning band frequency (Hz)	End band frequency (Hz)	Center of band (Hz)
A8	0	9.76	4.833
D8	9.76	19.531	14.649
D7	19.531	39.063	29.297
D6	39.063	78.128	58.594
D5	78.128	156.25	117.188
D4	156.25	312.5	234.375
D3	312.5	625	468.75
D2	625	1250	937.5
D1	1250	2500	1875

structure of the neural network and proposed BP algorithm are described.

In Figure 9, n_L is the number of layers, L is the layer number, and the activation function is defined as $a^{L+1} = f(z^{L+1})$, where $z^{L+1} = w^L a^L + b^L$, w^L is the weight matrix, b^L is the bias vector, and $L = 1, \dots, n_L - 1$. The overall function describing neural network is $h_{(w,b)}(x) = a^{n_L}$. λ is the training coefficient of BP; by choosing an appropriate value for λ , effect of large weights is weakened, and prevents from overfitting of the network.³⁵ Based on the batch gradient descent, weights and biases are updated as equations (8) and (9). w_{ij}^L denotes the weights between the i th neuron of layer L and j th neuron of layer $L + 1$. b_i^L denotes the bias of i th neuron of layer L as well.

$$w_{ij}^L = w_{ij}^L - \alpha \frac{\partial}{\partial w_{ij}^L} J(w, b) \quad (8)$$

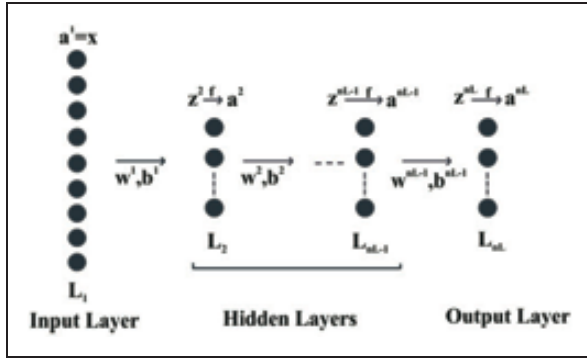
$$b_i^L = b_i^L - \alpha \frac{\partial}{\partial b_i^L} J(w, b) \quad (9)$$

Table 3. Results obtained from running neural network for a sensory condition monitoring.

Measurement (sensor) location	Fault location	Condition monitoring performance	Numbers of neurons in first hidden layer of ANN	Numbers of neurons in second hidden layer of ANN	Total training and testing time (s) ^a
M ₁ ^b	C ₅	98.33%	1	4	908.8620
C ₁ ^b	C ₅	100%	1	1	707.3260
M ₅	C ₅	100%	1	1	855.3686
M ₁₁	C ₅	97.5%	19	11	766.6893
C ₁₁	C ₅	98.33%	12	22	1.3059e + 03
M ₂	C ₅	94.17%	22	1	729.9423
C ₂	C ₅	95%	42	16	725.3852
M ₆	C ₅	90%	23	13	784.0735
C ₆	C ₅	96.67%	1	5	774.0304
M ₁₂	C ₅	97.5%	28	1	753.4494
C ₁₂	C ₅	100%	1	1	695.9175
C ₅	C ₅	93%	15	5	1.3898e + 03

^aComputations are performed on a 2.2 GHz Intel Core i7 V502L laptop, programming is done in MATLAB R14.

^bM₁ and C₁ imply that data measured on cylinder 1's intake manifold and cylinder 1's block, respectively.

**Figure 9.** Structure of the proposed neural network

Following procedure is applied in order to train the network, for each dataset (x^q, y^q) :

Step 1: Feed-forward running of the network with defined weights and biases.

Step 2: After calculating $h_{(w,b)}(x^q)$ and z_i^{nL} for the output neurons by feed-forward procedure, δ_i^{nL} is obtained as

$$\delta_i^{nL} = \frac{\partial}{\partial z_i^{nL}} \frac{1}{2} \|y^q - h_{(w,b)}(x^q)\|^2 = -(y_i^q - a_i^{nL}) \cdot f'(z_i^{nL}) \quad (10)$$

Step 3: Recursive error effect is applied to layers $L = n_L - 1, n_L - 1, \dots, 2$, respectively by equation (11), where w_{ji}^L is the weight from Step 1

$$\delta_i^L = \left(\sum_{j=1}^{S_{L+1}} w_{ji}^L \delta_j^{L+1} \right) \cdot f'(z_i^L) \quad (11)$$

Step 4: Terms $\frac{\partial}{\partial w_{ij}^L} J(w, b; x^q, y^q)$ and $\frac{\partial}{\partial b_i^L} J(w, b; x^q, y^q)$ are calculated based on equations (12) and (13), respectively

$$\frac{\partial}{\partial w_{ij}^L} J(w, b; x^q, y^q) = a_i^{L+1} \delta_j^{L+1} \quad (12)$$

$$\frac{\partial}{\partial b_i^L} J(w, b; x^q, y^q) = \delta_i^{L+1} \quad (13)$$

According to equations (12) and (13), batch method is used to calculate all $\frac{\partial}{\partial w_{ij}^L} J(w, b; x^q, y^q)$ by the mentioned procedure for all the training datasets, and then update the weights and biases based on the following equations

$$\frac{\partial}{\partial w_{ij}^L} J(w, b) = \frac{1}{m} \sum_{q=1}^m \frac{\partial}{\partial w_{ij}^L} J(w, b; x^q, y^q) + \lambda w_{ij}^L \quad (14)$$

$$\frac{\partial}{\partial b_i^L} J(w, b) = \frac{1}{m} \sum_{q=1}^m \frac{\partial}{\partial b_i^L} J(w, b; x^q, y^q) \quad (15)$$

In the training procedure, when epoch number crosses 1000, or network output converges to the desired output, the stopping criterion is triggered and training process is stopped.

Single-sensor condition monitoring

In this part, MLP ANN with two output neurons is being used for the condition monitoring purpose where vibration data were measured from one cylinder. Generally, ANNs have been employed through condition monitoring by training of the network with features extracted from data of both faulty and healthy conditions. Each dataset has a flag, which defines the condition or class it belongs to. For each

Table 4. Average condition monitoring performance based on the faulty side.

Measurement (sensor) locations	Fault location	Average condition monitoring performance	Measurement location
M ₁ –M ₅ –M ₁₁	C ₅	98.61%	Faulty side of engine
C ₁ –C ₅ –C ₁₁	C ₅	96.83%	Faulty side of engine
M ₂ –M ₆ –M ₁₂	C ₅	93.89%	Normal side of engine
C ₂ –C ₆ –C ₁₂	C ₅	97.22%	Normal side of engine

Table 5. Average condition monitoring performance based on distance to the fault location.

Measurement (sensor) location	Fault location	Average condition monitoring performance	Measurement location
C ₁ –C ₅	C ₅	96.5%	Close to the faulty cylinder
M ₁ –M ₅	C ₅	99.17%	Close to the faulty cylinder
C ₂ –C ₁₂	C ₅	97.5%	Far from the faulty cylinder
M ₂ –M ₁₂	C ₅	95.83%	Far from the faulty cylinder

fault and sensor location, MLP ANN is trained and the performance of the network for the test data is calculated. This process is repeated several times and the average of the performances (called average correct classification rate (ACCR)) is calculated and reported in Table 3. Then, number of neurons is changed and ACCR is calculated. The optimal number of neurons and final structure of MLP is obtained based on these ACCRs. Validation of condition monitoring, optimal neuron numbers and running time of networks are also reported in Table 3.

M_i and C_i refer to sensor location on cylinder i 's intake manifold and cylinder i 's block, respectively. The "total training and testing time" column shows the "computational expense" of the ANN. Table 3 shows that increasing number of the neurons does not necessarily leads to a better performance. For an improved interpretation, results of Table 3 are summarized into Tables 4 and 5 based on the faulty side of the engine and the distance of the sensor from the fault location, respectively. Both tables show that condition monitoring reaches a higher average performance by mounting sensors on intake manifold rather than cylinder block.

From Table 4, setting sensor on the faulty side of intake manifold has the best condition monitoring performance. Based on Table 5, when sensor location on intake manifold gets closer to the faulty cylinder, condition monitoring performance increases; however, results of the measured data from cylinder blocks show better validity when the faulty side data are not used and sensor location is far from the faulty cylinder.

Multi-sensor condition monitoring

In this section, data of simultaneous measurements of two vibration sensors were used for condition

monitoring. Training procedure of the ANN, validation of results, and obtaining the optimal number of neurons are similar to that described in the previous section. Validation of condition monitoring results depends on the number of sensors attached to the data logger and their location on the engine, but there are practical restrictions on the number of sensors and computational capability of the computer used for training networks based on sensors' data. Therefore, the challenge is to find the appropriate number of sensors installed on the engine and their best location on the engine.

From the first and third rows of Table 6, augmenting M_5 data to $\{M_1, M_{11}\}$ increases the condition monitoring performance, and the same happens for augmenting C_5 to $\{C_1, C_{11}\}$. However, augmenting M_6 data to $\{M_2, M_{12}\}$ and C_6 data to $\{C_2, C_{12}\}$ reduces the performance. On the other hand, in most cases, multi-sensor performance is less than the average performance of the same cylinders individually.

Considering the results of the single-sensor subsection, condition monitoring reaches higher average performance by mounting the sensor on the intake manifolds. On the other hand, sensor mounting on the faulty side or normal side of the engine yields different performance of condition monitoring. Since the faulty side is not known beforehand, sensors are supposed to be placed on both sides to obtain reliable condition monitoring. As a result, by putting one sensor on each side of the engine and on the intake manifolds, high and reliable performances are obtained as Table 7. For instance, by setting sensor on the intake manifold of cylinders 5 and 6, accurate condition of the engine was predicted by chance of 98.96%, whereas performances for each of them in the single sensor case were calculated as 100% and

Table 6. Results obtained from running neural network for multi-sensory condition monitoring (sensors are set on a single side of the engine).

Measurement location	Fault location	Condition monitoring performance	Number of neurons in the first hidden layer	Number of neurons in the second hidden layer	Total training and testing time (s)
Peng and Yam ^{29a}	C ₅	96.67%	40	3	849.9487
{M ₂ , M ₁₂ }	C ₅	92.22%	29	12	793.3366
{M ₁ , M ₅ , M ₁₁ }	C ₅	98.15%	31	25	878.4984
{M ₂ , M ₆ , M ₁₂ }	C ₅	90.37%	15	6	815.7967
{C ₁ , C ₁₁ }	C ₅	82.22%	4	28	728.2743
{C ₂ , C ₁₂ }	C ₅	98.33%	11	22	741.0951
{C ₂ , C ₆ , C ₁₂ }	C ₅	94.81%	41	6	807.3773
{C ₁ , C ₅ , C ₁₁ }	C ₅	94.07%	11	26	855.4415

^aIntegrating M₁ and M₁₁ data.

Table 7. Results obtained from running neural network for multi-sensory condition monitoring (sensors are set on both sides of the engine).

Measurement location	Fault location	Condition monitoring performance	Number of neurons in the first hidden layer	Number of neurons in the second hidden layer	Total training and testing time (s)
{M ₅ , M ₆ }	C ₅	98.96%	9	16	704.6328
{M ₁₁ , M ₆ }	C ₅	93.75%	23	7	769.9398
{M ₁ , M ₆ }	C ₅	97.92%	36	17	749.3865
{M ₅ , M ₂ }	C ₅	90.63%	27	29	713.8503
{M ₅ , M ₁₂ }	C ₅	95.31%	30	4	695.5757
{M ₁₁ , M ₂ }	C ₅	92.71%	40	6	708.2859
{M ₁ , M ₁₂ }	C ₅	91.16%	1	3	683.1001
{M ₁ , M ₂ }	C ₅	93.23%	23	23	705.3882
{M ₁₁ , M ₁₂ }	C ₅	96.35%	28	23	690.2536

90% (Table 3). In the presence of load, the condition monitoring is still possible, but the correct prediction percentage decreases due to disturbances and other engine vibrations.

Classification and fault detection

Classification methods are applied when no prior knowledge of the relation between symptoms and faults is available. Methods such as Naïve-Bayes (NB) classification, ANN, decision trees (DTs), k-nearest neighbor (k-NN),³⁶ and linear discriminant analysis (LDA) have been used widely for fault detection purposes. In this research, the objective is to determine the faulty side of the engine and then faulty cylinder with an acceptable CCR using ANNs. Also, it is known that the number of output neurons is equal based on the number of classes. In this paper, “fault side detection” is under consideration and two classes have been used that determine whether the fault is on the left or right side of the engine.

As mentioned earlier, Table 4 shows that the condition monitoring of the engine yields better performance by placing the sensor on the faulty cylinder side of the engine and on the intake manifold. Therefore, for detecting the side of the faulty cylinder, sensors are supposed to be placed on both sides of the engine. By comparing the overall results of Tables 3 and 6, and based on the already mentioned restrictions, the best choice is to mount one sensor on each side of the engine.

Table 8 shows the results of each paired sensors for fault side detection. Based on these results, best locations for paired sensors are found and side of fault will be determined thereafter with higher probability. Based on Table 5, setting sensors near the faulty places increases the capability of classification. Therefore, specifying faulty side helps to detect the fault location more easily.

This is a 2-step training method to detect faulty cylinders. Since each pairs of cylinders are synchronized and each side contains one of these cylinders, finding the exact faulty cylinder based on

Table 8. Results obtained from running neural network for classification and fault side detection.

Measurement location	Fault location	Fault side detection performance	Number of neurons in the first hidden layer	Number of neurons in the second hidden layer	Total training and testing time (s)
{M ₅ , M ₆ }	C ₅	92.38%	3	4	689.0072
{M ₁₁ , M ₆ }	C ₅	93.81%	35	29	718.9315
{M ₁ , M ₆ }	C ₅	97.14%	31	13	805.6078
{M ₅ , M ₂ }	C ₅	97.14%	16	19	825.2058
{M ₅ , M ₁₂ }	C ₅	95.71%	5	16	742.6408
{M ₁₁ , M ₂ }	C ₅	98.10%	37	6	712.2230
{M ₁ , M ₁₂ }	C ₅	96.67%	33	3	728.0262
{M ₁ , M ₂ }	C ₅	96.67%	11	7	650.6446
{M ₁₁ , M ₁₂ }	C ₅	94.76%	2	5	663.0755

Table 9. Confusion matrix plus classification accuracy (CA) results.

		Predicted class			CA ²³ (%)
		Normal	Fault in the measurement location	Fault in other locations	
Actual class	Normal	120	0	0	99.17
	Fault in the measurement location	0	120	0	99.17
	Fault in other locations	1	0	119	98.34

combustion signals at one step is not reliable. By detecting the faulty side, classifying sensors' data on the detected side lead to a reliable detection of the faulty cylinder location. For example, Table 8 for faulty side detection implies right side as the faulty one. In order to find whether faulty data of the sensor set on a cylinder is due to the fault of that cylinder or not, three classes are considered; The first class represents the normal engine, second and third classes are used to distinguish whether the sensor location is the faulty cylinder or not, respectively. According to Table 9, none of the first and second classes data were misclassified, only at the worst case, one of the data associated with fault on the other cylinders was misclassified as the healthy one. Therefore, by setting sensor on a cylinder of the faulty side, the classification specifies its condition with a high reliability. To compare between results of all sections, C₅ is selected as the faulty cylinder. On the other hand, selecting any cylinders as the fault location will not lead to any special change in the overall procedure.

Conclusions

An intelligent fault detection system for a high-power 12-cylinder trainset diesel engine was developed and implemented to pinpoint the combustion faults resulted from abnormal fuel injection. Vibration

signals were analyzed in time-, frequency-, and time–frequency domains. PSDs of the vibration signals were calculated and distinguished between normal and faulty engines. Nevertheless, PSDs cannot discriminate the faulty cylinders. Hence, DWT was utilized to overcome the problem. The energy spectrum not only reduced the data size of the DWT but also easily identified the difference of energy between normal and faulty conditions. The db4 of Daubechies wavelets provided high diagnosis efficiency for detection of combustion fault positions. Eventually, an MLP network with a well-formed, optimized structure, and remarkable accuracy was performed capable of identifying the faulty side, and then the faulty cylinder of the engine. The average condition monitoring performance was obtained to be from 93.89% up to 99.17%, based on the fault location and sensor placement, and CA was more than 98.34%. Therefore, this research properly verified the effectiveness of the DWT and the ANN in detecting the abnormal transient signals and showed that these techniques are promising for extracting proper features, fault detection, and fault diagnosis in complex trainset diesel engines.

Declaration of Conflicting Interests

The author(s) declared no potential conflicts of interest with respect to the research, authorship, and/or publication of this article.

Funding

The author(s) received no financial support for the research, authorship, and/or publication of this article.

ORCID iD

Moosa Ayati  <http://orcid.org/0000-0001-9943-739X>

References

- Jones N and Li YH. A review of condition monitoring and fault diagnosis for diesel engines. *Tribotest* 2000; 6: 267–2691.
- Traver ML, Atkinson RJ and Atkinson CM. Neural network-based diesel engine emissions prediction using in-cylinder combustion pressure. SAE Technical Paper, 1999.
- Li Z, Yan X, Yuan C, et al. Intelligent fault diagnosis method for marine diesel engines using instantaneous angular speed. *J Mech Sci Technol* 2012; 26: 2413–2423.
- Assanis DN and Friedmann FA. A thin-film thermocouple for transient heat transfer measurements in ceramic-coated combustion chambers. *Int Commun Heat Mass Transfer* 1993; 20: 459–468.
- Albarbar A, Gu F and Ball A. Diesel engine fuel injection monitoring using acoustic measurements and independent component analysis. *Measurement* 2010; 43: 1376–1386.
- Jiang K, Cao E and Wei L. NO_x sensor ammonia cross-sensitivity estimation with adaptive unscented Kalman filter for Diesel-engine selective catalytic reduction systems. *Fuel* 2016; 165: 185–192.
- Wang Y, Zhang F, Cui T, et al. Fault diagnosis for manifold absolute pressure sensor (MAP) of diesel engine based on Elman neural network observer. *Chin J Mech Eng* 2016; 29: 386–395.
- Ning D, Sun C, Gong YJ, et al. Extraction of fault component from abnormal sound in diesel engines using acoustic signals. *Mech Syst Signal Process* 2016; 75: 544–555.
- Moosavian A, Najafi G, Ghobadian B, et al. Piston scuffing fault and its identification in an IC engine by vibration analysis. *Appl Acoust* 2016; 102: 40–48.
- Chen J, Randall RB and Peeters B. Advanced diagnostic system for piston slap faults in IC engines, based on the non-stationary characteristics of the vibration signals. *Mech Syst Signal Process* 2016; 75: 434–454.
- Taghizadeh-Alisarai A, Ghobadian B, Tavakoli-Hashjin T, et al. Characterization of engine's combustion-vibration using diesel and biodiesel fuel blends by time-frequency methods: A case study. *Renew Energy* 2016; 95: 422–432.
- Heneghan C, Khanna SM, Flock A, et al. Investigating the nonlinear dynamics of cellular motion in the inner ear using the short-time Fourier and continuous wavelet transforms. *IEEE Trans Signal Process* 1994; 42: 3335–3352.
- Oehlmann H, Brie D, Tomczak M, et al. A method for analysing gearbox faults using time–frequency representations. *Mech Syst Signal Process* 1997; 11: 529–545.
- Staszewski WJ, Worden K and Tomlinson GR. Time–frequency analysis in gearbox fault detection using the Wigner–Ville distribution and pattern recognition. *Mech Syst Signal Process* 1997; 11: 673–692.
- Baydar N and Ball A. Detection of gear failures via vibration and acoustic signals using wavelet transform. *Mech Syst Signal Process* 2003; 17: 787–804.
- Butler-Purry KL and Bagriyanik M. Characterization of transients in transformers using discrete wavelet transforms. *IEEE Trans Power Syst* 2003; 18: 648–656.
- Geng Z and Chen J. Investigation into piston-slap-induced vibration for engine condition simulation and monitoring. *J Sound Vib* 2005; 282: 735–751.
- Teraguchi S, Suzuki W, Takiguchi M, et al. Effects of lubricating oil supply on reductions of piston slap vibration and piston friction. SAE Technical Paper, 2001.
- Gideon G, Gal de B BR and Eran S. Assessment of the quality of combustion in compression ignition engines through vibration signature analysis. Technical paper for students and young engineers, Fisita World Automotive Congress, Barcelona-Beer sheva, 2004, p. 2004.
- Carlucci A, Chiara F and Laforgia D. Analysis of the relation between injection parameter variation and block vibration of an internal combustion diesel engine. *J Sound Vib* 2006; 295: 141–164.
- Keskin A. The influence of ethanol–gasoline blends on spark ignition engine vibration characteristics and noise emissions. *Energy Sources A* 2010; 32: 1851–1860.
- Shirazi F and Mahjoob M. Application of discrete wavelet transform (DWT) in combustion failure detection of IC engines. In: *2007 ISPA 2007 5th international symposium on image and signal processing and analysis*, 2007, pp.482–486. New York: IEEE.
- Heywood JB. *Internal combustion engine fundamentals*. New York: McGraw-Hill, 1988.
- Liu S, Gu F and Ball A. Detection of engine valve faults by vibration signals measured on the cylinder head. *Proc IMechE, Part D: J Automobile Engineering* 2006; 220: 379–386.
- Jiang J, Gu F, Gennish R, et al. Monitoring of diesel engine combustions based on the acoustic source characterisation of the exhaust system. *Mech Syst Signal Process* 2008; 22: 1465–1480.
- Wang C, Zhang Y and Zhong Z. Fault diagnosis for diesel valve trains based on time–frequency images. *Mech Syst Signal Process* 2008; 22: 1981–1993.
- Flett J and Bone GM. Fault detection and diagnosis of diesel engine valve trains. *Mech Syst Signal Process* 2016; 72: 316–327.
- Cerna M and Harvey AF. The fundamentals of FFT-based signal analysis and measurement. National Instruments, Junho, 2000.
- Peng Y and Yam R. Wavelet analysis and envelope detection for rolling element bearing fault diagnosis—their effectiveness and flexibilities. *J Vib Acoust* 2001; 123: 303–310.
- Burrus CS, Gopinath RA and Guo H. *Introduction to wavelets and wavelet transforms: A primer*. Upper Saddle River: Prentice-Hall, 1997.
- Wu J-D, Hsu C-C and Wu G-Z. Fault gear identification and classification using discrete wavelet transform and adaptive neuro-fuzzy inference. *Expert Syst Appl* 2009; 36: 6244–6255.

32. Gaing Z-L. Wavelet-based neural network for power disturbance recognition and classification. *IEEE Trans Power Deliv* 2004; 19: 1560–1568.
33. Saravanan N and Ramachandran K. Incipient gear box fault diagnosis using discrete wavelet transform (DWT) for feature extraction and classification using artificial neural network (ANN). *Expert Syst Appl* 2010; 37: 4168–4181.
34. Ablameyko S. *Neural networks for instrumentation, measurement and related industrial applications*. Amsterdam, Netherlands: IOS Press, 2003.
35. Browne A. *Neural network analysis, architectures and applications*. Boca Raton, FL: CRC Press, 1997.
36. Lei Y, He Z and Zi Y. A combination of WKNN to fault diagnosis of rolling element bearings. *J Vib Acoust* 2009; 131: 064502.

Identification and Control of MIMO Linear Systems under Sufficient and Insufficient Excitation

Saeed Ansari-Rad^{*}, Sina Jahandari[†], Ahmad Kalhor[‡], Babak Nadjar Araabi[§]

Abstract— In closed-loop identification of unknown control systems, stability is a major concern. Particularly, when the system does not proceed with sufficient excitation. In this paper, a closed-loop identification strategy for Multi-Input Multi-Output (MIMO) linear systems is intended via a robust adaptive control law based on Sliding Mode Control (SMC). Under both sufficient and insufficient excitation of the system, Evolving Linear Models (ELMs) are deployed to identify and control the system. It is explained that under insufficient excitation, linear correlations between input and output signals and their derivatives can be removed. An equivalent reduced-order model of the original system results which can be identified as an ELM. Defining the control law based on the SMC and using appropriate adaptation rules for parameters of the model, the tracking errors converge to zero and the stability of the system is guaranteed. Meanwhile, the parameters of the model converge to their true values. Simulation results demonstrate the efficacy of the proposed approach.

I. INTRODUCTION

Multi variability and instability are two known challenges in identification which arise mainly in MIMO systems. Many works have tried to address identification of closed-loop MIMO systems in literature. Most of the methods guaranteeing closed-loop stabilities are based on Lyapunov theory such as the methods proposed for continuous nonlinear systems during identification [1-7] or the methods for discrete models [8] and the combination of recursive least square (RLS) and Lyapunov theory for discrete model identification [9, 10]. Only some of mentioned methods have considered multi-variability in their algorithms but none of them have guaranteed the convergence of parameters to their true values. On the other hand, approaches presented in [11-13] guarantee the tracking of desired signals based on the Lyapunov theory without guaranteeing stability. Robust adaptive techniques have been playing an important role in identification and control [14-17]. For nonlinear systems, on the other hand, SMCs have drawn attention in recent years [18]. Some of these works use adaptation rules with SMC or other control methods tracking both desired outputs and system parameters, but none offers a systematic procedure that also guarantees convergence of parameters to their actual values and stability of the closed-loop system.

Another important class of controllers in this domain are self-tuning regulators (STR) [19]. In indirect STR schemes,

the adaptive law generates online estimation of the parameters of the system. Due to its flexibility in choosing the controller design and adaptive law, indirect STRs are the most general class of adaptive control schemes [20]. The basic structure of this paper is emerged from indirect STRs: using SMC as the control methodology and continuous-time RLS as the adaptive law. In previous works, after the identification of parameters, tracking the desired behavior and the stability of the closed-loop system were feasible. Therefore, initializing the identification procedure and the speed of convergence of identified parameters were problematic. Avoiding these problems was a motivation to design the current structure. Moreover, tracking the desired output design of the proposed method is another advantage of the work compared to most STRs which are designed based on pole placement methods.

The proposed approach offers identification of parameters and control of the system simultaneously. Sliding mode technique reduces disturbances effects and leads to the tracking of desired signals asymptotically. Adaptation rules decrease energy of the Lyapunov function which is conceptually sum of parameters estimation error (PEE) in each channel and control efforts at any time.

Our key contributions are: 1- Combining SMC and adaptation rules in order to control the outputs and to identify parameters of the system simultaneously. 2- Introducing ELMs. ELMs consist of the basic model (a model with the same dynamic order of system channels that fits behaviors of the basic system) and switching R- reduced-order models (R-OMs). These linear models are used to model the behavior of the system when the excitation order of the user-defined signals are low. 3- Designing an algorithm in which identification and control are carried out simultaneously. These strategies, guarantee the convergence of the R-OMs' parameters to their real values and stability of the closed-loop system.

The remainder of the paper is organized as follows. Section II presents the main results and the identification algorithm through robust adaptive control laws. Simulation results are given in Section III. Concluding remarks are given in Section IV.

^{*} S. Ansari-Rad is M.Sc. student in Control and Intelligent Processing Center of Excellence, School of Electrical and Computer Engineering, University of Tehran, Tehran, Iran (e-mail: saeedansari71@ut.ac.ir).

[†] S. Jahandari is with Electrical Engineering and Computer Science Department of University of Tennessee, Knoxville, USA (e-mail: sj@utk.edu).

[‡] A. Kalhor is now with the Center of Excellence for Control and Intelligent Processing, School of Electrical and Computer Engineering, University of Tehran, Tehran, Iran (e-mail: akalhor@ut.ac.ir).

[§] B.N. Araabi is with the Center of Excellence for Control and Intelligent Processing, School of Electrical and Computer Engineering, University of Tehran, Tehran, Iran (e-mail: araabi@ut.ac.ir).

II. IDENTIFICATION OF MODELS VIA A ROBUST ADAPTIVE ALGORITHM

A. Time-invariant Models

In this part, basic models and R-OMs are suggested as a powerful alternative for modelling behavior of basic systems. Channel inputs and outputs data samples of the basic systems are used to identify the system.

The basic model for transfer functions of MIMO systems is considered as:

$$G(S) = \left[\frac{b_{qj}}{S^{n_q} - a_{qn_q} S^{n_q-1} \dots - a_{q1}} \right]_{N \times N} \quad (1)$$

$\forall q = 1, \dots, N, \forall j = 1, \dots, N,$

where the Laplace variable is denoted with symbol S . The index q is a general channel indicator and j refers to the index of input. Each output channel can be described by a differential equation:

$$y_q^{[n_q]} = a_q^T y_q + b_q^T \underline{u} = \theta_q^T \Phi_q, \quad (2)$$

where n_q denotes the dynamic rank of the q_{th} output. Also for each channel, vectors of denominator coefficients, output signal regressors, nominator coefficients, and transfer function parameters are denoted as $a_q^T \in \mathbb{R}^{n_q}$, $y_q^T \in \mathbb{R}^{n_q}$, $b_q^T \in \mathbb{R}^N$, $\theta_q^T \in \mathbb{R}^{N+n_q}$, respectively. The vector of input signals is shown as $\underline{u} \in \mathbb{R}^N$.

$$\begin{aligned} a_q^T &= [a_{qn_q}, a_{q(n_q-1)}, \dots, a_{q1}], b_q^T = [b_{qj}]_{1 \times N} \\ \theta_q^T &= [a_q^T, b_q^T], \underline{y}_q^T = [y_q^{[n_q-1]}, y_q^{[n_q-2]}, \dots, y_q^{[1]}, y_q] \\ \underline{u} &= [u_j]_{N \times 1} \end{aligned} \quad (3)$$

While regressors of each channel, $\Phi_q = \begin{bmatrix} y_q \\ \underline{u} \end{bmatrix}$, are linearly independent, the basic differential equation (2) governs the q_{th} channel. It is noteworthy to mention that input and output signals are measured from the basic system, not the model. This becomes important when we substitute identified parameters in models, where their output signal regressors are different from \underline{y}_q in each channel.

Assumption A1: The matrix $B = [b_{qj}]_{N \times N}$ is diagonally dominant if the condition $|b_{qq}| > \sum_{j \neq q} |b_{qj}|$ holds for the q_{th} output channel.

In the case of dependency between regressors of the i_{th} channel, we should switch its model to a R-OM. Therefore, the k_{th} regressor of the output signal, which is the most effective regressor in the dependency relation, is removed. By applying the dependency relation, the differential equation of the i_{th} channel can be written as follows.

$$y_i^{[n_i]} = \theta_i'^T \Phi_i'(t), \quad (4)$$

where

$$\Phi_i'^T(t) = [y_i^{[n_i-1]}, y_i^{[n_i-2]}, \dots, y_i^{[m]}, \dots, \underline{u}^T]$$

Basic models are MIMO square transfer functions with no zero elements. The characteristic equation of each output channel is different from others and should be minimum phase. Without any a priori knowledge about the system except the dynamic rank of each output ch

$$\theta_i'^T = [a'_{i n_i}, a'_{i(n_i-1)}, \dots, a'_{i(m+1)}, \dots, b_i'^T]$$

$$\forall m = 0, \dots, k-1, k+1, \dots, n_i-1. \quad (5)$$

Hence, (4) describes the reduced-order differential equation of the i_{th} channel, namely, the R-OM for the i_{th} channel. The accent ' distinguishes R-OM parameter from those of the basic model. The relationship between the j_{th} input and the i_{th} output can be described by the following transfer function:

$$g_{ij}(S) = \frac{b'_{ij}}{S^{n_i - a'_{i n_i}} S^{n_i-1} \dots - a'_{i(m+1)} S^m \dots - a'_{i1}}. \quad (6)$$

Remark 1: The number of removed regressors and their corresponding indices can be different from the mentioned scenario, but the result still holds.

B. Sliding Mode Control and Robust Adaptive Identification

In the following, equations governing the identifier are explained in details. Sliding rules force the system to gain our target features by sliding along a cross-section of the system's normal behavior. To track output signals and reduce output error, sliding rules at each channel are defined as follows.

$$s_q = \left(\frac{d}{dt} + \lambda_q \right)^{n_q-1} \tilde{y}_q = \Lambda \mu_q^T \tilde{y}_q \quad (7)$$

$$\Lambda \mu_q^T = [1, \dots, (n_q - 1)\lambda_q^{n_q-2}, \lambda_q^{n_q-1}]$$

$$\tilde{y}_q = y_q - y_{r_q}$$

Vectors of desired output regressors and output error regressors in each channel are, respectively, written as:

$$\underline{y}_{r_q}^T = [y_{r_q}^{[n_q-1]}, \dots, y_{r_q}^{[1]}, y_{r_q}], \tilde{y}_q^T = [\tilde{y}_q^{[n_q-1]}, \dots, \tilde{y}_q^{[1]}, \tilde{y}_q].$$

The scalar s_q denotes the sliding variable in each channel. Sliding rules are concerned with system signals, not the model's. Therefore, any changes in models do not affect sliding surfaces and the system will track desired outputs under any circumstances. To analyze sliding surfaces, the derivative of sliding variable in each channel will be studied. Based on these derivatives, control inputs are defined, which force the system to reach sliding surfaces. In the following, equations of the basic model are used to describe the role of models in the identifier.

Assumption A2: Desired signals are continuous and smooth.

Considering (2), the derivative of the q_{th} sliding variable is computed as follows.

$$\begin{aligned} \dot{s}_q &= \Lambda \mu_{s_q}^T \tilde{y}_q + \dot{\tilde{y}}_q^{[n_q]} = \Lambda \mu_{s_q}^T \tilde{y}_q + \theta_q^T \Phi_q(t) - y_{r_q}^{[n_q]} \\ &= \Lambda \mu_{s_q}^T \tilde{y}_q + a_q^T y_q + b_q^T \underline{u} - y_{r_q}^{[n_q]}. \end{aligned} \quad (8)$$

The derivative of the sliding vector, which is defined as $\mathbf{S} = \begin{bmatrix} s_1 \\ \vdots \\ s_N \end{bmatrix} \in \mathbb{R}^N$, can be written as:

$$\dot{\mathbf{S}} = \tilde{\Gamma} + \Gamma_a - \Gamma_r + B \mathbf{u}, \quad (9)$$

where

$$\tilde{\Gamma} = \begin{bmatrix} \Lambda \mu_{s_1}^T \underline{\tilde{y}}_1 \\ \vdots \\ \Lambda \mu_{s_N}^T \underline{\tilde{y}}_N \end{bmatrix} \in \mathbb{R}^N, \Gamma_a = \begin{bmatrix} a_1^T \underline{y}_1 \\ \vdots \\ a_N^T \underline{y}_N \end{bmatrix} \in \mathbb{R}^N$$

$$\Gamma_r = \begin{bmatrix} y_{r_1}^{[n_1]} \\ \vdots \\ y_{r_N}^{[n_N]} \end{bmatrix} \in \mathbb{R}^N, B = \begin{bmatrix} b_1^T \\ \vdots \\ b_N^T \end{bmatrix} \in \mathbb{R}^{N \times N}. \quad (10)$$

The vector of input signals is applied to the system based on:

$$\underline{\mathbf{u}} = \underline{\hat{\mathbf{u}}} - \eta \operatorname{sgn}(\mathbf{S}) \quad (11)$$

where

$$\underline{\hat{\mathbf{u}}} = -\hat{B}^{-1} (\tilde{\Gamma} + \Gamma_{\hat{a}} - \Gamma_r) \quad (12)$$

$$\eta = \begin{bmatrix} \eta_1 & 0 & 0 \\ 0 & \ddots & 0 \\ 0 & 0 & \eta_N \end{bmatrix} \in \mathbb{R}^{N \times N}, \hat{B} = \begin{bmatrix} \hat{b}_1^T \\ \vdots \\ \hat{b}_N^T \end{bmatrix} \in \mathbb{R}^{N \times N}, \Gamma_{\hat{a}} = \begin{bmatrix} \hat{a}_1^T \underline{y}_1 \\ \vdots \\ \hat{a}_N^T \underline{y}_N \end{bmatrix} \in \mathbb{R}^N.$$

Remark 2: The matrix η in (11) is determined such that $\eta_q b_{qq} > 0$.

Identified model parameters affect the vector of control inputs ($\underline{\hat{\mathbf{u}}}$) in (12). Conceptually, the force needed to keep the system on reaching surfaces, depends on model parameters. The accent $\hat{\cdot}$ on each parameter denotes the estimated value of that parameter by the identifier. Applying (11) to the derivative of the sliding vector results in (13), where $\tilde{a}_q = a_q - \hat{a}_q$. Likewise, the accent $\tilde{\cdot}$ on each parameter distinguishes the error value of the identified parameter from its basic value.

$$\dot{\mathbf{S}} = - \begin{bmatrix} \tilde{b}_1^T \\ \vdots \\ \tilde{b}_N^T \end{bmatrix} \underline{\hat{\mathbf{u}}} + \begin{bmatrix} \tilde{a}_1^T \underline{y}_1 \\ \vdots \\ \tilde{a}_N^T \underline{y}_N \end{bmatrix} - B \eta \operatorname{sgn}(\mathbf{S}) \quad (13)$$

To functionally separate the control and identification procedures, we need an energy function. This function shows how much energy the identifier needs to control system outputs and how much energy is needed to update model parameters. We introduce a Lyapunov function where we define $\tilde{\theta}_q^T = [\tilde{a}_q^T, \tilde{b}_q^T]$ for the q_{th} channel.

$$V(t) = \frac{1}{2} [\mathbf{S}^T \mathbf{S} + \sum_{q=1}^N \tilde{\theta}_q^T(t) P_q^{-1}(t) \tilde{\theta}_q^T(t)] \quad (14)$$

As it will be shown, the identifier at the beginning of the procedure spends much energy to reach sliding surfaces; eventually puts more efforts on tracking system parameters. To keep the closed-loop system stable, the identifier should decrease the energy of the Lyapunov function. To update identified model parameters, adaptation rules are used. By

designing suitable control inputs and adaptation rules, the stability of the closed-loop system can be guaranteed. The symmetric covariance matrix for each channel is denoted by $P_q^{-1}(t)$, where its initial value is set $P_q^{-1}(t=0) = g I_{n_q+N}$, $g \gg 1$ for the q_{th} channel.

RLS is an appropriate tool to update model parameters in order to decrease the identification error. The following updating rules are resulted from continuous RLS method,

$$\hat{\theta}_q(t) = P_q(t) \Phi_q(t) e_q(t) \quad (15)$$

where the scalar e_q is defined as:

$$e_q = \tilde{y}_q^{[n_q]} = y_q^{[n_q]} - y_{r_q}^{[n_q]} = \tilde{\theta}_q^T(t) \Phi_q(t).$$

Clearly, $e_q(t)$ is associated with system features, not the model. Based on RLS method, the online updating rule of matrix $P_q(t) \in \mathbb{R}^{N+n_q}$ can be expressed as follows:

$$\dot{P}_q(t) = \alpha_q P_q(t) - P_q(t) \Phi_q(t) \Phi_q^T(t) P_q(t) \quad (16)$$

where α_q denotes the forgetting factor of the q_{th} channel.

In RLS method, model parameters of the q_{th} channel are traceable if regressors of the channel (Φ_q) are at least persistent excited (PE) with order $n_q + N$, which is the number of parameters needed to be estimated in the channel. Equation (12) shows that desired output signals affect the vector of input signals and then output signals. Therefore, if all desired signals are sufficient PE (It can be shown that a persistent excitation with order n_q is sufficient excitation for the desired signal in channel q and any PE signals with order less than n_q are insufficient excitation for the channel), model parameters are traceable and covariance matrices always remain positive definite. Therefore, two time-invarying scalars $\underline{\sigma}_q$ and $\bar{\sigma}_q$ can be found such that $\exists \underline{\sigma}_q, \bar{\sigma}_q, \forall t \geq 0 : 0 < \underline{\sigma}_q I \leq P_q^{-1}(t) \leq \bar{\sigma}_q I$.

On the contrary, if at least for one channel (the i_{th} channel) desired output signal is not sufficient excited, the matrix $P_i^{-1}(t)$ becomes positive semi-defined after a while. Hence, some dependency relations occur between regressors of the i_{th} channel. Depending on the order of excitation signals in the channel, which determines the number of dependency relations, the identifier switches the basic model to a suitable R-OM, the same as (4), to fit the behavior of the i_{th} channel, while other channels remain intact. In this case, some correlated regressors are removed and related model parameters are reduced in order to adapt the model with insufficiency of excitation signals in the i_{th} channel. With these changes, the identifier carries on a partially identification method which is adapted to the excitation order of desired signals while controlling output signals. In this case, the floating rank is less than the dynamic rank of the i_{th} channel. (The floating rank of the i_{th} channel determines the number of denominator parameters which can be identified online.)

It is noteworthy to mention that by switching R-OMs, besides identification, the algorithm introduces much more sensible concept of the control theory: Desired signals can be determined by a user, not the identifier. Based on the desired

signal type and its excitation order, suitable models fit on system behaviors. Mathematical detail can be found in [21].

Suggested adaptation rules for basic model parameters are given by:

$$\forall t: \begin{bmatrix} \hat{a}_q \\ \hat{b}_q \end{bmatrix} = S_q(t)P_q(t) \begin{bmatrix} y_q \\ -\hat{u} \end{bmatrix} + \gamma_q P_q(t)\Phi_q(t)e_q(t) \quad (17)$$

The first term in the right hand-side of (17) is concerned with adaptive changes based on sliding values. After reaching sliding surfaces, this part vanishes and only the second term affects adaptation rules. The second term is mainly the same as (15); but parameter γ_q adjusts effects of RLS adaptation rules.

C. Stability and Convergence

As it was discussed, stability guarantees under any kinds of identification procedures is crucial. In the following, using the basic model and what we have explained so far, the stability of the closed-loop system is studied. Meanwhile, the convergence of model parameters to their true values will be shown.

Theorem 1: Regarding MIMO systems described in (1) and based on **A1** to **A3** and **Remark 2**, identification of the basic model is guaranteed. The closed-loop system remains asymptotically stable during identification procedure.

The Lyapunov function stated in (14) is being used to prove this theorem. Besides calculating the energy of the system in sliding surfaces, (14) shows the energy of identification error in the input-output space. So the derivative of this function should be negative definite in order to reduce identification errors.

$$\begin{aligned} \dot{V}(t) = & \frac{1}{2} \left[2\mathbf{S}^T \dot{\mathbf{S}} - 2 \sum_{q=1}^N \hat{\theta}_q^T(t) P_q^{-1}(t) \tilde{\theta}_q(t) \right. \\ & \left. + \sum_{q=1}^N \tilde{\theta}_q^T(t) \dot{P}_q^{-1}(t) \tilde{\theta}_q(t) \right] \end{aligned} \quad (18)$$

By substituting the derivative of the sliding vector into (18) we will have:

$$\begin{aligned} \dot{V}(t) = & \frac{1}{2} \left[-2\mathbf{S}^T \begin{bmatrix} \tilde{b}_1^T \\ \vdots \\ \tilde{b}_N^T \end{bmatrix} \hat{u} + 2\mathbf{S}^T \begin{bmatrix} \tilde{a}_1^T y_1 \\ \vdots \\ \tilde{a}_N^T y_N \end{bmatrix} \right. \\ & \left. - 2 \sum_{q=1}^N \hat{\theta}_q^T(t) P_q^{-1}(t) \tilde{\theta}_q(t) + \sum_{q=1}^N \tilde{\theta}_q^T(t) \dot{P}_q^{-1}(t) \tilde{\theta}_q(t) \right] \\ & - \mathbf{S}^T B \eta \text{sign}(\mathbf{S}). \end{aligned} \quad (19)$$

By writing (19) in a summation format, according to **Remark 2**, the following inequality can be obtained:

$$\begin{aligned} \dot{V}(t) \leq & \sum_{i=1}^N (s_q \left[y_q^T, -\hat{u}^T \right] - [\hat{a}_q^T(t), \hat{b}_q^T(t)] P_q^{-1}(t) \tilde{\theta}_q(t) \\ & + \frac{1}{2} \sum_{q=1}^N \tilde{\theta}_q^T(t) \dot{P}_q^{-1}(t) \tilde{\theta}_q(t) \\ & - \sum_{q=1}^N (|\eta_q| |s_q| (|b_{qq}| - \sum_{j=1, j \neq q}^N |b_{qj}|)). \end{aligned} \quad (20)$$

By imposing adaptation rules and some calculations, we will have:

$$\begin{aligned} \dot{V}(t) \leq & -\frac{1}{2} \sum_{q=1}^N \alpha_q \tilde{\theta}_q^T(t) P_q^{-1}(t) \tilde{\theta}_q(t) \\ & - \sum_{q=1}^N \left(\gamma_q - \frac{1}{2} \right) \tilde{\theta}_q^T(t) \Phi_q(t) \Phi_q^T(t) \tilde{\theta}_q(t) \\ & - \sum_{q=1}^N |\eta_q| |b_{qq}| |s_q|. \end{aligned} \quad (21)$$

Therefore,

$$\dot{V}(t) \leq -W_3(\|\mathbf{S}\|, \|\tilde{\theta}\|) = -\left(\frac{1}{2}a + \sigma\right) \|\tilde{\theta}\|^2 - \delta \|\mathbf{S}\| < 0 \quad (22)$$

with:

$$0 < a = \min_{\forall q=1, \dots, N} \alpha_q, \quad 0 < \delta = \min_{\forall q=1, \dots, N} (|\eta_q| |b_{qq}|).$$

According to (22), the derivative of the Lyapunov function remains negative definite for PEEs and sliding vector. Hence, based on Lyapunov theory, we conclude that the upper bound function $W_3(\|\mathbf{S}\|, \|\tilde{\theta}\|) \rightarrow 0$, asymptotically. As the result, estimated parameters of the basic model converge to their true values and output signals converge asymptotically to their corresponding desired signals. This completes the proof.

With few changes in the Lyapunov function, the same strategy can be applied with R-OMs. Using these strategies, the convergence of R-OM parameters to their actual values and stability of the closed-loop system can also be guaranteed.

III. SIMULATION

In the following, a handmade 2-input/2-output unstable and controllable system is studied; the transfer function of this system is shown in (23). The proposed robust adaptive algorithm is applied in order to identify the basic system. Considering these control parameters: $\lambda_1 = 1, \lambda_2 = [2 \ 1], \alpha_1 = \alpha_2 = 0.01, \gamma_1 = \gamma_2 = 1, \eta_1 = \eta_2 = 5, \overline{dt} = 0.001$, the result of the first simulation is shown in Fig. 1.

It is shown that the proposed algorithm is able to control the output behaviors and track system parameters, successfully; however, by applying an insufficient excitation to the second channel identified parameters diverge from their real values. The dynamic rank of the second channel is 3 and the model fitted on this channel needs higher excitation to be identified.

Here, some sinusoidal desired signals are applied with different frequencies and amplitudes. Ideally, for the second channel, a 2-sinusoidal signal with the excitation order of 4 is necessary and satisfies conditions of **Theorem 1**. Signals like a sinusoidal or a step, for this channel, are considered as insufficient excitation. In the second simulation, an independent sinusoidal signal is being applied for both channels. Hence, the first channel is sufficiently excited due to its dynamic rank of 2. Under these circumstances, the condition number of P_2^{-1} is increased and stability of the closed-loop system will be jeopardized.

To solve this problem, an R-OM switches with the basic model to reduce the number of identified parameters. The model switches based on a specified maximum limitation of the condition number of P_2^{-1} . Choosing this threshold, the switching time will be before vanishing σ_2 . To prevent any instabilities and control problems, this threshold is set 6000 in the simulation 2. So the system has enough time to react against insufficient excitations. The identifier chooses the worst regressor ($y_2^{[2]}$) of the second channel and removes it. Then, another model with floating rank of two fits the second

channel. In the switching moment, the identified R-OM for the channel 2 and input 2, is obtained as:

$$\hat{H}'_{22}(S) = \frac{1.3985}{S^3 - 2.5072 S + 0.6169}$$

while before switching, the model for the channel 2 was identified as:

$$\hat{H}_{22}(S) = \frac{1.3985}{S^3 - 1.0079 S^2 - 2.5072 S - 0.5926}$$

The characteristic equation of the R-OM for the second channel is calculated as $S^3 - 2.5088 S + 0.6261$, so identified parameters of the second channel converge asymptotically to these values. Since excitation of the second channel is now sufficient (1-sinusoidal signal can sufficiently excite an R-OM with floating rank of two.), the identifier does not switch the model and selects it as the best model for the second channel, in the presence of these excitation signals. Also, during these evolving procedures, the first channel with its basic model keeps tracking its parameters.

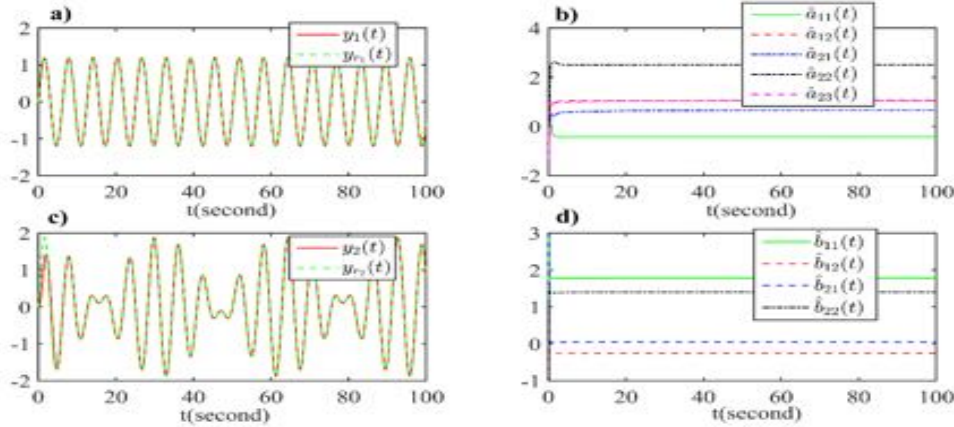


Figure 1. Simulation1: a) The first output and its desired signal b) The identified parameters of denominators c) The second output and its desired signal d) The identified parameters of nominators

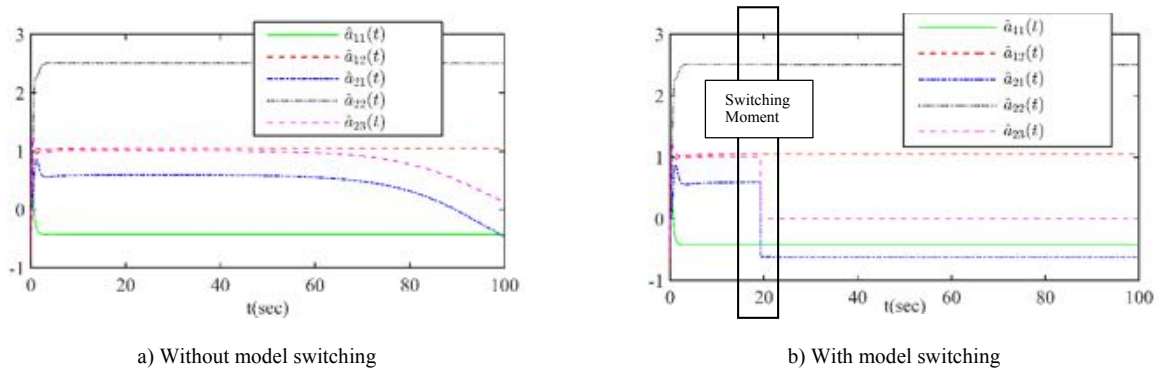


Figure 2. Simulation2: The identified denominator parameters under insufficient excitation

$$H(S) = \begin{bmatrix} \frac{1.7856}{S^2 - 1.0486 S + 0.4256} & \frac{-0.2567}{S^2 - 1.0486 S + 0.4256} \\ \frac{0.0533}{S^3 - 1.0635 S^2 - 2.5088 S - 0.6607} & \frac{1.3986}{S^3 - 1.0635 S^2 - 2.5088 S - 0.6607} \end{bmatrix}_{2 \times 2} \quad (23)$$

IV. CONCLUSION

The closed-loop identification and control of a MIMO linear system under both sufficient and insufficient excitation were investigated. Under the insufficient excitation of the system, by dropping out some input or output correlated variables, an equivalent R-OM of the original system was built which was identified as an ELM. Using SMC strategy and defining adaptation rules for parameters of the model, it was shown that the tracking errors converged to zero and the stability of the system was guaranteed. Moreover, the convergence of the parameters of the model to their true values was studied and discussed. Simulations showed that the proposed closed-loop identification approach works under different excitation signals.

REFERENCES

- [1] K. S. Narendra and P. Kudva, "Stable adaptive schemes for system identification and control-part I," *IEEE Transactions on Systems, Man, and Cybernetics*, pp. 542-551, 1974.
- [2] Y. Xu, W. Zhou, J. a. Fang, and W. Sun, "Adaptive lag synchronization and parameters adaptive lag identification of chaotic systems," *Physics Letters A*, vol. 374, pp. 3441-3446, 2010.
- [3] W. Xiao-Qun and L. Jun-An, "Parameter identification and backstepping control of uncertain Lü system," *Chaos, Solitons & Fractals*, vol. 18, pp. 721-729, 2003.
- [4] L. Yan, N. Sundararajan, and P. Saratchandran, "Nonlinear system identification using Lyapunov based fully tuned dynamic RBF networks," *Neural Processing Letters*, vol. 12, pp. 291-303, 2000.
- [5] S. Chen, J. Hu, C. Wang, and J. Lü, "Adaptive synchronization of uncertain Rössler hyperchaotic system based on parameter identification," *Physics Letters A*, vol. 321, pp. 50-55, 2004.
- [6] Jahandari, S., Beyglou, F. F., Kalhor, A., and Masouleh, M. T " A robust adaptive linear control for a ball handling mechanism," *In Robotics and Mechatronics (ICRoM), 2014 Second RSI/ISM International Conference on*, pp. 376-381, 2014.
- [7] J. de Jess Rubio and W. Yu, "Stability analysis of nonlinear system identification via delayed neural networks," *IEEE Transactions on Circuits and Systems II: Express Briefs*, vol. 54, pp. 161-165, 2007.
- [8] R. Johansson, "Global Lyapunov stability and exponential convergence of direct adaptive control," *International Journal of Control*, vol. 50, pp. 859-869, 1989.
- [9] Jahandari, S., Kalhor, A., and Araabi, B. N., " Online Forecasting of Synchronous Time Series Based on Evolving Linear Models," *IEEE Transactions on Systems, Man, and Cybernetics: Systems.*, vol. 48, doi: 10.1109/TSMC.2018.2789936 , 2018.
- [10] S. Akhtar and D. S. Bernstein, "Lyapunov- stable discrete- time model reference adaptive control," *International Journal of Adaptive Control and Signal Processing*, vol. 19, pp. 745-767, 2005.
- [11] Jahandari, S., Kalhor, A., and Araabi, B. N., " A self tuning regulator design for nonlinear time varying systems based on evolving linear models," *Evolving Systems.*, vol. 7(3), pp. 159-172, 2016.
- [12] C.-H. Lee and C.-C. Teng, "Identification and control of dynamic systems using recurrent fuzzy neural networks," *IEEE Transactions on fuzzy systems*, vol. 8, pp. 349-366, 2000.
- [13] X. Ren, A. B. Rad, P. Chan, and W. L. Lo, "Identification and control of continuous-time nonlinear systems via dynamic neural networks," *IEEE Transactions on Industrial Electronics*, vol. 50, pp. 478-486, 2003.
- [14] Jahandari, S., Kalhor, A., and Araabi, B.N., " Order determination and robust adaptive control of unknown deterministic input-affine systems: An operational controller," *In Decision and Control (CDC), 2016 IEEE 55th Conference on*, pp. 3831-3836. 2016.
- [15] M. Chen, S. S. Ge, and B. Ren, "Adaptive tracking control of uncertain MIMO nonlinear systems with input constraints," *Automatica*, vol. 47, pp. 452-465, 2011.
- [16] L. Lu and B. Yao, "Online constrained optimization based adaptive robust control of a class of MIMO nonlinear systems with matched uncertainties and input/state constraints," *Automatica*, vol. 50, pp. 864-873, 2014.
- [17] C. Nicol, C. Macnab, and A. Ramirez-Serrano, "Robust adaptive control of a quadrotor helicopter," *Mechatronics*, vol. 21, pp. 927-938, 2011.
- [18] C. Yin, Y. Chen, and S.-m. Zhong, "Fractional-order sliding mode based extremum seeking control of a class of nonlinear systems," *Automatica*, vol. 50, pp. 3173-3181, 2014
- [19] K. J. Åström and B. Wittenmark, *Adaptive control*: Courier Corporation, 2013.
- [20] P. A. Ioannou and J. Sun, *Robust adaptive control* vol. 1: PTR Prentice-Hall Upper Saddle River, NJ, 1996.
- [21] S. Ansari-Rad, A. Kalhor, and B. N. Araabi, "Partial identification and control of MIMO systems via switching linear reduced-order models under weak stimulations," *Evolving Systems*, pp. 1-18, 2017.



Experimental study on robust adaptive control with insufficient excitation of a 3-DOF spherical parallel robot for stabilization purposes

Saeed Ansari Rad^a, Mehran Ghafarian Tamizi^a, Mehdi Azmoon^a, Mehdi Tale Masouleh^{a,a,*}, Ahmad Kalhor^b

^a Human and Robotic Interaction Laboratory, School of Electrical and Computer Engineering, University of Tehran, Tehran, Iran

^b Control and Intelligent Processing Center of Excellence, School of Electrical and Computer Engineering, University of Tehran, Tehran, Iran

ARTICLE INFO

Article history:

Received 22 October 2019

Revised 20 May 2020

Accepted 3 July 2020

Available online xxx

Keywords:

Oscillation dampening
Insufficient excitations
Robust adaptive control
Singular value decomposition
Spherical parallel robot
Stabilization

ABSTRACT

In this paper, a robust adaptive control approach has been proposed for under insufficient excitation Multi-Input Multi-Output (MIMO) systems. The stability and performance of adaptive controllers are highly dependent on initial conditions and speed of convergence of identified parameters. Moreover, the corresponding adaptation rules suffer from system uncertainties, disturbances, and insufficient excitation. In order to overcome such crucial challenges, in this paper a robust adaptive control is proposed. By inspiring from the classic Damped Least Squares (DLS) and Singular Value Decomposition (SVD) methods, a novel algorithm namely, SVD-DLS, is introduced which obtains an optimal solution to the estimation wind-up. Above all, the proposed approach is implemented on a 3 degree-of-freedom spherical parallel robot for stabilization purposes. By avoiding from challenges of model-based approaches, the unknown parameters are obtained without having any prior knowledge which makes the proposed approach more interesting for robotic having complex models. Based on the practical implementation, the oscillations of identified parameters are dampened much smoother than other identification methods in which the ratio of end-effector to base orientation, as a stabilization index, is acquired as 0.134.

© 2020 Elsevier Ltd. All rights reserved.

1. Introduction

In recent decades, the widespread application of system identification theory in control contexts has been extended, significantly. Multi variability and instability are two known challenges in system identification. In order to address the aforementioned problems, adaptive controllers which deal with subjectives like the robustness, estimation of the parameters, and sufficient excitation have stimulated the interest of many researchers in the control system's field [1–3]. In this regard, the robust adaptive and robust tracking methods have been improved to control behaviors of system outputs [4–7]. Also, Sliding Mode Controllers (SMCs) have become more popular for controlling nonlinear systems [8–12]. From the literature, some researches have been conducted to the end of tracking both signals and involved parameters by combining several control approaches, namely, adaptive control but there is still a gap in proposing a systematic procedures with models

* Corresponding author.

E-mail addresses: saeedansari71@ut.ac.ir (S.A. Rad), mehran.ghafarian@ut.ac.ir (M.G. Tamizi), mehdi.azmoon@ut.ac.ir (M. Azmoon), m.t.masouleh@ut.ac.ir (M. Tale Masouleh), akalhor@ut.ac.ir (A. Kalhor).

whose parameters are guaranteed to converge to their true values while the closed-loop procedure is proven to remain stable.

Generally, robust adaptive control methods [13–15] have gained more attention recently due to their agility and robustness. However, most of these papers employ model-based method; therefore, the plant should be modeled comprehensively which is usually a delicate task, particularly, when the plant is a robot with non-linear equations. Moreover, having simplified models leads to less accuracy in control procedure and usually the model is not adaptable with disturbance and uncertainties which is a definite asset in the practice. In order to avoid these significant drawbacks, an algorithm which has ability to adapt with variation of surrounding environment and simultaneously performs identification and control of a system with unknown parameters is required. This considerable notion causes improvement in automatic control strategies based on the unknown parameters [16,17]. In this regard, employing learning-based algorithms [18,19] and neural networks [20,21] plays a major role. As a case, in [22] in order to solve a Linear Quadratic Regulator problem, an integral Q-learning algorithm is suggested. In [18], a novel policy iteration approach is proposed in order to acquire on-line adaptive controller for continuous time linear systems with unknown dynamics. Moreover, Jia et al. [19] suggested a learning algorithm which leads to a better result for identification procedure and has a more acceptable reaction to the changes of surrounding environment. Pomprapa et al. [23] employed policy iteration algorithm in order to solve the so-called Hamilton Jacobi Bellman equation. Most of these methods require lots of process and huge amounts of data which makes them not suitable for real-time control systems.

Another promising structure which merges the control concept during identification of the unknown parameter of the system is the so-called Self-Tuning Regulators (STR) [24]. From the STR point of view, the adaptive law generates online estimation of the parameters of the system which requires a control methodology in order to manipulate the behaviour of the system. Due to its flexibility in choosing the controller design methodology and adaptive law, indirect STRs can be classified as the most general class of adaptive control schemes [25]. In previous researches such as [26], upon identifying the desired parameters, tracking the desired behavior and the stability of the closed-loop system became possible. Therefore, initial conditions of the identification procedure and the speed of convergence of identified parameters play an important role [24].

From the study conducted in [27], it can be inferred that merging the indirect STRs approach with the novel design proposed in the latter study can be regarded as a remedy to the aforementioned problems. More precisely, in the foregoing approach, the SMC with robustness properties as the control methodology is blended with a continuous-time Recursive Least Squares (RLS) as the adaptive law which opens an avenue to identify the parameters and control of the system, simultaneously. Therefore, the identification of parameters and control of system behaviors become possible, simultaneously. In fact, it will be shown that the adaptation rules of the control structure can be extended to RLS estimation equations. The RLS is a well-known method in parameters estimation [28,29]. It is suitable for time-varying processes with sufficient excitation; otherwise, the singularity problem happens which is referred to as estimation wind up in the literature. In this case, the estimation gain increases exponentially and outputs of the estimator are sensitive to any disturbances in regressors [30].

By proposing Damped Least Squares (DLS) method, Lambert [29] changed the classical RLS approach in such way that parameters variation remained bounded. In some researches, such as [31–33], similar procedures were utilized. By improving the idea which has been introduced in [29], the Generalized DLS (GDLS) was proposed [28]. This algorithm systematically refines the estimation wind-up in a closed-loop control strategy. The additive term solves the singularity problem of the Covariance matrix in steady state which makes GDLS appropriate for tracking processes with slowly varying parameters and has been utilized in some researches as [34–36]. GDLS uses recursively the unitary matrix for avoiding the singularity which causes the same problem in the regularized constant-trace [37] and increases the output estimation error. On the other hand, some researches [38–40] used the Singular Value Decomposition (SVD) in order to solve the singularity problem in LS; however, they did not come up with a suitable solution to the estimation wind-up caused by these singularities. Similar to the RLS equations, by applying insufficient excitations to the proposed control structure, the adaptation rules face the estimation wind-up.

The main contribution of the paper is devoted to providing a mathematical solution to the aforementioned problems and falls into the following topics: Finding controllers which ensure stability of the nonlinear or time varying systems and identify the system's parameters while the sufficient excitation is not provided for identification can be considered as a hot topic. For the sake of quick reference, a summary of the recently published works is presented in Table 1 and is compared with the proposed Robust adaptive method which outperforms the other methods in the addressed subject. Moreover, by inspiring from DLS and using SVD, a novel algorithm is introduced in this paper, which is referred to as SVD-DLS. This algorithm is applicable to the Multi-Input Multi-Output (MIMO) systems whereas the classic DLS and GDLS are introduced for the single-output systems. The combination of the robust adaptive approach and the proposed algorithm provides a considerable approach for the automatic control context. The proposed approach is implemented on a 3 Degree-Of-Freedom (DOF) Spherical Parallel Robot (SPR). By avoiding from challenges of model-based approaches, the unknown parameters are obtained without having any prior knowledge on traditional kinematics or dynamic calculations. In this regard, the notion of suggested approach bears resemblance to the automatic control methods. Nonetheless, avoiding from designing complicated policies or heavy computational expenses, the proposed structure is applicable in the robotic field in which the aforementioned automatic algorithms encounter implementation difficulties.

Table 1

A comparison of the proposed method with some of its counterparts.

Reference	Proposed LF	Stability	Identification	LTV model	NL model	MIMO
[42]	$V = \frac{\alpha_1 + q_1^2 + (\alpha_1 q_2)^2}{2\alpha_1} \mathbf{e}_1^T \mathbf{e}_1 + \frac{1}{2} \mathbf{y}^T \mathbf{M}(\theta) \mathbf{y}$	✓			✓	
[43]	$V = \frac{1}{2} \mathbf{e}^T \mathbf{P}_m \mathbf{e} + \frac{1}{2\eta} \text{tr}(\boldsymbol{\phi}^T \boldsymbol{\phi})$	✓			✓	✓
[44]	$V = \frac{1}{2} (\sum_{i=1}^{2n} x_i^2 + \sum_{i=1}^n (\frac{1}{\hat{\alpha}_i} (\hat{\alpha}_i - \alpha_i)^2 + \dots))$	✓	✓		✓	
[45]	$V = \frac{1}{2} \gamma \tilde{\mathbf{I}}^T \tilde{\mathbf{I}} + \frac{1}{2} \tilde{\mathbf{s}}^T \tilde{\mathbf{s}}$	✓				✓
[46]	$V = \frac{1}{2} \tilde{\mathbf{s}}^T \tilde{\mathbf{s}} + \frac{1}{2\eta} \text{tr}(\tilde{\mathbf{W}}^T \tilde{\mathbf{W}})$	✓				
[47]	$V_k = \frac{1}{2} S_k^2 + \frac{1-\gamma}{2\beta} \boldsymbol{\phi}_k^T \boldsymbol{\phi}_k + \frac{1}{2\rho} (\psi_k - \hat{\psi})^2$	✓		✓	✓	
Proposed Method	$V = \frac{1}{2} (\mathbf{S}^T \mathbf{S} + \sum_{q=1}^N \tilde{\boldsymbol{\theta}}_q^T \mathbf{R}_q \tilde{\boldsymbol{\theta}}_q)$	✓	✓	✓		✓

The remainder of the paper is organized as follows: In Section 2, notions, some applied definitions and the basic MIMO model are briefly reviewed. In Section 3, the proposed robust adaptive method is explained. By mapping the correlated regressors to an orthogonal space, the problem of insufficient excitation is solved in Section 4. By employing SVD-DLS, an optimal estimation is obtained to dampen the oscillations in the adaptive controllers under insufficient excitation. In this case, only partially identification of system parameters can be guaranteed in the orthogonal space. In Section 5, the regularized constant-trace, Kaczmarz [41], and GDLS are compared with SVD-DLS in the robust adaptive method from varied indices point of view. In Section 6, the proposed approach is implemented on a 3-DOF SPR. Finally, the paper concludes with some hints and remarks as ongoing works.

2. Preliminaries

2.1. Notations and definitions

In the paper, \mathfrak{R}^n denotes a real n vectors, $\mathfrak{R}^{m \times n}$ denotes a real $m \times n$ matrices, \mathbf{I} represents the identity matrix with appropriate dimension. Moreover, $|\cdot|$ represents the absolute value of its scalar argument, $\|\cdot\|$ indicates the Euclidean norm of its vector argument, and $\text{tr}(\cdot)$ denotes the trace of its matrix argument. Also, $(\cdot)^T$ is written to denote the transpose operation. The hat mark ($\hat{\cdot}$) on each parameter stands for the estimated value of that parameter by the identifier. Likewise, the tilde mark ($\tilde{\cdot}$) on each parameter shows error value of the identified parameter from its real value. Finally, the sign function, $\text{sign}(z)$, is defined as $\text{sign}(z) = \begin{cases} 1 & z \geq 0 \\ -1 & z < 0 \end{cases}$.

2.2. Time-varying MIMO model

In the next part, a time-varying MIMO model is introduced in which a novel DLS method will be applied in order to solve the insufficient excitation problem.

In this part, in order to fit behaviors of basic systems in the identification procedure, models with MIMO square transfer functions with no element zeros are taken into account. Moreover, a system under these procedures should be minimum phase. In this paper, data of inputs and outputs of the basic system are utilized and the only pre-required information is the dynamic rank of each output channel. The basic time-varying model of MIMO systems is considered as:

$$\mathbf{G}(S) = \left[\frac{b_{qj}}{S^{n_q} - a_{qnq}(t)S^{n_q-1} - \dots - a_{q1}(t)} \right]_{N \times N} \tag{1}$$

$\forall q = 1, \dots, N, \forall j = 1, \dots, N$

where the Laplace variable is shown with symbol S . Also, q is a general channel indicator (in fact refers to all channels) and j refers to the index of input. Each output channel differential equation can be written as:

$$\mathbf{y}_q^{[n_q]} = \mathbf{a}_q^T(t) \mathbf{y}_q + \mathbf{b}_q^T(t) \mathbf{u} + d_q(t) = \boldsymbol{\theta}_q^T(t) \boldsymbol{\Phi}_q + d_q(t) \tag{2}$$

where n_q denotes the dynamic rank of q th output. d_q is a bounded disturbance in q th channel, whose upper bound is considered as \hat{d}_q . Also for each channel, vectors of denominator coefficients, nominator coefficients, system parameters, output signal regressors, input signals, and channel regressors are shown with $\mathbf{a}_q^T(t) \in \mathbb{R}^{n_q}$, $\mathbf{b}_q^T(t) \in \mathbb{R}^N$, $\boldsymbol{\theta}_q^T(t) \in \mathbb{R}^{N+n_q}$, $\mathbf{y}_q^T \in$

\mathbb{R}^{n_q} , $\mathbf{u} \in \mathbb{R}^N$, $\Phi_q \in \mathbb{R}^{N+n_q}$ respectively:

$$\begin{aligned} \mathbf{a}_q^T &= [a_{q_{n_q}}, a_{q_{n_q-1}}, \dots, a_{q_1}], \quad \mathbf{b}_q^T = [b_{qj}^T]_{1 \times N}, \quad \boldsymbol{\theta}_q^T = [\mathbf{a}_q^T, \mathbf{b}_q^T], \\ \mathbf{y}_q^T &= [y_q^{[n_q-1]}, y_q^{[n_q-2]}, y_q^{[1]}, y_q], \quad \mathbf{u} = [u_j]_{N \times 1}, \quad \Phi_q = \begin{bmatrix} \mathbf{y}_q \\ \mathbf{u} \end{bmatrix}. \end{aligned} \quad (3)$$

While there is no dependencies between regressors of each channel, Eq. (2) is the basic differential equation of q th channel.

Assumption 1. : The matrix $\mathbf{B} = [b_{qj}]_{N \times N}$ is diagonally dominant if condition $|b_{qq}| > \sum_{j \neq q} b_{qj}$ is established for q th output channel [48].

Assumption 2. The transfer function parameters are considered as slowly varying parameters with the following formulation:

$$\forall q, \forall t \geq 0 : \|\dot{\boldsymbol{\theta}}_q(t)\| < \rho_q \quad (4)$$

where, ρ_q is the upper bound of the parameters' variation in each output channel.

3. Identification of models via a robust adaptive algorithm

In the following, equations of the identifier are explained. Sliding rules force the system to gain the prescribed target features by sliding along a cross-section of the system's normal behavior. In order to track the output signals and reduce the output error, sliding rules at each channel are defined:

$$s_q = \left(\frac{d}{dt} + \lambda_q \right)^{n_q-1} \tilde{y}_q = \Lambda \mu_q^T \tilde{\mathbf{y}}_q \quad (5)$$

where

$$\Lambda \mu_q^T = [1, \dots, (n_q - 1)\lambda_q^{n_q-2}, \lambda_q^{n_q-1}] \quad (6)$$

and

$$\tilde{\mathbf{y}}_q = \mathbf{y}_q - \mathbf{y}_{r_q}. \quad (7)$$

The desired signals, y_{r_q} , are continuous and considerably smooth. Vectors of output desired regressors and output error regressors in each channel are shown with:

$$\mathbf{y}_{r_q}^T = [y_{r_q}^{[n_q-1]}, \dots, y_{r_q}^{[1]}, y_{r_q}] \quad (8)$$

and

$$\tilde{\mathbf{y}}_q^T = [\tilde{y}_q^{[n_q-1]}, \dots, \tilde{y}_q^{[1]}, \tilde{y}_q]. \quad (9)$$

In the above, s_q denotes the sliding variable in each channel. In order to analyze sliding surfaces, the derivative of sliding vector, $\dot{\mathbf{S}}$, in each channel should be studied. Based on these derivatives, control inputs, $\hat{\mathbf{u}}$, are defined, which force the system to reach the given sliding surfaces. The vector of input signals is applied to the system based on:

$$\mathbf{u} = \hat{\mathbf{u}} - \boldsymbol{\eta} \text{sign}(\mathbf{S}) \quad (10)$$

where,

$$\hat{\mathbf{u}} = -\hat{\mathbf{B}}^{-1}(\tilde{\boldsymbol{\Gamma}} + \boldsymbol{\Gamma}_{\hat{a}} - \boldsymbol{\Gamma}_r), \quad \mathbf{S} = \begin{bmatrix} s_1 \\ \vdots \\ s_N \end{bmatrix} \in \mathbb{R}^N, \quad \boldsymbol{\eta} = \begin{bmatrix} \eta_1 & 0 & 0 \\ 0 & \ddots & 0 \\ 0 & 0 & \eta_N \end{bmatrix} \quad (11)$$

and

$$\begin{aligned} \hat{\mathbf{B}} &= \begin{bmatrix} \hat{\mathbf{b}}_1^T \\ \vdots \\ \hat{\mathbf{b}}_N^T \end{bmatrix} \in \mathbb{R}^{N \times N}, \quad \tilde{\boldsymbol{\Gamma}} = \begin{bmatrix} \Lambda \mu_{s_1}^T \tilde{\mathbf{y}}_1 \\ \vdots \\ \Lambda \mu_{s_N}^T \tilde{\mathbf{y}}_N \end{bmatrix} \in \mathbb{R}^N, \\ \boldsymbol{\Gamma}_{\hat{a}} &= \begin{bmatrix} \hat{\mathbf{a}}_1^T \mathbf{y}_1 \\ \vdots \\ \hat{\mathbf{a}}_N^T \mathbf{y}_N \end{bmatrix} \in \mathbb{R}^N, \quad \boldsymbol{\Gamma}_r = \begin{bmatrix} y_{r_1}^{[n_1]} \\ \vdots \\ y_{r_N}^{[n_N]} \end{bmatrix} \in \mathbb{R}^N. \end{aligned} \quad (12)$$

Remark 1. The parameter, η , introduced in Eq. (11), is determined such that $\forall q: \eta_q b_{qq} > 0$ and $\forall q: |\eta_q| > \frac{\bar{d}_q}{|b_{qq}| - \sum_{j=1, j \neq q}^N |b_{qj}|}$ are simultaneously yielded.

The derivative of the sliding vector can be calculated as follows:

$$\dot{\mathbf{S}} = - \begin{bmatrix} \tilde{\mathbf{b}}_1^T \\ \vdots \\ \tilde{\mathbf{b}}_N^T \end{bmatrix} \hat{\mathbf{u}} + \begin{bmatrix} \tilde{\mathbf{a}}_1^T \tilde{\mathbf{y}}_1 \\ \vdots \\ \tilde{\mathbf{a}}_N^T \tilde{\mathbf{y}}_N \end{bmatrix} - \mathbf{B}\eta \text{sign}(\mathbf{S}) + \mathbf{d} \tag{13}$$

where, $\mathbf{d} = [d_1 \ \dots \ d_N]^T$ is the output disturbance vector. The error equation for each output channel is calculated by the following relation:

$$e_q(t) = y_{r_q}^{[n_q]}(t) - y_q^{[n_q]}(t) = \Phi_q^T(t) \tilde{\theta}_q(t) + d_q(t) \tag{14}$$

where $\tilde{\theta}_q(t) \in \mathbb{R}^{N+n_q}$ denotes the identification error of system parameters. The RLS method is the best candidate for estimation of the system parameters in each channel. In this regard, the symmetric Covariance matrix of each channel regressors is shown with:

$$\mathbf{R}_q(t) = \int_0^t e^{-\alpha_q(t-\tau)} \Phi_q(\tau) \Phi_q^T(\tau) d\tau \tag{15}$$

where the initial value is set $\mathbf{R}_q(0) = g \mathbf{I}_{N+n_q}$, $g \gg 1$ and the following dynamic equation is obtained for each channel:

$$\dot{\mathbf{R}}_q(t) = -\alpha_q \mathbf{R}_q(t) + \Phi_q(t) \Phi_q^T(t) \tag{16}$$

where α_q denotes forgetting factor of q th channel.

Remark 2. In RLS methods, the system parameters, θ_q , are traceable if the regressors of the system, $\Phi_q(t)$, are at least Persistent Excited (PE) with order $N + n_q$, which is the number of parameters required to be estimated at each channel [24]. Therefore, in the case that the system regressors are sufficient PE, model parameters are traceable and Covariance matrix, \mathbf{R}_q , always remains positive definite. On the other hand, any PE signal with order less than $N + n_q$ is considered as insufficient excitation.

Having sufficient excitation for all channels, the following inequalities hold:

$$\forall t > 0, \forall q: 0 < \underline{\sigma}_q \mathbf{I}_{N+n_q} \leq \mathbf{R}_q(t) \leq \bar{\sigma}_q \mathbf{I}_{N+n_q} \tag{17}$$

where, $\underline{\sigma}_q$ and $\bar{\sigma}_q$ are the smallest and largest singular values of \mathbf{R}_q .

Suggested adaptation rules as for estimation of model parameters are shown in Eq. (18). The first part is concerned with adaptive changes based on sliding values. After reaching sliding surfaces, this part is eliminated and only the second part affects adaptation rules. The second part states for the updating rule of continuous-time RLS:

$$\begin{bmatrix} \hat{\mathbf{a}}_q \\ \hat{\mathbf{b}}_q \end{bmatrix} = \mathbf{R}_q^{-1}(t) \left(\Phi_q(t) e_q(t) + \underbrace{\begin{bmatrix} \mathbf{y}_q \\ -\hat{\mathbf{u}} \end{bmatrix}}_{\phi_q(t)} s_q(t) \right), \forall q = 1, 2, \dots, N. \tag{18}$$

In Fig. 1, a diagram of the proposed controller is demonstrated, which comprises different function blocks. Each block represents an equation from the proposed approach trying to visualize the identification of MIMO models via the robust adaptive algorithm.

Theorem 1. Regarding to time-invariant version of the MIMO model described in Eq. (1), based on Assumption 1 and Remark 1, and for the sufficient excitation condition, perfect identification of the model and tracking the desired signals are guaranteed. Moreover, the closed-loop system remains asymptotically stable during the procedure [27].

In addition to the aforementioned theorem, it can be shown that the proposed controller is applicable in the case of having linear time-variant systems with bounded disturbance. The required theorems are presented as follows.

Theorem 2. Having the system presented in Eq. (1) with sufficient excitation condition and considering Assumption 1 and Assumption 2, the identification error of system parameters is guaranteed to be bounded with the following upper bound:

$$\|\tilde{\theta}\|_{\text{stv}}^{\max} = N \times \max_{q=1,2,\dots,N} \left(\frac{2\rho_q \bar{\sigma}_q}{\alpha_q \underline{\sigma}_q} \right) \tag{19}$$

Moreover, the tracking error of each output signal is guaranteed to be bounded, where the relating upper bound is formulated as follows:

$$\bar{c}_{\text{stv}}^q = \frac{\|\tilde{\theta}\|_{\text{stv}}^{\max} \sqrt{2\sigma}}{\lambda_q^{n_q-1}}$$

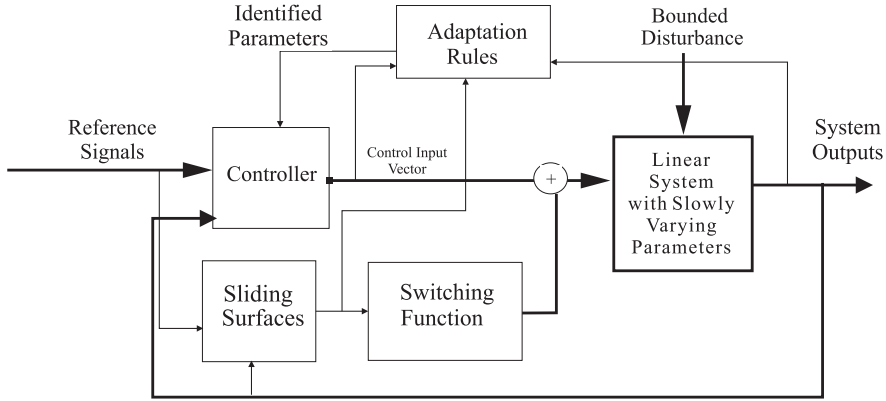


Fig. 1. The block diagram of the proposed robust adaptive control approach.

$$0 < \underline{\sigma} = \min\{\underline{\sigma}_1, \dots, \underline{\sigma}_N\}$$

and the closed-loop system stays Uniformly Ultimately Bounded (UUB) stable [49].

The corresponding proof is provided in Appendix Section, part A.

Theorem 3. For the considered system presented in Eq. (1) with sufficient excitation condition and an error upper bound as $\bar{\mathbf{d}} = [\bar{d}_q]_{N \times 1}$, and keeping with Assumption 1 and Remark 1, the identified parameters are guaranteed to converge to the vicinity of their real values:

$$\|\tilde{\boldsymbol{\theta}}(t \rightarrow \infty)\| \leq \|\tilde{\boldsymbol{\theta}}\|_{\text{dist}}^{\max} \quad (20)$$

where

$$\tilde{\boldsymbol{\theta}}^T = [\tilde{\boldsymbol{\theta}}_1^T, \dots, \tilde{\boldsymbol{\theta}}_N^T].$$

Furthermore, the tracking errors of the desired output signals are guaranteed to be bounded; the upper bounds are formulated as follows:

$$|\tilde{y}_q(t)| \leq \bar{c}_{\text{dist}}^q \quad (21)$$

where

$$\bar{c}_{\text{dist}}^q = \frac{\|\tilde{\boldsymbol{\theta}}\|_{\text{dist}}^{\max} \sqrt{2\underline{\sigma}}}{\lambda_q^{n_q-1}}$$

and the closed-loop system stays UUB stable.

Theorem 3 can be proved with some modifications in a similar procedure to what has been prepared in Appendix A for Theorem 2.

4. Robust adaptive scheme with SVD-DLS

In the following, a solution to improve the identification ability of the robust adaptive frame under insufficient excitations is presented. By taking Eq. (18) into account, the adaptation rules can be reformed as follows:

$$\hat{\boldsymbol{\theta}}_q(t) = \mathbf{R}_q^{-1}(t) \underbrace{(\boldsymbol{\Phi}_q(t)e_q(t) + \boldsymbol{\phi}_q(t)s_q(t))}_{\mathbf{E}_q(t)}. \quad (22)$$

The mutual vector of input-output regressors can be expressed as:

$$\mathbf{F}_q(t) = \int_{t_0}^t e^{-\alpha_q(t-\tau)} (\boldsymbol{\Phi}_q(\tau)y_{r_q}^{[n_q]}(\tau) + \boldsymbol{\phi}_q(\tau)s_q(\tau)) d\tau \quad (23)$$

where:

$$\dot{\mathbf{F}}_q(t) = -\alpha_q \mathbf{F}_q(t) + (\boldsymbol{\Phi}_q(t)y_{r_q}^{[n_q]}(t) + \boldsymbol{\phi}_q(t)s_q(t)). \quad (24)$$

In the case of having sufficient excitation, the Covariance matrix of q th channel remains invertible and the estimated parameters are considered as follows:

$$\hat{\boldsymbol{\theta}}_q(t) = \mathbf{R}_q^{-1}(t) \mathbf{F}_q(t). \quad (25)$$

By deriving $\hat{\boldsymbol{\theta}}_q(t)$ and using the error equation for each output channel in Eq. (14), the following calculations are obtained:

$$\begin{aligned} \dot{\hat{\boldsymbol{\theta}}}_q(t) &= -\mathbf{R}_q^{-1} \dot{\mathbf{R}}_q(t) \mathbf{R}_q^{-1} \mathbf{F}_q(t) + \mathbf{R}_q^{-1} \dot{\mathbf{F}}_q(t) \\ &= \alpha_q \mathbf{R}_q^{-1} \mathbf{F}_q(t) - \mathbf{R}_q(t) \boldsymbol{\Phi}_q(t) \boldsymbol{\Phi}_q^T(t) \mathbf{R}_q^{-1} \mathbf{F}_q(t) \\ &\quad - \alpha_q \mathbf{R}_q^{-1} \mathbf{F}_q(t) + \mathbf{R}_q^{-1} \left(\boldsymbol{\Phi}_q(t) y_{r_q}^{[n_q]}(t) + \boldsymbol{\phi}_q(t) s_q(t) \right) \\ &= \mathbf{R}_q^{-1}(t) \left(\boldsymbol{\Phi}_q(t) e_q(t) + \boldsymbol{\phi}_q(t) s_q(t) \right) = \mathbf{R}_q^{-1}(t) \mathbf{E}_q(t). \end{aligned} \quad (26)$$

It is demonstrated that the same adaptation rules in Eq. (22) are obtained. In fact, these rules can be regarded as an extended RLS estimation, which reduces both estimation errors and tracking errors during the adaptive control procedure. As in the classic version, this extended RLS (adaptation rules) faces estimation wind-up under insufficient excitations. If at least for one channel (the i th channel) desired output signal is not sufficient excited, the matrix $\mathbf{R}_i(t)$ becomes positive semi-defined after a while. Hence, some dependency relations happen between regressors of the i th channel.

Assumption 3. It is assumed that nullity of \mathbf{R}_i happens in the interval $[t_0, t]$, while $\mathbf{R}_{\forall q \neq i}(t)$ is positive definite in this interval. Moreover, $\mathbf{R}_i(t_0)$ is a full rank matrix and the nullity rank of \mathbf{R}_i equals n_w .

Predicated on Assumption 3, in $[t_0, t]$, the adaptation rules are not established, although for the rest of channels the following inequalities can be still formulated:

$$\forall t \in [t_0, t] : 0 < \underline{\sigma}_q \mathbf{I}_{N+n_q} \leq \mathbf{R}_{\forall q \neq i}(t) \leq \bar{\sigma}_q \mathbf{I}_{N+n_q}$$

where, $\underline{\sigma}_q$ and $\bar{\sigma}_q$ are the smallest and largest singular values of \mathbf{R}_q in the interval $[t_0, t]$.

Singular value decomposition of the symmetric Covariance matrix of i th channel leads to the following equation:

$$\mathbf{R}_i(t) = \underbrace{\begin{bmatrix} \mathbf{V}_{\text{nul}}^i(t) & \mathbf{V}_p^i(t) \end{bmatrix}}_{\mathbf{V}^i(t)} \begin{bmatrix} \boldsymbol{\Lambda}_{\text{nul}}^i & 0 \\ 0 & \boldsymbol{\Lambda}_p^i(t) \end{bmatrix} \underbrace{\begin{bmatrix} \mathbf{V}_{\text{nul}}^{i\text{T}}(t) \\ \mathbf{V}_p^{i\text{T}}(t) \end{bmatrix}}_{\mathbf{V}^{i\text{T}}(t)} \quad (27)$$

where, the diagonal matrix $\boldsymbol{\Lambda}_{\text{nul}}^i \in \mathbb{R}^{n_w^i \times n_w^i}$ contains the first n_w^i zero eigenvalues (n_w^i shows the rank deficiency of i th channel Covariance matrix) and the diagonal matrix $\boldsymbol{\Lambda}_p^i \in \mathbb{R}^{n_p^i \times n_p^i}$ contains the rest of eigenvalues (the next n_p^i) which means $\lambda_l^i > 0$, $l = n_w^i + 1, \dots, n_i$. Therefore, $\mathbf{R}_i(t)$ can be written as:

$$\mathbf{R}_i(t) = \underbrace{\mathbf{V}_p^i(t) \boldsymbol{\Lambda}_p^i(t) \mathbf{V}_p^{i\text{T}}(t)}_{\mathbf{R}_p^i(t)}. \quad (28)$$

By using $\mathbf{V}^i(t) \in \mathbb{R}^{n_i \times n_i}$ as a transformation matrix, regressors are mapped from the initial space to an orthogonal space:

$$\mathbf{Z}_i(\tau) = \mathbf{V}^{i\text{T}}(t) \boldsymbol{\Phi}_i(\tau) = \begin{bmatrix} \mathbf{V}_{\text{nul}}^{i\text{T}}(t) \boldsymbol{\Phi}_i \\ \mathbf{V}_p^{i\text{T}}(t) \boldsymbol{\Phi}_i \end{bmatrix} = \begin{bmatrix} 0 \\ \mathbf{Z}_{\text{red}}(\tau) \end{bmatrix} \quad (29)$$

$$\forall \tau \in [t_0, t]$$

where $\mathbf{Z}_i \in \mathbb{R}^{n_i}$ denotes the matrix of orthogonal regressors and $\mathbf{Z}_{\text{red}_i} \in \mathbb{R}^{n_p^i}$ denotes the matrix of orthogonal reduced-order regressors in channel i . Moreover, n_p^i is the dynamic rank of the i th channel in the orthogonal space.

The vector of reduced-order estimated system parameters is shown with $\hat{\boldsymbol{\zeta}}_{\text{red}_i}(t) \in \mathbb{R}^{n_p^i}$ and based on Eq. (29), can be related to the estimated system parameters $\hat{\boldsymbol{\theta}}_i(t)$ by the following equation: $\hat{\boldsymbol{\theta}}_i(t) = \mathbf{V}_p^i(t) \hat{\boldsymbol{\zeta}}_{\text{red}_i}(t)$. Using the least square estimation in the orthogonal space, the following equation is obtained:

$$\hat{\boldsymbol{\zeta}}_{\text{red}_i}(t) = \mathbf{R}_{\text{red}_i}^{-1} \mathbf{F}_{\text{red}_i} \quad (30)$$

where, $\mathbf{R}_{\text{red}_i}^{-1} \in \mathbb{R}^{n_p^i \times n_p^i}$ (the reduced-order Covariance matrix of regressors in i th channel) and $\mathbf{F}_{\text{red}_i}$ (the reduced-order mutual vector of input-output regressors in i th channel) are calculated according to the following equations:

$$\mathbf{R}_{\text{red}_i}(t) = \int_{t_0}^t e^{-\alpha_i(t-\tau)} \mathbf{Z}_{\text{red}_i}(\tau) \mathbf{Z}_{\text{red}_i}^T(\tau) d\tau$$

$$\begin{aligned}
&= \int_{t_0}^T e^{-\alpha_i(t-\tau)} \mathbf{V}_p^i{}^T(t) \Phi_i(\tau) \Phi_i^T(\tau) \mathbf{V}_p^i(t) d\tau \\
&= \mathbf{V}_p^i{}^T(t) \mathbf{R}_i(t) \mathbf{V}_p^i(t)
\end{aligned} \tag{31}$$

$$\begin{aligned}
\mathbf{F}_{z_{red_i}}(t) &= \int_{t_0}^T e^{-\alpha_i(t-\tau)} (\mathbf{Z}_{red_i}(\tau) y_{r_i}^{[n_i]}(\tau) + \phi_{z_i}(\tau) s_i(\tau)) d\tau \\
&= \int_{t_0}^T e^{-\alpha_i(t-\tau)} (\mathbf{V}_p^i{}^T(t) \Phi_i(\tau) y_{r_i}^{[n_i]}(\tau) \\
&\quad + \mathbf{V}_p^i{}^T(t) \phi_i(\tau) s_i(\tau)) d\tau \\
&= \mathbf{V}_p^i{}^T(t) \mathbf{F}_i(t).
\end{aligned} \tag{32}$$

Based on Eq. (31), $\mathbf{R}_{z_{red_i}}(t)$ remains positive definite in the interval $[t_0, t]$ and accordingly, the following inequalities are stated:

$$\forall t \in [t_0, t] : 0 < \underline{\sigma}_{z_i} \mathbf{I}_{n_p} \leq \mathbf{R}_{z_{red_i}}(t) \leq \bar{\sigma}_{z_i} \mathbf{I}_{n_p}$$

where, $\underline{\sigma}_{z_i}$ and $\bar{\sigma}_{z_i}$ are the smallest and largest singular values of $\mathbf{R}_{z_{red_i}}$ in the interval $[t_0, t]$. Therefore, utilizing the similar procedure in the Eq. (26), the adaptation rules are shown in the orthogonal space as follows:

$$\hat{\boldsymbol{\zeta}}_{red_i}(t) = \mathbf{R}_{z_{red_i}}^{-1} \mathbf{E}_{z_{red_i}} \tag{33}$$

where

$$\mathbf{E}_{z_{red_i}}(t) = \mathbf{Z}_{red_i}(t) e_i(t) + \phi_{z_i}(t) s_i(t) \tag{34}$$

In the aforementioned procedure, the derivative of reduced-order Covariance matrix of regressors in i th channel should be substituted from the following equation calculated from Eq. (31):

$$\dot{\mathbf{R}}_{z_{red_i}}(t) = -\alpha_i \mathbf{R}_{z_{red_i}}(t) + \mathbf{Z}_{red_i}(t) \mathbf{Z}_{red_i}^T(t). \tag{35}$$

By returning to the initial space, the following answers are estimated for system parameters:

$$\begin{aligned}
\hat{\boldsymbol{\theta}}_{\beta_i}(t) &= \mathbf{V}^i(t) \begin{bmatrix} \boldsymbol{\beta}_i(t) \\ \hat{\boldsymbol{\zeta}}_{red_i}(t) \end{bmatrix} \\
&= \mathbf{V}_{nul}^i \boldsymbol{\beta}_i(t) + \underbrace{\mathbf{V}_p^i(t) \mathbf{R}_{z_{red_i}}^{-1}(t) \mathbf{F}_{z_{red_i}}^T(t)}_{\hat{\boldsymbol{\theta}}_i(t)}.
\end{aligned} \tag{36}$$

From Eq. (26), the dynamic of $\hat{\boldsymbol{\theta}}_i(t)$ is calculated as:

$$\begin{aligned}
\dot{\hat{\boldsymbol{\theta}}}_i(t) &= \frac{d}{dt} \left(\mathbf{V}_p^i(t) \Lambda_p^{i-1}(t) \mathbf{V}_p^i{}^T(t) \right) \mathbf{F}_i(t) + \left(\mathbf{V}_p^i(t) \Lambda_p^{i-1}(t) \mathbf{V}_p^i{}^T(t) \right) \dot{\mathbf{F}}_i(t) \\
&= \mathbf{V}_p^i(t) \Lambda_p^{i-1}(t) \mathbf{V}_p^i{}^T(t) \mathbf{E}_i(t).
\end{aligned} \tag{37}$$

In the above, $\boldsymbol{\beta}_i(t)$ is utilized to damped the oscillations. In each moment, by selecting the optimal value of $\boldsymbol{\beta}_i(t)$, the variation of $\hat{\boldsymbol{\theta}}_{\beta_i}(t)$ is minimized:

$$\boldsymbol{\beta}_i^*(t) = \arg \min_{\boldsymbol{\beta}_i} \|\hat{\boldsymbol{\theta}}_{\beta_i}(t)\|. \tag{38}$$

Finally, the adaptation rules with SVD-DLS algorithm are calculated as:

$$\hat{\boldsymbol{\theta}}_{\beta_i}(t) = \hat{\boldsymbol{\theta}}_i(t) + \mathbf{V}_{nul}^i \boldsymbol{\beta}_i^*(t) \tag{39}$$

where:

$$\begin{aligned}
\dot{\boldsymbol{\beta}}_i^*(t) &= - \left(\mathbf{V}_{nul}^i{}^T \mathbf{V}_{nul}^i \right)^{-1} \mathbf{V}_{nul}^i{}^T \dot{\hat{\boldsymbol{\theta}}}_i(t), \quad \boldsymbol{\beta}_i^*(t_0) = \mathbf{0} \\
\hat{\boldsymbol{\theta}}_i(t) &= \mathbf{V}_p^i(t) \Lambda_p^{i-1}(t) \mathbf{V}_p^i{}^T(t) \mathbf{E}_i(t).
\end{aligned} \tag{40}$$

Theorem 4. For each MIMO system described in the output channel differential Eq. (2), by considering Assumptions 1, 2, 3, and Remark 1, and by mapping the regressors of the channel with rank deficiency to an orthogonal space and reducing its rank, the identified parameters are guaranteed to converge to the vicinity of an equivalent model:

$$\|\tilde{\boldsymbol{\theta}}_z(t \rightarrow \infty)\| \leq \|\tilde{\boldsymbol{\theta}}_z\|_{\max}$$

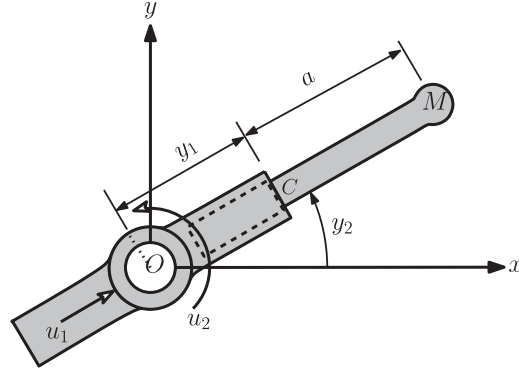


Fig. 2. A 2-DOF planar serial manipulator, the schematic is adopted from Ha et al. [41].

where

$$\tilde{\theta}_z^T = [\tilde{\theta}_1^T, \dots, \tilde{\zeta}_{\text{red}_i}^T, \dots, \tilde{\theta}_N^T]$$

Moreover, the tracking error of each channel (\tilde{y}_q) is guaranteed to be bounded:

$$\forall q : |\tilde{y}_q(t \rightarrow \infty)| \leq \bar{c}_z^q$$

where

$$\bar{c}_z^q = \|\tilde{\theta}_z\|_{\max} \frac{\sqrt{2\sigma_z}}{\lambda_q^{n_q-1}}$$

$$0 < \sigma_z = \min\{\sigma_1, \dots, \sigma_{z_i}, \dots, \sigma_N\}$$

and the closed-loop system stays UUB stable.

The corresponding proof is presented in Appendix Section, part B. Predicated on [Theorem 4](#), the proposed algorithm is an applicable method to simultaneously identification and control of LTV systems with bounded disturbance under insufficient excitation. In order to demonstrate its performance, in [Section 5](#), a numerical simulation is presented.

5. Numerical simulation

In this section, the application of SVD-DLS in the robust adaptive scheme is studied. Two-degree-of-freedom robot arms are applicable in the automation and factories. One-joint robots, as demonstrated in [Fig. 2](#), with the freedom of rotational angles and the length of arm are one of these robots. The dynamic equations of robot arms can be formulated as a nonlinear dynamic system [\[41\]](#) as below:

$$\begin{cases} y_1^{[2]} = \frac{[\mu y_1 + M(y_1 + a)]\dot{y}_2^2 + u_1}{\mu + M} \\ y_2^{[2]} = \frac{-2[\mu y_1 + M(y_1 + a)]\dot{y}_1\dot{y}_2 + u_2}{J_1 + J_2 + \mu y_1^2 + M(y_1 + a)^2} \end{cases} \quad (41)$$

In the above equation, y_1 is the variation of the arm length and y_2 shows the arm angle toward horizon. Also, u_1 is impeller force exerted on the arm and u_2 is the rotational force exerted on the joint. Mass of the arm and the located object on the arm are shown with μ and M , respectively. Also, the inertial moment of the arm toward the mass center and toward the arm origin are shown with J_1 and J_2 . The adaptive linear model of the nonlinear system is calculated as follows:

$$y_1^{[2]}(t) = a_{11}(t)y_1(t) + a_{12}(t)\dot{y}_1(t) + a_{13}(t)y_2(t) + a_{14}(t)\dot{y}_2(t) + b_{11}(t)u_1(t) + d_1(t) \quad (42)$$

where

$$\begin{aligned} a_{11}(t) &= \frac{[\mu + M]\dot{y}_2^2}{\mu + M}, \quad a_{12}(t) = a_{13}(t) = 0 \\ a_{14}(t) &= \frac{2[\mu y_1 + M(y_1 + a)]\dot{y}_2}{\mu + M}, \quad b_{11}(t) = \frac{1}{\mu + M} \end{aligned} \quad (43)$$

and

$$y_2^{[2]}(t) = a_{21}(t)y_2(t) + a_{22}(t)\dot{y}_2(t) + a_{23}(t)y_1(t) + a_{24}(t)\dot{y}_1(t) + b_{22}(t)u_2(t) + d_2(t) \quad (44)$$

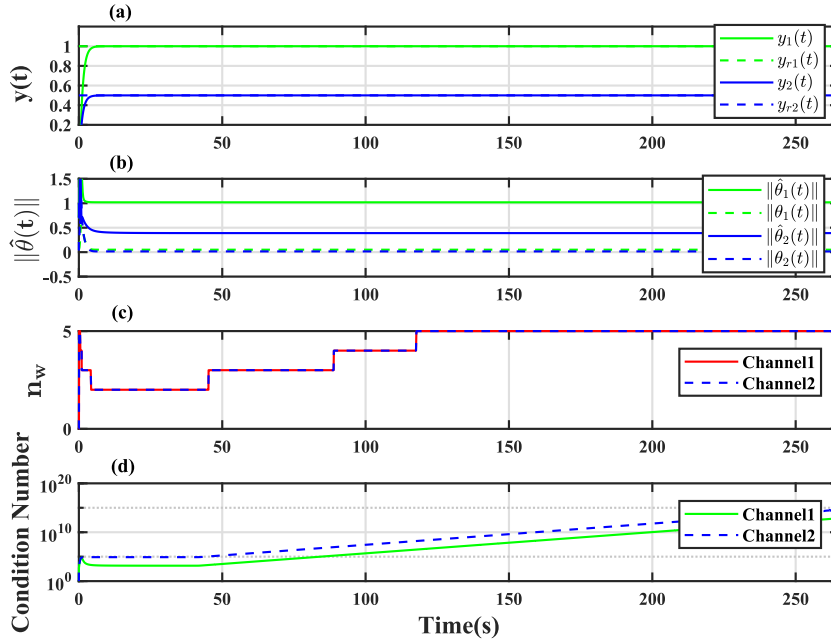


Fig. 3. The signals of robot arm by applying pulse desired outputs: (a) the system output signals (b) the norm of parameters vector (c) the nullity of \mathbf{R}_1 and \mathbf{R}_2 (d) the condition number of \mathbf{R}_1 and \mathbf{R}_2 .

where

$$\begin{aligned}
 a_{21}(t) &= 0, \quad a_{22}(t) = \frac{-2[\mu y_1 + M(y_1 + a)]\dot{y}_1}{J_1 + J_2 + \mu y_1^2 + M(y_1 + a)^2} \\
 a_{23}(t) &= \frac{-2[\mu + M]\dot{y}_1\dot{y}_2}{J_1 + J_2 + \mu y_1^2 + M(y_1 + a)^2} \\
 &\quad + \frac{-4[\mu y_1 + M(y_1 + a)]^2\dot{y}_1\dot{y}_2 + 2u_2[\mu y_1 + M(y_1 + a)]}{(J_1 + J_2 + \mu y_1^2 + M(y_1 + a)^2)^2} \\
 a_{24}(t) &= \frac{-2[\mu y_1 + M(y_1 + a)]\dot{y}_2}{J_1 + J_2 + \mu y_1^2 + M(y_1 + a)^2} \\
 b_{22} &= \frac{1}{J_1 + J_2 + \mu y_1^2 + M(y_1 + a)^2}
 \end{aligned} \tag{45}$$

and $d_1(t)$, $d_2(t)$ are unknown disturbances. By substitution of $\mu = M = 10$, $J_1 = J_2 = 10$, and $a = 1$ coefficients of the model are obtained. In the following by choosing $T = 0.001$, $\alpha_q = 0.1$, $\lambda_q = 1$, $\eta_q = 10$, and pulse desired signals, simulation results of the robust adaptive approach from Section 3 are demonstrated in Fig. 3.

Moreover, it is demonstrated that by applying persistent excitation to both channels, the output signals are controlled. Except in switching times, tracking the systems parameters is possible. Considering Fig. 3(c), the condition number of both channels remains bounded and the closed-loop system can be operated in this long-term situation. However, by applying insufficient excitation to channels, as shown in Fig. 4, the condition number increases gradually and makes the control and identification procedures impossible.

Considering Eqs. (43) and (45), most of coefficients vanish by applying constant signals and Covariance matrices gradually get closer to the singularity. Therefore, the identification error of system parameters increases and the adaptation rules are not able to converge to any bounded values. Consequently, the application of SVD-DLS in the robust adaptive scheme, described in Section 4, is adopted to tolerate ill-conditioned matrices. In Fig. 5, it is demonstrated that the nullity rank of Covariance matrices is considerable, but SVD-DLS decreases the identification error and forces the system remain under identification and control in the long-term procedure.

In order to analyze and compare varied algorithms quantitatively, Oscillation Number Index (ONI) of the system under study, introduced in [50,51] is employed. In this regard:

$$J_q^1 = \int \sqrt{\tilde{\theta}_q(\tau)^2 + \tilde{\theta}_q(\tau)^2} d\tau \tag{46}$$

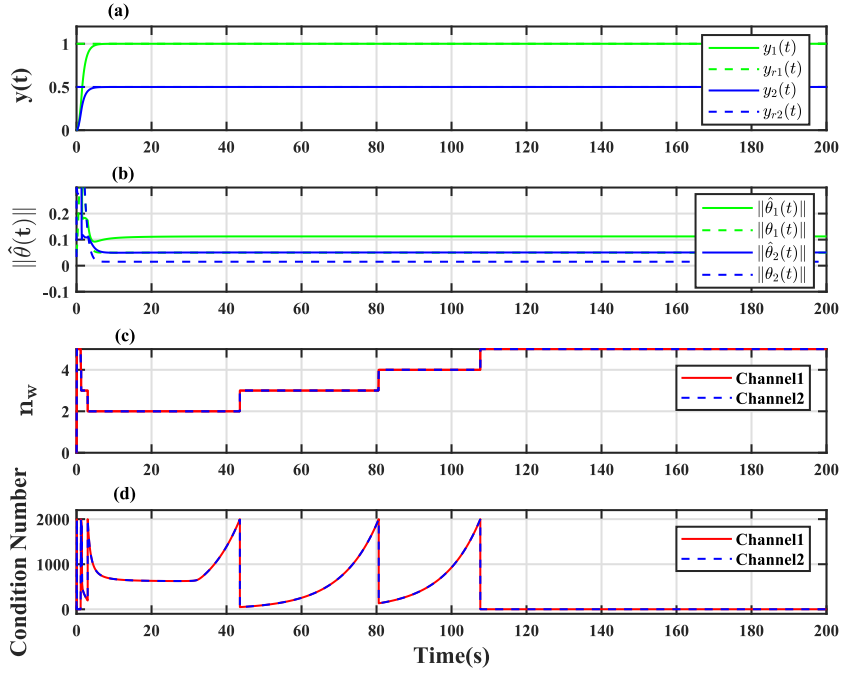


Fig. 4. The signals of robot arm by applying constant desired outputs: (a) the system output signals (b) the norm of parameters vector (c) the nullity of \mathbf{R}_1 and \mathbf{R}_2 (d) the condition number of \mathbf{R}_1 and \mathbf{R}_2 .

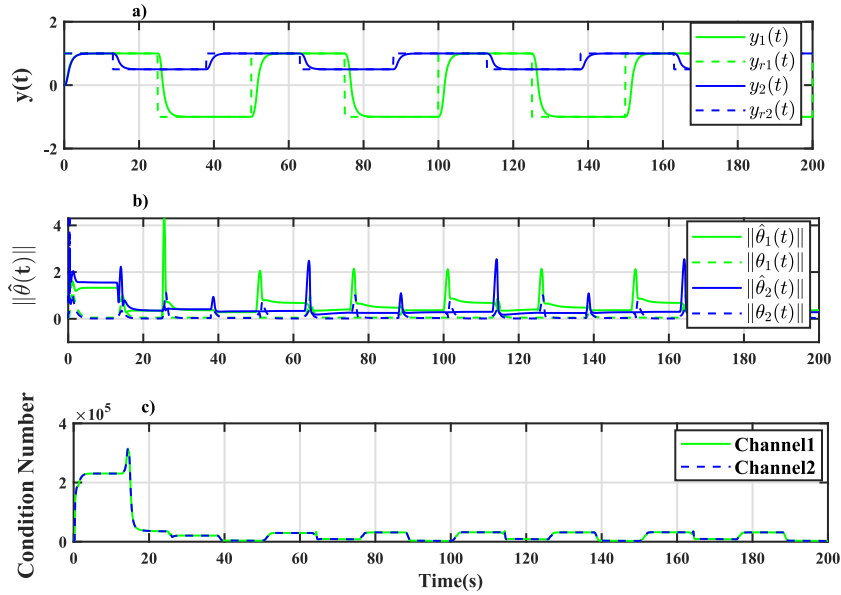


Fig. 5. The signals of robot arm under SVD-DLS algorithm by applying constant desired outputs: (a) the system output signals (b) the norm of parameters vector (c) the nullity of \mathbf{R}_1 and \mathbf{R}_2 .

is utilized to calculate oscillations of identified parameters. Furthermore,

$$J_q^2 = \int \|\tilde{\theta}_q(\tau)\|^2 d\tau \tag{47}$$

is utilized to calculate parameters identification error, and

$$J_q^3 = \int (y_q(\tau) - y_{r_q}(\tau))^2 d\tau \tag{48}$$

Table 2
Comparison between different solutions to tolerate under insufficient excitations.

Index	J_1^1	J_2^1	J_1^2	J_2^2	J_1^3	J_2^3
Applied Regularization	23.47	22.28	101.84	32.15	1.21	0.27
Applied Kaczmarz	24.97	25.32	40.28	10.58	1.19	0.26
Applied GDLS	22.52	21.76	18.17	04.62	1.17	0.24
Robust adaptive	27.71	22.67	107.08	23.43	1.13	0.23
Applied SVD-DLS	21.14	21.30	3.32	01.29	1.12	0.23

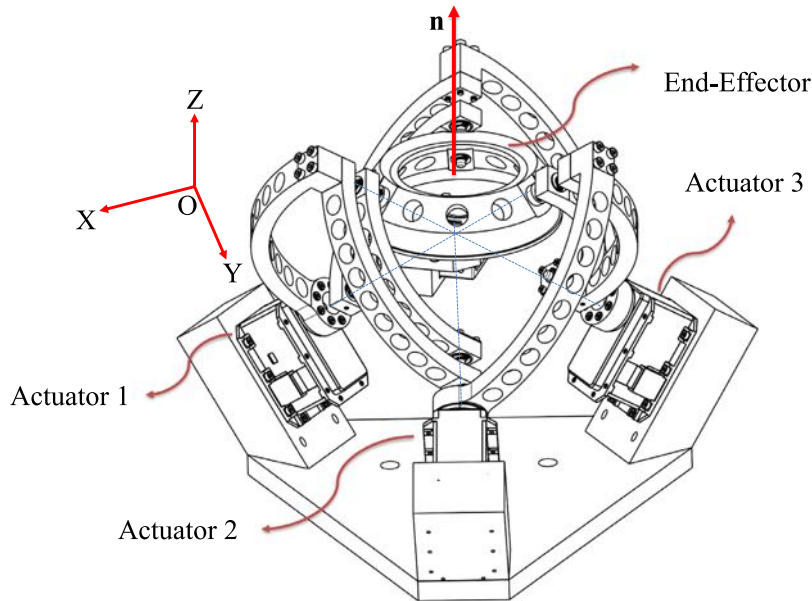


Fig. 6. CAD model of the under study 3-DOF SPR.

is utilized to calculate the tracking error of each channel. In Table 2, the effect of applying SVD-DLS to the robust adaptive approach is compared with the basic algorithm, Regularized constant-trace, GDLS, and Kaczmarz under. In the case of occurring high condition numbers, all the mentioned methods are applicable and improve the performance of the robust adaptive method under insufficient excitation. Based on Table 2, SVD-DLS not only decreases oscillations of identified parameters, but also makes the identification of system parameters possible under insufficient excitations.

From Table 2, it can be concluded that the performance of SVD-DLS in damping oscillations of identified parameters is better than the other method. Furthermore, from the identification point of view and in comparison with the basic robust adaptive algorithm, SVD-DLS has better performance. Based on quantitative results, SVD-DLS does not change the tracking error of output signals, while the other algorithms increase the tracking and identification error in compare with the proposed algorithm.

6. Practical implementation on the 3-DOF spherical parallel robot

In this section, the proposed approach is implemented on the 3-DOF SPR¹ which is built at the Human and Robot Interaction Laboratory, University of Tehran which can be adopted for image stabilization purposes. Parallel manipulators have many advantages over serial manipulators; they are more accurate and stiffer in compare to the serial manipulators. Due to these benefits, parallel manipulators are employed as a case study in several papers [52–55]. Specifically, this robot is utilized because of its low-moving inertia and inherent stiffness which leads to high performance dynamics and capability of high velocity and high acceleration [56]. Fig. 6 demonstrates the schematic of 3-DOF SPR. The main purpose of controlling this robot is to bound the Euler angles of End-Effector (EE). In fact, Roll and Pitch angles must be near zero and Yaw must be bounded to satisfy stabilization.

Setup components are shown in Fig. 7. Three Dynamixel MX-106R motors which have high accuracy and ability of control in both position and velocity mode, are utilized as actuators. It is worth noting that in this paper the stabilization of the under study robot is carried out in the velocity mode control; nonetheless, by resorting to some modifications, the position

¹ The results of the section are available in the following link: <https://youtube.com/watch?v=Tsh4mt7nJKo>.

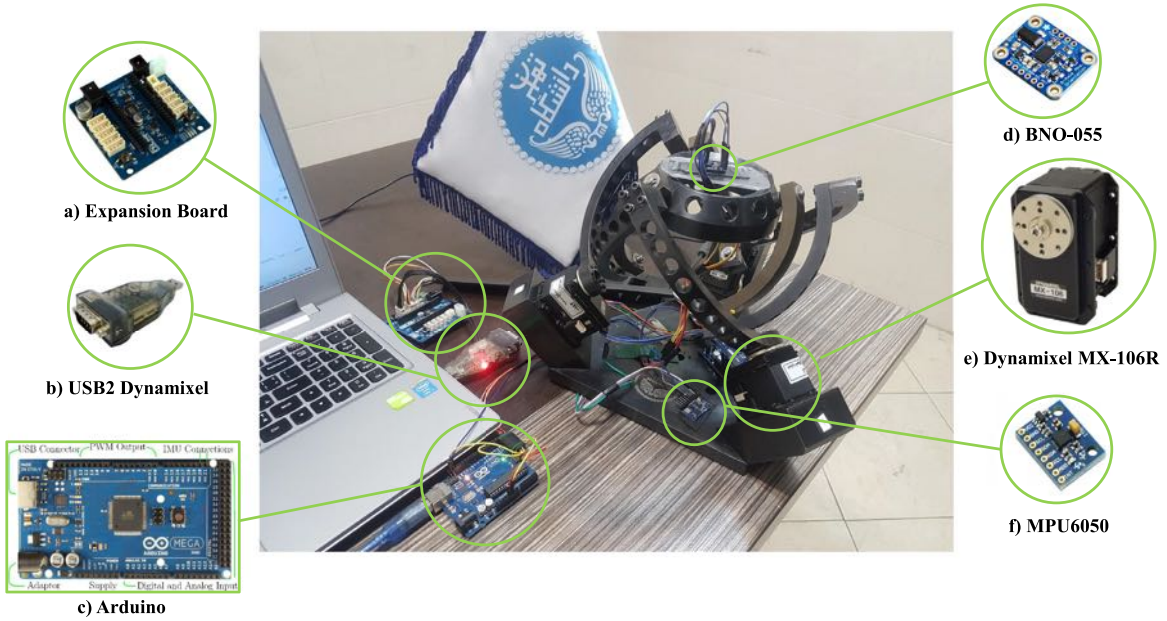


Fig. 7. Test setup of the under study 3-DOF SPR.

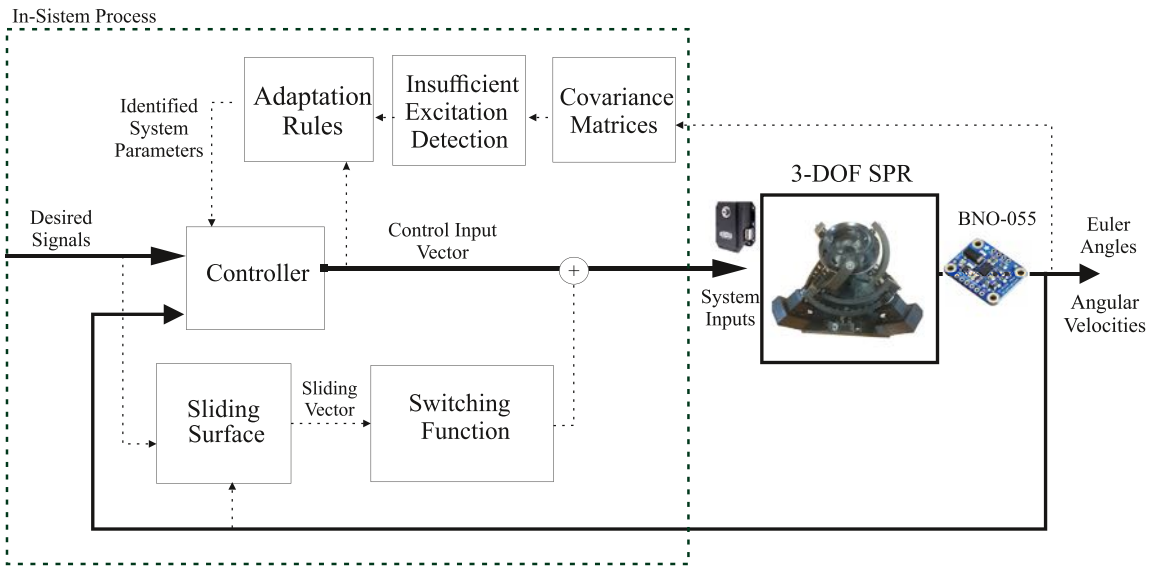


Fig. 8. The stabilization procedure of the under study SPR.

mode control is also applicable via the proposed approach. The motors are derived by adopting an Expansion board with a USB2Dynamixel device.

In Fig. 8, the relationship between various parts of the control procedure of the 3-DOF SPR is depicted. In this regard, intended to measure angular velocity and orientation of EE, a nine-axis navigation module, called BNO055, is mounted on the EE of the robot. This module is employed because of its high precision, high stability, and high performance. Then, the information is transferred to in-system process block. In this block, which represents the whole process of Procedure 1, the degree of excitation is checked in order to regulate the condition number of covariance matrix Eq. (16) in each output channel. In the next step, the measured data as well as the control input is employed by the adaptation rules, formulated in Eq. (18), in order to update the identified system parameters. On the other hand, in the case of detecting a correlated relation between the regressors, upon considering the orthogonal reduced-order models which are introduced in Section 4, the reduced-order parameters are acquired by employing the adaptation rules in Eq. (39) instead. Furthermore, the controller

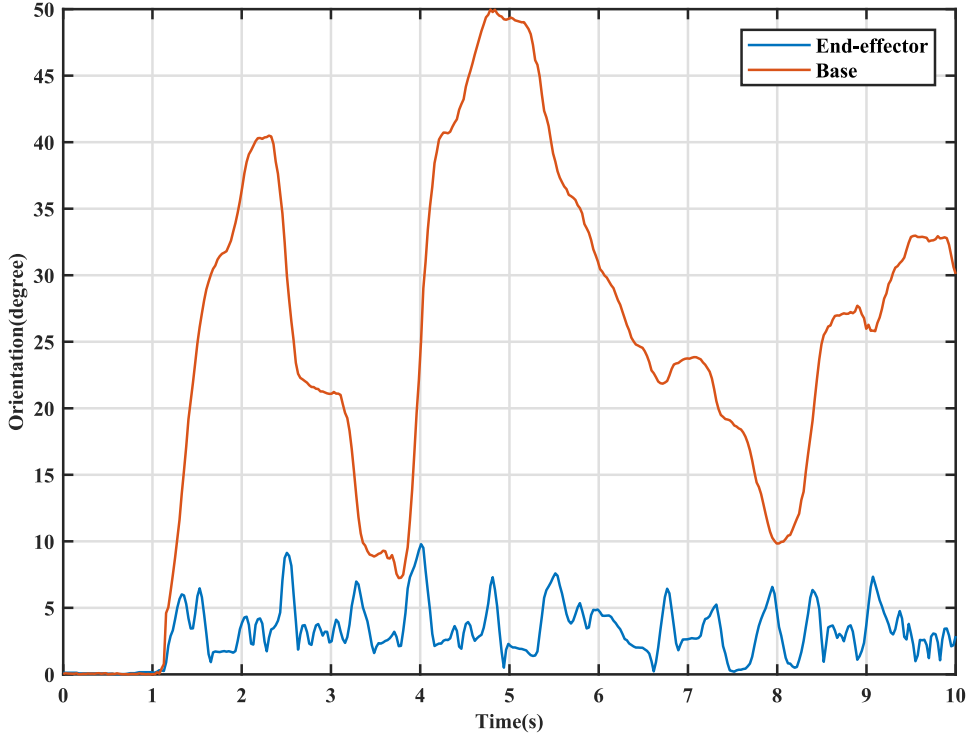


Fig. 9. Orientation of the EE and orientation of the base of the 3-DOF SPR.

adopts the desired signal values for the Euler angles and the angular velocities, which are obtained in such a way that stabilizes the condition of the robot. The control input vector is calculated based on these values in order to convey the system through the specified path by the sliding surface. The system inputs, which are applied to the actuators in the velocity mode, adopt the control input vectors and the switching values of the sliding surfaces. The whole process is done in PC and controller code is written in Python. The commands for servos are provided in PC by Python and are transmitted to servos by Expansion board and USB2Dynamixel.

In parallel manipulators, the time rate changes of the EE pose, namely the twist of EE, \mathbf{t} is mapped to the time rate changes of the joint space, $\dot{\boldsymbol{\theta}}$, through the so-called Jacobian matrix, \mathbf{J} , as follows [57]:

$$\dot{\boldsymbol{\theta}} = \mathbf{J}\mathbf{t} \quad (49)$$

In the case of the under study 3-DOF SPR, $\boldsymbol{\theta}$ is the position vector of the actuators, and the twist of the EE consists in only the angular velocity, $\boldsymbol{\omega}_e$, including ω_x , ω_y , and ω_z . Therefore, the following equation formulates the motion of the robot:

$$\dot{\boldsymbol{\theta}} = \mathbf{J}(\boldsymbol{\Omega}_e)\boldsymbol{\omega}_e \quad (50)$$

where $\boldsymbol{\Omega}_e$ denotes the measured position of the BNO055 module on the EE, including Ω_x , Ω_y , and Ω_z .

It is worth mentioning that the whole idea of the intelligent control, formulated in Sections 3 and 4, is provided for nonlinear time-continuous systems, among which, 3-DOF SPR is of importance. In fact, employing simple linear models rather than a complex one is followed in the intelligent control approaches due to their agility, having several analytical tools, and being easy to interpretation of the acquired results. Therefore, in spite of using the nonlinear model of the 3-DOF robot in Eq. (50), whose parameters are impossible to detect during any straight-forward approach, the simultaneous identification and control of the robot is carried out by resorting to the linear model, formulated in Eq. (51):

$$\omega_q = \sum_{j=x,y,z} a_{qj}\Omega_j + \mathbf{c}_q^T \dot{\boldsymbol{\theta}} + d_q, \quad q = x, y, z \quad (51)$$

where a_{qj} is the associated coefficient of the output interference from the j -axis in the q -axis of frame O, shown in Fig. 6. Extraction of these parameters from Eq. (50) requires great deal of effort which is time-consuming and somewhat impossible to directly acquire from Eq. (50). Moreover, \mathbf{c}_q denotes the associated vector of coefficients of the time rate changes of the actuators position vector toward the q -axis. The remaining non-modeled items of $\mathbf{J}(\boldsymbol{\Omega}_e)$ are represented by d_q in the q -axis. Subsequently, Eq. (51) is rewritten into the following form:

$$\omega_q = a_{qq}\Omega_q + \mathbf{b}_q^T \mathbf{u}_{\text{ext}} + d_q, \quad q = x, y, z \quad (52)$$

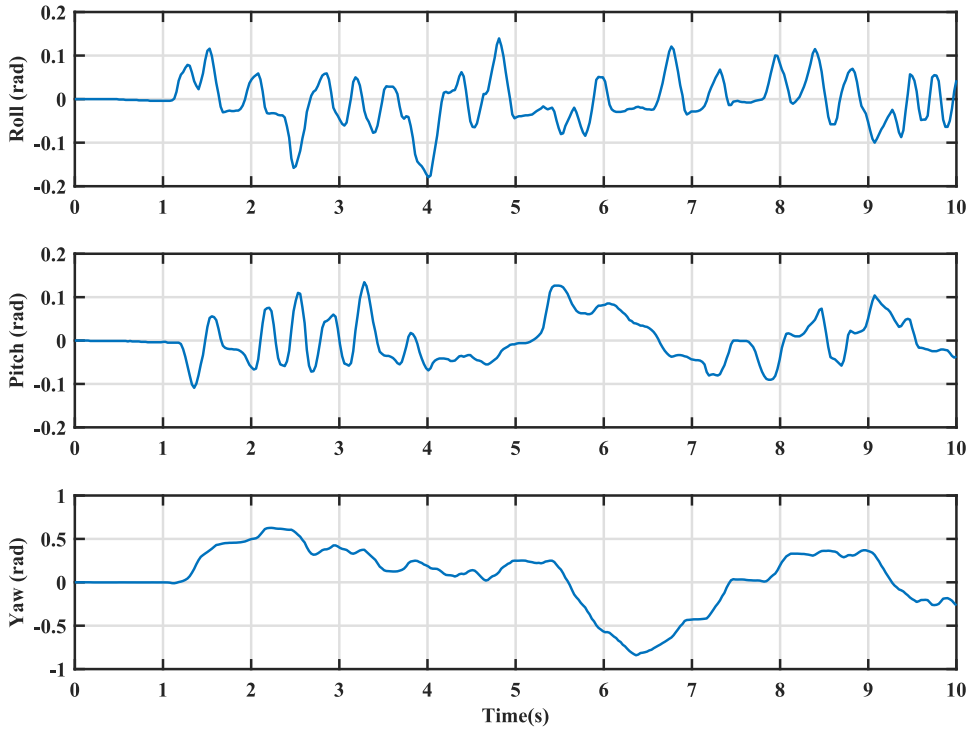


Fig. 10. Outputs of the 3-DOF SPR in three dimensions (Roll, Pitch, and Yaw).

in which \mathbf{u}_{ext} is comprised of the system input vector, $\mathbf{u} = \dot{\boldsymbol{\theta}}$, and the rest of items in Ω_j , $j = x, y, z$. Also, \mathbf{b}_q contains the corresponding vector of the coefficients of \mathbf{u}_{ext} . This acquired model, similar to the introduced equation in Eq. (2) in Section 3, behaves as a time-varying linear system influenced by the bounded disturbances. In this regard, $N = 3$ and $n_q = 1$ are set in order to match Eq. (52) to Eq. (2). Furthermore, Eq. (53) illustrates controller parameters which are employed in Eqs. (10) and (16):

$$\begin{aligned} \alpha_q &= 0.09 \quad q = 1, 2, 3 \\ \boldsymbol{\eta} &= \text{diag}(600, 600, 600) \end{aligned} \quad (53)$$

By choosing $n_q = 1$ for each channel, other control parameters such as λ_q are removed from the control procedure. Intended to simplifying identification stage, \mathbf{c}_q is set to fix values during the procedure and only the remaining parameters of \mathbf{b}_q , i.e. a_{qj} , $j \neq q$, as well as a_{qq} are updated by employing the adaptation rules. In this section, $[\mathbf{c}_1 \quad \mathbf{c}_2 \quad \mathbf{c}_3] = \mathbf{I}_{3 \times 3}$ is chosen which ultimately leads to acceptable results.

In the case of having sufficient excitation at each channel, Theorems 2 and 3 hold for the simultaneous control and identification of the system. Nonetheless, by detection of insufficient excited signals, the SVD-DLS algorithm will be applied to the robust adaptive controller. By so doing, notwithstanding the insufficient excitation condition, the proposed approach would succeed in the stabilization of the 3-DOF SPR, and Theorem 4 guarantees the stability of the system during the simultaneous control and identification.

In order to measure how much proposed method succeed in stabilization, orientation of the base and EE of the under study robot is compared. In order to calculate orientation of EE, denoted by $\boldsymbol{\theta}_e$, the angle between the vector perpendicular to the EE and the desired vector, $[0 \quad 0 \quad 1]^T$ in frame O should be measured. Similarly, orientation of the base, denoted by $\boldsymbol{\theta}_b$, can be obtained. Results of orientations are demonstrated in Fig. 9, where the proposed method succeeds to stabilize the objective EE in existence of considerable uncertainties and base movement. The orientation of the EE is bounded to 10 degrees. It is vital to note that external excitations are applied to the base of robot by hand movement. In order to illustrate how much this method has been successful in reducing disturbance, a new index is defined:

$$J_{\text{damped}} = \frac{\|\boldsymbol{\theta}_e\|}{\|\boldsymbol{\theta}_b\|} \quad (54)$$

Using the data plotted in Fig. 9, the value of this index is obtained as 0.134 which is acceptable for stabilization applications. It is vital to note that in the experimental tests it takes approximately 21 (ms) to 23 (ms) for each cycle of control loop of the written program in Python. Fig. 10 depicts the outputs of the system. Roll and Pitch angles are near zero, and Yaw angle is bounded; as a result, EE remains in an appropriate situation. Therefore, the desire condition for stabilizing is satisfied which proves Theorem 4 in this practical issue.

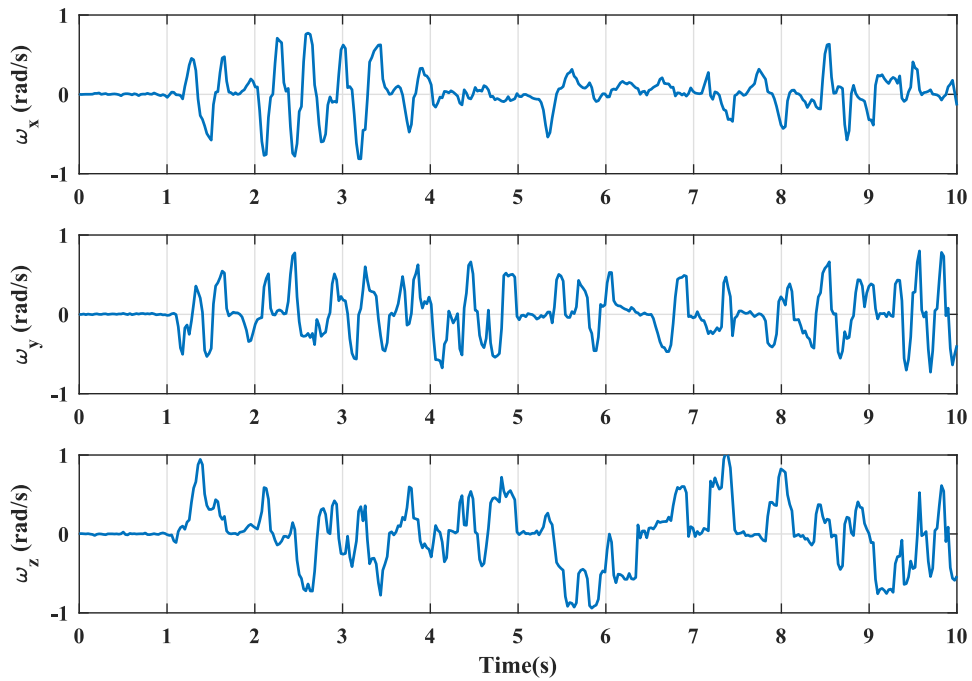


Fig. 11. Angular velocity of the EE in three dimensions.

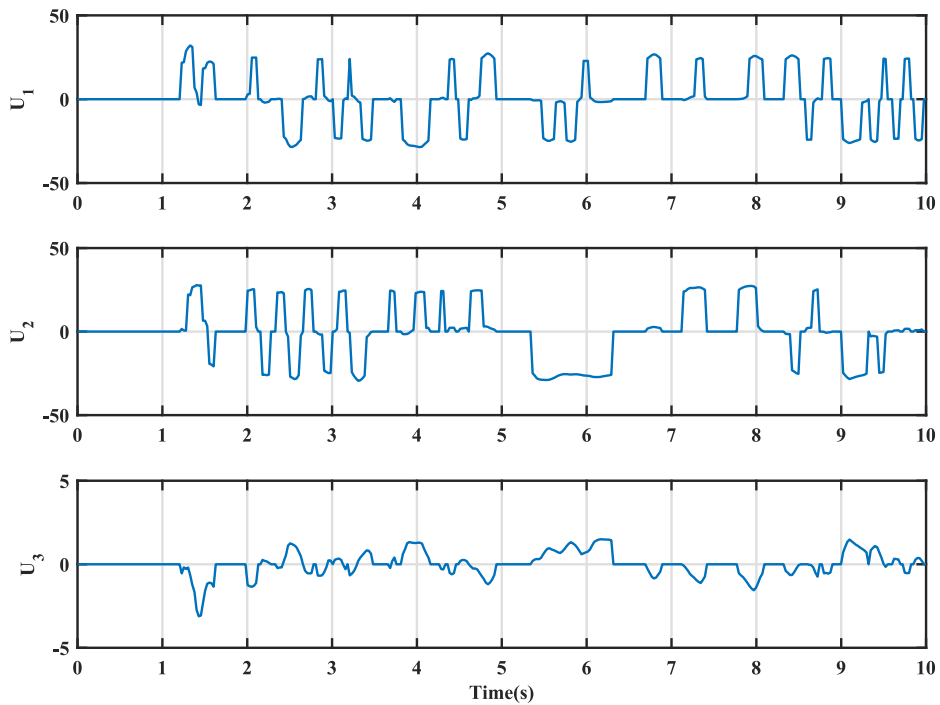


Fig. 12. Control inputs of the 3-DOF SPR.

Moreover, angular velocities of EE are shown in Fig. 11 and it is obvious that these velocities are not unstable and they are limited. Similarly, as it is shown in Fig. 12, the inputs, which are provided by controller, are bounded too. In Fig. 13, the identified parameters of the transfer function, defined in Eq. (1), are plotted during the implementation. Due to excitations

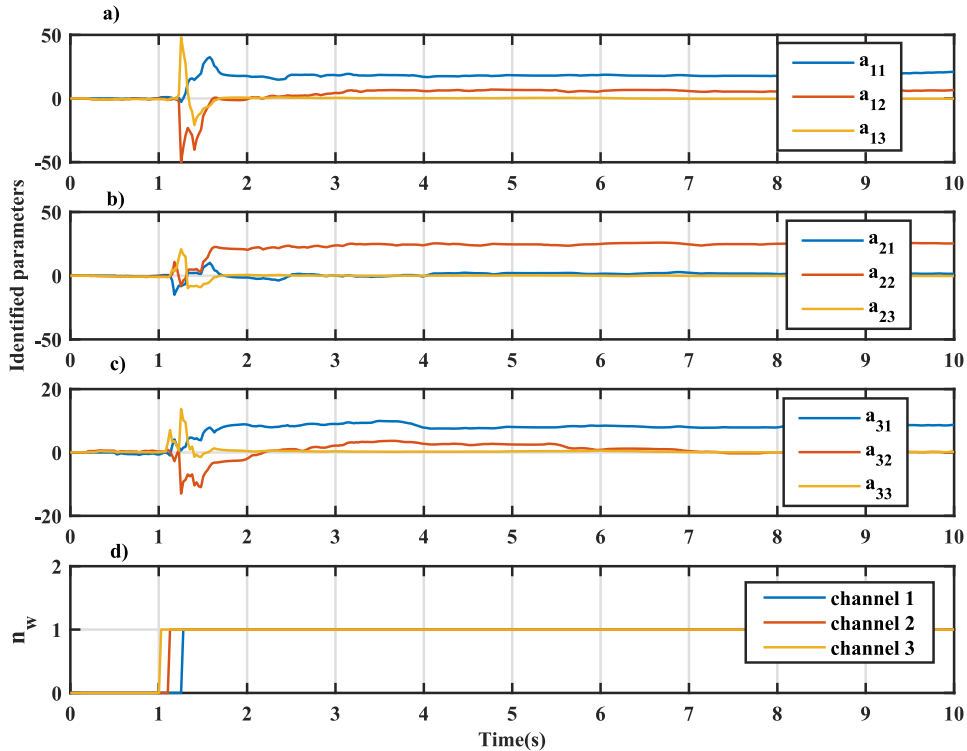


Fig. 13. Identified parameters of transfer function of the 3-DOF SPR. (a) channel 1, (b) channel 2, (c) channel 3. (d) nullity of channels

applied to the base of robot, [Assumption 3](#), as it is shown in [Fig. 13d](#), is satisfied for [Theorem 4](#) and convergence occurs for all of the parameters ([Fig. 13a-c](#)).

7. Conclusion

In this paper, the structure of a novel robust adaptive control method for MIMO systems was proposed which is experimentally implemented on a 3-DOF SPR for camera stabilization purposes. It was shown that adaptation rules of the robust adaptive method could be defined as an extended continuous-time RLS, which simultaneously reduces the identification and output tracking errors. Under insufficient excitations, the adaptive scheme led to estimation wind-up and the unlimited condition number of Covariance matrices. Therefore, a novel solution was proposed to dampen the oscillations of identified parameters. Unlike the classic DLS method, the model parameters were obtained much smoother in comparison to other possible methods. Based on these demonstrations, SVD-DLS method can be applied to the stabilization purposes as well. Adopting the SVD-DLS, the closed-loop system tolerated the insufficiency condition and remained stable. Also, the partially identification of system parameters was guaranteed and the oscillations of the identified parameters were dampened. Thereafter, the proposed algorithm was implemented on the 3-DOF SPR. Despite applying insufficient excitation to each actuator input, the robot succeeded to dampen the disturbance applied to the base of robot, which demonstrated the out-performance of the proposed automatic control method in the stabilization of the robot. As an ongoing work, improving the proposed automatic control method with concept of optimal control is of importance which in turn involves adopting the so-called reinforcement learning approach as to conforming to the behaviour of the surrounding environment in much more intelligent way.

Declaration of Competing Interest

The authors whose names are listed immediately below certify that they have NO affiliations with or involvement in any organization or entity with any financial interest (such as honoraria; educational grants; participation in speakers' bureaus; membership, employment, consultancies, stock ownership, or other equity interest; and expert testimony or patent-licensing arrangements), or non-financial interest (such as personal or professional relationships, affiliations, knowledge or beliefs) in the subject matter or materials discussed in this manuscript.

Saeed Ansari Rad, Mehran Ghafarian Tamizi, Mehdi Azmoun, Mehdi Tale Masouleh, Ahmad Kalhor

Procedure 1 Robust adaptive scheme with SVD-DLS.

```

1: Initialization:  $\forall q = 1, \dots, N : \hat{\mathbf{a}}_q(0) = \mathbf{0}_{n_q}, \hat{\mathbf{B}}(0) = \mathbf{I}_N, \mathbf{R}_q(0) = 0.01 \times \mathbf{I}_{N+n_q}$ 
2: while  $t < t_f$  do
3:   Calculate desired signals and their derivatives.
4:   Form  $\forall q = 1, \dots, N : \Phi_q = \begin{bmatrix} \mathbf{y}_q \\ \mathbf{u} \end{bmatrix}$ .
5:   Calculate sliding values regarding to Eq. (5).
6:    $\mathbf{u} = \tilde{\mathbf{u}} - \eta \text{sign}(\mathbf{S})$ .
7:   for  $q = 1, \dots, N$  do
8:      $e_q(t) = y_{r_q}^{[n_q]}(t) - y_q^{[n_q]}(t)$ 
9:      $\mathbf{E}_q(t) = \Phi_q(t)e_q(t) + \phi_q(t)s_q(t)$ 
10:     $\dot{\mathbf{R}}_q(t) = -\alpha_q \mathbf{R}_q(t) + \Phi_q(t)\Phi_q^T(t)$ 
11:     $\mathbf{R}_q(t + dt) = \mathbf{R}_q(t) + \dot{\mathbf{R}}_q(t)dt$ 
12:    Calculate  $n_w^q$  in regarding to  $\mathbf{R}_q(t)$ .
13:    if  $n_w^q = 0$  then
14:       $\hat{\boldsymbol{\theta}}_q(t) = \mathbf{R}_q^{-1}(t)\mathbf{E}_q(t)$ 
15:       $\hat{\boldsymbol{\theta}}_q(t + dt) = \hat{\boldsymbol{\theta}}_q(t) + \hat{\boldsymbol{\theta}}_q(t)dt$ 
16:    else
17:      Obtain:  $\mathbf{V}_{\text{nul}}^i(t), \mathbf{V}_p^i(t), \boldsymbol{\Lambda}_{\text{nul}}^i, \boldsymbol{\Lambda}_p^i(t)$ 
18:       $\hat{\boldsymbol{\theta}}_i(t) = \mathbf{V}_p^i(t)\boldsymbol{\Lambda}_p^{i-1}(t)\mathbf{V}_p^{i,T}(t)\mathbf{E}_i(t)$ 
19:       $\hat{\boldsymbol{\theta}}_i(t + dt) = \hat{\boldsymbol{\theta}}_i(t) + \hat{\boldsymbol{\theta}}_i(t)dt$ 
20:       $\dot{\boldsymbol{\beta}}_i^*(t) = -(\mathbf{V}_{\text{nul}}^{i,T}\mathbf{V}_{\text{nul}}^i)^{-1}\mathbf{V}_{\text{nul}}^{i,T}\hat{\boldsymbol{\theta}}_i(t)$ 
21:       $\boldsymbol{\beta}_i^*(t + dt) = \boldsymbol{\beta}_i^*(t) + \dot{\boldsymbol{\beta}}_i^*(t)dt$ 
22:       $\hat{\boldsymbol{\theta}}_{\beta_i}(t + dt) = \hat{\boldsymbol{\theta}}_i(t + dt) + \mathbf{V}_{\text{nul}}^i\boldsymbol{\beta}_i^*(t + dt)$ 
23:    end if
24:  end for
25:  put  $t = t + dt$ 
26: end while

```

Appendix A*A1. Proof of Theorem 2*

Proof. Consider the following Lyapunov function:

$$V(t) = \frac{1}{2} \left(\mathbf{S}^T \mathbf{S} + \sum_{q=1}^N \tilde{\boldsymbol{\theta}}_q^T(t) \mathbf{R}_q(t) \tilde{\boldsymbol{\theta}}_q(t) \right). \quad (\text{A.1})$$

The derivative of the Lyapunov function can be stated as the following equation:

$$\dot{V}(t) = \frac{1}{2} \left(2\mathbf{S}^T \dot{\mathbf{S}} + 2 \sum_{q=1}^N \tilde{\boldsymbol{\theta}}_q^T(t) \mathbf{R}_q(t) \dot{\tilde{\boldsymbol{\theta}}}_q(t) + \sum_{q=1}^N \tilde{\boldsymbol{\theta}}_q^T(t) \dot{\mathbf{R}}_q(t) \tilde{\boldsymbol{\theta}}_q(t) \right) \quad (\text{A.2})$$

With substitution of the derivation vector of the estimation error, one has:

$$\dot{V}(t) = \frac{1}{2} \left(2\mathbf{S}^T \dot{\mathbf{S}} + 2 \sum_{q=1}^N \tilde{\boldsymbol{\theta}}_q^T(t) \mathbf{R}_q(t) \dot{\tilde{\boldsymbol{\theta}}}_q(t) - 2 \sum_{q=1}^N \tilde{\boldsymbol{\theta}}_q^T(t) \mathbf{R}_q(t) \tilde{\boldsymbol{\theta}}_q(t) + \sum_{q=1}^N \tilde{\boldsymbol{\theta}}_q^T(t) \dot{\mathbf{R}}_q(t) \tilde{\boldsymbol{\theta}}_q(t) \right) \quad (\text{A.3})$$

By applying some mathematical calculation, it yields:

$$\begin{aligned} \dot{V}(t) \leq & \sum_{q=1}^N \dot{\boldsymbol{\theta}}_q^T(t) \mathbf{R}_q(t) \tilde{\boldsymbol{\theta}}_q(t) - \frac{1}{2} \sum_{q=1}^N \alpha_q \tilde{\boldsymbol{\theta}}_q^T(t) \mathbf{R}_q(t) \tilde{\boldsymbol{\theta}}_q(t) \\ & - \frac{1}{2} \sum_{q=1}^N \tilde{\boldsymbol{\theta}}_q^T(t) \boldsymbol{\Phi}_q(t) \boldsymbol{\Phi}_q^T(t) \tilde{\boldsymbol{\theta}}_q(t) \\ & - \sum_{q=1}^N |\eta_q| |s_q| (|b_{qq}| - \sum_{j=1, j \neq q}^N |b_{qj}|) \end{aligned} \quad (\text{A.4})$$

Predicated on [Assumption 1](#), [Eq. \(A.4\)](#) is reformulated as:

$$\begin{aligned} \dot{V}(t) \leq & - \sum_{q=1}^N \left(\frac{1}{2} \alpha_q \tilde{\boldsymbol{\theta}}_q^T(t) \mathbf{R}_q(t) \tilde{\boldsymbol{\theta}}_q(t) - \dot{\boldsymbol{\theta}}_q^T(t) \mathbf{R}_q(t) \tilde{\boldsymbol{\theta}}_q(t) \right) \\ & - \frac{1}{2} \sum_{q=1}^N \tilde{\boldsymbol{\theta}}_q^T(t) \boldsymbol{\Phi}_q(t) \boldsymbol{\Phi}_q^T(t) \tilde{\boldsymbol{\theta}}_q(t) - \sum_{q=1}^N |\eta_q| |b_{qq}| |s_q|. \end{aligned} \quad (\text{A.5})$$

If the following sufficient condition is satisfied:

$$|\dot{\boldsymbol{\theta}}_q^T(t) \mathbf{R}_q(t) \tilde{\boldsymbol{\theta}}_q(t)| < \frac{1}{2} |\alpha_q \tilde{\boldsymbol{\theta}}_q^T(t) \mathbf{R}_q(t) \tilde{\boldsymbol{\theta}}_q(t)| \quad (\text{A.6})$$

then:

$$\dot{V}(t) < - \frac{1}{2} \sum_{q=1}^N \tilde{\boldsymbol{\theta}}_q^T(t) \boldsymbol{\Phi}_q(t) \boldsymbol{\Phi}_q^T(t) \tilde{\boldsymbol{\theta}}_q(t) - \sum_{q=1}^N |\eta_q| |b_{qq}| |s_q|. \quad (\text{A.7})$$

By applying the sufficient conditions from [Eq. \(A.6\)](#), it is concluded that:

$$\dot{V}(t) < -W_1(\|\mathbf{S}\|, \|\tilde{\boldsymbol{\theta}}\|) = -\frac{1}{2} \underline{\sigma} \|\tilde{\boldsymbol{\theta}}\|^2 - \delta \|\mathbf{S}\| < 0 \quad (\text{A.8})$$

where

$$0 < \delta = \min_{q=1, \dots, N} (|\eta_q| |b_{qq}|).$$

Based on the sufficient conditions acquired in [Eq. \(A.6\)](#) and also based on [Assumption 2](#), one can calculate the following domain:

$$\begin{aligned} \bar{D}_1 = & \left\{ \forall \tilde{\boldsymbol{\theta}}(t), \tilde{\boldsymbol{\theta}} \in \mathbb{R}^{N+n_q}, \|\tilde{\boldsymbol{\theta}}(t)\| \right. \\ & \left. \geq N \times \underbrace{\max_{q=1, 2, \dots, N} \left(\frac{2\rho_q \bar{\sigma}_q}{\alpha_q \sigma_q} \right)}_{\|\tilde{\boldsymbol{\theta}}\|_{\text{stv}}^{\max}} \right\}. \end{aligned} \quad (\text{A.9})$$

which determines the area, where the model parameter identification error decreases such that $\|\tilde{\boldsymbol{\theta}}\| \leq \|\tilde{\boldsymbol{\theta}}\|_{\text{stv}}^{\max}$. Moreover, based on Final Value theorem and by exploiting [Eq. \(5\)](#), the following upper bound is calculated for the output tracking errors:

$$\forall q : |\tilde{y}_q(t)| \underset{t \rightarrow \infty}{\leq} \underbrace{\frac{\|\tilde{\boldsymbol{\theta}}\|_{\text{stv}}^{\max} \sqrt{2\sigma}}{\lambda_q^{n_q-1}}}_{\bar{c}_{\text{stv}}^q} \quad (\text{A.10})$$

Therefore, based on the Lyapunov theory, the intended closed-loop system is guaranteed to be UUB stable. \square

Appendix B. Proof of Theorem 4

Proof. According to [Assumption 3](#), it has been assumed that the channel i suffers from insufficient excitations, while the rest of channels are still under sufficient excitation in the interval $[t_0, t]$. Therefore, SVD-DLS method, the [Eqs. \(27\)](#) to [\(40\)](#),

is applied to the channel equations. Considering the positive definite Lyapunov function formulated in (B.1), it is required to be proven that the derivative of this function remains negative definite:

$$V(t) = \frac{1}{2} \left(\mathbf{S}^T \mathbf{S} + \tilde{\boldsymbol{\zeta}}_{\text{red}_i}^T(t) \mathbf{R}_{\text{red}_i}(t) \tilde{\boldsymbol{\zeta}}_{\text{red}_i}(t) + \sum_{q \neq i}^N \tilde{\boldsymbol{\theta}}_q^T(t) \mathbf{R}_q(t) \tilde{\boldsymbol{\theta}}(t) \right), \quad t \geq t_0 \quad (\text{B.1})$$

where, $\hat{\boldsymbol{\zeta}}_{\text{red}_i}(t) \in \mathbb{R}^{n_i}$ denotes the vector of error estimation of reduced-order parameters in the i th channel. Thereafter, the derivative of the Lyapunov function is computed as follow:

$$\begin{aligned} \dot{V}(t) = & \frac{1}{2} \left(2\mathbf{S}^T \dot{\mathbf{S}} + 2\dot{\boldsymbol{\zeta}}_{\text{red}_i}^T(t) \mathbf{R}_{\text{red}_i}(t) \tilde{\boldsymbol{\zeta}}_{\text{red}_i}(t) \right. \\ & - 2\tilde{\boldsymbol{\zeta}}_{\text{red}_i}^T(t) \dot{\mathbf{R}}_{\text{red}_i}(t) \tilde{\boldsymbol{\zeta}}_{\text{red}_i}(t) + \tilde{\boldsymbol{\zeta}}_{\text{red}_i}^T(t) \dot{\mathbf{R}}_{\text{red}_i}(t) \tilde{\boldsymbol{\zeta}}_{\text{red}_i}(t) \\ & + 2 \sum_{q \neq i}^N \dot{\boldsymbol{\theta}}_q^T(t) \mathbf{R}_q(t) \tilde{\boldsymbol{\theta}}(t) - 2 \sum_{q \neq i}^N \tilde{\boldsymbol{\theta}}_q^T(t) \dot{\mathbf{R}}_q(t) \tilde{\boldsymbol{\theta}}(t) \\ & \left. + \sum_{q \neq i}^N \tilde{\boldsymbol{\theta}}_q^T(t) \dot{\mathbf{R}}_q(t) \tilde{\boldsymbol{\theta}}(t) \right), \quad t \geq t_0 \end{aligned} \quad (\text{B.2})$$

where $\dot{\boldsymbol{\zeta}}_{\text{red}_i}(t)$ is the derivative of vector of reduced-order system parameters in the orthogonal space, which can be acquired from $\dot{\boldsymbol{\zeta}}_{\text{red}_i}(t) = \mathbf{V}_p^T(t) \dot{\boldsymbol{\theta}}_i(t)$.

Similarly, the vector of reduced-order system parameters is considered as slowly varying parameters with the following formulation:

$$\forall t \geq t_0 : \left\| \dot{\boldsymbol{\zeta}}_{\text{red}_i}(t) \right\| < \rho_{z_i} \quad (\text{B.3})$$

where, ρ_{z_i} is the upper bound of the parameters' variation in the orthogonal space. By substituting the derivative of sliding vector from Eq. (13) and reformulating (B.2) in summation format, the following formula is obtained:

$$\begin{aligned} \dot{V}(t) = & s_i^T \boldsymbol{\Phi}_{z_i}(t) \tilde{\boldsymbol{\zeta}}_{\text{red}_i}^T(t) + \tilde{\boldsymbol{\zeta}}_{\text{red}_i}^T(t) \mathbf{R}_{\text{red}_i}(t) \tilde{\boldsymbol{\zeta}}_{\text{red}_i}(t) \\ & + \frac{1}{2} \tilde{\boldsymbol{\zeta}}_{\text{red}_i}^T(t) \dot{\mathbf{R}}_{\text{red}_i}(t) \tilde{\boldsymbol{\zeta}}_{\text{red}_i}(t) + \sum_{q \neq i}^N \left(\dot{\boldsymbol{\theta}}_q^T(t) \mathbf{R}_q(t) \tilde{\boldsymbol{\theta}}(t) \right. \\ & + s_q \boldsymbol{\Phi}_q^T(t) \tilde{\boldsymbol{\theta}}_q(t) - \tilde{\boldsymbol{\theta}}_q^T(t) \mathbf{R}_q(t) \tilde{\boldsymbol{\theta}}(t) + \frac{1}{2} \tilde{\boldsymbol{\theta}}_q^T(t) \dot{\mathbf{R}}_q(t) \tilde{\boldsymbol{\theta}}(t) \left. \right) \\ & + \sum_{q=1}^N d_q s_q - \sum_{q=1}^N \left(\eta_q \sum_{j=1}^N b_{qj} s_q \text{sign}(a_j) \right), \quad t \geq t_0 \end{aligned} \quad (\text{B.4})$$

Using the given adaptation rules in Eq. (22) and (33) and according to Remark 1 and Assumption 1, the following inequality is obtained:

$$\begin{aligned} \dot{V}(t) \leq & \tilde{\boldsymbol{\zeta}}_{\text{red}_i}^T(t) \mathbf{R}_{\text{red}_i}(t) \tilde{\boldsymbol{\zeta}}_{\text{red}_i}(t) - e_i \mathbf{Z}_{\text{red}_i}^T(t) \tilde{\boldsymbol{\zeta}}_{\text{red}_i}(t) \\ & + \frac{1}{2} \tilde{\boldsymbol{\zeta}}_{\text{red}_i}^T(t) \dot{\mathbf{R}}_{\text{red}_i}(t) \tilde{\boldsymbol{\zeta}}_{\text{red}_i}(t) + \sum_{q \neq i}^N \left(\dot{\boldsymbol{\theta}}_q^T(t) \mathbf{R}_q(t) \tilde{\boldsymbol{\theta}}(t) \right. \\ & - e_q \boldsymbol{\Phi}_q^T(t) \tilde{\boldsymbol{\theta}}_q(t) + \frac{1}{2} \tilde{\boldsymbol{\theta}}_q^T(t) \dot{\mathbf{R}}_q(t) \tilde{\boldsymbol{\theta}}(t) \left. \right) + \sum_{q=1}^N |s_q| \bar{d}_q \\ & - \sum_{q=1}^N \left(|\eta_q| |s_q| (|b_{qq}| - \sum_{j=1, j \neq q}^N |b_{qj}|) \right), \quad t \geq t_0 \end{aligned} \quad (\text{B.5})$$

By substituting e_q from Eq. (14), it yields:

$$\begin{aligned} \dot{V}(t) \leq & \tilde{\boldsymbol{\zeta}}_{\text{red}_i}^T(t) \mathbf{R}_{\text{red}_i}(t) \tilde{\boldsymbol{\zeta}}_{\text{red}_i}(t) - d_i \mathbf{Z}_{\text{red}_i}^T(t) \tilde{\boldsymbol{\zeta}}_{\text{red}_i}(t) \\ & + \frac{1}{2} \tilde{\boldsymbol{\zeta}}_{\text{red}_i}^T(t) \dot{\mathbf{R}}_{\text{red}_i}(t) \tilde{\boldsymbol{\zeta}}_{\text{red}_i}(t) + \sum_{q \neq i}^N \left(\dot{\boldsymbol{\theta}}_q^T(t) \mathbf{R}_q(t) \tilde{\boldsymbol{\theta}}(t) \right. \\ & - d_q \boldsymbol{\Phi}_q^T(t) \tilde{\boldsymbol{\theta}}_q(t) - \tilde{\boldsymbol{\theta}}_q^T(t) \boldsymbol{\Phi}_q(t) + \frac{1}{2} \tilde{\boldsymbol{\theta}}_q^T(t) \dot{\mathbf{R}}_q(t) \tilde{\boldsymbol{\theta}}(t) \left. \right) \end{aligned}$$

$$+ \sum_{q=1}^N |s_q| \left(|\eta_q| \left(|b_{bb}| - \sum_{j=1, j \neq q}^N |b_{qj}| \right) - \bar{d}_q \right), \quad t \geq t_0 \tag{B.6}$$

According to Remark 1, the inequality of (B.7) is obtained. Also values of $\dot{\mathbf{R}}_q(t)$ and $\dot{\mathbf{R}}_{z_{red_i}}(t)$ are extracted from Eqs. (16) and (33), respectively.

$$\begin{aligned} \dot{V}(t) \leq & - \left(\frac{1}{2} \alpha_i \tilde{\boldsymbol{\zeta}}_{red_i}^T(t) \mathbf{R}_{z_{red_i}}(t) \tilde{\boldsymbol{\zeta}}_{red_i}(t) \right. \\ & - \dot{\boldsymbol{\zeta}}_{red_i}^T(t) \mathbf{R}_{z_{red_i}}(t) \tilde{\boldsymbol{\zeta}}_{red_i}(t) + d_i \mathbf{Z}_{red_i}^T(t) \tilde{\boldsymbol{\zeta}}_{red_i}(t) \left. \right) \\ & - \frac{1}{2} \tilde{\boldsymbol{\zeta}}_{red_i}^T(t) \mathbf{Z}_{red_i}(t) \mathbf{Z}_{red_i}^T(t) \tilde{\boldsymbol{\zeta}}_{red_i}(t) \\ & - \sum_{q \neq i}^N \left(\frac{1}{2} \alpha_q \tilde{\boldsymbol{\theta}}_q^T(t) \mathbf{R}_q(t) \tilde{\boldsymbol{\theta}}_q(t) - \dot{\boldsymbol{\theta}}_q^T(t) \mathbf{R}_q(t) \tilde{\boldsymbol{\theta}}_q(t) \right. \\ & + d_q \boldsymbol{\Phi}_q^T(t) \tilde{\boldsymbol{\theta}}_q(t) - \frac{1}{2} \sum_{q \neq i}^N \tilde{\boldsymbol{\theta}}_q^T(t) \boldsymbol{\Phi}_q(t) \boldsymbol{\Phi}_q^T(t) \tilde{\boldsymbol{\theta}}_q(t) \left. \right) \\ & - \sum_{q=1}^N |\eta_q| |b_{qq}| |s_q|, \quad t \geq t_0. \end{aligned} \tag{B.7}$$

Thereafter, the following sufficient conditions are considered for each output channel:

$$\begin{aligned} & \left| \frac{1}{2} \alpha_i \tilde{\boldsymbol{\zeta}}_{red_i}^T(t) \mathbf{R}_{z_{red_i}}(t) \tilde{\boldsymbol{\zeta}}_{red_i}(t) \right| \\ & > \left| d_i \mathbf{Z}_{red_i}^T(t) \tilde{\boldsymbol{\zeta}}_{red_i}(t) - \dot{\boldsymbol{\zeta}}_{red_i}^T(t) \mathbf{R}_{z_{red_i}}(t) \tilde{\boldsymbol{\zeta}}_{red_i}(t) \right| \\ \forall q \neq i : & \left| \frac{1}{2} \alpha_q \tilde{\boldsymbol{\theta}}_q^T(t) \mathbf{R}_q(t) \tilde{\boldsymbol{\theta}}_q(t) \right| \\ & > \left| d_q \boldsymbol{\Phi}_q^T(t) \tilde{\boldsymbol{\theta}}_q(t) - \dot{\boldsymbol{\theta}}_q^T(t) \mathbf{R}_q(t) \tilde{\boldsymbol{\theta}}_q(t) \right| \end{aligned} \tag{B.8}$$

By applying the sufficient conditions from Eq. (B.8), it is concluded that:

$$\dot{V}(t) < -W_2(\|\mathbf{S}\|, \|\tilde{\boldsymbol{\theta}}_z\|) = -\frac{1}{2} \underline{\sigma}_z \|\tilde{\boldsymbol{\theta}}_z\|^2 - \delta \|\mathbf{S}\| < 0 \tag{B.9}$$

where

$$\begin{aligned} 0 < \underline{\sigma}_z &= \min\{\underline{\sigma}_1, \dots, \underline{\sigma}_{z_i}, \dots, \underline{\sigma}_N\} \\ \tilde{\boldsymbol{\theta}}_z^T &= [\tilde{\boldsymbol{\theta}}_1^T, \dots, \tilde{\boldsymbol{\zeta}}_{red_i}^T, \dots, \tilde{\boldsymbol{\theta}}_N^T]. \end{aligned} \tag{B.10}$$

Therefore, based on the Lyapunov theory, the closed-loop system is guaranteed to be UUB stable. The sufficient conditions mentioned in Eq. (B.8) can be converted to the following sufficient conditions:

$$\begin{aligned} \frac{1}{2} \alpha_i \underline{\sigma}_{z_i} \|\tilde{\boldsymbol{\zeta}}_{red_i}\|^2 &> \|\tilde{\boldsymbol{\zeta}}_{red_i}\| \left\| d_i \mathbf{Z}_{red_i}^T - \dot{\boldsymbol{\zeta}}_{red_i}^T \mathbf{R}_{red_i}(t) \right\| \\ \xrightarrow{\forall q \neq i} \frac{1}{2} \alpha_q \underline{\sigma}_q \|\tilde{\boldsymbol{\theta}}_q\|^2 &> \|\tilde{\boldsymbol{\theta}}_q\| \left\| d_q \boldsymbol{\Phi}_q^T - \dot{\boldsymbol{\theta}}_q^T \mathbf{R}_q(t) \right\|. \end{aligned} \tag{B.11}$$

Considering Eq. (B.11), the following region is defined:

$$\begin{aligned} \bar{D}_2 = \left\{ \forall \tilde{\boldsymbol{\theta}}_z(t) \mid t_0 \leq t, \tilde{\boldsymbol{\theta}}_{vq \neq i} \in \mathbb{R}^{N+n_q}, \tilde{\boldsymbol{\zeta}}_{red_i} \in \mathbb{R}^{n_p}, \right. \\ \left. \|\tilde{\boldsymbol{\theta}}_z(t)\| \geq \underbrace{\max_{q=1, \dots, N} \left\{ \|\tilde{\boldsymbol{\theta}}_{vq \neq i}(t)\|_{\max}, \|\tilde{\boldsymbol{\zeta}}_{red_i}\|_{\max} \right\}}_{\|\tilde{\boldsymbol{\theta}}_z\|_{\max}} \right\} \end{aligned} \tag{B.12}$$

where

$$\|\tilde{\boldsymbol{\theta}}_{vq \neq i}\|_{\max} = \frac{2(\bar{d}_q \max_{t_0 \leq t} \|\boldsymbol{\Phi}_q(t)\| + \rho_q \bar{\sigma}_q)}{\alpha_q \underline{\sigma}_q}$$

$$\|\tilde{\xi}_{\text{red},i}\|_{\max} = \frac{2(\bar{d}_q \max_{t_0 \leq t} \|\mathbf{Z}_{\text{red},i}(t)\| + \rho_{z_i} \bar{\sigma}_{z_i})}{\alpha_i \sigma_{z_i}} \quad (\text{B.13})$$

\bar{D}_2 defines the region, where $\dot{V}(t)$ is guaranteed to be negative definite. Therefore, the estimation error of parameters, $\tilde{\theta}_z$, is diminished such that the ultimate value of $\tilde{\theta}_z(t)$ becomes less than or equal to $\|\tilde{\theta}_z\|_{\max}$. Therefore, it is proven that the identified parameters are guaranteed to converge to the vicinity of an equivalent model. If V^* defines the level set which $\exists t_1 < \infty : \forall t > t_1, \|\tilde{\theta}_z(t)\| < \|\tilde{\theta}_z\|_{\max}$ is entirely established in, then $\forall t > t_1, V(t) < V^*$. Moreover, the following equations can be written:

$$V^* = \underbrace{\frac{1}{2} \|\mathbf{S}^*\|^2}_{V_{\min}} = \sigma_z \|\tilde{\theta}_z\|_{\max}^2 \Rightarrow \|\mathbf{S}^*\| = \sqrt{2\sigma_z} \|\tilde{\theta}_z\|_{\max} \quad (\text{B.14})$$

Similarly, the following upper bound is calculated for the tracking error of each channel:

$$\forall q : |\tilde{y}_q(t_1 \leq t)| \leq \bar{c}_z^q = \frac{\sqrt{2\sigma_z} \|\tilde{\theta}_z\|_{\max}}{\lambda_q^{n_q-1}}. \quad (\text{B.15})$$

Consequently, it is proven that the tracking error of each channel is guaranteed to be bounded. \square

Supplementary material

Supplementary material associated with this article can be found, in the online version, at doi:[10.1016/j.mechmachtheory.2020.104026](https://doi.org/10.1016/j.mechmachtheory.2020.104026).

References

- [1] C. Rohrs, L. Valavani, M. Athans, G. Stein, Robustness of continuous-time adaptive control algorithms in the presence of unmodeled dynamics, *IEEE Trans. Autom. Control* 30 (9) (1985) 881–889.
- [2] A. Feuer, A. Morse, Adaptive control of single-input, single-output linear systems, *IEEE Trans. Autom. Control* 23 (4) (1978) 557–569.
- [3] J. Weimer, N. Bezzo, M. Pajic, G. Pappas, O. Sokolsky, I. Lee, Resilient adaptive control with application to vehicle cruise control, *Workshop on Control of Cyber-Physical Systems*, 2012.
- [4] H. Elmali, N. Olgac, Robust output tracking control of nonlinear MIMO systems via sliding mode technique, *Automatica* 28 (1) (1992) 145–151.
- [5] M. Chen, S.S. Ge, B. Ren, Adaptive tracking control of uncertain MIMO nonlinear systems with input constraints, *Automatica* 47 (3) (2011) 452–465.
- [6] I. Michailidis, S. Baldi, E.B. Kosmatopoulos, P.A. Ioannou, Adaptive optimal control for large-scale nonlinear systems, *IEEE Trans. Autom. Control* 62 (11) (2017) 5567–5577.
- [7] C. Nicol, C. Macnab, A. Ramirez-Serrano, Robust adaptive control of a quadrotor helicopter, *Mechatronics* 21 (6) (2011) 927–938.
- [8] M. Zeinali, L. Notash, Adaptive sliding mode control with uncertainty estimator for robot manipulators, *Mech. Mach. Theory* 45 (1) (2010) 80–90.
- [9] C.-S. Chiu, Derivative and integral terminal sliding mode control for a class of MIMO nonlinear systems, *Automatica* 48 (2) (2012) 316–326.
- [10] T.R. Oliveira, A.J. Peixoto, L. Hsu, Sliding mode control of uncertain multivariable nonlinear systems with unknown control direction via switching and monitoring function, *IEEE Trans. Autom. Control* 55 (4) (2010) 1028–1034.
- [11] S. Ansari-Rad, M. Zarei, M.G. Tamizi, S.M. Nejati, M.T. Masouleh, A. Kalhor, Stabilization of a 2-DOF spherical parallel robot via a novel adaptive approach, in: *Robotics and Mechatronics (ICROM)*, 2018 6th International Conference on, IEEE, 2018, pp. 1–7.
- [12] Y. Singh, M. Santhakumar, Inverse dynamics and robust sliding mode control of a planar parallel (2-PRP and 1-PPR) robot augmented with a nonlinear disturbance observer, *Mech. Mach. Theory* 92 (2015) 29–50.
- [13] H. Dou, S. Wang, Robust adaptive motion/force control for motion synchronization of multiple uncertain two-link manipulators, *Mech. Mach. Theory* 67 (2013) 77–93.
- [14] M. Begnini, D.W. Bertol, N.A. Martins, A robust adaptive fuzzy variable structure tracking control for the wheeled mobile robot: simulation and experimental results, *Control Eng. Pract.* 64 (2017) 27–43.
- [15] F.F. Bigelow, A. Kalhor, Robust adaptive controller based on evolving linear model applied to a ball-handling mechanism, *Control Eng. Pract.* 69 (2017) 85–98.
- [16] J.S.-H. Tsai, Y.-Y. Du, P.-H. Huang, S.-M. Guo, L.-S. Shieh, Y. Chen, Iterative learning-based decentralized adaptive tracker for large-scale systems: a digital redesign approach, *ISA Trans.* 50 (3) (2011) 344–356.
- [17] M.-B. Radac, R.-E. Precup, R.-C. Roman, Data-driven model reference control of MIMO vertical tank systems with model-free VRFT and Q-learning, *ISA Trans.* 73 (2018) 227–238.
- [18] Y. Jiang, Z.-P. Jiang, Computational adaptive optimal control for continuous-time linear systems with completely unknown dynamics, *Automatica* 48 (10) (2012) 2699–2704.
- [19] C. Jia, X. Li, K. Wang, D. Ding, Adaptive control of nonlinear system using online error minimum neural networks, *ISA Trans.* 65 (2016) 125–132.
- [20] A. Zabih-Hesari, S. Ansari-Rad, F.A. Shirazi, M. Ayati, Fault detection and diagnosis of a 12-cylinder trainset diesel engine based on vibration signature analysis and neural network, *Proce. Inst. Mech. Eng. Part C* 233 (6) (2019) 1910–1923.
- [21] M. Ayati, F.A. Shirazi, S. Ansari-Rad, A. Zabih-Hesari, Classification-based fuel injection fault detection of a trainset diesel engine using vibration signature analysis, *J. Dyn. Syst. Meas. Control* 142 (5) (2020).
- [22] J.Y. Lee, J.B. Park, Y.H. Choi, Integral Q-learning and explorized policy iteration for adaptive optimal control of continuous-time linear systems, *Automatica* 48 (11) (2012) 2850–2859.
- [23] A. Pomprapa, S. Leonhardt, B.J. Misgeld, Optimal learning control of oxygen saturation using a policy iteration algorithm and a proof-of-concept in an interconnecting three-tank system, *Control Eng. Pract.* 59 (2017) 194–203.
- [24] K.J. Åström, B. Wittenmark, *Adaptive Control*, Courier Corporation, 2013.
- [25] P.A. Ioannou, J. Sun, *Robust Adaptive Control*, vol. 1, PTR Prentice-Hall Upper Saddle River, NJ, 1996.
- [26] S. Jahandari, A. Kalhor, B.N. Araabi, A self tuning regulator design for nonlinear time varying systems based on evolving linear models, *Evolv. Syst.* 7 (3) (2016) 159–172.
- [27] S. Ansari-Rad, A. Kalhor, B.N. Araabi, Partial identification and control of MIMO systems via switching linear reduced-order models under weak stimulations, *Evolv. Syst.* (2017) 1–18.
- [28] C.K. Yoo, S.W. Sung, I.-B. Lee, Generalized damped least squares algorithm, *Comput. Chem. Eng.* 27 (3) (2003) 423–431.

- [29] E. Lambert, Process Control Applications of Long-Range Prediction, University of Oxford, 1987 Ph.D. thesis.
- [30] A. Argha, L. Ye, S.W. Su, H. Nguyen, B.G. Celler, Real-time modelling of heart rate response during exercise using a novel constrained parameter estimation method, in: Engineering in Medicine and Biology Society (EMBC), 2016 IEEE 38th Annual International Conference of the, IEEE, 2016, pp. 2680–2683.
- [31] C. Zengqiang, L. Maoqiong, Y. Zhuzhi, Convergence and stability of recursive damped least square algorithm, Appl. Math. Mech. 21 (2) (2000) 237–242.
- [32] E.M. Eksioğlu, A.K. Tanc, RLS Algorithm with convex regularization, IEEE Signal Process. Lett. 18 (8) (2011) 470–473.
- [33] R. Sadikov, P. Korba, G. Andersson, Self-tuning controller for damping of power system oscillations with facts devices, in: Power Engineering Society General Meeting, 2006. IEEE, IEEE, 2006, pp. 6–pp.
- [34] A. Zolghadrit, J. Cieslakt, P. Goupil, R. Dayre, Turning theory to practice in model-based FDI: successful application to new generation airbus aircraft, IFAC-PapersOnLine 50 (1) (2017) 12773–12778.
- [35] A. Padilla, Recursive Identification of Continuous-Time Systems with Time-Varying Parameters, Université de Lorraine, 2017 Ph.D. thesis.
- [36] A. Argha, L. Ye, K. Cao, S.W. Su, B.G. Celler, Real-time identification of heart rate responses via auxiliary-model-based damped RLS scheme, in: Engineering in Medicine and Biology Society (EMBC), 2017 39th Annual International Conference of the IEEE, IEEE, 2017, pp. 1312–1315.
- [37] V.-S. Nguyen, N. Im, Development of computer program for solving astronomical ship position based on circle of equal altitude equation and SVD-least square algorithm, J. Navig. Port Res. 38 (2) (2014) 89–96.
- [38] Y. Yan, Y. Cai, Precision PEP-II optics measurement with an SVD-enhanced least-square fitting, Nucl. Instrum. Methods Phys. Res. Sect. A 558 (1) (2006) 336–339.
- [39] F. Yaacoub, A. Abche, E. Karam, Y. Hamam, MRI Reconstruction using SVD in the least square sense, in: Computer-Based Medical Systems, 2008. CBMS'08. 21st IEEE International Symposium on, IEEE, 2008, pp. 47–49.
- [40] S. Kaczmarz, Approximate solution of systems of linear equations, Int. J. Control 57 (6) (1993) 1269–1271.
- [41] Q.P. Ha, D.C. Rye, H.F. Durrant-Whyte, Fuzzy moving sliding mode control with application to robotic manipulators, Automatica 35 (4) (1999) 607–616.
- [42] C. Ishii, T. Shen, Z. Qu, Lyapunov recursive design of robust adaptive tracking control with L2-gain performance for electrically-driven robot manipulators, Int. J. Control 74 (8) (2001) 811–828.
- [43] J. Lian, J. Hu, S.H. Zak, Adaptive robust control: a piecewise Lyapunov function approach, in: American Control Conference, 2009. ACC'09., IEEE, 2009, pp. 568–573.
- [44] S. Ghabraei, H. Moradi, G. Vossoughi, Finite time-Lyapunov based approach for robust adaptive control of wind-induced oscillations in power transmission lines, J. Sound Vib. 371 (2016) 19–34.
- [45] S. Mobayen, F. Tchier, A novel robust adaptive second-order sliding mode tracking control technique for uncertain dynamical systems with matched and unmatched disturbances, Int. J. Control Autom. Syst. 15 (3) (2017) 1097–1106.
- [46] W. Yan, S. Hou, Y. Fang, J. Fei, Robust adaptive nonsingular terminal sliding mode control of MEMS gyroscope using fuzzy-neural-network compensator, Int. J. Mach. Learn. Cybern. 8 (4) (2017) 1287–1299.
- [47] E. Ghotb Razmjou, S.K. Hosseini Sani, J. Sadati, Robust adaptive sliding mode control combination with iterative learning technique to output tracking of fractional-order systems, Trans. Inst. Meas. Control 40 (6) (2018) 1808–1818.
- [48] S. Ansari-Rad, S. Jahandari, A. Kalhor, B.N. Araabi, Identification and control of MIMO linear systems under sufficient and insufficient excitation, in: 2018 Annual American Control Conference (ACC), IEEE, 2018, pp. 1108–1113.
- [49] H.H. Khalil, High-Gain Observers in Nonlinear Feedback Control, vol. 31, SIAM, 2017.
- [50] M. Zarei, A. Aflakian, A. Kalhor, M.T. Masouleh, Oscillation damping of nonlinear control systems based on the phase trajectory length concept: an experimental case study on a cable-driven parallel robot, Mech. Mach. Theory 126 (2018) 377–396.
- [51] M. Zarei, A. Kalhor, M. Rastegar, Employing phase trajectory length concept as performance index in linear power oscillation damping controllers, Int. J. Electr. Power Energy Syst. 98 (2018) 442–454.
- [52] M. Sharifzadeh, A. Arian, A. Salimi, M.T. Masouleh, A. Kalhor, An experimental study on the direct & indirect dynamic identification of an over-constrained 3-DOF decoupled parallel mechanism, Mech. Mach. Theory 116 (2017) 178–202.
- [53] A. Karimi, M.T. Masouleh, P. Cardou, Avoiding the singularities of 3-RPR parallel mechanisms via dimensional synthesis and self-reconfigurability, Mech. Mach. Theory 99 (2016) 189–206.
- [54] S. Amine, M.T. Masouleh, S. Caro, P. Wenger, C. Gosselin, Singularity analysis of 3T2R parallel mechanisms using Grassmann–Cayley algebra and Grassmann geometry, Mech. Mach. Theory 52 (2012) 326–340.
- [55] M.T. Masouleh, C. Gosselin, M. Husty, D.R. Walter, Forward kinematic problem of 5-RPUR parallel mechanisms (3T2R) with identical limb structures, Mech. Mach. Theory 46 (7) (2011) 945–959.
- [56] C.M. Gosselin, É. St-Pierre, Development and experimentation of a fast 3-DOF camera-orienting device, Int. J. Robot. Res. 16 (5) (1997) 619–630.
- [57] C. Gosselin, J. Angeles, et al., Singularity analysis of closed-loop kinematic chains., IEEE Trans. Robot. Autom. 6 (3) (1990) 281–290.

Classification-Based Fuel Injection Fault Detection of a Trainset Diesel Engine Using Vibration Signature Analysis

Moosa Ayati

School of Mechanical Engineering,
College of Engineering,
University of Tehran,
Tehran 14399-55961, Iran
e-mail: m.ayati@ut.ac.ir

Farzad A. Shirazi¹

School of Mechanical Engineering,
College of Engineering,
University of Tehran,
Tehran 14399-55961, Iran
e-mail: fshirazi@ut.ac.ir

Saeed Ansari-Rad

School of Electrical and Computer Engineering,
College of Engineering,
University of Tehran,
Tehran 14399-55961, Iran
e-mail: saeedansari71@ut.ac.ir

Alireza Zabihhesari

School of Mechanical Engineering,
College of Engineering,
University of Tehran,
Tehran 14399-55961, Iran
e-mail: alireza_zabihhi@ut.ac.ir

Diesel engines are crucial components of trainsets. Automated fault detection of diesel engines can play an important role for increasing reliability of passenger trains. In this research, vibration-based fuel injection fault detection of a high-power 12-cylinder trainset diesel engine is studied. Vibration signals are analyzed in frequency and time-frequency domains to obtain possible patterns of faults. Fast Fourier transform (FFT) and wavelet packet transform (WPT) of vibration signals are used to extract several uncorrelated features. These features are chosen to increase the ability of classifiers to separate healthy and faulty engine sides, automatically. Different classification methods including multilayer perception (MLP), support vector machines (SVM), K-nearest neighbor (KNN), and local linear model tree (LOLIMOT) are used to process captured features; these methods are utilized in both “Single-sensor condition monitoring” and “Classification and fault detection” sections. It is shown that KNN networks are practical tools in the proposed fault detection procedure. The main novelty of this work comes from introducing a rich feature-extraction method based on a combination of FFT and db4 features. In addition, the complexity of computations and average running-time decrease while classification accuracy in the fuel injection fault detection procedure increases. [DOI: 10.1115/1.4046270]

Keywords: fault detection, wavelet transform, classification, vibration signal, fuel injection, trainset diesel engine

1 Introduction

In order to avoid expensive machine failures in transportation vehicles, it is imperative to keep the engine in its sound working conditions using nonintrusive monitoring and diagnostic approaches [1]. There are different probable faults in diesel engines for which appropriate measurement techniques must be applied to achieve an efficient condition monitoring and fault diagnosis system. Several types of signals can be measured and utilized for monitoring purposes including pressure [2], rotational angle speed [3], temperature [4], fuel and oil quality [5–7], and vibration [8–10]. Vibration monitoring is a reliable method for detecting machine abnormality, considering the fact that different faults especially those related to combustion are the source of vibration [11]. Vibration signals can be obtained by measuring different parameters including displacement, velocity, acceleration, and stress. Accelerometers are the best choice for vibration measurement due to their accuracy, lightweight, high temperature resistance, and wide frequency response [1]. Different mathematical tools are required to analyze accelerometer data and extract appropriate features from a primary vibration signal.

Fast Fourier transform (FFT) is one of the most popular feature-extraction tools in frequency domain. For instance Zhou et al. [12] extracted features based on FFT method and used them as inputs into different classification networks. Then, their approach of fault detection as ensemble rapid centroid estimation was compared with artificial neural network (ANN) and principal component analysis (PCA). Also, Liu et al. [13] introduced an approach for bearing fault diagnosis and for enabling the

extraction of bearing fault feature frequencies. These frequencies were identified by the FFT of Teager energy.

The wavelet transform (WT) has been widely used in signal processing and fault detection problems to analyze the vibration signals in the time-frequency domain. Many researches based on the use of discrete wavelet transform (DWT) have been conducted in recent years. There are three parameters with a decisive influence on the performance of DWT in fault detection including the sampling frequency, mother wavelet, and level of decomposition. Most researches use a particular combination of these parameters for a specific problem [14–16]. First, wavelet features are extracted and form the feature set used as input to the classifiers [17]. Atoui et al. [18] considered WT and FFT of vibration signals in order to detect and diagnose unbalance faults in rotating machinery. The condition and location of faults were successfully detected by WT-FFT for vibration measurements obtained from accelerometer sensors. In Ref. [19], DWT was employed to process the signals of a Pride gearbox in several conditions. Decomposition was made using Daubichies-5 (db5) wavelet with five levels. Koley et al. [20] presented a hybrid WT and modular ANN-based fault detector, classifier, and locator for six-phase transmission lines using single end data only. In Ref. [21], the vibration signals acquired from engine manifolds were preprocessed by the WT, and signal energy was considered as a distinguishing property to classify these faults.

Artificial neural networks are suitable for fault detection and identification applications because of their pattern recognition abilities. Ahmed et al. [22] introduced an engine fault detection and classification technique using vibration data. These data were used in ANNs to detect faults in a four-stroke gasoline engine. In Ref. [23], an unsupervised ANN was tested for fault detection and identification in an automated machine, and its performance was compared to a conventional rule-based method. Bangalore and Tjernberg [24] introduced a scheduler framework for maintenance management of wind turbines. In this framework, an ANN-based

¹Corresponding author.

Contributed by the Dynamic Systems Division of ASME for publication in the JOURNAL OF DYNAMIC SYSTEMS, MEASUREMENT, AND CONTROL. Manuscript received January 29, 2018; final manuscript received January 30, 2020; published online March 3, 2020. Assoc. Editor: Carrie Hall.

condition monitoring approach by using data from supervisory control and data acquisition system was proposed. Approaches for fault detection of wind turbines based on finite time and modified sliding mode observers were presented in Refs. [25] and [26]. The paper [27] presented a fault detection algorithm based on probabilistic neural network. This algorithm uses probabilistic neural network and back propagation neural network to train and test the mapping datasets. In Ref. [28], Janssens et al. proposed a feature learning model for condition monitoring based on convolutional neural networks. The goal of this approach was to autonomously learn useful features for bearing fault detection from the data itself.

For fault detection, many techniques have been employed among which the support vector machines (SVM) is a popular one owing to its attractive features like fast classification, good handling capability of nonlinear data, and providing a global optimum for classification. In Ref. [29], a multiclass SVM classified the type of present faults giving the final diagnosis. Seryasat et al. [30] proposed a method for detecting faults using WT and SVM for an electric motor that had two rolling bearings. The article [31] used the SVM and one of its variants for fault detection in a rotating machinery using vibrational signals.

Andre et al. [32] introduced a combination of SVM and *K*-nearest neighbor (KNN) to monitor rotational machines using vibrational data. Data were classified using a standard SVM, but for data within the SVM margin, where misclassifications are more likely, a KNN was used to reduce the false negative rate. The purpose of Ref. [33] was to develop an appropriate approach for detecting unbalanced fault in rotating machinery using KNN and SVM classifiers. The results demonstrated that the proposed approach can be used effectively for detecting unbalanced condition in rotating machinery. Moreover, a performance comparison was made between KNN and SVM in fault classification. In addition, this approach gave a high level of classification accuracy.

This paper investigates the application of FFT and DWT for feature extraction and well-known structures including SVM, multilayer perception (MLP), and KNN for classification in fault detection and diagnosis of a 12-cylinder trainset diesel engine subjected to abnormal fuel injection. Vibration signals are in frequency and time-frequency domains. Power spectral densities (PSD) of vibration signals are calculated and normal and faulty engine conditions are distinguished. Nevertheless, more details of the fault cannot be determined by this approach. Hence, FFT-based data features are introduced in order to overcome the problem. Conceptually, these features show the average of the frequency energy in selected intervals. Furthermore, wavelet packet transform (WPT)-based features are used to identify the difference of energy between normal and faulty conditions. In order to analyze derived features, different classifiers are applied in both “Single-sensor condition monitoring” and “Classification and fault detection” sections.

Even though the literature on fault detection and diagnosis methods is copious, relatively few papers have addressed the problem of abnormal fuel injection in diesel engines. In addition, the literature suffers from lack of papers in which sophisticated engines with more than six cylinders are investigated. As the number of cylinders increases in diesel engines, the fault detection and diagnosis process based on vibration signals becomes more complicated. Furthermore, well-known signal processing methods including FFT and WPT provide features with limited levels of accuracy in the classification phase. The main novelty of this work comes from the combination of FFT and db4-based features to increase the classification accuracy in the fault detection procedure. Meanwhile, this paper proposes a feature-extraction method based on FFT signals with higher separable features.

The remainder of the paper is organized as follows. The test bed and signal acquisition process are described in Sec. 2. Signal processing methods are presented in Sec. 3. Features analysis techniques are described in Sec. 4. Section 5 proceeds condition monitoring using one cylinder’s data. Section 6 describes the

classification and fault detection procedure. Finally, Sec. 7 concludes the paper.

2 Experimental Setup

2.1 Diesel Engine and Data Acquisition System. The experimental data have been acquired from a 12 cylinder, D 2842 LE 602 diesel engine commonly used in trainsets. The engine is a V-shaped, four-stroke diesel engine with a turbocharger and an intercooler. The major specifications of the engine are summarized in Table 1. All experiments have been done at zero-load and a constant speed of 600 rpm. Two DJB2784 accelerometers mounted on both intake manifold and cylinder heads have been used for vibration pickup. The accelerometers on the cylinder heads and intake manifold were firmly fixed by magnets and wax, respectively. In order to indicate the engine speed, a tachometer pointing to a reflective tape on the crankshaft pulley was utilized. Since the engine is a four-stroke type, two complete crankshaft revolutions (720 deg) represents a full thermodynamic cycle. The vibration signals, measured by accelerometers, and tachometer signals were transferred through cables into a data logger/analyzer and then to the computer for further analysis. The Bruel & Kajer-PULSE LABSHOP software version 12.5.1 was used in the course of data acquisition. The instrumented engine and the numbering of cylinders are shown in Fig. 1.

Combustion failure may be the result of malfunction in one or more cylinders. In order to test our proposed approach, faulty conditions must be introduced in the engine. In this work, the fuel valve of cylinders was opened to let the fuel partially enter the combustion chamber. Therefore, the combustion failure was modeled by disabling fuel valve of known cylinders.

2.2 Signal Acquisition. Vibration signals were obtained using two accelerometers mounted on either intake manifold or cylinder heads in two separate phases. The sampling frequency was chosen to be 8.192 kHz to acquire vibration data using a four-channel data logger. Each dataset comprised of 2 s of vibration signals with 16,384 data points. Using tachometer pulses, the engine vibration signals were split into segments with an equal length of 0.2 s corresponding to two crankshaft revolutions (a complete thermodynamic cycle). Throughout data acquisition process, the engine speed was set at 600 rpm (10 Hz) with zero load. The procedure of data acquisition and signal processing in this work is briefly illustrated in Fig. 2.

3 Signal Analysis

3.1 Principal Component Analysis. The principal component analysis is an optimal technique to reduce dimensionality based on variance of the data. PCA calculates loading vectors, which are a set of orthogonal vectors. These vectors are ordered by the values of variance explained in each vector direction. PCA analyses data matrix *X* consisting of *n* observations from *m*

Table 1 Engine specifications

Diesel Cycle	V 90 deg Four-stroke diesel with turbocharger and intercooler
Number of cylinders	12
Compression ratio	16.5:1
Bore	128 mm
Stroke	142 mm
Engine capacity	21,930 cm ³
Direction of rotation viewed on flywheel	Anticlockwise
Firing order	1-12-5-8-3-10-6-7-2-11-4-9
Firing interval	120 deg
Power based on DIN ISO 3046	588 kW at 2100 rpm

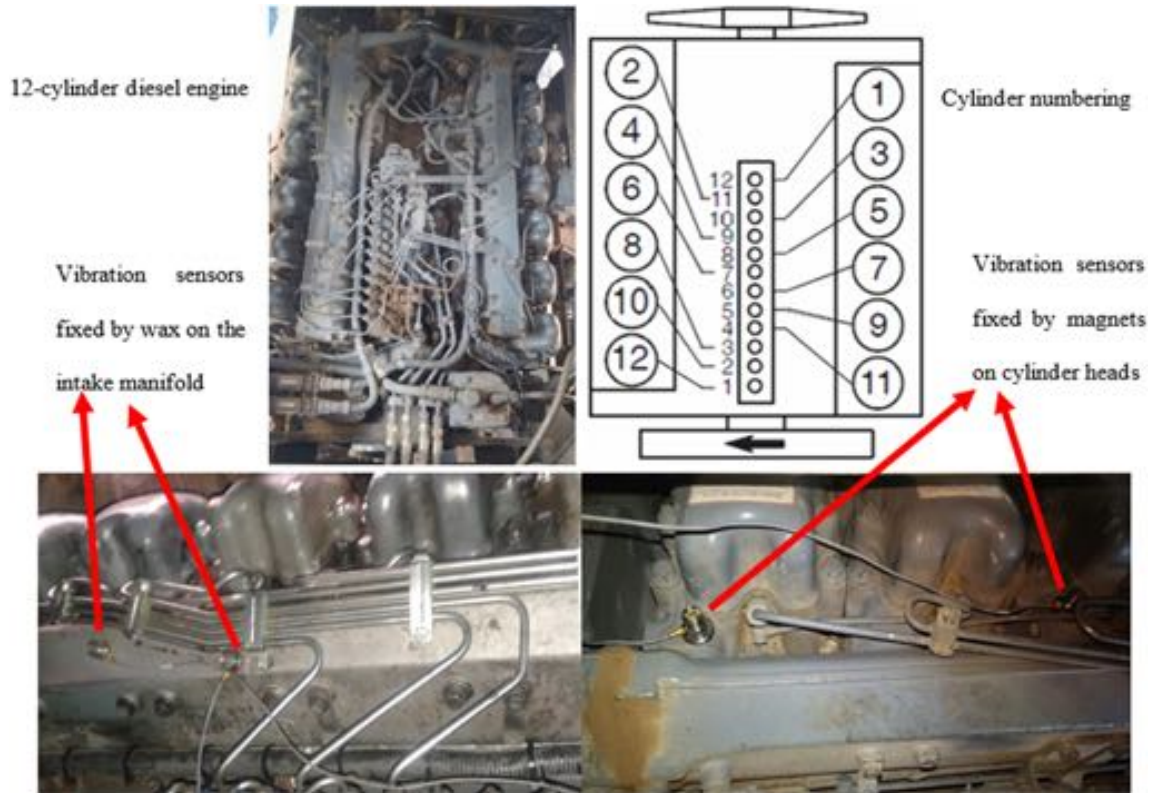


Fig. 1 The instrumented engine and cylinder numbering

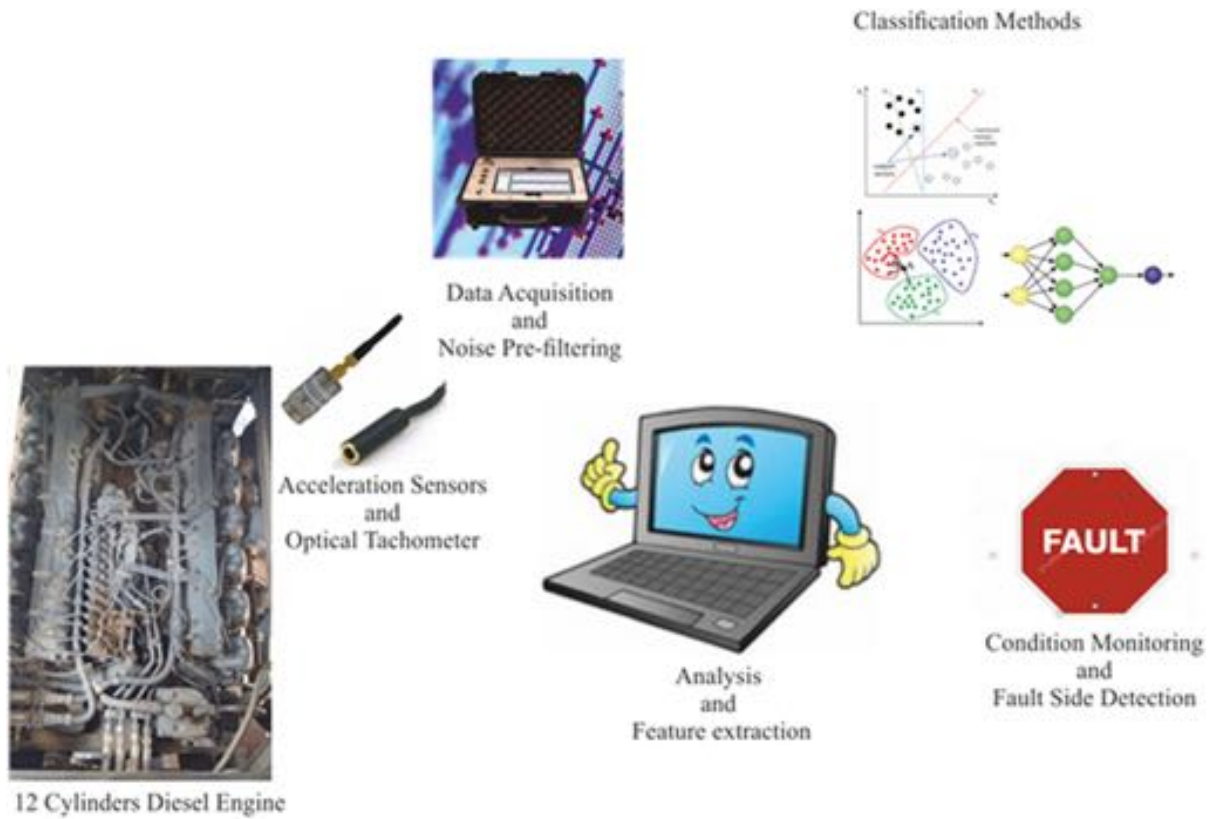


Fig. 2 Schematic of data acquisition and signal processing system

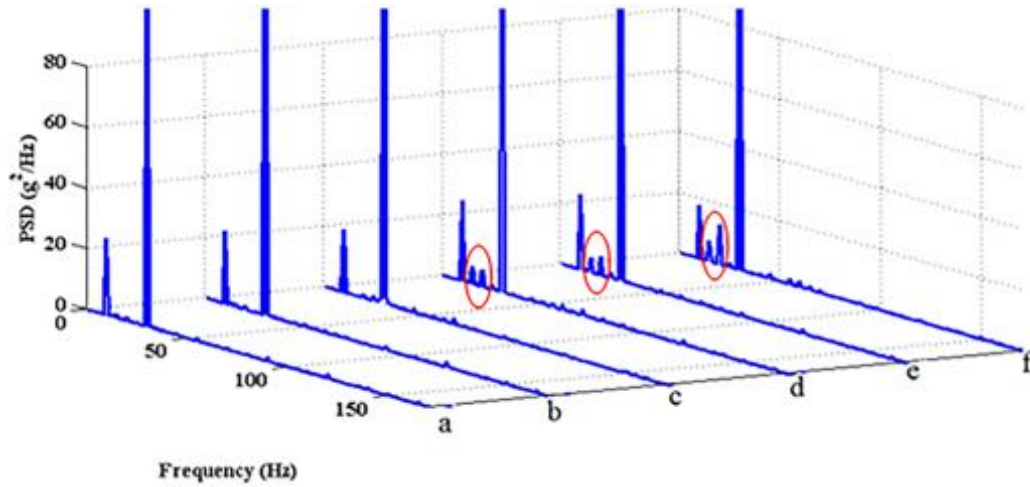


Fig. 3 PSD of engine vibrations of the intake manifold (a) in the vicinity of cylinder 1 for healthy condition, (b) in the vicinity of cylinder 3 for healthy condition, (c) in the vicinity of cylinder 8 for healthy condition, (d) in the vicinity of cylinder 1 when cylinder 9 is faulty, (e) in the vicinity of cylinder 3 when cylinder 9 is faulty, and (f) in the vicinity of cylinder 1 when cylinder 11 is faulty

Table 2 Frequency features of the extracted signals from wavelet bank and FFT

Feature index	Extracted signal from wavelet bank	Beginning frequency of band (Hz)	End frequency of band (Hz)	Center frequency of band (Hz)
1	cA ₈	0	12.5	6.25
2	cD ₈	12.5	25	18.75
3	cD ₇	25	50	37.5
4	cD ₆	50	100	75
5	cD ₅	100	200	150
6	cD ₄	200	400	300
7	cD ₃	400	800	600
8	cD ₂	800	1600	1200
9	cD ₁	1600	3200	2400

measurement variables. Computing the singularities of the following optimization problem gives loading vectors where $v \in \mathbb{R}^m$:

$$\max_{v \neq 0} \frac{v^T X^T X v}{v^T v} \quad (1)$$

The stationary points of above equation can be computed via singular value decomposition (SVD) as follows:

$$\frac{1}{\sqrt{n-1}} X = U \Sigma V^T \quad (2)$$

where $U \in \mathbb{R}^{n \times n}$ and $V \in \mathbb{R}^{m \times m}$ are unitary matrices and matrix $\Sigma \in \mathbb{R}^{n \times m}$ contains non-negative real singular values with decreasing magnitude ($\sigma_1 \geq \dots \geq \sigma_i \geq \dots \geq \sigma_{\min(m,n)} \geq 0$). The loading vectors are the orthonormal column vectors in the matrix V , and the variance of the dataset projected along the i th column of V is equal to σ_i^2 [34].

3.2 Frequency Domain Analysis. In this part, datasets are transferred from time domain to frequency domain using FFT. The autospectrum of a vibration signal is defined as [35]

$$P_{xx}(f) = X(f)X^*(f) = |X(f)|^2 \quad (3)$$

where $X(f)$ refers to FFT of the vibration signal, f is the frequency variable, and $*$ is the conjugate operator. Dividing $P_{xx}(f)$ by the sampling frequency (f_s) results in the PSD of the signal

$$\text{PSD} = \frac{P_{xx}(f)}{f_s} \quad (4)$$

The PSD of vibration signals from different locations on the intake manifold is depicted in Fig. 3. For a healthy engine (a, b, and c) power spectrum of vibration signals has the same pattern for different locations on the intake manifold. In this case, there are two peaks in the PSD of vibration signals in frequencies of 10 Hz and 30 Hz which refer to the engine speed (600 rpm) and the simultaneous combustion of a pair of cylinders in two complete revolutions of the crankshaft, respectively. We investigated the frequency domain analysis in a low-frequency interval of 0–180 Hz since it is more likely to distinguish between faulty and healthy conditions compared to a high-frequency range. Comparing PSDs of healthy and faulty peaks, it was revealed that in faulty conditions (d, e, and f) new peaks appeared between 10 Hz and 30 Hz in frequencies of 15 Hz and 20 Hz.

Therefore, it was concluded that any fault in combustion of cylinders changes the frequency patterns of PSD. According to the specified intervals in Table 2, average values of $P_{xx}(f)$ in these intervals were defined as features of dataset. Based on analysis of Fig. 3, values of the features in some intervals vary depending on location of fault and number of faulty cylinders

$$\text{Feature from interval } R_i = \frac{\int_{f \in R_i} |X(f)|^2 df}{\text{length}(R_i)} \quad 1 \leq i \leq 9 \quad (5)$$

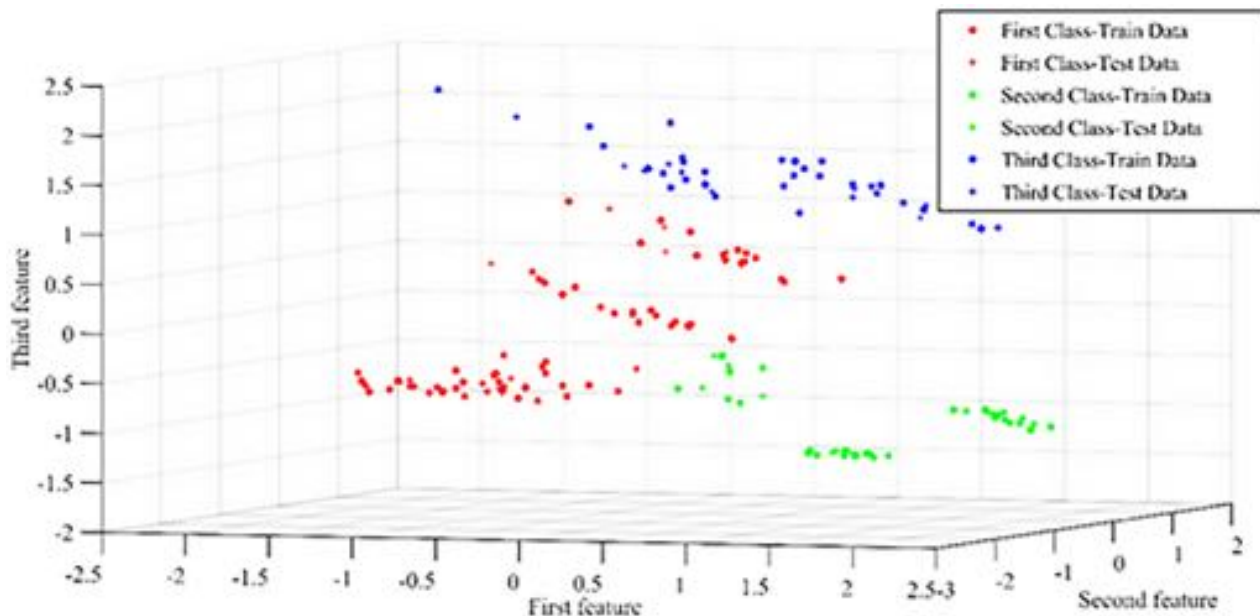


Fig. 4 Visualization of datasets with FFT-extracted features by applying PCA

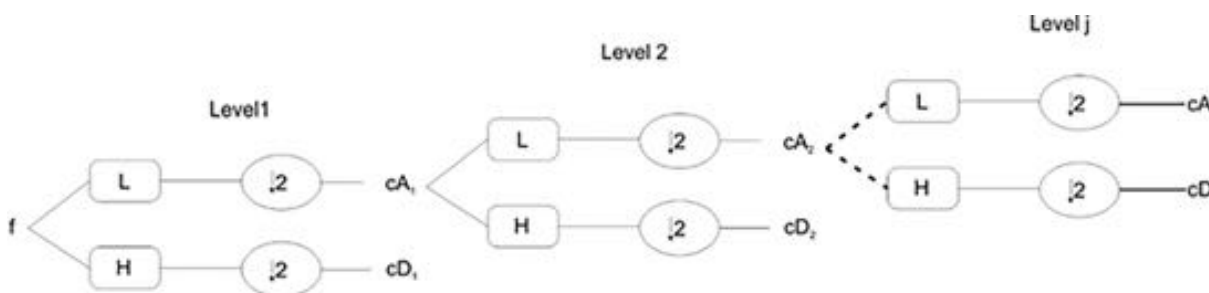


Fig. 5 Basic step of decomposition of WPT

In Fig. 4, to visualize introduced features, PCA was applied to data features of paired sensors {M5, M12}. Three features with higher singular values were chosen and then datasets were labeled based on three classes, which are explained with details in the “Fault side detection” section. Extracted data sets were whitened by using the average vector and covariance matrix. Therefore, Fig. 4 does not show actual distribution of data sets along axes. These illustrated classes are easy to separate and correct classification rate will be increased. Therefore, mentioned FFT-based features are classifiable and uncorrelated.

3.3 Time-Frequency Domain Analysis. In this section, wavelet-based feature extraction is presented. Wavelet transform has been widely used in signal processing and fault detection problems. The main idea is to convolve wavelets with spans of transient signal to extract valuable features of signal. The DWT method is an efficient way of analyzing data in time-frequency domain. To implement the DWT method, low-pass filter $h(k)$ and high-pass filter $g(k)$ are applied, which are related to the scaling function $\phi(t)$ and wavelet function $\Psi(t)$, respectively,

$$\begin{aligned} \phi_j(t) &= \sum_k h(k) \underbrace{2^{\frac{j+1}{2}} \phi(2^{j+1}t - k)}_{\phi_{(j+1,k)}(t)} = h(-k) * \phi_{(j+1,k)}(t) \\ \Psi_j(t) &= \sum_k g(k) 2^{\frac{j+1}{2}} \phi(2^{j+1}t - k) = g(-k) * \phi_{(j+1,k)}(t) \end{aligned} \quad (6)$$

$\phi_{(j,k)}(t)$ is a member of the set of expansion functions derived from a scaling function $\phi(t)$. Also, ϕ_j is the scaling function and Ψ_j is the wavelet function of scale j . Generalization of the DWT to more than one level results in the wavelet packet transform, where it is implemented based on wavelet filters. The following equations comprise WPT coefficients at each level:

$$\begin{aligned} W_{j+1}^{2K} &= W_j^K(n) * h(-2n) \\ W_{j+1}^{2K+1} &= W_j^K(n) * g(-2n) \end{aligned} \quad (7)$$

where, W_{j+1}^{2K} denotes the j th decomposed level of WPT coefficient at frequency band of $2k$ ($0 < k < 2^j - 1$). From above equations, it is obvious WPT is more efficient than DWT to describe faulty signals in different frequency bands of local information [36]. According to Fig. 5, at each level passing a signal through filters emerges as low-frequency (approximations (A’s)) and high-frequency [details (D’s)] signals. Hence, the signal $f(t)$ is written as

$$f(t) = cA_j + \sum_{j < J} cD_j \quad (8)$$

where cA_j and cD_j are the approximation and the detail coefficients of J th level. It is still hard to find the faulty conditions accurately visually or by classifier due to large size of coefficient signals produced at each level. The solution of this problem is to

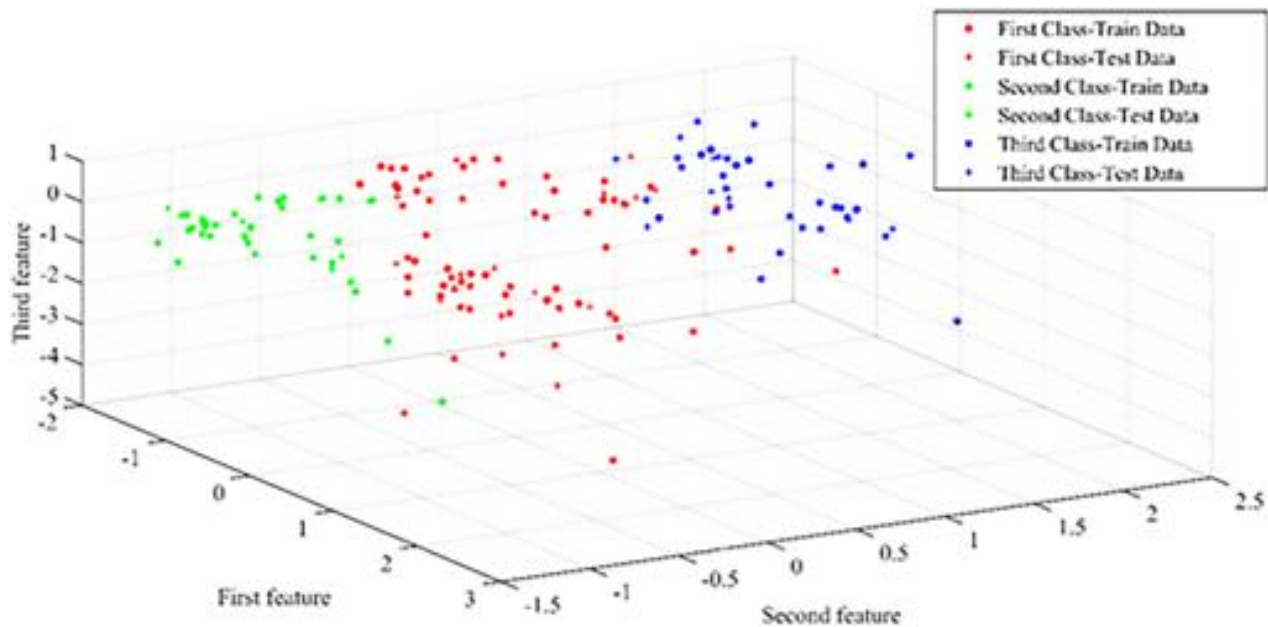


Fig. 6 Visualization of datasets with db4 extracted features by applying PCA

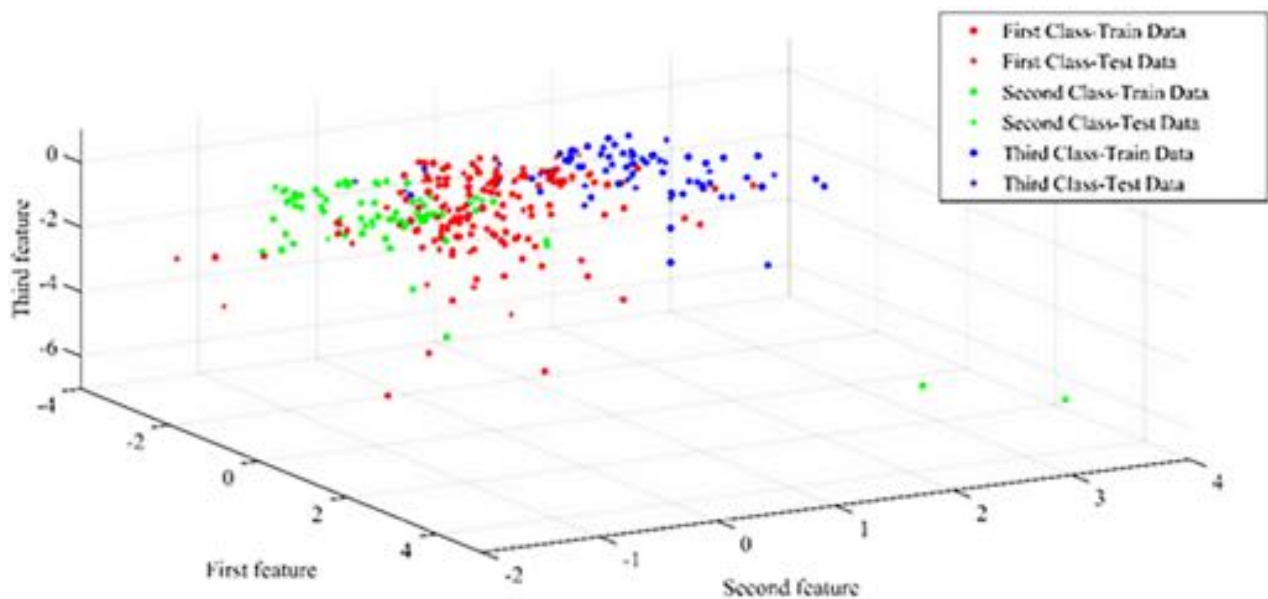


Fig. 7 Visualization of datasets with db8 extracted features by applying PCA

use energy spectrum based on Parseval's energy theorem [37] expressed as follows:

$$\sum_{t=0}^{N-1} |f(t)|^2 = \frac{1}{N} \sum_{f=0}^{N-1} |F(f)|^2 \quad (9)$$

where $f(t)$ is the time domain signal, $F(f)$ is the discrete form after applying discrete Fourier transform to the signal, and N is the sampling period. By substituting Eq. (8) into Eq. (9), signal features based on WPT and energy spectrum can be formulated as

$$\sum_{t=0}^{N-1} |f(t)|^2 = \frac{1}{N} \sum_{f=0}^{N-1} |cA_J(f)|^2 + \sum_{j \leq J} \left[\frac{1}{N} \sum_{f=0}^{N-1} |cD_j(f)|^2 \right] \quad (10)$$

where, $cA_J(f)$ and $cD_J(f)$ are discrete Fourier transformation of the approximation and the detail coefficients of J th level, respectively.

Daubechies wavelets are a family of orthogonal wavelets. There exists a scaling function for each wavelet type of this class that generates an orthogonal multiresolution analysis [38]. In next analyses, some of Daubechies scaling functions are considered as WPT method with eight levels. The average energy of signals in each frequency range is calculated as a proper feature which distinguishes between different sources of fault. The frequency intervals of a vibration signal are presented in Table 2.

In order to capture a good visualization, PCA was applied to db4 data features from paired sensors {M5, M12} and three features with higher singular values were selected and depicted in Fig. 6. These three classes are almost separable, but some datasets in the classes' borders make classification difficult. Figure 7

shows the same data but with features extracted from db8. It was observed that it is difficult for classifiers to separate these three classes completely. By comparing Figs. 4, 6, and 7, we expect that performance of classifiers in Sec. 4 would be enhanced for data features extracted from FFT signals. In addition, comparing wavelet-based features, db4 was determined to be an acceptable choice for classification and condition monitoring purposes.

4 Feature Analysis Methods

4.1 Multilayer Perceptron. The way the human brain works, encourages researchers to develop artificial models based on learning process of a biological neuron. As a result, artificial neural networks have been developed from a number of richly interconnected artificial processing neurons called nodes, integrated in layers forming a network [39].

In this research, an MLP network was used to process data features indicating the average energy of signals in each frequency range. These signals were obtained from FFT and wavelet analyses. The feature values were normalized to increase the network performance.

The basic structure of an MLP network consists of an input layer (with neuron numbers equal to the number of features), two hidden layers, and an output layer (the number of output layer neurons is equal to the number of classes). The best structure of the network is found by searching through neuron numbers of hidden layers. The tangent sigmoid was chosen as the activation function. The training of the MLP network is based on the back propagation algorithm [40]. As test data, 20% of datasets were selected randomly as the test dataset, the rest were used as the train dataset.

4.2 Local Linear Model Tree. As information about the inner physical model structure of the system is not well-known, neural networks are embraced for condition monitoring purposes. The local linear model tree (LOLIMOT) method developed by Nelles and Isermann [41], is a structure of linear models. These linear models are identified by an orthogonal divided input space and properties of each model are represented with radial basis functions. The input space is partitioned by a tree construction algorithm. The local models are interpolated by overlapping local basis functions. The resulting structure is equivalent to a Sugeno-Takagi fuzzy system and a local model network and can therefore be interpreted correspondingly. The LOLIMOT algorithm is simple, easy to implement, and fast.

The local model parameters are calculated using least square method which leads to decrement of running time of the network and training procedures. The model structure of LOLIMOT is updated from one local model to the best adaptive number of local models, iteratively. The input space of the worst performing local model is divided in two local models, resulting in a growing number of local models. This algorithm is stopped when a given number of local models are reached or the training error falls below a given limit [42].

4.3 Support Vector Machine. The SVM is a novel learning method based on statistical learning theory which specializes in the case of a small number of samples. SVM theory is the extension of the optimal separating plane under linearly separable condition.

To formulating the problem, it is assumed $X_i = (x_{1i}, x_{2i}, \dots, x_{ni})^T$, $i = 1, \dots, M$, is a sample of $x \in R_n$ in the n -dimension space which belongs to classes I or II. M is the number of data points in the dataset. For linearly separable data, the hyper-plane described as Eq. (13) can separate two classes

$$f(x) = w^T x + b = \sum_{j=1}^n w_j x_j + b = 0 \quad (11)$$

The vector w and the scalar b delimitate the locality of the hyper-plane. By assigning $y_i = 1$ for the class I and $y_i = -1$ for

the class II, appropriate label is defined for the data point X_i . The mentioned hyper-plane should satisfy the constraint $f(x_i) \geq 0$, if X_i belongs to the class I and $f(x_i) < 0$, if X_i belongs to the class II. For linearly separable case, solving the following convex quadratic optimization problem results in an optimal hyper-plane which classifies two classes, completely. This convex quadratic problem keeps the weights of the hyper-plane under mentioned constraint

$$\begin{aligned} \text{minimize } \gamma &= \frac{1}{2} \|w\|^2 \\ \text{subject to } &y_i(w^T x_i + b) \geq 1 \end{aligned} \quad (12)$$

For nonlinear classification problem, two classes are not well-separable due to nonlinearity of the boundary in the input space. By using nonlinear mapping $\phi(x)$ onto a high-dimensional feature space, the nonlinearly separable dataset is mapped from the original space to a high-dimensional space where dataset is linearly separable. This nonlinear mapping is called kernel functions which are usually linear functions, polynomials functions, radial basis functions, multilayered perceptron, or sigmoid functions [43].

4.4 K-Nearest Neighbor. The KNN classification method is one of the most popular and efficient fault detection methods. Unlike other methods in this research, both train and test samples are represented in a D-dimensional space according to the value of each of their features and then, K -nearest neighbors are selected. In other word, the test cases are classified based on the Euclidean distance of majority of K -nearest neighbors. However, all of the computations must be done during test procedure which makes this method slow for large test datasets. The class with the most "votes" is selected as the class of a testing sample [44]. By searching through different neighbors, the optimal number of neighbors is obtained in this study for K-NN classifiers.

5 Single-Sensor Condition Monitoring

In this part, MLP with two output neurons will be used for condition monitoring purpose where vibration data were measured from one cylinder. The basic procedure of condition monitoring is organized as the left part of Fig. 8. Generally, ANNs have been employed through condition monitoring by training of the network with features extracted from data of both faulty and healthy conditions. Each dataset has a flag which defines the condition or class it belongs to. For each fault and sensor location, MLP was trained and the performance of the network for the test data was calculated. This process was repeated several times and the average of the performances (called average correct classification rate (ACCR)) was calculated and reported in Table 3. Then, the number of the neurons was changed and ACCR was recalculated. Based on backward elimination process [45], different subsets of FFT extracted features were analyzed, and in case of removing any feature it is listed in sixth column of the table. Validation of condition monitoring, optimal neuron numbers, and running time of networks are also reported in Table 3.

In addition, support vector machines were used in this research for condition monitoring. The classes were separated by one-against-one approach. For each case of sensor location, performance of SVM and the best kernel scale for the radial basis function (RBF) kernel are reported in Table 4. The total time of training and testing in search of the best kernel scale and also deleted feature(s) of FFT analysis, based on the backward elimination method, are written in fifth and sixth columns of the table.

Local linear model trees are another structure that has been used repeatedly in model-based fault detection. Nonetheless, we used LOLIMOTs in this problem with similar structures. In search of optimal number of linear models, correlated features were removed; therefore, any subset selection procedures are

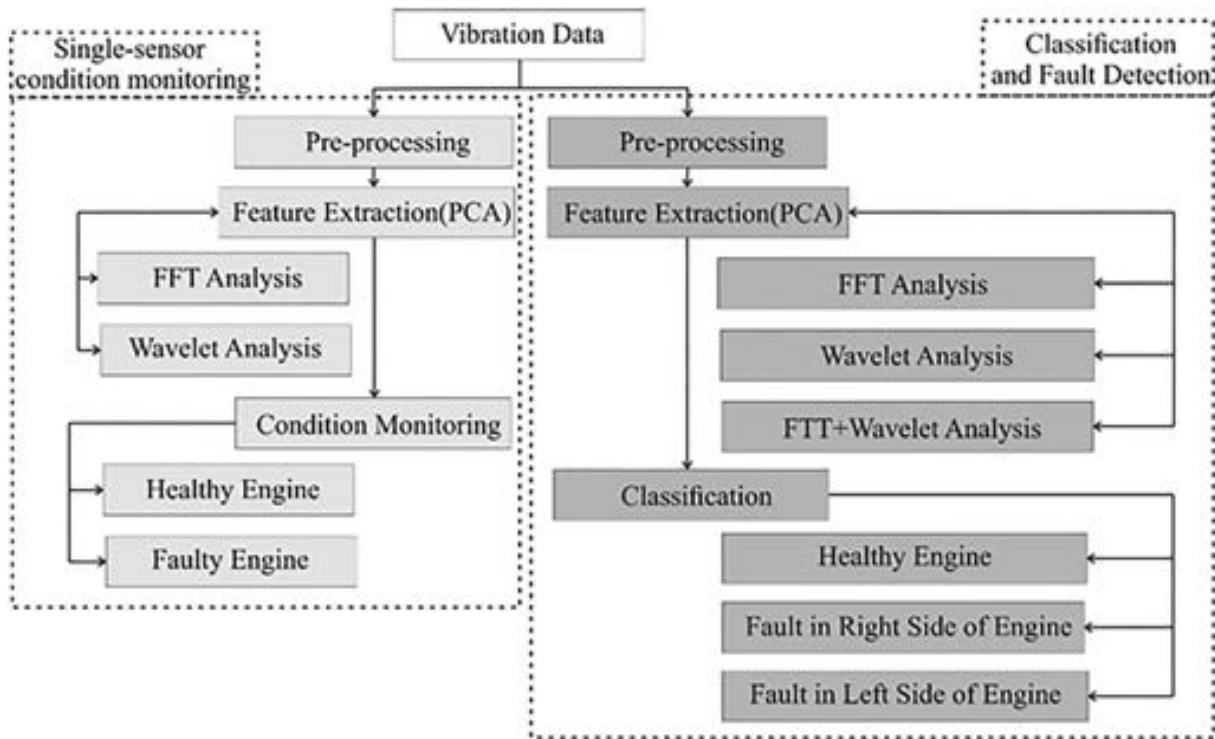


Fig. 8 High-level representation of the proposed algorithms' architectures

Table 3 Results obtained from running MLP on FFT-based features for a sensory condition monitoring

Measurement (sensor) location	Fault location	Average condition monitoring performance (%)	Numbers of neurons in first hidden layer of ANN	Numbers of neurons in second hidden layer of ANN	Average training and testing time (s)	Deleted features
M_1	C_5	100	1	2	22.4083	1
M_5	C_5	100	1	1	22.9484	—
M_{11}	C_5	100	1	1	23.8483	—
M_2	C_5	100	1	1	20.2418	—
M_6	C_5	100	1	1	24.8963	—
M_{12}	C_5	100	1	1	19.9249	—

Table 4 Results obtained from running SVM on FFT-based features for a sensory condition monitoring

Measurement (sensor) location	Fault location	Condition monitoring performance (%)	Best kernel scale	Total training and testing time (s)	Deleted features
M_1	C_5	100	0.0853	2.2866	—
M_5	C_5	100	0.1083	1.4498	—
M_{11}	C_5	100	0.1743	1.4533	—
M_2	C_5	100	0.1374	1.4297	—
M_6	C_5	100	0.1083	1.4386	—
M_{12}	C_5	100	0.1083	1.4272	—

unnecessary. The number of linear models and running time of each sensory condition monitoring are mentioned in Table 5.

In KNN structure, test cases were classified based on the majority of its K -nearest neighbors' distances. As shown in Table 6, the closest neighbor of each point is enough for obtaining high performance, because features extracted from FFT signals are well-separable and uncorrelated.

Figure 9 gives a better standpoint to evaluate performance of mentioned classifiers. It was shown the KNN structure is a better choice for condition monitoring of sensors mounted on the intake manifolds. Also, KNNs are more suitable from "computational expense" criteria viewpoint based on overall calculated times in Tables 3–6. Among different sets of features, extracted FFT features seemed to be uncorrelated and more linearly separable; in

most cases, it was not required to remove extracted features from FFT method.

6 Classification and Fault Detection

Classification methods are applied when no prior knowledge of the relation between symptoms and faults is available. Methods such as SVM, MLP, LOLIMT, and KNN have been used widely for fault detection purposes. In this research, the objective is to determine faulty side of the engine and then the faulty cylinder with a high correct classification rate using the best classification method. Figure 9 shows data stream in classification procedure. Here, "fault side detection" is under consideration and we have used two classes that determine whether the fault is on the left or

Table 5 Results obtained from running LOLIMOT on FFT-based features for a sensory condition monitoring

Measurement (sensor) location	Fault location	Condition monitoring performance (%)	Best number of LLMs	Total training and testing time (s)
M ₁	C ₅	95	3	1.6417
M ₅	C ₅	100	2	1.2752
M ₁₁	C ₅	100	2	1.2667
M ₂	C ₅	100	2	1.2592
M ₆	C ₅	100	2	1.3176
M ₁₂	C ₅	100	2	1.2756

Table 6 Results obtained from running KNN on FFT-based features for a sensory condition monitoring

Measurement (sensor) location	Fault location	Condition monitoring performance (%)	Best number of neighbors	Total training and testing time (s)	Deleted features
M ₁	C ₅	100	1	0.0968	—
M ₅	C ₅	100	1	0.1007	—
M ₁₁	C ₅	100	1	0.1040	—
M ₂	C ₅	100	1	0.1011	—
M ₆	C ₅	100	1	0.0942	—
M ₁₂	C ₅	100	1	0.0945	—

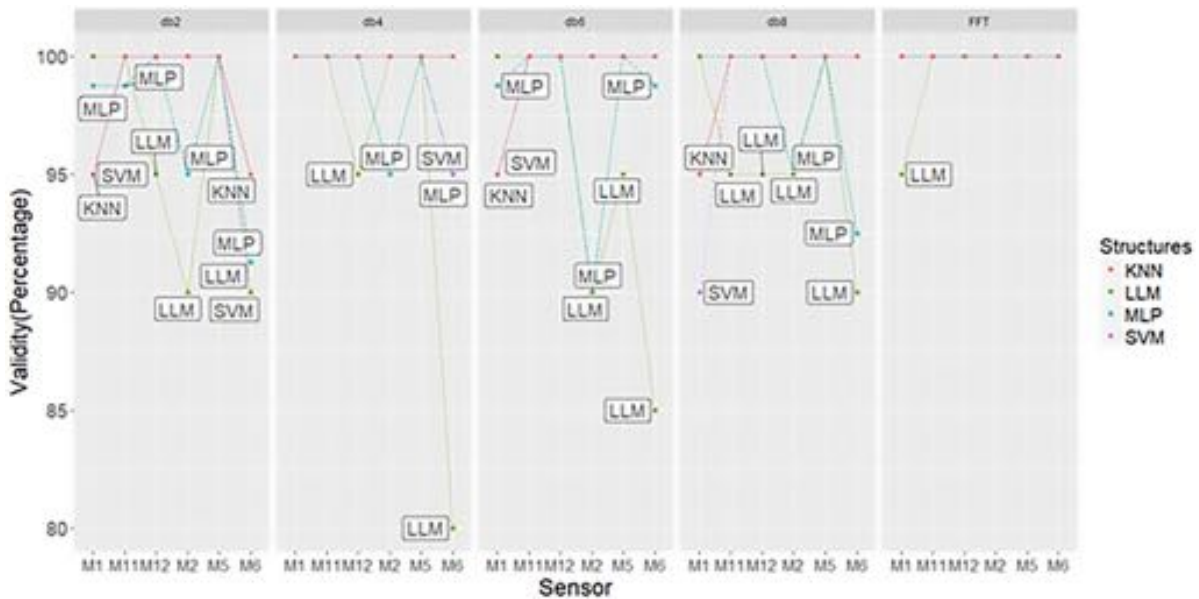


Fig. 9 Performance comparison of different structures for the single-sensor condition monitoring purpose

Table 7 Results obtained from running MLP on FFT-based features for classification and fault side detection

Measurement location	Fault location	Fault side detection performance (%)	Numbers of neurons in first hidden layer	Numbers of neurons in second hidden layer	Average training and testing time (s)	Deleted features
{M ₅ ,M ₆ }	C ₅	100	7	9	32.8729	—
{M ₁₁ ,M ₆ }	C ₅	100	2	5	38.3669	9,4
{M ₁ ,M ₆ }	C ₅	95	9	7	32.7400	3,1
{M ₅ ,M ₂ }	C ₅	100	12	7	31.1036	8
{M ₅ ,M ₁₂ }	C ₅	100	2	3	23.2595	—
{M ₁₁ ,M ₂ }	C ₅	100	5	9	29.6589	—
{M ₁ ,M ₁₂ }	C ₅	98.125	4	2	32.4077	3,8
{M ₁ ,M ₂ }	C ₅	99.375	5	3	31.5059	5
{M ₁₁ ,M ₁₂ }	C ₅	100	3	3	33.2315	—

right side of the engine. Also, sensors are supposed to be placed on both sides of the engine and the best choice is to mount one sensor on each side (and on intake manifolds).

Table 7 reports the results of fault side detection using MLP neural networks. ACCR of each paired sensors was calculated and the best results based on subset selection are mentioned. The

Table 8 Results obtained from running SVM on FFT-based features for classification and fault side detection

Measurement location	Fault location	Fault side detection performance (%)	Best kernel scale	Average training and testing time (s)	Deleted features
{M ₅ ,M ₆ }	C ₅	100	0.2807	3.8364	—
{M ₁₁ ,M ₆ }	C ₅	100	1.8874	3.7765	—
{M ₁ ,M ₆ }	C ₅	97.5	0.1374	3.7592	5,3
{M ₅ ,M ₂ }	C ₅	100	0.2212	3.7513	—
{M ₅ ,M ₁₂ }	C ₅	100	0.1743	3.7573	—
{M ₁₁ ,M ₂ }	C ₅	100	0.1743	3.7370	—
{M ₁ ,M ₁₂ }	C ₅	97.5	0.1743	3.7676	—
{M ₁ ,M ₂ }	C ₅	100	0.1743	3.8617	—
{M ₁₁ ,M ₁₂ }	C ₅	100	0.1743	3.7969	—

Table 9 Results obtained from running KNN on FFT-based features for classification and fault side detection

Measurement location	Fault location	Fault side detection performance (%)	Best number of neighbors	Average training and testing time (s)	Deleted features
{M ₅ ,M ₆ }	C ₅	100	2	0.1459	—
{M ₁₁ ,M ₆ }	C ₅	100	2	0.0972	—
{M ₁ ,M ₆ }	C ₅	97.5	5	0.0948	3,9
{M ₅ ,M ₂ }	C ₅	100	1	0.1081	—
{M ₅ ,M ₁₂ }	C ₅	100	1	0.1176	—
{M ₁₁ ,M ₂ }	C ₅	100	1	0.1173	—
{M ₁ ,M ₁₂ }	C ₅	100	1	0.1203	3
{M ₁ ,M ₂ }	C ₅	100	1	0.1001	—
{M ₁₁ ,M ₁₂ }	C ₅	100	1	0.1086	—

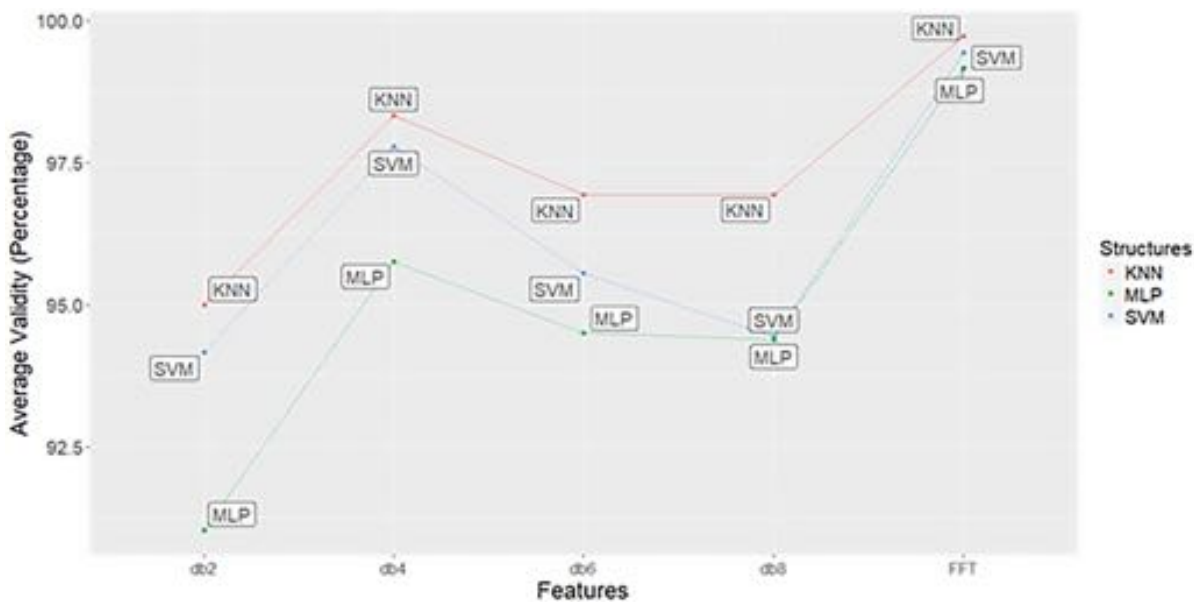


Fig. 10 Performance comparison of different structures for the fault side detection purpose

Table 10 Results obtained from running SVM on FFT+db4-based features by applying PCA for fault side detection

Measurement location	Fault location	Fault side detection performance (%)	Best kernel scale	Average training and testing time (s)
{M ₅ ,M ₆ }	C ₅	100	0.5736	3.6341
{M ₁₁ ,M ₆ }	C ₅	100	1.1721	3.7871
{M ₁ ,M ₆ }	C ₅	100	0.2212	3.7024
{M ₅ ,M ₂ }	C ₅	100	0.2807	3.9206
{M ₅ ,M ₁₂ }	C ₅	100	0.4520	3.5777
{M ₁₁ ,M ₂ }	C ₅	100	0.1743	3.6572
{M ₁ ,M ₁₂ }	C ₅	100	0.4520	3.5451
{M ₁ ,M ₂ }	C ₅	100	0.9237	3.8256
{M ₁₁ ,M ₁₂ }	C ₅	100	0.3562	4.0446

Table 11 Results obtained from running KNN on FFT+db4-based features by applying PCA for fault side detection

Measurement location	Fault location	Fault side detection performance (%)	Best number of neighbors	Average training and testing time (s)
{M ₅ ,M ₆ }	C ₅	100	1	0.1140
{M ₁₁ ,M ₆ }	C ₅	100	2	0.1333
{M ₁ ,M ₆ }	C ₅	100	3	0.0944
{M ₅ ,M ₂ }	C ₅	100	1	0.1448
{M ₅ ,M ₁₂ }	C ₅	100	1	0.0952
{M ₁₁ ,M ₂ }	C ₅	100	2	0.0946
{M ₁ ,M ₁₂ }	C ₅	100	3	0.0951
{M ₁ ,M ₂ }	C ₅	100	5	0.1810
{M ₁₁ ,M ₁₂ }	C ₅	100	1	0.1189

classification procedure by SVM and KNN methods is same as “Single-sensor condition monitoring” section. The results of classification based on FFT extracted features are listed in Tables 7–9.

In Fig. 10, validity label shows average performance of whole rows, which is an appropriate indicator of paired sensors’ result. According to the figure, KNN classifiers are the best choice for fault side detection purposes; in each set of features, they reach higher validity with less computational cost. In small size of datasets, KNNs still have an acceptable performance.

Between wavelet-based features, db4 gives classifiable features. Comparing with wavelet-based features, FFT-based features are more reliable and they lead to higher performances. But still in Tables 7–9, some features seem to be correlated and data points are nonseparable. In order to attain higher performance, we require to gain much separable and rich features: combined FFT and db4-based features. Then, PCA is applied and reduces number of features, effectively.

Based on Tables 10 and 11, the whitened data provides an improved separability and the highest performance for detection of the fault side can be obtained. On the other hand, the complexity of computations and the average running time decrease.

7 Conclusions

A classification-based fault detection system for a high-power 12-cylinder trainset diesel engine was developed and implemented to pinpoint the combustion faults resulted from abnormal fuel injection. Vibration signals were analyzed in frequency and time-frequency domains. PSDs of the vibration signals were calculated and distinguished between normal and faulty engines. Nevertheless, PSDs cannot discriminate the faulty cylinders. Hence, FFT-based data features were introduced in order to overcome the problem. Conceptually, these features show the average energy in selected intervals. Furthermore, WPT-based features were used to identify the energy difference between normal and faulty conditions. Between wavelet-based features, the db4 of Daubechies wavelets provided classifiable features in order to enhance performance of the condition monitoring and fault detection procedures. In order to analyze the derived features, well-known classifiers including SVM, MLP, and KNN were utilized in both “Single-sensor condition monitoring” and “Classification and fault detection” sections. FFT extracted features were more classifiable and uncorrelated rather than DWT-based features. Therefore, the average performance reached up to 99.72%, based on these features. The initiative of this research was to introduce well-separable features based on FFT analyses and to combine these features with db4 extracted features. By applying PCA, the combination of features raised ACCR to almost perfect percentage. In addition, use of this feature extraction method resulted in decreasing the complexity of computations and average running time for fault detection.

Acknowledgment

Authors would like to thank Iranian Raja Rail Transportation Company for helping the research team acquire the test datasets.

Conflict of Interest Statement

The authors certify that they have no affiliations with or involvement in any organization or entity with any financial interest, or non-financial interest in the subject matter or materials discussed in this paper.

References

- [1] Jones, N. B., and Li, Y.-H., 2000, “A Review of Condition Monitoring and Fault Diagnosis for Diesel Engines,” *Tribotest*, 6(3), pp. 267–291.
- [2] Traver, M. L., Atkinson, R. J., and Atkinson, C. M., 1999, “Neural Network-Based Diesel Engine Emissions Prediction Using in-Cylinder Combustion Pressure,” *SAE Paper No. 1999-01-1532*.
- [3] Li, Z., Yan, X., Yuan, C., and Peng, Z., 2012, “Intelligent Fault Diagnosis Method for Marine Diesel Engines Using Instantaneous Angular Speed,” *J. Mech. Sci. Technol.*, 26(8), pp. 2413–2423.
- [4] Assanis, D. N., and Friedmann, F. A., 1993, “A Thin-Film Thermocouple for Transient Heat Transfer Measurements in Ceramic-Coated Combustion Chambers,” *Int. Commun. Heat Mass Transfer*, 20(4), pp. 459–468.
- [5] Albarbar, A., Gu, F., and Ball, A. D., 2010, “Diesel Engine Fuel Injection Monitoring Using Acoustic Measurements and Independent Component Analysis,” *Measurements*, 43(10), pp. 1376–1386.
- [6] Jiang, K., Cao, E., and Wei, L., 2016, “NO_x Sensor Ammonia Cross-Sensitivity Estimation With Adaptive Unscented Kalman Filter for Diesel-Engine Selective Catalytic Reduction Systems,” *Fuel*, 165, pp. 185–192.
- [7] Wang, Y., Zhang, F., Cui, T., and Zhou, J., 2016, “Fault Diagnosis for Manifold Absolute Pressure Sensor (MAP) of Diesel Engine Based on Elman Neural Network Observer,” *Measurement and Fault Diagnosis*, 29(2), pp. 386–395.
- [8] Chen, J., Randall, R. B., and Peeters, B., 2016, “Advanced Diagnostic System for Piston Slap Faults in IC Engines, Based on the Non-Stationary Characteristics of the Vibration Signals,” *Mech. Syst. Signal Process.*, 75, pp. 434–454.
- [9] Dayong, N., Changle, S., Yongjun, G., Zengmeng, Z., and Jiaoyi, H., 2016, “Extraction of Fault Component From Abnormal Sound in Diesel Engines Using Acoustic Signals,” *Mech. Syst. Signal Process.*, 75, pp. 544–555.
- [10] Moosavian, A., Najafi, G., Ghobadian, B., Mirsalim, M., Jafari, S. M., and Sharghi, P., 2016, “Piston Scuffing Fault and Its Identification in an IC Engine by Vibration Analysis,” *Appl. Acoust.*, 102, pp. 40–48.
- [11] Taghizadeh-Alisaraei, A., Ghobadian, B., Tavakoli-Hashjin, T., Mohtasebi, S. S., Rezaei-Asl, A., and Azadbakht, M., 2016, “Characterization of Engine’s Combustion-Vibration Using Diesel and Biodiesel Fuel Blends by Time-Frequency Methods: A Case Study,” *Renewable Energy*, 95, pp. 422–432.
- [12] Zhou, J., Qin, Y., Kou, L., Yuwono, M., and Su, S., 2015, “Fault Detection of Rolling Bearing Based on FFT and Classification,” *J. Adv. Mech. Des. Syst. Manuf.*, 9(5), pp. 1–5.
- [13] Liu, H., Wang, J., and Lu, C., 2013, “Rolling Bearing Fault Detection Based on the Teager Energy Operator and Elman Neural Network,” *Math. Probl. Eng.*, 2013, p. 498385.
- [14] Qi, P., Lezama, J., Jovanovic, S., and Schweitzer, P., 2014, “Adaptive Real-Time DWT-Based Method for Arc Fault Detection,” *27th International Conference on Electrical Contacts*, Dresden, Germany, June 22–26 pp. 1–6.
- [15] Zabihi-Hesari, A., Ansari-Rad, S., Shirazi, F. A., and Ayati, M., 2019, “Fault Detection and Diagnosis of a 12-Cylinder Trainset Diesel Engine Based on Vibration Signature Analysis and Neural Network,” *Proc. Inst. Mech. Eng. Part C*, 233(6), pp. 1910–1923.
- [16] Shirazi, F. A., Ayati, M., Zabihi-Hesari, A., and Ansari-Rad, S., 2018, “Fuel Injection Fault Detection in a Diesel Engine Based on Vibration Signature Analysis,” *Fifth Iranian International NDT Conference*, Tehran, Iran, pp. 1–7.
- [17] Muralidharan, V., and Sugumaran, V., 2016, “A Comparative Study Between Support Vector Machine (SVM) and Extreme Learning Machine (ELM) for Fault Detection in Pumps,” *Indian J. Sci. Technol.*, 9(48), pp. 1–8.
- [18] Atoui, I., Meradi, H., Boulkroune, R., and Saidi, R., 2013, “Fault Detection and Diagnosis in Rotating Machinery by Vibration Monitoring Using FFT and Wavelet Techniques,” *Eighth International Workshop on Systems, Signal Processing and Their Applications (WoSSPA)*, Algiers, Algeria, May 12–15, pp. 401–406.

- [19] Reza Asadi Asad Abad, M., Ahmadi, H., Moosavian, A., Khazaei, M., Ranjbar Kohan, M., and Mohammadi, M., 2013, "Discrete Wavelet Transform and Artificial Neural Network for Gearbox Fault Detection Based on Acoustic Signals," *J. Vibroeng.*, **15**(1), pp. 459–463.
- [20] Koley, E., Verma, K., and Ghosh, S., 2015, "An Improved Fault Detection Classification and Location Scheme Based on Wavelet Transform and Artificial Neural Network for Six Phase Transmission Line Using Single End Data Only," *Springerplus*, **4**(1), p. 551.
- [21] Khajavi, M. N., Nasiri, S., and Eslami, A., 2014, "Combined Fault Detection and Classification of Internal Combustion Engine Using Neural Network," *J. Vibroeng.*, **16**(8), pp. 3912–3921.
- [22] Ahmed, R., El Sayed, M., Gadsden, S. A., Tjong, J., and Habibi, S., 2015, "Automotive Internal-Combustion-Engine Fault Detection and Classification Using Artificial Neural Network Techniques," *IEEE Trans. Veh. Technol.*, **64**(1), pp. 21–33.
- [23] Fernando, H., and Surgenor, B., 2017, "An Unsupervised Artificial Neural Network Versus a Rule-Based Approach for Fault Detection and Identification in an Automated Assembly Machine," *Rob. Comput. Integr. Manuf.*, **43**, pp. 79–88.
- [24] Bangalore, P., and Tjernberg, L. B., 2015, "An Artificial Neural Network Approach for Early Fault Detection of Gearbox Bearings," *IEEE Trans. Smart Grid*, **6**(2), pp. 980–987.
- [25] Rahnavard, M., Ayati, M., Yazdi, M. R. H., and Mousavi, M., 2019, "Finite Time Estimation of Actuator Faults, States, and Aerodynamic Load of a Realistic Wind Turbine," *Renewable Energy*, **130**, pp. 256–267.
- [26] Rahnavard, M., Ayati, M., and Yazdi, M. R. H., 2019, "Robust Actuator and Sensor Fault Reconstruction of Wind Turbine Using Modified Sliding Mode Observer," *Trans. Inst. Meas. Control*, **41**(6), pp. 1504–1518.
- [27] Zhang, K., Du, K., and Ju, Y., 2014, "Algorithm of Railway Turnout Fault Detection Based on PNN Neural Network," *Seventh International Symposium on Computational Intelligence and Design*, Hangzhou, China, Dec. 13–15, pp. 544–547.
- [28] Janssens, O., Slavkovikj, V., Vervisch, B., Stockman, K., Loccufier, M., Verstockt, S., de Walle, R., and Van Hoecke, S., 2016, "Convolutional Neural Network Based Fault Detection for Rotating Machinery," *J. Sound Vib.*, **377**, pp. 331–345.
- [29] González, J. P. N., 2018, "Vehicle Fault Detection and Diagnosis Combining an AANN and Multiclass SVM," *Int. J. Interact. Des. Manuf.*, **12**(1), pp. 273–279.
- [30] Seryasat, O. R., Habibi, M., Ghane, M., and Taherkhani, H., 2014, "Fault Detection of Rolling Bearings Using Discrete Wavelet Transform and Neural Network of SVM," *Adv. Environ. Biol.*, **8**(6), pp. 2175–2184.
- [31] Amir, R. B., Gul, S. T., and Khan, A. Q., 2016, "A Comparative Analysis of Classical and One Class SVM Classifiers for Machine Fault Detection Using Vibration Signals," *International Conference on Emerging Technologies (ICET)*, Islamabad, Pakistan, Oct. 18–19, pp. 1–6.
- [32] Andre, A. B., Beltrame, E., and Wainer, J., 2013, "A Combination of Support Vector Machine and K-Nearest Neighbors for Machine Fault Detection," *Appl. Artif. Intell.*, **27**(1), pp. 36–49.
- [33] Moosavian, A., Ahmadi, H., Sakhaei, B., and Labbafi, R., 2014, "Support Vector Machine and K-Nearest Neighbour for Unbalanced Fault Detection," *J. Qual. Maint. Eng.*, **20**(1), pp. 65–75.
- [34] Chiang, L. H., Russell, E. L., and Braatz, R. D., 2000, "Fault Diagnosis in Chemical Processes Using Fisher Discriminant Analysis, Discriminant Partial Least Squares, and Principal Component Analysis," *Chemom. Intell. Lab. Syst.*, **50**(2), pp. 243–252.
- [35] Cerna, M., and Harvey, A. F., 2000, "The Fundamentals of FFT-Based Signal Analysis and Measurement," National Instrument, Application Note 041.
- [36] Hemmati, F., Orfali, W., and Gadala, M. S., 2016, "Roller Bearing Acoustic Signature Extraction by Wavelet Packet Transform, Applications in Fault Detection and Size Estimation," *Appl. Acoust.*, **104**, pp. 101–118.
- [37] Gaing, Z.-L., 2004, "Wavelet-Based Neural Network for Power Disturbance Recognition and Classification," *IEEE Trans. Power Deliv.*, **19**(4), pp. 1560–1568.
- [38] Saravanan, N., and Ramachandran, K. I., 2010, "Incipient Gear Box Fault Diagnosis Using Discrete Wavelet Transform (DWT) for Feature Extraction and Classification Using Artificial Neural Network (ANN)," *Expert Syst. Appl.*, **37**(6), pp. 4168–4181.
- [39] Paya, B. A., Esat, I. I., and Badi, M. N. M., 1997, "Artificial Neural Network Based Fault Diagnostics of Rotating Machinery Using Wavelet Transforms as a Preprocessor," *Mech. Syst. Signal Process.*, **11**(5), pp. 751–765.
- [40] Browne, A., 1997, *Neural Network Analysis, Architectures and Applications*, CRC Press, Nene College, UK.
- [41] Nelles, O., and Isermann, R., 1996, "Basis Function Networks for Interpolation of Local Linear Models," *35th IEEE Conference on Decision and Control*, Kobe, Japan, Dec. 13, pp. 470–475.
- [42] Kimmich, F., Schwarte, A., and Isermann, R., 2005, "Fault Detection for Modern Diesel Engines Using Signal-and Process Model-Based Methods," *Control Eng. Pract.*, **13**(2), pp. 189–203.
- [43] Vapnik, V., 2013, *The Nature of Statistical Learning Theory*, Springer Science & Business Media, New York.
- [44] Wang, J., Neskovic, P., and Cooper, L. N., 2006, "Neighborhood Size Selection in the K-Nearest-Neighbor Rule Using Statistical Confidence," *Pattern Recognit.*, **39**(3), pp. 417–423.
- [45] Bjørnstad, J. F., and Butler, R. W., 1988, "The Equivalence of Backward Elimination and Multiple Comparisons," *J. Am. Stat. Assoc.*, **83**(401), pp. 136–144.

